EMERGING INFECTIOUS DISEASES®

Mycobacterial Infections

March 2021

Gutzon Borglum. The Saranac Lake Stevenson Memorial at Baker Cottage, 1915. Bronze. 31 in x 18 in. Wikimedia Commons. Holding institution: The Stevenson Society of America, Memorial Cottage at Saranac Lake, New York, USA.

EMERGING INFECTIOUS DISEASES®

EDITOR-IN-CHIEF
D. Peter Drotman

ASSOCIATE EDITORS

Charles Ben Beard, Fort Collins, Colorado, USA
Ermias Belay, Atlanta, Georgia, USA
David M. Bell, Atlanta, Georgia, USA
Sharon Bloom, Atlanta, Georgia, USA
Richard Bradbury, Melbourne, Australia
Mary Brandt, Atlanta, Georgia, USA
Corrie Brown, Athens, Georgia, USA
Benjamin J. Cowling, Hong Kong, China
Michel Drancourt, Marseille, France
Paul V. Effler, Perth, Australia
David O. Freedman, Birmingham, Alabama, USA
Peter Gerner-Smidt, Atlanta, Georgia, USA
Stephen Hadler, Atlanta, Georgia, USA
Matthew J. Kuehnert, Edison, New Jersey, USA
Nina Marano, Atlanta, Georgia, USA
Martin I. Meltzer, Atlanta, Georgia, USA
David Morens, Bethesda, Maryland, USA
J. Glenn Morris, Jr., Gainesville, Florida, USA
Patrice Nordmann, Fribourg, Switzerland
Johann D.D. Pitout, Calgary, Alberta, Canada
Ann Powers, Fort Collins, Colorado, USA
Didier Raoult, Marseille, France
Pierre E. Rollin, Atlanta, Georgia, USA
Frederic E. Shaw, Atlanta, Georgia, USA
David H. Walker, Galveston, Texas, USA
J. Todd Weber, Atlanta, Georgia, USA
J. Scott Weese, Guelph, Ontario, Canada

Associate Editor Emeritus
Charles H. Calisher, Fort Collins, Colorado, USA

Managing Editor
Byron Breedlove, Atlanta, Georgia, USA

Copy Editors Deanna Altomara, Dana Dolan, Karen Foster, Thomas Gryczan, Amy Guinn, Shannon O'Connor, Tony Pearson-Clarke, Jill Russell, Jude Rutledge, P. Lynne Stockton, Deborah Wenger

Production Thomas Eheman, William Hale, Barbara Segal, Reginald Tucker

Journal Administrator Susan Richardson

Editorial Assistants Jane McLean Boggess, Kaylyssa Quinn

Communications/Social Media Heidi Floyd, Sarah Logan Gregory

Founding Editor
Joseph E. McDade, Rome, Georgia, USA

EDITORIAL BOARD

Barry J. Beaty, Fort Collins, Colorado, USA
Martin J. Blaser, New York, New York, USA
Andrea Boggild, Toronto, Ontario, Canada
Christopher Braden, Atlanta, Georgia, USA
Arturo Casadevall, New York, New York, USA
Kenneth G. Castro, Atlanta, Georgia, USA
Christian Drosten, Charité Berlin, Germany
Anthony Fiore, Atlanta, Georgia, USA
Isaac Chun-Hai Fung, Statesboro, Georgia, USA
Kathleen Gensheimer, College Park, Maryland, USA
Rachel Gorwitz, Atlanta, Georgia, USA
Duane J. Gubler, Singapore
Scott Halstead, Arlington, Virginia, USA
David L. Heymann, London, UK
Keith Klugman, Seattle, Washington, USA
S.K. Lam, Kuala Lumpur, Malaysia
Shawn Lockhart, Atlanta, Georgia, USA
John S. Mackenzie, Perth, Australia
John E. McGowan, Jr., Atlanta, Georgia, USA
Jennifer H. McQuiston, Atlanta, Georgia, USA
Tom Marrie, Halifax, Nova Scotia, Canada
Nkuchia M. M'ikanatha, Harrisburg, Pennsylvania, USA
Frederick A. Murphy, Bethesda, Maryland, USA
Barbara E. Murray, Houston, Texas, USA
Stephen M. Ostroff, Silver Spring, Maryland, USA
W. Clyde Partin, Jr., Atlanta, Georgia, USA
Mario Raviglione, Milan, Italy and Geneva, Switzerland
David Relman, Palo Alto, California, USA
Connie Schmaljohn, Frederick, Maryland, USA
Tom Schwan, Hamilton, Montana, USA
Rosemary Soave, New York, New York, USA
Robert Swanepoel, Pretoria, South Africa
David E. Swayne, Athens, Georgia, USA
Kathrine R. Tan, Atlanta, Georgia, USA
Phillip Tarr, St. Louis, Missouri, USA
Duc Vugia, Richmond, California, USA
Mary Edythe Wilson, Iowa City, Iowa, USA

Emerging Infectious Diseases is published monthly by the Centers for Disease Control and Prevention, 1600 Clifton Rd NE, Mailstop H16-2, Atlanta, GA 30329-4027, USA. Telephone 404-639-1960; email, eideditor@cdc.gov

The conclusions, findings, and opinions expressed by authors contributing to this journal do not necessarily reflect the official position of the U.S. Department of Health and Human Services, the Public Health Service, the Centers for Disease Control and Prevention, or the authors' affiliated institutions. Use of trade names is for identification only and does not imply endorsement by any of the groups named above.

All material published in *Emerging Infectious Diseases* is in the public domain and may be used and reprinted without special permission; proper citation, however, is required.

Use of trade names is for identification only and does not imply endorsement by the Public Health Service or by the U.S. Department of Health and Human Services.

EMERGING INFECTIOUS DISEASES is a registered service mark of the U.S. Department of Health & Human Services (HHS).

EMERGING INFECTIOUS DISEASES®

Mycobacterial Infections **March 2021**

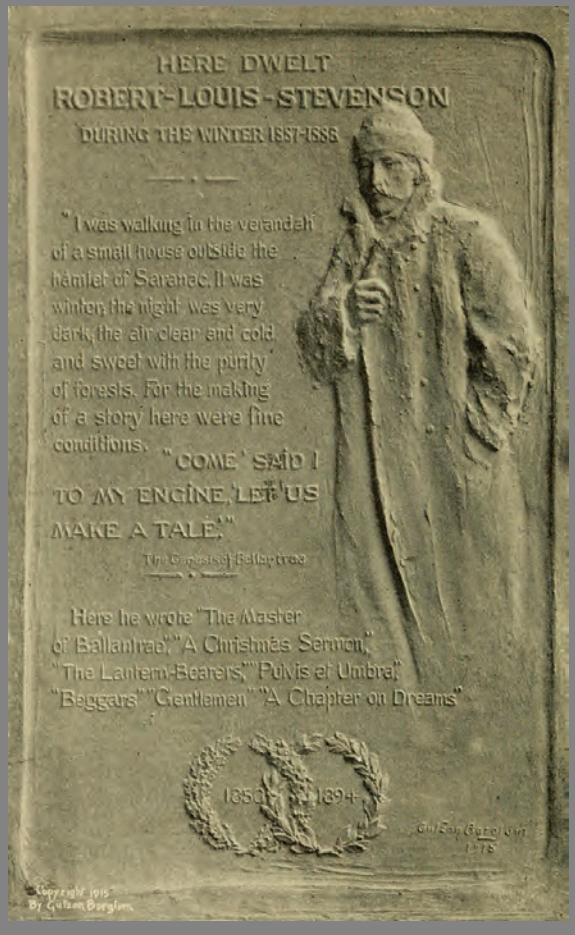

On the Cover

Gutzon Borglum. *The Saranac Lake Stevenson Memorial at Baker Cottage*, 1915. Bronze. 31 in x 18 in. Wikimedia Commons. Holding institution: The Stevenson Society of America, Memorial Cottage at Saranac Lake, New York, USA

About the Cover p. 994

Perspective

Synopses

Research

EMERGING INFECTIOUS DISEASES®
March 2021

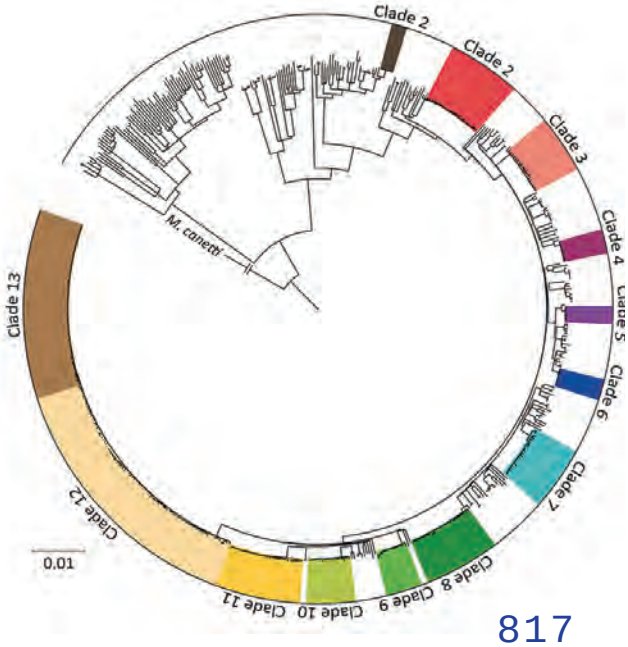

Dispatches

EMERGING INFECTIOUS DISEASES®
March 2021

Another Dimension

Research Letters

Books and Media

About the Cover

Etymologia

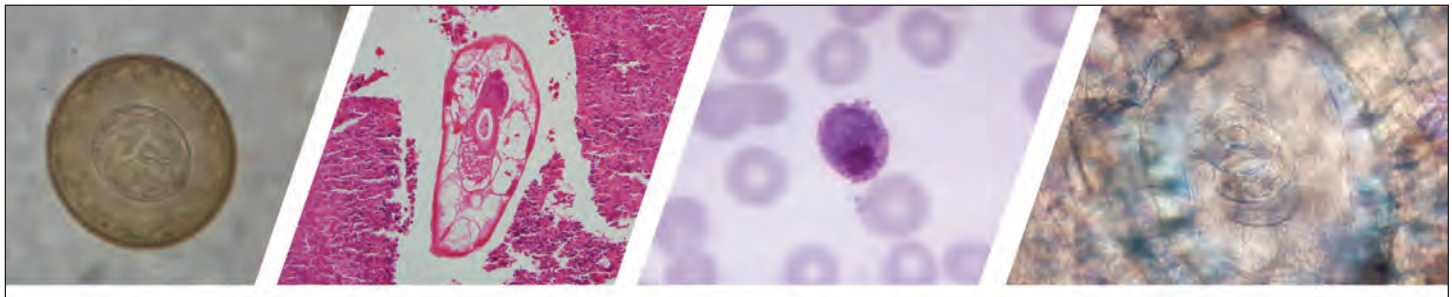

DPDx

Diagnostic Assistance and Training in Laboratory Identification of Parasites

A free service of CDC available to laboratorians, pathologists, and other health professionals in the United States and abroad

- Diagnosis from photographs of worms, histological sections, fecal, blood, and other specimen types
- Expert diagnostic review
- Formal diagnostic laboratory report
- Submission of samples via secure file share

Visit the DPDx website for information on laboratory diagnosis, geographic distribution, clinical features, parasite life cycles, and training via Monthly Case Studies of parasitic diseases.

www.cdc.gov/dpdx
dpdx@cdc.gov

U.S. Department of Health and Human Services
Centers for Disease Control and Prevention

CS272346-DE

Parallels and Mutual Lessons in Tuberculosis and COVID-19 Transmission, Prevention, and Control

Philip C. Hopewell, Lee B. Reichman, Kenneth G. Castro

The coronavirus disease (COVID-19) pandemic has had unprecedented negative effects on global health and economies, drawing attention and resources from many other public health services. To minimize negative effects, the parallels, lessons, and resources from existing public health programs need to be identified and used. Often underappreciated synergies relating to COVID-19 are with tuberculosis (TB). COVID-19 and TB share commonalities in transmission and public health response: case finding, contact identification, and evaluation. Data supporting interventions for either disease are, understandably, vastly different, given the diseases' different histories. However, many of the evolving issues affecting these diseases are increasingly similar. As previously done for TB, all aspects of congregate investigations and preventive and therapeutic measures for COVID-19 must be prospectively studied for optimal evidence-based interventions. New attention garnered by the pandemic can ensure that knowledge and investment can benefit both COVID-19 response and traditional public health programs such as TB programs.

In addition to having devastating effects on the economies of the world, the pandemic of coronavirus disease (COVID-19) itself and the responses entailed in containment and mitigation efforts could have disastrous consequences for existing public health programs, with the impacts being most pronounced in high-burden, low-income settings (*1*,*2*). Modeling of the impact of the COVID-19 pandemic conducted by Imperial College London (London, UK) suggests that in high-burden settings, disease-related deaths over 5 years might be increased by up to 10% for HIV, 20% for TB, and 36% for malaria (*1*).

To minimize the adverse consequences of COVID-19 on overall public health services, synergies between COVID-19 response and traditional public health programs should be sought and the lessons and resources developed in any of the programs should be used for the benefit of the others. In this regard, approaches to TB control might hold lessons for the public health response to COVID-19 and vice-versa.

Synergies and Commonalities for COVID-19 and TB

Several commonalities exist between COVID-19 and TB, most notably transmission of their etiologic agents, severe acute respiratory syndrome coronavirus 2 (SARS-CoV-2) and *Mycobacterium tuberculosis*. Both pathogens are transmitted through secretions from the respiratory tract (*3*–*5*). Moreover, protecting healthcare workers and other susceptible patients and contact identification and evaluation are key components of the public health response to both infections. An understanding of the routes of and factors influencing transmission is necessary to develop effective and efficient measures to control the diseases. For TB, many years of clinical and experimental studies have provided a wealth of information on which to base contact identification, prioritization, and evaluation (*4*). Investigations of TB outbreaks have been especially informative (*6*). Not surprisingly, this level of understanding of SARS-CoV-2 transmission does not exist, and the relative contributions to transmission of large respiratory droplets, fomites, and aerosols remain controversial (*7*). Notably, transmission of both pathogens has been associated with superspreader events (*8*–*10*).

The clinical manifestations of COVID-19 were initially described as mainly involving the respiratory tract, with cough as a predominant symptom along

Author affiliations: Zuckerberg San Francisco General Hospital, University of California, San Francisco, California, USA (P.C. Hopewell); Rutgers New Jersey Medical School, Rutgers University, Newark, New Jersey, USA (L.B. Reichman); Emory University Rollins School of Public Health, Atlanta, Georgia, USA (K.G. Castro); Emory University School of Medicine, Atlanta (K.G. Castro)

DOI: https://doi.org/10.3201/eid2703.203456

with fever, but knowledge of its full natural history, with both immediate and potential long-term consequences, is still increasing rapidly (*3*,*11*). Both the degree of infectiousness and the severity of SARS-CoV-2 infection dictate rapid and effective implementation of healthcare facility infection prevention and control to minimize transmission. These measures include administrative, engineering, and personal measures (i.e., personal protective equipment) and community-based public health activities, even without strong empirical evidence on which to base these interventions.

Seeking COVID-19 Mitigation and Control Strategies

Unquestionably, the package of community-based mitigation measures put into place for the current pandemic has had a major effect in reducing cases and deaths, as shown by Hsiang et al. (*12*). However, uncertainties remain concerning the most effective individual or combinations of measures. These uncertainties preclude the ability to readily identify more targeted and efficient control strategies. Thus, an urgent need exists for a more detailed understanding of SARS-CoV-2 transmission routes and patterns.

Of particular importance is the implementation of monitoring and rapid case identification as current mitigation measures are relaxed. General agreement exists that rapid case identification through PCR-based testing quickly followed by contact identification and evaluation (generally called contact tracing in the context of COVID-19) is the key strategy in reducing transmission in settings where the epidemic curve is flattened or declining (*13*,*14*). Earlier in the pandemic, after the spring 2020 surge subsided, this approach, which closely resembles strategies used for TB, was being scaled up and implemented rapidly. The core actions involve identifying persons with the disease (index case-patients) and identifying and evaluating persons exposed to the index case-patient (contacts) to find additional cases and offer contacts preventive interventions. However, rapid increases in cases in late fall and winter 2020 made contact tracing impractical, simply because of volume. Now, as the pandemic wanes, a trend that we hope will continue, contract tracing is again becoming feasible.

Value of Contact Identification and Evaluation

Contact identification and evaluation have been key components of TB-control measures in most low TB–incidence countries for at least the past 75 years, and a strong scientific basis exists for most, but not all, elements of this activity (*15*,*16*). Although the same information and approaches apply in generally resource-poor, high TB–incidence countries and although international guidelines exist, implementation of routine contact investigations has been very limited (*17*,*18*). In the setting of TB, effective contact investigations have addressed stigma, community engagement, training of interviewers, and use of specific operational guidelines (*17*,*19*). These same elements will likely prove crucial to the effectiveness of COVID-19 contact tracing.

At least 3 important differences exist between factors that should be considered when engaging in contact identification and evaluation for COVID-19 compared with TB. First, because of the short interval between exposure and disease onset, estimated to be a median of 4.1 days for COVID-19, the timeframe for contact identification and evaluation is much shorter than for TB (*20*). In addition, infection with *M. tuberculosis* in immunocompetent hosts most commonly results in latent infection, which can last decades and in most cases never progresses to active TB disease. Second, persons with COVID-19 are most infectious in the immediate presymptomatic and early symptomatic phases, when the viral titers are at their peak, again indicating the need for speed in the contact process for maximal effectiveness (*20*). Third, SARS-CoV-2 clearly is transmitted from person to person predominantly through respiratory secretions that may be inhaled, settling on the mucosal lining of large airways, or be self-inoculated onto nasal mucosa or into the eyes (*7*,*11*,*21*). Unlike TB, the droplets with the SARS-CoV-2 viral cargo might also contaminate and persist on surfaces, although the role played by surface or fomite transmission is not well-quantified (*22*). However, increasing controversies and concerns exist as to the relative contribution of aerosols to overall transmission (*7*,*11*).

The Role of Droplet Nuclei and Acquisition of Infection

M. tuberculosis is transmitted nearly exclusively by aerosolized droplet nuclei, particles <5 μm in aerodynamic diameter (*23*). Large droplets per se are not effective vehicles for transmission of *M. tuberculosis*; however, as the water content of large droplets evaporates, droplet nuclei are formed. The closeness and duration of exposure to a person with infectious TB, as well as the ventilation of the space in which the exposure occurs, influence the likelihood of transmission. Nevertheless, TB outbreaks have been documented with more casual exposures in churches, schools, nursing homes, prisons and jails, and long airplane flights, as well as in other congregate settings, many of which have also been locations of documented SARS-CoV-2 transmission (*6*,*23*–*27*).

Direct and indirect evidence that SARS-CoV-2 may also be transmitted by aerosols with droplet nuclei (i.e., fine particles that remain suspended in air) carrying infectious particles (*5*,*7*,*28*) is increasing. A description of an outbreak of COVID-19, associated with a restaurant in Guangzhou, China, strongly suggested transmission through an airborne route (*29*), as did case distribution and additional studies of air circulation, also in this restaurant in Guangzhou (Y. Li, unpub. data, https://doi.org/10.1101/2020.04.16.20067728).

For both TB and COVID-19, cough is a predominant symptom, and airborne droplets are produced by any forced expiratory maneuver, especially coughing; at least for TB, the severity of cough is an indicator of transmission risk. For TB, several additional indicators assist in quantifying the risk for transmission from the index case and, thus, in assigning priority to a contact investigation. These indicators include the bacillary burden, as indicated by the radiographic extent of the disease in the lungs and the presence or absence of cavitary lesions and qualitative sputum smear positivity (*16*,*30*). No such assessment is routinely used for COVID-19, although quantification of viral load in nasal or pharyngeal swab specimens and an assessment of the severity and duration of respiratory symptoms could provide such information (*31*,*32*). Reduction in viral inoculum by widespread wearing of masks has been postulated to result in less severe manifestations of SARS-CoV-2 infection (*33*).

For TB, because of the increasing risk for acquisition of infection with the closeness and duration of exposure to persons with this disease, contact evaluation can be structured, beginning in the home, workplace, or school, and places of leisure and working outward in a manner that conceptually resembles concentric circles. The number and percentage of close contacts with evidence of disease, or recent infection, inform the need to expand the investigation to contacts in outer ring circles. This iterative approach optimizes the use of resources for investigations and testing (*16*,*30*). For SARS-CoV-2, data strongly suggest that the virus is highly transmissible even with casual contact, so the duration of exposure might not be relevant (*14*,*20*,*32*).

All of the foregoing indicates that in conducting contact identification and evaluation for persons exposed to persons with COVID-19, a wide net must be cast. Moreover, given the incubation period and pace of the disease, the process must be accomplished much more quickly than is necessary for TB. Unfortunately, much of the knowledge base that is used to guide TB contact identification and evaluation does not yet exist for COVID-19. To generate the necessary information, investigators studying the epidemiology of COVID-19 and, in particular, those charged with investigating outbreaks and conducting contact tracing, should be certain that the data being collected will enable analyses directed toward identifying factors that influence viral transmission. A recent report of nationwide contact tracing for COVID-19 in South Korea indicated both the need to investigate ≈10 contacts per index case and that 11.8% of household contacts had COVID-19, >6 times the 1.9% prevalence of COVID-19 in nonhousehold contacts (*34*).

Using the Investigation of TB on the USS Byrd as a Template

Essentially all infection control and public health measures for TB are based on the understanding, backed by strong empirical and experimental evidence, that *M. tuberculosis* is transmitted nearly exclusively by aerosols (*23*,*35*). Some of the strongest evidence of *M. tuberculosis* transmission through aerosols has been derived from several TB outbreak investigations. Perhaps the most notable and informative outbreak investigation was conducted in response to a single crew member who was found the have cavitary pulmonary TB during the course of a long sea tour by the US Navy vessel the USS Richard Byrd in 1965 (*36*). A thorough assessment of the patterns of air circulation and their relationship to new cases and infections was conducted aboard the ship. The investigation found that all new cases and infections occurred in crew members who had either direct personal contact with the index case-patient or were exposed through recirculated air in a closed ventilation system. The investigators were able to establish what might be viewed as a dose-response curve based on the exposure to different amounts of recirculated air and the proportion exposed crew members who were infected (*36*). Of particular note, several of the newly infected sailors (indicated by a new positive tuberculin skin test) who were asymptomatic and had negative chest radiographs were found to have *M. tuberculosis* in their sputum, raising the possibility of transmission from persons without the usual symptoms of TB, as is the case with COVID-19 (*20*,*32*). This finding is consistent with findings from national TB prevalence surveys of a substantial proportion of study subjects who were found to have *M. tuberculosis* in their sputum but had no symptoms (e.g., cough >2 weeks) (*37*).

Outbreaks of COVID-19 on a cruise ship (Diamond Princess) in late January 2020 and the USS Theodore Roosevelt in March 2020 provide unique opportunities, similar to those provided by the USS Byrd, to gain a more detailed understanding of transmission patterns for SARS-CoV-2. To date, published assessments of COVID-19 outbreaks in these 2 separate settings consist of initial assessments, 1 documenting the

occurrence of 700 cases of COVID-19 among nearly 3,700 passengers and crew members in the cruise ship (*38*). The investigation identified that 15 of 20 cases in crew members were in food workers, and 16 of these 20 persons slept in cabins on deck 3. No details were provided for the distribution of COVID-19 cases in passengers, nor of the ventilation system in this cruise ship (*38*). A follow-up assessment was limited to 215 Hong Kong passengers after quarantine and disembarkation; 9 tested positive for SARS-CoV-2 (*39*). No berthing information is available for those passengers. The USS Roosevelt outbreak investigation was a serostudy of a convenience sample of 382 crew members (*40*). Although the sample was not representative of the entire crew, 60% of the participants had antibodies to SARS-CoV-2, indicating prior infection. Notably, 20% of the seropositive group denied having symptoms. Also, as is the case with asymptomatic TB, the degree to which these asymptomatic persons transmitted the infection is not known. Examination of crew member duty rosters and assessment of ventilation patterns in areas inhabited by infected and noninfected persons could provide important information concerning aerosol transmission and the role of spread of the virus by asymptomatic persons. Although the outbreak on the USS Byrd occurred >50 years ago, its assessment is a model for advancing knowledge by thorough investigations, including environmental studies to examine the role of air circulation. With increasing speculation and uncertainty about basic questions such as relative importance of different transmission modes for SARS-CoV-2 (*5*,*7*), the Diamond Princess and USS Roosevelt outbreaks present opportunities, similar to that provided by the USS Byrd, that should not be overlooked.

As noted, although contact identification and evaluation are widely used in high-income, low TB–incidence countries, implementation is limited in low- and middle-income countries. Given the experience with TB, considerable patience, skill, and ingenuity are needed in the implementation of contact tracing for COVID-19. Digital and other automated technologies have been applied to COVID-19 contact tracing in different country settings (*41*,*42*). This new thinking, coupled with innovative tools, will likely hold lessons and examples for improvements in TB prevention and control.

Avoiding Past Mistakes and Seizing Present Opportunities

In response to COVID-19, countries are having to reassign or recruit and train staff, as well as to establish a robust laboratory diagnostic testing capacity to deliver timely quality-assured results. Early reports from the United States have documented that the COVID-19 response has diverted resources away from essential TB services (*43*). This scenario must be avoided; investments required should be used to improve all public health programs and be sustained over time. Thirty-five years ago, TB provided a dramatic example of the impact of inattention to, and disinvestments in, basic public health programs. During 1985–1992, a reversal of longstanding downward trends occurred as well as and 20% increase in cases (*44*,*45*).

We now have a rare opportunity to seize the moment and use the attention garnered by this novel virus pandemic to ensure that new investments contribute not only to the control of COVID-19, but also to the strengthening of older, yet very relevant public health programs, and to recognize that lessons learned from those programs benefit those at risk for COVID-19. In the United States and in other parts of the world, TB served as the impetus for the establishment of public health programs, and these programs were geared to deal with TB as a public health problem (*46*,*47*). Public health approaches to COVID-19, relying as they do on accelerated responses, digital technologies, and large numbers of trained community-based contact investigators, could establish a new more comprehensive paradigm for the public health programs of the future.

About the Author

Dr. Castro is Professor of Global Health, Epidemiology, and Infectious Diseases, Rollins School of Public Health and School of Medicine, Emory University, Atlanta, GA, and Senior Tuberculosis Scientific Advisor to the US Agency for International Development, Washington, DC. His primary research interests are in the rapid diagnosis, optimal clinical management, and epidemiology of persons with HIV and tuberculosis, including those with drug-resistant forms of tuberculosis.

References

1. Hogan AB, Jewell B, Sherrard-Smith E, Vesga J, Watson OJ, Whittaker C, et al. The potential impact of the COVID-19 epidemic on HIV, TB and malaria in low- and middle-income countries. Imperial College London. May 2020 [cited 2020 Oct 27]. https://www.imperial.ac.uk/media/imperial-college/medicine/mrc-gida/2020-05-01-COVID19-Report-19.pdf
2. The Global Fund to Fight AIDS. Tuberculosis and malaria. Mitigating the impact of COVID 19 on countries affected by HIV, tuberculosis and malaria. June 2020 [cited 2020 Oct 27]. https://www.theglobalfund.org/media/9819/covid19_mitigatingimpact_report_en.pdf
3. Wu F, Zhao S, Yu B, Chen YM, Wang W, Song ZG, et al. A new coronavirus associated with human respiratory disease

in China. Nature. 2020;579:265–9. https://doi.org/10.1038/s41586-020-2008-3
4. Hopewell PC. Factors influencing the transmission and infectivity of *Mycobacterium tuberculosis*: implication for clinical and public health management of tuberculosis. In: Sande MA, Root RK, Hudson LD, editors. Respiratory Infections. New York: Churchill Livingstone Inc.; 1986. P. 191–216.
5. Meyerowitz EA, Richterman A, Gandhi RT, Sax PE. Transmission of SARS-CoV-2: a review of viral, host, and environmental factors. Ann Intern Med. 2020 Sep 17 [Epub ahead of print].
6. Hadler SC, Castro KG, Dowdle W, Hicks L, Noble G, Ridzon R. Epidemic Intelligence Service investigations of respiratory illness, 1946–2005. Am J Epidemiol. 2011;174(Suppl):S36–46. https://doi.org/10.1093/aje/kwr309
7. Morawska L, Milton DK. Is it time to address airborne transmission of COVID-19. Clin Infect Dis. 2020 Jul 6 [Epub ahead of print].
8. Kline SE, Hedemark LL, Davies SF. Outbreak of tuberculosis among regular patrons of a neighborhood bar. N Engl J Med. 1995;333:222–7. https://doi.org/10.1056/NEJM199507273330404
9. Valway SE, Sanchez MPC, Shinnick TF, Orme I, Agerton T, Hoy D, et al. An outbreak involving extensive transmission of a virulent strain of *Mycobacterium tuberculosis*. N Engl J Med. 1998;338:633–9. https://doi.org/10.1056/NEJM199803053381001
10. Frieden TR, Lee CT. Identifying and interrupting superspreading events-implications for control of severe acute respiratory syndrome coronavirus 2. Emerg Infect Dis. 2020;26:1059–66. https://doi.org/10.3201/eid2606.200495
11. Wiersinga WJ, Rhodes A, Cheng AC, Peacock SJ, Prescott HC. Pathophysiology, transmission, diagnosis, and treatment of coronavirus disease 2019 (COVID-19): a review. JAMA. 2020;324:782–93.
12. Hsiang S, Allen D, Annan-Phan S, Bell K, Bolliger I, Chong T, et al. The effect of large-scale anti-contagion policies on the COVID-19 pandemic. Nature. 2020;584:262–7.
13. World Health Organization. Contact tracing in the context of COVID 19: interim guidance, 10 May 2020 [cited 2020 Oct 27]. https://www.who.int/publications/i/item/contact-tracing-in-the-context-of-covid-19
14. CDC. Interim guidance on developing a COVID-19 case investigation & contact tracing plan: overview [cited 2020 Oct 27]. https://www.cdc.gov/coronavirus/2019-ncov/php/contact-tracing/contact-tracing-plan/overview.html
15. Erkins CGM, Kamphorst M, Abubakar I, Bothamley GH, Chemtob D, Haas W, et al. Tuberculosis contact investigation in low prevalence countries: a European consensus. Eur Resp J 2010;36:925–49.
16. National Tuberculosis Controllers Association; Centers for Disease Control and Prevention (CDC). Guidelines for the investigation of contacts of persons with infectious tuberculosis. Recommendations from the National Tuberculosis Controllers Association and CDC. MMWR Recomm Rep. 2005;54(No. RR-15):1–47.
17. Fair E, Miller CR, Ottmani S-E, Fox GJ, Hopewell PC. Tuberculosis contact investigation in low- and middle-income countries: standardized definitions and indicators. Int J Tuberc Lung Dis. 2015;19:269–72. https://doi.org/10.5588/ijtld.14.0512
18. Reichman LB. The tuberculosis taboo. Int J Tuberc Lung Dis. 2017;21:251–5. https://doi.org/10.5588/ijtld.16.0621
19. Marangu D, Mwaniki H, Nduku S, Maleche-Obimbo E, Jaoko W, Babigumira J, et al. Stakeholder perspectives for optimization of tuberculosis contact investigation in a high-burden setting. PLoS One. 2017;12:e0183749. https://doi.org/10.1371/journal.pone.0183749
20. Cheng H-Y, Jian S-W, Liu D-P, Ng TC, Huang WT, Lin HH; Taiwan COVID-19 Outbreak Investigation Team. Contact tracing assessment of COVID-19 transmission dynamics in Taiwan and risk at different exposure periods before and after symptom onset. JAMA Intern Med. 2020;180:1156–63. https://doi.org/10.1001/jamainternmed.2020.2020
21. Ong SWX, Tan YK, Chia PY, Lee TH, Ng OT, Wong MSY, et al. Air, surface environmental, and personal protective equipment contamination by severe acute respiratory syndrome coronavirus 2 (SARS-CoV-2) from a symptomatic patient. JAMA. 2020;323:1610–2. https://doi.org/10.1001/jama.2020.3227
22. Chin AWH, Chu JTS, Perera MRA, Hui KPY, Yen HL, Chan MCW, et al. Stability of SARS-CoV-2 in different environmental conditions. Lancet Microbe. 2020;1:e10. https://doi.org/10.1016/S2666-5247(20)30003-3
23. Churchyard G, Kim P, Shah NS, Rustomjee R, Gandhi N, Mathema B, et al. What we know about tuberculosis transmission: an overview. J Infect Dis. 2017;216(suppl_6):S629–35. https://doi.org/10.1093/infdis/jix362
24. Kenyon TA, Valway SE, Ihle WW, Onorato IM, Castro KG. Transmission of multidrug-resistant *Mycobacterium tuberculosis* during a long airplane flight. N Engl J Med. 1996;334:933–8. https://doi.org/10.1056/NEJM199604113341501
25. Driver CR, Valway SE, Morgan WM, Onorato IM, Castro KG. Transmission of *Mycobacterium tuberculosis* associated with air travel. JAMA. 1994;272:1031–5. https://doi.org/10.1001/jama.1994.03520130069035
26. Khanh NC, Thai PQ, Quach H-L, Thi NA-H, Dinh PC, Duong TN, et al. Transmission of severe acute respiratory syndrome coronavirus 2 during long flight. Emerg Infect Dis. 2020 Sep 18 [Epub ahead of print]. https://doi.org/10.3201/eid2611.203299
27. Choi EM, Chu DKW, Cheng PKC, Tsang DNC, Peiris M, Bausch DG, et al. In-flight transmission of severe acute respiratory syndrome coronavirus 2. Emerg Infect Dis. 2020;26:2617–24.
28. Tellier R, Li Y, Cowling BJ, Tang JW. Recognition of aerosol transmission of infectious agents: a commentary. BMC Infect Dis. 2019;19:101. https://doi.org/10.1186/s12879-019-3707-y
29. Lu J, Gu J, Li K, Xu C, Su W, Lai Z, et al. COVID-19 outbreak associated with air conditioning in restaurant, Guangzhou, China, 2020. Emerg Infect Dis. 2020;26:1628–31. https://doi.org/10.3201/eid2607.200764
30. Young KH, Ehman M, Reves R, Peterson Maddox BL, Khan A, Chorba TL, et al. Tuberculosis contact investigations—United States, 2003–2012. MMWR Morb Mortal Wkly Rep. 2016;64:1369–74. https://doi.org/10.15585/mmwr.mm6450a1
31. Wölfel R, Corman VM, Guggemos W, Seilmaier M, Zange S, Müller MA, et al. Virological assessment of hospitalized patients with COVID-2019. Nature. 2020;581:465–9. https://doi.org/10.1038/s41586-020-2196-x
32. Furukawa NW, Brooks JT, Sobel J. Evidence supporting transmission of severe acute respiratory syndrome coronavirus 2 while presymptomatic or asymptomatic. Emerg Infect Dis. 2020;26:26. https://doi.org/10.3201/eid2607.201595
33. Gandhi M, Rutherford GW. Facial Masking for Covid-19 - Potential for "variolation" as we await a vaccine. N Engl J Med. 2020 Sep 8 [Epub ahead of print].
34. Park YJ, Choe YJ, Park O, Park SY, Kim YM, Kim J, et al.; COVID-19 National Emergency Response Center,

Epidemiology and Case Management Team. Contact tracing during coronavirus disease outbreak, South Korea, 2020. Emerg Infect Dis. 2020;26:2465–8. https://doi.org/10.3201/eid2610.201315
35. Riley RL, Wells WF, Mills CC, Nyka W, McLean RL. Air hygiene in tuberculosis: quantitative studies of infectivity and control in a pilot ward. Am Rev Tuberc. 1957;75:420–31.
36. Houk VN, Baker JH, Sorensen K, Kent DC. The epidemiology of tuberculosis infection in a closed environment. Arch Environ Health. 1968;16:26–35. https://doi.org/10.1080/00039896.1968.10665011
37. Onozaki I, Law I, Sismanidis C, Zignol M, Glaziou P, Floyd K. National tuberculosis prevalence surveys in Asia, 1990–2012: an overview of results and lessons learned. Trop Med Int Health. 2015;20:1128–45. https://doi.org/10.1111/tmi.12534
38. Kakimoto K, Kamiya H, Yamagishi T, Matsui T, Suzuki M, Wakita T. Initial investigation of transmission of COVID-19 among crew members during quarantine of a cruise ship—Yokohama, Japan, February 2020. MMWR Morb Mortal Wkly Rep. 2020;69:312–3. https://doi.org/10.15585/mmwr.mm6911e2
39. Hung IFN, Cheng VCC, Li X, Tam AR, Hung DLL, Chiu KHY, et al. SARS-CoV-2 shedding and seroconversion among passengers quarantined after disembarking a cruise ship: a case series. Lancet Infect Dis. 2020;20:1051–60. https://doi.org/10.1016/S1473-3099(20)30364-9
40. Payne DC, Smith-Jeffcoat SE, Nowak G, Chukwuma U, Geibe JR, Hawkins RJ, et al.; CDC COVID-19 Surge Laboratory Group. SARS-CoV-2 infections and serologic responses from a sample of U.S. Navy service members—USS Theodore Roosevelt, April 2020. MMWR Morb Mortal Wkly Rep. 2020;69:714–21. https://doi.org/10.15585/mmwr.mm6923e4
41. Lin C, Braund WE, Auerbach J, Chou JH, Teng JH, Tu P, et al. Policy decisions and use of information technology to fight COVID-19, Taiwan. Emerg Infect Dis. 2020;26:1506–12. https://doi.org/10.3201/eid2607.200574
42. Braithwaite I, Callender T, Bullock M, Aldridge RW. Automated and partly automated contact tracing: a systematic review to inform the control of COVID-19. Lancet Digit Health. 2020;2:e607–21. https://doi.org/10.1016/S2589-7500(20)30184-9
43. Cronin AM, Railey S, Fortune D, Wegener DH, Davis JB. Notes from the field: effects of the COVID-19 response on tuberculosis prevention and control efforts—United States, March–April 2020. MMWR Morb Mortal Wkly Rep. 2020;69:971–2. https://doi.org/10.15585/mmwr.mm6929a4
44. Reichman LB. The U-shaped curve of concern. Am Rev Respir Dis. 1991;144:741–2. https://doi.org/10.1164/ajrccm/144.4.741
45. Cantwell MF, Snider DE Jr, Cauthen GM, Onorato IM. Epidemiology of tuberculosis in the United States, 1985 through 1992. JAMA. 1994;272:535–9. https://doi.org/10.1001/jama.1994.03520070055038
46. McKenna MT, McCray E, Jones JL, Onorato IM, Castro KG. The fall after the rise: tuberculosis in the United States, 1991 through 1994. Am J Public Health. 1998;88:1059–63. https://doi.org/10.2105/AJPH.88.7.1059
47. Castro KG, Marks SM, Chen MP, Hill AN, Becerra JE, Miramontes R, et al. Estimating tuberculosis cases and their economic costs averted in the United States over the past two decades. Int J Tuberc Lung Dis. 2016;20:926–33. https://doi.org/10.5588/ijtld.15.1001

Address for correspondence: Kenneth G. Castro, Rollins School of Public Health, Emory University, 1518 Clifton Rd NE (CNR 6013), Atlanta, GA 30322, USA; email: kcastro@emory.edu

EID Podcast

Telework during Epidemic Respiratory Illness

The COVID-19 pandemic has caused us to reevaluate what "work" should look like. Across the world, people have converted closets to offices, kitchen tables to desks, and curtains to videoconference backgrounds. Many employees cannot help but wonder if these changes will become a new normal.

During outbreaks of influenza, coronaviruses, and other respiratory diseases, telework is a tool to promote social distancing and prevent the spread of disease. As more people telework than ever before, employers are considering the ramifications of remote work on employees' use of sick days, paid leave, and attendance.

In this EID podcast, Dr. Faruque Ahmed, an epidemiologist at CDC, discusses the economic impact of telework.

Visit our website to listen:
https://go.usa.gov/xfcmN

EMERGING INFECTIOUS DISEASES®

Genomic Evidence of In-Flight Transmission of SARS-CoV-2 Despite Predeparture Testing

Tara Swadi,[1] Jemma L. Geoghegan,[1] Tom Devine, Caroline McElnay, Jillian Sherwood, Phil Shoemack, Xiaoyun Ren, Matt Storey, Sarah Jefferies, Erasmus Smit, James Hadfield, Aoife Kenny, Lauren Jelley, Andrew Sporle, Andrea McNeill, G. Edwin Reynolds, Kip Mouldey, Lindsay Lowe, Gerard Sonder, Alexei J. Drummond, Sue Huang, David Welch, Edward C. Holmes, Nigel French, Colin R. Simpson, Joep de Ligt

Since the first wave of coronavirus disease in March 2020, citizens and permanent residents returning to New Zealand have been required to undergo managed isolation and quarantine (MIQ) for 14 days and mandatory testing for severe acute respiratory syndrome coronavirus 2 (SARS-CoV-2). As of October 20, 2020, of 62,698 arrivals, testing of persons in MIQ had identified 215 cases of SARS-CoV-2 infection. Among 86 passengers on a flight from Dubai, United Arab Emirates, that arrived in New Zealand on September 29, test results were positive for 7 persons in MIQ. These passengers originated from 5 different countries before a layover in Dubai; 5 had negative predeparture SARS-CoV-2 test results. To assess possible points of infection, we analyzed information about their journeys, disease progression, and virus genomic data. All 7 SARS-CoV-2 genomes were genetically identical, except for a single mutation in 1 sample. Despite predeparture testing, multiple instances of in-flight SARS-CoV-2 transmission are likely.

Author affiliations: New Zealand Ministry of Health, Wellington, New Zealand (T. Swadi, T. Devine, A. Kenny); University of Otago, Dunedin, New Zealand (J.L. Geoghegan); Institute of Environmental Science and Research, Porirua, New Zealand (J.L. Geoghegan, J. Sherwood, X. Ren, M. Storey, S. Jefferies, E. Smit, L. Jelley, A. McNeill, G. Sonder, S. Huang, J. de Ligt); New Zealand Ministry of Health, Wellington (C. McElnay); Bay of Plenty District Health Board, Tauranga, New Zealand (P. Shoemack, K. Mouldey, L. Lowe); Fred Hutchinson Cancer Research Centre, Seattle, Washington, USA (J. Hadfield); University of Auckland, Auckland, New Zealand (A. Sporle, A.J. Drummond, D. Welch); iNZight Analytics Ltd., Auckland (A. Sporle); Auckland District Health Board, Auckland (G.E. Reynolds); The University of Sydney, Sydney, New South Wales, Australia (E.C. Holmes); Massey University, Palmerston North, New Zealand (N. French); Victoria University of Wellington, Wellington (C.R. Simpson); University of Edinburgh, Edinburgh, UK (C.R. Simpson)

DOI: https://doi.org/10.3201/eid2703.204714

In response to the growing international risks associated with importation of coronavirus disease (COVID-19), on March 20, 2020, New Zealand closed its borders to all but New Zealand citizens, permanent residents, and persons with an exemption (*1*). On April 9, 2020, to better control importation risks, New Zealand implemented a system of managed isolation and quarantine (MIQ) at the border. Persons arriving in New Zealand were required to stay in a government-assigned MIQ facility for at least 14 days before entering the New Zealand community. In June 2020, a system of testing persons who were returning to New Zealand and staying in MIQ facilities was instituted; nasopharyngeal swabs were taken on approximately the third and the twelfth day of the quarantine period and from anyone in whom symptoms developed or those identified as close contacts of persons with severe acute respiratory syndrome coronavirus 2 (SARS-CoV-2) positive test results.

On September 29, 2020, flight EK448, which originated in Dubai, United Arab Emirates, with a stop in Kuala Lumpur, Malaysia, landed in Auckland, New Zealand. During the required 14-day MIQ period, 7 passengers who had traveled on the flight received positive SARS-CoV-2 test results. The 7 passengers had begun their journeys from 5 different countries before a layover in Dubai; predeparture SARS-CoV-2 test results were negative for 5 (Figure 1). These 7 passengers had been seated within 4 rows of each other during the ≈18-hour flight from Dubai to Auckland. Because recent studies have reported conflicting findings of the risks associated with in-flight transmission (*2*–*4*), we undertook a comprehensive investigation to determine the potential source of infection of these travelers.

[1]These authors contributed equally to this article.

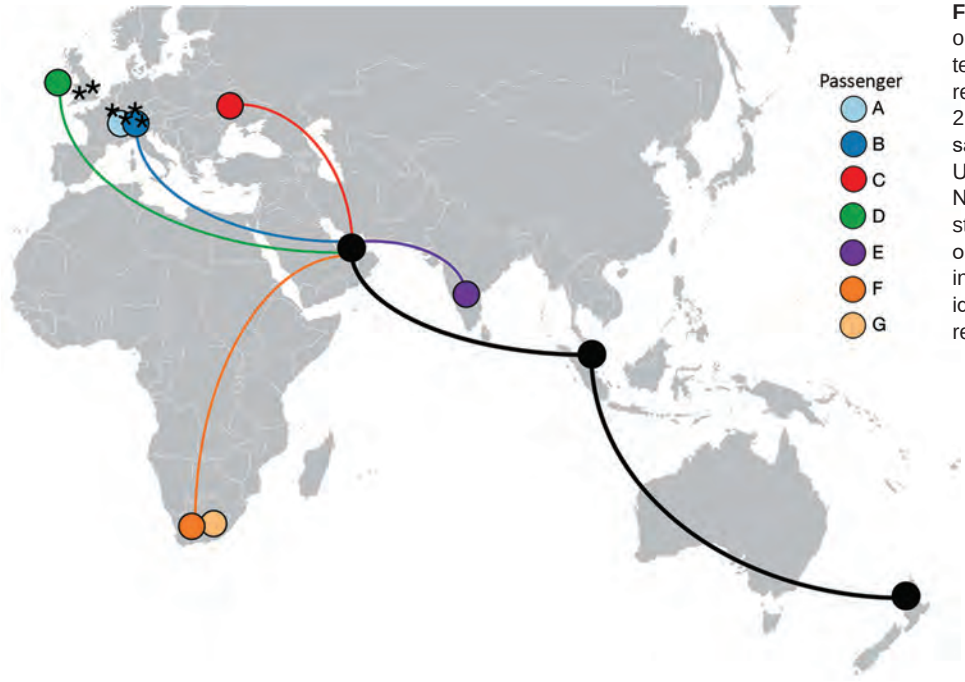

Figure 1. Countries of travel origins for 7 passengers who tested positive for severe acute respiratory syndrome coronavirus 2 infection after traveling on the same flight (EK448) from Dubai, United Arab Emirates, to Auckland, New Zealand, with a refueling stop in Kuala Lumpur, Malaysia, on September 29, 2020. Asterisks indicate where 6 other genetically identical genomes have been reported (*5*).

Methods

Case Details and Consent

In New Zealand, COVID-19 is a notifiable disease; all positive cases are reported to the national surveillance system, enabling further public health investigation. All persons with COVID-19 described in this article were contacted, and they provided written or verbal consent for their data to be used in this article. Case data were collected under the Ministry of Health contract for epidemic surveillance. The 7 persons with COVID-19 are denoted here as passengers A–G (Tables 1, 2).

Clinical Data and Sample Collection

Case details were sourced from the national notifiable diseases database, EpiSurv (https://surv.esr.cri.nz/episurv/index.php). While in MIQ, all 86 passengers on the flight underwent real-time reverse transcription PCR (rRT-PCR) diagnostic testing for SARS-CoV-2 on day 3 and again on day 12 if the previous test result was negative. Cabin crew members departed New Zealand soon after their arrival and were therefore not tested. Investigations used information from rRT-PCR testing by using the Cepheid GeneXpert system (https://www.cepheid.com) and BD Max (https://www.bd.com). We determined seating plans by consulting the flight manifest for the Boeing 777–300ER aircraft and confirmed them by administering a questionnaire to passengers, asking where they actually sat.

Genome Sequencing

Independent viral extracts were prepared by the Institute of Environmental Science and Research (Porirua, New Zealand) from the 7 positive respiratory tract samples in which SARS-CoV-2 was initially detected by rRT-PCR. We extracted RNA from SARS-CoV-2–positive samples and subjected it to whole-genome sequencing by following the 1,200-bp amplicon protocol (*6*) and Oxford Nanopore Rapid barcoding R9.0 sequencing (*7*). Genomic data are available on GISAID (*5*) (Table 1).

Phylogenetic Analysis of SARS-CoV-2 Genomes

The lineage of the genomes obtained from the 7 passengers was determined by using pangolin version 2.0.8 (https://pangolin.cog-uk.io) and compared with genomes from the same lineage available on GISAID (*5*). Genomes were aligned by using MAFFT version 7 (*8*) and using the FFT-NS-2 progressive alignment algorithm. We estimated a maximum-likelihood phylogenetic tree by using IQ-TREE version 1.6.8 (*9*) and the Hasegawa-Kishino-Yano nucleotide substitution model (*10*) with a gamma distributed rate variation among sites (HKY+Γ), the best-fit model as determined by ModelFinder (*11*), and branch support assessment by using the ultrafast bootstrap method (*12*).

Analysis of Disease Transmission Data

All times and dates reported here were converted to New Zealand daylight savings time (Greenwich mean time + 13 hours) (Table 2). The mean incubation

period, defined as the duration between estimated dates of infection and reported symptom onset, has been reported as 5–6 days (range 1–14 days) (*13*). We assumed a 5-day incubation period for passengers A, B, D, E, F, and G, and a 3-day incubation period for passenger C. We considered the median presymptomatic infectious period to be <1–4 days unless a negative PCR result indicated otherwise (*14*).

Results

The Flight

Flight EK448 from Dubai, UAE to Auckland, New Zealand, was an 18-hour, 2-minute flight on a Boeing 777–300ER aircraft. It departed Dubai on September 28, 2020, at 5:29 PM; arrived in Kuala Lumpur on September 29 at 12:11 AM to refuel; and departed Kuala Lumpur on September 29 at 2:03 AM. No passengers entered or exited the aircraft during the 2-hour refueling period in Kuala Lumpur. The flight arrived in Auckland on September 29 at 11:31 AM. During the flight and before departure in Dubai airport, mask use was not mandatory; passengers A, B, D, F, and G self-reported mask and glove use while on the airplane but passengers C and E did not. In the days before the flight, these 7 passengers (other than the 2 travel groups, 1 of which comprised passengers A and B and the other passengers F and G) had been in different countries and did not have any form of contact (Figure 1). Similarly, none of the passengers reported having been in close contact at the Dubai airport. Passengers F and G were part of a family travel group of 4, all of whom reported having changed seats within their row during the flight.

All passengers, with the exception of passenger E, were transferred by bus to an MIQ facility in Rotorua, New Zealand. All passengers reported wearing masks during the bus journeys. Passengers A, B, and D were on bus 1; passengers F and G were on bus 2. Passenger C was initially seated on bus 1 but was transferred to bus 2 before transit. Both buses departed Auckland at 12:05 PM and arrived in Rotorua at 3:00 PM. Passenger E traveled on bus 3 to an MIQ facility in Auckland. Seating on all buses was physically distanced where possible, and mask use was mandated.

Testing and Disease Progression

Five passengers reported having received negative test results before departure (Table 1). A negative test result was mandatory according to airline regulations for passenger C, who traveled from Ukraine.

The first 3 passengers to receive positive SARS-CoV-2 test results (passengers A, B, and C) were

Table 1. Detailed information for 7 passengers with SARS-CoV-2 infection detected after being on flight EK448, Dubai, United Arab Emirates, to Auckland, New Zealand, September 29, 2020*

Variable	Passenger						
	A	B	C	D	E	F	G
Genome	Identical	Identical	Identical†	1 additional mutation	Identical	Identical	Identical
Genome ID (GISAID accession no.) (*5*)	20CV0408 (EPI_ISL_582019)	20CV0409 (EPI_ISL_582020)	20CV0410 (EPI_ISL_582021)	20CV0401 (EPI_ISL_582018)	20CV0398 (EPI_ISL_582017)	20CV0414 (EPI_ISL_582022)	20CV0415 (EPI_ISL_582023)
Preflight testing result (date)‡	Negative (Sep 24)	Negative (Sep 24)	Negative (Sep 25)	Negative (Sep 24)	Not tested	Negative (Sep 25)	Not tested
Symptom onset date	Oct 1	Oct 2	Asymptomatic	Oct 4	Asymptomatic	Oct 3	Oct 9
Date tested positive	Oct 2	Oct 2	Oct 2	Oct 7	Oct 6	Oct 8	Oct 8
Technology§ and C_t	GeneXpert, E-gene C_t 14.3, N2-gene C_t 16.4	GeneXpert, E-gene C_t 27, N2-gene C_t 29.3	GeneXpert, E-gene C_t 33.3, N2-gene C_t 36.8	GeneXpert, E-gene C_t 18.5 N2-gene C_t 20.4	GeneXpert, E-gene C_t 18.5, N2 gene C_t 22.3	BD Max, N1-gene C_t 22.0 N2-gene C_t 22.3	BD Max, N1-gene C_t 22.1, N2-gene C_t 19.1
Country of origin	Switzerland	Switzerland	Ukraine	Ireland	India	South Africa	South Africa
Layover time in Dubai	9 h 27 min	9 h 27 min	11 h 30 min	8 h 18 min	70 h 54 min	5 h 44 min	5 h 44 min
Seat no. on flight	26G	26D	24C	27D	28G	24D/E/F/G	
PPE worn on airplane and bus‡	Face mask and gloves¶	Face mask and gloves¶	Not reported	Face mask and gloves	Not reported	Face mask	Face mask
Bus from airport to MIQ#	Bus 1	Bus 1	Bus 1 briefly, transported on bus 2	Bus 1	Bus 3	Bus 2	Bus 2

*GISAID, https://www.gisaid.org. C_t, cycle threshold; MIQ, managed isolation and quarantine; PPE, personal protective equipment.
†Partial genome obtained (1 amplicon failed, resulting in 1,200 ambiguous nucleotide bases) but has the 5 defining mutations of the cluster.
‡Self-reported.
§GeneXpert, https://www.cepheid.com; BD Max, https://www.bd.com.
¶Reportedly removed when sleeping and seated.
#Social distancing and mandated mask wearing on all buses.

Table 2. Travel times for 7 passengers with SARS-CoV-2 infection detected after being on flight EK448, Dubai, United Arab Emirates, to Auckland, New Zealand, September 29, 2020

Variable	Date and time of departure country	Date and time of New Zealand arrival*
Flight EK448	Departed Dubai Sep 28, 08:29 AM Arrived Kuala Lumpur, Malaysia, Sep 28, 7:11 PM Departed Kuala Lumpur Sep 28, 9:03 PM Arrived Auckland, Sep 29, at 11:31 AM	Departed Dubai, Sep 28, 5:29 PM Arrived Kuala Lumpur, Sep 29,12:11 AM Departed Kuala Lumpur, Sep 29, 2:03 AM Arrived Auckland, Sep 29, 11:31 AM
Passengers A and B	Depart Zurich, Switzerland, Sep 27, 3:25 PM Arrived Dubai, Sep 27, 11:02 PM	Departed Zurich Sep 28, 2:25 AM Arrived Dubai, Sep 28, 8:02 AM
Passenger C	Departed Kiev, Ukraine, Sep 27, 3:16 PM† Arrived Dubai, Sep 27, 8:59 PM	Departed Kiev Sep 28, 1:16 AM† Arrived Dubai, Sep 28, 5:59 AM
Passenger D	Departed Dublin, Ireland, Sep 27, 2:10 PM‡ Arrived Dubai Sep 28, 12:05 AM	Departed Dublin Sep 28, 2:10 AM‡ Arrived Dubai Sep 28, 9:05 AM
Passenger E	Departed Kochi, India, Sep 25, 8:21 AM§ Arrived Dubai, Sep 25, 10:35 AM	Departed Kochi Sep 25, 2:51 PM§ Arrived Dubai Sep 25, 6:35 PM
Passengers F and G	Departed Johannesburg, South Africa, Sep 27, 5:10 PM¶ Arrived Dubai Sep 28, 02:45 AM	Departed Johannesburg Sep 28, 4:10 AM¶ Arrived Dubai Sep 28, 11:45 AM

*Daylight savings time zone (Greenwich mean time +13 hours).
†Flight EK2354.
‡Flight EK162.
§Flight 6E67.
¶Flight EK762, seats 29 D, E, F, and G.

identified through routine surveillance testing on the third day of the quarantine period in New Zealand (Figure 2). Passengers A and B traveled together from Switzerland; both reported having had negative test results in their country of origin, ≤72 hours before boarding the flight. They departed Zurich, Switzerland, and arrived in Dubai on September 28, 2020, at 08:02 AM. Passenger A reported symptom onset (general weakness and muscle pain) while in MIQ on October 1, and passenger B reported symptom onset (rhinorrhea, general weakness, cough, and muscle pain) on October 2. Test results for samples collected on October 2 from both persons were positive.

Test results for passenger C were also positive on October 2, but the passenger did not report symptoms at any time during the infection. This person had traveled from Kiev, Ukraine, and arrived in Dubai on September 28 at 5:59 AM.

Test results for passenger D were negative on October 2, but the passenger reported symptoms on the fifth day after arrival in New Zealand. The symptoms progressively worsened, and another test on October 7 returned a positive result. Reported symptoms included coryza, headache, muscle pain, general weakness, irritability, confusion, and a head cold. This passenger had departed from Dublin, Ireland, and arrived in Dubai on September 28 at 9:05 AM.

Test results for passenger E were negative on October 2, but the passenger was retested on October 6 as a potential close contact of those on the airplane and found to be positive for SARS-CoV-2. This passenger was not in the same MIQ facility (nor the same city) in New Zealand as the other passengers with reported

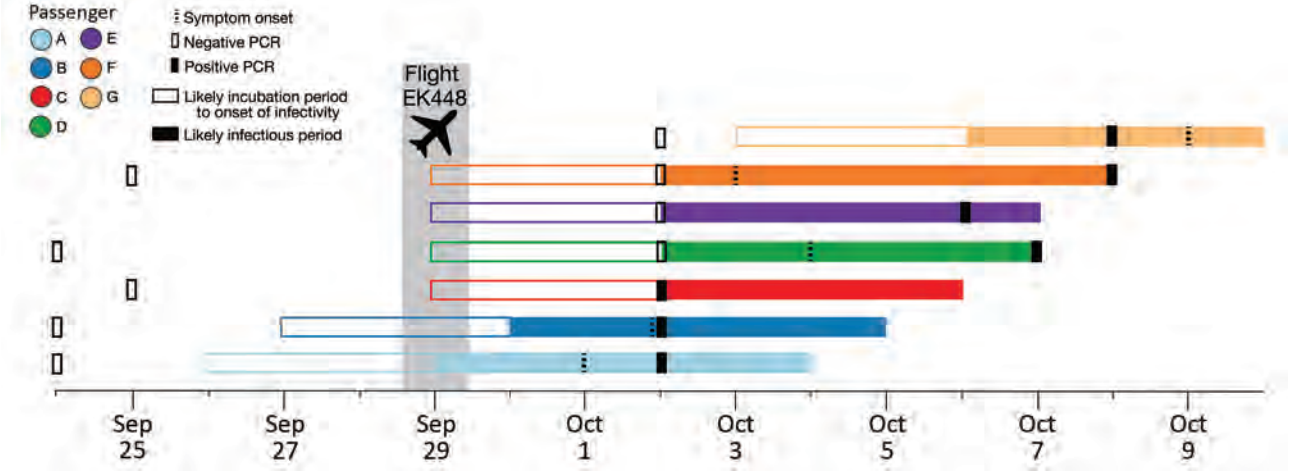

Figure 2. Timeline of likely incubation and infectious periods, indicating testing dates, for 7 passengers who tested positive for severe acute respiratory syndrome coronavirus 2 infection after traveling on the same flight (EK448) from Dubai, United Arab Emirates, to Auckland, New Zealand, with a refueling stop in Kuala Lumpur, Malaysia, on September 29, 2020.

cases and did not report symptoms during the infection. This passenger had departed from Kochi, India, and arrived in Dubai on September 25 at 6:35 PM.

Test results for passengers F and G (part of a group of 4 family members traveling together) were negative on October 2 in New Zealand. Passenger F became mildly symptomatic (coryza and a cough) on October 2 and self-reported having had a negative test result before leaving South Africa. The group was retested as potential contacts of those on the flight with positive results, and on October 8, results were positive for passengers F and G. Passenger G reported coryza and a sore throat on October 9. The 4-person travel group had departed from Johannesburg, South Africa, and arrived in Dubai on September 28 at 11:45 AM. The 4 family members were seated in 4 adjacent seats in row 24 but interchanged seats within the row, such that no specific seat can be determined for each passenger (Figure 2). Test results were positive for only 2 of the 4 family members; after receiving the positive results, the persons were separated in the MIQ facility.

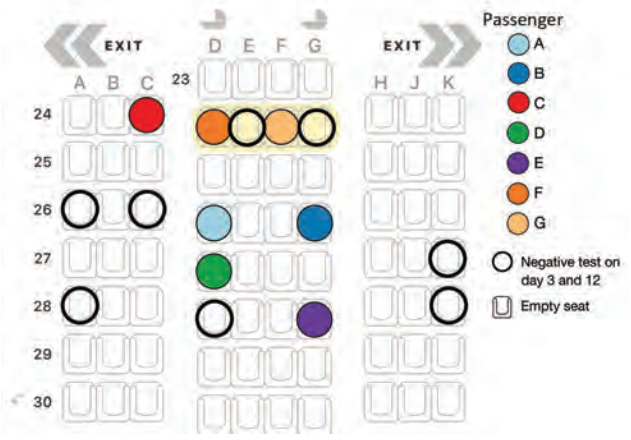

Figure 3. Seating arrangement (Boeing 777–300ER) for 7 passengers who tested positive for severe acute respiratory syndrome coronavirus 2 (SARS-CoV-2) infection on flight EK448 from Dubai, United Arab Emirates, to Auckland, New Zealand, with a refueling stop in Kuala Lumpur, Malaysia, on September 29, 2020. Passengers F and G interchanged seats within row 24. Open circles represent nearby passengers who were negative for SARS-CoV-2 on days 3 and 12 while in managed isolation and quarantine. All other seats shown remained empty.

Timeline of Transmission Events

The first person to experience symptoms was passenger A on October 1, consistent with having been infectious while on flight EK448 2 days earlier (Figure 3). The second person to experience symptoms, on October 2, was passenger B, a travel companion of passenger A, which may represent shared exposure to a source A, such that passenger B's infection is not considered a case of in-flight transmission. Passenger C was asymptomatic and received a positive test result on day 3. Symptom onset and positive test result dates for passengers D, E, and F were all consistent with in-flight transmission. Passenger G was a travel companion of passenger F, and their date of symptom onset was consistent with infection during their stay in an MIQ facility, where they resided in the same room. As such, passenger G's infection was not considered a result of in-flight transmission.

Viral Genomic Data

All SARS-CoV-2 samples from the 7 passengers were subjected to whole-genome sequencing for surveillance purposes. The sequences obtained were assigned to lineage B.1 and were genetically identical, apart from 1 mutation for the sample from passenger D (Figure 4) (*15*). By comparing these 7 genomes to the international database (GISAID), we identified 6

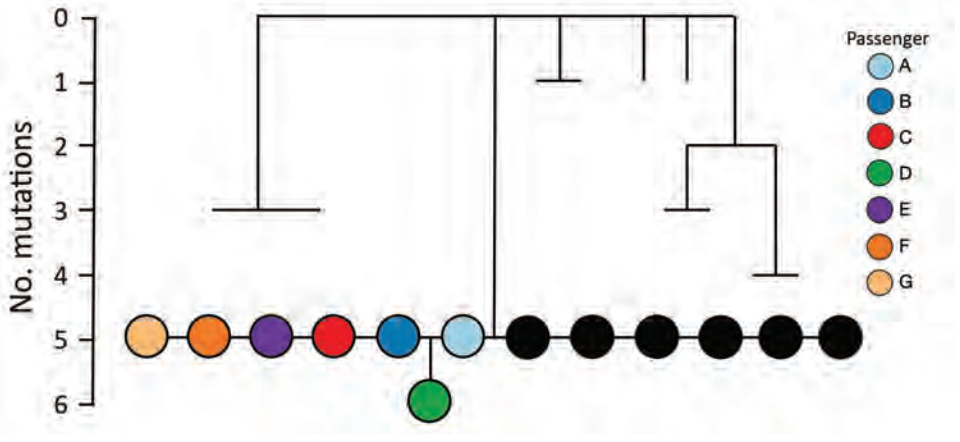

Figure 4. Simplified maximum-likelihood phylogenetic tree of genomes from severe acute respiratory syndrome coronavirus 2 from 7 passengers who traveled on flight EK448 (Boeing 777–300ER) from Dubai, United Arab Emirates, to Auckland, New Zealand, with a refueling stop in Kuala Lumpur, Malaysia, on September 29, 2020. Tree shows positive cases along with their closest genomic relatives sampled from the global dataset. Black circles illustrate cases obtained from the global dataset that are genetically identical, sampled September 2–23, 2020. Scale bar shows the number of mutations relative to the closest reconstructed ancestor from available global data.

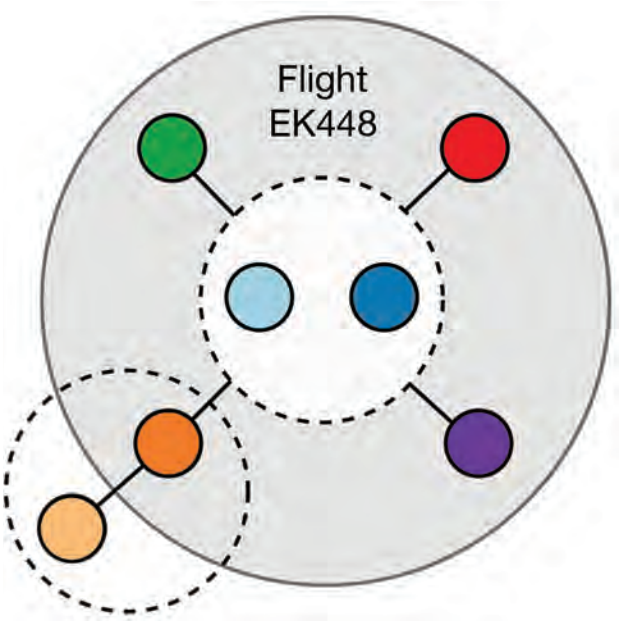

Figure 5. Network of likely severe acute respiratory syndrome coronavirus 2 (SARS-CoV-2) transmission among 7 passengers who traveled on flight EK448 (Boeing 777–300ER) from Dubai, United Arab Emirates, to Auckland, New Zealand, with a refueling stop in Kuala Lumpur, Malaysia, on September 29, 2020. The gray shaded area illustrates likely in-flight virus transmission. Dashed circles represent likely virus transmission between travel companions.

additional identical genomes: 4 from Switzerland and 2 from the United Kingdom, sampled during September 2–23. These findings were consistent with virus introduction onto the airplane from Switzerland by passenger A, B, or both (Figure 5). Nevertheless, accurately identifying the source of this outbreak may be impeded by substantial biases and gaps in global sequencing data (J. Geoghegan, unpub. data, https://www.medrxiv.org/content/10.1101/2020.10.28.20221853v1); hence, we cannot explicitly exclude passenger C as the source.

Discussion

Evidence of in-flight transmission on a flight from the United Arab Emirates to New Zealand is strongly supported by the epidemiologic data, in-flight seating plan, symptom onset dates, and genomic data for this group of travelers who tested positive for SARS-CoV-2 (passengers A–G). Among the 7 passengers, 2 (A and B) were probably index case-patients infected before the flight, 4 (C, D, E, and F) were probably infected during the flight, and the remaining passenger (G) was probably infected while in MIQ. All 7 passengers were seated in aisle seats within 2 rows of where the presumed index case-patient(s) were seated.

Combined, these data present a likely scenario of ≥4 SARS-CoV-2 transmission events during a long-haul flight from Dubai to Auckland. These transmission events occurred despite reported in-flight use of masks and gloves. Further transmission between travel companions then occurred after the flight, in an MIQ facility.

These conclusions are supported by genome sequencing, an in-flight seating plan, and dates of disease onset. These data do not definitively exclude an alternative exposure event, such as virus transmission at the Dubai airport before boarding (e.g., during check-in or in boarding queues). However, the close proximity of the relevant passengers on board suggests that in-flight transmission is plausible.

Similar reports of SARS-CoV-2 being transmitted during flight have recently been published (*3*,*4*,*16*,*17*). Those reports, along with the findings we report, demonstrate the potential for SARS-CoV-2 to spread on long-haul flights. It must also be noted that the auxiliary power unit of the flight EK448 aircraft was reported as having been inoperative for ≈30 minutes during the 2-hour refueling stop in Kuala Lumpur, such that the environmental control system would not have been working during this period.

That 3 passengers had positive test results on day 3 of their 14-day quarantine period indicates some of the complexities of determining the value of predeparture testing, including the modality and timing of any such testing. Although not definitive, these findings underscore the value of considering all international passengers arriving in New Zealand as being potentially infected with SARS-CoV-2, even if predeparture testing was undertaken, social distancing and spacing were followed, and personal protective equipment was used in-flight.

This work was funded by the New Zealand Ministry of Health, Ministry of Business, Innovation and Employment (CIAF-0470), the New Zealand Health Research Council (20/1018), and ESR Strategic Innovation Fund.

About the Authors

Dr. Swadi is the chief advisor in COVID-19 at the Ministry of Health New Zealand and was a lead on the internal investigation into this series of cases. Dr. Geoghegan is an evolutionary virologist with a strong research focus on understanding how viruses emerge and spread in new populations.

References

1. Jefferies S, French N, Gilkison C, Graham G, Hope V, Marshall J, et al. COVID-19 in New Zealand and the impact of the national response: a descriptive epidemiological study. Lancet Public Health. 2020;5:e612–23. https://doi.org/10.1016/S2468-2667(20)30225-5
2. International Air Transport Association. Low risk of transmission [cited 2020 Nov 1]. https://www.iata.org/en/youandiata/travelers/health/low-risk-transmission
3. Freedman DO, Wilder-Smith A. In-flight transmission of SARS-CoV-2: a review of the attack rates and available data on the efficacy of face masks. J Travel Med. 2020 Sep 25 [Epub ahead of print]. https://doi.org/10.1093/jtm/taaa178
4. Murphy N, Boland M, Bambury N, Fitzgerald M, Comerford L, Dever N, et al. A large national outbreak of COVID-19 linked to air travel, Ireland, summer 2020. Euro Surveill. 2020;25:200162. https://doi.org/10.2807/1560-7917.ES.2020.25.42.2001624
5. Elbe S, Buckland-Merrett G. Data, disease and diplomacy: GISAID's innovative contribution to global health. Glob Chall. 2017;1:33–46. https://doi.org/10.1002/gch2.1018
6. Quick J. nCoV-2019 sequencing protocol V3 [cited 2020 Nov 1]. https://www.protocols.io/view/ncov-2019-sequencing-protocol-v3-locost-bh42j8y
7. Freed NE, Vlková M, Faisal MB, Silander OK. Rapid and inexpensive whole-genome sequencing of SARS-CoV-2 using 1200 bp tiled amplicons and Oxford Nanopore Rapid Barcoding. Biol Methods Protoc. 2020;5:bpaa014. https://doi.org/10.1093/biomethods/bpaa014
8. Katoh K, Standley DM. MAFFT multiple sequence alignment software version 7: improvements in performance and usability. Mol Biol Evol. 2013;30:772–80. https://doi.org/10.1093/molbev/mst010
9. Nguyen LT, Schmidt HA, von Haeseler A, Minh BQ. IQ-TREE: a fast and effective stochastic algorithm for estimating maximum-likelihood phylogenies. Mol Biol Evol. 2015;32:268–74. https://doi.org/10.1093/molbev/msu300
10. Hasegawa M, Kishino H, Yano T. Dating of the human-ape splitting by a molecular clock of mitochondrial DNA. J Mol Evol. 1985;22:160–74. https://doi.org/10.1007/BF02101694
11. Kalyaanamoorthy S, Minh BQ, Wong TKF, von Haeseler A, Jermiin LS. ModelFinder: fast model selection for accurate phylogenetic estimates. Nat Methods. 2017;14:587–9. https://doi.org/10.1038/nmeth.4285
12. Hoang DT, Chernomor O, von Haeseler A, Minh BQ, Vinh LS. UFBoot2: improving the ultrafast bootstrap approximation. Mol Biol Evol. 2018;35:518–22. https://doi.org/10.1093/molbev/msx281
13. World Health Organization. Novel coronavirus situation report [cited 2020 Nov 1]. https://www.who.int/docs/default-source/coronaviruse/situation-reports/20200121-sitrep-1-2019-ncov.pdf
14. Byrne AW, McEvoy D, Collins AB, Hunt K, Casey M, Barber A, et al. Inferred duration of infectious period of SARS-CoV-2: rapid scoping review and analysis of available evidence for asymptomatic and symptomatic COVID-19 cases. BMJ Open. 2020;10:e039856. https://doi.org/10.1136/bmjopen-2020-039856
15. Rambaut A, Holmes EC, O'Toole Á, Hill V, McCrone JT, Ruis C, et al. A dynamic nomenclature proposal for SARS-CoV-2 lineages to assist genomic epidemiology. Nat Microbiol. 2020;5:1403–7. https://doi.org/10.1038/s41564-020-0770-5
16. Choi EM, Chu DKW, Cheng PKC, Tsang DNC, Peiris M, Bausch DG, et al. In-flight transmission of SARS-CoV-2. Emerg Infect Dis. 2020;26:2713–6. https://doi.org/10.3201/eid2611.203254
17. Speake H, Phillips A, Chong T, Sikazwe C, Levy A, Lang J, et al. Flight-associated transmission of severe acute respiratory syndrome coronavirus 2 corroborated by whole-genome sequencing. Emerg Infect Dis. 2020;26:2872–80. https://doi.org/10.3201/eid2612.203910

Address for correspondence: Joep de Ligt, Institute of Environmental Science and Research Ltd, Health, Bioinformatics & Genomics, 34 Kenepuru Dr, Porirua, Wellington 5022, New Zealand; email: joep.deligt@esr.cri.nz; Jemma L. Geoghegan, University of Otago Division of Health Sciences, Microbiology and Immunology, 720 Cumberland St, Dunedin, Otago 9054, New Zealand; email: jemma.geoghegan@otago.ac.nz

Evaluation of National Event-Based Surveillance, Nigeria, 2016–2018

Kazim Beebeejaun, James Elston, Isabel Oliver, Adachioma Ihueze, Chika Ukenedo, Olusola Aruna, Favour Makava, Ejezie Obiefuna, Womi Eteng, Mercy Niyang, Ebere Okereke, Bola Gobir, Elsie Ilori, Olubunmi Ojo, Chikwe Ihekweazu

Nigeria Centres for Disease Control and Prevention established an event-based surveillance (EBS) system in 2016 to supplement traditional surveillance structures. The EBS system is comprised of an internet-based data mining tool and a call center. To evaluate the EBS system for usefulness, simplicity, acceptability, timeliness, and data quality, we performed a descriptive analysis of signals received during September 2017–June 2018. We used questionnaires, semistructured interviews, and direct observation to collect information from EBS staff. Amongst 43,631 raw signals detected, 138 (0.3%) were escalated; 63 (46%) of those were verified as events, including 25 Lassa fever outbreaks and 13 cholera outbreaks. Interviewees provided multiple examples of earlier outbreak detections but suggested notifications and logging could be improved to ensure action. EBS proved effective in detecting outbreaks, but we noted clear opportunities for efficiency gains. We recommend improving signal logging, standardizing processes, and revising outputs to ensure appropriate public health action.

In resource-limited settings, classical indicator-based surveillance approaches can be limited by available diagnostic capacity and surveillance architecture (*1*–*3*). The Ebola outbreak in West Africa during 2014–2016 highlighted surveillance needs and generated sustained commitment to global health security with a focus on the implementation of the International Health Regulations (IHR 2005) (*4*). The World Health Organization considers implementation of event-based surveillance (EBS) a major priority for developing countries worldwide and a critical component for meeting IHR (2005) commitments (*5*,*6*).

Author affiliations: Public Health England, London, UK (K. Beebeejaun, J. Elson, I. Oliver, O. Aruna, E. Okereke); University of Maryland Baltimore, Abuja, Nigeria (A. Ihueze, C. Ukenedo, F. Makava, M. Niyang, B. Gobir); Nigeria Centre for Disease Control, Abuja (E. Obiefuna, W. Eteng, E. Ilori, O. Ojo, C. Ihekweazu)

DOI: https://doi.org/10.3201/eid2703.200141

EBS is the organized and rapid capture of information about events that are a potential risk to public health (*7*). Information captured by EBS can include rumors and other ad hoc reports from indirect channels, such as news organizations or social media, and direct channels, such as reporting by members of the public or healthcare workers. Events of interest include those related to the occurrence of disease in humans, including clustered cases of a disease or syndrome; unusual disease patterns or unexpected deaths identified by health workers and other key informants; diseases and deaths in animals; contaminated food products; and water and environmental hazards (*7*).

EBS systems have been implemented across Africa but most are at the community level (*8*–*11*). Supporting the implementation of EBS at a national level is a priority for the Africa Centres for Disease Control and Prevention (Africa CDC), which aims for ≥60% of member states to have an established EBS system by 2021. Africa CDC has proposed frameworks to support this implementation (*12*). Sharing knowledge and best practices from the few existing national EBS systems implemented in Africa is crucial for informing this process.

The Nigeria Centres for Disease Control and Prevention (NCDC) introduced EBS in 2016. NCDC EBS was supported by the University of Maryland Baltimore (UMB) through a grant from the US Centers for Disease Control and Prevention (CDC). The aim of the EBS is to rapidly collect and organize information about signals and trigger public health action by NCDC and its partners. Nigeria's EBS system uses data actively mined from internet sources by Tatafo, a software platform developed by UMB for NCDC; data collected from incoming calls from the public and healthcare professionals at NCDC's Connect Centre; and information collected by systematic and ad hoc searches of social media, blogs, health tracking websites, and the news media.

The evaluation was undertaken as part of a 4-year partnership between Public Health England (PHE), UK Department of Health (UK DoH), and NCDC to strengthen capabilities for compliance with IHR (2005). The purpose of the project was to describe the NCDC EBS system and the nature of signals and events detected; evaluate the system against its objectives and provide recommendations to improve effectiveness and efficiency and maximize utility of the system.

Methods

Study Design and Evaluation Period

The evaluation was performed over a 4-week period in July 2018 and informed by CDC guidelines for the evaluation of public health surveillance systems (*13*). We used a mixed methods approach comprising quantitative and qualitative data collection using semistructured interviews, document reviews, observations, questionnaires, and analysis of routinely collected data.

We conducted 19 semistructured interviews by purposive sampling of key NCDC staff members directly involved in or receiving outputs from the EBS system. Staff included call handlers, surveillance officers, data management staff, department heads, and NCDC senior leadership.

We used a bespoke topic guide to capture views on functionality, usefulness, and efficiency of the EBS. We used a questionnaire to capture specific information for certain attributes, such as ease of use, production of outputs, and acceptability of processes.

Describing the System, Signals, and Events Detected

Existing documentation included internal guidance on implementation of EBS and technical documents on how signals were detected. Semistructured interviews explored the structure of teams, steps in escalation of signals, and data flows. Documentation was supplemented with hands-on experience working alongside and observing practices of EBS staff for 3 weeks.

Data Sources and Links

During November 1, 2016–June 30, 2018, raw signal data were exported from the Web-based systems Tatafo and SugarCRM (https://info.sugarcrm.com). During September 1, 2017–June 30, 2018, escalated signal data were available through paper logbooks, which were digitized before analysis. We manually linked escalated signals to raw source signals. We linked escalated signals to raw source signals if the following were consistent: disease or syndrome; location or geography, such as state and town for which location information were recorded; time ±5 days; and source, such as newspaper or social media. To estimate the number of unique raw signals detected, we defined a signal cluster as linked signals on the same disease or syndrome that occurred ±2 days in the same geography (Table 1).

Evaluation

Data Quality

We assessed data quality by reviewing completeness of data collected by EBS. These data included the date of raw signal detection, geolocation of the signal source, URLs of relevant websites, the related disease or nature of the event suspected, and estimated numbers of cases associated with the signal.

Acceptability and Simplicity

We used questionnaires and semistructured staff interviews to investigate the ease of use of EBS system components, including data entry, logging of calls, prioritization of signals, escalation, and ease of producing routine outputs. We assessed acceptability by examining routine tasks performed by staff and the usefulness of routine outputs. We used Likert scales

Table 1. Definition for terms used in evaluation of national event-based surveillance, Nigeria, 2016–2018*

Term	Definition
Raw signal	Communication received or retrieved from EBS system that contains data with potential to meet the WHO definition for a signal (*7*)
Signal	Raw signal reviewed by EBS technical staff who considered the signal to represent a potential acute risk to human health requiring investigation or verification according to the WHO definition†
Signal cluster	Group of signals detected by EBS system relating to same disease or syndrome and occurring within ±2 d in the same state
Escalated signal	A signal escalated and recorded by EBS technical staff to a senior surveillance officer for investigation and verification
Senior surveillance officer	Nominated member of the surveillance team responsible for investigating and verifying escalated signals
Event	A signal verified by SSO and surveillance team as an event that has potential for disease spread

*Terminology listed in order of appearance during EBS monitoring. EBS, event-based surveillance; SSO, senior surveillance officer; WHO, World Health Organization.
†WHO definition states: Data and/or information considered by the Early Warning and Response system as representing a potential acute risk to human health. Signals may consist of reports of cases or deaths (individual or aggregated), potential exposure of human beings to biological, chemical, or radiological and nuclear hazards, or occurrence of natural or man-made disasters (*7*).

to query staff on their level of agreement to statements regarding the EBS.

Timeliness

We assessed timeliness by measuring the number of days between individual steps in EBS processes from the initial detection of a signal indicating a potential event, to escalation, and then to investigation. We retrieved dates from relevant EBS Web-based platforms or paper logbooks, where available.

Usefulness

We assessed usefulness by using semistructured staff interviews. We asked interviewees for their views on the usefulness of the EBS system, particularly regarding detection of events and the related public health action. We asked staff to provide examples to support their responses, where practical.

Analysis

We manually entered questionnaire data in Excel (Microsoft Corp. https://www.microsoft.com). We used Stata version 14 (StataCorp LLC, https://www.stata.com) and Excel to clean and analyze data. We manually reviewed qualitative data from interviews and organized data into themes according to evaluation attributes by 2 investigators.

Results

Description of the EBS System

Detection of Signals

In accordance with the World Health Organization definition of a signal of interest (*7*), NCDC's EBS detected signals by using 3 key receptors: Tatafo, the NCDC Connect Centre, and manual searches (Figure 1). Tatafo is an automated internet-based data system that uses text mining, text analysis, and natural language processing to detect the occurrence of events of interest from internet feeds. The system uses a list of keywords related to the 41 notifiable diseases for Nigeria (*14*). Tatafo also is customized to search for signals by using alternate terminology, such as slang and pidgin English.

The NCDC Connect Centre is the focal point of communications to and from NCDC, facilitating communications with the public, healthcare workers, and surveillance officers. The Connect Centre operated telephone, text messaging, and WhatsApp (https://www.whatsapp.com) platforms to receive signals. All communications were logged on SugarCRM.

Manual searches of online media sources included online news media websites, television, and radio. Daily online media searches were performed using a news aggregator website (http://ww38.latestnigerianews.com), which includes all major newspapers in Nigeria. Staff logged searches that had identified a signal of interest on SugarCRM.

Prioritization

Signals received through these channels were individually reviewed and prioritized by EBS staff according to relevance and urgency based on the potential for public health effects. Signals prioritized for escalation were forwarded to the surveillance team for further investigation and relevant public health action.

Escalation

Escalation was primarily performed by using a signal escalation email with details of the event sent to a predetermined distribution list that included senior surveillance officers (SSOs), technical working group (TWG) leads for the relevant disease, surveillance department leads, and the director general. SSOs acted as focal points for investigating and establishing the authenticity of an escalated signal or otherwise and performing a risk assessment. When an escalated signal was verified after initial information gathering, the verified signal was considered an event. The SSO was responsible for initiating or undertaking further investigation or public health action as appropriate for the event and recording and communicating related actions.

Staffing

EBS was staffed by 7 members: 2 information officers, 4 NCDC Connect Centre agents, and 1 public health analyst. These staff were funded by UMB and assigned to NCDC.

As part of their roles in EBS, 2 senior NCDC surveillance officers acted as the surveillance focal point responsible for the follow up of escalated signals. A further 12 staff were part of the surveillance department.

Evaluation

Data Quality

Among raw signals detected over the 20-month evaluation period, most computer automated fields were complete, but the geolocation field was only 29% complete (20,045/69,722) (Table 2). However, a further review identified an additional 2,444 (3.5%) records that had the name of a state recorded in descriptive text fields, such as in newspaper headlines.

Logs of escalated signals were maintained in Excel during September 1, 2017–December 1, 2017, and then replaced by paper logbooks. Both Excel and the paper log contained records of escalated signals detected by Tatafo or manual searches. No records of escalated signals originated from the NCDC Connect Centre, despite observations of escalations by the study team. Among the 103 escalated signals recorded by the EBS team over the evaluation period, 99 (96%) included data concerning the source of the information, 97 (94%) included the date the signal was detected, 94 (91%) contained information on action taken, 72 (70%) contained information on subsequent verification of the event, and 57 (50%) had details on the numbers of cases.

During the 20-month evaluation, SSOs kept a separate paper log containing information concerning the verification of escalated signals. Information logged included date of signal escalation, signal details, source of information, source person, investigation outcomes, and action taken. During the evaluation, SSOs logged 12 records, of which 11 (92%) contained date of signal escalation, 6 (50%) included source of information, and 5 (42%) included the name of the staff member escalating the signal. However, the original unique source identifier (ID), such as Tatafo ID or SugarCRM ID, was not logged.

Raw Signals Detected

During November 1, 2016–June 30, 2018, the EBS system detected 69,831 raw signals. Peaks in raw signals were observed during periods of known national disease outbreaks, including the peak of a meningitis outbreak during March–April 2017, a cholera outbreak during September 2017, a monkeypox outbreak during October 2017, and a Lassa fever outbreak during January–March 2018 (Table 3). Among raw signals, most (69,722; 99.8%) were detected by Tatafo, denoting ≈4,571 signal clusters. A mean of 3,486 raw signals (410 signal clusters) were detected by Tatafo each month. The Connect Centre received and categorized 92 communications as raw signals, of which 45% (41/92) were from phone calls and 31% (28/91) from WhatsApp messages.

Among raw 69,831 signals, 99.8% (69,722) included pathogen information. Of raw signals with pathogen information 18% (12,429) related to Lassa fever, 12% (8,679) related to HIV/AIDS, 11% (7,990) to meningitis or cerebrospinal meningitis, 10% (7,230) to Ebola, and 7% (5,131) to cholera (Table 3).

Only 20,045 (29%) records included with geographic information, among which 22,489 referenced states (multiple states were recorded in 1,428 records). Niger State was most frequently referenced (6,032/22,489; 27%), along with Borno State (2,016/22,489; 9%), Lagos (1,928/22,489; 9%), and Federal Capital Territory (1,476/22,489; 7%). Akwa Ibom and Cross River States had no recorded signals during the study period, likely indicating a problem with search configurations in Tatafo.

Escalated signals

During September 1, 2017–June 30, 2018, when records were available from both EBS and SSOs, the EBS detected 43,631 raw signals, among which 138 (0.3%) were escalated to the SSOs for investigation and 75% (103/138) had details of escalation recorded. Of escalated events, 61 (44%) were from the Connect Centre,

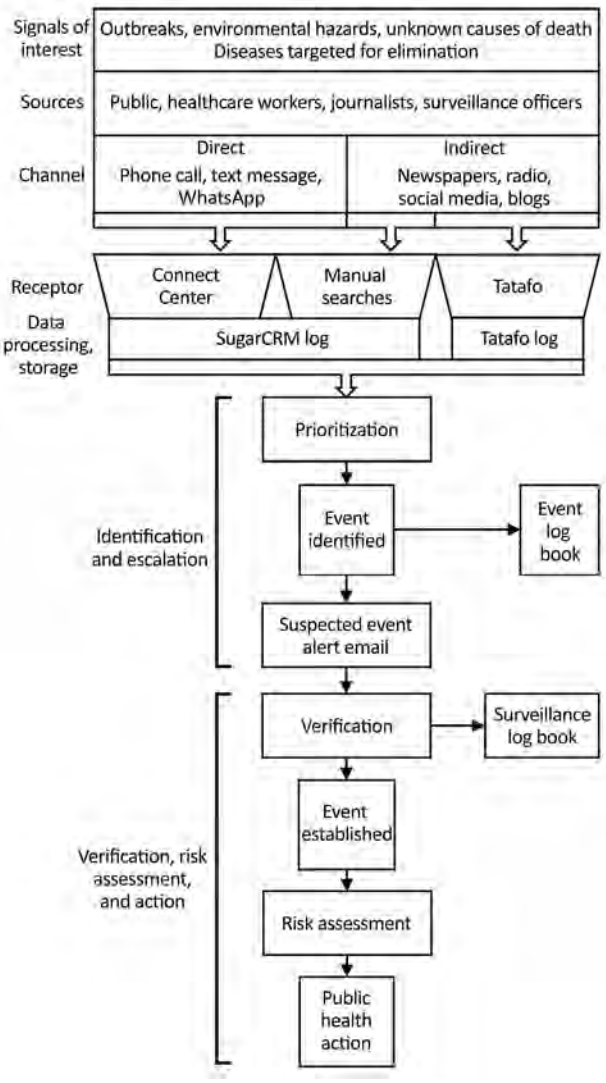

Figure 1. Data sources and flow of signals from detection to public health action in Nigeria Centres for Disease Control and Prevention event-based surveillance system, 2016–2018. SugarCRM, https://info.sugarcrm.com.

Table 2. Completeness of key fields in online event-based surveillance system, Nigeria, November 1, 2016–June 30, 2018*

EBS source	Field name	Total no. entries	No. complete entries	% Completeness
Tatafo†	Unique ID	69,722	69,722	100
	Date received	69,722	69,722	100
	Topic	69,722	69,722	100
	Headline text	69,722	69,722	100
	Website address (url)	69,722	69,722	100
	Location	69,722	20,045	29
Connect Centre	Unique ID	92	92	100
	Call category	92	92	100
	Case method	92	92	100
	Date created	92	92	100
	Date modified	92	92	100
	Description	92	92	100
	Subject	92	92	100

*EBS, event-based surveillance; ID, identification.
†Tatafo is an internet data mining software platform developed by the University of Maryland Baltimore for Nigeria Centres for Disease Control and Prevention's event-based surveillance system.

60 (43%) from Tatafo, 2 (1%) from manual searches, and 15 (11%) had no source recorded.

Among escalated signals, EBS team logs recorded 72 (52%) for which an investigation or follow up was begun and the SSO took steps to verify the signal, but only 4 (6%) were recorded in equivalent SSO records. Among 72 recorded escalated signals, 63 (46%) were recorded as verified events in EBS team logs. The ratio of signals:verified events was 693:1 (Figure 2). Of 138 signals escalated, 66 (48%) had a record of prioritization being performed before escalation so that a record indicated that the original raw signal was triaged and logged appropriate for escalation.

Simplicity

In semistructured interviews, all 3 users of the Tatafo web platform agreed that the user interface was easy to navigate, data could be exported easily, and the system was reliable. However, only 2/3 users agreed that the process to prioritize raw signals for escalation was clear.

Semistructured interviews of all 4 Connect Centre staff found the system was easy or very easy to use for completing routine tasks, such as logging calls, updating records, and assigning priority levels to signals. Interviewees also indicated that it was easy to identify which senior staff members should be sent escalated signals.

Table 3. Number of signals detected Tatafo for top infectious disease topics, November 1, 2016–June 30, 2018*

Date raw signal detected	Top infectious disease topics											
	Lassa fever	HIV/ AIDS	Meningitis, CSM	Ebola	Cholera	Polio	Malaria	Monkey pox	Yellow fever	TB	Other	Total
2016												
Nov	6	269	4	118	33	206	166	0	3	20	496	1,321
Dec	83	727	1	51	17	63	42	0	2	3	170	1,159
2017												
Jan	206	54	3	56	1	368	39	0	6	10	437	1,180
Feb	479	440	6	42	7	79	91	0	7	7	184	1,342
Mar	749	279	832	148	102	319	83	0	12	167	200	2,891
Apr	255	385	5,116	113	44	101	372	0	9	40	288	6,723
May	374	270	1,035	1,768	76	93	210	0	11	6	178	4,021
Jun	266	469	384	106	154	167	112	0	9	37	256	1,960
Jul	215	470	89	81	215	116	199	0	14	59	389	1,847
Aug	1,308	269	48	208	116	138	241	0	10	26	262	2,626
Sep	254	266	33	152	2,100	95	166	4	209	37	470	3,786
Oct	130	300	38	268	231	399	157	3,034	357	59	1,408	6,381
Nov	36	524	18	116	102	126	331	316	42	85	716	2,412
Dec	23	1,267	43	114	210	100	186	123	400	47	485	2,998
2018												
Jan	1,494	335	49	150	92	371	115	25	615	15	379	3,640
Feb	2,008	363	67	190	41	105	186	19	152	38	436	3,605
Mar	2,812	442	91	350	139	231	212	11	104	204	742	5,338
Apr	1,216	476	48	158	244	302	1,072	33	215	45	554	4,363
May	407	585	30	2,777	676	172	456	20	40	39	705	5,907
Jun	108	489	55	264	531	195	176	35	66	63	793	2,775

*Tatafo is an internet data mining software platform developed by the University of Maryland Baltimore for Nigeria Centres for Disease Control and Prevention's event-based surveillance system. CSM, cerebrospinal meningitis; TB, tuberculosis.

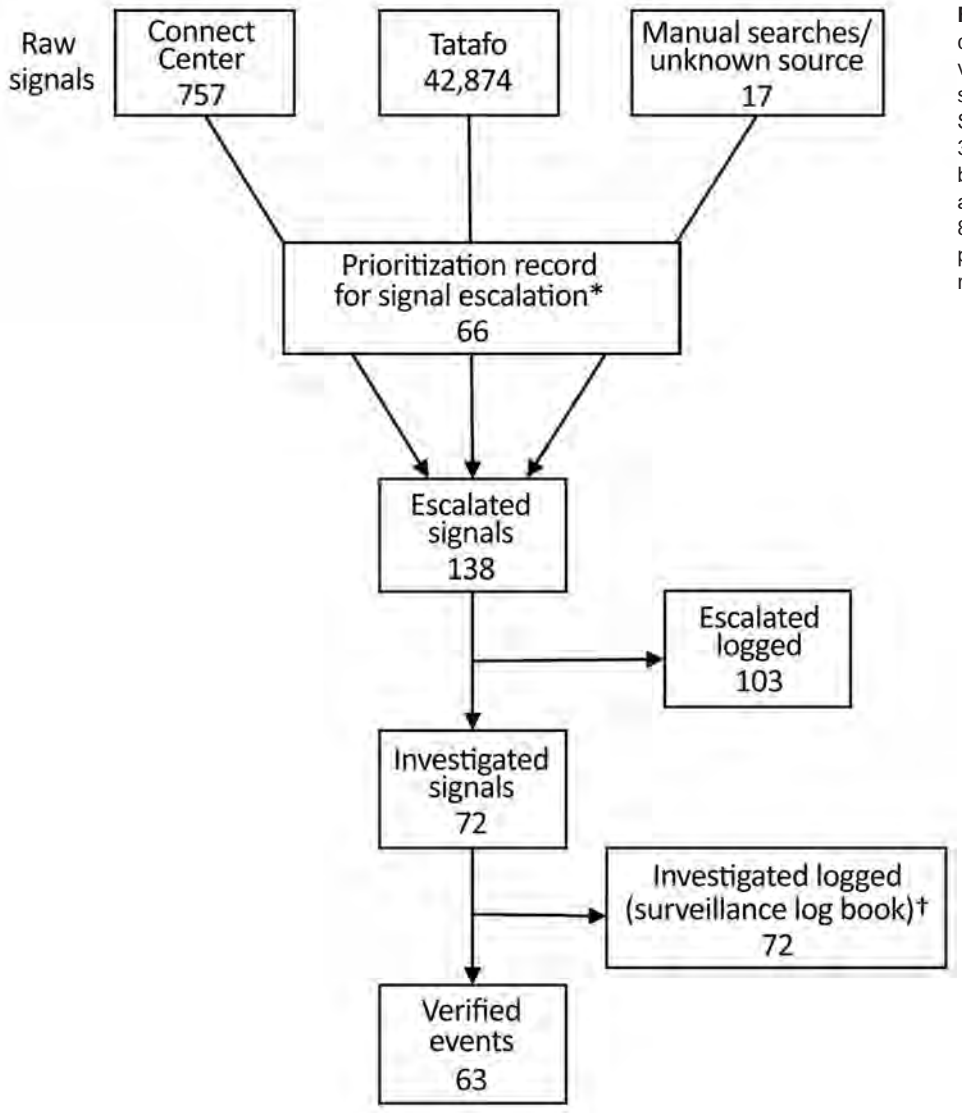

Figure 2. Logged recording of signals from detection to verification in event-based surveillance system, Nigeria, September 1, 2017–June 30, 2018. *Record of signal being prioritized and logged as appropriate for escalation. †For 8 additional records, it was not possible to link back to original raw signals.

Acceptability

Interviews with EBS staff working with Tatafo and or in the Connect Centre indicated a high level of satisfaction with the systems. Tatafo was viewed by staff to be an effective system and that it detected appropriate signals of interest. Primary EBS staff were satisfied with their roles and procedures for escalation to senior staff. However, EBS staff reported that they did not consistently receive feedback on appropriateness of escalation, progress of investigation, or outcome of escalated signals.

User satisfaction with the outputs of EBS varied according to job role. A high level of satisfaction was expressed by interviewees for the signal escalation email notifications, which were critical for action. However, several interviewees considered that notifications, although vital, were often unstructured and lacked targeting to ensure action.

Staff considered manual searches time-consuming and resource intensive. Senior staff expressed concern that the time spent on manual searches potentially wasted limited resources. EBS staff reported intermittent internet connectivity to Tatafo, and they typically lost connection once daily for ≤1 hour. To avoid missing signals due to intermittent connectivity, staff reported spending extra time at the office to undertake manual searches outside work hours.

Timeliness

Delays between detection of a raw signal and logging in Tatafo were few because the process was automated; most delays in raw signal detection could be attributed to network connectivity issues. Similarly, no delays were found between the receipt of a call by the Connect Centre and logging because phone lines

were directly linked to SugarCRM. However, time of receipt of WhatsApp or text messages were not logged. Similarly, the time interval between performing a manual search and logging data could not be established due to lack of recording.

Among 79 records from which an escalated signal could be linked back to its raw signal, the median time from signal detection to escalation was 1 day (range 0–5 days) and we did not observe any date conflicts. The longest interval between signal detection and escalation observed was in February 2018 during the peak of a national Lassa fever outbreak, during which we also observed a large increase in escalated signals.

Usefulness

Several themes on the usefulness of the EBS emerged from interviews. Although EBS was viewed to be valuable in detecting outbreaks, users noted that a lack of recording limited oversight and assurance of action (Table 4).

Discussion

Our findings indicate that the NCDC EBS system detected events of public health concern and appropriately triggered public health investigation. Interviewees considered the EBS system useful for disease surveillance, particularly given limitations in routine integrated disease surveillance and response reporting in Nigeria. Interviewees reported that several large outbreaks were detected earlier or exclusively by EBS, primarily by Tatafo, including early detection of a large monkeypox outbreak that would not have been subject to routine surveillance. However, comparison of EBS with integrated disease surveillance and response is not practical due to lack of detailed recording of outbreaks investigated in relation to either source.

Table 4. Assessments of national event-based surveillance system in Nigeria derived from excerpts of staff interviews*

Assessment	Staff quote (staff role)
EBS system enabled early detection of outbreaks and largely met its objectives for providing information to enable prompt identification of appropriate signals for verification and public health action	A lot of outbreaks across Nigeria are underreported. For example, if you are reported of five cases of a certain disease happening in one area, it is likely that there are actually a lot more cases in the community. The other issue is that some health facilities do not report routine data. EBS helps fill that gap. (Data manager)
Underdetection of events in areas where English was not the main spoken language	Language translation in Nigeria is an issue. There are three main languages that are competing with English. There is a large population that know how to speak and write in Hausa but cannot read or understand English. (Director)
Suboptimal recording limited effective oversight	We need something better to record what happens. When something is escalated… there needs to be an electronic record of it where I can view it and see what it is concerning and whether it has been followed up and what the action taken was. (Deputy director)

*EBS, event-based surveillance.

The EBS system detected signals from a range of sources, particularly from Twitter (https://www.twitter.com) and news media websites. The large number of signals verified by routine reporting and coincident surges in signals during known national outbreaks suggests the system was sensitive, however our study did not formally assess this. Of note, print newspapers, radio, and television were outside the reach of the Tatafo and the reliance of our study on internet-based media introduced some bias toward urban areas. Further, Nigeria has >520 different spoken languages; limitation to English, the official language of Nigeria spoken by ≈53% of the population, also introduced a selection bias (*15*). The fact that no signals were detected in 2 states, Akwa Ibom and Cross River, likely indicates a problem in the geographical search configurations in Tatafo. Sensitivity and timeliness of detection were therefore limited given some events would not have been detected or subject to delay until signals were in English. However, language restrictions are not unique to Nigeria's EBS system (*16*).

Of note, no standard operating procedures (SOPs) were available, but staff appeared to have a firm understanding of data flow and communications. EBS staff had limited feedback on progress and outcomes of suspected events, verifications, and investigations, which hindered their awareness of the response. Further, prioritization of raw signals was not performed consistently, and signals often were escalated without evidence of prioritization.

During out study, only a small number of escalated signals were recorded as investigated or verified. Although our observations suggest that most escalated signals were investigated, recording was suboptimal, likely due to resource constraints and lack of SOPs. Lack of recording had implications for providing assurance of response and ensuring oversight. Suboptimal recording also limited our ability to link escalated signals to their raw signals and likely underestimated EBS related activity.

Outputs were valued by senior staff, although they considered that outputs could be better targeted

to relevant persons to inform public health action. A centrally maintained directory of key staff and their disease focal points was not available to EBS staff, but a directory could have made messaging to appropriate responders more efficient.

Although interviewees indicated that several major outbreaks were detected earlier than would have been evident via routine indicator surveillance, if detected at all, we could not quantify this information by using the Salzburg standards (*17*). Time between signal detection and escalation was short, but the lack of consistent recording prevented us from estimating the time to investigation, verification, and public health intervention or action. Timeliness decreased during major outbreaks, presumably a consequence of limited resources and resource diversion from EBS to outbreak response activities. Manual searches were time consuming, resource intensive, and they yielded limited data, with only 2 signals from manual searches recorded as being escalated during the 20-month study period.

Our evaluation draws on the strengths of a mixed-methods approach to evaluate a complex surveillance system and permitted triangulation of findings. Our evaluation was subject to several limitations. The context and available data and records posed challenges in conducting a robust evaluation. For example, inclusion of a relatively small number of users introduced greater subjectivity than might have been desirable. Reporting bias is possible because staff might have avoided expressing critical opinions or might have modified aspects of their behavior in response to being observed. Although interviewees were selected purposely, a small number of senior staff were unable to be interviewed; thus, an element of selection bias could be present because of an over representation of surveillance staff. We were unable to assess the sensitivity or validity of signals because we could not establish which signals were missed by the system. Additionally, the lack of recording and volume of signals also made it difficult to determine which signals should have been investigated and required public health action. Some signals requiring investigation likely were not identified by the EBS surveillance system.

Conclusions

Our evaluation found the NCDC EBS system to be effective in detecting relevant signals and users deemed it a valued asset for national surveillance. According to its users and NCDC leadership, the EBS system helped trigger public health action to address events of concern that otherwise might not have been detected or for which response might have been delayed. However, the extent to which investigation and response improved was difficult to establish in view of limitations in recording. EBS tasks, such as prioritization, were not performed consistently and a lack of recording hindered oversight in ensuring appropriate public health action occurred. The lack of documented SOPs potentially compromised quality and consistency of practice. Furthermore, our evaluation found that routine outputs could have been more optimally targeted to ensure action and we identified several potential inefficiencies, such as the lack of a centralized list of disease focal points.

While a valued asset, implementation and maintenance of the NCDC EBS system required funding and investments in resources, including software systems, staff, training materials. At the time of our evaluation the EBS was supported by funds from UMB and financial and personnel investments should be relevant considerations for other countries looking to adopt national EBS.

To optimize the EBS system in Nigeria, we recommended implementation of SOPs, centralized event and response logging, targeted outputs, and continuous quality improvement processes. In addition, Tatafo should be enhanced to include non-English languages. We recommend public health organizations with surveillance needs similar to those in Nigeria use our evaluation to inform implementation of national EBS systems.

K.B., J.E., I.O., C.I., O.O., E.I., E.O., and O.A. formulated objectives of evaluation and first draft of manuscript. A.I., C.U., F.M., E.O., W.E., M.N., and B.G. contributed to conducting evaluation, identifying key improvements and subsequent drafts of manuscript. All authors agreed on all aspects of the work for the final manuscript.

About the Author

Mr. Beebeejaun was an epidemiologist with Public Health England at the time of this research. His research interests include infectious disease epidemiology and building surveillance capacity in developing country settings.

References

1. Chretien J-P, Lewis SH. Electronic public health surveillance in developing settings: meeting summary. BMC Proc. 2008;2 Suppl 3(Suppl 3):S1. https://doi.org10.1186/1753-6561-2-s3-s1
2. Heymann DL, Rodier GR; WHO Operational Support Team to the Global Outbreak Alert and Response Network. Hot spots in a wired world: WHO surveillance of emerging and re-emerging infectious diseases. Lancet

Infect Dis. 2001;1:345–53. https://doi.org/10.1016/S1473-3099(01)00148-7
3. Butler D. Disease surveillance needs a revolution. Nature. 2006;440:6–7. https://doi.org/10.1038/440006a
4. World Health Organization. International health regulations (2005) [cited 2020 Aug 8]. http://www.who.int/ihr/publications/978924159
5. United Nations Office for Coordination of Humanitarian Affairs. Africa Centres for Disease Control and Prevention and partners plan new approach to detect and respond to outbreaks: press release 21 Jun 2017 [cited 2020 Aug 8]. https://reliefweb.int/report/world/africa-centres-disease-control-and-prevention-and-partners-plan-new-approach-detect-and
6. Hii A, Chughtai AA, Housen T, Saketa S, Kunasekaran MP, Sulaiman F, et al. Epidemic intelligence needs of stakeholders in the Asia-Pacific region. Western Pac Surveill Response J. 2018;9:28–36. https://doi.org/10.5365/wpsar.2018.9.2.009
7. World Health Organization. Early detection, assessment and response to acute public health events: implementation of early warning and response with a focus on event-based surveillance [cited 2020 Aug 8]. https://www.who.int/ihr/publications/WHO_HSE_GCR_LYO_2014.4/en
8. Ratnayake R, Crowe SJ, Jasperse J, Privette G, Stone E, Miller L, et al. Assessment of community event-based surveillance for Ebola virus disease, Sierra Leone, 2015. Emerg Infect Dis. 2016;22:1431–7. https://doi.org/10.3201/eid2208.160205
9. Toyama Y, Ota M, Beyene BB. Event-based surveillance in north-western Ethiopia: experience and lessons learnt in the field. Western Pac Surveill Response J. 2015;6:22–7. https://doi.org/10.5365/wpsar.2015.6.2.002
10. Stone E, Miller L, Jasperse J, Privette G, Diez Beltran JC, Jambai A, et al. Community event-based surveillance for Ebola virus disease in Sierra Leone: implementation of a national-level system during a crisis. PLoS Curr. 2016;8: ecurrents.outbreaks.d119c71125b5cce312b9700d744c56d8. https://doi.org/10.1371/currents.outbreaks.d119c71125b5cce312b9700d744c56d8
11. Fall IS, Rajatonirina S, Yahaya AA, Zabulon Y, Nsubuga P, Nanyunja M, et al. Integrated Disease Surveillance and Response (IDSR) strategy: current status, challenges and perspectives for the future in Africa. BMJ Glob Health 2019;4:e001427. https://doi.org/10.1136/bmjgh-2019-001427
12. Africa Centres for Disease Control and Prevention. Africa CDC strategic plan 2017–2021 [cited 2020 Aug 8]. https://africacdc.org/download/africa-cdc-strategic-plan-2017-2021
13. German RR, Lee LM, Horan JM, Milstein RL, Pertowski CA, Waller MN; Guidelines Working Group Centers for Disease Control and Prevention (CDC). Updated guidelines for evaluating public health surveillance systems: recommendations from the Guidelines Working Group. MMWR Recomm Rep. 2001;50(RR-13):1–35.
14. Nigerian Federal Ministry of Health. Technical guidelines for integrated disease surveillance and response in Nigeria [cited 2020 Aug 8]. https://ncdc.gov.ng/themes/common/docs/protocols/4_1476085948.pdf
15. Ethnologue. Languages of Nigeria 2017 [cited 2020 Aug 8]. https://www.ethnologue.com/country/NG/languages
16. Alruily M. A review on event-based epidemic surveillance systems that support the Arabic language. Int J Adv Comput Sci. 2018;9:711–18.
17. Salzburg Global Seminar. Finding outbreaks faster: how do we measure progress? Session 613; 2018 Nov 4–8 [cited 2020 Aug 8]. https://www.salzburgglobal.org/fileadmin/user_upload/Final_Summary_EP_Outbreak_Timeliness_Metrics.pdf

Address for correspondence: Kazim Beebeejaun, Hertfordshire Public Health Department, County Hall, Pegs Ln, Hertford SG13 8DQ UK; email: k.beebeejaun@nhs.net

Clinical Features and Comparison of *Kingella* and Non-*Kingella* Endocarditis in Children, Israel

Alexander Lowenthal,[1] Hila Weisblum-Neuman,[1] Einat Birk, Liat Ashkenazi-Hoffnung, Itzhak Levy, Haim Ben-Zvi, Gabriel Amir, Georgy Frenkel, Elchanan Bruckheimer, Havatzelet Yarden-Bilavsky, Dafna Marom, Eran Shostak, Elhanan Nahum, Tamir Dagan, Gabriel Chodick, Oded Scheuerman

Kingella spp. have emerged as an important cause of invasive pediatric diseases. Data on *Kingella* infective endocarditis (KIE) in children are scarce. We compared the clinical features of pediatric KIE cases with those of *Streptococcus* species IE (StIE) and *Staphylococcus aureus* IE (SaIE). A total of 60 patients were included in the study. Throughout the study period, a rise in incidence of KIE was noted. KIE patients were significantly younger than those with StIE and SaIE, were predominately boys, and had higher temperature at admission, history of oral aphthae before IE diagnosis, and higher lymphocyte count ($p<0.05$). Pediatric KIE exhibits unique features compared with StIE and SaIE. Therefore, in young healthy children <36 months of age, especially boys, with or without a congenital heart defect, with a recent history of oral aphthae, and experiencing signs and symptoms compatible with endocarditis, *Kingella* should be suspected as the causative pathogen.

Infective endocarditis (IE) is a rare but potentially life-threatening disease in children and has an incidence of 0.8–3.3 cases/1,000 pediatric hospital admissions (*1*). Although early reports described IE exclusively in children whose hearts were structurally abnormal because of congenital heart disease or acquired rheumatic heart disease, this infection has more recently been reported in diverse groups of patients. In addition to children with congenital heart disease, other groups of children have emerged as being at high risk for IE, including children born prematurely; those with noncardiac congenital malformations, genetic syndromes, and malignancies; and, in particular, children with central venous catheters and those who have been treated by invasive procedures or intravenous medications (*1*–*3*).

The most common IE pathogens in children are gram-positive cocci, especially the α-hemolytic viridans group streptococci (e.g., *Streptococcus sanguis, S. mitis* group, and *S. mutans*), staphylococci, and enterococci. In patients with IE who are >1 year of age, the viridans group streptococci are the most commonly isolated organisms. *Staphylococcus aureus* is the second most common cause of IE in children but the most common cause of acute bacterial endocarditis (*2*). The HACEK group (*Haemophilus parainfluenzae, H. aphrophilus, H. paraphrophilus, Aggregatibacter actinomycetemcomitans, Cardiobacterium hominis, Eikenella* spp., and *Kingella kingae*) is a rare cause of IE, accounting for ≈1.4% of all cases of endocarditis (*2*,*4*).

Kingella spp. are carried asymptomatically in the oropharynx and disseminate through close interpersonal contact. These gram-negative bacteria (especially *K. kingae*) are commonly the etiology of pediatric bacteremia and the leading cause of osteomyelitis and septic arthritis in children 6–36 months of age (*5*). Invasive *K. kingae* disease usually affects previously healthy children <4 years of age, whereas older children and adults frequently have predisposing conditions (*6*).

Kingella IE (KIE) is estimated to account for 0%–6% of all IE cases in the general population (*7*–*10*). Similar numbers have been described in the pediatric population in a few published reports. *Kingella*

Author affiliations: Tel-Aviv University, Tel-Aviv, Israel (A. Lowenthal, H. Weisblum-Neuman, E. Birk, L. Ashkenazi-Hoffnung, I. Levy, H. Ben-Zvi, G. Amir, G. Frenkel, E. Bruckheimer, H. Yarden-Bilavsky, D. Marom, E. Shostak, E. Nahum, T. Dagan, G. Chodick, O. Scheuerman); Schneider Children's Medical Center of Israel, Petach-Tikva, Israel (A. Lowenthal, H. Weisblum-Neuman, E. Birk, L. Ashkenazi-Hoffnung, I. Levy, G. Amir, G. Frenkel, E. Bruckheimer, H. Yarden-Bilavsky, E. Shostak, E. Nahum, T. Dagan, O. Scheuerman); Rabin Medical Center, Beilinson Hospital, Petach-Tikva (H. Ben-Zvi); Tel Aviv Sourasky Medical Center, Tel Aviv (D. Marom)

DOI: https://doi.org/10.3201/eid2703.203022

[1]These authors contributed equally to this article.

appears to cause an even higher number of endocardial infections in children and was the etiologic agent of 4 (7.8%) of 51 episodes in a tertiary-care pediatric hospital in Israel (*3*) and of 6 (7.1%) of 85 cases among New Zealand children (*11*). However, lower rates of KIE have also been reported; a recent study of 53 cases of IE in Belgium described no cases of KIE (*12*). Serious cardiovascular and central nervous system complications and a need for emergent cardiac surgery for life-threatening complications that do not respond to conservative medical treatment have been described in the pediatric population (*13*). *Kingella* spp. as a causative pathogen of endocarditis has been poorly studied, and the number of studies regarding the pediatric population is limited (*3*,*11*,*14*–*20*). Therefore, we examined the characteristics of pediatric KIE case-patients to compare these cases with IE cases caused by other common pathogens.

Methods

We retrospectively reviewed all files of children with IE admitted to Schneider Children's Medical Center of Israel (Petach-Tikva, Israel) during 1994–2019. We included children ≤18 years of age with history and physical findings consistent with possible or definite diagnosis of IE according to the Duke criteria (*21*). Culture-negative IE cases were excluded because some might represent undiagnosed KIE. We also excluded cases of endocarditis that were attributed to coagulase-negative staphylococci species and other rare enteric gram-negative bacteria, because these consist of only nosocomial cases or IE cases associated with foreign bodies or intravenous catheters, which are epidemiologically distinct from the general IE pediatric population. A pediatric cardiologist and a pediatric infectious diseases specialist reviewed all files. Cases were divided into 2 groups on the basis of bacterial etiology: KIE (*K. kingae* and *K. dentrificans*) and non-*Kingella* IE (non-KIE, including *Streptococcus* species and *S. aureus*).

Each isolate was identified by using the VITEK 2 system (bioMérieux, https://www.biomerieux.com) or MALDI Biotyper System (Bruker, https://www.bruker.com), in accordance with the manufacturers' instructions for bacteria identification. Antimicrobial-susceptibility profiles of the isolates were determined by the disk diffusion method (Oxoid, http://www.oxoid.com), Etest (bioMérieux), or VITEK 2 as needed and interpreted based on the Clinical and Laboratory Standards Institute criteria for other non-*Enterobacteriaceae* (*22*). Data retrieved from patients' charts included demographics, past medical history, clinical manifestations, laboratory findings, imaging studies, treatment, and outcome. The characteristics of KIE were compared with characteristics of *Streptococcus* species IE (StIE) and *S. aureus* IE (SaIE). The study was approved by the local institutional review board.

Statistical Analysis

To compare baseline correlates between case categories, we employed a χ^2 test for categorical variables, analysis of variance test for parametric continuous data, and Kruskal–Wallis test for nonparametric continuous data. We calculated p values for the post hoc comparison with Bonferroni correction for the number of comparisons. Statistical analyses were performed by using SPSS Statistics 23.0 software (IBM, https://www.ibm.com) and the tableone package (*23*) in R version 3.6.1 (R Foundation for Statistical Computing, https://www.r-project.org).

Results

Study Population

During the study period, IE was diagnosed in 114 admitted patients, yielding an incidence rate of 1.4 cases/1,000 admissions. A total of 60 patients with IE caused by *Kingella* species, *Streptococcus* species, or *S. aureus* were included in this study. In 19 patients (14% of total IE admissions), the causative pathogen was *Kingella* species (*K. kingae* [n = 18] and *K. dentrificans* [n = 1]); in 25 patients (19%), the causative pathogen was *Streptococcus* species (*S. viridans* [n = 17], *S. pneumoniae* [n = 6], and *S. pyogenes* [n = 2]); and in 16 patients (12%), the causative pathogen was *S. aureus*.

Baseline Characteristics

The baseline characteristics of study participants with KIE and non-KIE are detailed in Table 1. Patients with KIE were significantly younger than those with non-KIE (16 ± SD 10.29 months vs. 91 ± SD 74.11 months; p<0.001). Although the difference was not statistically significant, congenital heart disease was previously diagnosed in fewer patients with KIE than in patients with non-KIE (53% vs. 78%; p = 0.09). Based on queries regarding a previous heart murmur, far fewer patients with KIE had a history of a known murmur than those with non-KIE (37% vs. 71%; p = 0.027). All KIE cases were community-acquired. No statistically significant differences were observed in previous noncardiac disease and previous interventions (surgery, cardiac catheterization, and dental procedures) between the groups. Median time (weeks) between prior cardiac catheterization to infection was shorter

Table 1. Comparison of baseline demographics and characteristics of pediatric infective endocarditis case-patients by causative pathogen, Israel, 1994–2019*

Characteristic	*Kingella*, n = 19 (32%)	Non-*Kingella*, n = 41 (68%)	p value
Age, mo, mean (SD)	16 (± 10.29)	91.4 (± 74.11)	<0.001
Sex			
F	6 (32)	25 (61)	0.065
M	13 (68)	16 (39)	
Congenital heart disease	10 (52)	32 (78.0)	0.09
Known heart murmur	7 (37)	29 (71)	0.027
Recent dental procedure†	0 (0)	6 (15)	0.195
Long-term CVL	0 (0)	5 (12)	0.277
Recent catheterization†	4 (21)	6 (15)	0.804
Time from catheterization to infection, wk	14.50 (10–23)‡	6.00 (2.9–14)‡	0.24
Community-acquired infection	19 (100)	33 (80)	0.097

*Values are no. (%) except as indicated. CVL, central venous line.
†Recent catheterization or dental procedures defined as ≤6 mo before diagnosis of infective endocarditis.
‡Median (interquartile range).

for the non-KIE group than the KIE group but was not statistically significant.

Clinical, Laboratory, and Imaging Characteristics

We compiled the clinical, laboratory, and imaging characteristics of case-patients with KIE compared with non-KIE case-patients (Table 2). Patients with KIE had significantly higher fever when first examined (40°C [range 39.45°C–40°C] vs. 39°C [range 38.6°C–39.8°C]; p = 0.003). No difference was observed in duration of febrile disease before admission. Hepatosplenomegaly was more common among non-KIE patients. Approximately a quarter of KIE patients reported previous oral aphthae, significantly more than those in the non-HIE group (5 patients vs. 0 patients; p = 0.003). No additional differences in clinical findings were noted.

The leukocyte count at admission differed significantly in lymphocyte counts: 4.27 K cells/mL (3.04) among KIE case-patients vs. 2.21 K cells/mL (1.81) in non-KIE case-patients (p = 0.002). Study groups approached significance (p = 0.055) in neutrophil–lymphocyte ratio; patients with KIE had the lowest ratio (4.7), whereas non-KIE patients had a higher ratio (10.7). No differences were observed in other parameters of the complete blood count or the level of inflammatory markers between the 2 groups. The number of positive cultures differed significantly between the 2 groups; most patients with KIE had 1–2 positive blood cultures, and none had ≥4 positive cultures, compared with an average of 4 in the non-KIE group (p<0.001). Days to blood-culture sterilization were fewer in the KIE group (2 days [2–3] vs. 3 days [2–5]; p = 0.017). The chest radiography or echocardiography findings did not exhibit differential features between the 2 groups.

Duke criteria findings are listed in Table 2. Only 37% of those patients with KIE versus 98% in the non-KIE group (p<0.001) fulfilled the Duke major clinical criterion blood culture component. However, blood-culture positivity as a minor clinical criterion was far more prevalent in the KIE group than the non-KIE group (11 patients [58] vs. 1 patient [2]; p<0.001).

A post hoc comparison of the 3 pathogen groups (Table 3) showed that KIE differed significantly from the StIE group in a few parameters. Previous diagnosis of a heart murmur (p = 0.027) and hepatosplenomegaly (p<0.001) were less prevalent in patients with KIE. The absolute leukocyte count was significantly higher in the KIE group than in the StIE group (p<0.005). KIE was significantly more likely to be community-acquired than SaIE (p<0.012). Absolute neutrophil count was significantly lower in the KIE group than the SaIE group (p<0.001).

Outcome

Complications and mortality rates are shown in Table 4. No statistically significant differences were found between case-patients with KIE and those with non-KIE. Urgent surgery ≤10 days after admission was more common in the KIE group but did not reach statistical significance. No deaths occurred in the KIE group, whereas the non-KIE group had an intrahospitalization death rate of 17%.

Discussion

In this study we described the distinct features of pediatric KIE in a large cohort. We found that pediatric patients with KIE have similar characteristics, enabling the suspicion of *Kingella* as a causative pathogen when patients seek care. KIE is community-acquired and occurs in children (mean age 16 months) who are experiencing hyperpyrexia and have no history of previous structural heart disease. A quarter of patients in this study had a history of oral aphthae. This finding is consistent with previous studies indicating that *Kingella* are often carried in the oropharynx of toddlers and that oral aphthae are the port of entry resulting in bacteremia (*5*,*6*).

Relative lymphocytosis was found to be significantly more prevalent in the KIE group than the non-KIE group (4.27 K leukocytes/mL vs. 2.21 K leukocytes/mL). This finding is probably because of the younger age of KIE case-patients. Children with KIE had fewer positive blood cultures and shorter duration of positive cultures. When examining the Duke criteria, we found that a minority of KIE case-patients fulfilled microbiologic major criteria compared with non-KIE case-patients. Because the infection was community-acquired in all patients with KIE and only about half had structural heart disease, in most cases only 1 culture was drawn, probably because of the low level of suspicion. This practice might explain why culture positivity as a minor criterion was far more prevalent in the KIE group than the non-KIE group (57.9% vs. 2.4%). We can therefore assume that, in most cases of KIE, the diagnosis was not clear at admission and that non-KIE pathogens require prolonged antimicrobial regimens for eradication.

A previous study in Israel suggests that the proportion of pediatric KIE cases in Israel is rising, from 4.2% of total IE cases during 1980–1991 to 14% during 1994–2019 (*24*), consistent with the findings in our study. This high proportion of KIE has not been described previously in other countries (*15*,*25*). A probable explanation is the improved detection of this fastidious bacterium, combined with the tertiary nature of our medical center. In addition, a higher prevalence of *Kingella* infection in Israel is a plausible explanation (*5*,*6*).

Data characterizing the course of disease and fatal outcomes were not very helpful in differentiating between the groups, apart from deaths noted

Table 2. Comparison of clinical, laboratory, and imaging characteristics of pediatric infective endocarditis case-patients by causative pathogen, Israel, 1994–2019*

Characteristic	*Kingella*, n = 19 (32%)	Non-*Kingella*, n = 41 (68%)	p value
Temperature, °C, median (IQR)	40 (39.45–40)	39 (38.6–39.8)	0.003
Fever duration before admission, d, median (IQR)	7 (4.50–14)	6 (3–14)	0.43
Hepatosplenomegaly	4 (21)	24 (58)	0.015
Oral aphthae	5 (26)	0 (0)	0.003
Ocular findings	1 (5)	8 (19)	0.294
Systemic emboli	7 (37)	14 (34)	1
Pulmonary emboli	0 (0.0)	2 (5)	0.837
Seizures	3 (16)	6 (15)	1
New onset murmur	7 (37)	10 (24)	0.492
Conduction disturbance	1 (5)	2 (5)	1
Microhematuria	5 (26)	23 (56)	0.061
Leukocyte count K/mL, mean (SD)	20.87 (± 12.39)	16.39 (± 9.58)	0.131
Neutrophils K/mL, mean (SD)	12.98 (± 8.49)	12.43 (± 8.67)	0.821
Lymphocytes K/mL, mean (SD)	4.27 (± 3.04)	2.21 (± 1.81)	0.002
NLR, mean (SD)	4.7 (6.71)	10.7 (11.3)	0.055
Hemoglobin, mean (SD)	10.00 (± 1.36)	10.39 (± 2.27)	0.489
Platelets (100 K/mL), mean (SD)	220.16 (± 203.30)	243.85 (± 178.53)	0.649
C-reactive protein, mean (SD)	12.56 (± 6.79)	12.49 (± 10.75)	0.979
ESR, mean (SD)	65.92 (± 38.86)	64.19 (± 34.34)	0.89
No. positive blood cultures, median (IQR)	1 (1–2)	4 (3–5)	<0.001†
Time to eradication, d, median (IQR)	2 (2–3)	3 (2–5)	0.017
Echocardiography			
Mural thrombus	1 (5)	2 (5)	1
Reduced ventricular function	4 (21)	11 (27)	0.873
Vegetation	12 (63)	20 (49)	0.447
Left-sided involvement‡	12 (80)	15 (65)	0.297
Major Duke criteria			
Culture	7 (37)	40 (98)	<0.001
Echocardiography	16 (84)	23 (56)	0.067
Minor Duke criteria			
Fever	19 (100)	39 (95)	0.837
Congenital heart disease	10 (52)	31 (76)	0.138
Vascular	8 (42)	14 (34)	0.759
Immunologic	0 (0)	9 (22)	0.068
Blood culture	11 (58)	1 (2)	<0.001
Summary			
Definite	14 (74)	30 (73)	0.768
Possible	5 (23)	11 (27)	0.768

*Values are no. (%) except as indicated. All laboratory results are at admission apart from temperature, which we recorded as the highest in the 24 h before admission. ESR, erythrocyte sedimentation rate; IQR, interquartile range; NLR, neutrophil–lymphocyte ratio.
†By Mann–Whitney test.
‡Percentage of left-sided involvement in patients with echocardiographic findings.

Table 3. Comparison of the characteristics of case-patients with infective endocarditis by specific causative pathogen, Israel, 1994–2019*

Characteristic	*Kingella species,* n = 19	*Streptococcus* species, n = 25	*Staphylococcus aureus* species, n = 16	p value
Age, mo, mean (SD)	16 (± 10.29)	106.3 (± 70.43)	68 (± 75.89)	**<0.001**†
Sex				
F	6 (32)	15 (60)	10 (62)	0.104
M	13 (68)	10 (40)	6 (38)	
Congenital heart disease	10 (52)	21 (84)	11 (69)	0.079
Known murmur	7 (37)	19 (76)	10 (62.5)	**0.031**‡
Recent surgery	3 (16)	2 (8)	6 (37)	0.055
Recent dental procedure	0	5 (20)	1 (6.2)	0.077
Community-acquired infection	19 (100.0)	23 (92.0)	10 (62.5)	**0.003**§
Temperature, °C, median (IQR)	40 (39.45–40)	39 (39–39.6)	39 (38.4–40)	**0.013**†
Fever duration, d, median (IQR)	7 (4.5–14)	7 (2–21)	5 (3–7)	0.514
Hepatosplenomegaly	4 (21)	15 (60)	9 (56)	**0.025**‡
Oral aphthae	5 (26)	0	0	**0.002**†
Musculoskeletal infection	2 (11.8)	0	0	0.111
Microhematuria	5 (26.3)	13 (52.0)	10 (62.5)	0.08
Leukocyte count, K/mL, mean (SD)	20.87 (± 12.39)	12.68 (± 4.77)	22.18 (± 12.23)	**0.005**‡
Neutrophils, K/mL, mean (SD)	12.98 (± 8.49)	9.34 (± 4.30)	17.27 (± 11.41)	**0.012**§
Lymphocytes, K/mL, mean (SD)	4.27 (± 3.04)	2.09 (± 1.36)	2.40 (± 2.38)	**0.007**†
NLR, mean (SD)	4.7 (6.7)	7.8 (10.4)	15.2 (11.5)	**0.01**‡
C-reactive protein, mean (SD)	12.56 (± 6.79)	10.67 (± 10.21)	15.23 (± 11.33)	0.385
Reduced ventricular function	4 (21)	4 (16)	7 (44)	0.12
Central nervous system involvement	4 (21)	5 (21)	3 (19)	0.983
Death	0	3 (12.5)	3 (25)	0.074
Culture positivity as major Duke criteria	7 (37)	24 (96)	16 (100)	**<0.001**†
Echocardiography as major Duke criteria	16 (84)	13 (52)	10 (62)	0.083
Immunologic involvement as minor Duke criteria	0	5 (20)	4 (25)	0.078
Culture as minor Duke criteria	11 (58)	1 (4)	0	**<0.001**†
Vegetation	10 (53)	6 (24)	8 (50)	0.1

*Values are no. (%) except as indicated. Bold indicates statistical significance (p<.05). IE, infective endocarditis; NLR, neutrophil–lymphocyte ratio.
†Denotes statistical significance between *Kingella* IE and both *Streptococcus* IE and *Staphylococcus aureus* IE.
‡Denotes statistical significance between *Kingella* IE and *Streptococcus* IE.
§Denotes statistical significance between *Kingella* IE and *Staphylococcus aureus* IE.

only in the non-KIE cohort, which probably signify that most KIE case-patients were healthier before contracting IE. We discovered some similarities between the KIE group and the SaIE subgroup; however, larger numbers are needed to draw significant conclusions. The similar trends observed in these groups emphasize the high risk for major complications in KIE as observed in previous studies (*16*,*26*). For reasons unknown, KIE causes devastating damage to the valve tissue in some cases but not others. This range of severity is probably explained by the different *Kingella* strains, which cause varying clinical syndromes (*27*). Unfortunately, *K. kingae* isolates of the patients in our study were not kept in our laboratory for further genotyping. A recent study postulated that a certain major virulence factor of *K. kingae* RtxA, a toxin that belongs to the RTX (repeats in toxin) group of secreted pore-forming toxins, is found in some *K. kingae* strains and causes cellular death by pore formation (*28*). Of note, *S. aureus*–derived α-toxin, a pore-forming exotoxin, has also been implicated as a major cause of cardiac tissue damage in SaIE (*29*).

The limitations of our study include its retrospective data gathering and the relatively small cohort. We did not include cases of IE caused by coagulase-negative staphylococci and enteric gram-negative bacteria in the study. These pathogens cause only

Table 4. Complications and mortality rates among pediatric infective endocarditis case-patients, Israel, 1994–2019*

Complication	No. (%) *Kingella* IE	No. (%) Non-*Kingella* IE	p value
Surgical intervention	8 (42)	15 (37)	0.958
Urgent surgical intervention†	4 (8)	4 (15)	0.07
Congestive heart failure	7 (37)	7 (17)	0.192
Valvular impairment	11 (58)	15 (37)	0.233
Central nervous system involvement	4 (21)	8 (20)	1
Intrahospital death	0 (0)	6 (17)	0.131

*IE, infective endocarditis.
†≤10 days after diagnosis.

nosocomial and foreign body–associated endocarditis and occur in a distinct hospital-associated population. Including those bacteria would have biased this study by further emphasizing *Kingella* as a community-acquired cause of IE. We also excluded culture-negative cases of endocarditis because these could have included partially treated cases of *Kingella* endocarditis. An additional limitation is a selection bias of the population because our medical center is a tertiary-care center. Therefore, patients in whom endocarditis is diagnosed, patients with congenital heart disease, and patients with serious complications are referred to our center from other hospitals. Conversely, this bias is preserved in all 3 groups because most pediatric patients with IE are referred to a tertiary-care center.

In conclusion, this study shows that pediatric KIE has typical features compared with StIE and SaIE. Clinical cases of high fever in young healthy children (<36 months of age), especially boys, with or without congenital heart defects and with a recent history of oral aphthae should raise the suspicion for KIE.

About the Author

Dr. Lowenthal is a staff pediatric cardiologist at Schneider Children's Medical Center of Israel. His main research interests are fetal echocardiography, echocardiography, and acquired pediatric heart disease.

References

1. Day MD, Gauvreau K, Shulman S, Newburger JW. Characteristics of children hospitalized with infective endocarditis. Circulation. 2009;119:865–70. https://doi.org/10.1161/CIRCULATIONAHA.108.798751
2. Ferrieri P, Gewitz MH, Gerber MA, Newburger JW, Dajani AS, Shulman ST, et al. Unique features of infective endocarditis in childhood. Pediatrics. 2002;109:931–43. https://doi.org/10.1542/peds.109.5.931
3. Marom D, Levy I, Gutwein O, Birk E, Ashkenazi S. Healthcare-associated versus community-associated infective endocarditis in children. Pediatr Infect Dis J. 2011;30:585–8. https://doi.org/10.1097/INF.0b013e31820f66c7
4. Chambers ST, Murdoch D, Morris A, Holland D, Pappas P, Almela M, et al.; International Collaboration on Endocarditis Prospective Cohort Study Investigators. HACEK infective endocarditis: characteristics and outcomes from a large, multi-national cohort. PLoS One. 2013;8:e63181. https://doi.org/10.1371/journal.pone.0063181
5. Yagupsky P. *Kingella kingae*: carriage, transmission, and disease. Clin Microbiol Rev. 2015;28:54–79. https://doi.org/10.1128/CMR.00028-14
6. Dubnov-Raz G, Ephros M, Garty BZ, Schlesinger Y, Maayan-Metzger A, Hasson J, et al. Invasive pediatric *Kingella kingae* infections: a nationwide collaborative study. Pediatr Infect Dis J. 2010;29:639–43. https://doi.org/10.1097/INF.0b013e3181d57a6c
7. Berbari EF, Cockerill FR III, Steckelberg JM. Infective endocarditis due to unusual or fastidious microorganisms. Mayo Clin Proc. 1997;72:532–42. https://doi.org/10.4065/72.6.532
8. Chambers ST, Murdoch D, Morris A, Holland D, Pappas P, Almela M, et al.; International Collaboration on Endocarditis Prospective Cohort Study Investigators. HACEK infective endocarditis: characteristics and outcomes from a large, multi-national cohort. PLoS One. 2013;8:e63181. https://doi.org/10.1371/journal.pone.0063181
9. Geraci JE, Wilson WR. Symposium on infective endocarditis. III. Endocarditis due to gram-negative bacteria. Report of 56 cases. Mayo Clin Proc. 1982;57:145–8.
10. Thekekara AG, Denham B, Duff DF. Eleven-year review of infective endocarditis. Ir Med J. 1994;87:80–2.
11. Webb R, Voss L, Roberts S, Hornung T, Rumball E, Lennon D. Infective endocarditis in New Zealand children 1994-2012. Pediatr Infect Dis J. 2014;33:437–42. https://doi.org/10.1097/INF.0000000000000133
12. Kelchtermans J, Grossar L, Eyskens B, Cools B, Roggen M, Boshoff D, et al. Clinical characteristics of infective endocarditis in children. Pediatr Infect Dis J. 2019;38:453–8. https://doi.org/10.1097/INF.0000000000002212
13. Amir G, Frenkel G, Rotstein A, Nachum E, Bruckheimer E, Lowenthal A, et al. Urgent surgical treatment of aortic endocarditis in infants and children. Pediatr Cardiol. 2019;40:580–4. https://doi.org/10.1007/s00246-018-2030-5
14. Berkun Y, Brand A, Klar A, Halperin E, Hurvitz H. *Kingella kingae* endocarditis and sepsis in an infant. Eur J Pediatr. 2004;163:687–8. https://doi.org/10.1007/s00431-004-1520-z
15. Brachlow A, Chatterjee A, Stamato T. Endocarditis due to *Kingella kingae*: a patient report. Clin Pediatr (Phila). 2004;43:283–6. https://doi.org/10.1177/000992280404300311
16. Foster MA, Walls T. High rates of complications following *Kingella kingae* infective endocarditis in children: a case series and review of the literature. Pediatr Infect Dis J. 2014;33:785–6. https://doi.org/10.1097/INF.0000000000000303
17. Martínez Olorón P, Romero Ibarra C, Torroba Álvarez L, Pérez Ocón A. *Kingella kingae* endocarditis [in Spanish]. An Pediatr (Barc). 2011;74:274–5. https://doi.org/10.1016/j.anpedi.2010.10.018
18. Rabin RL, Wong P, Noonan JA, Plumley DD. *Kingella kingae* endocarditis in a child with a prosthetic aortic valve and bifurcation graft. Am J Dis Child. 1983;137:403–4.
19. Rotstein A, Konstantinov IE, Penny DJ. *Kingella*-infective endocarditis resulting in a perforated aortic root abscess and fistulous connection between the sinus of Valsalva and the left atrium in a child. Cardiol Young. 2010;20:332–3. https://doi.org/10.1017/S1047951110000314
20. Youssef D, Henaine R, Di Filippo S. Subtle bacterial endocarditis due to *Kingella kingae* in an infant: a case report. Cardiol Young. 2010;20:448–50. https://doi.org/10.1017/S1047951110000351
21. Li JS, Sexton DJ, Mick N, Nettles R, Fowler VG Jr, Ryan T, et al. Proposed modifications to the Duke criteria for the diagnosis of infective endocarditis. Clin Infect Dis. 2000;30:633–8. https://doi.org/10.1086/313753
22. Clinical and Laboratory Standards Institute. Performance standards for antimicrobial susceptibility testing: 25th edition informational supplement (M100–S25). Wayne (PA): The Institute; 2015.
23. Yoshida K, Bohn J. tableone-package: create "Table 1" to describe baseline characteristics [cited 2020 Jul 26]. https://rdrr.io/cran/tableone/man/tableone-package.html
24. Marom D, Birk E, Ashkenazi S. Trends in pediatric infective endocarditis in a tertiary pediatric center in Israel [in Hebrew]. Harefuah. 2012;151:464–8, 98, 97.

25. Gupta S, Sakhuja A, McGrath E, Asmar B. Trends, microbiology, and outcomes of infective endocarditis in children during 2000–2010 in the United States. Congenit Heart Dis. 2017;12:196–201. https://doi.org/10.1111/chd.12425
26. Baddour LM, Wilson WR, Bayer AS, Fowler VG Jr, Tleyjeh IM, Rybak MJ, et al.; American Heart Association Committee on Rheumatic Fever, Endocarditis, and Kawasaki Disease of the Council on Cardiovascular Disease in the Young, Council on Clinical Cardiology, Council on Cardiovascular Surgery and Anesthesia, and Stroke Council. Infective endocarditis in adults: diagnosis, antimicrobial therapy, and management of complications: a scientific statement for healthcare professionals from the American Heart Association. Circulation. 2015;132:1435–86. https://doi.org/10.1161/CIR.0000000000000296
27. Amit U, Porat N, Basmaci R, Bidet P, Bonacorsi S, Dagan R, et al. Genotyping of invasive *Kingella kingae* isolates reveals predominant clones and association with specific clinical syndromes. Clin Infect Dis. 2012;55:1074–9. https://doi.org/10.1093/cid/cis622
28. Bárcena-Uribarri I, Benz R, Winterhalter M, Zakharian E, Balashova N. Pore forming activity of the potent RTX-toxin produced by pediatric pathogen *Kingella kingae*: Characterization and comparison to other RTX-family members. Biochim Biophys Acta. 2015;1848:1536–44. https://doi.org/10.1016/j.bbamem.2015.03.036
29. Hoerr V, Franz M, Pletz MW, Diab M, Niemann S, Faber C, et al. *S. aureus* endocarditis: Clinical aspects and experimental approaches. Int J Med Microbiol. 2018;308:640–52. https://doi.org/10.1016/j.ijmm.2018.02.004

Address for correspondence: Oded Scheuerman, Schneider Children's Medical Center of Israel, 14 Kaplan St, PO Box 559, Petach Tikva 49202, Israel; email: odedshv@clalit.org.il

The Public Health Image Library (PHIL)

The Public Health Image Library (PHIL), Centers for Disease Control and Prevention, contains thousands of public health–related images, including high-resolution (print quality) photographs, illustrations, and videos.

PHIL collections illustrate current events and articles, supply visual content for health promotion brochures, document the effects of disease, and enhance instructional media.

PHIL images, accessible to PC and Macintosh users, are in the public domain and available without charge.

Visit PHIL at:
http://phil.cdc.gov/phil

Use of US Public Health Travel Restrictions during COVID-19 Outbreak on Diamond Princess Ship, Japan, February–April 2020

Alexandra M. Medley, Barbara J. Marston, Mitsuru Toda, Miwako Kobayashi, Michelle Weinberg, Leah F. Moriarty, M. Robynne Jungerman, Amethyst Clare A. Surpris, Barbara Knust, Anna M. Acosta, Caitlin E. Shockey, David Daigle, Zachary D. Schneider, Julia Charles, Atsuyoshi Ishizumi, Andrea Stewart, Laura A Vonnahme, Clive Brown, Stefanie White, Nicole J. Cohen, Marty Cetron[1]

Public health travel restrictions (PHTR) are crucial measures during communicable disease outbreaks to prevent transmission during commercial airline travel and mitigate cross-border importation and spread. We evaluated PHTR implementation for US citizens on the Diamond Princess during its coronavirus disease (COVID-19) outbreak in Japan in February 2020 to explore how PHTR reduced importation of COVID-19 to the United States during the early phase of disease containment. Using PHTR required substantial collaboration among the US Centers for Disease Control and Prevention, other US government agencies, the cruise line, and public health authorities in Japan. Original US PHTR removal criteria were modified to reflect international testing protocols and enable removal of PHTR for persons who recovered from illness. The impact of PHTR on epidemic trajectory depends on the risk for transmission during travel and geographic spread of disease. Lessons learned from the Diamond Princess outbreak provide critical information for future PHTR use.

Public health travel restrictions (PHTR) have been used by the United States to reduce the likelihood of transmission of selected communicable diseases aboard aircraft (*1*). US federal mechanisms used to implement PHTR include the public health Do Not Board (DNB) list and the Public Health Border Lookout (PHLO) record (*2*,*3*). The DNB, established in 2007, prevents travelers who are contagious or potentially contagious with a communicable disease of public health concern from obtaining a boarding pass for any commercial flight within, to, or from the United States (*2*–*4*). The PHLO alerts Customs and Border Protection officials to notify the Centers for Disease Control and Prevention (CDC) when a person on PHTR attempts to enter the United States by any port of entry so public health action can be taken, if needed (*2*). The public health aspects are managed by CDC and implemented under the legal authority of the Department of Homeland Security (DHS) (*2*). State or local health departments, other federal agencies, or international partners may initiate PHTR requests by contacting CDC (*4*).

Certain criteria must be met before implementing PHTR (*2*). Primarily, the person must be known or believed to be infectious with, or at risk for becoming infectious with, a serious communicable disease that poses a public health threat to others during travel. If not, then ≥1 of the additional criteria must be met: the person is unaware of his or her diagnosis and cannot be notified by public health authorities, is not following public health recommendations, cannot be located, or is likely to travel on a commercial flight or travel internationally by any means; or PHTR are needed to respond to a public health outbreak or to help enforce a public health order. PHTR are removed when the person is no longer considered infectious or at risk for becoming infectious (*2*).

The outbreak of severe acute respiratory syndrome coronavirus 2 (SARS-CoV-2) infection on the Diamond Princess cruise ship in Japan in February 2020 was the earliest large-scale use of US PHTR applied to a cohort on the basis of a common exposure. A total of 111 individual PHTR were placed in

Author affiliation: Centers for Disease Control and Prevention, Atlanta, Georgia, USA

DOI: https://doi.org/10.3203/eid2703.203820

[1]Authors make up the Centers for Disease Control and Prevention COVID-19 Response Team.

1 day, compared with 556 during the 10-year period 2007–2016 (*1*,*3*). Furthermore, placement of the largest single cohort on US federal PHTR previously comprised 14 persons identified as having had a high-risk exposure to Ebola virus during December 2014–April 2015 (*1*).

PHTR generally apply to both US citizens and foreign nationals and can be applied to persons located within the United States or abroad (*2*). CDC decided to limit use of PHTR to US citizens and residents on the Diamond Princess on the assumption that these persons had reason to return to the United States. In addition, the DHS implemented and managed travel restrictions for non–US citizens on the Diamond Princess, which are outside of the scope of this article. The use of PHTR for US citizens and residents on the Diamond Princess should also be differentiated from travel restrictions imposed by the US government by presidential proclamation under section 212(f) of the Immigration and Nationality Act that apply to certain immigrants or nonimmigrants (*5*).

Coronavirus Disease Outbreak on the Diamond Princess

On February 3, 2020, the Diamond Princess cruise ship arrived in Yokohama, Japan, carrying 2,666 passengers and 1,045 crew (*6*). Two days earlier, 1 symptomatic passenger who departed the ship in Hong Kong had tested positive for severe acute respiratory syndrome coronavirus 2 (SARS-CoV-2), the causative agent of coronavirus disease (COVID-19). By February 5, additional passengers on the cruise ship tested positive for the virus; Japanese authorities instituted a 14-day onboard quarantine for all passengers. Effective quarantine of the crew was challenged by communal living quarters, few single-occupancy rooms for isolation, and the need for crew to continue performing essential duties (*7*). Passengers and crew testing positive for SARS-CoV-2 were transferred to hospital isolation wards, along with some of their family members who had not been tested or had tested negative. During Japan's 14-day quarantine, public health authorities relocated passengers ≥80 years of age or with underlying conditions, along with passengers residing in windowless cabins, to land-based quarantine facilities (*7*).

Preliminary data suggested that although most transmission occurred before quarantine implementation, there was residual risk for transmission among crew members and among passengers sharing cabins (*8*,*9*). By February 18, Japan reported 531 confirmed cases (65 crew, 466 passengers) on the Diamond Princess, representing 14% of those on board; additional test results were pending. Concurrently, positive tests among passengers were declining, but positive cases were increasing among the crew (*7*). The overall infection rate on the Diamond Princess (19.2% of passengers and crew) exceeded the reported infection rate (110/100,000 population) in Hubei Province, and viral exposure risk was considered high for Diamond Princess passengers and crew (*6*;*10*–*14*). At that time, the United States had reported 15 confirmed cases of COVID-19 in 7 states, all imported or travel related, and travelers from Hubei Province were subject to mandatory quarantine (*15*). CDC decided that US citizens and residents on the Diamond Princess should not travel to the United States by commercial carrier until those testing positive for SARS-CoV-2 were no longer infectious and those never testing positive were no longer at risk of becoming infectious (*16*).

In light of the apparent continuing spread of COVID-19 aboard the ship during the quarantine, and to prioritize US citizen welfare and safety, the US government offered a large-scale voluntary repatriation involving controlled movement of US citizens, permanent residents, and their partners from the Diamond Princess to the United States and encouraged all eligible to participate. A total of 329 persons disembarked the ship on February 16, evacuating by 2 chartered aircraft configured to prevent and control transmission on board. Except for 1 individual who recovered from COVID-19 in Japan, persons were placed in federally supervised mandatory quarantine by the US government for 14 days after arrival in the United States (*6*,*17*).

PHTR for US Citizens from Diamond Princess in Japan

To prevent commercial travel to the United States by infectious persons, CDC placed all US citizens and residents remaining in Japan on PHTR. Before the repatriation, the US Embassy Tokyo, Mission Japan (USEMB Japan), informed US citizens and residents that those electing to remain in Japan would be placed on PHTR (*18*). CDC rapidly established an active monitoring process to confirm that persons not testing positive for SARS-CoV-2 remained asymptomatic and to enable PHTR removal for each person as soon as CDC's criteria were met. More than 100 US citizens and residents remained in Japan. More than half were hospitalized for medical care due to SARS-CoV-2 infection or underlying health problems; others were spouses or travel companions of hospitalized patients, crew members, or persons who declined repatriation. Operational challenges of PHTR implementation for large cohorts during an epidemic have not been described. To evaluate the use of PHTR in this context and inform future use, we describe

PHTR implementation during the Diamond Princess COVID-19 outbreak, including successes, challenges, and lessons learned.

Methods

Implementation and Removal of PHTR

We reconciled manifests from the US repatriation flights and the cruise ship and worked with USEMB Japan to identify and locate US citizens remaining in Japan, whether in hospitals, government quarantine facilities, or hotels; aboard the ship; or as residents of Japan. On February 19, the ship quarantine imposed by Japan's authorities ended. All identified US citizens and legal permanent residents who had been on the Diamond Princess but declined repatriation were placed on PHTR; they were notified of the PHTR through the USEMB Japan and cruise ship by both email and letter.

For passengers and crew who had not tested positive for SARS-CoV-2, CDC determined that commercial travel would be allowed after they had been off the ship for 14 days, provided they remained asymptomatic and had not tested positive for SARS-CoV-2 in the interim. To ensure these criteria were met, CDC implemented an active monitoring system until 14 days after the last potential exposure (i.e., disembarkation or close contact) (Figure 1; Appendix Figure 1, panel A, https://wwwnc.cdc.gov/EID/article/27/3/20-3820-App1.pdf). For those who experienced symptoms during the monitoring period, CDC and USEMB Japan facilitated medical evaluation in coordination with authorities in Japan.

For persons who tested positive for SARS-CoV-2, criteria to remove PHTR and discontinue isolation were based on CDC criteria in effect at the time: documentation of negative results in 2 consecutive sets of both oropharyngeal (OP) and nasopharyngeal (NP)

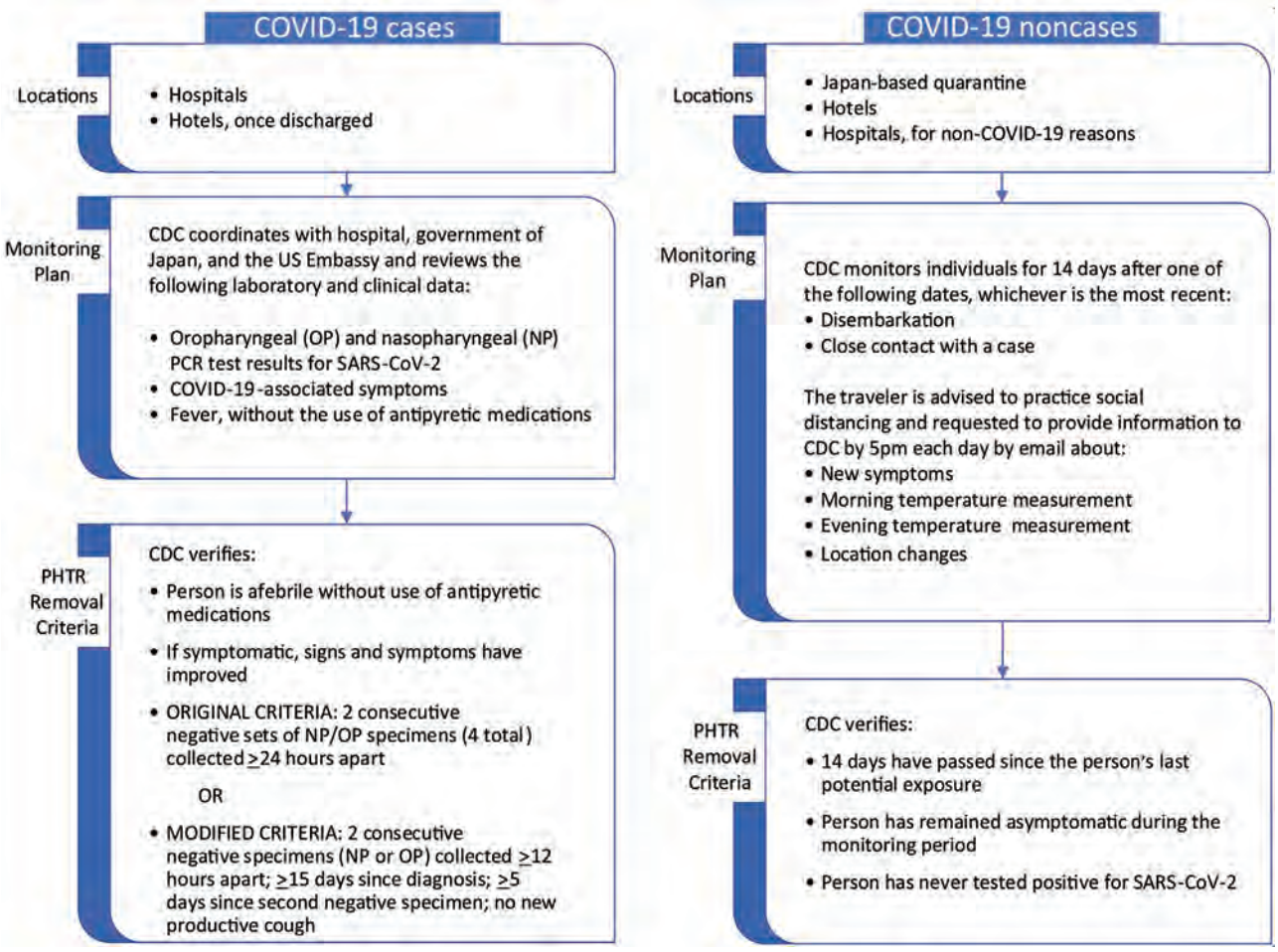

Figure 1. Implementation of PHTR for Diamond Princess cruise ship passengers and crew during the coronavirus disease outbreak, Japan, February 2020, including locations, monitoring plans, and criteria for PHTR removal for persons who tested positive for the virus (cases) and those who did not (non-cases). CDC, US Centers for Disease Control and Prevention; COVID-19, coronavirus disease; PHTR, public health travel restrictions; SARS-COV-2, severe acute respiratory syndrome coronavirus 2.

specimens collected ≥24 hours apart; absence of fever without the use of antipyretic medications; and improvement in other symptoms (Figure 1; Appendix Figure 1, panel B). Hospital discharge criteria in use in Japan at the time required either 2 NP or 2 OP specimens collected ≥12 hours apart. For some patients, CDC was able to request the additional testing and sampling timeframe needed to meet CDC's criteria. However, testing for SARS-CoV-2 in Japan at the time was covered under public funding and required approval of local public health centers (*19*,*20*). Obtaining additional tests to meet CDC criteria (criteria 1; Appendix Figure 1) was challenging for many hospitals, and CDC adopted modified criteria (criteria 2) on February 27 that accepted Japan's testing strategy but added as criteria the times since first positive test (≥15 days) and second negative test result (≥5 days) and absence of a productive cough (Figure 1; Appendix Figure 1, panel C). Time-based criteria were determined from available CDC data that suggested viable virus was rarely recovered from patients later in their clinical course (*21*).

CDC coordinated with USEMB Japan and the cruise line to provide passengers, crew, and hospitals with the criteria and procedures for removal of PHTR (Appendix Figure 1). USEMB Japan consular staff monitored clinical status of all hospitalized US citizens, coordinating directly with hospitals and patients, and provided daily updates to CDC response team, which verified when patients met the criteria for discontinuation of PHTR and the anticipated date of removal. Japanese health workers, in close communication with USEMB Japan, assisted CDC active monitoring efforts for 9 passengers hospitalized for non–COVID-19 health concerns.

Evaluation of PHTR

Using a database consolidating data from the cruise ship, the government of Japan, USEMB Japan, and CDC that was originally used for PHTR implementation, we described characteristics of persons subject to PHTR: US state of residence; sex; age; crew or passenger; history of close contact with a case (e.g., infected cabin mate); number of cabin mates; initial SARS-CoV-2 test result; presence of symptoms at the time of testing (symptomatic or asymptomatic), and disposition (entered monitoring or hospitalized). For those with COVID-19, we described their clinical severity and types of samples collected to meet the discharge criteria (OP, NP, or both), comparing proportions of those meeting original CDC criteria for PHTR removal to the modified criteria. We described outcomes, successes, and challenges of the monitoring process to identify lessons learned, based on our professional judgment and expertise on containing infectious diseases. We analyzed data using R (R Foundation for Statistical Computing, https://www.r-project.org).

Results

Demographics and Dispositions of Persons with PHTR

CDC initially placed 108 US citizen passengers and crew on PHTR on February 19, 2020. One additional passenger self-declared as a legal permanent resident of the United States, and USEMB Japan identified 2 additional persons with dual citizenship, for a total of 111 PHTR. Thirteen persons did not live in the United States but reported secondary residences in or frequent travel to the United States. Of the 98 persons residing in the United States, 30 (31%) resided in California.

From the 111 US citizens and residents remaining in Japan, 44 entered active monitoring after disembarking the ship. Three of these persons were tested for SARS-CoV-2 during the active monitoring period, 1 because of a fever, 1 because of hospitalization for other reasons, and 1 for close contact to a confirmed case; 2 tested positive for SARS-CoV-2. Overall, 69 US citizens had positive test results for SARS-CoV-2 and were hospitalized in 35 hospitals in Japan (Table). Of these patients, 39 (57%) were symptomatic at the time of testing; some asymptomatic but ultimately testing positive US citizens disembarked the ship with test results still pending. Fourteen percent of all persons with COVID-19 were critically ill at any timepoint, including 1 patient with COVID-19 who became critically ill unrelated to COVID-19. The median age of COVID-19 patients was 71 years (range 25–92 years); median age of those testing negative for SARS-CoV-2 was 63 years (range 3–85 years; p = 0.005).

Removal of the PHTR

US citizen and resident passengers disembarked February 19–22 and crew on February 27 (Figure 2). Of the 42 persons (37 passengers, 5 crew) never testing positive for SARS-CoV-2 (Figure 3), 40 (95.2%) completed active monitoring until 14 days after their last potential exposure, spending a median of 16 days with PHTR in place (range 6–34) depending on their disembarkation date (Appendix Figure 2). Two persons were unreachable, and CDC removed their PHTR 28 days (2 incubation periods) after the date of disembarkation.

Of the 69 patients with COVID-19, 40 recovered patients were able to meet the original criteria for PHTR removal, and 29 met the modified criteria. The

Table. Characteristics of Diamond Princess passengers and crew who remained in Japan after US repatriation with public health travel restrictions, 2020*

Characteristic	SARS-CoV-2 positive, no. (%), n = 69	SARS-CoV-2 negative, no. (%), n = 33	Odds ratio (95% CI)	p value
Sex				
F	38 (55)	18 (55)	Referent	None
M	31 (45)	15 (45)	1.02 (0.44–2.37)	0.96
Median age, y (range)	71 (25–92)	63 (3–85)		0.005†
Crew or passenger				
Passenger	66 (96)	33 (100)	ND	ND
Crew	3 (4)	0 (0)	ND	ND
Close contact				
Index patient in cabin	42 (63)	ND	ND	ND
Close contact	25 (37)	9 (100)	ND	ND
Room occupancy				
1	2 (3)	1 (3)	Referent	None
2	58 (88)	23 (70)	0.75 (0.06–24.36)	0.84
3	4 (6)	5 (15)	2.22 (0.13–87.42)	0.59
4	2 (3)	4 (12)	3.28 (0.17–144.84)	0.45
Disposition				
Entered monitoring	0	33 (100)	ND	ND
Criteria 1	40 (58)	0 (0)	ND	ND
Criteria 2	29 (42)	0 (0)	ND	ND

*Data were compiled for 111 US citizens and residents through April 7, 2020. The following characteristics were missing values: sex (2), age (3), room occupancy (11), SARS-CoV-2 test result (9). ND, no data; SARS-COV-2, severe acute respiratory syndrome coronavirus 2.
†By Wilcoxon rank-sum test.

median time from PHTR placement to removal was 17 days (range 7–57 days) (Appendix Figure 2). The median time from notification of a positive test to PHTR removal was 25 days (range 12–62 days) (Figure 4). Multiple persons reported persistent positive test results after symptom resolution; complete information was not available for the full cohort. CDC removed all PHTR by April 15.

Discussion

The Diamond Princess COVID-19 outbreak represents a unique event in public health history: the quarantine of thousands of persons aboard a cruise ship for a newly identified disease at a time when most countries had few imported cases but the epidemic rapidly became a pandemic. Lessons learned from the experience of implementing PHTR on an unprecedented scale can inform the future use of PHTR in outbreaks with pandemic potential.

The first critical lesson is that during a novel disease epidemic, the lack of information about the disease challenges the general practice that ethical use of PHTR requires evidence-based decisions regarding when persons may be contagious or at risk of becoming contagious (*6*). CDC routinely uses PHTR for diseases such as infectious tuberculosis or measles, in which case definitions and criteria for determining noninfectiousness are well established (*3*). During this incident, little was known about SARS-CoV-2 transmission; transmission dynamics in Wuhan, China, and during the severe acute respiratory syndrome coronavirus (2003) and Middle Eastern respiratory syndrome coronavirus (since 2012) epidemics were used in establishing criteria for PHTR removal.

As the COVID-19 epidemic unfolded, we observed notable challenges in identifying persons who might transmit SARS-CoV-2 during travel or contribute to cross-border spread of disease (*22*). Limited information was available to determine whether potentially exposed persons who remained asymptomatic were no longer at risk of becoming infected or when infected persons were no longer infectious because the optimal monitoring period had not yet been determined and it was possible to persistently test positive (*23*). Particular challenges included differences in strategies for discontinuing isolation between the United States and Japan, differences in SARS-CoV-2 testing procedures between hospitals and laboratories in Japan and obtaining medical records and English translations (*24*). These challenges highlight the importance of multinational coordination at all levels and sectors. CDC used the best available data to modify criteria as needed through the event, ensuring that PHTR removal criteria were both evidence based and feasible in the international setting. The modified criteria simplified the PHTR removal process for many infected persons, and the time to remove PHTR was only 5 days longer for those meeting modified criteria (Figure 4). In this experience, clear and consistently applied criteria for removal of PHTR were essential, as was the flexibility to overcome the systemic challenges to meeting those criteria.

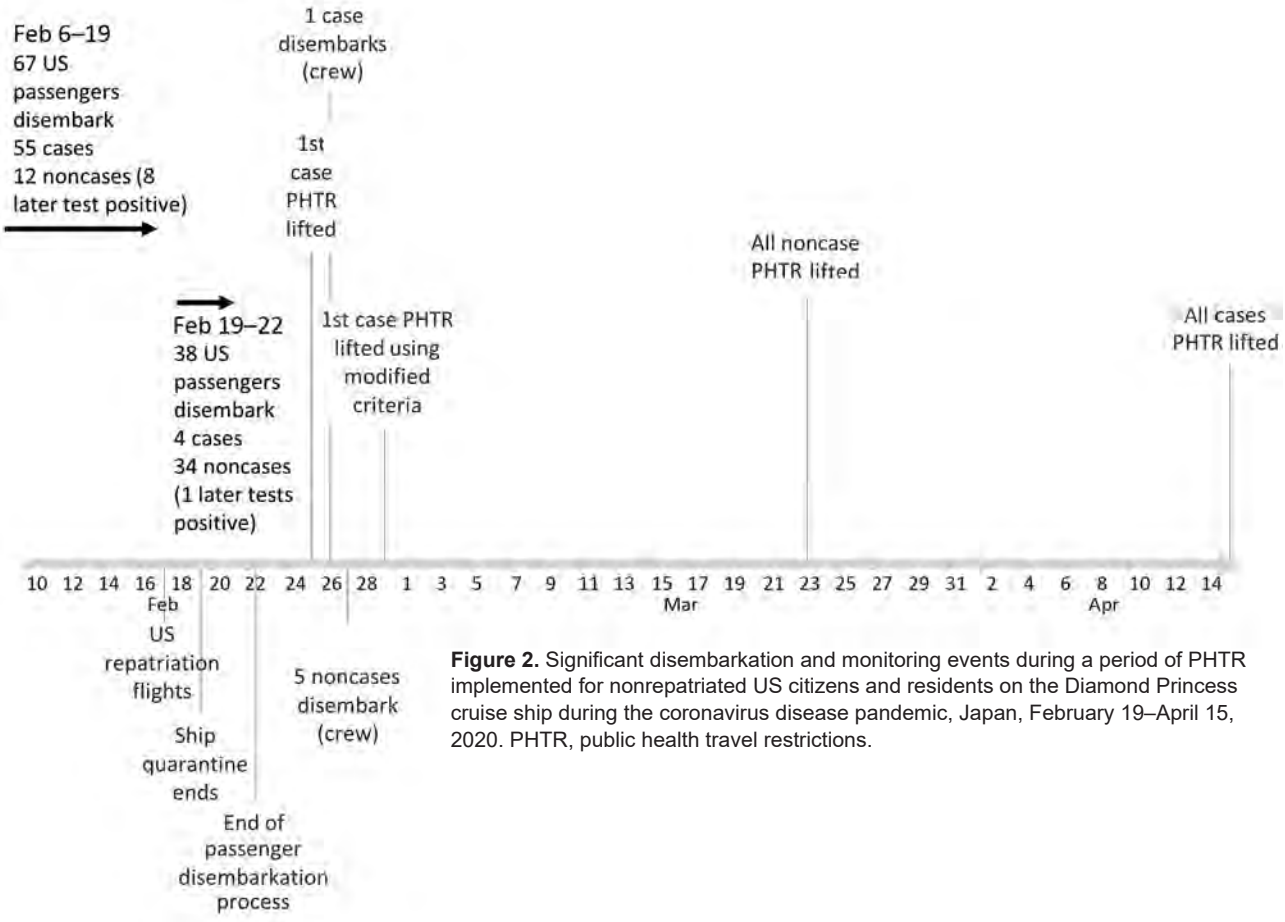

Figure 2. Significant disembarkation and monitoring events during a period of PHTR implemented for nonrepatriated US citizens and residents on the Diamond Princess cruise ship during the coronavirus disease pandemic, Japan, February 19–April 15, 2020. PHTR, public health travel restrictions.

Second, there are logistical challenges in applying and monitoring travel restrictions on this scale. US government personnel had to identify each person for whom travel restrictions were warranted, verify their identities against federal databases, add them individually to the DNB and PHLO, document that criteria for removal of PHTR were met, and ensure timely removal of PHTR once the criteria were met. Because this situation took place on a cruise ship that kept detailed passenger and crew manifests, it was relatively straightforward to identify, notify, and obtain contact information for the persons at risk. If exposure had occurred in a less well-defined situation, identification would have been particularly challenging. However, the complex process to add >100 persons to the DNB and PHLO in the compressed timeframe of 24–48 hours required substantial federal resources.

Typically, documenting criteria for PHTR removal is completed by US jurisdictions or foreign public health authorities (*1*–*3*). For this event, CDC independently created a mechanism to document that exposed persons remained asymptomatic at the end of the 14-day period through an active monitoring process that continued past the end of Japan's mandated quarantine period. Despite rapid implementation, CDC's monitoring process worked well: most travelers had access to email either directly through their personal smartphones or phones provided by the cruise line or through family members in the United States who could communicate with them, and they responded to daily CDC information requests. The USEMB Japan could track the status of hospitalized patients, although this process required substantial resources for translation. Monitored persons and the involved agencies coordinated a large volume of communication both in managing emails with active monitoring information from Diamond Princess travelers and responding to individual travelers' queries about their situations. However, in situations in which this level of coordination is unlikely or persons are difficult to contact, active monitoring for the purposes of PHTR may be challenging to accomplish (*25*,*26*). Before considering use of PHTR, especially on a large scale, implementors should evaluate what resources or capacity are available for identifying persons to be placed on PHTR, personnel required across

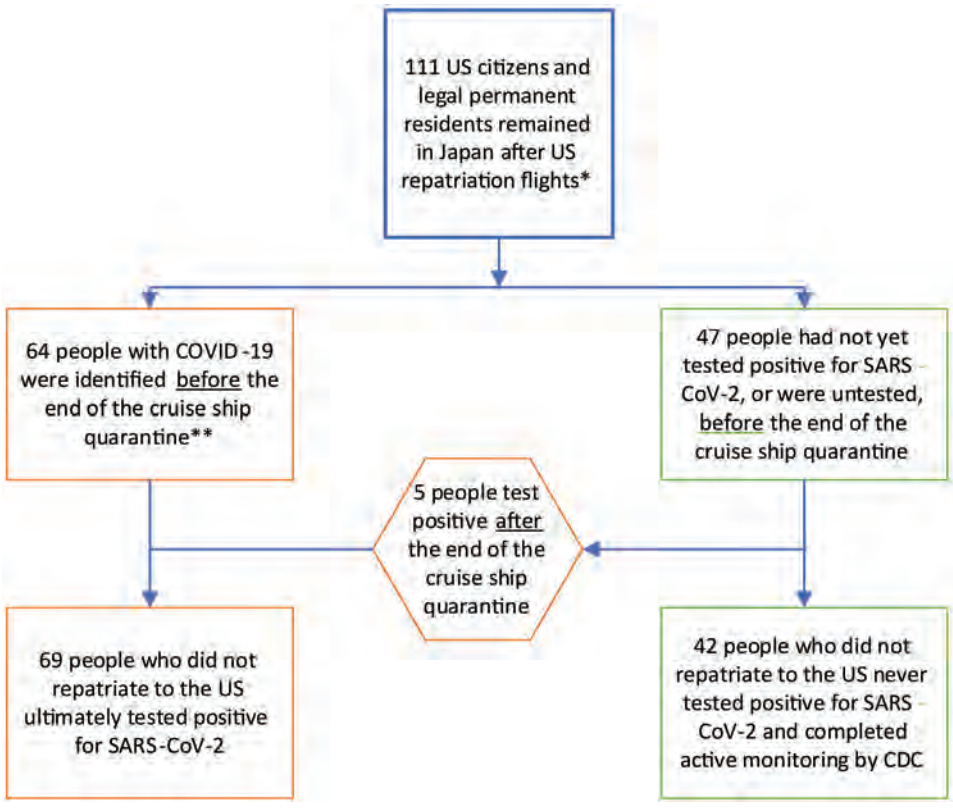

Figure 3. Final disposition (hospitalized for COVID-19 vs. entered active monitoring) of US citizen passengers and crew of the Diamond Princess cruise ship who remained in Japan following US repatriation flights and were subject to public health travel restrictions during the COVID-19 outbreak, 2020. Repatriation flights occurred on February 17, 2020. The Diamond Princess cruise ship quarantine mandated by Japan ended on February 19, 2020; by that date, 67 persons had disembarked, 3 of whom had not tested positive for SARS-CoV-2 at that time. CDC, US Centers for Disease Control and Prevention; COVID-19, coronavirus disease; SARS-COV-2, severe acute respiratory syndrome coronavirus 2.

all relevant agencies and countries to monitor travelers' status and document when they are eligible for removal of PHTR, diagnostic testing capacity, and communications channels.

Third, it is critical that travel restrictions do not create undue risk to affected persons. Persons with positive tests or who became ill could access high-quality medical care in Japan; ethics considerations could be different for persons seeking medical care in areas with inadequate medical infrastructure. In such situations, charter travel or medical evacuation may be options for US citizens and residents to return safely to the United States (*1*), but this option is challenging on a large scale and may have been especially difficult in this situation, in which some of the patients remaining in Japan had complex medical needs. In this situation, the cruise line covered most travel expenses incurred by restricted travelers; CDC can assist travelers whose travel is restricted or delayed for public health reasons by requesting airlines to waive rebooking fees.

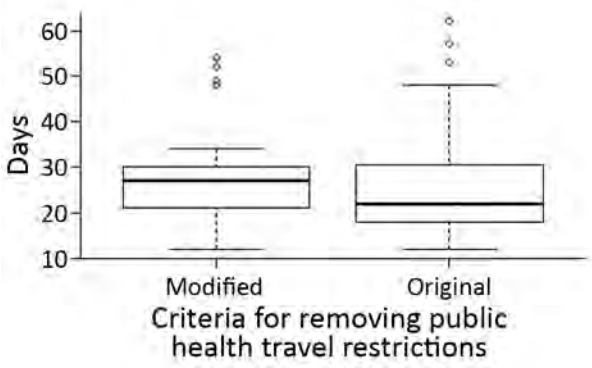

Figure 4. Whisker plot for days between notification of a positive SARS-CoV-2 test result and removal of PHTR for passengers and crew on board the Diamond Princess cruise ship who remained in Japan after US repatriation flights, by type of criteria met for PHTR removal. Horizontal line within the box is the median; bottom line of box is first quartile (25%), top line of box is third quartile (75%). Whiskers represent the minimum (bottom) and maximum (top) number of days. Dots represent outliers. PHTR, public health travel restrictions; SARS-COV-2, severe acute respiratory syndrome coronavirus 2.

Limitations of the analysis were incomplete information, including hospital locations and clinical severity, and inability to obtain the specimen collection date. We approximated date of positive test result by the date of notification.

As with all decisions, overall costs and benefits should be considered when determining whether to use PHTR. Protection of the public, individual civil liberties, and increasing risk for disease transmission are all considerations that can inform use of PHTR (*7*). Costs and benefits may vary as outbreaks or pandemics progress; the benefit was evident in

this event when the United States had only 15 cases. By mid-March 2020, the United States had reported over 6,000 confirmed cases of COVID-19. Most states implemented community mitigation measures such as social distancing requirements and cancellation of mass gatherings, especially once the World Health Organization declared COVID-19 a pandemic on March 11 (*27*,*28*).

PHTR implementation may have prevented transmission via air travel among Diamond Princess travelers under active monitoring and never tested. Transmission on the cruise ship was possible for many days before the vessel quarantine began; it is likely there were many asymptomatic but SARS-CoV-2–positive persons aboard (*6*). As the domestic outbreak grew, CDC shifted to different containment strategies for cruise ships on which COVID-19 cases occurred, including requirements for noncommercial travel after disembarkation and a No Sail Order for all cruise ships operating in US waters (*29*–*31*).

CDC continues to use individual-level PHTR for persons with known or suspected COVID-19 or high-risk exposures and advises persons who are symptomatic, test positive for SARS-CoV-2, or have been exposed to someone with COVID-19 to delay travel until no longer infectious or at risk of becoming infectious. CDC shares information and considerations for use of PHTR with health authorities of other countries but recognizes that many countries may not have the resources to manage similar systems. Lessons learned from the Diamond Princess outbreak are essential in planning future PHTR use during this pandemic or future outbreaks of novel diseases.

Acknowledgments

We thank the Japanese Ministry of Health, Labor and Welfare, the Japanese National Institute of Infectious Diseases, USEMB Japan, the Holland America Group Health Services Team, the CDC Travel Restrictions and Intervention Activity Team, and Elizabeth Wessel, Karin Lang, Timothy Smith, Jason Dyer, Anthony Kujawa, Mami Itami, Tokiko Asada, Akiko Matsuyoshi, Atsuko Morohoshi, Cleatus Hunt, Cody Walsh, Martin Robinson, Grant Tarling, Will Chang, James Misrahi, William Bower, Mateusz Plucinski, Joanna Regan, Carolyn Herzig, Sarah Poser, Robin Rinker, and Ashley Brooks.

About the Author

Dr. Medley is a veterinarian and an Epidemic Intelligence Service officer with the Division of Global Migration and Quarantine, National Center for Emerging and Zoonotic Diseases, Centers for Disease Control and Prevention. Her work focuses primarily on building border health strategies to prevent disease importation in the global setting and the role of population mobility in the cross-border spread of disease.

References

1. Vonnahme LA, Jungerman MR, Gulati RK, Illig P, Alvarado-Ramy F. US federal travel restrictions for persons with higher-risk exposures to communicable diseases of public health concern. Emerg Infect Dis. 2017;23. https://doi.org/10.3201/eid2313.170386
2. Criteria for requesting federal travel restrictions for public health purposes, including for viral hemorrhagic fevers. 80 C.F.R. 16400. 2015 Mar 27 [cited 2020 Dec 17]. https://www.federalregister.gov/documents/2015/03/27/2015-07118/criteria-for-requesting-federal-travel-restrictions-for-public-health-purposes-including-for-viral
3. Jungerman MR, Vonnahme LA, Washburn F, Alvarado-Ramy F. Federal travel restrictions to prevent disease transmission in the United States: an analysis of requested travel restrictions. Travel Med Infect Dis. 2017;18:30–5. https://doi.org/10.1016/j.tmaid.2017.06.007
4. Penfield S, Flood J, Lang W, Zanker M, Haddad MB, Alvarado-Ramy F; Centers for Disease Control and Prevention (CDC). Federal air travel restrictions for public health purposes—United States, June 2007–May 2008. MMWR Morb Mortal Wkly Rep. 2008/57;57:1009–12.
5. Suspension of entry as immigrants and nonimmigrants of persons who pose a risk of transmitting 2019 novel coronavirus and other appropriate measures to address this risk. 85 C.F.R. 6709. 2020 Feb 5 [cited 2020 Dec 30]. https://www.federalregister.gov/documents/2020/02/05/2020-02424/suspension-of-entry-as-immigrants-and-nonimmigrants-of-persons-who-pose-a-risk-of-transmitting-2019
6. Moriarty LF, Plucinski MM, Marston BJ, Kurbatova EV, Knust B, Murray EL, et al.; CDC Cruise Ship Response Team; California Department of Public Health COVID-19 Team; Solano County COVID-19 Team. Public health responses to COVID-19 outbreaks on cruise ships—worldwide, February–March 2020. MMWR Morb Mortal Wkly Rep. 2020;69:347–52. https://doi.org/10.15585/mmwr.mm6912e3
7. Nakazawa E, Ino H, Akabayashi A. Chronology of COVID-19 cases on the Diamond Princess cruise ship and ethical consideration: a report from Japan. Disaster Med Public Health Prep. 2020;14:506–13. https://doi.org/10.1017/dmp.2020.50
8. Kakimoto K, Kamiya H, Yamagishi T, Matsui T, Suzuki M, Wakita T. Initial investigation of transmission of COVID-19 among crew members during quarantine of a cruise ship—Yokohama, Japan, February 2020. MMWR Morb Mortal Wkly Rep. 2020;69:312–3. https://doi.org/10.15585/mmwr.mm6911e2
9. National Institute for Infectious Diseases (NIID). Field briefing: Diamond Princess COVID-19 cases. February 19, 2020 [cited 2020 Dec 30]. https://www.niid.go.jp/niid/en/2019-ncov-e/9407-covid-dp-fe-01.html
10. Liu D. Insistence on prevention and treatment—Hubei's combat against COVID-19 outbreak. Health Commission of Hubei Province. March 12, 2020 [cited 2020 Dec 17]. https://www.who.int/docs/default-source/wpro—documents/countries/china/covid-19-briefing-nhc/14-slides-from-hubei-province.pdf?sfvrsn=3fa3c892_2

11. Nishiura H. Backcalculating the incidence of infection with COVID-19 on the Diamond Princess. J Clin Med. 2020;9:657. https://doi.org/10.3390/jcm9030657
12. Mizumoto K, Chowell G. Transmission potential of the novel coronavirus (COVID-19) onboard the Diamond Princess cruises ship, 2020. Infect Dis Model. 2020;5:264–70. https://doi.org/10.1016/j.idm.2020.02.003
13. Rocklöv, J, Sjödin H, Wilder-Smith A. COVID-19 outbreak on the Diamond Princess cruise ship: estimating the epidemic potential and effectiveness of public health countermeasures, J Travel Med https://doi.org/10.1093/jtm/taaa030
14. Sanche S, Lin YT, Xu C, Romero-Severson E, Hengartner N, Ke R. High contagiousness and rapid spread of severe acute respiratory syndrome coronavirus 2. Emerg Infect Dis. 2020;26:1470–77.
15. Patel A, Jernigan DB; 2019-nCoV CDC Response Team. Initial public health response and interim clinical guidance for the 2019 novel coronavirus outbreak—United States, December 31, 2019–February 4, 2020. MMWR Morb Mortal Wkly Rep. 2020;69:140–6. https://doi.org/10.15585/mmwr.mm6905e1
16. Centers for Disease Control and Prevention. Update on the Diamond Princess cruise ship in Japan. February 18, 2020 [cited 2020 Dec 30] https://www.cdc.gov/media/releases/2020/s0218-update-diamond-princess.html
17. US Embassy Tokyo. Message to US citizen Diamond Princess passengers and crew. February 15, 2020 [cited 2020 Dec 17]. https://japan2.USembassy.gov/pdfs/alert-20200215-diamond-princess.pdf https://jp.USembassy.gov/updates-on-diamond-princess-quarantine
18. US Embassy Tokyo. Information for US citizens—Diamond Princess. February 16, 2020 [cited 2020 Dec 17]. https://japan2.USembassy.gov/pdfs/alert-20200216-diamond-princess.pdf
19. Ministry of Health, Labour and Welfare Japan, Tuberculosis and Infectious Diseases Control Division, Health Service Bureau (MHLW). PCR testing system for novel coronavirus covered by medical insurance. 2020 [cited 2020 Dec 30]. https://www.mhlw.go.jp/content/10900000/000606696.pdf
20. Takahashi R. Coronavirus testing now covered by Japan's national insurance. Japan Times. 2020 [cited 2020 Dec 30]. https://www.japantimes.co.jp/news/2020/03/06/national/science-health/covid-19-tests-japan-national-insurance
21. Kujawski SA, Wong KK, Collins JP, Epstein L, Killerby ME, Midgley CM; COVID-19 Investigation Team. Clinical and virologic characteristics of the first 12 patients with coronavirus disease 2019 (COVID-19) in the United States. Nat Med. 2020;26:861–8. https://doi.org/10.1038/s41591-020-0877-5
22. Furukawa NW, Brooks JT, Sobel J. Evidence supporting transmission of severe acute respiratory syndrome coronavirus 2 while presymptomatic or asymptomatic. Emerg Infect Dis. 2020;26. https://doi.org/10.3201/eid2607.201595
23. Wei WE, Li Z, Chiew CJ, Yong SE, Toh MP, Lee VJ. Presymptomatic transmission of SARS-CoV-2—Singapore, January 23–March 16, 2020. MMWR Morb Mortal Wkly Rep. 1 April 2020;69:411–15. https://doi.org/10.15585/mmwr.mm6914e1.
24. Ministry of Health, Labour and Welfare Japan, Tuberculosis and Infectious Diseases Control Division, Health Service Bureau (MHLW). Handling discharge and work restrictions for patients infected with the novel coronavirus in the context of the law regarding infection prevention and health-care for patients with infectious diseases (partially modified) [in Japanese]. February 18, 2020 [cited 2020 Dec 17]. https://www.mhlw.go.jp/content/10900000/000597947.pdf
25. Millman AJ, Chamany S, Guthartz S, Thihalolipavan S, Porter M, Schroeder A, et al. Active monitoring of travelers arriving from Ebola-affected countries—New York City, October 2014–April 2015. MMWR Morb Mortal Wkly Rep. 2016;65:51–54. https://doi.org/10.15585/mmwr.mm6503a3
26. Saffa A, Tate A, Ezeoke I, Jacobs-Wingo J, Iqbal M, Baumgartner J, et al. Active monitoring of travelers for Ebola virus disease—New York City, October 25, 2014–December 29, 2015. Health Secur. 2018;16:8–13. https://doi.org/10.1089/hs.2017.0077
27. COVID-19 Response Team. Geographic differences in COVID-19 cases, death, and incidence—United States, February 12–April 7, 2020. MMWR Morb Mortal Wkly Rep. 2020;69:465–71. https://doi.org/10.15585/mmwr.mm6915e4
28. World Health Organization. WHO Director-General's opening remarks at the media briefing on COVID-19—11 March 2020. 2020 [cited 2020 Dec 17]. https://www.who.int/director-general/speeches/detail/who-director-general-s-opening-remarks-at-the-media-briefing-on-covid-19---11-march-2020
29. No Sail Order and suspension of further embarkation. 85 C.F.R. 16628. 2020 Mar 14 [cited 2020 Dec 30]. https://www.federalregister.gov/documents/2020/03/24/2020-06166/no-sail-order-and-suspension-of-further-embarkation
30. No Sail Order and suspension of further embarkation; notice of modification and extension and other measures related to operations. 85 C.F.R. 21004. 2020 Apr 15 [cited 2020 Dec 30]. https://www.federalregister.gov/documents/2020/04/15/2020-07930/no-sail-order-and-suspension-of-further-embarkation-notice-of-modification-and-extension-and-other
31 Myers JF, Snyder RE, Porse CC, Tecle S, Lowenthal P, Danforth ME, et al.; Traveler Monitoring Team. Identification and monitoring of international travelers during the initial phase of an outbreak of COVID-19—California, February 3–March 17, 2020. MMWR Morb Mortal Wkly Rep. 2020;69:599–602. https://doi.org/10.15585/mmwr.mm6919e4

Address for correspondence: Alexandra M. Medley, Centers for Disease Control and Prevention, 1600 Clifton Rd NE, Mailstop V24-5, Atlanta, GA 30329-4027, USA; email: amedley2@cdc.gov

Systematic Review of Pooling Sputum as an Efficient Method for Xpert MTB/RIF Tuberculosis Testing during COVID-19 Pandemic

Luis E. Cuevas, Victor S. Santos, Shirley Verônica Melo Almeida Lima, Konstantina Kontogianni, John S. Bimba, Vibol Iem, Jose Dominguez, Emily Adams, Ana Cubas Atienzar, Thomas Edwards, S. Bertel Squire, Patricia J. Hall, Jacob Creswell

GeneXpert-based testing with Xpert MTB/RIF or Ultra assays is essential for tuberculosis diagnosis. However, testing may be affected by cartridge and staff shortages. More efficient testing strategies could help, especially during the coronavirus disease pandemic. We searched the literature to systematically review whether GeneXpert-based testing of pooled sputum samples achieves sensitivity and specificity similar to testing individual samples; this method could potentially save time and preserve the limited supply of cartridges. From 6 publications, we found 2-sample pools using Xpert MTB/RIF had 87.5% and 96.0% sensitivity (average sensitivity 94%; 95% CI 89.0%–98.0%) (2 studies). Four-sample pools averaged 91% sensitivity with Xpert MTB/RIF (2 studies) and 98% with Ultra (2 studies); combining >4 samples resulted in lower sensitivity. Two studies reported that pooling achieved 99%–100% specificity and 27%–31% in cartridge savings. Our results show that pooling may improve efficiency of GeneXpert-based testing.

Xpert MTB/RIF (Cepheid, https://www.cepheid.com) is a cartridge-based nucleic amplification assay for use with Cepheid's GeneXpert diagnostic instrument systems that detects both *Mycobacterium tuberculosis* complex (MTB) and resistance to rifampin (RIF). In 2010, the World Health Organization endorsed Xpert MTB/RIF for laboratory detection of tuberculosis (TB) (*1*), signaling a sea change for diagnosing TB. Xpert MTB/RIF increased sensitivity over microscopy and its ability to simultaneously detect rifampin resistance led to its rapid adoption in low- and middle-income countries. Within the first 5 years, 23 million cartridges were procured at the negotiated price of $9.98/each (P. Jacon, Cepheid, pers. comm., email, April 2020). In 2017, the Cepheid Xpert MTB/RIF Ultra assay (Ultra) was released for use on GeneXpert instruments and results determined to be comparable to those from the Xpert MTB/RIF assay, with an even lower limit for detection (*1*).

Coronavirus disease (COVID-19) is severely disrupting health systems and is threatening progress made by national TB control programs. The new Xpert Xpress SARS-CoV-2 test is run on the same GeneXpert instruments as those for Xpert MTB/RIF and Ultra testing; it is being expedited for large-scale production and deployment. Consequently, TB-testing capacity, already limited by the availability of necessary staff, testing modules, and Xpert MTB/RIF and Ultra cartridges, may be further reduced by the increased demand for GeneXpert for COVID-19 testing (*3*). There is an urgent need to develop laboratory testing approaches to expand TB diagnostic and case-finding services in preparation for crises, such as the COVID-19 pandemic.

GeneXpert-based testing for TB requires 1 cartridge per sputum sample. However, screening for other infectious diseases has used sample pooling methods, in which samples from several patients are

Author affiliations: Liverpool School of Tropical Medicine, Liverpool, UK (L.E. Cuevas, K. Kontogianni, V. Iem, E. Adams, A.T. Atienzar, T. Edwards, S.B. Squire); Federal University of Alagoas, Arapiraca, Brazil (V.S. Santos); Federal University of Sergipe, Aracaju, Brazil (S.V.M. Almeida Lima); Bingham University, Karu, Nigeria (J.S. Bimba); National TB Control Program, Vientiane, Laos (V. Iem); Institut d'Investigació Germans Trias i Pujol and Universitat Autònoma de Barcelona, Badalona, Spain (J. Dominguez); Centers for Disease Control and Prevention, Atlanta, Georgia, USA (P.J. Hall); Stop TB Partnership, Innovations and Grants, Geneva, Switzerland (J. Creswell)

DOI: https://doi.org/10.3201/eid2703.204090

pooled together for a single test to optimize processing. If a pooled-sample test is negative, all samples in the pool are considered negative; if the pooled-sample test is positive, all samples in the pool are retested individually to identify the samples that are positive. This method is routinely used in situations where the prevalence of disease is low (e.g., blood banks screening donated blood for hepatitis and syphilis) (*4*–*9*). The method can substantially reduce workload and cost and, for TB, could more efficiently process samples for diagnosis. We reviewed the literature to determine the accuracy of pooling for Xpert MTB/RIF and Ultra detection of pulmonary TB, with the aim of supporting TB programs as they continue to test for TB in the context of increased resource constraints during the COVID-19 pandemic.

Methods

We conducted a systematic review following the Cochrane Collaboration's Diagnosis Test Accuracy Working Group protocol (https://methods.cochrane.org). Our primary aim was to describe whether testing using GeneXpert for pulmonary TB on pooled samples would result in similar numbers of patients being confirmed with TB as testing samples individually. Secondarily, we aimed to describe the advantages and disadvantages reported, such as savings in cartridges used and time required to process samples.

We searched PubMed, CINAHL, Global Health, and Web of Science for publications from January 2010–March 2020 with no regional or language restrictions. We used the terms "GeneXpert" OR "Xpert" OR "Ultra" AND "tuberculos*" AND "pool*" AND "diagnos*" with associated subject headings and search terms without filters (Appendix Table, https://wwwnc.cdc.gov/EID/article/27/3/20-4090-App1.pdf). S.V.M.A.L. and K.K. eliminated duplicates, screened titles and abstracts, and read full texts to determine eligibility. We also searched for article references manually and for abstracts published at the 2019 Union World Conference of Lung Health. Studies were included if they presented original data, if data were not duplicated in other publications, and if the articles were not reviews or opinions. We excluded studies that pooled several samples from the same patient to increase the yield and those that included samples other than sputum. Given the paucity of studies, we included both those that directly processed patient samples and those that used leftover samples to prepare a specimen repository for bench evaluation of the pooling method. We read selected studies in full for data extraction; L.E.C. and V.S.S. resolved disagreements by consensus.

Data extracted included study identifiers (author, year, country, and setting), methods (study design, pooling methods, number of participants, pooling ratio, number of pools, and type of test), and whether the pooled positive and negative test results coincided with those obtained through individual testing. Data are presented as sensitivity and specificity values, considering the individual GeneXpert test as the reference. Sensitivity was defined as the proportion of pooled samples correctly identified as positive when the pool contained at least 1 sample with a positive individual GeneXpert test. Specificity was defined as the proportion of pooled samples correctly identified as negative when all samples in the pool were negative in individual GeneXpert tests. Data are presented with 95% confidence intervals and ranges.

We assessed the quality of the studies based on a further reference standard, the use of TB culture by any method, whether pooled results were recorded blind to the individual results and whether participants had been recruited consecutively to represent the range of disease severity. The quality of studies and the risk of bias were assessed by 2 independent reviewers (authors) using the QUADAS-2 (Quality Assessment of Diagnostic Accuracy Studies) guidelines (https://www.bristol.ac.uk/media-library/sites/quadas/migrated/documents/quadas2.pdf). We used Cochrane Collaboration Rev-Man 5.3 software (https://training.cochrane.org/online-learning/core-software-cochrane-reviews/revman/revman-5-download) to generate the graphs on the risk of bias (Appendix Figures 1, 2). Because the studies were highly heterogeneous and most (4/6) did not present data on specificity, we were unable to perform a meta-analysis to estimate the pooled sensitivity and specificity or to explore the reasons for heterogeneity through meta-regression. Institutional review board approval was not required because all data sources and publications were in the public domain and in aggregate format.

Results

We identified 33 publications through the initial publication search. After screening titles and abstracts, we assessed 5 full-text articles for eligibility and initially included 2 in data syntheses. In addition, 4 studies were identified from other sources: 1 conference report, 1 preprint article, and 2 articles from the reference lists of other studies. We included 6 articles in the final data synthesis (Figure 1). One study was conducted in South America (*10*), 2 in Africa (*11*,*12*), and 3 in Asia (*13*–*15*); all were published during 2014–2020, before the COVID-19 pandemic.

We assessed the quality of the studies and the risk of bias (Appendix Figures 1, 2). Three studies used samples collected directly from patients with presumptive TB, and 3 studies used previously collected stored samples with known GeneXpert results. Studies pooling direct clinical samples were conducted in high-burden settings in which the proportion of patients that tested GeneXpert-positive was high (15%, 16%, and 38.6%), whereas stored samples were used to prepare pools varying the proportion of positive specimens in each pool to explore the effect on sensitivity. Pools were prepared with clinical samples from consecutive patients in 5 studies and in bench-prepared spiked sputum in a laboratory setting in 1 study. The latter study had also prepared the pool using combinations of smear-positive/culture-positive and smear-negative/culture-positive samples. Generally, the studies followed a similar approach to pooling: a sample was collected from patients with presumptive TB and split into aliquots for Xpert MTB/RIF or Ultra testing following the manufacturer's guidelines. Studies that processed and homogenized sputum used the same steps for the individual and pooled GeneXpert tests. One aliquot was used to obtain an individual result, which was considered the reference result; and the second aliquot was mixed with aliquots from other patients and then tested as a pooled sample. All studies reported that laboratory technicians were blind to whether they were testing pooled versus individual samples. One study collected smear and culture results from all participants in addition to the GeneXpert result (*11*). Four studies tested sputum using Xpert MTB/RIF (*11*–*14*) and 2 with Ultra (*10*,*15*) (Table 1).

These 6 studies tested 1,878 individual samples. Participants were recruited from hospitals (n = 262), ambulatory clinics (n = 914), and outreach activities (n = 702). The percentage of individual patients with Xpert MTB/RIF-positive tests included in the pools ranged from 8.9% to 37%, except for 1 in vitro study, which used spiked samples and prepared pools with up to 64% of positive samples. Only 15 (0.8%) participants across all studies had rifampin resistance (Table 1). Overall, of the 690 pools tested, 117 pooled 2 samples, 28 pooled 3 samples, 364 pooled 4 samples, 37 pooled 5 samples, 16 pooled 6 samples, 36 pooled 8 samples, 16 pooled 10 samples, 36 pooled 12 samples, and 40 pooled 16 samples. Most of the pools with high numbers of samples (≥6) per pool were in the bench-based study. Only 2 studies reported specificity, 1 in which pools were tested with Xpert MTB/RIF (99%, 95% CI 94%–100%) and 1 in which pools were tested with Ultra (100%, 95% CI 96%–100%; Table 2) (*12*,*15*).

The 2 studies (*13*,*14*) combining 2 sputum samples per pool reported 87.5% and 96.0% Xpert MTB/RIF sensitivity relative to individual testing (Figure 2, panel A). The 4 studies combining 4 samples per pool reported sensitivities of 88% (*10*) and 96% (*12*) for Xpert MTB/RIF and 95% (*13*) and 100% (*15*) for Ultra (Figure 2, panel B). In 2 studies (*10*,*13*), pools combining >4 sputum samples reported lower sensitivity ranges for Xpert MTB/RIF (63%–81%) and for Ultra (80%–100%) (Table 2).

Given that all studies had <200 pools, we combined the results from all studies with similar pool sizes and test type (e.g., all studies that pooled 4 samples and test them using Xpert MTB/RIF) to evaluate the effect of the number of pooled samples on accuracy. Although this approach has limitations due to variations in study design and proportion of sample positivity, we believe the benefit of this preliminary analysis of the potential use of pooling during the COVID-19 pandemic outweighs these limitations. After combination, when using Xpert MTB/RIF, 114/117 2-sputa pools

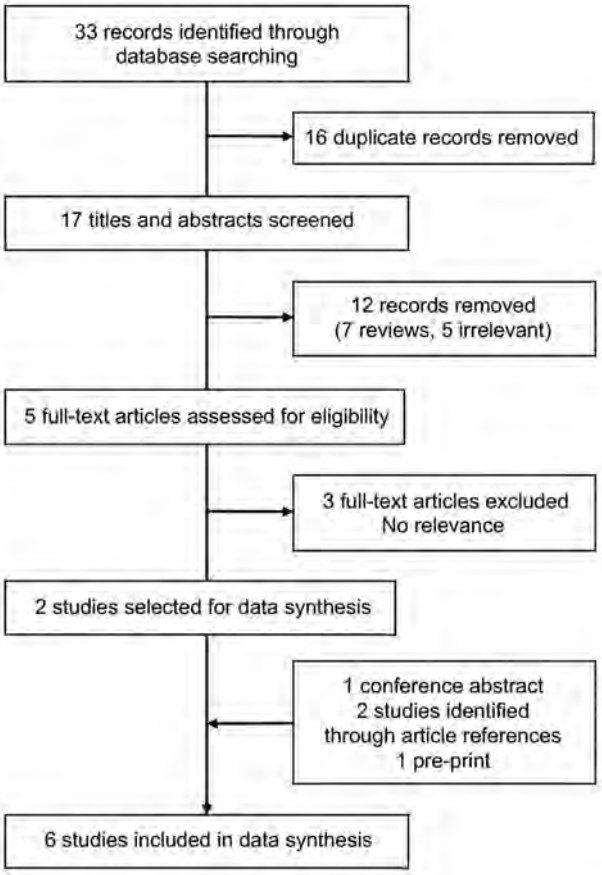

Figure 1. Flow diagram of study selection for a systematic review of pooling sputum as an efficient method for Xpert MTB/RIF and Ultra (Cepheid, https://www.cepheid.com) testing for tuberculosis during the coronavirus disease pandemic.

Table 1. Characteristics of the studies, number of participants, and pool size used in a systematic review of pooling sputum as an efficient method for Xpert MTB/RIF and Ultra testing for tuberculosis during the coronavirus disease pandemic*

Study	Country	Participants recruited from	No. samples	Culture	GX cartridge used	Pooling ratio	No. pools	GX-pos,† no. (%)	GX-neg,† no. (%)	RIF-pos, no.	Comments
(*11*)	South Africa	Reference laboratory	100	Yes	MTB/RIF	1:5	20	20 (20.6)	80 (79.4)	5	Culture and SM pos
			85			1:5	17	17 (20)	68 (32)	3	Culture pos/SM neg
(*12*)	Nigeria	OPD	729	No	MTB/RIF	1:4	185‡	115 (15.8)	614 (84.2)	4	Compared active and passive case finding
(*13*)	Vietnam	SS	118	No	MTB/RIF	1:2	16	75 (63.6)	43 (36.4)	NR	None
						1:4	16				
						1:6	16				
						1:8	16				
						1:10	16				
						1:12	16				
(*14*)	Vietnam	Hospitals	262	No	MTB/RIF	1:2	101§	99 (37.7)	163 (62.3)	NR	Pools constructed 1 pos/1 neg
(*15*)	Cambodia	ACF	584	No	ULTRA	1:4	125	91 (15.6)	493 (84.4)	3	Used chest radiograph to screen
						1:3	28				
(*10*)	Brazil	Prisons, SS	1,120	Yes	ULTRA	1:4	20	100 (8.9)	1,020 (91.1)	NR	None
						1:8	20				
						1:12	20				
						1:16	40				

*Xpert MTB/RIF and Ultra, Cepheid (https://www.cepheid.com). ACF, active case finding; GX, GeneXpert; hosp, hospitalized patients; neg, negative; NR, not reported; OPD, outpatient department; pos, positive; RIF, rifampin; SM, smear; SS, spiked samples.
†Single tests.
‡3 had failed results.
§2 had failed results.

and 101/201 4-sputa pools tested contained an Xpert MTB/RIF-positive sputum; when using Ultra, 93/173 4-sputa pools tested contained an Ultra-positive sputum. If only pools containing a positive sputum sample were considered, 109/114 2-sputa pools tested by Xpert MTB/RIF had a MTB-positive result (sensitivity 93.2%, 95% CI 87.0%–96.4%), and 94/101 4-sputa pools tested by Xpert MTB/RIF had a MTB-positive result (sensitivity 93.0%, 95% CI 86.4%–96.6%). Lastly, 92/93 of the 4-sputa pools tested by Ultra had an MTB-positive result (sensitivity 98.9%, 95% CI 94.1%–99.9%), an increase in sensitivity over those tested by Xpert MTB/RIF.

Studies reported slight changes in the cycle threshold (C_t) values of the pooled samples compared with the individual tests. Most of the C_t changes were relatively small, although studies were not sufficiently powered to determine statistical significance. One study reported that the pooled Xpert MTB/RIF test was negative in 5/10 samples with very low individual Xpert MTB/RIF semiquantitative results (*12*). The South African study that used reconstituted processed sputa to generate pools reported that 20 pools containing 1 smear-positive and 4 smear-negative, but culture-positive, samples yielded a median Xpert MTB/RIF C_t value increase of 12 (IQR 0.3–20.0), and 22 pools containing only smear-negative/culture-positive samples had a median C_t increase of 6.2 (IQR 3.2–16.0) (*11*). Another study (*13*) also reported that Xpert MTB/RIF C_t values increased slightly with increasing pool ratios and, although most pools had C_t values similar to the individual sample tests, pools containing >12 sputum samples had a median increase in C_t value of 2.1 (IQR 0.0–4.5).

A study from South Africa (*11*) reported 5 five-sample pools in which 1 was smear-positive/culture-positive and RIF-resistant and 3 five-sample pools in which 1 was smear-negative/culture-positive and RIF-resistant. All 8 pools containing RIF-resistant samples tested positive for RIF-resistance (*11*). However, in Chry et al. (*15*), of the 3 MTB-positive/RIF-resistant samples subjected to Ultra testing, the pools containing the samples yielded MTB-positive but RIF-sensitive results. Abdurrahman et al. (*12*) included MTB-positive/RIF-resistant samples in all 4 pools, of which 3 were detected by Xpert MTB/RIF as MTB-positive/RIF-resistant and 1 as MTB-positive/RIF-sensitive.

Only 2 studies (*12*–*15*) reported on the operational effects of using a pooling method, including cartridge costs and time savings. The 2 studies (*12,15*) using 4 samples per pool reported savings in cartridge costs alone of 31% ($2,295 on 230 Xpert MTB/RIF

Table 2. Tuberculosis Xpert results of pools composed of positive and negative samples, with sensitivity and specificity, in a systematic review of pooling sputum as an efficient method for Xpert MTB/RIF and Ultra testing for tuberculosis during the coronavirus disease pandemic

Study	Pooling ratio	Test results, no.				Sensitivity, % (95% CI)	Specificity, % (95% CI)
		True pos†	False pos‡	False neg†	True neg‡		
(*11*)	1:5 (Cult neg/SM pos)	20	NA	0	NA	100 (80–100)	NR
	1:5 (Cult pos/SM neg)	13	NA	4	NA	76 (50–92)	NR
(*12*)	1:4	80	1	5	96	94 (87–98)	99 (94–100)
(*13*)	1:2	14	NA	2	NA	88 (62–98)	NR
	1:4	14	NA	2	NA	88 (62–98)	NR
	1:6	11	NA	5	NA	69 (41–98)	NR
	1:8	10	NA	6	NA	63 (35–85)	NR
	1:10	13	NA	3	NA	81 (54–96)	NR
	1:12	13	NA	3	NA	81 (54–96)	NR
(*14*)	1:2	95	NA	4	NA	96 (90–99)	NR
(*15*)	1:4	73	0	0	80	100 (95–100)	100 (96–100)
(*10*)	1:4	19	NA	1	NA	95 (75–100)	NR
	1:8	20	NA	0	NA	100 (83–100)	NR
	1:12	16	NA	4	NA	80 (56–94)	NR
	1:16	39	0	1	0	98 (87–100)	NR

*Xpert MTB/RIF and Ultra, Cepheid (https://www.cepheid.com). Cult, culture, NA, not applicable; neg, negative; NR, not reported; pos, positive; SM, smear.
†At least one of the patients included in the pool had an Xpert-positive test.
‡All patients included in the pool were Xpert-negative in the individual tests.

cartridges) and 27% ($2,092 on 202 Ultra cartridges). These 2 studies also reported reductions of 377 (62%) and 226 (26%) hours in the staff time required to process and run samples (Table 3). All 6 studies included comments indicating the pooling procedure was feasible and beneficial. The study from South Africa (*11*) noted the lower sensitivity found among smear-negative/culture-positive patients. Several studies mentioned the need for specific training on the pooling procedure. The only negative effect, reported anecdotally, was the need to process samples more carefully to avoid handling and reporting errors. No studies included data on patient outcomes, such as treatment initiation.

Discussion

This systematic review synthesizes the available literature on the performance of the pooling method using sputum for GeneXpert testing for detecting pulmonary TB. Although the number of studies is small, the studies reported high sensitivity and specificity for 1:2 and 1:4 pooling ratios, replicating single test results, but pooling >4 samples decreased sensitivity. Studies reporting C_t values consistently reported a slight increase in C_t values and corresponding lower MTB/RIF semiquantitative results for pooled samples. This result is to be expected because testing samples together necessarily dilutes individual samples. Efficiency gained by pooling samples could increase the resilience of TB diagnostic services in a time when health system resources are being challenged by the COVID-19 pandemic.

The Xpert MTB/RIF Ultra cartridge was expected to help improve the sensitivity of pooled tests because the new assay has a much lower limit for detection than Xpert MTB/RIF (*16*). Ultra's improved

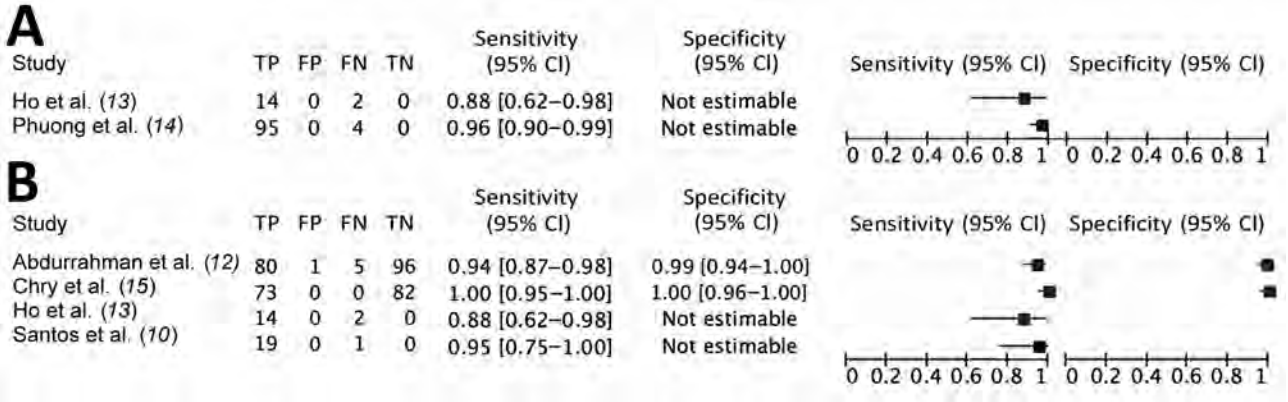

Figure 2. Sensitivity and specificity for pooling sputum in the ratio of 1:2 (A) and pooling sputum in the ratio of 1:4 (B) in a systematic review of pooling sputum as an efficient method for Xpert MTB/RIF and Ultra testing (Cepheid, https://www.cepheid.com) for tuberculosis during the coronavirus disease pandemic.

Table 3. Potential cost and time savings and positive and negative effects of pooling in a systematic review of pooling sputum as an efficient method for Xpert MTB/RIF and Ultra testing for tuberculosis during the coronavirus disease pandemic*

Study	Cartridge savings	Time savings, h (%)	Negative effects	Positive effects
(*11*)	Model of 1,000 patients with TB prevalence rate of 3% found 67.5% cartridge savings	NR	Lower sensitivity for smear-negative tuberculosis; requires laboratory infrastructure and training	Processes higher volume of samples with fewer materials; time savings
(*12*)	11% cartridge savings for hospital-based patients	377 (62%)	Steps involved heighten potential for errors	High-level agreement with individual Xpert results at reduced cost; substantial time savings to process hospital samples
	41% cartridge savings for patients identified through active case finding	NR	NR	Higher savings on cartridge cost and processing time for patients identified through active case finding
(*13*)	NR	NR	NR	Improved feasibility and cost-effectiveness of large-scale testing; reduced number of cartridges
(*14*)	NR	NR	Increase in "error" results when using less buffer for pooling compared with standard buffer technique	Reduced costs and number of cartridges
(*15*)	27% (lower savings estimate using combination of approaches)	226/876 (26%) for all samples; 300/876 (30%) if hybrid approach used	NR	Method feasible; potential to reduce costs, increase throughput. Pooling can be used selectively if another screening test (e.g., radiograph) used for additional savings (hybrid approach)
	34.5% (if used in patients with normal chest x-rays)	NR	NR	Higher savings if only samples from patients without abnormal chest radiographs are included
(*10*)	NR	NR	NR	Method sensitive and cost-effective

*NR, not reported.

performance was confirmed by the higher sensitivities reported in 2 studies included in this review, suggesting that Ultra may be preferred over Xpert MTB/RIF for pooled sample testing (*10*,*15*). Moreover, the only 2 studies reporting specificity (of 99% and 100%) indicated that almost all pools containing all negative individual samples correctly reported negative results for the pooled samples (*12*–*15*). This is an important consideration because the additional steps required to split sputum samples and the need to keep track of sputum batches with a link between individual samples could be prone to cross contamination and error. Further studies are needed to replicate these findings under operational conditions.

Regarding the reproducibility of RIF resistance results in pooled samples, in 1 study from South Africa, all 8 individual RIF-resistant results were detected as pooled RIF-resistant (*11*). However, in a study in Cambodia, 3 samples with RIF-resistant results from individual testing were reported as RIF-susceptible in the pooled testing (*15*) and in a study from Nigeria, pooling missed 1 of 4 RIF-resistant results (*12*). Although pooling seems to be an unreliable method to detect RIF resistance, in practice all samples from MTB-positive pools would be retested individually, which should replicate RIF resistance results from individual samples.

Almost all studies reported anecdotal positive feedback from laboratory staff, and 2 studies (*12*,*15*) quantified savings in cartridge costs and staff time required to process samples. Although both of those studies reported substantial savings, they were conducted in populations with a high proportion of patients testing positive. If a high proportion of presumptive TB patients is expected to be positive, presumably a greater proportion of pools would test positive and require follow-up testing of individual samples. Savings therefore would be more substantial when applied within outreach case-finding activities in the community, where typically around 5% of samples are Xpert MTB/RIF-positive (*12*) and lower in referral and congregate centers (e.g., prisons), where patients might have a higher probability of having TB. The expected proportion of positive samples may therefore guide the pooling ratio selected for evaluation. For example, in active case finding, it is likely a pool ratio of 1:4 would be highly efficient and generate substantial savings, whereas a ratio of 1:2 would be more suitable for busy TB diagnostic centers where the proportion of samples that are positive can be as high as 15%. Pooling is not likely to be useful at a much higher prevalence than 20%, because most of the pools would be positive and samples would have to be retested individually (B.G. Williams, unpub. data, https://arxiv.org/abs/1007.4903). Moreover, there are operational issues that need further study, as it is unclear whether the timing of sputum splitting

could affect results. For example, splitting samples before adding the GeneXpert buffers requires dividing thick and infectious samples, which are likely to have unevenly distributed bacilli, whereas splitting after adding the buffers could increase the risk of cross contamination but provide a safer and more liquid sample with more evenly distributed bacilli.

To inform national programs, further research is needed to determine the effects on time savings from pooled testing, from sample collection to notification and treatment initiation. Two studies quantified large reductions in testing time from pooling (*12*,*15*), which could shorten turnaround times for patient notification, but time to notification was not reported in any of the studies. Quality management of the pooling process is critical, as reflected in discussions in the studies highlighting the importance of sample management and procedure training. As with routine testing procedures, ensuring that pooling is implemented in a biosafe and quality-assured manner would help mitigate risk to laboratorians from increased sample manipulation and prevent errors in sample handling and testing, which could reduce efficiency and benefit to both patients and programs.

Our findings are especially relevant during the ongoing global COVID-19 pandemic, which is severely disrupting health services, the availability of diagnostic and treatment resources, supply chains, and other disease control efforts. Although the diagnosis of COVID-19 takes precedence, steps can be taken to preserve key services for diagnosing and treating patients with presumptive TB. Quarantine and restriction of movement during the pandemic have limited accessibility to services and reduced the numbers of patients attending TB diagnostic and treatment centers. Confinement of the population to households and the resulting increase in contact with other household members in crowded conditions could increase TB transmission. A surge in undetected cases, together with increases in treatment interruptions, will likely lead to increases in incident cases. Demand for testing also may cause severe resource constraints. Preparing for this scenario, such as by introducing pooling strategies, may result in more efficient use of limited resources.

Before the COVID-19 pandemic, the World Health Organization issued guidelines promoting a rapid diagnostic test, such as a GeneXpert-based test, for all persons with presumptive TB (*17*). However, <20% of the GeneXpert TB tests necessary to test the estimated 100 million people who develop presumptive TB each year have been procured (*2*). Individual rapid molecular diagnostic testing for all patients with presumptive TB remains the standard of care and a goal for national TB programs worldwide, but the cost of individually testing all estimated symptomatic persons using GeneXpert would have been more than US $1 billion in cartridges alone in 2018 (*2*), more than the total amount of funding provided by international donors globally for TB in 2019 (*18*). Moreover, although passive case finding has long been the standard approach in many countries, it is becoming apparent that outreach beyond health facilities is needed to identify those with TB missed by programs (*19*). Increasing outreach activities usually means more testing, requiring more cartridges, will be needed. However, a typically greater negative-to-positive testing ratio in persons identified through outreach activities means that pooling strategies might decrease costs.

Despite the potential usefulness of our findings, the quality of evidence we present remains insufficient to support wide adoption of the pooling method. Because the 6 studies were heterogeneous, we were unable to conduct a meta-analysis, and we considered all the studies together with bench evaluations of the technical sensitivity and specificity of the methods; our findings should therefore be considered hypothesis-generating to promote and inform further studies. Moreover, all studies were underpowered for investigating the performance of the pooled testing method in subpopulations (e.g., HIV-positive vs. HIV-negative, men vs. women), and very few samples tested rifampin resistant. C_t values also need to be interpreted with caution.

Although both Xpert MTB/RIF and Ultra tests report C_t values, the test algorithms that determine their C_t and semiquantitative results differ, which impacts the interpretation of C_t-based analyses. Moreover, because C_t ranges vary between multiple tests on the same homogenized sample, it would have been preferable to describe changes in positivity relative to the semiquantitative results. However, semiquantitative results were not reported in most studies. Similarly, although culture was used in some of the studies, this information was not used to stratify analyses. A second reference method would have been useful to further investigate whether discordant results were potentially due to improper sample management, cross-contamination in the laboratory, or random variation due to the bacilli not being homogeneously distributed in the sputum sample.

Despite these limitations, we propose that the pooling method be considered as an interim option to strengthen capacity of TB laboratories during times of crisis, such as during the COVID-19 pandemic. Our

team is currently conducting accelerated evaluations of the pooling method in Laos and Nigeria. We encourage the TB community to conduct studies on the pooling strategy and other resource-saving strategies for TB diagnostic testing that generates data for open access databases to inform national programs.

This research was funded in part by the European and Developing Countries Clinical Trial Partnership (grant no. DRIA2014-309) and its cofunders, Medical Research Council UK and Instituto de Salud Carlos III, Spain; Coordenação de Aperfeiçoamento de Pessoal de Nível Superior, Brazil, as a travel scholarship for SVMAL (process no. 88881.187327/2018–01); TB REACH grant (STBP/TBREACH/GSA/2020-04) supported by Global Affairs Canada; UK Department for International Development, LIGHT Health Research Programme Consortium (contract pending); UK National Institute for Health Research, Health Protection Research Unit in Emerging and Zoonotic Infections, Centre of Excellence in Infectious Diseases Research; and the Alder Hey Charity.

About the Author

Luis Cuevas is professor of international health and epidemiology at the Liverpool School of Tropical Medicine. His main research focus is the evaluation of diagnostics for high burden and emerging infections for use in locations with limited resources, with a primary interest in tuberculosis.

References

1. World Health Organization. WHO monitoring of Xpert MTB/RIF roll-out. Geneva: The Organization; 2019 [cited 2020 Apr 1]. https://www.who.int/tb/areas-of-work/laboratory/mtb-rif-rollout/en
2. Van Deun A, Tahseen S, Affolabi D, Hossain MA, Joloba ML, Angra PK, et al. Sputum smear microscopy in the Xpert® MTB/RIF era. Int J Tuberc Lung Dis. 2019;23:12–8. https://doi.org/10.5588/ijtld.18.0553
3. World Health Organization. WHO: Global TB progress at risk. Geneva: The Organization; 2020. [cited 2020 Nov 1]. https://www.who.int/news/item/14-10-2020-who-global-tb-progress-at-risk
4. Emmanuel JC, Bassett MT, Smith HJ, Jacobs JA. Pooling of sera for human immunodeficiency virus (HIV) testing: an economical method for use in developing countries. J Clin Pathol. 1988;41:582–5. https://doi.org/10.1136/jcp.41.5.582
5. Morandi PA, Schockmel GA, Yerly S, Burgisser P, Erb P, Matter L, et al. Detection of human immunodeficiency virus type 1 (HIV-1) RNA in pools of sera negative for antibodies to HIV-1 and HIV-2. J Clin Microbiol. 1998;36:1534–8. https://doi.org/10.1128/JCM.36.6.1534-1538.1998
6. Peeling RW, Toye B, Jessamine P, Gemmill I. Pooling of urine specimens for PCR testing: a cost saving strategy for *Chlamydia trachomatis* control programmes. Sex Transm Infect. 1998;74:66–70. https://doi.org/10.1136/sti.74.1.66
7. Mine H, Emura H, Miyamoto M, Tomono T, Minegishi K, Murokawa H, et al.; Japanese Red Cross NAT Research Group. High throughput screening of 16 million serologically negative blood donors for hepatitis B virus, hepatitis C virus and human immunodeficiency virus type-1 by nucleic acid amplification testing with specific and sensitive multiplex reagent in Japan. J Virol Methods. 2003;112:145–51. https://doi.org/10.1016/S0166-0934(03)00215-5
8. Lindan C, Mathur M, Kumta S, Jerajani H, Gogate A, Schachter J, et al. Utility of pooled urine specimens for detection of *Chlamydia trachomatis* and *Neisseria gonorrhoeae* in men attending public sexually transmitted infection clinics in Mumbai, India, by PCR. J Clin Microbiol. 2005;43:1674–7. https://doi.org/10.1128/JCM.43.4.1674-1677.2005
9. Westreich DJ, Hudgens MG, Fiscus SA, Pilcher CD. Optimizing screening for acute human immunodeficiency virus infection with pooled nucleic acid amplification tests. J Clin Microbiol. 2008;46:1785–92. https://doi.org/10.1128/JCM.00787-07
10. Santos P, Santos A, Verma R, Oliveira R, Camioli C, Lemos E, et al. The utility of pooling sputum samples for mass screening for tuberculosis in prisons using Xpert MTB/RIF Ultra. In: 50th World Conference on International Union Against Tuberculosis and Lung Disease; 2019 Oct 30–Nov 2; Hyderabad, India. Abstract SOA-01-1001-31. Int J Tuberc Lung Dis. 2019;23:S110–1 [cited 2020 Mar 30]. https://hyderabad.worldlunghealth.org/wp-content/uploads/2019/11/20191101_UNION2019_Abstracts_Final.pdf
11. Zishiri V, Chihota V, McCarthy K, Charalambous S, Churchyard GJ, Hoffmann CJ. Pooling sputum from multiple individuals for Xpert® MTB/RIF testing: a strategy for screening high-risk populations. Int J Tuberc Lung Dis. 2015;19:87–90. https://doi.org/10.5588/ijtld.14.0372
12. Abdurrahman ST, Mbanaso O, Lawson L, Oladimeji O, Blakiston M, Obasanya J, et al. Testing pooled sputum with Xpert MTB/RIF for diagnosis of pulmonary tuberculosis to increase affordability in low-income countries. J Clin Microbiol. 2015;53:2502–8. https://doi.org/10.1128/JCM.00864-15
13. Ho J, Jelfs P, Nguyen PTB, Sintchenko V, Fox GJ, Marks GB. Pooling sputum samples to improve the feasibility of Xpert® MTB/RIF in systematic screening for tuberculosis. Int J Tuberc Lung Dis. 2017;21:503–8. https://doi.org/10.5588/ijtld.16.0846
14. Phuong NTB, Anh NT, Van Son N, Sintchenko V, Ho J, Fox GJ, et al. Effect of two alternative methods of pooling sputum prior to testing for tuberculosis with Genexpert MTB/RIF. BMC Infect Dis. 2019;19:347. https://doi.org/10.1186/s12879-019-3778-9
15. Chry M, Smelyanskaya M, Ky M, Codlin AJ, Cazabon D, Tan Eang M, et al. Can the high sensitivity of Xpert MTB/RIF Ultra be harnessed to save cartridge costs? Results from a pooled sputum evaluation in Cambodia. Trop Med Infect Dis. 2020;5:27. https://doi.org/10.3390/tropicalmed5010027
16. Chakravorty S, Simmons AM, Rowneki M, Parmar H, Cao Y, Ryan J, et al. The new Xpert MTB/RIF Ultra: improving detection of *Mycobacterium tuberculosis* and resistance to rifampin in an assay suitable for point-of-care testing. MBio. 2017;8:e00812–7. https://doi.org/10.1128/mBio.00812-17
17. World Health Organization. Automated real-time nucleic acid amplification technology for rapid and simultaneous detection of tuberculosis and rifampicin resistance: Xpert

MTB/RIF assay for the diagnosis of pulmonary and extrapulmonary TB in adults and children: policy update. Geneva: The Organization; 2013 [cited 2020 Apr 1]. https://apps.who.int/iris/bitstream/handle/10665/112472/9789241506335_eng.pdf

18. World Health Organization. Global tuberculosis report 2019. Geneva: The Organization; 2019. [cited 2020 Apr 1]. https://apps.who.int/iris/bitstream/handle/10665/329368/9789241565714-eng.pdf

19. Dowdy DW, Basu S, Andrews JR. Is passive diagnosis enough? The impact of subclinical disease on diagnostic strategies for tuberculosis. Am J Respir Crit Care Med. 2013;187:543–51. https://doi.org/10.1164/rccm.201207-1217OC

Address for correspondence: Luis E. Cuevas, Liverpool School of Tropical Medicine, Pembroke Place, Liverpool L3 5QA, UK; email: Luis.Cuevas@lstmed.ac.uk

January 2020

Viruses

- Spatial Epidemiologic Trends and Hotspots of Leishmaniasis, Sri Lanka, 2001–2018
- *Candidatus* Mycoplasma haemohominis in Human, Japan
- Nutritional Care for Patients with Ebola Virus Disease
- Paid Leave and Access to Telework as Work Attendance Determinants during Acute Respiratory Illness, United States, 2017–2018
- Preclinical Detection of Prions in Blood of Nonhuman Primates Infected with Variant Creutzfeldt-Jakob Disease
- Effect of Acute Illness on Contact Patterns, Malawi, 2017
- Outbreak of Peste des Petits Ruminants among Critically Endangered Mongolian Saiga and Other Wild Ungulates, Mongolia, 2016–2017
- Elephant Endotheliotropic Herpesvirus Hemorrhagic Disease in Asian Elephant Calves in Logging Camps, Myanmar
- Risk Factors for and Seroprevalence of Tickborne Zoonotic Diseases among Livestock Owners, Kazakhstan
- High Azole Resistance in *Aspergillus fumigatus* Isolates from Strawberry Fields, China, 2018
- Tick-Borne Encephalitis Virus, United Kingdom
- Phenotypic and Genotypic Correlates of Penicillin Susceptibility in Nontoxigenic *Corynebacterium diphtheriae*, British Columbia, Canada, 2015–2018

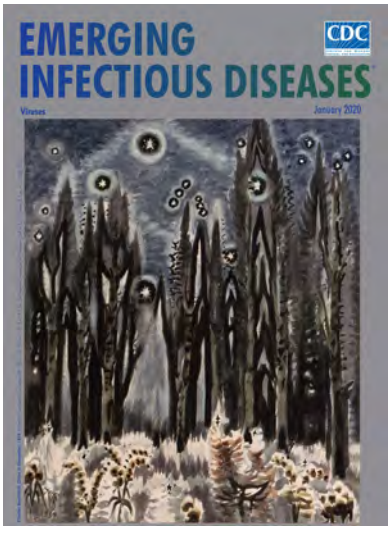

- High Pathogenicity of Nipah Virus from *Pteropus lylei* Fruit Bats, Cambodia
- Varicella in Adult Foreigners at a Referral Hospital, Central Tokyo, Japan, 2012–2016
- Geographic Distribution and Incidence of Melioidosis, Panama
- *Shigella* Bacteremia, Georgia, USA, 2002–2012
- Distribution of Japanese Encephalitis Virus, Japan and Southeast Asia, 2016–2018
- Novel Reassortant Highly Pathogenic Avian Influenza A(H5N2) Virus in Broiler Chickens, Egypt
- Infectivity of Norovirus GI and GII from Bottled Mineral Water during a Waterborne Outbreak, Spain
- Effect of Pediatric Influenza Vaccination on Antibiotic Resistance, England and Wales
- Locally Acquired Human Infection with Swine-Origin Influenza A(H3N2) Variant Virus, Australia, 2018
- Use of Ambulance Dispatch Calls for Surveillance of Severe Acute Respiratory Infections
- Hantavirus Pulmonary Syndrome in Traveler Returning from Nepal to Spain
- Visceral Leishmaniasis, Northern Somalia, 2013–2019
- Autochthonous Human Fascioliasis, Belgium
- Recombinant Nontypeable Genotype II Human Noroviruses in the Americas
- *Legionella pneumophila* as Cause of Severe Community-Acquired Pneumonia, China
- Training for Foodborne Outbreak Investigations by Using Structured Learning Experience
- Emergence of *Vibrio cholerae* O1 Sequence Type 75 in Taiwan
- Diabetes Mellitus, Hypertension, and Death among 32 Patients with MERS-CoV Infection, Saudi Arabia
- Influenza D Virus of New Phylogenetic Lineage, Japan
- Diagnosis of Syphilitic Bilateral Papillitis Mimicking Papilloedema
- Influenza A Virus Infections in Dromedary Camels, Nigeria and Ethiopia, 2015–2017

EMERGING INFECTIOUS DISEASES®

To revisit the January 2020 issue, go to:
https://wwwnc.cdc.gov/eid/articles/issue/26/1/table-of-contents

Decentralized Care for Rifampin-Resistant Tuberculosis, Western Cape, South Africa

Sarah V. Leavitt, Karen R. Jacobson, Elizabeth J. Ragan, Jacob Bor, Jennifer Hughes, Tara C. Bouton, Tania Dolby, Robin M. Warren, Helen E. Jenkins

In 2011, South Africa implemented a policy to decentralize treatment for rifampin-resistant tuberculosis (TB) to reduce durations of hospitalization and enable local treatment. We assessed policy implementation in Western Cape Province, where services expanded from 6 specialized TB hospitals to 406 facilities, by analyzing National Health Laboratory Service data on TB during 2012–2015. We calculated the percentage of patients who visited a TB hospital ≤1 year after rifampin-resistant TB diagnosis, the median duration of their hospitalizations, and the total distance between facilities visited. We assessed temporal changes with linear regression and stratified results by location. Of 2,878 patients, 65% were from Cape Town. In Cape Town, 29% visited a TB hospital; elsewhere, 68% visited a TB hospital. We found that hospitalizations and travel distances were shorter in Cape Town than in the surrounding areas.

South Africa has a high tuberculosis (TB) prevalence, complicated by multidrug resistance to rifampin and isoniazid (*1*). In 2018, multidrug-resistant (MDR) and rifampin-resistant (RR) TB accounted for 3.4% of new and 7.1% of previously treated cases in South Africa (*1*). These forms of TB require more complex and lengthy treatments than drug-susceptible TB. Before 2011, most patients with MDR/RR TB in South Africa were hospitalized in dedicated TB hospitals, which were considered better than other facilities for managing infection control, regimen complexities, and side effects. However, centralized care might have contributed to delayed initiation of second-line drugs for MDR/RR TB, high pretreatment death rates caused by limited bed capacity, and patient loss to follow-up because of long-term hospitalization of clinically stable patients (*2*,*3*).

A 2009 pilot program in Khayelitsha township, Cape Town (*4*), South Africa, demonstrated that community-based care improved case detection. It also reduced death, health system costs, and treatment delays (*3*,*5*–*11*). In 2011, the South African National Department of Health implemented a national policy to decentralize and deinstitutionalize MDR/RR TB care (*2*). In Western Cape, MDR/RR TB care decentralization enabled clinically stable patients to initiate second-line TB treatment at 1 of 406 local facilities offering TB care instead of the province's 6 specialized TB hospitals (*12*). The policy also reduced the required duration of TB hospitalizations for patients who required hospitalization (*2*). Because of the reduced density of TB hospitals outside Cape Town, the potential policy effects are largest in rural areas. However, long distances between facilities and lack of resources and experienced providers pose challenges to implementation in rural areas.

Despite these demonstrated benefits of decentralization, data analyzing its effects on hospitalization rates, duration, and travel distance in Western Cape are scarce. The National Health Laboratory Service (NHLS) conducts and records most laboratory tests in South Africa. We used NHLS data to track where patients received care for RR TB in the year after their diagnoses. We identified temporal trends in patient

Author affiliations: Boston University, Boston, Massachusetts, USA (S.V. Leavitt, K.R. Jacobson, E.J. Ragan, J. Bor, T.C. Bouton, H.E. Jenkins); Boston Medical Center, Boston (K.R. Jacobson, E.J. Ragan, T.C. Bouton); University of the Witwatersrand, Johannesburg, South Africa (J. Bor); Stellenbosch University, Stellenbosch, South Africa (J. Hughes, R.M. Warren); Brown University, Providence, Rhode Island, USA (T.C. Bouton); Green Point Tuberculosis Laboratory, Cape Town, South Africa (T. Dolby); South African Medical Research Council Centre for Tuberculosis Research, Cape Town (R.M. Warren); Department of Science and Technology–National Research Foundation Centre of Excellence for Biomedical Tuberculosis Research, Cape Town (R.M. Warren)

DOI: https://doi.org/10.3201/eid2703.203204

contact with TB hospitals, estimated hospital stay duration and distance traveled between facilities during early implementation of the national decentralization policy in Western Cape. We compared these metrics between Cape Town and more rural Western Cape districts.

Methods

Data Source

We extracted records of TB laboratory tests conducted on clinical samples at the NHLS TB laboratory in Green Point, Cape Town, during January 1, 2012–July 31, 2015. These tests were used to diagnose and monitor TB cases in the Western Cape. Samples originated from patients at various facilities, including specialized TB hospitals, primary healthcare clinics, mobile clinics, regional hospitals, and district hospitals. The NHLS records data on patients receiving tests through the public healthcare system, which conducts 93% of all TB tests nationally (*13*). The study was approved by Stellenbosch University's Health Research Ethics Committee (protocol no. N09/11/296) and Boston University's Institutional Review Board (no. H-38441). Given the study's retrospective nature, an informed consent waiver was granted.

During the study period, the Western Cape's TB investigation policy required that facilities submit 2 clinical samples from each patient to the nearest NHLS laboratory (*14*). Usually, the first sample was tested with Xpert MTB/RIF (Cepheid, https://www.cepheid.com). If RR TB was detected, the second sample was sent to the Green Point laboratory for smear microscopy, culturing with the mycobacterial growth indicator tube (Becton, Dickinson, and Company, https://www.bd.com), and drug susceptibility testing (DST). Line probe assays (LPAs) conducted by using GenoType MTBDR*plus* (Hain Lifescience GmbH, https://www.hain-lifescience.de) confirmed the presence of *Mycobacterium tuberculosis* and genes for resistance to rifampin and other first-line drugs. Phenotypic DST was used to detect genes conferring second-line drug (SLD) resistance. Although samples from tertiary (non-TB) hospitals with their own culture laboratories are not included in this dataset, the laboratory in Green Point conducts most culture-based and LPA confirmatory testing for TB in the Western Cape; therefore, this dataset includes most patients with RR TB in this province (Appendix, https://wwwnc.cdc.gov/EID/article/27/3/20-3204-App1.pdf).

Each NHLS record represents a single laboratory test but lacks a unique patient identifier. Therefore, to track patients over time, we used a patient matching algorithm to link samples belonging to the same patient. This algorithm, previously applied to NHLS HIV data, estimates the probability that records belong to the same patient on the basis of name, birthdate, sex, and facility data (*15*; J. Bor, unpub. data, https://www.biorxiv.org/content/early/2018/11/02/450304) (Appendix).

Definitions

We defined a patient with RR TB as someone who submitted ≥1 clinical sample with bacteriological confirmation of *M. tuberculosis* and rifampin resistance according to Xpert MTB/RIF, LPA, phenotypic DST, or a combination of these testing methods at the NHLS laboratory in Green Point. We defined the taken date as the date the sample was obtained from a patient. We considered the taken date of the first RR TB–positive sample to be the patient's initial sample date and the diagnosis date (Appendix). We defined a visit as a unique day in which a patient submitted ≥1 laboratory sample. Time in care was defined as 1 year from the initial RR TB sample or until the most recent sample in the study timeframe, whichever was earlier.

Study Population

We analyzed each patient's TB laboratory samples in the year after that patient's initial RR TB sample was submitted to the NHLS during January 1, 2012–July 31, 2015. Using specific exclusion criteria (Figure 1), we excluded samples that were from locations outside Western Cape, collected for research purposes, submitted with invalid identifying data (e.g., names containing the words "control," "staff," "Ecoli", etc.), or had facility codes that could not be linked to a physical location.

After linking samples to individual patients, we excluded patients whose initial RR TB sample was submitted after July 1, 2014, enabling us to study 12 months of follow-up for each patient. Some patients might have had less time in care if they died, moved out of the province, or were otherwise lost to follow-up, after which point these patients would no longer be included in the Western Cape public healthcare system. Because we could not correlate laboratory results with clinical records, we excluded patients whose initial RR TB sample was submitted during the first 3 months of the study (January 1–March 31, 2012) because this sample might not have been their diagnostic sample. We excluded patients who had no subsequent laboratory samples submitted to the NHLS because we assumed that those patients were less

likely to have initiated treatment or stayed in care. Finally, we excluded patients who were less likely to have been affected by the decentralization policy: those in correctional facilities, those with documented SLD resistance, and children <15 years of age at diagnosis.

Mapping Patient Movement

In the NHLS database, each sample is registered with a collecting facility code. We determined the facility name, type, and geocoordinates from NHLS and National Department of Health reference lists. We grouped facilities into 3 categories: specialized TB hospitals, non-TB hospitals (i.e., all other hospitals), and clinics (i.e., all other location types). We validated geocoordinates on Google Maps (https://maps.google.com); researchers and healthcare providers in South Africa resolved discrepancies. We combined facilities of the same type and geographic location into a single entity. We used the code associated with the samples from each patient to track patient movement between facilities.

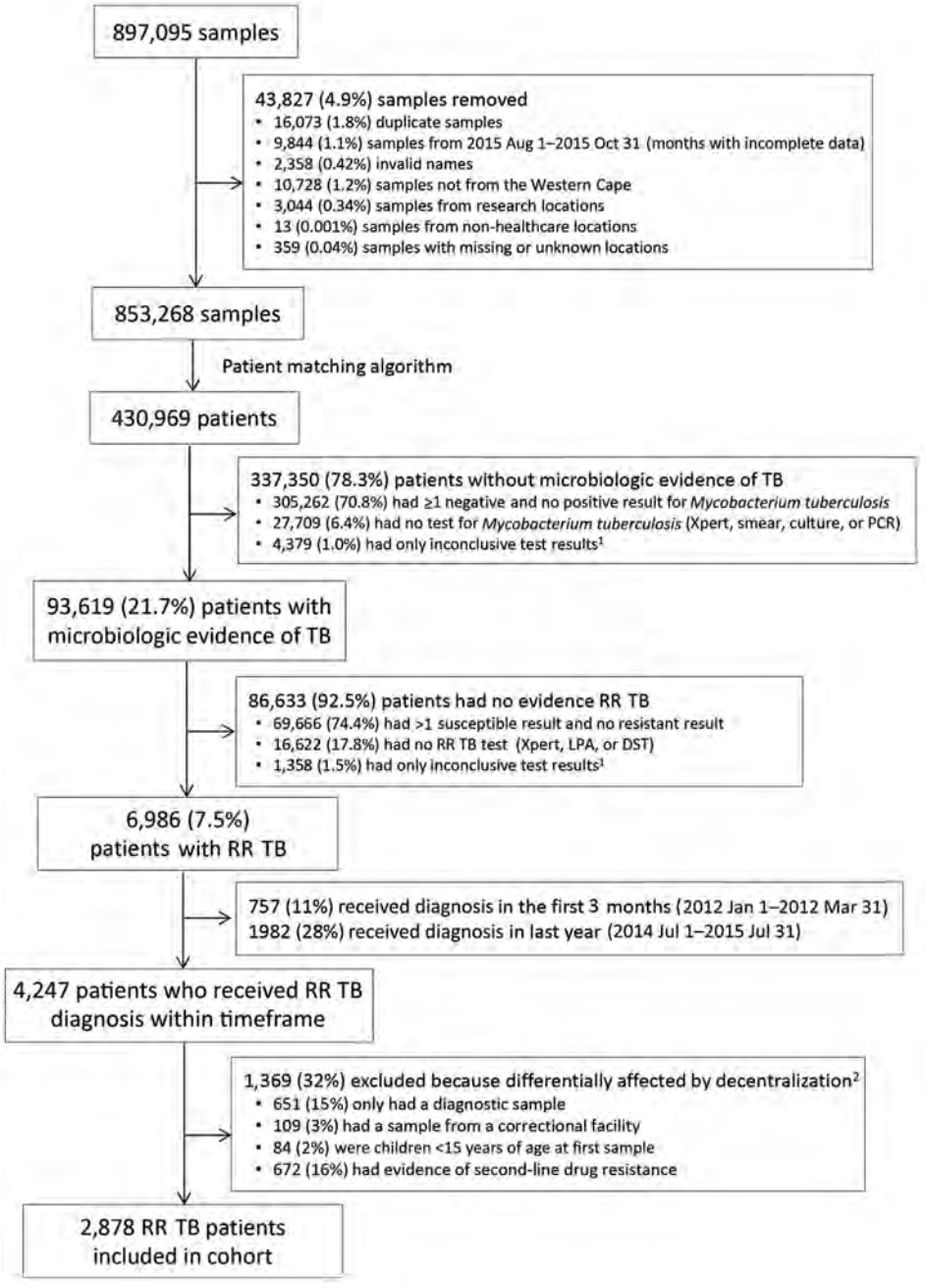

Figure 1. Flow diagram showing identification of adult patients with RR TB, Western Cape, South Africa, 2012–2014. Patients did not have second-line drug resistance and attended ≥2 clinic visits. The following test results were classed as inconclusive: inconclusive, error, unsuccessful, specimen container received empty, no result, lost viability, contaminated, specimen accidentally destroyed, insufficient specimen, or leaky specimen. The total number of patients excluded does not equal the sum of the individual categories because some patients belonged to multiple groups. RR, rifampin-resistant; TB, tuberculosis.

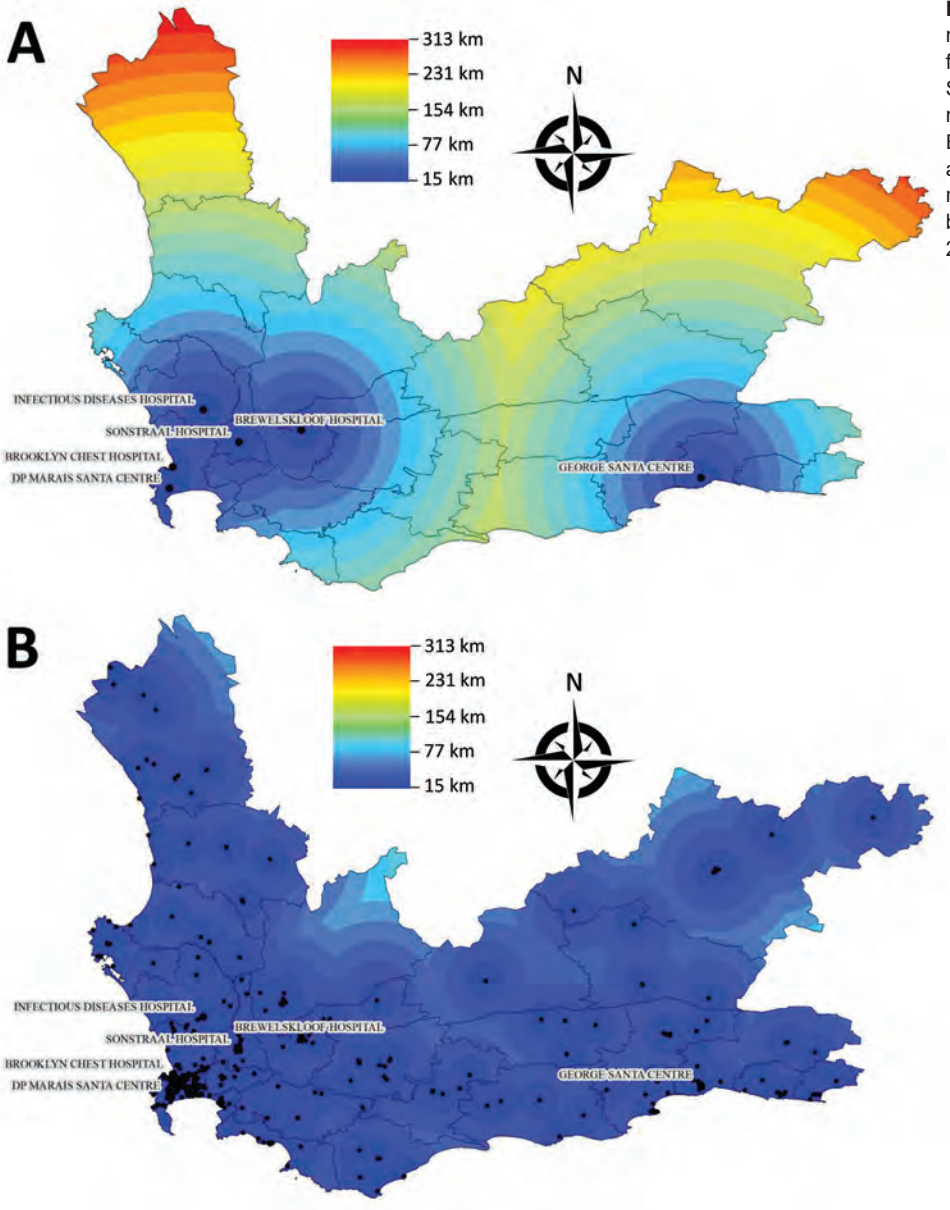

Figure 2. Distances to the nearest tuberculosis healthcare facility, Western Cape Province, South Africa. A) Distance to nearest specialized TB hospital. B) Distance to nearest facility of any type: TB hospital, clinic, or non-TB hospital that was visited by patients in this study during 2012–2015. TB, tuberculosis.

Decentralization Analysis

The national decentralization policy stated that clinically stable patients with no SLD resistance could initiate treatment at local hospitals and clinics designated as decentralized treatment initiation sites (2). According to this policy, although a small proportion of patients would still be hospitalized for clinical or psychosocial reasons, most patients with RR TB would be treated outside specialized TB hospitals. In addition, hospitalized patients would have shorter hospital stays (2).

We first summarized cohort characteristics regarding sex, age, TB type, type of facility submitting the initial RR TB sample, smear status, number of visits, and time in care. To assess decentralization implementation, we calculated the percentage of patients with ≥1 sample submitted from a TB hospital ≤1 year after diagnosis; we stratified these results by facility type (i.e., TB hospital, non-TB hospital, clinic). We calculated the percentage of patients who transitioned to care outside a TB hospital (i.e., patients who submitted samples from a non-TB hospital or clinic ≤3 months after their most recent sample from a TB hospital). For these patients, we estimated duration of TB hospitalization as the time between the date of the first sample submitted from the TB hospital to the midpoint between the most recent sample submitted from the TB hospital and the date

of the first subsequent sample submitted from a clinic or non-TB hospital.

We then used simple linear regression to estimate temporal trends of all outcomes by quarter (i.e., 3-month period) of initial RR TB sample during April 2012–June 2014, for a total of 9 quarters. We ran 2 models for each outcome: 1 stratified by diagnosis location and 1 combined model with an interaction term to assess the differences in trend between locations. In addition, we used multivariable logistic regression to test the association between whether or not a patient submitted a sample from a TB hospital and quarter of initial RR TB sample adjusting for sex, age (15–34, 35–54, ≥55 years of age), TB type (pulmonary, extrapulmonary, both), smear status within 1 month of initial RR TB sample, and number of visits ≤1 year after diagnosis. For this analysis only, we excluded patients missing data on age, sex, or both.

One decentralization goal was to enable treatment closer to patients' homes (*2*). We calculated the percentage of patients that had samples from ≥2 facilities, indicating movement between facilities. To estimate travel distance without home addresses, we calculated the total Euclidean distance between all facilities from which a patient submitted samples during the first year after diagnosis. For multiple visits, we counted distances multiple times. Because the number of visits could affect the total distance between facilities, we also determined each patient's number of visits in the first year after diagnosis. We then controlled for the number of visits by calculating the median distance between facilities visited consecutively for each patient. We used linear regressions to assess temporal trends in these travel outcomes.

We stratified analyses by whether patients' initial RR TB samples were from Cape Town or outside Cape Town (i.e., the rest of Western Cape) to identify differential implementation of decentralization. To demonstrate the potential travel benefit for patients receiving RR TB treatment in a clinic or local hospital compared with a specialized TB hospital, we mapped the distance to the nearest TB hospital from anywhere in the province and compared this distance to the distance to the nearest facility of any kind that submitted samples recorded in this study (Figure 2). We used R version 3.6.1 (*16*) for analyses and ArcMap version

Table 1. Characteristics of patients with RR TB, Western Cape, South Africa, 2012–2014*

Characteristic†	Overall, n = 2,878	Cape Town, n = 1,878	Outside Cape Town n = 1,000	p value‡
Sex§				0.32
F	1,245 (43.4)	825 (44.1)	420 (42.0)	
M	1,626 (56.6)	1,047 (55.9)	579 (58.0)	
Age group, y¶				<0.01
15–34	1,420 (50.1)	978 (53.0)	442 (44.9)	
35–54	1,232 (43.5)	761 (41.2)	471 (47.8)	
≥55	180 (6.4)	108 (5.8)	72 (7.3)	
Type of TB				0.72
Pulmonary only	2,685 (93.3)	1,747 (93.0)	938 (93.8)	
Extrapulmonary only	70 (2.4)	47 (2.5)	23 (2.3)	
Both	123 (4.3)	84 (4.5)	39 (3.9)	
Results of closest smear within 30 d of first RR TB–positive sample				0.93
Negative	1,396 (48.5)	913 (48.6)	483 (48.3)	
Scanty positive	310 (10.8)	202 (10.8)	108 (10.8)	
Positive +	262 (9.1)	178 (9.5)	84 (8.4)	
Positive ++	181 (6.3)	118 (6.3)	63 (6.3)	
Positive +++	499 (17.3)	321 (17.1)	178 (17.8)	
Unknown	230 (8.0)	146 (7.8)	84 (8.4)	
Setting of first RR TB–positive result				<0.01
TB hospital	103 (3.6)	43 (2.3)	60 (6.0)	
Clinic	2,361 (82.0)	1,554 (82.7)	807 (80.7)	
Non-TB hospital	414 (14.4)	281 (15.0)	133 (13.3)	
Median time in care** in first year after RR TB diagnosis, mos (IQR)	11 (5–12)	11 (5–12)	11 (6–12)	<0.01#
Median number of visits†† in the first year after RR TB diagnosis, (IQR)	9 (5–12)	8 (4–12)	10 (5–12)	<0.01#

*Patients without second-line drug resistance who attended ≥2 visits. RR, rifampin-resistant; TB, tuberculosis.
†Data are no. (%), except where otherwise indicated.
‡p values determined by χ^2 test of patients in Cape Town versus outside Cape Town.
§A total of 7 patients were missing data on sex: 6 from Cape Town and 1 from outside of Cape Town.
¶A total of 46 patients were missing data on age: 31 from Cape Town and 15 from outside of Cape Town.
#p values determined by Wilcoxon rank-sum test of patients in Cape Town versus outside Cape Town.
**Time in care is defined as the time between the first and most recent RR TB–positive sample or 1 y from the first RR TB–positive sample, whichever was earlier.
††Defined as unique days in which a patient submitted ≥1 sample.

Table 2. Magnitude and duration of hospitalization and movement of patients with RR TB, Western Cape, South Africa, 2012–2014*

Description	Overall, n = 2,878	Cape Town, n = 1,878	Outside Cape Town, n = 1,000	p value†
Hospitalization in TB hospital, no. (%) No. patients with ≥1 sample from a specialized TB hospital in the first year after RR TB diagnosis	1,228 (42.7)	545 (29.0)	683 (68.3)	<0.01
Moved to care outside TB hospital, no. (%) No. patients with a sample from a TB hospital who had a subsequent sample from a non-TB hospital <3 mo after the most recent sample in the TB hospital	837 (68.2)	317 (58.2)	520 (76.1)	<0.01
Median length of TB hospital stay, d (IQR) Median hospitalization period of patients who moved to care outside of a TB hospital in the first year after RR TB diagnosis	99 (61–136)	79 (50–118)	108 (72–144)	<0.01‡
Any movement, no. (%) No. patients who had samples from ≥2 different facilities in first year after RR TB diagnosis	1,765 (61.3)	1,012 (53.9)	753 (75.3)	<0.01
Median no. of visits (IQR) No. unique days with ≥1 laboratory sample in the first year after RR TB diagnosis	9 (5–12)	8 (4–12)	10 (5–12)	<0.01‡
Median total distance, km (IQR) Total Euclidian distance between all facilities visited by each patient in the first year after RR TB diagnosis	4.4 (0.0–41)	1.5 (0.0–20)	46.0 (0.2–122)	<0.01‡
Median distance between consecutive visits, km (IQR) Median distance between facilities visited consecutively by each patient in the first year after RR TB diagnosis	2.7 (0.0–19.8)	1.4 (0.0–12.2)	24.0 (0.2–64.8)	<0.01‡

*Patients without second-line resistance who attended ≥2 clinic visits. RR, rifampin-resistant; TB, tuberculosis.
†χ^2 p values of patients in Cape Town versus outside Cape Town.
‡p values determined by Wilcoxon rank-sum test.

10.6 (Environmental Systems Research Institute, Inc., https://desktop.arcgis.com) for mapping.

Results

Cohort Description

After excluding ineligible patients, we analyzed a cohort of 2,878 patients who received a diagnosis of RR TB during April 1, 2012–June 30, 2014 (Figure 1). The exclusions included 651 (15.3%) patients with only a diagnostic sample recorded (14.0% of patients in Cape Town and 17.7% outside Cape Town; Appendix Table 1). Of the 2,878 patients, 1,878 (65%) submitted their initial RR TB sample from Cape Town and 1,000 (35%) from outside Cape Town. The mean age was 36 years (SD ±12 years), and 57% were men. Most (93%) patients had RR TB detected from sputum or lung samples, suggesting pulmonary disease, and 49% had negative smear microscopy results when RR TB was detected (Table 1).

Samples from Specialized TB Hospitals

In total, 2,361 (82%) patients submitted initial RR TB samples from clinics, 414 (14%) from non-TB hospitals, and 103 (4%) from TB hospitals. Although only 4% of patients submitted their initial RR TB sample from a TB hospital, 1,228 (43%) patients submitted ≥1 sample from a TB hospital ≤1 year after diagnosis. In particular, 894 (38%) patients who submitted their initial sample from a clinic and 231 (56%) who submitted their initial sample from a non-TB hospital submitted ≥1 additional sample from a TB hospital (Appendix Table 2). Patients in Cape Town were significantly less likely to submit a sample from a TB hospital than patients outside Cape Town (29% vs. 68%; p<0.01). Of the 545 patients from Cape Town who submitted a TB hospital sample, 317 (58%) transitioned to care outside of the TB hospital compared with 520 (76%) of the 683 patients outside Cape Town (p<0.01). We estimated that the median first TB hospital stay for those who transitioned to care outside of the TB hospital was 79 days (interquartile range [IQR] 50–118 days) in Cape Town and 108 days (IQR 72–144 days) outside Cape Town (Table 2).

In Cape Town, the percentage of patients who submitted a TB hospital sample in the first year on average decreased by 1 percentage point (95% CI 0.2%–1.7%; p = 0.02) per quarter, representing a 9 percentage point decrease during the study period; we observed no statistically significant trend outside Cape Town (Table 3). During the study period, the percentage of patients who transitioned to care outside of a TB hospital stayed constant in and outside Cape Town. In Cape Town, the estimated first TB hospital stay duration decreased by 3.6 days per quarter (95% CI –8.7 to 1.5 days; p = 0.14), for a total decrease of 32 days during the study. Outside Cape Town, the duration stayed constant (Table 3; Figure 3). Visual inspection of all trends indicated that linear trends were appropriate.

Table 3. Linear temporal trends in magnitude and duration of movement for adult patients with RR TB, Western Cape, South Africa, 2012–2014*

Description	Overall, n = 2,878		Cape Town, n = 1,878		Outside Cape Town, n = 1,000		
	Slope (95% CI)	p value	Slope (95% CI)	p value	Slope (95% CI)	p value	Interaction p value†
Hospitalization in TB hospital, no. (%) No. patients with ≥1 sample from a specialized TB hospital in the first year after RR TB diagnosis	−0.4 (−1.2 to 0.5)	0.33	−1.0 (−1.7 to −0.2)	0.02	1.1 (−0.9 to 3.1)	0.23	0.03
Moved to care outside TB hospital, no. (%) No. patients with a sample from a TB hospital who had a subsequent sample from a non-TB hospital <3 mo after the most recent sample in the TB hospital	0.2 (−0.9 to 1.3)	0.69	0.1 (−1.3 to 1.6)	0.84	−0.01 (−1.8 to 1.8)	0.99	0.89
Median length of TB hospital stay, d (IQR) Median hospitalization period of patients who moved to care outside of a TB hospital in the first year after RR TB diagnosis	−1.5 (−5.7 to 2.6)	0.42	−3.6 (−8.7 to 1.5)	0.14	−0.28 (−4.3 to 3.7)	0.87	0.24
Any movement, no. (%) No. patients who had samples from ≥2 different facilities in first year after RR TB diagnosis	−0.5 (−1.2 to 0.3)	0.19	−0.9 (−1.7 to −0.06)	0.04	0.5 (−1.2 to 2.3)	0.50	0.10
Median no. of visits (IQR) No. unique days with ≥1 laboratory sample in the first year after RR TB diagnosis	0.04 (−0.01 to 0.1)	0.12	0.0 (−0.2 to 0.2)	>0.99	0.1 (−0.01 to 0.2)	0.06	0.22
Median total distance, km (IQR) Total Euclidian distance between all facilities visited by each patient in the first year after RR TB diagnosis	−0.1 (−0.4 to 0.2)	0.43	−0.3 (−0.5 to −0.01)	0.04	4.7 (−1.3 to 10.6)	0.10	0.07
Median distance between consecutive visits, km (IQR) Median distance between facilities visited consecutively by each patient in the first year after RR TB diagnosis	−0.06 (−0.2 to 0.04)	0.21	−0.18 (−0.4 to −0.02)	0.07	2.5 (−0.5 to 5.6)	0.09	0.05

*Patients without second-line drug resistance who attended ≥2 visits. Estimates are change per quarter (i.e., 3 mos). RR, rifampin-resistant; TB, tuberculosis.
†p value of interaction term between quarter of diagnosis and location.

We included 2,831 patients in the individual-level multivariable logistic regression analysis and adjusted for number of visits. In Cape Town, the odds of submitting a sample from a TB hospital decreased by 5% per quarter (p = 0.02); outside Cape Town, we found no statistically significant association. Outside Cape Town, increasing smear grade (i.e., scanty, +, ++, +++) was associated with increasing odds of submitting a sample from a TB hospital (Table 4).

Distance Traveled

In the first year after diagnosis, patients with RR TB had samples submitted from 315 different facilities: 268 clinics, 41 non-TB hospitals, and 6 TB hospitals (Appendix Table 3). Most patient movements between different facilities involved a TB hospital (Figure 4). A total of 1,765 (61%) patients submitted samples from ≥2 different facilities. Patients outside Cape Town were more likely to transition between facilities than those in Cape Town (75% vs. 54%; p<0.01) (Table 2). Overall, the median Euclidean distance traveled between facilities was 4.4 km (IQR 0–41 km). The median distance traveled was significantly shorter in Cape Town (1.5 km, IQR 0–20 km) than outside Cape Town (46 km, IQR 0.2–122 km; p<0.01). This disparity remained after controlling for the number of visits per patient (Table 2).

In Cape Town, the percentage of patients who transitioned between facilities decreased by 0.9 percentage points per quarter (95% CI 0.1%–1.7%; p = 0.04) and the total distance between all facilities visited decreased by 0.3 km per quarter (95% CI 0.01–0.5 km; p = 0.04). However, outside Cape Town, this distance increased by 4.7 km each quarter (95% CI –1.3 to 10.6 km; p = 0.10). We observed no statistically significant change in median number of visits. Trends in median distance between consecutive visits were consistent with total distance trends (Table 3; Figure 3). In Cape Town, the distances to the nearest TB hospital compared with the nearest clinic or non-TB hospital were similar. Outside Cape Town, clinics and non-TB hospitals were often much closer than the nearest TB hospital (Figure 2).

Discussion

We used routinely collected laboratory data from Western Cape, South Africa to evaluate implementation of a national policy to decentralize MDR/RR TB care. Patients with RR TB in Cape Town facilities were less likely to have samples submitted from a TB hospital than patients outside Cape Town (29% vs. 68%, p<0.01), suggesting that persons in Cape Town were less likely to be hospitalized for RR TB. In addition, the percentage of patients who were likely hospitalized decreased significantly in Cape Town but not outside Cape Town. In Cape Town, the estimated average duration of TB hospitalization was nearly a month shorter and decreased over time compared with stays outside Cape Town, where duration remained constant.

These findings suggest that after the decentralization policy was implemented, more decentralization occurred in Cape Town than outside Cape Town. Loveday et al. (*9*) showed that treatment outcomes across decentralized sites in KwaZulu-Natal varied greatly and were highly influenced by health system performance. Health system factors such as long distances between facilities and limited provision of resources, training, and support from TB hospitals might have slowed decentralized care uptake in more rural areas. Furthermore, the large distances between patients in rural areas posed challenges to in-home medication administration. Additional outreach efforts such as mobile clinics have facilitated RR TB diagnosis. However, because mobile clinics might not be staffed in the same location each day, they are unable to administer SLDs, suggesting that broader access to new oral second-line TB drugs is needed in these settings (*17*).

Although the national policy change was introduced in 2011, Cape Town subdistricts had already begun decentralizing RR TB care after the success of the pilot program in Khayelitsha in 2009 (*2*,*4*). Our findings are consistent with previous work showing substantial challenges to healthcare access in rural areas of South Africa (*18*–*21*). The limited timeframe (2012–2015) of our study might have hindered our ability to detect slow changes in referral patterns outside Cape Town. However, Hill et al. (*18*) showed that in 2016, Cape Town patient travel patterns were still more consistent with a decentralized model than those elsewhere in the Western Cape.

In our study, patients outside Cape Town traveled 30 times further than patients in Cape Town (46 km vs. 1.5 km). Over the study period, travel distance decreased significantly for patients in Cape Town and increased for those outside Cape Town. This pattern of longer travel distances for healthcare in more rural

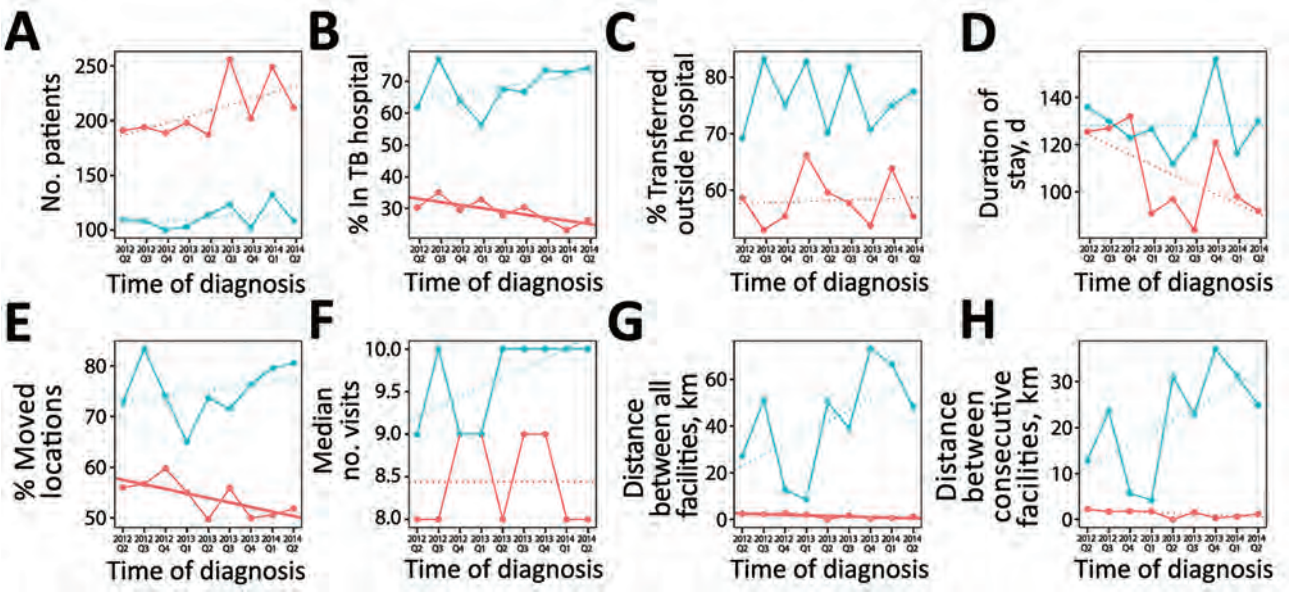

Figure 3. Linear time trends in magnitude and duration of movement for adult patients with RR TB, Western Cape, South Africa, 2012–2014. Patients did not have second-line drug resistance and attended ≥2 clinic visits. Linear regression trendlines are colored based on district of diagnosis (red indicates Cape Town; blue indicates other districts) and styled based on significance (solid line indicates p<0.05; dotted line indicates p≥0.05). A) Number of patients diagnosed with RR TB. B) Percentage of patients who submitted a sample from a TB hospital ≤1 year after diagnosis. C) Percentage of patients who transitioned to care outside a TB hospital. D) Median duration of first stay in a TB hospital. E) Percentage of patients who transitioned to different facilities. F) Median number of visits in which patient submitted ≥1 sample. G) Median total Euclidean distance traveled between locations. H) Median Euclidean distance between consecutive visits. RR, rifampin-resistant; TB, tuberculosis.

Table 4. Multivariable logistic regression for factors associated with sample submitted from a TB hospital ≤1 y after diagnosis of RR TB, Western Cape, South Africa, 2012–2014*

	Overall, n = 2,831		Cape Town, n = 1,846		Outside Cape Town, n = 985	
Characteristic	OR (95% CI)	p value	OR (95% CI)	p value	OR (95% CI)	p value
Location						
Cape Town	Referent		Referent		Referent	
Other	5.7 (4.8–6.8)	<0.01	NA		NA	
Sex						
F	Referent		Referent		Referent	
M	1.2 (1.0–1.4)	0.03	1.2 (1.0–1.5)	0.07	1.2 (0.9–1.6)	0.27
Age, y						
15–34	Referent		Referent		Referent	
35–54	1.1 (0.9–1.3)	0.43	1.2 (0.9–1.5)	0.14	0.9 (0.7–1.3)	0.55
≥55	0.8 (0.6–1.2)	0.24	1.0 (0.6–1.6)	0.95	0.6 (0.3–1.0)	0.05
Type of TB						
Pulmonary only	Referent		Referent		Referent	
Extrapulmonary only	1.0 (0.5–1.7)	0.98	0.8 (0.4–1.7)	0.63	1.3 (0.5–3.5)	0.53
Both	2.7 (1.8–4.2)	<0.01	3.7 (2.3–5.9)	<0.01	1.1 (0.5–2.4)	0.85
Results of most recent smear from ≤30 d of first RR TB–positive sample						
Negative	Referent		Referent		Referent	
Scanty positive	1.4 (1.0–1.8)	0.03	1.7 (1.2–2.4)	<0.01	1.0 (0.6–1.6)	>0.99
Positive +	1.5 (1.1–2.1)	<0.01	1.6 (1.1–2.2)	0.02	1.5 (0.9–2.8)	0.16
Positive ++	1.8 (1.3–2.5)	<0.01	1.5 (1.0–2.3)	0.06	3.0 (1.5–6.4)	<0.01
Positive +++	2.1 (1.7–2.7)	<0.01	1.9 (1.4–2.5)	<0.01	3.5 (2.2–5.8)	<0.01
Unknown	1.2 (0.9–1.7)	0.19	1.2 (0.8–1.9)	0.29	1.2 (0.7–2.1)	0.56
Quarter of RR TB diagnosis†	0.98 (0.95–1.02)	0.29	0.95 (0.92–0.99)	0.02	1.04 (0.98–1.10)	0.20

*Patients without second-line drug resistance who attended ≥2 visits. All analyses adjusted for no. of visits ≤1 y after diagnosis. Excludes 47 patients who are missing data on age, sex, or both. NA, not applicable; OR, odds ratio; RR, rifampin-resistant; TB, tuberculosis.
†Estimated change per quarter (i.e., 3 mos).

areas of South Africa is well-documented (*18*–*20*). Although rural areas face more challenges to decentralization, the spread of local facilities throughout Western Cape indicates the potential for a reduction in travel distances for patients outside Cape Town (*12*). Shorter travel distances decrease treatment-related challenges for patients, enable local clinics to provide more patient support, and decrease risk for transmission during travel (*22*).

Although NHLS data are reliable for assessing aspects of TB and HIV care, its use introduces limitations to our study (*18*,*23*–*29*). These data lack information regarding treatment initiation, hospitalization, admission and discharge dates, and treatment outcomes. We therefore focused on where patients submitted samples and assumed repeat samples implied treatment prescription and monitoring (*29*,*30*). We also assumed that providing a sample at a TB hospital implied inpatient admission, which we believe is reasonable given that TB hospitals in the Western Cape only provide inpatient care (*12*). To focus on patients most likely to have started and continued RR TB treatment, we excluded patients without subsequent samples after the initial RR TB sample. However, this criterion might have excluded patients with extrapulmonary TB or those unable or unwilling to produce sputum samples. Furthermore, we could not account for patients who moved or transferred care to other provinces.

Without admission and discharge dates, our TB hospital stay duration estimate is a proxy for true hospital stay. In addition, without residential addresses, our distance traveled measure is a proxy for total travel distance. We also measured simple Euclidean distance between facilities, which might not reflect true traveling distance. Despite these limitations, the relative differences between Cape Town and outside Cape Town and the time trends should represent differences and trends in true hospital stays and travel distances.

Our study is also limited by its timeframe (2012–2015), which does not extend before the decentralization policy or to the present day, and by our inability to attribute causality between the decentralization policy and our estimated measures. Therefore, these results reflect patterns observed during early policy implementation and are a proof-of-concept that routinely collected laboratory data can be used to assess care patterns following policy implementation. However, other interventions, such as the introduction of GeneXpert, occurred in 2011 and 2012, which might also have affected TB diagnostic use and care. Our results might not be generalizable to all of South Africa because the Western Cape has more decentralized TB care units than other provinces (*12*), and Hill et al. (*18*) showed that in 2016 patients in Eastern Cape and KwaZulu-Natal had more centralized care patterns than patients in Western Cape.

The benefits of the decentralization of MDR/RR TB care have been documented in South Africa and elsewhere. In Khayelitsha, Cox et al. (*5*–*7*) found that decentralized care resulted in higher case detection, better outcomes, and lower costs. In KwaZulu-Natal, Loveday et al. (*9*–*11*) observed that decentralized sites had shorter time to treatment initiation and higher culture conversion rates; however, outcomes were poorer where decentralized services were not integrated into existing services. These studies concluded that regular monitoring and support were needed to optimize outcomes (*9*–*11*). Although Western Cape was the forerunner for implementing community-based MDR/RR TB care in South Africa, we have shown that locations

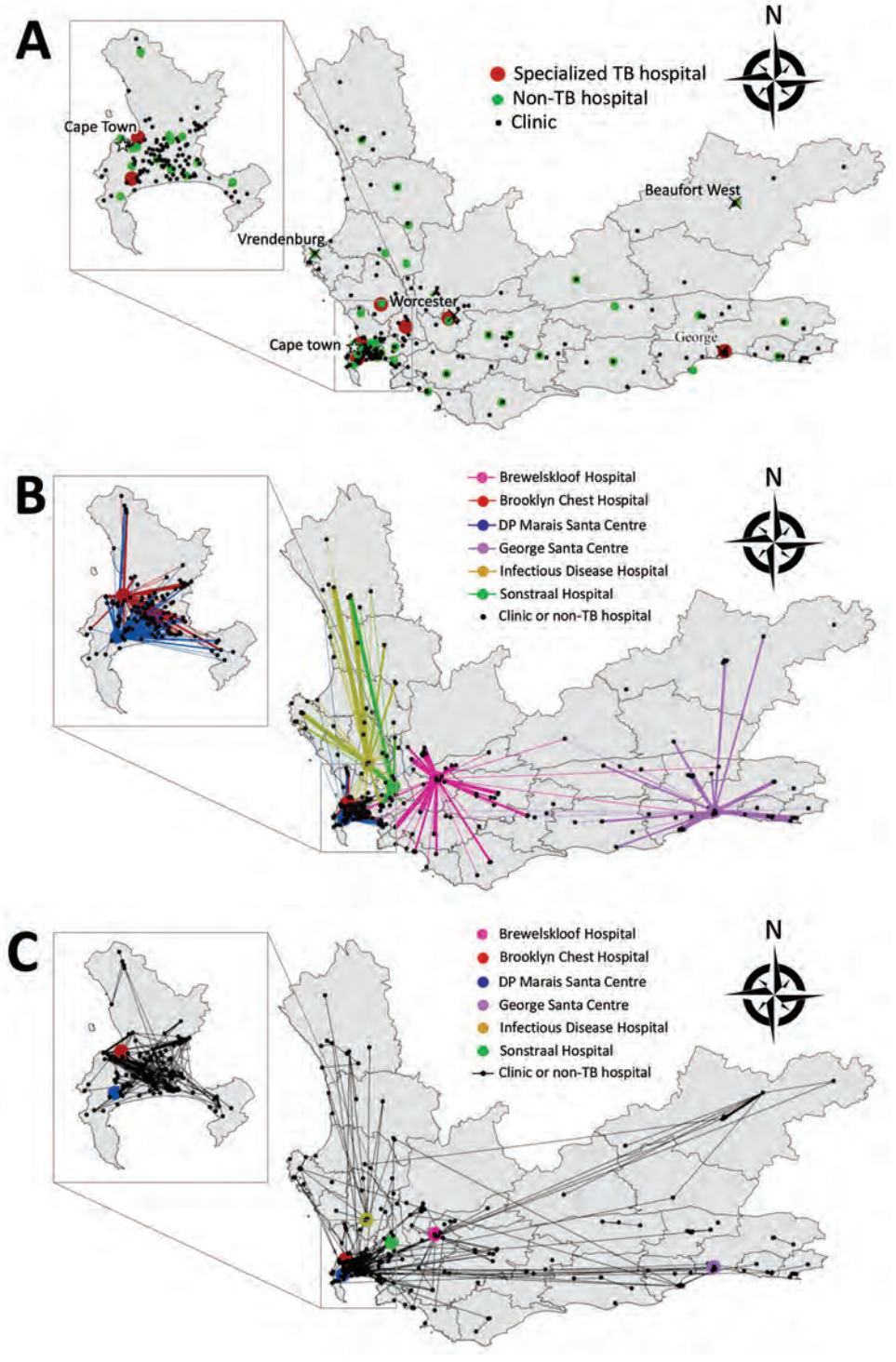

Figure 4. Healthcare facilities visited and movements between hospitals by patients in RR TB cohort, Western Cape Province, South Africa, 2012–2014. Inset maps show the Cape Town Metropole. A) All healthcare facilities visited ≤1 y after diagnosis. B) All movements made ≤1 y after diagnosis that involved TB hospitals. C) All movements made ≤1 y after diagnosis that did not involve a TB hospital. RR, rifampin-resistant; TB, tuberculosis.

outside Cape Town, and likely rural areas in general, need more support for implementing these policies (*12*,*18*). We have demonstrated a proof-of-concept that laboratory data can be used to assess policy implementation. As we work toward TB elimination, we must maximize our use of available, routinely collected data as a cost-effective, rapid method for evaluating policy implementation. Laboratory data can contribute to evidence-based expansion of policies to improve TB treatment and reduce incidence.

S.V.L. and H.E.J. were funded by the US National Institutes of Health (NIH) (grant no. NIH R03AI144335). S.V.L. was funded by the US NIH (Interdisciplinary Training grant no. NIHGMS T32GM074905) and the Providence/Boston Center for AIDS Research (grant no. P30AI042853), which is co-funded by the National Institute of Allergy and Infectious Diseases, the National Institute on Aging, the Eunice Kennedy Shriver National Institute of Child Health and Human Development, the National Institute on Drug Abuse, the National Institute of Diabetes and Digestive and Kidney Diseases, the National Institute on Minority Health and Health Disparities, the National Institute of Mental Health, the National Cancer Institute, the National Institute of General Medical Sciences, the National Institute of Dental and Craniofacial Research, and the National Heart, Lung, and Blood Institute. H.E.J. was also funded by the US NIH (grant nos. NIH K01AI102944 and NIH R01AI152126). T.C.B. was funded by NIH (NIH T32DA013911) and the Burroughs Wellcome Fund/ American Society for Tropical Medicine and Hygiene Postdoctoral Fellowship in Tropical Infectious Diseases. K.R.J. was funded by the US NIH (grant nos. K01TW009213, R01AI119037). R.M.W. was supported by the South African Medical Research Council.

About the Author

Dr. Leavitt is a postdoctoral associate at Boston University, Boston. Her research interests include using laboratory data to study tuberculosis care patterns and developing methods to estimate infectious disease transmission probabilities.

References

1. World Health Organization. Global tuberculosis report 2019. Geneva: World Health Organization; 2019.
2. National Department of Health. Multi-drug resistant tuberculosis: a policy framework on decentralised and deinstitutionalized management for South Africa. Pretoria (South Africa): National Department of Health; 2011.
3. Evans D, Sineke T, Schnippel K, Berhanu R, Govathson C, Black A, et al. Impact of Xpert MTB/RIF and decentralized care on linkage to care and drug-resistant tuberculosis treatment outcomes in Johannesburg, South Africa. BMC Health Serv Res. 2018;18:973. https://doi.org/10.1186/s12913-018-3762-x
4. Medecins Sans Frontiers. Scaling up diagnosis and treatment of drug-resistant tuberculosis in Khayelitsha, South Africa. 2011 [cited 2020 Apr 15]. http://www.msfaccess.org/sites/default/files/MSF_assets/TB/Docs/TB_report_ScalingUpDxTxKhaye_ENG_2011.pdf
5. Cox H, Ramma L, Wilkinson L, Azevedo V, Sinanovic E. Cost per patient of treatment for rifampicin-resistant tuberculosis in a community-based programme in Khayelitsha, South Africa. Trop Med Int Health. 2015;20:1337–45. https://doi.org/10.1111/tmi.12544
6. Cox H, Hughes J, Daniels J, Azevedo V, McDermid C, Poolman M, et al. Community-based treatment of drug-resistant tuberculosis in Khayelitsha, South Africa. Int J Tuberc Lung Dis. 2014;18:441–8. https://doi.org/10.5588/ijtld.13.0742
7. Cox HS, Daniels JF, Muller O, Nicol MP, Cox V, van Cutsem G, et al. Impact of decentralized care and the Xpert MTB/RIF test on rifampicin-resistant tuberculosis treatment initiation in Khayelitsha, South Africa. Open Forum Infect Dis. 2015;2:ofv014 https://doi.org/10.1093/ofid/ofv014
8. Evans D, Schnippel K, Govathson C, Sineke T, Black A, Long L, et al. Treatment initiation among persons diagnosed with drug resistant tuberculosis in Johannesburg, South Africa. PLoS One. 2017;12:e0181238. https://doi.org/10.1371/journal.pone.0181238
9. Loveday M, Padayatchi N, Wallengren K, Roberts J, Brust JCM, Ngozo J, et al. Association between health systems performance and treatment outcomes in patients co-infected with MDR-TB and HIV in KwaZulu-Natal, South Africa: implications for TB programmes. PLoS One. 2014;9:e94016. https://doi.org/10.1371/journal.pone.0094016
10. Loveday M, Wallengren K, Reddy T, Besada D, Brust JCM, Voce A, et al. MDR-TB patients in KwaZulu-Natal, South Africa: cost-effectiveness of 5 models of care. PLoS One. 2018;13:e0196003. https://doi.org/10.1371/journal.pone.0196003
11. Loveday M, Wallengren K, Voce A, Margot B, Reddy T, Master I, et al. Comparing early treatment outcomes of MDR-TB in decentralised and centralised settings in KwaZulu-Natal, South Africa. Int J Tuberc Lung Dis. 2012;16:209–15. https://doi.org/10.5588/ijtld.11.0401
12. National Department of Health. Summary report on decentralized and multi-drug resistant tuberculosis services in South Africa. 2017 [cited 2019 Aug 23]. https://tinyurl.com/Leavitt2021
13. TB Diagnostics Market Analysis Consortium. Market assessment of tuberculosis diagnostics in South Africa, 2012–2013. Int J Tuberc Lung Dis. 2015;19:216–22. https://doi.org/10.5588/ijtld.14.0565
14. National Department of Health. National tuberculosis management guidelines 2014. Pretoria (South Africa): Fishwicks PTA; 2014. p. 28.
15. Fox MP, Bor J, Brennan AT, MacLeod WB, Maskew M, Stevens WS, et al. Estimating retention in HIV care accounting for patient transfers: a national laboratory cohort study in South Africa [Erratum in: PLoS Med. 2018;15:e1002643]. PLoS Med. 2018;15:e1002589. https://doi.org/10.1371/journal.pmed.1002589
16. R Core Team. R: a language and environment for statistical computing. Vienna (Austria): R Foundation for Statistical Computing; 2019 [cited 2020 Apr 15]. https://www.r-project.org/
17. Udwadia Z, Furin J. Quality of drug-resistant tuberculosis care: gaps and solutions [Erratum in: J Clin Tuberc Other Mycobact Dis. 2020;21:100177]. J Clin Tuberc Other

Mycobact Dis. 2019;16:100101. https://doi.org/10.1016/j.jctube.2019.100101
18. Hill J, Dickson-Hall L, Grant AD, Grundy C, Black J, Kielmann K, et al. Drug-resistant tuberculosis patient care journeys in South Africa: a pilot study using routine laboratory data. Int J Tuberc Lung Dis. 2020;24:83–91. https://doi.org/10.5588/ijtld.19.0100
19. McLaren ZM, Ardington C, Leibbrandt M. Distance decay and persistent health care disparities in South Africa. BMC Health Serv Res. 2014;14:541. https://doi.org/10.1186/s12913-014-0541-1
20. Harris B, Goudge J, Ataguba JE, McIntyre D, Nxumalo N, Jikwana S, et al. Inequities in access to health care in South Africa. J Public Health Policy. 2011;32:S102–23. https://doi.org/10.1057/jphp.2011.35
21. van Rensburg HCJ. South Africa's protracted struggle for equal distribution and equitable access—still not there. Hum Resour Health. 2014;12:26. https://doi.org/10.1186/1478-4491-12-26
22. Kapwata T, Morris N, Campbell A, Mthiyane T, Mpangase P, Nelson KN, et al. Spatial distribution of extensively drug-resistant tuberculosis (XDR TB) patients in KwaZulu-Natal, South Africa. PLoS One. 2017;12:e0181797. https://doi.org/10.1371/journal.pone.0181797
23. Bassett IV, Huang M, Cloete C, Candy S, Giddy J, Frank SC, et al. Using national laboratory data to assess cumulative frequency of linkage after transfer to community-based HIV clinics in South Africa. J Int AIDS Soc. 2019;22:e25326. https://doi.org/10.1002/jia2.25326
24. Bassett IV, Huang M, Cloete C, Candy S, Giddy J, Frank SC, et al. Assessing the completeness and accuracy of South African National Laboratory CD4 and viral load data: a cross-sectional study. BMJ Open. 2018;8:e021506. https://doi.org/10.1136/bmjopen-2018-021506
25. McLaren ZM, Brouwer E, Ederer D, Fischer K, Branson N. Gender patterns of tuberculosis testing and disease in South Africa. Int J Tuberc Lung Dis. 2015;19:104–10. https://doi.org/10.5588/ijtld.14.0212
26. Dlamini-Mvelase NR, Werner L, Phili R, Cele LP, Mlisana KP. Effects of introducing Xpert MTB/RIF test on multi-drug resistant tuberculosis diagnosis in KwaZulu-Natal South Africa. BMC Infect Dis. 2014;14:442. https://doi.org/10.1186/1471-2334-14-442
27. Nanoo A, Izu A, Ismail NA, Ihekweazu C, Abubakar I, Mametja D, et al. Nationwide and regional incidence of microbiologically confirmed pulmonary tuberculosis in South Africa, 2004–12: a time series analysis. Lancet Infect Dis. 2015;15:1066–76. https://doi.org/10.1016/S1473-3099(15)00147-4
28. McIntosh AI, Jenkins HE, White LF, Barnard M, Thomson DR, Dolby T, et al. Using routinely collected laboratory data to identify high rifampicin-resistant tuberculosis burden communities in the Western Cape Province, South Africa: a retrospective spatiotemporal analysis. PLoS Med. 2018;15:e1002638. https://doi.org/10.1371/journal.pmed.1002638
29. Cox H, Dickson-Hall L, Ndjeka N, Van't Hoog A, Grant A, Cobelens F, et al. Delays and loss to follow-up before treatment of drug-resistant tuberculosis following implementation of Xpert MTB/RIF in South Africa: a retrospective cohort study. PLoS Med. 2017;14:e1002238. https://doi.org/10.1371/journal.pmed.1002238
30. Naidoo P, Theron G, Rangaka MX, Chihota VN, Vaughan L, Brey ZO, et al. The South African tuberculosis care cascade: estimated losses and methodological challenges. J Infect Dis. 2017;216:S702–13. https://doi.org/10.1093/infdis/jix335

Address for correspondence: Sarah V. Leavitt, Boston University School of Public Health, Department of Biostatistics, Crosstown Bldg, 801 Massachusetts Ave, 3rd Fl, Boston, MA 02118, USA; email: sv1205@bu.edu

Transmission of Antimicrobial-Resistant *Staphylococcus aureus* Clonal Complex 9 between Pigs and Humans, United States

Pranay R. Randad, Jesper Larsen, Hülya Kaya, Nora Pisanic, Carly Ordak, Lance B. Price, Maliha Aziz, Maya L. Nadimpalli, Sarah Rhodes, Jill R. Stewart, Dave C. Love, David Mohr, Meghan F. Davis, Lloyd S. Miller, Devon Hall, Karen C. Carroll, Trish M. Perl, Christopher D. Heaney

Transmission of livestock-associated *Staphylococcus aureus* clonal complex 9 (LA-SA CC9) between pigs raised on industrial hog operations (IHO) and humans in the United States is poorly understood. We analyzed whole-genome sequences from 32 international *S. aureus* CC9 isolates and 49 LA-SA CC9 isolates from IHO pigs and humans who work on or live near IHOs in 10 pig-producing counties in North Carolina, USA. Bioinformatic analysis of sequence data from the 81 isolates demonstrated 3 major LA-SA CC9 clades. North Carolina isolates all fell within a single clade (C3). High-resolution phylogenetic analysis of C3 revealed 2 subclades of intermingled IHO pig and human isolates differing by 0–34 single-nucleotide polymorphisms. Our findings suggest that LA-SA CC9 from pigs and humans share a common source and provide evidence of transmission of antimicrobial-resistant LA-SA CC9 between IHO pigs and humans who work on or live near IHOs in North Carolina.

Livestock-associated *Staphylococcus aureus* (LA-SA) has emerged among pigs raised in industrial hog operations (IHOs) and persons who work on or live near IHOs globally, including in the United States (*1*–*4*). IHO workers who are occupationally exposed to pigs are at increased risk for intranasal carriage of *S. aureus*, including methicillin-resistant *S. aureus* (MRSA), multidrug-resistant *S. aureus* (MDRSA), and LA-SA (*3*,*5*). Furthermore, persons exposed to LA-SA are at risk of developing mild-to-severe infections, including skin and soft tissue infections (SSTIs), pneumonia, endocarditis, osteomyelitis, and bacteremia (*5*–*8*). Recent evidence supports emergence of diverse clones associated with IHOs. *S. aureus* clonal complex 9 (CC9), for example, has been reported as a dominant LA-SA lineage in Asia and has been described as an emerging clone in some areas with intensive industrial livestock production in the United States (*9*–*11*).

The population structure and transmission dynamics of emerging LA-SA CC9 strains in the United States remains poorly understood. Previous epidemiologic studies in the top 10 pig-producing counties in North Carolina, the second leading US pig-producing state, showed a high prevalence of LA-SA CC9 nasal carriage among IHO pigs and IHO workers (*3*,*12*). Epidemiologic findings provide support for potential transmission of LA-SA CC9 between IHO workers and their household contacts, including minor children (<18 years of age; IHO minors), based on nasal carriage of LA-SA CC9 with concordant *spa* types at the same time point (*3*). Epidemiologic studies have also identified instances of LA-SA CC9 nasal carriage among community residents with no known exposure to livestock in high-density IHO areas of North Carolina (*2*). Whole-genome sequencing (WGS) analysis provides an opportunity to characterize the population structure and transmission dynamics of LA-SA CC9 in the United States. The objectives of this study were to use WGS and phylogenetic analyses to elucidate the population structure of *S. aureus* CC9 from various regions in North America, South America,

Author affiliations: Johns Hopkins University, Baltimore, Maryland, USA (P.R. Randad, N. Pisanic, C. Ordak, D.C. Love, D. Mohr, M.F. Davis, L.S. Miller, K.C. Carroll, T.M. Perl, C.D. Heaney); Statens Serum Institut, Copenhagen, Denmark (J. Larsen, H. Kaya); George Washington University, Washington, DC, USA (L.B. Price, M. Aziz); Tufts University, Boston, Massachusetts, USA (M.L. Nadimpalli); University of North Carolina at Chapel Hill, Chapel Hill, North Carolina, USA (S. Rhodes, J.R. Stewart); Rural Empowerment Association for Community Help (REACH), Warsaw, North Carolina, USA (D. Hall); University of Texas Southwestern Medical Center, Dallas, Texas, USA (T.M. Perl)

DOI: https://doi.org/10.3201/eid2703.191775

Europe, and Asia and to investigate potential transmission of antimicrobial-resistant LA-SA CC9 among IHO pigs and humans who work on or live near IHOs in North Carolina.

Methods

Sources of *S. aureus* Isolates from Humans and from Pigs Raised on IHOs in North Carolina

S. aureus isolates from IHO pigs were collected from a convenience sample of a single IHO in North Carolina (IHO-1), as described previously (*12*). We collected additional pig samples by hanging a length of undyed, unbleached cotton rope in pig pens of 20 IHOs in North Carolina (IHO-2–IHO-21) (Appendix). Pig isolates were recovered from IHO-2, IHO-3, IHO-4, IHO-5, and IHO-6 for a total of 6 IHOs (IHO-1–IHO-6). Isolates from IHO-2–IHO-6 have not been published previously. The *spa* type for all IHO pig isolates was characterized, as previously described (*12*), and used to assign each isolate to a putative multilocus sequence type (MLST).

S. aureus isolates from humans were collected from participants who were previously enrolled into 1 of 3 separate epidemiologic studies (study 1, study 2, and study 3) and screened for nasal carriage of *S. aureus* (Appendix, https://wwwnc.cdc.gov/EID/article/27/3/19-1775-App1.pdf). Sample collection, sample processing, and *S. aureus* isolation methods were described previously (*1*–*3*). MLST was previously determined for all study 1 isolates (*1*). The *spa* type was previously characterized for study 2 and study 3 isolates and used to assign a putative MLST based on previously published associations between *spa* types and MLSTs (*2*,*3*).

Selection of *S. aureus* CC9 Isolates for WGS Analysis

A total of 236 putative or MLST-confirmed *S. aureus* CC9 isolates were recovered from IHO pigs (n = 91) and humans (n = 145) in North Carolina during 2011–2016 (Appendix). For this study, a convenience sample of 49 isolates from North Carolina were subjected to WGS analysis, including 10 isolates from pigs raised on 4 different IHOs, 34 isolates from 25 IHO workers, 1 isolate each from 3 IHO minors, and 1 isolate each from 2 community resident adults (Appendix). For comparative purposes, we also included an international collection of 32 *S. aureus* CC9 genomes available as of August 1, 2018, from the National Center for Biotechnology Information (NCBI) Reference Sequence Database (http://www.ncbi.nlm.nih.gov/RefSeq), which included information on source, geographic location, and collection year.

WGS and Bioinformatic Analyses

We prepared DNA for multiplexed, paired-end sequencing by preparing libraries using either the Nextera XT DNA Library Preparation Kit (Illumina, Inc.), according to manufacturer instructions, or the Kapa Hyper Prep Kit (Kapa Biosystems, Inc., https://www.sigmaaldrich.com) and uniquely barcoded adaptors from NEXTFLEX-96 Unique Dual Index barcodes (Bioo Scientific, https://www.biooscientific.com). We prepared equimolar pools of *S. aureus* libraries at a concentration of 2 nmol and sequenced on a MiSeq (Illumina, Inc., https://ww.illumina.com) at 2 × 300 bp. WGS data are available in the NCBI Sequence Read Archive (http://www.ncbi.nlm.nih.gov; BioProject no. PRJNA574434).

We used SPAdes (*13*) to generate de novo assemblies and compared these against the *S. aureus* MLST database (*14*) to assign MLSTs. We used ABRicate (https://github.com/tseemann/abricate) to search the ResFinder database for antimicrobial-resistance (AMR) genes (*15*). We used BLASTN (https://blast.ncbi.nlm.nih.gov/Blast.cgi) to detect genes in the phage-associated immune evasion cluster (IEC), including *scn*, *chp*, *sak*, *sea* (GenBank accession no. NC_009641), and *sep* (GenBank accession no. BA000018) (*16*).

We used the NASP pipeline (*17*) to map sequence reads against the de novo-assembled genome of North Carolina isolate IHOW6.1 (BioProject accession no. PRJNA574434) and to perform single-nucleotide polymorphism (SNP) calling, as described previously (*8*). We used Gubbins version 2.3.1 (*18*) to remove recombination from the SNP alignment and used the remaining SNPs in the core genome to construct a midpoint-rooted maximum-likelihood tree by using PhyML (*19*) with a general time-reversible model of nucleotide substitution and 100 bootstrap replicates (*20*). We used the same methods to perform a separate SNP analysis of the cluster containing the North Carolina isolates (clade 3) to improve the resolution of the transmission analysis. We calculated pairwise SNP differences by using MEGA5 (*21*). To define a SNP-based threshold for assigning isolates into putative transmission clusters, we used the maximum within-farm pairwise SNP distance among *S. aureus* CC9 isolates from IHO-1, in which all isolates were collected from the same IHO at the same sampling time.

Antimicrobial Susceptibility Testing

Isolates in the North Carolina collection previously were assessed for susceptibility to a panel of antimicrobial drugs by using the Phoenix Automated Microbiology System (Becton Dickinson, https://www.

bd.com) or the Kirby-Bauer disk diffusion method (Appendix Table 2). Testing was completed by the Clinical Microbiology Laboratory at the Johns Hopkins Hospital based on Clinical Laboratory Standards Institute (CLSI; https://clsi.org) guidelines specified in the source studies (*1*–*3*) (Appendix Table 2). We defined MDRSA as *S. aureus* isolates resistant to ≥3 classes of antimicrobial drugs (*22*). We defined MRSA as *S. aureus* harboring the *mecA* gene.

Statistical analysis

We used the χ^2 test to compare AMR and IEC genes between groups. We performed all statistical analyses by using Stata version 14.2 (StataCorp LLC, https://www.stata.com).

Results

All 49 isolates from the North Carolina collection used in WGS analysis were classified as sequence type 9 by MLST. Among 81 *S. aureus* CC9 isolates analyzed, 95% (77/81) were located in 3 major clades, C1, C2, and C3 (Figure 1; Appendix Tables 3, 4). Despite the small number of pig isolates, each clade contained both pig and human isolates (Figure 1; Appendix Table 3).

Among C1–C3 isolates, 61% (47/77) contained tetracycline resistance genes. By contrast, only 1 (1.3%) of the isolates in C1–C3 contained IEC genes (Figure 1; Appendix Table 4). The presence of pig isolates coupled with the absence of IEC genes and presence of tetracycline resistance genes in C1–C3 suggest that C1–C3 isolates may be members of a larger LA-SA CC9 clade. LA-MRSA CC9, which harbored the *mecA* gene, was present in C1 and C2 but absent from C3.

C1 was composed of isolates primarily originating from Asia (12/13 isolates; 92%), of which 46% (6/13) were from China and 46% (6/13) were from Taiwan (Figure 1; Appendix Table 3). All of C2 (14/14 isolates) was composed of isolates originating from Europe, of which 71% (10/14) were from Germany, 21% (3/14) were from the Netherlands, and 7% (1/14) were from Denmark (Figure 1; Appendix Table 3). C3 included 100% (49/49) of the North Carolina isolates, which made up 98% (49/50) of all C3 isolates (Figure 1; Appendix Table 3). Only 2 isolates grouped into a clade that did not correspond to the continent of predominance within the clade. A single isolate from Colombia (South America) grouped into C3 with isolates from North Carolina, and a single isolate from the Netherlands grouped into C1 with isolates from Asia (Figure 1; Appendix Table 3).

High-resolution phylogenetic analysis of C3 revealed multiple distinct subclades, one of which contained all 6 IHO-1 pig isolates from North Carolina (Figure 2). The pairwise SNP distance among IHO pig isolates from IHO-1 ranged from 0–43 SNPs. Thus, we used 43 SNPs as the threshold to identify putative transmission clusters and found that 19 isolates fell into 2 distinct putative transmission clusters (Figure 2). The minimum pairwise SNP distance between IHO pig and human isolates within putative transmission clusters ranged from 12–34 SNPs.

Almost all (94.7%) transmission cluster isolates were classified as MDRSA (Figure 2). Among 19 putative transmission cluster isolates, 14 were recovered from IHO workers, all of which were classified as MDRSA. Among IHO worker isolates, 2 differed from an IHO pig isolate by only 12 SNPs. An IHO worker isolate that was associated with a recent SSTI differed from an IHO pig isolate by only 20 SNPs (Figure 2). One transmission cluster isolate was from an adult community resident with no known exposure to livestock; this isolate also was classified as MDRSA (Figure 2). The minimum SNP distance between this isolate and the closest IHO pig isolate was 25 SNPs and it was 22 SNPs from the closest IHO worker isolate. Among 3 isolates from minors, 2 were identical (0 SNP differences) to an isolate from an IHO worker in the same household (Figure 2); 1 of the isolates from a minor was collected at the same sampling time as the IHO worker isolate. Among C3 isolates, we noted genetic determinants conferring resistance to tetracyclines, including *tet*(K), *tet*(L), *tet*(T); macrolides, including *erm*(A), *erm*(C); lincosamides, including *lnu*(A); aminoglycosides, including *aac6′-aph2″*, *spc*, and *aadD*; and streptogramins, including $vga(A)_{LC}$ (Figure 2).

We noted abundant genetic determinants conferring resistance to several antimicrobial classes among C3 isolates, including tetracyclines in 50% (25/50), macrolides in 56% (28/50), and aminoglycosides in 62% (31/50) of C3 isolates (Figure 2; Appendix Table 4). Among LA-SA CC9 clades, 50% (25/50) of C3 isolates were uniquely enriched for *erm*(A) genes, 16% (8/50) for $vga(A)_{LC}$, 42% (21/50) for *lnu*(A), and 54% (27/50) for *spc* (Figure 1; Appendix Table 4). The *mecA* gene was absent from C3 but common among C1 and C2 isolates.

Discussion

Our WGS analysis suggests that the clonal expansion of LA-SA CC9 in North Carolina is distinct from that in Asia and Europe and that LA-SA CC9 from IHO pigs and humans in high-density pig-producing counties of North Carolina come from a common pool. Considering the high degree of phylogenetic relatedness among intermingled IHO pig and human

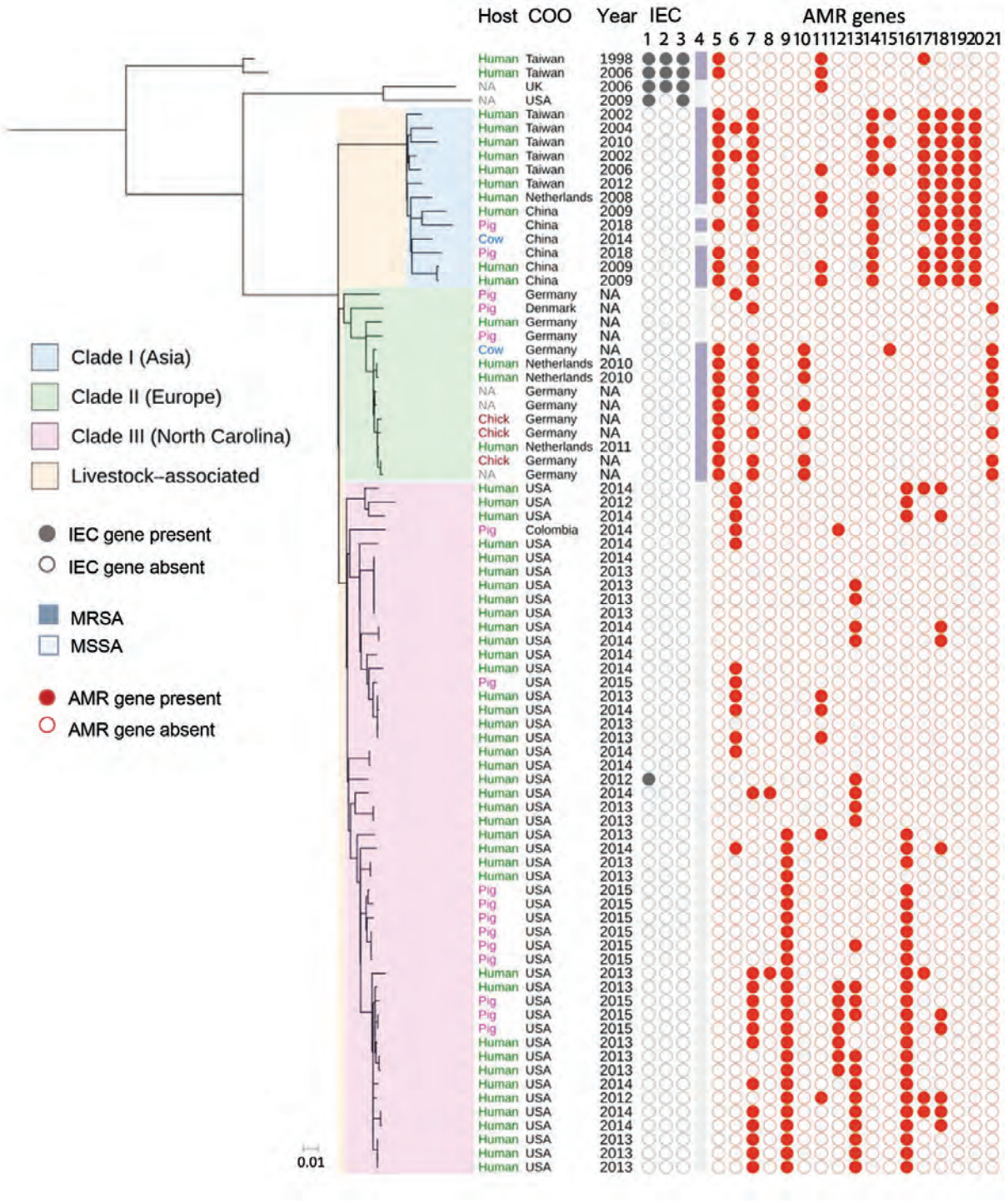

Figure 1. Maximum-likelihood tree demonstrating population structure of *Staphylococcus aureus* clonal complex (CC) 9 isolates from humans and livestock in North Carolina, USA, and reference sequences. A total of 81 *S. aureus* CC9 isolates from human and livestock specimens were included in this midpoint-rooted maximum-likelihood phylogeny based on 3,847 core genome single-nucleotide polymorphisms. *S. aureus* isolates belonged to 3 phylogeographically distinct clades (C1–C3). All the North Carolina collection isolates were included in C3. IEC genes are shown in columns 1, *scn*; 2, *sak*; and 3, *chp.* MRSA is shown in column 4. AMR genes are shown in columns 5, *mecA*; 6, *tet*(K); 7, *tet*(L); 8, *tet*(T); 9, *erm*(A); 10, *erm*(B); 11, *erm*(C); 12, *vga*(A)$_{LC}$; 13, *lnu*(A); 14, *lnu*(B); 15, *str*; 16, *spc*; 17, *aadD*; 18, *aac*(6); 19, *ant*(6)-1a; 20, *dfr*G; and 21, *dfr*K. Scale bar indicates nucleotide substitutions per site. AMR, antimicrobial resistance; Chick, chicken; COO, country of origin; IEC, immune evasion cluster; MRSA, methicillin-resistant *S. aureus*; MSSA, methicillin-susceptible *S. aureus*; NA, not applicable.

isolates in putative transmission clusters, the results of this study support potential transmission of antimicrobial-resistant LA-SA CC9 between IHO pigs and humans in the United States.

Our results also provide evidence of household-level transmission of LA-SA CC9 between IHO workers and minors and suggest that potential LA-SA CC9 transmission is not limited to the occupational setting. Dissemination of LA-SA CC9 into the general human population represents a public health concern for 2 reasons. Globally, communities include a higher proportion of children, the elderly, and probably immunocompromised persons, who are at higher risk of developing invasive staphylococcal infections, compared with IHO workers who are predominantly healthy adults of working age. Our analysis revealed an 11-year-old child and an IHO worker residing in the same household who were carrying identical

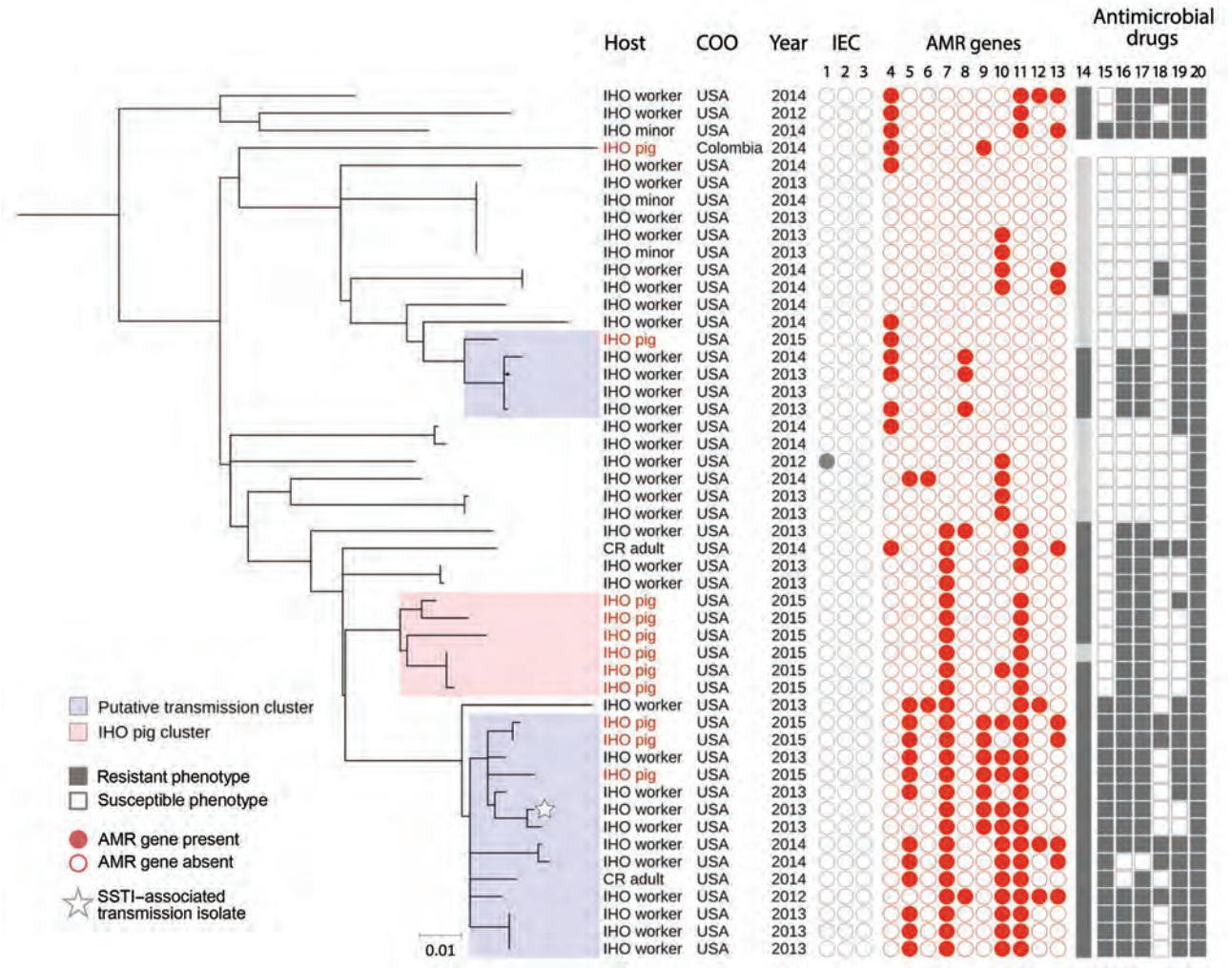

Figure 2. High-resolution population structure of clade 3 livestock-associated *Staphylococcus aureus* clonal complex (CC) 9 isolates from humans and livestock in North Carolina, USA, and reference isolates. A subset of 50 livestock-associated *S. aureus* CC9 isolates that were collected from IHO pigs, IHO workers, IHO minors, and CR adults were included in this midpoint-rooted maximum-likelihood phylogeny based on 1,198 core genome single-nucleotide polymorphisms. A single subclade, denoted as the IHO pig cluster, included only pig isolates from IHO-1 and was used to set a threshold of 43 SNPs for identifying transmission clusters; clusters of IHO pig and human isolates separated by ≤43 SNPs are considered transmission clusters. Two subclades included intermingled human and IHO pig isolates with a high degree of phylogenetic relatedness and were considered transmission clusters. IEC isolates are shown in columns 1, *scn*, 2, *sak*, and 3, *chp*. AMR genes are shown in columns 4, *tet*(K); 5, *tet*(L); 6, *tet*(T); 7, *erm*(A); 8, *erm*(C); 9, *vga*(A)$_{LC}$; 10, *lnu*(A); 11, *spc*; 12, *aadD*; and 13, *aac*(6). MDRSA is shown in column 14. Antimicrobial drug resistance is shown in columns 15, fluoroquinolone resistance, considered phenotypic resistance to moxifloxacin; 16, lincosamide resistance, considered phenotypic resistance to clindamycin; 17, macrolide resistance, considered phenotypic resistance to erythromycin; 18, aminoglycoside resistance, considered phenotypic resistance to gentamicin; 19, tetracycline resistance, considered phenotypic resistance to tetracycline; and 20, penicillin resistance. Scale bar indicates nucleotide substitutions per site. AMR, antimicrobial resistance; CR, community resident, a person with no known exposure to livestock; IHO, industrial hog operation; MDRSA, multidrug resistant *S. aureus;* SSTI, skin and soft tissue infection.

LA-SA CC9 isolates (0 SNP differences) at the same sampling time, which provides strong evidence of household transmission of LA-SA CC9 between IHO workers and their children. Second, clinical implications might arise regarding treatment regimens for LA-MDRSA CC9 colonization and infection. Most (63.3%; 31/49) LA-SA CC9 isolates from North Carolina were multidrug-resistant and carried multiple genes conferring resistance to antimicrobial drug classes critical for human medicine (*23*). Of note, the single LA-SA CC9 isolate from an IHO worker who reported a recent SSTI belonged to a putative transmission cluster, displayed an MDRSA phenotype, and previously was reported to display a high degree of pathogenicity compared with a hypervirulent community-associated MRSA strain, USA300 (GenBank accession no. CP000255), in a mouse model of SSTI (*24*).

Our results support potential transmission of LA-SA CC9 between IHO pigs and humans, and between humans and other humans, in the top 10 pig-producing counties in North Carolina. These findings are consistent with previous publications on LA-SA CC9 and other lineages of LA-SA. First, a separate analysis of LA-MRSA CC9 recovered from IHO pigs in China suggested potential transmission of LA-MRSA CC9 between pigs, humans, and cows (*11*). Second, an abundance of previous epidemiologic and WGS analyses support transmission of diverse lineages of LA-SA from pigs to humans, which can result in human SSTI and bloodstream infections (*8*,*10*,*25*). Last, prior WGS analyses and epidemiologic studies have provided support for household transmission of LA-SA CC9 and CC398 between persons based on spatial, temporal, and genotypic overlap (*2*,*3*,*26*). In our analysis, the exact transmission pathway remains unclear because we did not ascertain the direction of transmission or whether transmission occurred through direct or indirect contact.

Previous studies have suggested a *S. aureus* mutation rate of 5–10 SNPs per year per genome (*27*–*30*), but our threshold of 43 SNPs was justified for 2 reasons. First, our empirically derived SNP threshold was consistent with SNP-based thresholds used by others to identify suspected transmission of MRSA in clinical settings (*31*) and previous measures of within-person *S. aureus* diversity (*32*). The robustness of our findings was supported when we used the median (32 SNPs), rather than maximum (43 SNPs), pairwise SNP distance among IHO pig cluster isolates as the SNP threshold for identification of putative transmission clusters. We excluded only 1 isolate from an IHO worker from putative transmission clusters, and the excluded isolate was not the SSTI-associated isolate (data not shown). Second, the aim of this study was to clarify whether any SNP-based evidence of transmission between IHO pig and human populations in North Carolina exists, rather than provide evidence of recent or incident transmission or to identify specific pathways of transmission. Using 43 SNPs as the threshold enabled us to observe potential direct or indirect transmission that might not be observed by using epidemiologic data alone. Investigations of *S. aureus* transmission conventionally combine epidemiologic and strain typing data, but these methods can fail to identify transmission links in cases in which spatial and temporal overlap is lacking (*31*). Using the epidemiologic data that were available to us, such as multiple *S. aureus* CC9 isolates from the same IHO, household, or individual, we observed SNP-based evidence of *S. aureus* CC9 clustering that would be expected biologically (Appendix Table 5).

Since 2016, tetracyclines have been the most heavily used antimicrobial drug class in the US pig production system, followed distantly by macrolides, lincosamides, aminoglycosides, streptogramins, and fluoroquinolones (*33*,*34*). If antimicrobial-resistant CC9 strains were enriched through selective pressure, antimicrobial use in pig production possibly has played a role in the clonal expansion of LA-SA CC9 in North Carolina and other regions of the world. Of note, resistance to several of these antimicrobial drug classes was conferred by different AMR genes in C1, C2, and C3 (Figure 1; Appendix Table 4), highlighting different evolutionary pathways for adaptation to antimicrobial selection pressures in different regions of the world. Continued surveillance of IHO pigs and humans, including during and after regulatory and policy restrictions on antimicrobial use in animal agriculture, could provide critical insight into the potential contribution of antimicrobial use in the clonal expansion of LA-SA CC9 and its associated AMR genes in the United States.

The strengths of our study included using SNP-based analyses to examine the population structure and transmission dynamics of LA-SA CC9 among pigs and humans in a region of North Carolina with the highest density of IHOs in the United States (*35*), a region in which residents and IHO workers are actively expressing concerns about IHO-related exposures (*36*). Second, our study used SNP distance to classify human isolates closely related to IHO pig isolates, which is an improvement on previous studies that used *spa*-typing, MLST typing, absence of IEC genes (specifically *scn*), phenotypic AMR determination, or combinations of these techniques, to classify *S. aureus* isolates as livestock-associated (*2*,*3*,*12*).

Third, the use of a SNP-based definition for cluster analysis can capture the potential for transmission between animal and human populations that would have been missed by using more conventional epidemiologic methods alone (*31*).

Limitations of our study included that we were not able to provide evidence for directionality of transmission. We rooted our high-resolution phylogenetic tree at the midpoint; therefore, we are unsure if the most ancestral clade of *S. aureus* CC9 is of human or animal origin. In addition, whereas the SNP-based evidence for pig-to-human transmission could have been strengthened by spatial or temporal data linking pigs and workers at the same IHO, these data were not available because of efforts to protect the privacy of participants enrolled in the epidemiologic studies and because of limited access to IHOs in the United States (*37*). In contrast to countries in Europe, the lack of access to IHOs prevents us from assessing the generalizability of our results in the United States. We hypothesize that we would see even closer genetic relatedness between IHO worker and IHO pig LA-SO CC9 isolates collected from the same IHO at the same time. Last, our collection of *S. aureus* CC9 isolates was limited. The North Carolina collection was a convenience sample that identified *S. aureus* CC9 isolates from only 6 IHOs, which does not represent the full population of IHOs or pigs in North Carolina. Also, we excluded many isolates selected for WGS from SNP-analysis because they did not pass our quality control criteria (Appendix), potentially introducing bias into the studied isolate sample. Additional *S. aureus* CC9 isolates likely are available now in the NCBI Reference Sequence Database, but publicly available LA-SA CC9 sequence data were limited when we accessed the database for this study. A more representative dataset could provide more refined estimates on frequency of transmission in North Carolina and other regions of the world.

Despite these limitations, our results show a high degree of phylogenetic relatedness between IHO pig and human LA-SA CC9 isolates in the top 10 pig-producing counties in North Carolina. The presence of a highly pathogenic SSTI-associated LA-SA CC9 isolate with an MDRSA phenotype in a putative transmission cluster warrants future investigations into the disease burden associated with these strains in the United States. Future research could further improve or build on our findings by including environmental isolates and considering WGS analysis in conjunction with spatial and temporal data analysis to investigate the frequency of transmission, environmental exposure routes, and geographic extent of LA-SA CC9. Our reference dataset might be useful in future investigations of worker and community health concerns related to LA-SA CC9 dissemination and acquisition, both in North Carolina and in other regions of the United States with high densities of IHOs.

Acknowledgments

The authors thank Aaron Milstone for intellectual contributions to the manuscript drafts; the Rural Empowerment Association for Community Help (REACH) for their assistance with participant enrollment and collection of human nasal samples; and William Flowers, Sarah Blacklin, Asher Wright, Alexis Brown, Haley Keller, and Ralph A. Tripp for their assistance with collection of samples from pigs in North Carolina.

This study was funded by the Sherrilyn and Ken Fisher Center for Environmental Infectious Diseases Discovery Program at the Johns Hopkins University, School of Medicine, Department of Medicine, Division of Infectious Diseases (award no. 018HEA2013); a gift from the GRACE Communications Foundation; the National Institute for Occupational Safety and Health (NIOSH) pilot award from the Johns Hopkins NIOSH Education and Research Center (grant no. T42OH008428); and NIOSH grant no. K01OH010193 and National Science Foundation (NSF) grant no. 1316318 as part of the joint NSF-NIH-USDA Ecology and Evolution of Infectious Diseases program. P.R.R. was supported by NIOSH (grant no. T42OH008428) and a gift from the GRACE Communications Foundation. J.L., L.B.P., and M.A. received funding support from the National Institute of Allergy and Infectious Diseases (NIAID; grant no. R01AI101371). C.D.H. received funding from NIOSH (grant no. K01OH010193). E.W. received funding from "AI" Thrasher Award 10287; a gift from the GRACE Communications Foundation; the National Institute of Environmental Health Sciences (grant no. R01ES026973); NIAID (grant nos. R21AI139784, R43AI141265, and R01AI130066); and the National Science Foundation (grant no. 1316318), as part of the joint NSF-NIH-USDA Ecology and Evolution of Infectious Diseases program. M.L.N. received funding support as part of a Royster Society fellowship and a US Environmental Protection Agency Science to Achieve Results fellowship. M.F.D. received funding support from NIH (grant no. K01OD019918). L.S.M received funding support from NIH (grant nos. R01AR069502 and R01AR073665). D.C.L. received funding support through a gift from the GRACE Communications Foundation. The funders had no role in study design, data collection and analysis, decision to publish, or preparation of the manuscript.

D.H. is the program manager and co-founder of the Rural Empowerment Association for Community Help (REACH), a 501(c)(3) not-for-profit organization located in Duplin County, North Carolina, and was a complainant in a Title VI administrative complaint against the North Carolina Department of Environmental Quality related to its statewide hog operation lagoon and spray field liquid waste management permitting system; D.H. has no potential personal financial gain from this administrative complaint, which is not directly related to the research described in this manuscript and is not a lawsuit or litigation.

L.S.M. is a full-time employee of Janssen Pharmaceuticals and may hold Johnson & Johnson stock and stock options. He performed all work at his prior affiliation at Johns Hopkins University School of Medicine; has received prior grant support from AstraZeneca, Pfizer, Boehringer Ingelheim, Regeneron Pharmaceuticals, and Moderna Therapeutics; was a paid consultant for Armirall and Janssen Research and Development; was on the scientific advisory board of Integrated Biotherapeutics; and is a shareholder of Noveome Biotherapeutics, which are all developing therapeutics against infections, including S. aureus and other pathogens, and inflammatory conditions. All other authors declare that they have no actual or potential competing financial interests.

About the Author

Dr. Randad is a postdoctoral fellow in the department of Environmental Health and Engineering at Johns Hopkins University Bloomberg School of Public Health. His research focuses on infectious disease epidemiology and diagnostic development.

References

1. Rinsky JL, Nadimpalli M, Wing S, Hall D, Baron D, Price LB, et al. Livestock-associated methicillin and multidrug resistant *Staphylococcus aureus* is present among industrial, not antibiotic-free livestock operation workers in North Carolina. PLoS One. 2013;8:e67641. https://doi.org/10.1371/journal.pone.0067641
2. Hatcher SM, Rhodes SM, Stewart JR, Silbergeld E, Pisanic N, Larsen J, et al. The prevalence of antibiotic-resistant *Staphylococcus aureus* nasal carriage among industrial hog operation workers, community residents, and children living in their households: North Carolina, USA. Environ Health Perspect. 2017;125:560–9. https://doi.org/10.1289/EHP35
3. Nadimpalli ML, Stewart JR, Pierce E, Pisanic N, Love DC, Hall D, et al. Face mask use and persistence of livestock-associated *Staphylococcus aureus* nasal carriage among industrial hog operation workers and household contacts, USA. Environ Health Perspect. 2018;126:127005. https://doi.org/10.1289/EHP3453
4. Casey JA, Curriero FC, Cosgrove SE, Nachman KE, Schwartz BS. High-density livestock operations, crop field application of manure, and risk of community-associated methicillin-resistant Staphylococcus aureus infection in Pennsylvania. JAMA Intern Med. 2013;173:1980–90. https://doi.org/10.1001/jamainternmed.2013.10408
5. Wardyn SE, Forshey BM, Farina SA, Kates AE, Nair R, Quick MK, et al. Swine farming is a risk factor for infection with and high prevalence of carriage of multidrug-resistant staphylococcus aureus. Clin Infect Dis. 2015;61:59–66. https://doi.org/10.1093/cid/civ234
6. Wardyn SE, Stegger M, Price LB, Smith TC. Whole-genome analysis of recurrent *Staphylococcus aureus* t571/ST398 infection in farmer, Iowa, USA. Emerg Infect Dis. 2018;24:153–4. https://doi.org/10.3201/eid2401.161184
7. Nadimpalli M, Stewart JR, Pierce E, Pisanic N, Love DC, Hall D, et al. Livestock-associated, antibiotic-resistant *Staphylococcus aureus* nasal carriage and recent skin and soft tissue infection among industrial hog operation workers. PLoS One. 2016;11:e0165713. https://doi.org/10.1371/journal.pone.0165713
8. Larsen J, Petersen A, Larsen AR, Sieber RN, Stegger M, Koch A, et al.; Danish MRSA Study Group. Emergence of livestock-associated methicillin-resistant *Staphylococcus aureus* bloodstream infections in Denmark. Clin Infect Dis. 2017;65:1072–6. https://doi.org/10.1093/cid/cix504
9. Butaye P, Argudín MA, Smith TC. Livestock-associated MRSA and its current evolution. Curr Clin Microbiol Rep. 2016;3:19–31. https://doi.org/10.1007/s40588-016-0031-9
10. Chuang Y-Y, Huang Y-C. Livestock-associated methicillin-resistant *Staphylococcus aureus* in Asia: an emerging issue? Int J Antimicrob Agents. 2015;45:334–40. https://doi.org/10.1016/j.ijantimicag.2014.12.007
11. Zhou W, Li X, Osmundson T, Shi L, Ren J, Yan H. WGS analysis of ST9-MRSA-XII isolates from live pigs in China provides insights into transmission among porcine, human and bovine hosts. J Antimicrob Chemother. 2018;73:2652–61. https://doi.org/10.1093/jac/dky245
12. Davis MF, Pisanic N, Rhodes SM, Brown A, Keller H, Nadimpalli M, et al. Occurrence of *Staphylococcus aureus* in swine and swine workplace environments on industrial and antibiotic-free hog operations in North Carolina, USA: a One Health pilot study. Environ Res. 2018;163:88–96. https://doi.org/10.1016/j.envres.2017.12.010
13. Bankevich A, Nurk S, Antipov D, Gurevich AA, Dvorkin M, Kulikov AS, et al. SPAdes: a new genome assembly algorithm and its applications to single-cell sequencing. J Comput Biol. 2012;19:455–77. https://doi.org/10.1089/cmb.2012.0021
14. Enright MC, Day NPJ, Davies CE, Peacock SJ, Spratt BG. Multilocus sequence typing for characterization of methicillin-resistant and methicillin-susceptible clones of *Staphylococcus aureus*. J Clin Microbiol. 2000;38:1008–15. https://doi.org/10.1128/JCM.38.3.1008-1015.2000
15. Zankari E, Hasman H, Cosentino S, Vestergaard M, Rasmussen S, Lund O, et al. Identification of acquired antimicrobial resistance genes. J Antimicrob Chemother. 2012;67:2640–4. https://doi.org/10.1093/jac/dks261
16. Altschul SF, Gish W, Miller W, Myers EW, Lipman DJ. Basic local alignment search tool. J Mol Biol. 1990;215:403–10. https://doi.org/10.1016/S0022-2836(05)80360-2
17. Sahl JW, Lemmer D, Travis J, Schupp JM, Gillece JD, Aziz M, et al. NASP: an accurate, rapid method for the identification of SNPs in WGS datasets that supports flexible input and output formats. Microb Genom. 2016;2:e000074. https://doi.org/10.1099/mgen.0.000074
18. Croucher NJ, Page AJ, Connor TR, Delaney AJ, Keane JA, Bentley SD, et al. Rapid phylogenetic analysis of large samples of recombinant bacterial whole genome sequences

using Gubbins. Nucleic Acids Res. 2015;43:e15–15. https://doi.org/10.1093/nar/gku1196
19. Guindon S, Dufayard J-F, Lefort V, Anisimova M, Hordijk W, Gascuel O. New algorithms and methods to estimate maximum-likelihood phylogenies: assessing the performance of PhyML 3.0. Syst Biol. 2010;59:307–21. https://doi.org/10.1093/sysbio/syq010
20. Guindon S, Gascuel O. A simple, fast, and accurate algorithm to estimate large phylogenies by maximum likelihood. Syst Biol. 2003;52:696–704. https://doi.org/10.1080/10635150390235520
21. Tamura K, Peterson D, Peterson N, Stecher G, Nei M, Kumar S. MEGA5: molecular evolutionary genetics analysis using maximum likelihood, evolutionary distance, and maximum parsimony methods. Mol Biol Evol. 2011;28:2731–9. https://doi.org/10.1093/molbev/msr121
22. Magiorakos A-P, Srinivasan A, Carey RB, Carmeli Y, Falagas ME, Giske CG, et al. Multidrug-resistant, extensively drug-resistant and pandrug-resistant bacteria: an international expert proposal for interim standard definitions for acquired resistance. Clin Microbiol Infect. 2012;18:268–81. https://doi.org/10.1111/j.1469-0691.2011.03570.x
23. World Health Organization. Critically important antimicrobials for human medicine, 6th revision. Geneva: The Organization; 2018 [cited 2020 Dec 18]. https://www.who.int/foodsafety/publications/antimicrobials-sixth
24. Randad PR, Dillen CA, Ortines RV, Mohr D, Aziz M, Price LB, et al. Author correction: comparison of livestock-associated and community-associated *Staphylococcus aureus* pathogenicity in a mouse model of skin and soft tissue infection. Sci Rep. 2019;9:12811. https://doi.org/10.1038/s41598-019-46940-z
25. Price LB, Stegger M, Hasman H, Aziz M, Larsen J, Andersen PS, et al. *Staphylococcus aureus* CC398: host adaptation and emergence of methicillin resistance in livestock. mBio. 2012;3:e00305–11. https://doi.org/10.1128/mBio.00305-11
26. Bosch T, Verkade E, van Luit M, Landman F, Kluytmans J, Schouls LM. Transmission and persistence of livestock-associated methicillin-resistant *Staphylococcus aureus* among veterinarians and their household members. Appl Environ Microbiol. 2015;81:124–9. https://doi.org/10.1128/AEM.02803-14
27. Harris SR, Feil EJ, Holden MTG, Quail MA, Nickerson EK, Chantratita N, et al. Evolution of MRSA during hospital transmission and intercontinental spread. Science. 2010;327:469–74.
28. Nübel U, Dordel J, Kurt K, Strommenger B, Westh H, Shukla SK, et al. A timescale for evolution, population expansion, and spatial spread of an emerging clone of methicillin-resistant *Staphylococcus aureus*. PLoS Pathog. 2010;6:e1000855. https://doi.org/10.1371/journal.ppat.1000855
29. Smyth DS, McDougal LK, Gran FW, Manoharan A, Enright MC, Song J-H, et al. Population structure of a hybrid clonal group of methicillin-resistant *Staphylococcus aureus*, ST239-MRSA-III. PLoS One. 2010;5:e8582. https://doi.org/10.1371/journal.pone.0008582
30. Young BC, Golubchik T, Batty EM, Fung R, Larner-Svensson H, Votintseva AA, et al. Evolutionary dynamics of *Staphylococcus aureus* during progression from carriage to disease. Proc Natl Acad Sci U S A. 2012;109:4550–5. https://doi.org/10.1073/pnas.1113219109
31. Price JR, Golubchik T, Cole K, Wilson DJ, Crook DW, Thwaites GE, et al. Whole-genome sequencing shows that patient-to-patient transmission rarely accounts for acquisition of *Staphylococcus aureus* in an intensive care unit. Clin Infect Dis. 2014;58:609–18. https://doi.org/10.1093/cid/cit807
32. Golubchik T, Batty EM, Miller RR, Farr H, Young BC, Larner-Svensson H, et al. Within-host evolution of *Staphylococcus aureus* during asymptomatic carriage. PLoS One. 2013;8:e61319. https://doi.org/10.1371/journal.pone.0061319
33. US Food and Drug Administration. 2016 summary report on antimicrobials sold or distributed for use in food-producing animals [cited 2020 Dec 18]. https://www.fda.gov/media/109457/download
34. US Food and Drug Administration. 2017 summary report on antimicrobials sold or distributed for use in food-producing animals [cited 2020 Dec 18]. https://www.fda.gov/media/119332/download
35. US Department of Agriculture, North Carolina Department of Agriculture and Consumer Services. 2018 North Carolina agricultural statistics [cited 2020 Dec 18]. https://quickstats.nass.usda.gov
36. Cole D, Todd L, Wing S. Concentrated swine feeding operations and public health: a review of occupational and community health effects. Environ Health Perspect. 2000;108:685–99. https://doi.org/10.1289/ehp.00108685
37. Ceryes CA, Heaney CD. "Ag-Gag" laws: evolution, resurgence, and public health implications. NEW Solut. 2019.28:664–82. https://doi.org/10.1177/1048291118808788

Address for correspondence: Pranay R. Randad, Department of Environmental Health and Engineering, Bloomberg School of Public Health, Johns Hopkins University, 615 N Wolf St, Baltimore, MD 21205, USA; email: prandad1@jhmi.edu

Epidemiology and Clinical Course of First Wave Coronavirus Disease Cases, Faroe Islands

Marnar F. Kristiansen, Bodil H. Heimustovu, Sanna á Borg, Tróndur Høgnason Mohr., Hannes Gislason, Lars Fodgaard Møller, Debes H. Christiansen, Bjarni á Steig, Maria Skaalum Petersen, Marin Strøm, Shahin Gaini

The Faroe Islands was one of the first countries in the Western Hemisphere to eliminate coronavirus disease (COVID-19). During the first epidemic wave in the country, 187 cases were reported between March 3 and April 22, 2020. Large-scale testing and thorough contact tracing were implemented early on, along with lockdown measures. Transmission chains were mapped through patient history and knowledge of contact with prior cases. The most common reported COVID-19 symptoms were fever, headache, and cough, but 11.2% of cases were asymptomatic. Among 187 cases, 8 patients were admitted to hospitals but none were admitted to intensive care units and no deaths occurred. Superspreading was evident during the epidemic because most secondary cases were attributed to just 3 infectors. Even with the high incidence rate in early March, the Faroe Islands successfully eliminated the first wave of COVID-19 through the early use of contact tracing, quarantine, social distancing, and large-scale testing.

The World Health Organization declared coronavirus disease (COVID-19) a pandemic on March 12, 2020 (*1*). Initial outbreaks were reported in China during late 2019, and by February 2020 COVID-19 had spread globally and caused clusters of contagion in Europe (*2*).

Author affiliations: National Hospital of the Faroe Islands, Tórshavn, Faroe Islands (M.F. Kristiansen, B.H. Heimustovu, S. á Borg, T.H. Mohr, B. á Steig, S. Gaini); Ministry of Health COVID-19 Task Force, Tórshavn (M.F. Kristiansen, B.H. Heimustovu, B. á Steig); University of the Faroe Islands, Tórshavn (M.F. Kristiansen, H. Gislason, M.S. Petersen, M. Strøm, S. Gaini); Office of the Chief Medical Officer, Tórshavn (L.F. Møller); Faroese Food and Veterinary Authority, Tórshavn (D.H. Christiansen); The Faroese Hospital System, Tórshavn (M.S. Petersen); Statens Serum Institut, Copenhagen, Denmark (M. Strøm); Odense University Hospital, Odense, Denmark (S. Gaini); University of Southern Denmark, Odense (S. Gaini)

DOI: https://doi.org/10.3201/eid2703.202589

The first confirmed case of COVID-19 in the Faroe Islands was identified on March 3. The Faroe Islands, located in the North Atlantic Ocean, is a high-income self-governing country in the Kingdom of Denmark with a population of 52,428 (*3*). During March 3–April 22, 2020, 187 persons in the Faroe Islands tested positive for COVID-19 (Figure 1). The last case was diagnosed on April 22 and recovered on May 8, at which point the first wave of COVID-19 ended in the country. To eliminate COVID-19, the Faroe Islands used an active suppression strategy that included large-scale testing, contact tracing, quarantine, and social distancing measures.

We describe the epidemiology and clinical course of COVID-19 during March 3–May 8, 2020, and the successful elimination of the first wave of COVID-19 in the Faroe Islands. We assessed the effects of contact tracing, quarantine, and social distancing. We also estimated the average and observed number of secondary cases caused by each infector at the date of diagnosis during various stages of the epidemic.

Methods

Identification of COVID-19 Cases and Contacts

The government of Faroe Islands implemented lockdown on March 12, 2020, when only 3 confirmed cases were known in the country. The main nonpharmaceutical interventions were closing schools, childcare centers, and nonessential public workplaces. The government discouraged unnecessary travel and reduced transport to and from the country to a minimum. The government also promoted social distancing, frequent handwashing and use of hand sanitizers, and avoiding large gatherings. After March 12, all travelers arriving in the Faroe Islands were asked to self-quarantine for 14 days (Figure 2). Government authorities implemented all measures

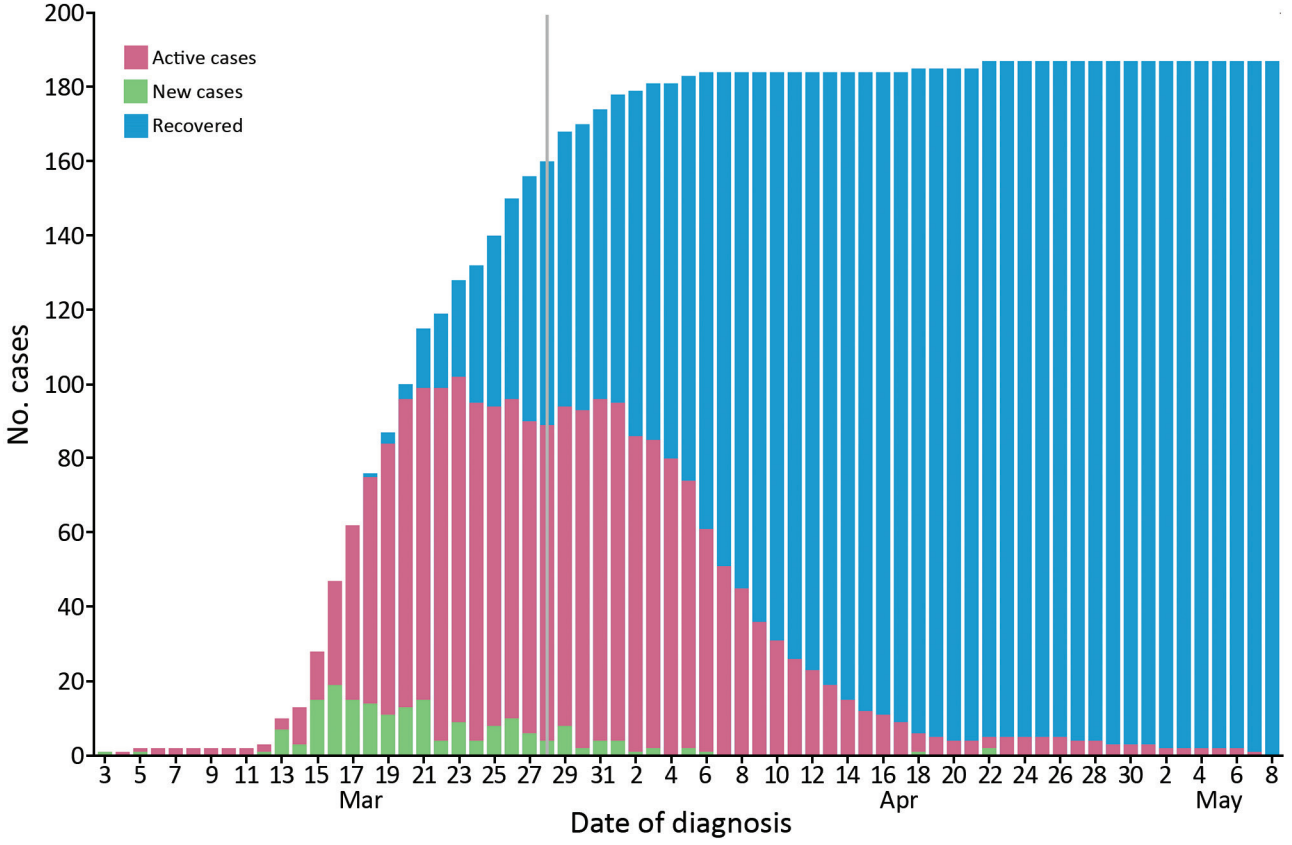

Figure 1. All confirmed cases of coronavirus disease in the Faroe Islands as of May 8, 2020. Active cases, recovered cases, new cases per day, and cumulative cases are shown. Vertical gray line indicates change in recovery criteria on March 28, which prolonged the required time for recovery to ≥14 days.

as nonmandatory recommendations, which the public generally followed.

The Faroe Islands quickly adapted diagnostic real-time reverse transcription PCR (RT-PCR) resources to test for severe acute respiratory syndrome coronavirus 2 (SARS-CoV-2), the virus that causes COVID-19. RT-PCR resources normally used in salmon farming by the Food and Veterinary Authority were adapted to implement a large-scale COVID-19 testing strategy early in the epidemic. This strategy enabled high testing capacity per capita; 600 tests per day were administered during the first days of the outbreak, and test results were available within 1–2 days.

The Office of the Chief Medical Officer performed contact tracing by requesting that all persons with positive RT-PCR test results self-isolate and list persons with whom they had close contact ≤48 hours before symptom onset. Asymptomatic positive persons were asked to list all contacts ≤48 hours before diagnosis. For contact tracing, close contacts were persons who had face-to-face contact ≤2 meters of a positive case for ≥15 minutes; direct physical contact with a case; direct care of a COVID-19 patient without using proper personal protective equipment; or other equally assessed exposures, such as living in a household with, having face-to-face contact for >15 minutes with, or riding in a vehicle with a confirmed COVID-19 case-patient (*4*). The Office of the Chief Medical Officer contacted all reported close contacts and requested that they quarantine for 14 days. If persons could not quarantine at home, the government offered hotel rooms free of charge to both cases and contacts.

The Ministry of Health established a COVID-19 task force (CTF) of medical doctors to maintain contact with all isolated COVID-19 cases and quarantined contacts. To monitor for symptom development and clinically evaluate whether cases needed to be hospitalized, task force members contacted diagnosed cases at intervals of ≤48 hours during isolation until the end of the quarantine period. CTF recorded information on the infection source, including whether the case was contracted from a known infector, an imported case, or an unknown source. CTF also recorded information on quarantine before RT-PCR testing and the

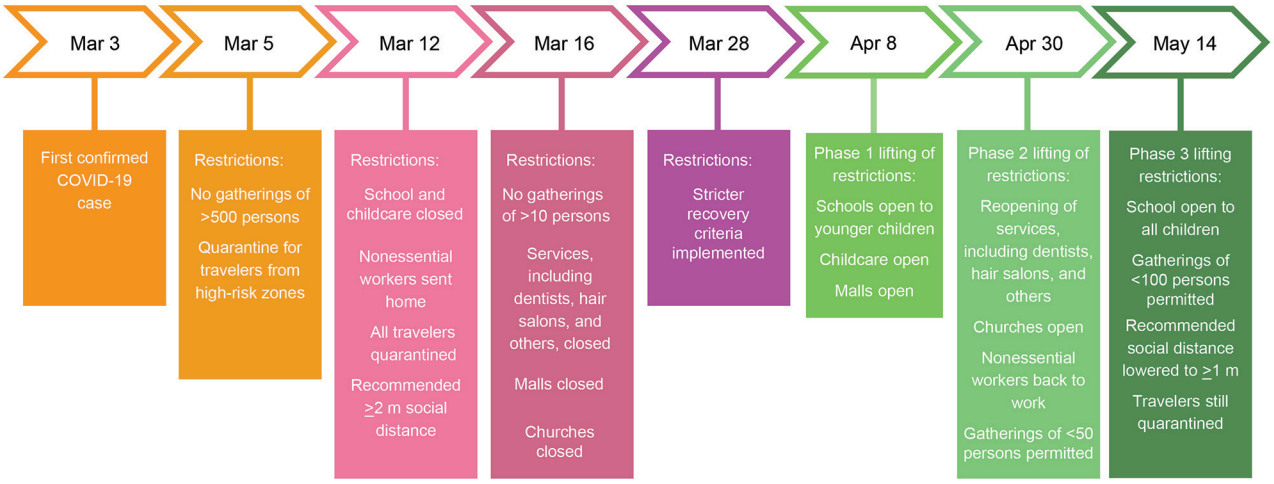

Figure 2. Timeline of government actions taken against COVID-19, Faroe Islands. Restrictions were not mandatory but generally were followed by the public. It is difficult to conclude which effect every specific nonpharmaceutical intervention had on the Faroese epidemic as several were implemented successively and some in parallel, although these interventions in concordance with contact tracing and quarantine managed to eliminate the first wave of the epidemic. COVID-19, coronavirus disease.

number of close contacts asked to quarantine. CTF recorded symptoms for all patients prospectively. Reported symptoms included cough, headache, throat pain, dyspnea, and fever. CTF also recorded the dates of illness onset, end of acute symptoms, and end of quarantine for patients.

Quarantined contacts were given a telephone number to call if symptoms developed. Shortly before the end of their quarantine, contacts were asked again whether symptoms had developed to determine whether they should be tested. Some asymptomatic contacts also were tested, but this was not done routinely. Testing required a referral from a doctor.

During the initial epidemic period, recovery criteria in the Faroe Islands followed guidelines from Denmark and considered persons who were without symptoms for ≥48 hours recovered. However, because observations indicated that 48 hours without symptoms did not ensure that the infectious period was over, recovery criteria were changed on March 28 to ≥14 days after a positive RT-PCR. Retesting was not recommended for positive cases and negative tests were not used as part of the recovery criteria.

Statistical Analyses

The serial interval is the time from symptom onset in a primary case to symptom onset in a secondary case. The generation time is the time between infection events in a primary case and a secondary case. Generation time is difficult to observe but is expected to be approximately equal to the serial interval (*5*,*6*). We chose to use the serial interval in all cases in this study and we estimated the mean serial interval by using the EpiEstim package in R (R Foundation for Statistical Computing, https://www.r-project.org). We assumed a gamma distributed model on 124 identified infector–infectee pairs for which symptom onset was known for both cases.

The reproduction number (R_0) is the average number of secondary cases each case will infect. A time-varying reproduction number (R_t) is the average number of secondary cases caused by each primary case at different times in the epidemic. R_t can be affected by government interventions, behavior changes, or when a certain fraction of the population is no longer susceptible to the pathogen because of immunity. We estimated R_t by using sliding 1-week windows, which assumes the transmission potential at given time t is the same as in the time window that ends at time t. We used the default 1-week window of the EpiEstim package (*7*) and took the average of the transmission potential of that sliding window to estimate R_t. Using sliding windows reduces noise while retaining the possibility to show changes in real-time in different phases in the epidemic. We used local serial interval data and the distribution of local and imported case counts as input data.

We determined the observed individual reproductive number (R_{obs}) by using transmission chains in the Faroe Islands. R_{obs} is the average number of observed secondary infections caused by each primary case at different times in the epidemic by date of diagnosis.

We made 2 adjustments to make R_t and R_{obs} data comparable. For cases of unknown transmission, we set the infector as diagnosed 5 days earlier by rounding the serial interval from 5.35 to 5 days to avoid

underestimating R_{obs} by censoring these cases. Because R_{obs} is based on the infector and R_t is based on the infectee, we displaced R_{obs} forward by the serial interval of 5 days to facilitate visual comparison of R_{obs} and R_t.

Determining Transmission Chains

We determined transmission chains by interviewing newly diagnosed patients about their contacts and whereabouts 2 weeks before symptom onset and linking this with information on previously known cases. If multiple exposures were known for a case and the most likely infector was uncertain, we chose the earliest diagnosed case as infector. Persons who had been abroad during the previous 14 days were classified as imported cases if no better explanation was known. When cases could not be linked to previous cases and had no recent travel history, we classified the transmission as unknown.

All study procedures were in accordance with the Declaration of Helsinki. The study was approved by the Data Protection Authority of the Faroe Islands (approval no. 20/00096-12).

Results

In the first wave of COVID-19, 187 cases were identified; the first case on March 3 and the last on April 22. On May 8, the Faroe Islands had no active COVID-19 cases. No fatalities or admissions to the intensive care unit occurred during this first wave. By May 8, a total of 7,653 RT-PCR tests for SARS-CoV-2 had been performed on 6,957 persons and the Faroe Islands had a per capita testing rate of 13,339/100,000 population, the highest globally (*8*,*9*). Furthermore, at that time, the Faroe Islands had the 12th highest confirmed cases per capita, 357/100,000 population (*8*,*9*) (Table).

Among identified case-patients, 88.8% experienced symptoms, the most prevalent of which were fever (63.1%), headache (47.6%), and cough (44.4%) (Table). More asymptomatic cases occurred among persons <18 (25%) and ≥65 years of age (30%) than among persons 18–64 years of age (6.3%) (Table). The mean time from symptom onset to diagnosis was 3.06 days (range <1–17 days; 95% CI 2.67–3.45 days); 6 cases were diagnosed before the onset of symptoms. The median age among case-patients was 40 years (range 0–92 years) (Table).

Among 187 cases, 8 patients were hospitalized, and the median length of hospitalization was 2 days (range 0–11 days). The median age of hospitalized case-patients was 57 years (range 37–92 years); and 1 patient was hospitalized twice. Among the 8 hospitalized case-patients, 7 had ≥1 underlying condition, including hypertension, emphysema, asthma, ulcerative colitis, diabetes, and cardiovascular disease.

We noted 10 cases of unknown or uncertain origin and 9 from known contact with a person who was not tested or who tested negative (Figure 3). We classified 30 cases as imported; 62 cases were acquired in a household, 39 in a workplace, 11 during an event, and 45 in other or unknown settings. Among imported cases, 20 did not cause further infections. We noted 4 large transmission chains that led to 105 other cases. We also noted 3 superspreading cases, each of which infected ≥10 secondary cases.

We estimated the serial interval by fitting a gamma distribution on symptom onset of infector–infectee pairs, resulting in a mean of 5.36 days (95% CI 4.63–6.09

Table. Occurrence, characteristics, and symptoms of 187 coronavirus disease cases during March 3–May 8, 2020, Faroe Islands*

	COVID-19 cases					
		Sex		Age range, y		
Variable	All cases	Male	Female	0–17	18–64	≥65
All cases	187	88 (47.1)	99 (52.9)	24 (12.8)	143 (76.5)	20 (10.7)
Cases/100,000 population	357	324	393	184	478	218
Cases tested by RT-PCR	6,957	3,091 (45.5)	3,866 (54.5)	1,132 (19.3)	4,965 (68.4)	860 (12.3)
RT-PCR tests/100,000 population	13,339	11,377	15,305	8,660	16,597	9,381
Reported symptoms						
Asymptomatic	21 (11.2)	11 (12.5)	10 (10.1)	6 (25.0)	9 (6.3)	6 (30.0)
Fever	118 (63.1)	55 (62.5)	63 (63.6)	12 (50.0)	94 (65.7)	12 (60.0)
Cough	83 (44.4)	47 (53.4)	36 (36.4)	4 (16.7)	71 (49.7)	8 (40.0)
Headache	89 (47.6)	36 (40.9)	53 (53.5)	5 (20.8)	78 (54.5)	6 (30.0)
Sore throat	56 (29.9)	24 (27.3)	32 (32.3)	3 (12.5)	51 (35,7)	2 (10.0)
Dyspnea	20 (10.7)	7 (8.0)	13 (13.1)	1 (4.2)	19 (13.3)	0 (0.0)
Loss of smell or taste†	63 (33.7)	23 (26.1)	40 (40.4)	3 (12.5)	56 (39.2)	4 (20.0)
Fatigue†	26 (13.9)	11 (12.5)	15 (15.2)	0 (0.0)	23 (16.1)	3 (15.0)
Rhinorrhea†	44 (23.5)	21 (23.9)	23 (23.2)	4 (16.7)	35 (24.5)	5 (25.0)
Body aches†	36 (19.3)	22 (25.0)	14 (14.1)	1 (4.2)	30 (21)	5 (25.0)
Chest tightness†	15 (8.0)	8 (9.1)	7 (7.1)	1 (4.2)	14 (9.8)	0 (0.0)
Diarrhea†	11 (5.9)	2 (2.3)	9 (9.1)	2 (8.3)	6 (4.2)	3 (15.0)
Abdominal pain†	11 (5.9)	4 (4.5)	7 (7.1)	3 (12.5)	4 (2.8)	4 (20.0)

*Values are no. (%) except as indicated. COVID-19, coronavirus disease; RT-PCR, reverse transcription PCR.
†Only recorded when mentioned by patients. Other symptoms were systematically collected.

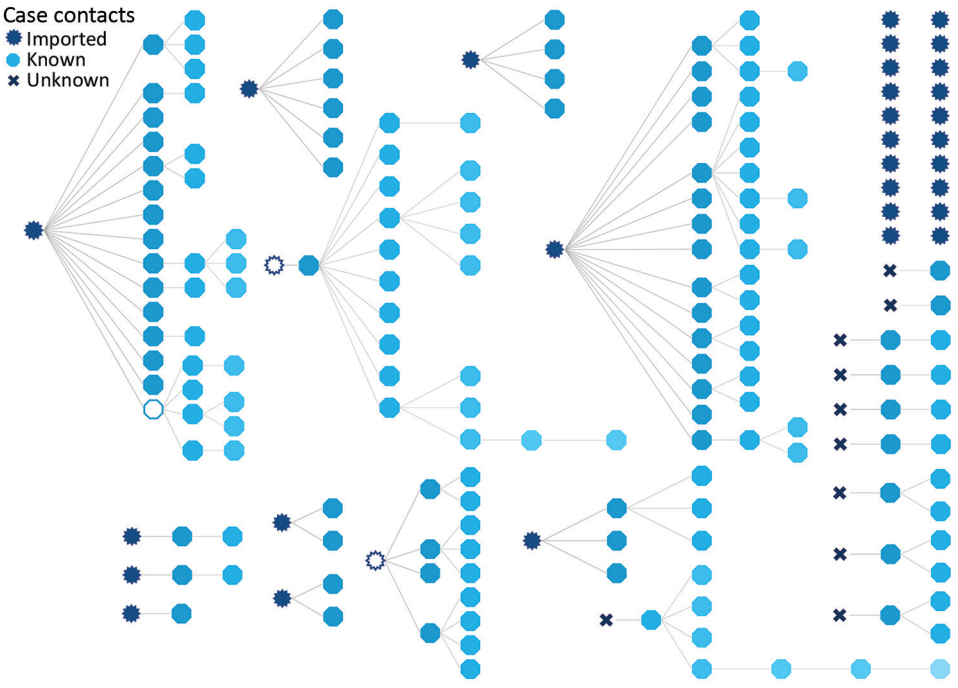

Figure 3. Transmission chains of coronavirus disease, Faroe Islands. All transmission chains are shown but are not represented chronologically. Transmission is based on persons, not events. The 3 open symbols represent known cases that were not tested or that tested negative for coronavirus. Blue shading in hectogons denotes secondary, tertiary, and quaternary cases infected from primary case. When multiple exposures were known for a case, the first exposure was chosen as the source of infection; this choice might slightly overestimate the number of secondary cases caused some infectors. The 20 cases shown in the top right were imported and led to no further infections. Among 9 cases that originated from contact with known but untested persons or persons with negative test results (denoted by open circles), we presume the tests were false negative; those who were not tested had relevant symptoms and contact with later cases but had left the country or the course of the disease was over before their case was discovered. We classified cases that caused ≥10 secondary infections superspreading cases.

days; SD 4.12 days, 95% CI 3.56–4.93 days). R_t peaked at 4.88 on March 16, after which it fell to <1 from March 24 onward. On April 22, we saw a short peak of >1 with the last case. After the last case, R_t rose to >1 again on May 4, even though no new cases were detected, but the 95% CI was quite large (95% CI 0.06–2.99). R_{obs} roughly followed R_t when displaced by the serial interval with a peak of 4.0 on March 17 (Figure 4).

During March 2–April 22, a total of 854 persons were quarantined because of close contact with a COVID-19 case; 132 (15%) were later confirmed as having COVID-19 cases. Fourteen persons were quarantined before diagnosis because of recent travel (Figure 5). For each identified case, the mean number of contacts quarantined was 5.1 (Figure 6).

Discussion

The Faroe Islands were one of the first countries in the Western Hemisphere to eliminate COVID-19, showing the feasibility of elimination in a country with well-defined borders, even starting with a high incidence. Testing, contact tracing, quarantine, and social distancing measures were instrumental to success in the Faroe Islands. These strategies have proven effective in suppressing the infection in other countries, including Iceland, Taiwan, Switzerland, and New Zealand (*10*–*13*). A notable success is that only 10.7% of COVID-19 cases in the Faroe Islands were among persons ≥65 years of age, even though this group constitutes 17.6% of the population (*3*). Low incidence among persons ≥65 years of age reflects the timely government restrictions on access to care homes, nursing homes, and hospitals, which might explain why no COVID-19 deaths or intensive care unit admissions occurred and only 8 case-patients were admitted to hospitals during the first wave in the Faroe Islands.

After the initial success of eliminating COVID-19, government travel restrictions remained strict, and a 14-day quarantine was recommended for travelers arriving in the country. Travel restrictions were loosened on June 15, quarantine was no longer requested, and only 1 test was required at the border. Lifting travel restrictions did not lead to an instant influx of cases, but some sporadic cases were found among tourists at the borders and foreign workers at harbors in the Faroe Islands. However, on August 4, two locally transmitted cases of unknown origin put an end to a streak of 104 days without locally transmitted cases.

The number of close contacts put in quarantine fell quickly after government recommendations were implemented (Figure 6). After the outbreak's initial

days, implemented restrictions resulted in quarantine of most new cases before diagnosis because of travel or contact with a previous case (Figure 5). This finding demonstrates that contact tracing and quarantine were effective strategies, despite some cases persisting without quarantine. Unquarantined cases were among cases of unknown origin or contacts not included in the close contact quarantine guidelines. Cases diagnosed outside of quarantine might indicate that contact tracing and quarantine would not have been enough to eliminate the epidemic without simultaneously implementing social distancing measures.

Mapping the transmission chains of COVID-19 revealed that most cases infected few or no secondary contacts, whereas 3 superspreading cases set off long, aggressive chains that led to most of the identified secondary locally transmitted cases. When we mapped transmission chains, among cases that had multiple exposures but the most likely infector was unclear, we chose the first diagnosed case in the chain as the infector, which might slightly overestimate the number of secondary cases caused by some infectors.

The observation of superspreading persons aligns with previous findings in many infectious disease outbreaks, including the 2002–2003 SARS outbreaks, in which a small percentage of cases in a population caused most transmission events, known as the 20/80 rule (*14*). Our observations support other reports that indicated super-spreading has played a major role in the current outbreak of COVID-19 (*15*).

Variation in demonstrated infectiousness can be affected by host, pathogen, or the environment. The 3

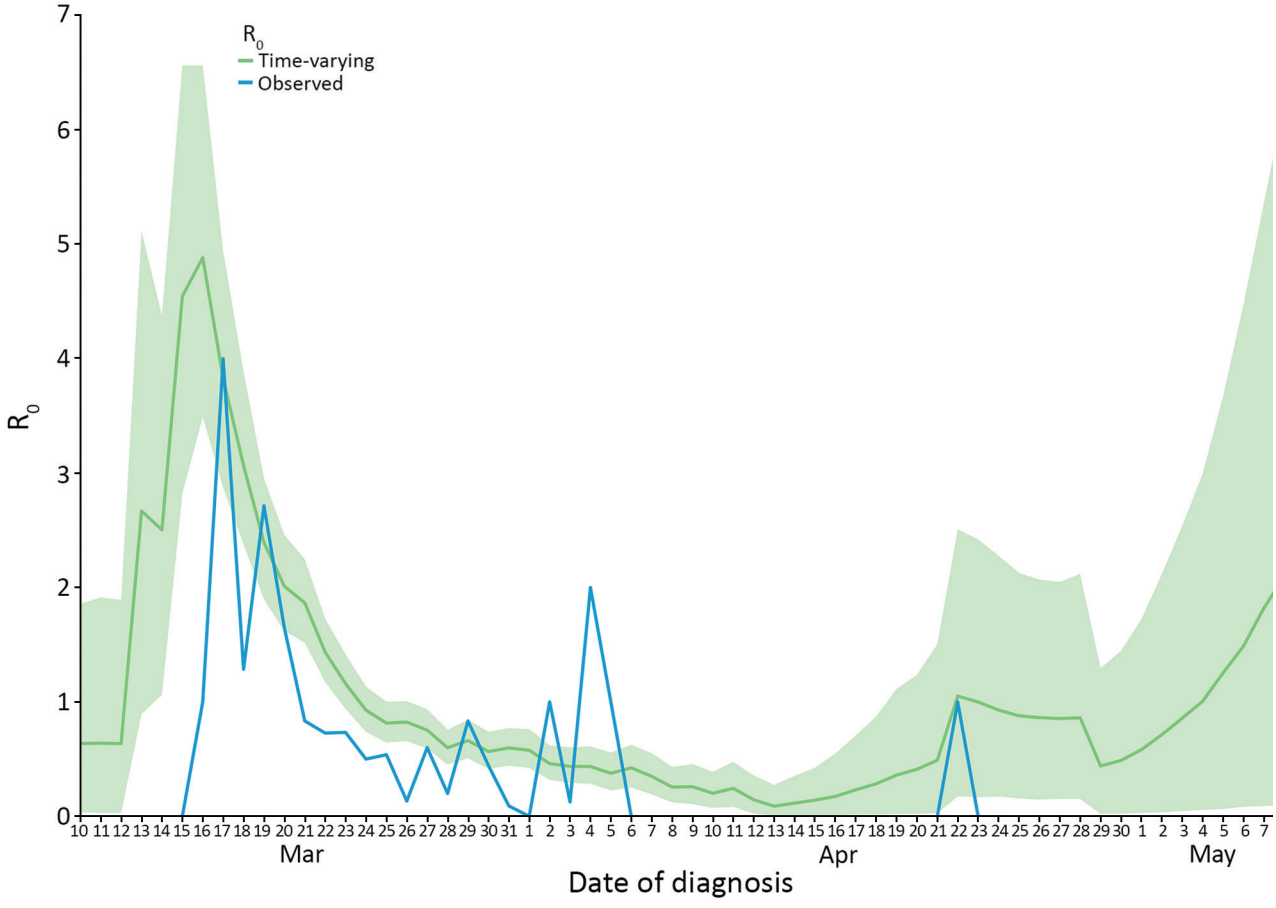

Figure 4. Time-varying reproduction number (R_t) and observed reproduction number (R_{obs}) for coronavirus disease by date, Faroe Islands. Green shading indicates 95% CI for R_t. We noted a rapid decrease in R_t, from 4.88 on March 16. From March 24 onward, R_t and R_{obs} were <1 until April 22 when the last case was confirmed in the Faroe Islands. After May 4, R_t rose >1 due to increasing uncertainty in the estimate. We calculated R_t by using the EpiEstim package in R (R Foundation for Statistical Computing, https://www.r-project.org) and local data on serial interval and imported cases. R_{obs} was determined by information from the transmission chains. We made 2 adjustments to compare R_{obs} to R_t: we moved R_{obs} 5 days forward (equal to the serial interval) because R_{obs} is measured on the infector; and we set R_t on the infected case. When the infector was unknown, we set transmission as 5 days earlier, equal to the serial interval, to avoid underestimating R_{obs} by censoring those cases. R_0, reproduction number; R_{obs}, observed reproduction number; R_t, time-varying reproduction number.

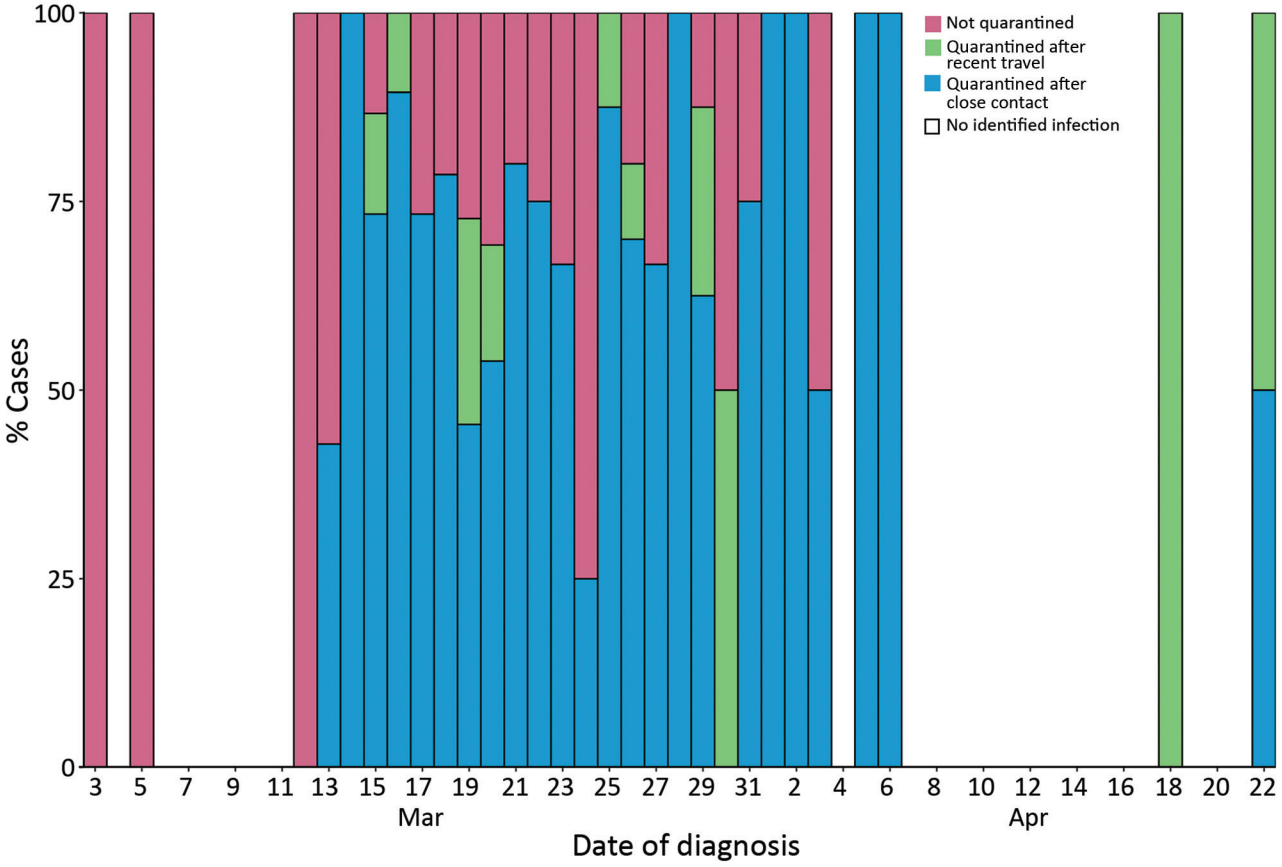

Figure 5. Percentage of known coronavirus disease cases quarantined by date, Faroe Islands. During March 3–12, 2020, no cases were quarantined because no previous infection was diagnosed in the Faroe Islands and travel quarantine was not enforced yet. After March 12, most cases were quarantined, either as a result of recent travel or close contact with a positive case. However, some nonquarantined cases persisted and an unquarantined case was identified on April 3.

superspreading cases in our study had many sporadic contacts, were of varying ages and of both sexes, and had no underlying conditions. Although we do not have data to speculate on why these persons spread the disease more effectively than others, known risk factors for superspreading described in the literature for other infectious disease epidemics include co-infections, a higher viral load in superspreaders, or that superspreaders had more close contacts than other cases (*14*,*16*). Other hypotheses for these apparent differences in COVID-19 spread could be that some transmission chains in the Faroe Islands had more contagious strains of SARS-CoV-2 than others, which other preliminary studies might support (*17*,*18*). Further studies, including sequencing of SARS-CoV-2 viruses from the Faroe Islands, will further investigate these aspects.

Of note, infection in the Faroe Islands appears to have been spread by a small number of quarantined children who tested negative, presumably because of false-negative tests. The children were exposed independently and were quarantined with their family members who later tested positive for SARS-CoV-2 without exposure to positive cases themselves. The children continued to test negative with repeated tests.

The Faroe Islands are a unique place to investigate the effects of COVID-19. Because of large-scale testing in the country, few unrecorded cases would be expected, and this was confirmed by seroprevalence study. The study, conducted during April–May in a representative 2% sample of the population, assessed SARS-CoV-2 seroprevalence at 0.7%, indicating only a few unrecorded cases (*19*). The performance and sensitivity of RT-PCR tests in community settings has been in doubt because the likelihood of a false-negative test is assumed to be higher among persons with mild or no symptoms compared with hospitalized patients. However, our practical experience shows that elimination is possible with large-scale testing, even if some cases might be missed due to false-negative results. One consequence of the intensive testing regime in the Faroe Islands is that clinical data reflect symptoms in the milder spectrum of COVID-19

disease. Studies in other countries might overestimate the prevalence of severe symptoms because severe cases are more likely to be tested in those settings, and some milder cases might be missed.

Studies from other countries have shown proportions of asymptomatic cases ranging from 11.9% to 51.7% (*12*,*20*–*22*). We found 11.2% of cases in our study were asymptomatic. One reason for the difference might be that COVID-19 symptoms initially were used as criteria for testing in the Faroe Islands and some asymptomatic cases might have been missed. Another explanation of the different proportion of asymptomatic cases might be misclassification of symptoms in previous reports from the country, meaning COVID-19 cases categorized as asymptomatic patients were presymptomatic. The most prevalent symptoms reported by COVID-19 cases in our study were fever, headache, and cough, similar to findings in other studies (*12*,*21*,*23*,*24*).

In the Faroe Islands, both R_t and R_{obs} showed a rapid decrease as effects of social distancing, contact tracing, and quarantine were established, which indicates that the measures had the desired effect. Toward the end of the epidemic, after May 4, R_t increased to >1 and had an increasingly high 95% CI, even though no new cases were detected after April 22. R_t should not increase without new cases, but the increase seen here is likely due to the small size of the dataset and increasing uncertainty.

If R_0 falls to <1, an epidemic will die out, indicating that measures to suppress the spread are working. Changes in R_0 should be interpreted with caution, and assigning causal effects to specific government measures is challenging because several measures were implemented at the same time or over short periods (Figure 2); their effects on the contagion only can be seen after some delay. The changes in individual behavior caused by the media focus on the pandemic probably also have had an independent effect from any government measures. Furthermore, the statistical methods we used frequently overestimate R_0 in the early stages of an epidemic, which would make the decrease in R_0 seem more rapid than it was (*25*).

Most countries have pursued a strategy to mitigate the spread of COVID-19 and flatten the epidemic curve, but others, such as New Zealand, announced a goal to eliminate COVID-19 (*13*,*26*). The Faroe Islands successfully eliminated COVID-19 on May 8, 2020,

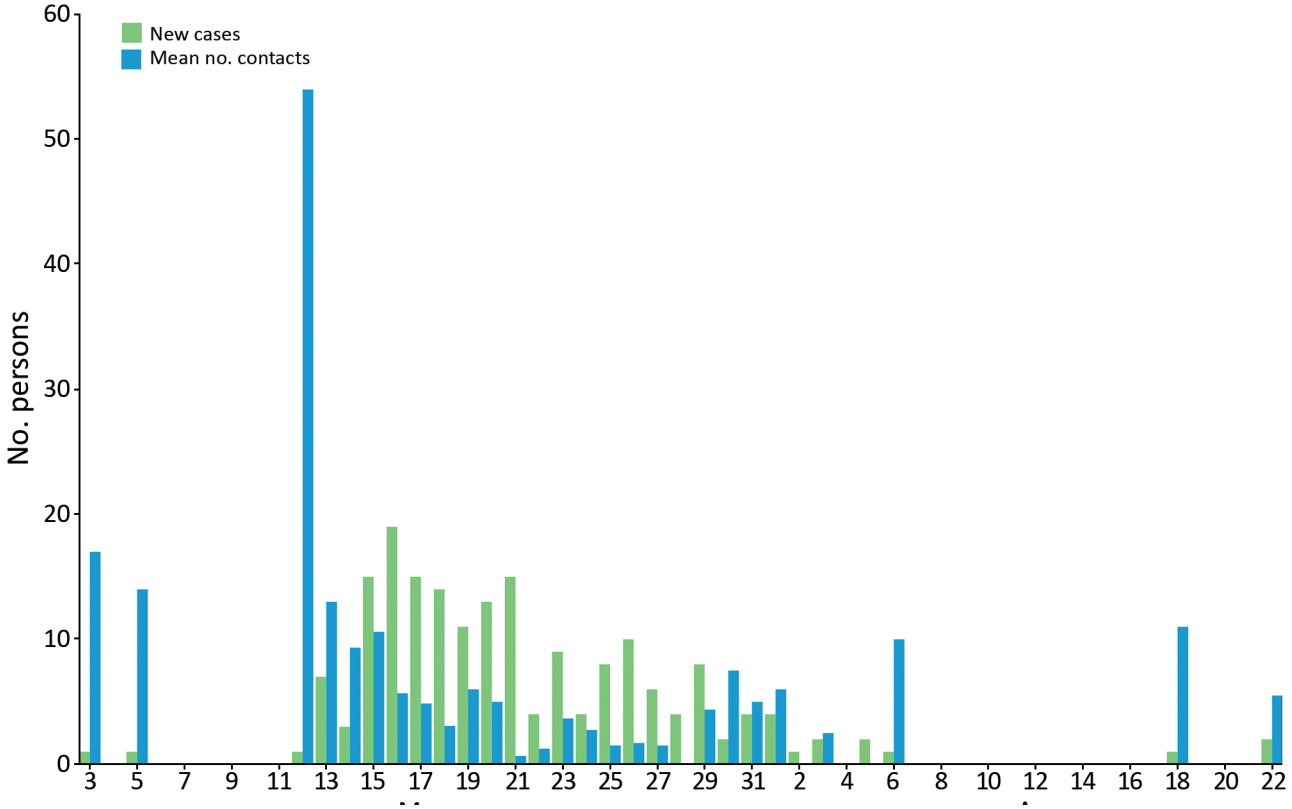

Figure 6. Mean number of contacts per coronavirus disease case placed in quarantine each day, Faroe Islands. The number of close contacts per case quickly dropped after March 12, 2020, and the effects of social distancing due to government measures, changes in social behaviors, and quarantine is apparent.

but because controls on incoming travelers were reduced, elimination did not last (*27*).

A strength of this study is the use of nationwide data that includes all confirmed cases and prospective reporting of symptoms, which gives a more accurate description of COVID-19 symptoms compared with studies focusing on admitted patients. Furthermore, because the Faroe Islands had some of the world's highest per capita testing rates, few unreported cases could be expected, strengthening the representation of the general course of the illness in the country.

Limitations of our study include the limited sensitivity of oropharyngeal swabs used for RT-PCR, which might lead to false-negative test results and, thus, underestimating the total number of cases. However, a follow-on seroprevalence study in the Faroe Islands indicated few unrecorded infections (*19*). With 187 cases, no fatalities, and few hospital admissions, ascertaining much about severe COVID-19 in the Faroe Islands is difficult, but the country shows a good representation of the most general course of disease. The Faroe Islands only have sea borders, and COVID-19 elimination here might not be readily generalizable to countries with land borders because control of incoming travelers can be more difficult in such settings.

In conclusion, our study includes all nationwide cases during the first wave of COVID-19 in the Faroe Islands, adds to the knowledge of COVID-19 symptoms in mild cases, and further supports to the role of superspreading in the pandemic. An effective suppression strategy led to eliminating the first wave of COVID-19 in the Faroe Islands, but the infection reappeared after the borders were reopened. This reemergence is indicative that other countries with easily monitored borders could feasibly eliminate COVID-19 by using a combination of large-scale testing, contact tracing, social distancing measures, and border restrictions. The rise of a second COVID-19 wave also is a warning that relaxing border restrictions will lead to a rise in infections.

Acknowledgments

We thank the doctors in the COVID-19 task force for collecting data and Lív Joensen for proofreading and editing the manuscript.

The project was funded partly by the special COVID-19 funding from the Faroese Research Council and partly by in-kind contributions by the participating institutions.

M.F.K., S.G., M.S., and M.S.P. drafted the manuscript; M.F.K., B.H.H., S.á B., and D.H.C. curated data; and M.F.K. and H.G. analyzed the data. All authors contributed to the revision of the manuscript and approved the final version.

About the Author

Dr. Kristiansen is a medical doctor and PhD student at the University of the Faroe Islands. His research interests include epidemiology, cancer, and COVID-19.

References

1. World Health Organization. WHO Director-General's opening remarks at the media briefing on COVID-19—11 Mar 2020 [cited 2021 Jan 12]. https://www.who.int/director-general/speeches/detail/who-director-general-s-opening-remarks-at-the-media-briefing-on-covid-19---11-march-2020
2. Spiteri G, Fielding J, Diercke M, Campese C, Enouf V, Gaymard A, et al. First cases of coronavirus disease 2019 (COVID-19) in the WHO European Region, 24 January to 21 February 2020. Euro Surveill. 2020;25:2000178. https://doi.org/10.2807/1560-7917.ES.2020.25.9.2000178
3. Hagstova Føroya. Population statistics, Faroe Islands [cited 2021 Jan 12]. https://hagstova.fo/en/population/population/population-0
4. World Health Organization. Coronavirus disease 2019 (COVID-19) situation report–61; 2020 Mar 21 [cited 2021 Jan 12]. https://apps.who.int/iris/handle/10665/331605
5. Griffin J, Casey M, Collins Á, Hunt K, McEvoy D, Byrne A, et al. Rapid review of available evidence on the serial interval and generation time of COVID-19. BMJ Open. 2020;10:e040263. https://doi.org/10.1136/bmjopen-2020-040263
6. Ma S, Zhang J, Zeng M, Yun Q, Guo W, Zheng Y, et al. Epidemiological parameters of COVID-19: case series study. J Med Internet Res. 2020;22:e19994. https://doi.org/10.2196/19994
7. Thompson RN, Stockwin JE, van Gaalen RD, Polonsky JA, Kamvar ZN, Demarsh PA, et al. Improved inference of time-varying reproduction numbers during infectious disease outbreaks. Epidemics. 2019;29:100356. https://doi.org/10.1016/j.epidem.2019.100356
8. Roser M, Ritchie H, Ortiz-Ospina E, Hasell J. Coronavirus pandemic (COVID-19). Our World in Data [cited 2021 Jan 12]. https://ourworldindata.org/covid-cases
9. Coronavirus in the Faroe Islands—statistics [in Danish] [cited 2021 Jan 12]. https://corona.fo/statistics
10. Salathé M, Althaus CL, Neher R, Stringhini S, Hodcroft E, Fellay J, et al. COVID-19 epidemic in Switzerland: on the importance of testing, contact tracing and isolation. Swiss Med Wkly. 2020;150:w20225. https://doi.org/10.4414/smw.2020.20225
11. Cheng H-Y, Jian S-W, Liu D-P, Ng T-C, Huang W-T, Lin H-H; Taiwan COVID-19 Outbreak Investigation Team. Contact tracing assessment of COVID-19 transmission dynamics in Taiwan and risk at different exposure periods before and after symptom onset. JAMA Intern Med. 2020;180:1156–63. https://doi.org/10.1001/jamainternmed.2020.2020
12. Gudbjartsson DF, Helgason A, Jonsson H, Magnusson OT, Melsted P, Norddahl GL, et al. Spread of SARS-CoV-2 in the Icelandic population. N Engl J Med. 2020;382:2302–15. https://doi.org/10.1056/NEJMoa2006100
13. Baker MG, Wilson N, Anglemyer A. Successful elimination of Covid-19 transmission in New Zealand. N Engl J Med. 2020;383:e56. https://doi.org/10.1056/NEJMc2025203
14. Stein RA. Super-spreaders in infectious diseases. Int J Infect Dis. 2011;15:e510–3. https://doi.org/10.1016/j.ijid.2010.06.020

15. Gómez-Carballa A, Bello X, Pardo-Seco J, Martinón-Torres F, Salas A. Mapping genome variation of SARS-CoV-2 worldwide highlights the impact of COVID-19 super-spreaders. Genome Res. 2020;30:1434–48. https://doi.org/10.1101/gr.266221.120
16. Shen Z, Ning F, Zhou W, He X, Lin C, Chin DP, et al. Superspreading SARS events, Beijing, 2003. Emerg Infect Dis. 2004;10:256–60. https://doi.org/10.3201/eid1002.030732
17. Tang X, Wu C, Li X, Song Y, Yao X, Wu X, et al. On the origin and continuing evolution of SARS-CoV-2. Natl Sci Rev. 2020 Mar 3;nwaa036. https://doi.org/10.1093/nsr/nwaa036
18. Koyama T, Platt D, Parida L. Variant analysis of COVID-19 genomes. Bull World Health Organ. 2020 Feb 24 [Epub ahead of print]. http://dx.doi.org/10.2471/BLT.20.253591
19. Petersen MS, Strøm M, Christiansen DH, Fjallsbak JP, Eliasen EH, Johansen M, et al. Seroprevalence of SARS-CoV-2–specific antibodies, Faroe Islands. Emerg Infect Dis. 2020;26:2761–3. https://doi.org/10.3201/eid2611.202736
20. Mizumoto K, Kagaya K, Zarebski A, Chowell G. Estimating the asymptomatic proportion of coronavirus disease 2019 (COVID-19) cases on board the Diamond Princess cruise ship, Yokohama, Japan, 2020. Euro Surveill. 2020;25:2000180. https://doi.org/10.2807/1560-7917.ES.2020.25.10.2000180
21. Zhu J, Ji P, Pang J, Zhong Z, Li H, He C, et al. Clinical characteristics of 3062 COVID-19 patients: A meta-analysis. J Med Virol. 2020;92:1902–14. https://doi.org/10.1002/jmv.25884
22. Lavezzo E, Franchin E, Ciavarella C, Cuomo-Dannenburg G, Barzon L, Del Vecchio C, et al.; Imperial College COVID-19 Response Team. Suppression of a SARS-CoV-2 outbreak in the Italian municipality of Vo′. Nature. 2020;584:425–9. https://doi.org/10.1038/s41586-020-2488-1
23. Guan WJ, Ni ZY, Hu Y, Liang WH, Ou CQ, He JX, et al.; China Medical Treatment Expert Group for Covid-19. Clinical characteristics of coronavirus disease 2019 in China. N Engl J Med. 2020;382:1708–20. https://doi.org/10.1056/NEJMoa2002032
24. Bi Q, Wu Y, Mei S, Ye C, Zou X, Zhang Z, et al. Epidemiology and transmission of COVID-19 in 391 cases and 1286 of their close contacts in Shenzhen, China: a retrospective cohort study. Lancet Infect Dis. 2020;20:911–9. https://doi.org/10.1016/S1473-3099(20)30287-5
25. O'Driscoll M, Harry C, Donnelly CA, Cori A, Dorigatti I. A comparative analysis of statistical methods to estimate the reproduction number in emerging epidemics with implications for the current COVID-19 pandemic. Clin Infect Dis. 2020 Oct 20 [Epub ahead of print]. https://doi.org/10.1093/cid/ciaa1599
26. Baker M, Kvalsvig A, Verrall AJ, Telfar-Barnard L, Wilson N. New Zealand's elimination strategy for the COVID-19 pandemic and what is required to make it work. N Z Med J. 2020;133:10–4.
27. Strøm M, Kristiansen MF, Christiansen DH, Weihe P, Petersen MS. Elimination of COVID-19 in the Faroe Islands: effectiveness of massive testing and intensive case and contact tracing. Lancet Reg Heal–Eur. 2020 Dec 29 [Epub ahead of print]. https://doi.org/10.1016/j.lanepe.2020.100011

Address for correspondence: Marnar Fríðheim Kristiansen, University of the Faroe Islands, Faculty of Health Sciences, J.C. Svabos gøta 14, Tórshavn FO-100, Faroe Islands; email: marfr@ls.fo

EID Podcast

Livestock, Phages, MRSA, and People in Denmark

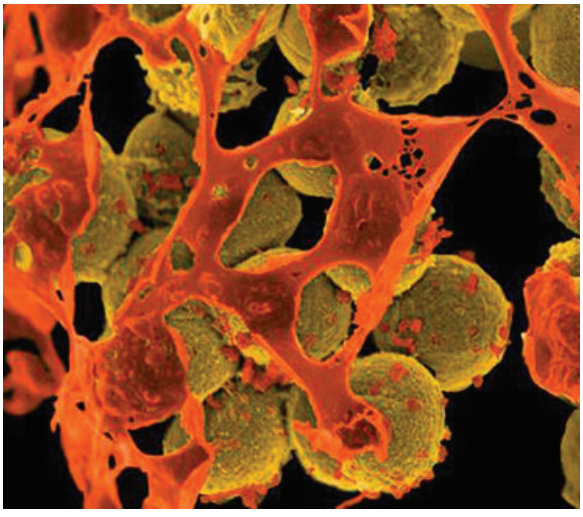

Methicillin-resistant *Staphylococcus aureus*, better known as MRSA, is often found on human skin. But MRSA can also cause dangerous infections that are resistant to common antimicrobial drugs. Epidemiologists carefully monitor any new mutations or transmission modes that might lead to the spread of this infection.

Approximately 15 years ago, MRSA emerged in livestock. From 2008 to 2018, the proportion of infected pigs in Denmark rocketed from 3.5% to 90%.

What happened, and what does this mean for human health?

In this EID podcast, Dr. Jesper Larsen, a senior researcher at the Statens Serum Institut, describes the spread of MRSA from livestock to humans.

Visit our website to listen:
https://go.usa.gov/x74Jh

EMERGING INFECTIOUS DISEASES®

Oral Human Papillomavirus Infection in Children during the First 6 Years of Life, Finland

Stina Syrjänen, Marjut Rintala, Marja Sarkola, Jaana Willberg, Jaana Rautava, Hanna Koskimaa, Anna Paaso, Kari Syrjänen, Seija Grénman,[1] Karolina Louvanto[1]

Human papillomavirus (HPV) infections are found in children, but transmission modes and outcomes are incompletely understood. We evaluated oral samples from 331 children in Finland who participated in the Finnish Family HPV Study from birth during 9 follow-up visits (mean time 51.9 months). We tested samples for 24 HPV genotypes. Oral HPV prevalence for children varied from 8.7% (at a 36-month visit) to 22.8% (at birth), and 18 HPV genotypes were identified. HPV16 was the most prevalent type to persist, followed by HPV18, HPV33, and HPV6. Persistent, oral, high-risk HPV infection for children was associated with oral HPV carriage of the mother at birth and seroconversion of the mother to high-risk HPV during follow-up (odds ratio 1.60–1.92, 95% CI 1.02–2.74). Children acquire their first oral HPV infection at an early age. The HPV status of the mother has a major impact on the outcome of oral HPV persistence for her offspring.

Cutaneous warts are common in children and are acquired mostly through horizontal transmission, but also through vertical transmission; lesions can persist asymptomatically for years (*1*). Unlike human papillomavirus (HPV) infections of the skin, mucosal HPV infections have mostly been regarded as sexually transmitted diseases. However, certain mucosal HPVs (α-HPVs) have also been found in virgins, infants, and children in oral and genital mucosa, implicating a nonsexual mode of transmission (*2*–*6*). From the clinical point of view, virus clades 7, 9, and 10, which include high-risk HPV genotypes, are the major subgroups of α-HPVs. These high-risk HPVs are known to be involved in development of anogenital and head and neck cancers, and estimated to be causally associated with ≈4.5% of all human cancers (*7*).

Author affiliations: University of Turku, Turku, Finland (S. Syrjänen, M. Rintala, J. Willberg, J. Rautava, H. Koskimaa, A. Paaso, S. Grenman, K. Louvanto); Central Hospital of Lahti, Lahti, Finland (M. Sarkola); Biohit Oyj, Helsinki, Finland (K. Syrjänen)

DOI: https://doi.org/10.3201/eid2703.202721

Nonsexual HPV transmission modes includes vertical or horizontal transmission and autoinoculation (i.e., multisite HPV infections, which can spread from 1 site to another within an individual). Vertical transmission can be further categorized as periconceptual (time around fertilization), prenatal (during pregnancy), and perinatal (during birth or immediately thereafter) (*3*,*8*). Perinatal transmission has been regarded as the most likely explanation for HPV detection in newborns. Several studies have shown that children born to HPV-positive mothers have a higher risk of becoming HPV positive (*9*–*14*). Meta-analysis of 3,128 mother–child pairs showed that children born to HPV-positive mothers were 33% more likely to be HPV positive than children born to HPV-negative mothers (*6*). This risk was even higher (45%) when only high-risk HPV infections were considered (*6*).

Periconceptual transmission could theoretically occur through infected oocytes or spermatozoa. HPV DNA has been detected in semen, sperm, seminal plasma, spermatozoa, and vas deferens (*15*). Studies have shown that the placenta is not a sterile microenvironment; instead, it has been shown to harbor both viruses and bacteria, which can further influence the maternal part of periconceptual transmission (*16*). HPV has been found in the placenta and shown to replicate in trophoblasts, which could feasibly explain prenatal transmission (*2*). A recent systematic review on intrauterine HPV transmission showed that the pooled percentage of antenatal vertical HPV transmission was 4.9% (95% CI 1.65%–9.85%), and the mode of delivery had no effect on this transmission (*17*).

Elucidation of the early HPV infections is needed to generate a comprehensive overview on the natural history of HPV infections. The main aims of this study were to characterize oral HPV prevalence and genotype variation in children in Finland and determine infection outcomes during the first 6 years of life.

[1]These senior authors contributed equally to this article.

Material and Methods

Participants

The Finnish Family HPV Study is a prospective cohort study conducted at the University of Turku and Turku University Hospital, Turku, Finland, since 1998. Members of 329 families were enrolled (329 mothers, 131 fathers, and 331 newborns) as described (*13*,*14*,*18*). Women were enrolled at a minimum of 36 weeks of their index pregnancy and subsequently followed up for 6 years. HPV status of mothers was not available before enrollment. All parents provided written, informed consent at the first visit for the study. The Research Ethics Committee of Turku University Hospital approved the study protocol and its amendments (#2/1998 and #2/2006).

We collected demographic data from parents by using structured questionnaires at baseline and at 3-year and 6-year visits. General health of children was recorded at the 36-month visit (Appendix Table 1, https://wwwnc.cdc.gov/EID/article/27/3/20-2721-App1.pdf), and examination of oral mucosa was performed at the 6-year follow-up visit.

Samples and HPV Genotyping

Oral scrapings for HPV testing were obtained at birth; at day 3 before leaving the hospital; and at 1-, 2-, 6-, 12-, 24-, and 36-month and 6-year follow-up visits. Oral scrapings were obtained by using a brush (Cytobrush; MedScan Medical AB, https://www.diapath.com) and covering the entire oral mucosa as described (*13*). HPV DNA was extracted from oral scrapings by using the high salt method, as described (*13*). For HPV testing, we used nested PCR (MY09/MY11 external primers and GP05+/bioGP06+ internal primers) because the viral load/cell and the number of infected cells among uninfected cells was expected to be low in oral samples.

After nested PCR, HPV genotyping was performed by using the Multimetrix Kit (Progen Biotechnik GmbH, https://www.progen.com), which detected 24 low-risk, putative high-risk, and high-risk HPV genotypes as follows: 6 low-risk genotypes (HPV6, 11, 42, 43, 44, and 70); 3 putative high-risk genotypes (HPV26, 53 and 66); and 15 high-risk genotypes (HPV16, 18, 31, 33, 35, 39, 45, 51, 52, 56, 58, 59, 68, 73, and 82 (*19*). Blood samples from the mother and father were taken at baseline and at 12, 24, and 36 months of the follow-up and stored as described (*20*). Antibodies to the major capsid protein L1 of HPV6, 11, 16, 18, and 45 were analyzed by using multiplex HPV serologic analysis based on glutathione S-transferase fusion protein capture on fluorescent beads, as described (*21*). Serum samples were scored as positive when antigen-specific medium fluorescence intensity values exceeded the cutoff level of 200 for L1 antigen of individual HPV types.

Statistical Analysis

Times in months to incident oral HPV infections were calculated from the baseline visit to the first incident event. Genotype-specific HPV persistence was recorded whenever $\geq$2 consecutive follow-up samples were positive for the same individual HPV genotype as a single infection or as part of a multiple-type infection. Clearance was defined as an event at any follow-up visit for which a previously HPV-positive test result turned out to be negative and remained HPV negative to the end of the follow-up. Times in months to the first clearance event were calculated as the time of the first visit by an HPV-positive patient to the first clearance event.

Predictors of incident HPV infection and genotype-specific HPV clearance or persistence were analyzed by using the most prevalent high-risk HPV types (species α7: HPV18, 39, 45, 59, 68, and 70; species α9: HPV16, 31 ,33, 35, 52, and 58). To model incident infections and genotype-specific HPV clearance, Poisson regression analysis was used. For persistence, a generalized estimating equation (GEE) modeling was used. In the univariate GEE model, all covariates recorded at baseline and previously implicated as potential risk factors for HPV infections were tested (*13*,*14*). The following risk factors were analyzed for the both parents: age; age at time of first sexual encounter; number of lifetime sexual partners; smoking; use of alcohol; history of skin warts, oral/genital warts, and papillomas; history of sexually transmitted infections; drug consumption; oral and genital HPV DNA status; and HPV serologic results at baseline before the birth of the index child. For the mother, the risk factors were a Pap test at baseline, delivery mode, rupture of membrane, and breast-feeding. In the multivariate GEE model, only variables that were significant in the univariate model were entered and adjusted for age. All statistical tests performed were 2-sided, and a p value <0.05 indicated significance. Statistical analyses were performed by using SPSS (https://www.ibm.com) and Stata version 15 (https://www.stata.com) software packages.

Results

Our study focused on oral HPV infections among the 331 infants born to the 329 mothers in the Finnish Family HPV Study cohort. The mean ± SD age of the mothers at enrollment was 25.5 ± 3.35 years. Of the

331 newborns, 5 did not participate in oral samplings at any visit, and 2 others had only 1 visit, resulting in a longitudinal cohort of 324 (171 girls and 153 boys) children (Figure). Participants had a follow-up mean ± SD age of 51.9 ± 28.9 months (range 0.03–99.7 months). Of these children, 77.6% were born by vaginal delivery and 22.4% by cesarean section.

We collected general background information for the general health of the children recorded at the 36-month visit as given by their parents (Table 1). Hand warts were reported only for 3 children, and a common childhood viral disease (molluscum contagiosum) was reported in for 18 children (n = 203). Allergy/atopic symptoms were identified in 26.6% of the children at the 36-month visit. For 54% of the index families, the child was a firstborn. At the 6-year follow-up visit, 11% (20/180) of the children had clinical lesions on their oral mucosa. The most common lesions were small hyperplastic lesions (3.9%), aphtous ulcers (2.8%), and red lesions (2.2%). Only 1 child had a papillary lesion; this child was positive for HPV16 at day 3, month 1, and month 24 and subsequently HPV negative at other visits. Hand warts at the time of examination were detected in 3% of the children. There was no correlation recorded between the presence of hand warts and oral HPV at the 6-year visit.

We also provide an overview of oral HPV infections in children who had HPV genotypes and their point prevalence during the follow-up period (Table 1). The prevalence of oral HPV varied from 8.7% to 22.8% over time, and was lowest at the 3-year visit and highest at birth. Altogether, 18 different HPV genotypes were identified in the oral mucosa. HPV16 was the most prevalent genotype, followed by HPV18, 6, 33, and 31. The prevalence of multiple-type infections varied from 0.3% to 3.7%. Overall, 22.9% of the oral samples collected immediately after birth were positive for HPV DNA. At that time point, the genotype distribution was also the widest (15 different HPV types), and the frequency of multiple-type infections was the highest (3.7%). At the 36-month visit, only 8.7% of the oral samples were positive for HPV, and only 4 genotypes (HPV6, 11, 16, and 18) were identified. At the 6-year visit, HPV prevalence increased again to 20.4%, and 8 different HPV genotypes were identified. A total of 25 different combinations of HPV co-infections (with ≥2 genotypes) were recorded, HPV16 was present in 56% (14/25) of these samples. When analyzed by sex, we found differences in HPV prevalence at 1-, 2-, 12-, and 36-month visits, but none at the 6-year visit. HPV positivity at birth or later was unrelated to the mode of delivery. Overall, 41.4% (135/329) of

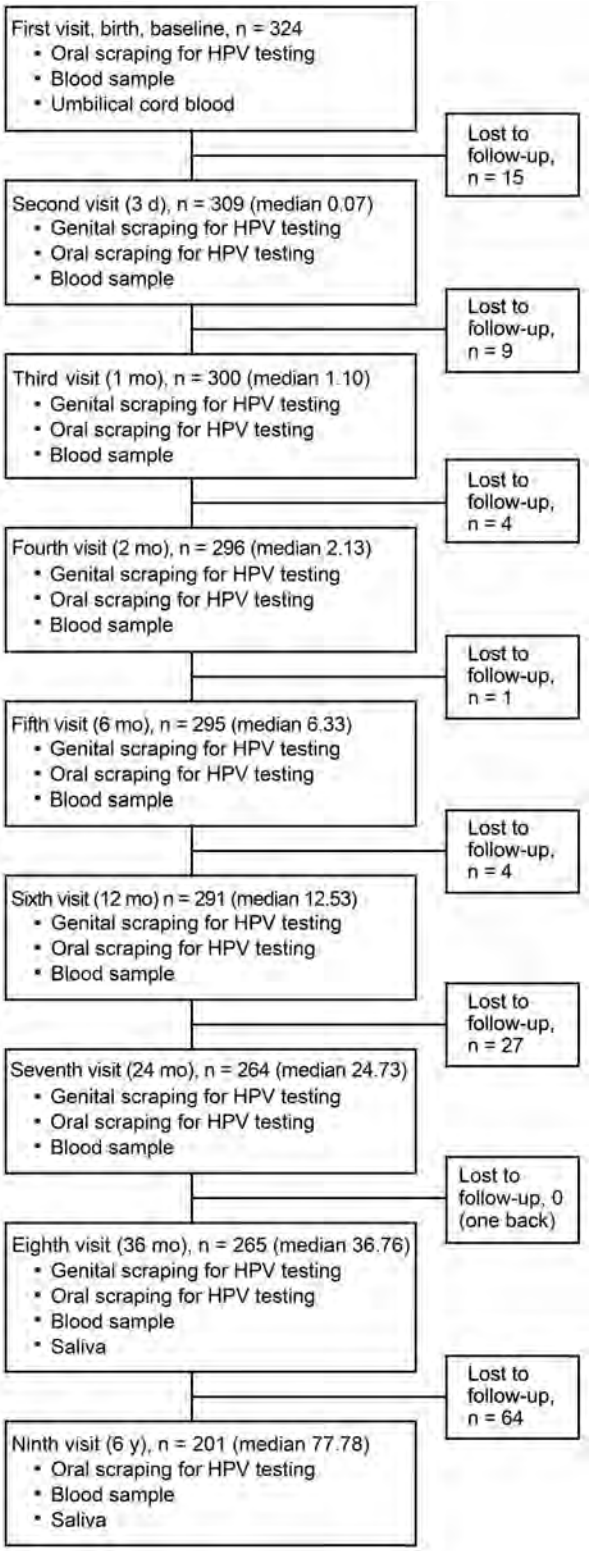

Figure. Oral HPV infection in 324 children in the Finnish Family HPV Study during the first 6 years of life. Each visit shows the number of children who participated in the specific follow-up, timeline of the visit, and samples obtained at each visit. HPV, human papillomavirus.

Table 1. Prevalence and genotype variation of oral HPV infections among 324 children from birth to 6 y of age*

Variable	At birth	3 d	1 mo	2 mo	6 mo	12 mo	24 mo	36 mo	6 y
Oral sample	324	309	300	296	295	291	264	265	201
Mean ± SD age, mo	0	0.08 ± 0.37	1.14 ± 0.18	2.23 ± 0.33	6.41 ± 0.45	12.61 ± 0.67	24.90 ± 1.01	36.98 ± 1.31	77.47 ± 11.01
Any HPV+	74 (22.8)	41 (13.3)	57 (19)	48 (16.2)	44 (14.9)	34 (11.7)	25 (9.5)	23 (8.7)	41 (20.4)
Girls, any HPV+	35 (47.9)	19 (46.3)	25 (43.9)	29 (60.4)	20 (46.5)	20 (58.5)	14 (56.0)	10 (43.5)	20 (49.9)
Boys, any HPV+	39 (52.1)	22 (53.7)	32 (56.1)	19 (39.6)	24 (53.5)	14 (51.5)	9 (44.0)	13 (56.5)	21 (51.2)
Single HPV+	62 (19.1)	36 (11.7)	55 (18.3)	44 (14.8)	36 (12.2)	33 (11.0)	20(7.6)	21 (7.9)	35 (17.4)
Multiple HPV (>2)	12 (3.7)	5 (1.6)	2 (0.7)	4 (1.4)	8 (2.7)	1 (0.3)	4 (1.5)	2 (0.8)	6 (3.0)
No. HPV genotypes	15	5	8	7	9	10	7	4	8
Low-risk HPV									
HPV6	11 (3.4)	5 (1.6)	3 (1.0)	7 (2.4)	4 (1.4)	3 (1.0)	1 (0.4)	2 (0.8)	4(2.0)
HPV11	1(0.3)	–	1 (1.0)	5 (1.7)	4 (1.4)	1 (0.3)	–	1 (0.4)	–
HPV70	2 (0.6)	–	–	1 (0.3)	1 (0.3)	1 (0.3)	2 (0.8)	–	–
High-risk HPV									
HPV16	25 (7.7)	28 (9.1)	30 (10)	16 (5.4)	14 (4.7)	14 (4.8)	9 (3.4)	17 (6.4)	20(10)
HPV18	4 (1.2)	1 (0.3)	9 (3.0)	11 (3.7)	7 (2.4)	8 (2.7)	4 (1.5)	1 (0.4)	2 (1.0)
HPV31	31 (0.9)	–	–	2 (0.7)	–	1 (0.3)	–	–	3 (1.5)
HPV33	2 (0.6)	–	8 (2.7)	2 (0.7)	1 (0.3)	–	2 (0.8)	–	2 (1.0)
HPV39	1 (0.3)	–	1 (0.3)	–	–	–	–	–	2 (1.0)
HPV45	1 (0.3)	–	1 (0.3)	–	1 (0.3)	–	–	–	1 (0.5)
HPV51	–	–	–	–	1 (0.3)	1 (0.3)	–	–	–
HPV52	–	–	–	–	–	1 (0.3)	–	–	–
HPV53	1 (0.3)	1 (0.3)	–		–	…	–	–	–
HPV56	3 (0.9)	–	–	–	–	1 (0.3)	1 (0.4)	–	–
HPV58	2 (0.6)	–	–	–	–	1 (0.3)	–	–	1 (0.5)
HPV66	4 (1.2)	1 (0.3)	2 (0.7)	–	1 (0.3)	–	1 (0.4)	–	–
HPV68	1 (0.3)	–	–	–	–	–	–	–	–
HPV82	1 (0.3)	–	–	–	–	–	–	–	–

*Values are no. (%) unless indicated otherwise. Two cases where excluded because of missing sample at birth. HPV, human papillomavirus. –, HPV genotype not found at that visit.

the children remained negative for all oral samples collected during the follow-up.

Incident HPV infection (baseline negative) was determined for 107 (32.8%) of 326 children: 107 cases/5,754 person-months at risk (PMR), which resulted in an incidence rate of 18.6 cases/1,000 PMR. Ten children (9.4%) had multiple-type infections among this group of incident infections. Kaplan-Meier analysis showed that there were no significant differences in the acquisition of oral HPV between the different species (Appendix Figure). The incidence of new HPV genotypes during the follow-up were also investigated by HPV clades. The results indicated that none of the HPV genotypes present at birth would promote acquisition of another specific HPV genotype, not even an HPV from the same clade. However, newborns with oral HPV6 or HPV11 (n = 4) acquired only HPV16 or HPV18 genotypes. We provide the type distribution of children who were positive at 6-year visit across different time points (Appendix Table 2). The results showed that 63% (26/41) had the same genotype detectable already at birth, and 14.6% (6/41) of the children had the same genotype at some visit during the follow-up, but not at birth. Of the children, 22% (9/41) had the genotype present only at most recent (6-year) follow-up visit. Four of the children positive for HPV6 at birth still had this genotype at their 6-year follow-up visit.

A total of 99 children cleared their oral HPV infection during the follow-up, resulting in a clearance rate of 19.1 cases/1,000 PMR (99/5,183). The mean clearance times for clades 10 (HPV6/11 and their closest relative), 9 (HPV16 group), and 7 (HPV18) genotypes were not significantly different: 28.6, 34.2, and 30 months, respectively (Appendix Figure).

A total of 14.9% (48/323) of the children had persistent oral HPV infection. The mean time of persistence was 20.6 months (range 0.1–92.2 months). We provide type-specific HPV persistence times (Table 2). The most prevalent type to persist was HPV16, which had a persistence time of 19.8 months, followed by multiple-type infections (persistence time 14.2 months), HPV18 (persistence time 11.8 months), HPV33 (persistence time 14.2 months), and HPV6 (persistence time 19.7 months). The 6 children who had multiple-type HPV infections at birth still had them at the most recent visit. Our results show that clade α9 resulted most frequently in the full-time persistence of oral HPV infection in early childhood, followed by clade α7.

We summarized the predictors of incident, cleared, and persistent oral high-risk HPV infections in these children (Table 3). All established or implicated

Table 2. Duration of genotype and species-specific persistence of oral HPV infection in children*

HPV genotypes/clades	No.	Mean persistence, mo (range)
HPV6	2	19.7 (1.8–37.5)
HPV16	36	19.8 (0.1–82)
HPV18	3	11.8 (5.0–18.6)
HPV31	1	92.2 (92.2)
HPV33	3	14.2 (1.0–40.6)
HPV39	1	89.0 (89.0)
HPV58	1	88.7 (88.7)
Multiple-type infections (≥2)	20	14.2 (1.0–91.0)
Clade A7: HPV18, 39, 45, 59, 68, 70, 85	4	31.2 (5.0–89.0)
Clade A9: HPV16, 31, 33, 35, 52, 58	41	22.8 (0.1–92.2)
Clade A10: HPV6, 11, 13, 44, 55, 74	2	19.7 (1.8–37.7)

*Persistence is defined as having ≥2 consecutive visit HPV-positive results for the same HPV genotype or clade. HPV, human papillomavirus.

risk factors in our previous studies were tested as covariates, but we report only those that showed any significant predictive value (Table 3). Demographic data obtained at the 36-month visit for children did not show any association for oral HPV (Appendix Table 1). High-risk HPV seropositivity was associated with oral high-risk HPV incidence for fathers and clearance for children. Incidence rates were 3.32 (95% CI 1.24–8.91) for fathers and 5.84 (95% CI 2.09–16.32) for children. Conversely, baseline oral carriage for mothers, as well as high-risk HPV seroconversion, were associated with persistent oral high-risk HPV infection for children. Odds ratios were 1.92 (95% CI 1.35–2.74) for baseline oral carriage and 1.60 (95% CI 1.02–2.50) for high-risk HPV seroconversion.

Discussion

HPV infections in the oral cavity have been detected in young children, but the outcome of these infections has remained unknown. We found that the prevalence of HPV and multiple-type infections was highest and the spectrum of HPV genotypes was widest at birth. The mode of delivery had no association with oral HPV carriage, and some sex differences were found in oral HPV prevalence during the early months, but not at the end of the follow-up period. Results indicate that none of the HPV genotypes present at birth would promote acquiring another specific HPV genotype, not even an HPV from the same clade. Although most of the oral HPV infections were cleared during the 6-year follow-up period, persistent oral HPV infection was found in 14.9% of these children. The 6 children who had multiple-type HPV infections at birth still harbored those infections at the most recent visit. Thus, clade α9 resulted most frequently in the full-time persistence of oral HPV infection during the early childhood, followed by α7 as the second most frequent clade.

HPV acquisition at birth has been regarded to be caused by vertical transmission, although controversial opinions have been reported (*3*,*5*,*6*). The debate is ongoing, particularly regarding the magnitude of risk, as well as route and timing, and whether mother-to-child transmission of HPV is a major infection route. Neonatal HPV infection through vertical transmission is believed to be transient, although there have been only a few follow-up studies (*5*,*11*,*12*,*22*). One of those studies showed that 37% (39/106) of

Table 3. Predictors of incident, cleared, and persistent high-risk HPV infection in oral mucosa of children*

	Oral high-risk HPV infection		
Predictor	Incident, IRR (95% CI)†	Clearance, IRR (95% CI)†	Persistence,‡ OR (95% CI)†
Oral HPV DNA			
Mother	1.05 (0.49–2.27)	1.72 (0.95–3.10)	**1.92 (1.35–2.74)**
Father	1.80 (0.79–4.08)	1.60 (0.70–3.65)	1.39 (0.57–3.39)
Seropositive to high-risk HPV at baseline			
Mother	1.67 (0.67–4.12)	1.76 (0.74–4.20)	1.15 (0.75–1.76)
Father	**3.32 (1.24–8.91)**	**5.84 (2.09–16.32)**	1.25 (0.61–2.53)
Seroconversion to high-risk HPV			
Mother	2.20 (0.90–5.36)	**2.86 (1.15–7.10)**	**1.60 (1.02–2.50)**
Father	1.10 (0.57–2.10)	1.44 (0.46–4.49)	0.92 (0.39–2.17)
Child	0.83 (0.56–1.23)	1.48 (0.55–3.95)	0.93 (0.58–1.48)

*Values in bold are significant. Analyses were performed by using generalized estimating equation modeling (persistence) and Panel Poisson (incident and cleared) restricted to high-risk HPV types from species 7 (HPV genotypes: 18, 39, 45, 59, 68, 70, 85) and 9 (HPV genotypes: 16, 31, 33, 35, 52, 58). HPV70 was also included in the analyses even if labeled as a low-risk HPV genotype in the insert of the Multiplex Kit (Progen Biotechnik GmbH, https://www.progen.com). HPV70 can be a possible carcinogen (limited evidence according to International Agency for Research on Cancer classification. HPV, human papillomavirus; IRR, incidence rate ratio; OR, odds ratio.
†Adjusted for age and all significant (and borderline significant) univariates in the model.
‡Binary outcome (persistent/not persistent), as defined by persistence of the 2 original HPV species (same genotype) during the follow-up.

nasopharyngeal aspirates of newborns were HPV positive, and concordance between HPV types in the mother (genital tract) and newborn was 69% (*12*). In a few days, HPV positivity disappeared in 38% of these newborns. However, 10.4% of the infants had the same HPV type detectable at birth and after 3 months to 3 years (*12*). Another study reported that 32% (31/98) of the children (age range 3.6 months–11.6 years) born to mothers who had cervical HPV infections at the time of delivery had HPV detectable in their oral mucosa (*11*). A total of 52% of these children had an HPV type identical with that of their mothers; HPV16/18 was most prevalent (81%).

Our results are consistent with previous results because they show that oral HPV is detectable in 22.8% of newborns. This HPV detection rate is almost identical to what Castellsague et al. reported in 2009, showing that the overall oral HPV prevalence at any visit was 18.2% during the mean follow-up of 14 months, by using PCR (MY09/MY11 primers), followed by subsequent hybridization with specific probes for HPV6, 11, 16, 18, 31, 33, and 39 (*22*). That study reported HPV positivity of 12.7% (14/110) at 6 weeks of age; in our study, HPV positivity at month 2 was 16.2% (48/296). Similar to our present results, HPV16 was the most frequent genotype, followed by HPV6/11, HPV18, and HPV31 (*22*) and in this study by HPV18, 6, 31, and 33.

Our results are derived from a longitudinal study rather than a cross-sectional study, in which autocorrelation (intrasubject variability) has been controlled by models for panel data (GEE and panel Poisson). Trottier et al. published their first results from the HERITAGE study on perinatal transmission and risk for HPV persistence in children (*23*). The design of their study is nearly identical with that of our study, but they extended sampling to conjunctival, pharyngeal, and genital sites. Their preliminary results on 75 HPV-positive participating mothers and their 67 infants sampled at birth and at 3-month visits showed that overall HPV positivity in children was 11% (range 5%–22%). Site-specific HPV positivity for conjunctival and genital areas were 4.8% and 4.8%, respectively (*23*). However, the HPV detection rate was only 8.1% for oral sites and 1.6% for oropharyngeal sites, which was lower than that reported in our study. Oral sampling (brushing of the entire oral mucosa vs. Dacron swab of buccal mucosa) and HPV amplification (nested vs. single PCR) might explain the differences in oral HPV detection rates between these 2 studies.

HPV data for mothers were not included in our report because these data have been reported in other studies (*14*,*20*,*24*,*25*). In brief, HPV DNA was detected in 17.9% of baseline oral samples from newborns and in 16.4% of maternal cervical samples (*14*). The HPV genotype-specific concordance between the newborns at delivery and the mothers was almost perfect (weighted $\kappa = 0.988$; 95% CI 0.951–0.997), but this concordance disappeared in 2 months (*14*). We have also shown that oral HPV carriage in newborns was most significantly associated with HPV presence in the placenta or cord blood (*9*,*14*). Together with these previous baseline data, our study strongly supports the hypothesis that HPV can be transmitted vertically and cause a true infection of oral mucosa of the newborn. Some of these oral HPV infections acquired at birth can also persist for years without any major clinical lesions. We reported the detection of HPV16-specific cell-mediated immunity in a small number of sexually inexperienced children from this cohort (*25*,*26*). However, we cannot determine by detection of HPV DNA the time when HPV-evoked immune recognition occurred. It has also been shown that half of healthy adults demonstrate HPV-specific cell-mediated immunity, irrespective of their partner/sexual status (*27*,*28*).

Oral HPV persistence during the 6-year follow-up period was predicted by oral HPV infection and seroconversion to high-risk HPV of the mother during the follow-up. We have recently shown that human leukocyte antigen G has a role in predicting the likelihood of the newborn for oral HPV infection at birth (*29*). However, human leukocyte antigen G had no association with HPV genotype-specific concordance between the mother and her child at birth or influence on perinatal HPV status of the child. This finding suggests that some persistent oral HPV infections after birth are not caused by vertical transmission but are acquired horizontally from the mother. This finding also indicates that transmission from a mother to her child continues during early childhood. In addition, some of the so-called persistent HPV infections could be reinfections among the family, and the incident HPV infections for a child were predicted by HPV seropositivity of the father. However, reinfection of the child needs to be further studied.

In our study, 41% of children remained constantly HPV negative during the follow-up period ($\leq$9 consequent oral samples). We do not know yet whether these children will continue to remain HPV negative later in life. We suspect that these children might be less prone to HPV infections in general, and would be interesting to evaluate again later in life.

In conclusion, our results indicate that HPV infection can be acquired nonsexually and is already

common at an early age. The oral cavity is the common site of the first HPV exposure, and the mother is the most likely source of first HPV infection in her child. These results have several major implications in HPV vaccination programs. If a subgroup of children can acquire a persistent HPV infection, the timing of prophylactic HPV vaccination is imperative. Maternal HPV antibodies, irrespective of whether they are acquired by natural HPV infection or vaccination, might protect the fetus, newborn, and young child against early HPV infection. In addition, children who have persistent HPV infections (caused by immunologic tolerance) might also benefit from vaccination, as has been the case with hepatitis B virus–infected newborns or children (*30*).

Acknowledgments

We thank Elisa Hovimäki for participating in the enrollment of the women in the Finnish Family HPV study and their clinical follow-up and Tatjana Peskova, Mariia Valkama, and Ketlin Adel for providing skillful technical assistance.

This study was supported by the Academy of Finland (grants 116438/2006 and 0204/2008), the Finnish Cancer Foundation, and the Sohlberg Foundation.

About the Author

Dr. Stina Syrjänen is a professor and chairman emerita in the Department of Oral Pathology, Faculty of Medicine, University of Turku, Turku, Finland, and chief physician in the Department of Pathology, Turku University Hospital. Her primary research interests are HPV, its transmission mode, and its role in early carcinogenesis.

References

1. Weissenborn SJ, De Koning MN, Wieland U, Quint WG, Pfister HJ. Intrafamilial transmission and family-specific spectra of cutaneous betapapillomaviruses. J Virol. 2009;83:811–6. https://doi.org/10.1128/JVI.01338-08
2. Rombaldi RL, Serafini EP, Mandelli J, Zimmermann E, Losquiavo KP. Perinatal transmission of human papilomavirus DNA. Virol J. 2009;6:83. https://doi.org/10.1186/1743-422X-6-83
3. Syrjänen S. Current concepts on human papillomavirus infections in children. APMIS. 2010;118:494–509. https://doi.org/10.1111/j.1600-0463.2010.02620.x
4. D'Souza G, Kluz N, Wentz A, Youngfellow RM, Griffioen A, Stammer E, et al. Oral human papillomavirus (HPV) infection among unvaccinated high-risk young adults. Cancers (Basel). 2014;6:1691–704. https://doi.org/10.3390/cancers6031691
5. Liu Z, Rashid T, Nyitray AG. Penises not required: a systematic review of the potential for human papillomavirus horizontal transmission that is non-sexual or does not include penile penetration. Sex Health. 2016;13:10–21. https://doi.org/10.1071/SH15089
6. Merckx M, Liesbeth WV, Arbyn M, Meys J, Weyers S, Temmerman M, et al. Transmission of carcinogenic human papillomavirus types from mother to child: a meta-analysis of published studies. Eur J Cancer Prev. 2013;22:277–85. https://doi.org/10.1097/CEJ.0b013e3283592c46
7. de Martel C, Plummer M, Vignat J, Franceschi S. Worldwide burden of cancer attributable to HPV by site, country and HPV type. Int J Cancer. 2017;141:664–70. https://doi.org/10.1002/ijc.30716
8. Chatzistamatiou K, Sotiriadis A, Agorastos T. Effect of mode of delivery on vertical human papillomavirus transmission: a meta-analysis. J Obstet Gynaecol. 2016;36:10–4. https://doi.org/10.3109/01443615.2015.1030606
9. Sarkola ME, Grénman SE, Rintala MA, Syrjänen KJ, Syrjänen SM. Human papillomavirus in the placenta and umbilical cord blood. Acta Obstet Gynecol Scand. 2008;87:1181–8. https://doi.org/10.1080/00016340802468308
10. Smith EM, Parker MA, Rubenstein LM, Haugen TH, Hamsikova E, Turek LP. Evidence for vertical transmission of HPV from mothers to infants. Infect Dis Obstet Gynecol. 2010;2010:326369. https://doi.org/10.1155/2010/326369
11. Puranen M, Yliskoski M, Saarikoski S, Syrjänen K, Syrjänen S. Vertical transmission of human papillomavirus from infected mothers to their newborn babies and persistence of the virus in childhood. Am J Obstet Gynecol. 1996;174:694–9. https://doi.org/10.1016/S0002-9378(96)70452-0
12. Puranen MH, Yliskoski MH, Saarikoski SV, Syrjänen KJ, Syrjänen SM. Exposure of an infant to cervical human papillomavirus infection of the mother is common. Am J Obstet Gynecol. 1997;176:1039–45. https://doi.org/10.1016/S0002-9378(97)70399-5
13. Rintala MA, Grénman SE, Puranen MH, Isolauri E, Ekblad U, Kero PO, et al. Transmission of high-risk human papillomavirus (HPV) between parents and infant: a prospective study of HPV in families in Finland. J Clin Microbiol. 2005;43:376–81. https://doi.org/10.1128/JCM.43.1.376-381.2005
14. Koskimaa HM, Waterboer T, Pawlita M, Grénman S, Syrjänen K, Syrjänen S. Human papillomavirus genotypes present in the oral mucosa of newborns and their concordance with maternal cervical human papillomavirus genotypes. J Pediatr. 2012;160:837–43. https://doi.org/10.1016/j.jpeds.2011.10.027
15. Laprise C, Trottier H, Monnier P, Coutlée F, Mayrand MH. Prevalence of human papillomaviruses in semen: a systematic review and meta-analysis. Hum Reprod. 2014;29:640–51. https://doi.org/10.1093/humrep/det453
16. Aagaard K, Ma J, Antony KM, Ganu R, Petrosino J, Versalovic J. The placenta harbors a unique microbiome. Sci Transl Med. 2014;6:237ra65. https://doi.org/10.1126/scitranslmed.3008599
17. Zouridis A, Kalampokas T, Panoulis K, Salakos N, Deligeoroglou E. Intrauterine HPV transmission: a systematic review of the literature. Arch Gynecol Obstet. 2018;298:35–44. https://doi.org/10.1007/s00404-018-4787-4
18. Louvanto K, Rintala MA, Syrjänen KJ, Grénman SE, Syrjänen SM. Genotype-specific persistence of genital human papillomavirus (HPV) infections in women followed for 6 years in the Finnish Family HPV study. J Infect Dis. 2010;202:436–44. https://doi.org/10.1086/653826
19. Schmitt M, Bravo IG, Snijders PJ, Gissmann L, Pawlita M, Waterboer T. Bead-based multiplex genotyping of human papillomaviruses. J Clin Microbiol. 2006;44:504–12. https://doi.org/10.1128/JCM.44.2.504-512.2006

20. Syrjänen S, Waterboer T, Sarkola M, Michael K, Rintala M, Syrjänen K, et al. Dynamics of human papillomavirus serology in women followed up for 36 months after pregnancy. J Gen Virol. 2009;90:1515–26. https://doi.org/10.1099/vir.0.007823-0
21. Waterboer T, Sehr P, Michael KM, Franceschi S, Nieland JD, Joos TO, et al. Multiplex human papillomavirus serology based on in situ-purified glutathione s-transferase fusion proteins. Clin Chem. 2005;51:1845–53. https://doi.org/10.1373/clinchem.2005.052381
22. Castellsagué X, Drudis T, Cañadas MP, Goncé A, Ros R, Pérez JM, et al. Human papillomavirus (HPV) infection in pregnant women and mother-to-child transmission of genital HPV genotypes: a prospective study in Spain. BMC Infect Dis. 2009;9:74. https://doi.org/10.1186/1471-2334-9-74
23. Trottier H, Mayrand MH, Coutlée F, Monnier P, Laporte L, Niyibizi J, et al. Human papillomavirus (HPV) perinatal transmission and risk of HPV persistence among children: design, methods and preliminary results of the HERITAGE study. Papillomavirus Res. 2016;2:145–52. https://doi.org/10.1016/j.pvr.2016.07.001
24. Rintala MA, Grénman SE, Järvenkylä ME, Syrjänen KJ, Syrjänen SM. High-risk types of human papillomavirus (HPV) DNA in oral and genital mucosa of infants during their first 3 years of life: experience from the Finnish HPV Family study. Clin Infect Dis. 2005;41:1728–33. https://doi.org/10.1086/498114
25. Koskimaa HM, Paaso AE, Welters MJ, Grénman SE, Syrjänen KJ, van der Burg SH, et al. Human papillomavirus 16 E2-, E6- and E7-specific T-cell responses in children and their mothers who developed incident cervical intraepithelial neoplasia during a 14-year follow-up of the Finnish Family HPV cohort. J Transl Med. 2014;12:44. https://doi.org/10.1186/1479-5876-12-44
26. de Jong A, van der Burg SH, Kwappenberg KM, van der Hulst JM, Franken KL, Geluk A, et al. Frequent detection of human papillomavirus 16 E2-specific T-helper immunity in healthy subjects. Cancer Res. 2002;62:472–9.
27. Koskimaa HM, Paaso A, Welters MJ, Grénman S, Syrjänen K, van der Burg SH, et al. Human papillomavirus 16-specific cell-mediated immunity in children born to mothers with incident cervical intraepithelial neoplasia (CIN) and to those constantly HPV negative. J Transl Med. 2015;13:370. https://doi.org/10.1186/s12967-015-0733-4
28. Welters MJ, de Jong A, van den Eeden SJ, van der Hulst JM, Kwappenberg KM, Hassane S, et al. Frequent display of human papillomavirus type 16 E6-specific memory t-Helper cells in the healthy population as witness of previous viral encounter. Cancer Res. 2003;63:636–41.
29. Louvanto K, Roger M, Faucher MC, Syrjänen K, Grenman S, Syrjänen S. HLA-G and vertical mother-to-child transmission of human papillomavirus infection. Hum Immunol. 2018; 79:471–6. https://doi.org/10.1016/j.humimm.2018.03.002
30. Qu C, Chen T, Fan C, Zhan Q, Wang Y, Lu J, et al. Efficacy of neonatal HBV vaccination on liver cancer and other liver diseases over 30-year follow-up of the Qidong hepatitis B intervention study: a cluster randomized controlled trial. PLoS Med. 2014;11:e1001774. https://doi.org/10.1371/journal.pmed.1001774

Address for correspondence: Stina Syrjänen, Department of Oral Pathology and Oral Radiology, Institute of Dentistry, Faculty of Medicine, University of Turku, Lemminkäisenkatu 2, 20520 Turku, Finland; e-mail: stisyr@utu.fi

EID Podcast
Enterovirus D68 and Acute Flaccid Myelitis, 2020

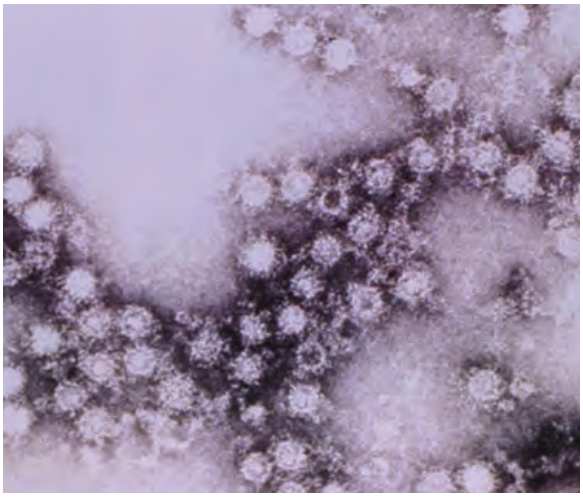

Around 2014, a mysterious, polio-like illness emerged in California and Colorado. Acute flaccid myelitis (AFM) primarily infects children, and if untreated, can lead to paralysis and respiratory failure. Despite extensive surveillance and research campaigns, the true cause of this debilitating disease remains unknown.

New research has shed light on a possible connection between AFM and a pathogen called enterovirus D68.

In this EID podcast, Dr. Sarah Kidd, a medical epidemiologist at CDC, and Sarah Gregory discuss what is known—and unknown—about AFM.

Visit our website to listen:
https://go.usa.gov/x7CkY

EMERGING INFECTIOUS DISEASES®

Daily Forecasting of Regional Epidemics of Coronavirus Disease with Bayesian Uncertainty Quantification, United States

Yen Ting Lin, Jacob Neumann, Ely F. Miller, Richard G. Posner, Abhishek Mallela, Cosmin Safta, Jaideep Ray, Gautam Thakur, Supriya Chinthavali, William S. Hlavacek

To increase situational awareness and support evidence-based policymaking, we formulated a mathematical model for coronavirus disease transmission within a regional population. This compartmental model accounts for quarantine, self-isolation, social distancing, a nonexponentially distributed incubation period, asymptomatic persons, and mild and severe forms of symptomatic disease. We used Bayesian inference to calibrate region-specific models for consistency with daily reports of confirmed cases in the 15 most populous metropolitan statistical areas in the United States. We also quantified uncertainty in parameter estimates and forecasts. This online learning approach enables early identification of new trends despite considerable variability in case reporting.

Coronavirus disease (COVID-19), caused by severe acute respiratory syndrome coronavirus 2 (SARS-CoV-2) (*1*), was detected in the United States in January 2020 (*2*). Researchers documented deaths in the United States caused by COVID-19 in February (*3*). Thereafter, surveillance testing expanded nationwide (*4*). These and other efforts revealed community spread across the United States and exponential growth of new COVID-19 cases throughout most of March. Growth of cases during February–April had a doubling time of 2–3 days (*5*), similar to the doubling time of the initial outbreak in China (*6*). The rapid increase in cases prompted broad adoption of social distancing practices such as teleworking, travel restrictions, use of face masks, and government mandates prohibiting public gatherings (*7*). The United States soon became a hotspot of the COVID-19 pandemic. In the United States, detection of new cases peaked in late April and steadily declined until mid-June (*4*). The decline in case numbers suggest that mandates and social distancing interventions effectively slowed COVID-19 transmission. Efforts to quantify the effects of these measures indicate that they substantially reduced disease prevalence (*8*,*9*).

In mid-June and mid-September 2020, the daily incidence of COVID-19 cases in the United States increased a second and third time (*4*). Public health officials must effectively monitor ongoing COVID-19 transmission to quickly respond to dangerous upticks in disease. To contribute to situational awareness of COVID-19 transmission dynamics, we developed a mathematical model for the daily incidence of COVID-19 in each of the 15 most populous US metropolitan statistical areas (MSAs) (*10*). Each model is composed of ordinary differential equations (ODEs) characterizing the dynamics of various populations, including subpopulations that did or did not practice social distancing.

We used online learning to calibrate our models for consistency with historical case reports. We also applied Bayesian methods to quantify uncertainties in predicted detection of new cases. This approach enabled identification of new epidemic trends despite variability in case detection. These findings can inform policymakers designing evidence-based responses to regional COVID-19 epidemics in the United States.

Methods

Data Used in Online Learning

We obtained reports of new confirmed cases from the GitHub repository maintained by The New York Times newspaper (*11*). Each day, at varying times

Author affiliations: Los Alamos National Laboratory, Los Alamos, New Mexico, USA (Y.T. Lin, W.S. Hlavacek); Northern Arizona University, Flagstaff, Arizona, USA (J. Neumann, E.F. Miller, R.G. Posner); University of California, Davis, California, USA (A. Mallela); Sandia National Laboratories, Livermore, California, USA (C. Safta, J. Ray); Oak Ridge National Laboratory, Oak Ridge, Tennessee, USA (G. Thakur, S. Chinthavali)

DOI: https://doi.org/10.3201/eid2703.203364

of day, we updated the model using cumulative data since January 21, 2020. The data in this analysis is from January 21–June 26, 2020. We aggregated county-level data to obtain case counts for each of the 15 most populous US MSAs, which encompass the following cities: New York City, New York; Los Angeles, California; Chicago, Illinois; Dallas, Texas; Houston, Texas; Washington, DC; Miami, Florida; Philadelphia, Pennsylvania; Atlanta, Georgia; Phoenix, Arizona; Boston, Massachusetts; San Francisco, California; Riverside, California; Detroit, Michigan; and Seattle, Washington.

The political entities comprising each MSA are those delineated by the federal government (*10*). The number of political units (i.e., counties and independent cities) in the MSAs of interest ranged from 2 (for the Los Angeles and Riverside MSAs) to 29 (for the Atlanta MSA). The median number of counties in an MSA was 7; the mean was 10. The number of states encompassing an MSA ranged from 1 (for 8/15 MSAs) to 4 (for Philadelphia). The median number of encompassing states was 1; the mean was 2.

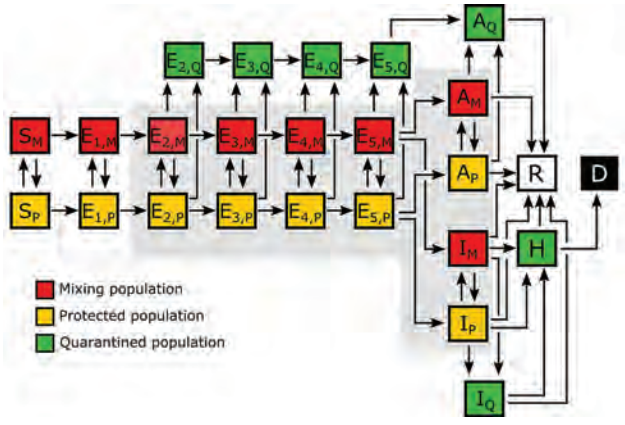

Figure 1. Illustration of the populations and processes considered in a mechanistic compartmental model of coronavirus disease daily incidence during regional epidemics, United States, 2020. The model accounts for susceptible persons (*S*), exposed persons without symptoms in the incubation phase of disease (*E*), asymptomatic persons in the immune clearance phase of disease (*A*), mildly ill symptomatic persons (*I*), severely ill persons in hospital or at home (*H*), recovered persons (*R*), and deceased persons (*D*). The model also accounts for social distancing, which establishes mixing ($_M$) and protected ($_P$) subpopulations; quarantine driven by testing and contact tracing, which establishes quarantined subpopulations ($_Q$); and self-isolation spurred by symptom awareness. Persons who are self-isolating because of symptoms are considered to be members of the I_Q population. The incubation period is divided into 5 stages (E_1–E_5), which enables the model to reproduce an empirically determined (nonexponential) Erlang distribution of waiting times for the onset of symptoms after infection (*12*). The exposed population consists of persons incubating virus and is comprised of presymptomatic and asymptomatic persons. The *A* populations consist of asymptomatic persons in the immune clearance phase. The gray background indicates the populations that contribute to disease transmission. An auxiliary measurement model (Appendix Equations 23, 24, https://wwwnc.cdc.gov/EID/article/27/3/20-3364-App1.pdf) accounts for imperfect detection and reporting of new cases. Only symptomatic cases are assumed to be detectable in surveillance testing. Red indicates the mixing population; yellow indicates the protected population; green indicates the quarantined population; white indicates the recovered population; black indicates the deceased population.

COVID-19 Transmission Model and Parameters

We used daily reports of new cases to parameterize a compartmental model for the regional COVID-19 epidemic in each of the 15 MSAs of interest. Until June 2020, we also parameterized curve-fitting models. However, curve-fitting models can generate only single-peak epidemic curves, so we abandoned this approach after the MSAs of interest all experienced multiple waves of disease (Appendix 1, https://wwwnc.cdc.gov/EID/article/27/3/20-3364-App1.pdf).

Each MSA-specific model accounted for 25 populations (Figure 1; Appendix 1 Figure 1). We considered infectious persons to be exposed and incubating virus (i.e., presymptomatic), asymptomatic while clearing virus, or symptomatic. The parameter ρ_E characterized the relative infectiousness of exposed persons and ρ_A characterized that of asymptomatic persons compared with symptomatic persons. In our model, infected persons quarantined with rate constant k_Q and symptomatic persons with mild disease quarantined with rate constant j_Q. We modeled social distancing by enabling the movement of susceptible and infectious persons between mixing and socially distanced (i.e., protected) populations. The size of the protected population was determined by 2 parameters: λ_i, a rate constant; and p_i, a steady-state population setpoint, where index i refers to the current social distancing period. The model accounts for varying adherence to social distancing practices over time by using n distinct social distancing periods after an initial period of social distancing. Persons in the protected population were less likely to be infected and less likely to transmit disease by a factor m_b. Within the mixing population, disease was transmitted with rate constant β. The model reproduced a nonexponentially distributed incubation period by dividing the incubation period into 5 sequential stages of equal mean duration, given by $1/k_L$. We considered infected persons in the first stage of the incubation period to be noninfectious and undetectable. A fraction of exposed persons, f_A, left the incubation period without symptoms. The remaining persons left with symptoms. The other symptomatic persons, f_H, progressed to severe disease; the

remainder had mild disease and recovered. The fraction of persons with severe disease who recovered is denoted as f_R; the others died. We considered hospitalized persons (or those at home with severe disease) to be quarantined. Persons left the asymptomatic state with rate constant c_A, left the mild disease state with rate constant c_I, and left the severe disease/hospitalized state with rate constant c_H.

The model consisted of 25 ODEs (Appendix 1 Equations 1–17). Each state variable of the model represented the size of a population. In addition to the 25 ODEs, we considered an auxiliary 1-parameter measurement model that related state variables to expected case reporting (Appendix 1 Equations 23, 24) and a negative binomial model for variability in new case detection (Appendix 1 Equations 25–27). We designed the model to consider multiple periods of social distancing with distinct setpoints for the quasistationary protected population size. The model always included an initial period of social distancing. The number of additional social distancing periods was given by n. Here, we considered only 2 cases: $n = 0$ and $n = 1$. We determined the best value of n by using model selection (Appendix 1).

The compartmental model and the auxiliary measurement model for $n = 0$ had a total of 20 parameters. We considered 6 of these parameters to have adjustable values (Table 1) and 14 to have fixed values (Tables 2, 3) (*12*–*20*; Appendix 1). The adjustable model parameters were t_0, the start time of the local epidemic; $\sigma > t_0$, the time at which the initial social distancing period began; p_0, the quasistationary fraction of the total population practicing social distancing; λ_0, an eigenvalue characterizing the rate of movement between the mixing and protected subpopulations and establishing a timescale for population-level adoption of social distancing practices; and β, which characterized the rate of disease transmission in the absence of social distancing. The measurement model parameter f_D represented the time-averaged fraction of new cases detected. Inference of adjustable parameter values was based on a negative binomial likelihood function (Appendix 1 Equation 27). The dispersal parameter r of the likelihood was adjustable; its value was jointly inferred with those of t_0, σ, p_0, λ_0, β, and f_D.

The compartmental model had 3 adjustable parameters for each additional social distancing period after the initial. For 1 additional period of social distancing ($n = 1$), the additional adjustable parameters were $\tau_1 > \sigma$, the onset time of second-phase social distancing; p_1, the second-phase quasistationary setpoint; and λ_1, which determined the timescale for transition from first- to second-phase social distancing behavior. For a second social distancing period, we replaced p_0 with p_1 and λ_0 with λ_1 at time $t = \tau_1$. If adherence to effective social distancing practices began to relax at time $t = \tau_1$, then $p_1 < p_0$.

Table 1. Inferred values of parameters in models for forecasting regional epidemics of coronavirus disease, United States

Parameter*	Estimate†	Definition
t_0	33 d	Start of transmission
σ	33 d	Start of social distancing
p_0	0.87	Social distancing setpoint
λ_0	0.10/d	Social distancing rate
β	2.0/d	Disease transmission rate
f_D	0.12	Fraction of active cases reported
r	12	Dispersal parameter of NB(r,p)‡

*t_0, σ, p_0, λ_0, and β are adjustable parameters of the compartmental model; f_D is a parameter of the auxiliary measurement model; and r is a parameter for the associated statistical model for noise in case detection and reporting.
†All estimates are region-specific and inference-time-dependent. Inferences were conducted daily. These findings reflect the maximum a posteriori estimates inferred for the New York City metropolitan statistical area using all confirmed coronavirus disease case count data available in the GitHub repository maintained by The New York Times newspaper (*11*) for January 21–June 21, 2020. Time $t = 0$ corresponds to midnight on January 21, 2020.
‡The probability parameter of NB(r,p) is constrained (i.e., its reporting-time-dependent value is determined by Appendix 1 Equation 26, https://wwwnc.cdc.gov/EID/article/27/3/20-3364-App1.pdf).

Statistical Model for Noisy Case Reporting

We used a deterministic compartmental model to predict the expected number of new confirmed COVID-19 cases reported daily. In other words, we assumed that the number of new cases reported over a 1-day period was a random variable and that the expected value would follow a deterministic

Table 2. Estimates for the fixed parameters of compartmental model for forecasting regional epidemics of coronavirus disease, United States

Parameter	Estimate	Source
S_0	19,216,182*	US Census Bureau (*13*)
I_0	1	Assumption
n	0†	Assumption
m_b	0.1	Assumption
ρ_E	1.1	Arons et al. (*14*)
ρ_A	0.9	Nguyen et al. (*15*)
k_L	0.94/d	Lauer et al. (*12*)
k_Q	0.0038/d	Assumption
j_Q	0.4/d	Assumption
f_A	0.44	(*16*,*17*)
f_H	0.054	Perez-Saez et al. (*18*)
f_R	0.79	Richardson et al. (*19*)
c_A	0.26/d	Sakurai et al. (*17*)
c_I	0.12/d	Wölfel et al. (*20*)
c_H	0.17/d	Richardson et al. (*19*)

*All estimates listed in this table are considered to apply to all regions of interest except for n, the number of distinct social distancing periods after an initial social distancing period, and S_0, the region-specific initial number of susceptible persons. The value given here for S_0 is the US Census Bureau estimated total population of the New York City metropolitan statistical area.
†$n = 0$, unless stated otherwise.

Table 3. Description of the fixed parameters of the compartmental model for forecasting regional epidemics of coronavirus disease, United States

Parameter	Definition
S_0	Initial size of susceptible population*
I_0	Initial no. infected individuals†
n	No. prior social distancing periods (e.g., 0 or 1)
m_b	Protective effect of social distancing‡
ρ_E	Relative infectiousness of an exposed person without symptoms during the incubation period§
ρ_A	Relative infectiousness of an asymptomatic person in the immune clearance phase of infection§
k_L	Rate constant for progression through each stage of the incubation period¶
k_Q	Rate constant for entry into quarantine for a person without symptoms
j_Q	Rate constant for entry into quarantine for a person with mild symptoms
f_A	Fraction of all cases that are asymptomatic
f_H	Fraction of all cases of severe disease (including patients requiring hospitalization or isolation at home)
f_R	Fraction of persons with severe disease who eventually recover
c_A	Rate constant for recovery of asymptomatic persons in the immune clearance phase of infection
c_I	Rate constant for recovery of symptomatic persons with mild disease or progression to severe disease#
c_H	Rate constant for recovery of symptomatic persons with severe disease or progression to death**

*Initial susceptible population within a given region is assumed to be the total regional population.
†Assuming that there is initially a single infected, symptomatic person.
‡This parameter defines the reduction in disease transmission caused by the protective effects of social distancing.
§This parameter characterizes infectiousness relative to a symptomatic person with all other factors being equal (i.e., a symptomatic person exhibiting the same social distancing behavior).
¶The incubation period is divided into 5 stages, each of equal duration on average.
#In the model, after a mean waiting time of $1/c_I$, symptomatic persons with mild disease recover or progress to severe disease.
**In the model, after a mean waiting time of $1/c_H$, symptomatic persons with severe disease recover or die.

trajectory. We further assumed that day-to-day fluctuations in the random variable were independent and characterized by a negative binomial distribution, denoted as NB(r,p). We used NB(r,p) to model noise in reporting and case detection. The support of this distribution is the nonnegative integers, which is natural for populations. Furthermore, the shape of NB(r,p) is flexible enough to recapitulate an array of unimodal empirical distributions. With these assumptions, we obtained a likelihood function (Appendix 1 Equation 27) in the form of a product of probability mass functions of NB(r,p). Formulation of a likelihood is a prerequisite for standard Bayesian inference; however, some related methods, such as approximate Bayesian computation, do not rely on a likelihood function.

Online Learning of Model Parameter Values through Bayesian Inference

We used Bayesian inference to identify adjustable model parameter values for each MSA of interest. In each inference, we assumed a uniform prior and used an adaptive Markov chain Monte Carlo algorithm (*21*) to generate samples of the posterior distribution for the adjustable parameters (Appendix 1).

The maximum a posteriori (MAP) estimate of a parameter is the value corresponding to the mode of its marginal posterior, where probability mass is highest. Because we assumed a uniform prior, our MAP estimates were maximum-likelihood estimates.

Forecasting with Quantification of Prediction Uncertainty: Bayesian Predictive Inference

In addition to inferring parameter values, we quantified uncertainty in predicted trajectories of daily case reports. We obtained a predictive inference of the expected number of new cases detected on a given day by parameterizing a model using a randomly-chosen parameter posterior sample generated in Markov chain Monte Carlo sampling. We then predicted the number of cases detected by adding a noise term, drawn from NB(r,p), where r is set at the randomly sampled value and p is set using an equation (Appendix 1 Equation 26).

We used LSODA (*22*; SciPy, https://scipy.org) to numerically integrate the described ODEs and obtain a prediction of the compartmental model for any given (1-day) surveillance period and specified settings for parameter values (Appendix 1 Equations 1–17, 23). The initial condition was defined by the inferred value of t_0 (Table 1) and the fixed settings for S_0 and I_0 (Tables 2, 3). We predicted the actual number of new cases detected by entering the predicted expected number of new cases into an equation (Appendix 1 Equation 29).

The 95% credible interval (CrI) for the predicted number of new case reports on a given day is the central part of the marginal predictive posterior capturing 95% of the probability mass. This region is bounded above by the 97.5th percentile and below by the 2.5th percentile.

Results

The objective of our study was to detect notable new trends in daily COVID-19 incidence as early as possible. We achieved this goal by systematically and regularly updating mathematical models capturing historical trends in regional COVID-19 epidemics using Bayesian inference and making forecasts with Bayesian uncertainty quantification.

Our analysis focused on the populations of US cities and their MSAs instead of regional populations within other political boundaries, such as those of US states. The boundaries of MSAs are based on social and economic interactions (*10*), which suggests that the population of an MSA is likely to be more uniformly affected by the COVID-19 pandemic than, for example, the population of a state. Accordingly, daily reports of new COVID-19 cases for the New York City MSA (Figure 2, panel A) are more temporally correlated than for the 3 states that make up the New York City MSA: New York (Figure 2, panel B), New Jersey (Figure 2, panel C), and Pennsylvania (Figure 2, panel D). Daily case counts for New Jersey resembled those for New York City because the 2 populations overlap considerably: ≈74% of New Jersey's population is part of the New York City MSA and ≈32% of the population of the New York City MSA is part of New Jersey (*13*).

For each of the 15 most populous US MSAs, we defined parameters for a compartmental model using MSA-specific surveillance data, namely aggregated county-level reports indicating the number of new confirmed COVID-19 cases within a given MSA each day. We made daily predictions by using Bayesian parameterization and forecasting with uncertainty quantification (UQ) for each of the 15 MSAs (Figure 3). Predictions took the form of a predictive posterior distribution and varied because of the uncertainties in adjustable model parameter estimates, which were characterized quantitatively through Bayesian inference. For these inferences we used the complete time series of available daily new case counts for the region of interest.

We conducted predictive inferences for all 15 MSAs of interest (Figure 4). We conditioned our predictions on the compartmental model with $n = 0$.

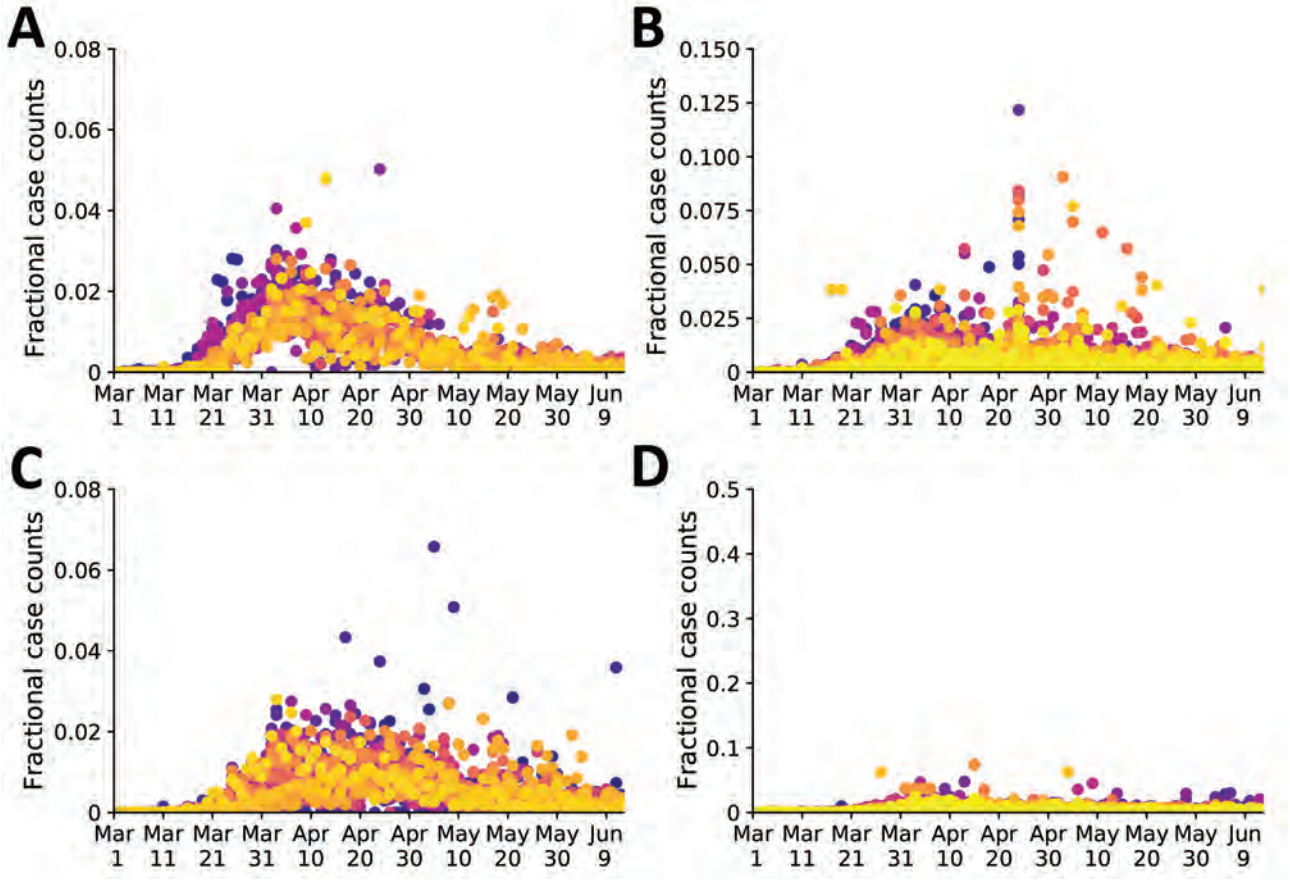

Figure 2. Temporal correlations of fractional case counts of coronavirus disease in and around the New York City, New York, metropolitan statistical area, United States, March 1–June 13, 2020. The fractional case count for a county on a given date is defined as the reported number of cases on that date divided by the total reported number of cases in the county over the entire time period of interest. Panels show the fractional cast counts for: A) the 23 counties comprising the New York City metropolitan statistical area (Fano factor 0.0026); B) the 62 counties comprising New York state (Fano factor 0.021); C) the 21 counties comprising New Jersey (Fano factor 1.2); and D) the 67 counties comprising Pennsylvania (Fano factor 0.028). Within each plot, different colors indicate the data points from each distinct county. Purple–yellow gradient indicates alphabetical order of the counties. A smaller Fano factor indicates less county-to-county variability.

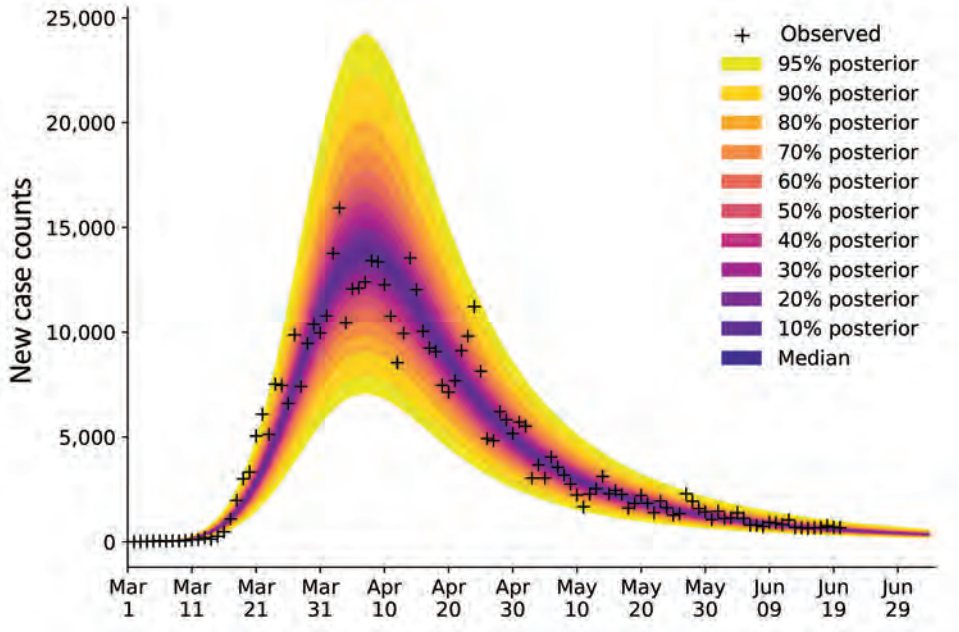

Figure 3. Illustration of Bayesian predictive inference for daily new case counts of coronavirus disease in the New York City, New York, metropolitan statistical area, United States, March 1–June 21, 2020. Daily reports of new cases forecasted with rigorous uncertainty quantification through online Bayesian learning of model parameters. Each day considers all daily case-reporting data available up to that point. We conducted Markov chain Monte Carlo sampling of the posterior distribution for a set of adjustable parameters. Subsampling of the posterior samples enabled the relevant model to generate trajectories of the epidemic curve that account for parametric and observation uncertainty. Crosses indicate observed daily case reports. The shaded region indicates the 95% credible interval for predictions of daily case reports. The color-coded bands within the shaded region indicate alternate credible intervals. The model was parametrized with uncertainty quantification data from January 21–June 21, 2020. The uncertainty bands/inferred model was used to make predictions for 14 days after the last observed data: the last prediction date was July 5, 2020.

These results demonstrate that, for the timeframe of interest, the compartmental model with $n = 0$ can reproduce many of the empirical epidemic curves for the MSAs of interest, which vary in shape.

We also calculated predictive inferences for the New York City and Phoenix MSAs over time (Figure 5; Appendix 2 Videos 1, 2, https://wwwnc.cdc.gov/EID/article/27/3/20-3364-App2.pdf). These results illustrate that accurate short-term predictions are possible; however, continual updating of parameter estimates is required to maintain accuracy.

We found that the adjustable parameters of the compartmental model had identifiable values, meaning that their marginal posteriors were unimodal (Figure 6). In the context of a deterministic model, the significance of identifiability is that, despite uncertainties in parameter estimates, we can expect predictive inferences of daily new case reports to cluster around a central trajectory. The results are representative (Figure 6); we routinely recovered unimodal marginal posteriors. However, we do not have a mathematical proof of identifiability for our model.

Usually, when we forecasted with UQ, the empirical new case count for the day immediately following our inference (+1), and often for each of several additional days, fell within the 95% CrI of the predictive posterior. When the reported number of new cases falls outside the 95% CrI and above the 97.5 percentile, we interpret this upward-trending rare event to have a probability of <0.025, assuming the model is both explanatory (i.e., consistent with historical data) and predictive of the near future. If the model is predictive of the near future, the probability of 2 consecutive rare events is far smaller, <0.001. Thus, consecutive upward-trending rare events, called upward-trending anomalies, can indicate that the model is not predictive. An anomaly suggests that the rate of COVID-19 transmission has increased beyond what can be explained by the model.

We did not observe upward-trending anomalies for the New York City MSA (Figure 7, panel A). However, for the Phoenix MSA, we observed several anomalies that preceded rapid and sustained growth in the number of new cases reported per day in June (Figure 7, panel B).

We assumed these anomalies arose from behavioral changes. To explain them, we enabled the compartmental model to account for a second social distancing period by increasing the setting for n from 0 to 1. With this change, the number of adjustable parameters increased from 7 to 10. One of the new parameters was τ_1, the start time of the second social distancing period. The other new parameters, λ_1 and p_1, replaced λ_0 and p_0 at time $t = \tau_1$. The compartmental model with 2 social distancing periods better explained the data from Phoenix than the compartmental model with only 1

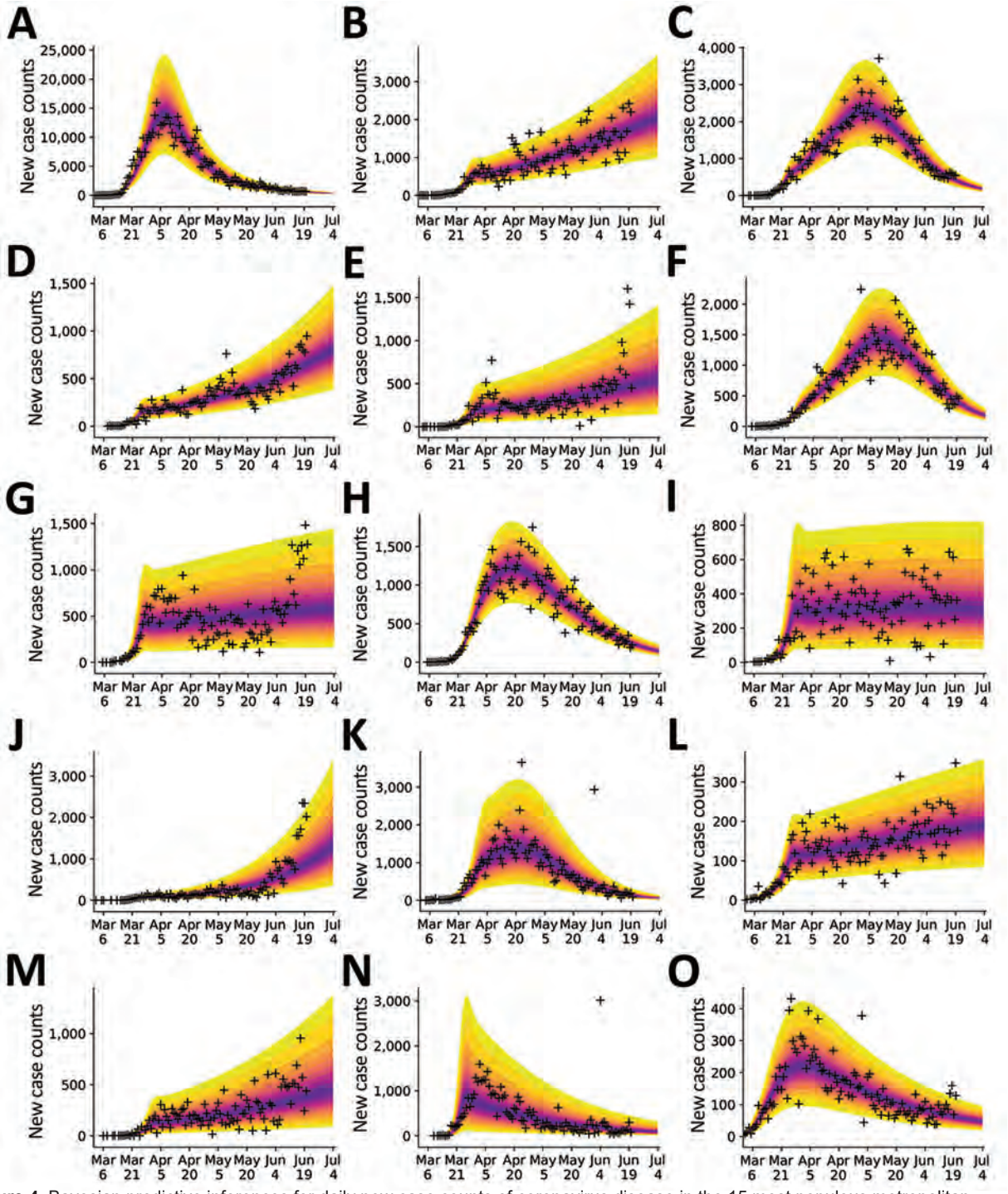

Figure 4. Bayesian predictive inferences for daily new case counts of coronavirus disease in the 15 most populous metropolitan statistical areas, United States, March 1–June 21, 2020. Predictions conditioned on the compartmental model with structure defined by *n* = 0, which accounts for a single initial period of social distancing. Inferences shown for the metropolitan statistical areas for the following cities: A) New York City, New York; B) Los Angeles, California; C) Chicago, Illinois; D) Dallas, Texas; E) Houston, Texas; F) Washington, DC; G) Miami, Florida; H) Philadelphia, Pennsylvania; I) Atlanta, Georgia; J) Phoenix, Arizona; K) Boston, Massachusetts; L) San Francisco, California; M) Riverside, California; N) Detroit, Michigan; and O) Seattle, Washington. Crosses indicate observed daily case reports. The shaded region indicates the 95% credible interval for predictions of daily case reports. The color-coded bands within the shaded region indicate alternate credible intervals. The model had parameters set by using uncertainty quantification by using data from January 21–June 21, 2020. The uncertainty bands/inferred model was used to make predictions for 14 days after the last observed data: the last prediction date was July 5, 2020.

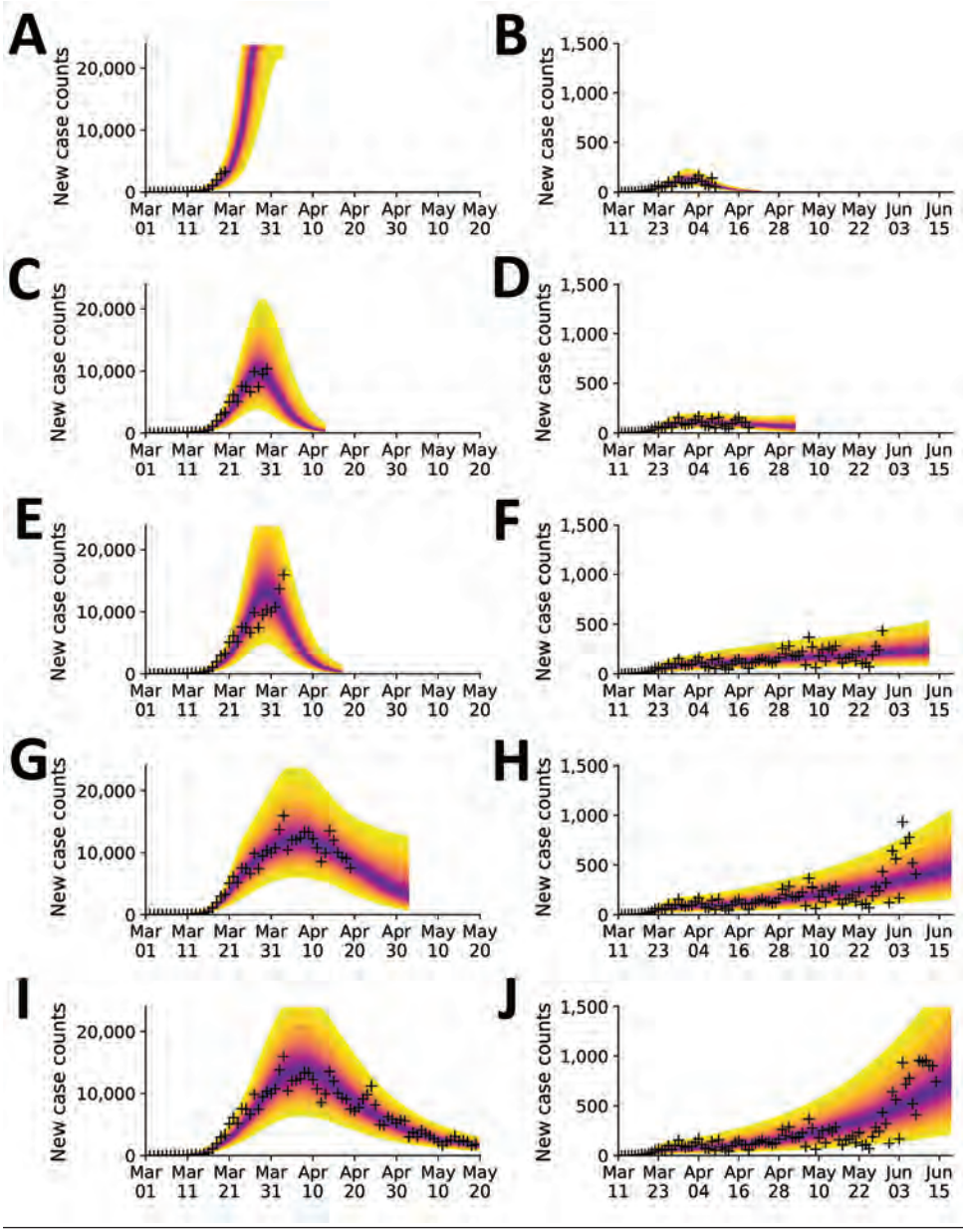

Figure 5. Illustration of the need for online learning for modeling daily new case counts of coronavirus disease in the New York City, New York, and Phoenix, Arizona, metropolitan statistical areas, United States, 2020. Predictions made over a series of progressively later dates as indicated for the New York City area (A, C, E, G, I) and the Phoenix area (B, D, F, H, J). Predictive inferences are data driven and conditioned on a compartmental model. Crosses indicate observed daily case reports. The shaded region indicates the 95% credible interval for predictions of daily case reports. The color-coded bands within the shaded region indicate alternate credible intervals. Predictions are accurate but only over a finite period of time into the future. New data must be considered as these data become available to maintain prediction accuracy. The model had parameters set by using uncertainty quantification using all data up to a terminal date, which differs in each panel. The uncertainty bands/inferred model was used to make predictions for 14 days after the last observed data point. For the New York City area, visualization began on March 1, 2020; the terminal dates were A) March 20, C) March 30, E) April 3, G) April 19, and I) May 19, 2020. For the Phoenix area, visualization began on March 11, 2020; the terminal dates were B) April 9, D) April 19, F) May 29, H) June 8, and J) June 18, 2020.

social distancing period (Figure 8, panels A and B). This conclusion is supported by the Akaike and Bayesian information criteria values for the 2 scenarios (Appendix 1 Table 1). Although these criteria are crude model selection tools in the context of non-Gaussian posteriors, we decided that they were adequately discriminatory. Each strongly indicates that the model with 2 social distancing periods better represented the data than the model with 1 social distancing period. Furthermore, the MAP estimate for p_1 (≈0.38) was less than that for p_0 (≈0.49) (Figure 8, panels C, D) and the marginal posteriors for these parameters were largely nonoverlapping (Figure 8, panel D). These findings suggest that the increase in COVID-19 cases in Phoenix can be explained by relaxation in social distancing practices, quantified by our estimates for p_0 and p_1. The MAP estimate of the start time of the second period of social distancing corresponds to May 24, 2020 (95% CrI May 20–28, 2020). Overall, 8 of the 9 observed anomalies occurred after this period, the first of which occurred on June 2, 2020 (Figure 8, panel B).

We hypothesized that a single event generating thousands of new infections, such as a mass gathering, might prompt a new upward trend in COVID-19 transmission. However, simulations for New York City and Phoenix did not support this hypothesis (Appendix 1 Figure 2). In each of these simulations, we moved a specified number of persons from the

mixing susceptible population S_M into the exposed population E_1 at the indicated time, May 30, 2020. Each perturbation increased disease incidence but had minimal effect on the slope of the trajectory of new case detection.

In addition to Phoenix, 4 other MSAs had contemporaneous trends explainable by relaxation of social distancing (Appendix 1 Table 1, Figure 3). MAP estimates for τ_1 indicate that the second social distancing period began on May 27, 2020 in Houston; April 19, 2020 in Miami; May 24, 2020 in Phoenix; June 12, 2020 in San Francisco; and June 7, 2020 in Seattle (Appendix 1 Figure 3). We detected upward-trending anomalies for these 5 MSAs (Appendix 1 Figure 4, panels A–D), but not for 3 of 4 other MSAs that had epidemic curves consistent with sustained social distancing (Appendix 1 Figure 4, panels E–H; Appendix 2 Videos 3–10). We assessed the overall prediction accuracy of the region-specific compartmental models (Appendix 1 Figure 5).

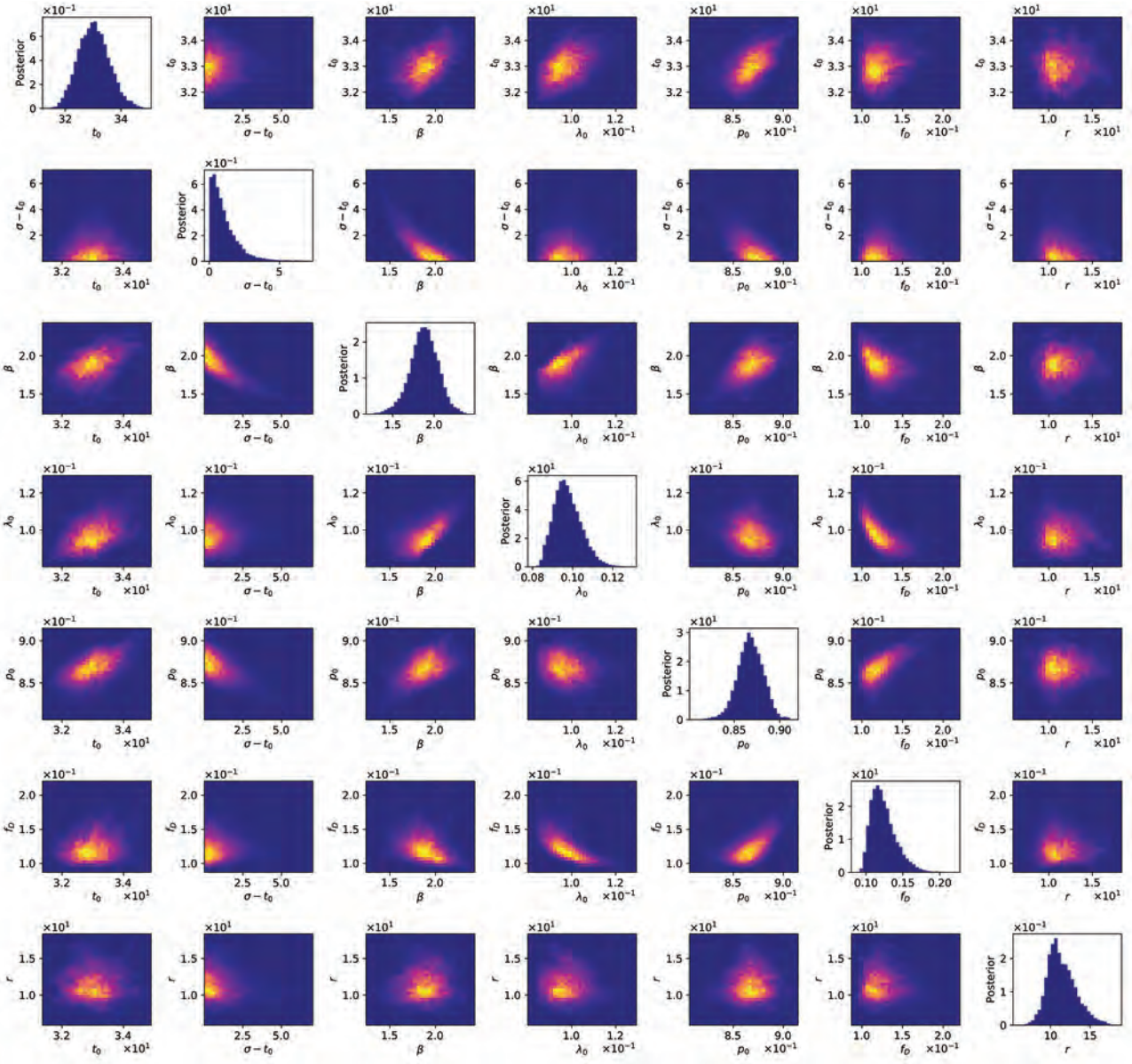

Figure 6. Matrix of 1- and 2-dimensional projections of the 7-dimensional posterior samples obtained for the adjustable parameters associated with the compartmental model (n = 0) for daily new case counts of coronavirus disease in the New York City, New York, metropolitan statistical area, United States, January 21–June 21, 2020. Plots of marginal posteriors (1-dimensional projections) are shown on the diagonal from top left to bottom right. Other plots are 2-dimensional projections indicating the correlations between parameter estimates. Brightness indicates higher probability density. A compact bright area indicates absence of or relatively low correlation. An extended, asymmetric bright area indicates relatively high correlation.

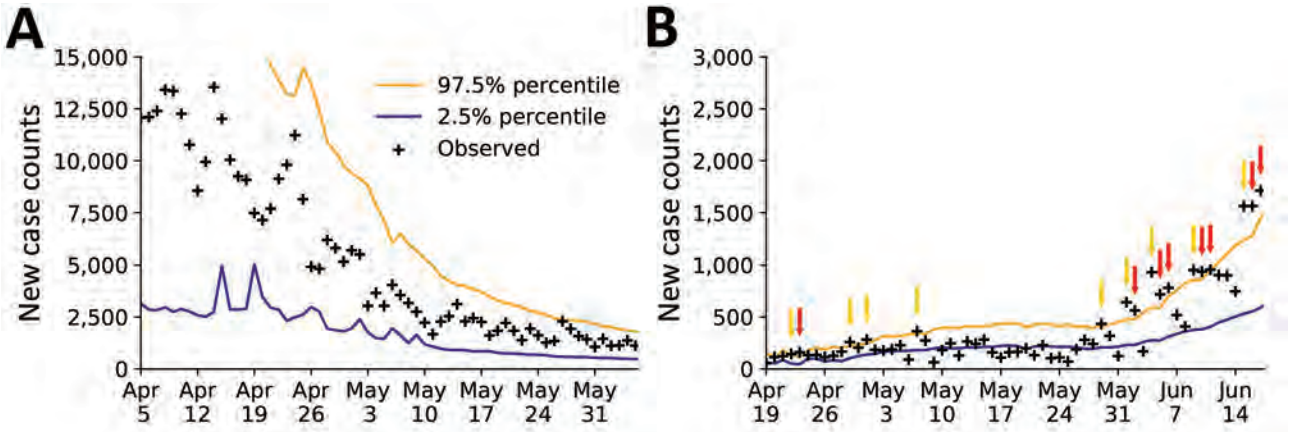

Figure 7. Rare events and anomalies in daily new case counts of coronavirus disease in (A) the New York City, New York metropolitan statistical area during April 5–June 4, 2020 and (B) Phoenix, Arizona, metropolitan statistical area during April 19–June 18, 2020, United States. Crosses indicate observed daily case reports. Orange line indicates 97.5% probability percentile; blue line indicates 2.5% probability percentile. Yellow arrows mark upward-trending rare events. Red arrows mark upward-trending anomalies.

Discussion

We found that online learning of model parameter values from real-time surveillance data is feasible for mathematical models of COVID-19 transmission. Furthermore, we found that predictive inference of the daily number of new cases reported is feasible for regional COVID-19 epidemics occurring in multiple US MSAs. We are continuing to perform daily forecasts and to disseminate the results (*23*,*24*). Inferences are computationally expensive and the cost increases as new data become available; thus, daily inferences using these methods might be impractical in some circumstances.

These predictive inferences can be used to identify harbingers of future growth in COVID-19 transmission rates. We found that 2 consecutive upward-trending rare events in which the number of new cases reported is above the upper limit of the 95% CrI of the predictive posterior might indicate potential for increased transmission during the following days to weeks. This feature might be especially predictive when anomalies are accompanied by increasing prediction uncertainty, as seen in Phoenix (Figure 7, panel B).

We found that the June increase in transmission rate of COVID-19 in the Phoenix metropolitan area can be explained by a reduction in the percentage of the population adhering to effective social distancing practices from ≈49% to ≈38% (Figure 8, panel D). However, our study sheds no light on which social distancing practices are effective at slowing COVID-19 transmission. We inferred that relaxation of

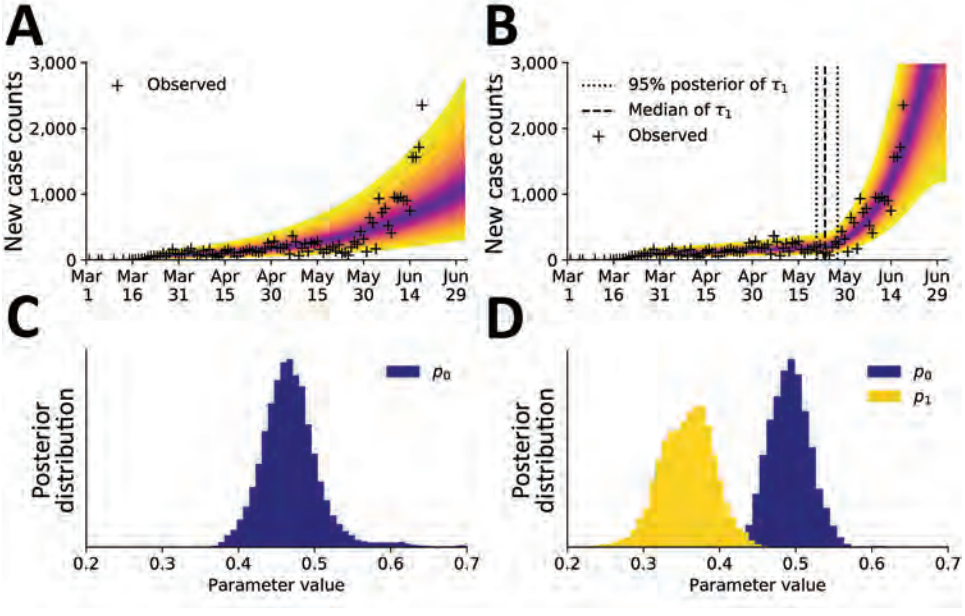

Figure 8. Predictions of the compartmental model for daily new case counts of coronavirus disease in the Phoenix, Arizona, metropolitan statistical area, United States, January 21–June 18, 2020. A) Model using 1 initial period of social distancing (n = 0). B) Model using an initial period of social distancing and a subsequent period of reduced adherence to social distancing practices (n = 1). C) The marginal posteriors for the social-distancing setpoint parameter p_0 inferred in panel A. D) The marginal posteriors for the social-distancing parameters p_0 and p_1 inferred in panel B.

social distancing measures began around May 24, 2020 (Figure 8, panel B). Contemporaneous upward trends in the rate of COVID-19 transmission in the Houston, Miami, San Francisco, and Seattle MSAs can also be explained by relaxation of social distancing (Appendix 1 Table 1, Figure 3). These findings are qualitatively consistent with earlier studies indicating that social distancing is effective at slowing the transmission of COVID-19 (*7*,*8*). These results also suggest that the future course of the pandemic is controllable, especially with accurate recognition of when stronger nonpharmaceutical interventions are needed to slow COVID-19 transmission.

One limitation of our study is that trend detection is data-driven, which means that a new trend cannot be detected until enough evidence has accumulated. Our analysis used reports of new cases, which reflect transmission dynamics of the past days to weeks rather than the current moment. Other types of surveillance data, such as assays of viral RNA in wastewater samples, also might improve situational awareness. Another limitation is that our inferences are based on a mathematical model associated with considerable structure and fixed parameter uncertainties and simplifications. Among the simplifications is the replacement of certain time-varying parameters, such as those characterizing testing capacities, with constants, which are assumed to provide an adequate time-averaged characterization. In this study, we used a deterministic compartmental model. If disease prevalence decreases, a stochastic version of the model might be more appropriate for forecasting efforts. Although the model can reproduce historical data and make accurate short-term forecasts, its structure and fixed parameters are subject to revision as we learn more about COVID-19. Furthermore, the model will need to be revised to account for vaccination. Results from serologic studies and estimates of excess deaths should enable model improvements.

This article was preprinted at https://arxiv.org/abs/2007.12523.

Y.T.L. received financial support from the Laboratory Directed Research and Development Program at Los Alamos National Laboratory (Project XX01); this support enabled early feasibility studies. Y.T.L., C.S., J.R., G.T., S.C., and W.S.H. were supported by the US Department of Energy Office of Science through the National Virtual Biotechnology Laboratory, a consortium of national laboratories (Argonne, Los Alamos, Oak Ridge, and Sandia) focused on responding to COVID-19, with funding provided by the Coronavirus CARES Act. J.N., E.M., and R.G.P. were supported by the National Institute of General Medical Sciences of the National Institutes of Health (grant no. R01GM111510). A.M. received financial support from the 2020 Mathematical Sciences Graduate Internship program, which is sponsored by the Division of Mathematical Sciences of the National Science Foundation. Computational resources were from the Darwin cluster at Los Alamos National Laboratory, which is supported by the Computational Systems and Software Environment subprogram of the Advanced Simulation and Computing program at Los Alamos National Laboratory, which is funded by National Nuclear Security Administration of the US Department of Energy. Computational resources also came from Northern Arizona University's Monsoon computer cluster, which is funded by Arizona's Technology and Research Initiative Fund.

About the Author

Dr. Lin is a scientist in the Information Sciences Group of the Computer, Computational, and Statistical Sciences Division at Los Alamos National Laboratory. His primary research interest is the development and application of advanced data science methods in the modeling of biological systems.

References

1. Gorbalenya AE, Baker SC, Baric RS, de Groot RJ, Drostetn C, Gulyaeva AA, et al.; Coronaviridae Study Group of the International Committee on Taxonomy of Viruses. The species *Severe acute respiratory syndrome-related coronavirus*: classifying 2019-nCoV and naming it SARS-CoV-2. Nat Microbiol. 2020;5:536–44. https://doi.org/10.1038/s41564-020-0695-z
2. Ghinai I, McPherson TD, Hunter JC, Kirking HL, Christiansen D, Joshi K, et al.; Illinois COVID-19 Investigation Team. First known person-to-person transmission of severe acute respiratory syndrome coronavirus 2 (SARS-CoV-2) in the USA. Lancet. 2020;395:1137–44. https://doi.org/10.1016/S0140-6736(20)30607-3
3. Holshue ML, DeBolt C, Lindquist S, Lofy KH, Wiesman J, Bruce H, et al.; Washington State 2019-nCoV Case Investigation Team. First case of 2019 novel coronavirus in the United States. N Engl J Med. 2020;382:929–36. https://doi.org/10.1056/NEJMoa2001191
4. The Atlantic Monthly Group. The COVID Tracking Project. 2020 [cited 2020 Jul 1]. https://covidtracking.com/data/national
5. Silverman JD, Hupert N, Washburne AD. Using influenza surveillance networks to estimate state-specific prevalence of SARS-CoV-2 in the United States. Sci Transl Med. 2020;12:eabc1126. https://doi.org/10.1126/scitranslmed.abc1126
6. Sanche S, Lin YT, Xu C, Romero-Severson E, Hengartner N, Ke R. High contagiousness and rapid spread of severe acute respiratory syndrome coronavirus 2. Emerg Infect Dis. 2020;26:1470–7. https://doi.org/10.3201/eid2607.200282
7. Coronavirus Resource Center, Johns Hopkins University. Timeline of COVID-19 policies, cases, and deaths in your

state: a look at how social distancing measures may have influenced trends in COVID-19 cases and deaths. 2020 [2020 Jul 1]. https://coronavirus.jhu.edu/data/state-timeline
8. Courtemanche C, Garuccio J, Le A, Pinkston J, Yelowitz A. Strong social distancing measures in the United States reduced the COVID-19 growth rate. Health Aff (Millwood). 2020;39:1237–46. https://doi.org/10.1377/hlthaff.2020.00608
9. Hsiang S, Allen D, Annan-Phan S, Bell K, Bolliger I, Chong T, et al. The effect of large-scale anti-contagion policies on the COVID-19 pandemic. Nature. 2020;584:262–7. https://doi.org/10.1038/s41586-020-2404-8
10. Executive Office of the President. OMB bulletin no. 15-01. 2020 [cited 2020 Jul 1]. https://www.bls.gov/bls/omb-bulletin-15-01-revised-delineations-of-metropolitan-statistical-areas.pdf
11. The New York Times. Coronavirus (Covid-19) data in the United States. 2020 [cited 2020 Jul 1]. https://github.com/nytimes/covid-19-data
12. Lauer SA, Grantz KH, Bi Q, Jones FK, Zheng Q, Meredith HR, et al. The incubation period of coronavirus disease 2019 (COVID-19) from publicly reported confirmed cases: estimation and application. Ann Intern Med. 2020;172:577–82. https://doi.org/10.7326/M20-0504
13. United States Census Bureau. Metropolitan and micropolitan statistical areas population totals and components of change: 2010–2019. 2020 [cited 2020 Jul 1]. https://www.census.gov/data/tables/time-series/demo/popest/2010s-total-metro-and-micro-statistical-areas.html
14. Arons MM, Hatfield KM, Reddy SC, Kimball A, James A, Jacobs JR, et al.; Public Health–Seattle and King County; CDC COVID-19 Investigation Team. Presymptomatic SARS-CoV-2 infections and transmission in a skilled nursing facility. N Engl J Med. 2020;382:2081–90. https://doi.org/10.1056/NEJMoa2008457
15. Nguyen VVC, Vo TL, Nguyen TD, Lam MY, Ngo NQM, Le MH, et al. The natural history and transmission potential of asymptomatic SARS-CoV-2 infection. Clin Infect Dis 2020 Jun 4 [Epub ahead of print]. https://doi.org/10.1093/cid/ciaa711
16. Ministry of Health, Labour and Welfare of Japan. Official report on the cruise ship *Diamond Princess*, May 1, 2020. 2020 [cited 2020 Jul 1]. https://www.mhlw.go.jp/stf/newpage_11146.html
17. Sakurai A, Sasaki T, Kato S, Hayashi M, Tsuzuki SI, Ishihara T, et al. Natural history of asymptomatic SARS-CoV-2 infection. N Engl J Med. 2020;383:885–6. https://doi.org/10.1056/NEJMc2013020
18. Perez-Saez J, Lauer SA, Kaiser L, Regard S, Delaporte E, Guessous I, et al. Serology-informed estimates of SARS-COV-2 infection fatality risk in Geneva, Switzerland. Lancet Infect Dis. 2020 Jul 14 [Epub ahead of print]. https://doi.org/10.1016/S1473-3099(20)30584-3
19. Richardson S, Hirsch JS, Narasimhan M, Crawford JM, McGinn T, Davidson KW, et al.; the Northwell COVID-19 Research Consortium. Presenting characteristics, comorbidities, and outcomes among 5700 patients hospitalized with COVID-19 in the New York City area. JAMA. 2020;323:2052–9. https://doi.org/10.1001/jama.2020.6775
20. Wölfel R, Corman VM, Guggemos W, Seilmaier M, Zange S, Müller MA, et al. Virological assessment of hospitalized patients with COVID-2019. Nature. 2020;581:465–9. https://doi.org/10.1038/s41586-020-2196-x
21. Andrieu C, Thoms J. A tutorial on adaptive MCMC. Stat Comput. 2008;18:343–73. https://doi.org/10.1007/s11222-008-9110-y
22. Hindmarsh AC. ODEPACK, a systematized collection of ODE solvers. In: Stepleman RS, editor. Scientific computing: applications of mathematics and computing to the physical sciences. Amsterdam: North-Holland Publishing Company; 1983. p. 55–64.
23. U.S. Department of Energy. COVID-19 pandemic modeling and analysis. 2020 [cited 2020 Jul 1]. https://covid19.ornl.gov
24. Lin YT, Neumann J, Miller EF, Posner RG, Mallela A, Safta C, et al. Los Alamos COVID-19 city predictions. 2020 [cited 2020 Jul 1]. https://github.com/lanl/COVID-19-Predictions.

Address for correspondence: Yen Ting Lin, CCS-3, Los Alamos National Laboratory, Mailstop B256, 1 Bikini Atoll, Los Alamos, NM 87545, USA; email: yentingl@lanl.gov

Fluconazole-Resistant *Candida glabrata* Bloodstream Isolates, South Korea, 2008–2018

Eun Jeong Won,[1] Min Ji Choi,[1] Mi-Na Kim, Dongeun Yong, Wee Gyo Lee, Young Uh, Taek Soo Kim, Seung Ah Byeon, Seung Yeob Lee, Soo Hyun Kim, Jong Hee Shin

Medscape EDUCATION ACTIVITY

In support of improving patient care, this activity has been planned and implemented by Medscape, LLC and Emerging Infectious Diseases. Medscape, LLC is jointly accredited by the Accreditation Council for Continuing Medical Education (ACCME), the Accreditation Council for Pharmacy Education (ACPE), and the American Nurses Credentialing Center (ANCC), to provide continuing education for the healthcare team.

Medscape, LLC designates this Journal-based CME activity for a maximum of 1.00 ***AMA PRA Category 1 Credit(s)™***. Physicians should claim only the credit commensurate with the extent of their participation in the activity.

Successful completion of this CME activity, which includes participation in the evaluation component, enables the participant to earn up to 1.0 MOC points in the American Board of Internal Medicine's (ABIM) Maintenance of Certification (MOC) program. Participants will earn MOC points equivalent to the amount of CME credits claimed for the activity. It is the CME activity provider's responsibility to submit participant completion information to ACCME for the purpose of granting ABIM MOC credit.

All other clinicians completing this activity will be issued a certificate of participation. To participate in this journal CME activity: (1) review the learning objectives and author disclosures; (2) study the education content; (3) take the post-test with a 75% minimum passing score and complete the evaluation at http://www.medscape.org/journal/eid; and (4) view/print certificate. For CME questions, see page 997.

Release date: February 17, 2021; Expiration date: February 17, 2022

Learning Objectives

Upon completion of this activity, participants will be able to:

- Assess the mortality and antifungal resistance (including fluconazole resistance) of *C. glabrata* bloodstream isolates, based on a study of South Korean multicenter surveillance cultures collected during an 11-year period (2008–2018)
- Evaluate antifungal resistance molecular mechanisms, including amino acid substitutions of fluconazole-resistant *C. glabrata* bloodstream isolates, based on a study of South Korean multicenter surveillance cultures collected during an 11-year period (2008–2018)
- Determine the clinical and public health implications of outcomes and antifungal-resistant molecular mechanisms of fluconazole-resistant *C. glabrata* bloodstream isolates, based on a study of South Korean multicenter surveillance cultures collected during an 11-year period (2008–2018)

CME Editor

Jude Rutledge, BA, Technical Writer/Editor, Emerging Infectious Diseases. *Disclosure: Jude Rutledge has disclosed no relevant financial relationships.*

CME Author

Laurie Barclay, MD, freelance writer and reviewer, Medscape, LLC. *Disclosure: Laurie Barclay, MD, has disclosed no relevant financial relationships.*

Authors

Disclosures: ***Eun Jeong Won, MD, PhD; Min Ji Choi, PhD; Mi-Na Kim, MD, PhD; Dongeun Yong, MD, PhD; Wee Gyo Lee, MD, PhD; Young Uh, MD, PhD; Taek Soo Kim, MD; Seung Ah Byeon, MS; Seung Yeob Lee, MD, PhD; Soo Hyun Kim, MD, PhD;*** *and* ***Jong Hee Shin, MD, PhD,*** *have disclosed no relevant financial relationships.*

Author affiliations: Chonnam National University Medical School, Gwangju, South Korea (E.J. Won, M.J. Choi, S.A. Byeon, S.Y. Lee, S.H. Kim, J.H. Shin); Asan Medical Center, University of Ulsan College of Medicine, Seoul, South Korea (M.-N. Kim); Yonsei University College of Medicine, Seoul (D. Yong); Ajou University School of Medicine, Suwon, South Korea (W.G. Lee); Yonsei University Wonju College of Medicine, Wonju, South Korea (Y. Uh); Seoul National University College of Medicine, Seoul (T.S. Kim)

DOI: https://doi.org/10.3201/eid2703.203482

[1]These first authors contributed equally to this article.

We investigated the clinical outcomes and molecular mechanisms of fluconazole-resistant (FR) *Candida glabrata* bloodstream infections. Among 1,158 isolates collected during multicenter studies in South Korea during 2008–2018, 5.7% were FR. For 64 patients with FR bloodstream infection isolates, the 30-day mortality rate was 60.9% and the 90-day mortality rate 78.2%; these rates were significantly higher than in patients with fluconazole-susceptible dose-dependent isolates (30-day mortality rate 36.4%, 90-day mortality rate 43.8%; p<0.05). For patients with FR isolates, appropriate antifungal therapy was the only independent protective factor associated with 30-day (hazard ratio 0.304) and 90-day (hazard ratio 0.310) mortality. Sequencing of pleiotropic drug-resistance transcription factor revealed that 1–2 additional Pdr1p amino acid substitutions (except genotype-specific Pdr1p amino acid substitutions) occurred in 98.5% of FR isolates but in only 0.9% of fluconazole-susceptible dose-dependent isolates. These results highlight the high mortality rate of patients infected with FR *C. glabrata* BSI isolates harboring Pdr1p mutations.

Candida glabrata is a commensal yeast in the human gut, genitourinary tract, or oral cavity; however, it can cause serious bloodstream infections (BSIs) that result in substantial illness and death (*1*). Unlike other common *Candida* species, *C. glabrata* exhibits intrinsically low susceptibility to azole drugs, especially fluconazole, and rapidly acquires antifungal resistance in response to azole or echinocandin exposure (*1*–*3*). Although the incidence of echinocandin- and multidrug-resistant (MDR) *C. glabrata* BSIs is low, fluconazole resistant (FR) *C. glabrata* BSI isolates have been increasingly reported worldwide, typically at rates of 2.6%–10.6%, although these rates can reach 17% (*4*–*6*). Fluconazole resistance in *C. glabrata* is of particular concern because of the increased incidence of BSIs caused by this species in various locations worldwide (*1*,*4*,*5*). Acquired azole resistance in *C. glabrata* is most commonly mediated by overexpression of the drug-efflux transporter genes *CgCDR1*, *CgCDR2*, and *CgSNQ2* through a gain-of-function (GOF) mutation in the transcription factor pleiotropic drug-resistance (*PDR1*) (*2*,*7*,*8*), although other mechanisms might contribute (*9*–*11*).

PDR1 mutations in *C. glabrata* associated with azole resistance have been shown to cause hypervirulence in a mouse model of systemic candidiasis, suggesting the need for careful monitoring of FR *C. glabrata* BSI isolates and their *PDR1* mutations (*7*,*12*). To date, little substantial research has been conducted on *PDR1* mutation incidence among FR *C. glabrata* BSI isolates from multicenter surveillance cultures or on mortality rates of patients infected with these *PDR1* mutants. This deficit might be attributable to Pdr1p amino acid substitutions (AAS) found in FR and fluconazole-susceptible dose-dependent (F-SDD) isolates (*7*,*13*,*14*), which can impede determination of whether specific Pdr1p AAS result in fluconazole resistance. Therefore, the aim of this study was to investigate the clinical outcomes, molecular mechanisms, and genotypes associated with antifungal-resistant BSI isolates of *C. glabrata* collected during multicenter studies in South Korea during an 11-year period (2008–2018). We focused on the mortality rates of patients infected with FR *C. glabrata* BSI isolates harboring the Pdr1p mutation.

Materials and Methods

Microorganisms and Antifungal Susceptibility Testing

A total of 1,158 BSI isolates of *C. glabrata* were collected from 19 university hospitals in South Korea during January 2008–December 2018 (Appendix Table 1, https://wwwnc.cdc.gov/EID/article/27/3/20-3482-App1.pdf). All isolates were collected from routine blood cultures by using methods that varied among laboratories; only the first isolate from each patient was included. The hospitals participating in this laboratory-based nationwide multicenter surveillance system differed each year. All *C. glabrata* isolates were submitted to Chonnam National University Hospital (Gwangju, South Korea) for testing. Species identification was based on matrix-assisted laser desorption/ionization time-of-flight mass spectrometry (Biotyper; Bruker Daltonics, https://www.bruker.com) with library version 4.0, or sequencing of the D1/D2 domains of the 26S rRNA gene, to differentiate *C. glabrata* from cryptic species (*C. nivariensis* and *C. bracarensis*) within the *C. glabrata* complex (*15*). In vitro testing of susceptibility to fluconazole, micafungin, caspofungin, voriconazole, and amphotericin B was performed for all isolates according to the Clinical and Laboratory Standards Institute broth microdilution method (*16*). MICs were determined after 24 hours of incubation. Two reference strains, *Candida parapsilosis* ATCC 22019 and *Candida krusei* ATCC 6258, were included in each antifungal susceptibility test as quality-control isolates. The MIC interpretive criteria included species-specific Clinical and Laboratory Standards Institute clinical breakpoints for fluconazole, micafungin, and caspofungin (*17*), as well as epidemiologic cutoff values (ECVs) for voriconazole and amphotericin B (*18*). Echinocandin resistance was confirmed through DNA sequence analysis of *FKS* genes to identify resistance hot-spot mutations in *FKS1* and *FKS2* (*19*).

Multidrug resistance was defined as resistance to both fluconazole and echinocandins (*2*).

Clinical Characteristics

Candidemia was defined as the isolation of *Candida* from ≥1 blood culture (*20*), and cases with invasive candidiasis without candidemia or colonization were excluded. All demographic characteristics and clinical conditions potentially related to candidemia mortality rates at the time of candidemia onset were investigated (*21*–*23*). Previous use of antifungal agents was defined as administration within 3 months before the onset of candidemia. A lack of antifungal therapy was defined as no antifungal therapy or treatment with antifungals for <3 days; appropriate antifungal therapy was defined as the administration of ≥1 in vitro–active antifungal (according to the susceptibility pattern of the isolate) for ≥72 hours (*23*,*24*). Therapeutic failure was defined as either persistence of *Candida* in the bloodstream despite ≥72 hours of antifungal therapy or development of breakthrough fungemia during treatment with the indicated antifungal agents for ≥72 hours (*23*,*24*). All-cause mortality rates were assessed at 30 and 90 days after the first positive blood culture result. Mortality rates also were analyzed for patients with candidemia who were infected with 297 SDD isolates of *C. glabrata* as controls. This study was approved by the Institutional Review Board of Chonnam National University Hospital (approval no. CNUH-2020-117).

Multilocus Sequence Typing and Molecular Mechanisms

Multilocus sequence typing (MLST) and *PDR1* sequencing were performed for all antifungal-resistant isolates of *C. glabrata* and for 212 F-SDD control isolates by using methods described previously (*14*,*21*,*25*). *PDR1* sequences of each isolate were compared and analyzed on the basis of the reference *PDR1* sequence of *C. glabrata* (GenBank accession no. FJ550269) (*14*). The *FKS1* and *FKS2* sequences of 79 isolates that exhibited full or intermediate resistance to micafungin (MIC ≥0.12 mg/L) or caspofungin (MIC ≥0.25 mg/L) were compared with those of *C. glabrata* (GenBank reference sequence nos. FKS1 XM_446406 and FKS2 XM_448401) (*14*). The expression levels of *CgCDR1*, *CgCDR2*, and *CgSNQ2* were evaluated for 30 FR isolates of *C. glabrata* harboring FR-specific Pdr AAS and for 65 F-SDD control isolates without FR-specific Pdr AAS, as described previously (*26*,*27*). The cycle threshold (C_t) of each gene was normalized to that of *URA3* to determine the ΔC_t value. For all isolates, relative gene expression ($\Delta\Delta C_T$) was reported as fold change calculated as the mean normalized expression level relative to that of *C. glabrata* ATCC 90030 (fluconazole MIC 8 mg/L, set as 1.0).

Statistical Analysis

Quantitative variables are expressed as means with standard deviations, whereas categorical variables are expressed as counts and percentages. Categorical variables were compared by using the χ^2 test or Fisher exact test, Student *t*–test or the Mann–Whitney U test to compare quantitative variables, as appropriate. Cox proportional hazards models were used to evaluate potential risk factors for 30- and 90-day mortality rates by calculating the hazard ratio (HR). The Kaplan–Meier and log–rank (Mantel–Cox) tests were used to calculate the 30- and 90-day survival probabilities in subgroup analyses. All data were analyzed by using SPSS Statistics 26.0 (IBM, https://www.ibm.com). Statistical significance was determined at a level of $p<0.05$.

Results

Incidence of Antifungal Resistance

The annual proportion of *C. glabrata* BSI isolates among all *Candida* BSI isolates increased from 11.7% to 23.9% (mean 18.6%) during the study period (Table 1). The rate of fluconazole resistance (MIC ≥64 mg/L) increased from 0% (0/68 isolates) to 8.3% (14/168 isolates) during the study period. Among the 1,158 BSI isolates of *C. glabrata*, 66 (5.7%) were resistant to fluconazole, 16 (1.4%) were resistant to echinocandin, and 6 (0.5%) were resistant to multiple drugs. Of the 16 echinocandin-resistant isolates, 6 (37.5%) were also resistant to fluconazole; thus, these isolates were MDR. Isolates of echinocandin-resistant and MDR *C. glabrata* were initially found in 2013 and then annually from 2016 to 2018. Resistance to amphotericin B (MIC >2 mg/L) was not detected in any isolate, but 79 (6.8%) isolates had voriconazole MICs that exceeded the ECV (0.25 mg/L). All 64 FR isolates were associated with a voriconazole MIC ≥0.5 mg/L.

Mortality Rate of FR *Candida glabrata* BSIs

The mortality rate for 64 patients with FR *C. glabrata* BSI isolates was 60.9% at 30 days (Appendix Table 2). Univariate Cox regression analyses revealed that a high Charlson comorbidity index ($p = 0.051$), liver disease ($p = 0.015$), intensive-care unit admission ($p = 0.071$), severe sepsis ($p = 0.039$), lack of antifungal therapy ($p<0.001$), azole monotherapy ($p = 0.005$), any combination antifungal therapy ($p = 0.014$), and appropriate antifungal therapy

Table 1. Incidence of antifungal resistance in *Candida glabrata* BSI isolates, based on cultures collected during a multicenter surveillance study, South Korea, 2008–2018*

Study year	No. participating hospitals†	% *C. glabrata* of all *Candida* BSI isolates	No. BSI isolates of *C. glabrata* tested	No. (%) *C. glabrata* BSI isolates‡		
				Fluconazole resistance	Echinocandin resistance§	Multidrug resistance¶
2008	13	11.7	68	0	0	0
2009	8	16.0	67	4 (6.0)	0	0
2010	8	16.8	60	4 (6.7)	0	0
2011	10	16.0	85	4 (4.7)	0	0
2012	11	17.0	108	3 (2.8)	0	0
2013	7	16.9	73	4 (5.5)	1 (1.4)	1 (1.4)
2014	7	22.1	123	11 (8.9)	0	0
2015	10	17.2	110	5 (4.5)	3 (2.7)	0
2016	10	21.2	123	4 (3.3)	4 (3.3)	2 (1.6)
2017	13	21.6	173	13 (7.5)	4 (2.3)	1 (0.6)
2018	13	23.9	168	14 (8.3)	4 (2.4)	2 (1.2)
Total	19	18.6	1158	66 (5.7)	16 (1.4)	6 (0.5)

*BSI, bloodstream infection.
†Hospitals participating in this laboratory-based nationwide multicenter surveillance system differed each year.
‡Antifungal susceptibility was determined by using the Clinical and Laboratory Standards Institute M27–4ED broth microdilution method (*16*). Interpretive categories of resistance were determined by using Clinical and Laboratory Standards Institute document M60-ED (*17*). We deposited 76 antifungal-resistant isolates of *C. glabrata* in the Korea Collection for Type Culture (KCTC; Jeongeup-si, Korea), including those showing resistance to fluconazole alone (60 isolates, KCTC nos. 37113–37172), echinocandin alone (10 isolates, KCTC nos. 37176–37185), and both fluconazole and echinocandin (6 multidrug-resistant isolates, KCTC nos. 37110–37112, 37173–37175). All 76 isolates were identified as *C. glabrata* by sequence analysis using the D1/D2 domain (GenBank accession nos. MW349716–90 and MW351777).
§Echinocandin resistance was confirmed by the identification of resistance hot-spot mutations in *FKS1* and *FKS2* in isolates that exhibited full or intermediate resistance to micafungin (MIC ≥0.12 mg/L) or caspofungin MIC (≥0.25 mg/L).
¶Multidrug resistance was defined as resistance to both fluconazole and echinocandins.

(p = 0.001) were associated with the 30-day mortality rate. The 30-day mortality rates were 88.9% (8/9) in patients with azole monotherapy, 69.2% (9/13) in patients with echinocandin monotherapy, 70% (7/10) in patients with amphotericin B monotherapy, 36.4% (8/22) in patients with combination antifungal therapy, 90% (18/20) in patients with inadequate antifungal therapy, and 47.7% (21/44) in patients with appropriate antifungal therapy. Patients treated with azole monotherapy or inadequate antifungal therapy showed significantly higher 30-day mortality rates than those receiving combination therapy or appropriate antifungal therapy (all p<0.05). In multivariate Cox regression analysis, no independent risk factors for 30-day mortality were identified, but appropriate antifungal therapy (HR 0.304 [95% CI 0.134–0.689]; p = 0.004) was independently protective with respect to 30-day mortality. The mortality rate for 64 patients with FR *C. glabrata* BSI isolates was 78.2% at 90 days; appropriate antifungal therapy (HR 0.31 [95% CI 0.138–0.695]; p = 0.004) was the only protective factor with respect to 90-day mortality (Appendix Table 3). Kaplan–Meier survival analysis showed that the mortality dynamics of the FR group (64 patients) decreased during the study period, whereas the F-SDD group (297 patients) exhibited a plateau period of decreasing cumulative survival from 30 to 90 days, which was similar in each of the 4 years of the study period (Figure). The median survival of patients with FR *C. glabrata* BSI was significantly shorter than that of patients with F-SDD *C. glabrata* (17 days for FR vs. 90 days for F-SDD; p<0.001 by log-rank test).

MLST Genotypes and AAS in Pdr1p

MLST revealed that 56.1% (37/66) of FR, 56.3% (9/16) of echinocandin-resistant, and 100% (6/6) of MDR isolates belonged to sequence type (ST) 7. Table 2 lists the sequencing results for *PDR1* and the MLST genotypes for the 66 FR isolates of *C. glabrata*, as well as 212 control F-SDD isolates. In total, 68 types of AAS in Pdr1p were found in the 278 isolates of *C. glabrata* tested. When Pdr1p polymorphisms were compared between ≥2 isolates in the same ST (257 isolates in 11 STs), excluding 21 STs that were unique to a single isolate, all 50 ST3 isolates harbored the same 3 Pdr1p AAS (P76S, P143T, and D243N), all 8 ST55 isolates harbored E259G, and all 4 ST59 isolates harbored T745A, irrespective of FR. However, these 5 Pdr AAS were not found in any ST7 isolates or any isolates of the other 7 ST groups, each of which contained ≥2 isolates. Excluding 5 Pdr1 AAS (P76S, P143T, D243N, E259G, and T745A), 1 additional Pdr1p AAS was found in each of 2 F-SDD isolates (0.9%, n = 212); 1 (59 FR isolates) or 2 (6 FR isolates) additional Pdr1p AAS was found in 65/66 (98.5%) FR isolates.

AAS in Pdr1p Shown in Only FR isolates

Each of the 49 Pdr1p AAS was found alone in 59 FR isolates of *C. glabrata* and their MLST genotypes (Table 3). In 38 (64.4%) isolates, AAS were found in 3 domains of Pdr1p, the inhibition (33.9%), fungal-specific

transcription factor (11.9%), and activation (18.6%) domains; AAS were outside the main domains in 21 (35.6%) isolates. Of 49 Pdr1p AAS, 16 were described previously for FR isolates, whereas 33 (67.3%) were newly found in this study. Of these potentially novel Pdr1p AAS, 5 (P327L, G346S, H576Y, T607A, and G788W) were shared by 2 isolates with the same genotype. Among these, 2 AAS (G346S [ST2] and H576Y [ST7]), were shared by 2 isolates from the same hospital in the same year. Quantitative reverse transcription PCR revealed that 30 FR isolates harboring the Pdr mutation exhibited significantly higher mean expression levels of *CgCDR1*, *CgCDR2*, and *CgSNQ2* than 65 control F-SDD isolates (FR vs. F-SDD; 11.5- vs. 1.5-fold for *CgCDR1*, p<0.0001; 43.4- vs. 27.0-fold for *CgCDR2*, p = 0.0408; and 4.9- vs. 3.5-fold for *CgSNQ2*, p = 0.0174) (Appendix Figure).

Discussion

After *C. albicans, C. glabrata* is the most common *Candida* species isolated from BSI in North America and in countries of central and northern Europe (*1*,*4*). *C. glabrata* was the fourth most common BSI-causing *Candida* species in many countries in Asia besides South Korea (*6*,*28*,*29*); however, increasing rates of *C. glabrata* with FR have been reported in China (*30*), and this strain is now the second most common species in South Korea (*31*). In this study, the FR rate of BSI isolates of *C. glabrata* were found to have increased from 0% (0/68) in 2008 to 8.3% (14/168) in 2018. No *C. glabrata* isolate collected during 2008–2012 was resistant to echinocandins, whereas 2%–3% were resistant to echinocandins during 2015–2018. The emergence of echinocandin-resistant BSI isolates of *C. glabrata* in South Korea might reflect the increased use of echinocandin antifungals as the initial option for candidemia after insurance coverage for echinocandins began in 2014 (*32*). Of 16 echinocandin-resistant isolates, 6 (37.5%) were also resistant to fluconazole, indicating multidrug resistance. Overall, our 11-year nationwide surveillance revealed an increasing incidence of *C. glabrata* causing BSI and an increasing propensity for development of antifungal resistance in South Korea, consistent with surveillance data from other countries (*1*,*2*,*4*,*5*,*30*).

Data are scarce regarding the mortality rates for patients with candidemia who are infected with FR *C. glabrata* BSI isolates. The 30-day mortality rates in patients infected with *C. glabrata* BSI isolates are 21.3%–48.6% (*16*,*33*–*37*) but can reach 50%–60% among patients in intensive care units (*38*,*39*). However, few FR *C. glabrata* isolates were included in previous studies. We found that FR BSI isolates of *C. glabrata* in South Korea were associated with significantly higher 30-day (60.9%) and 90-day (78.2%) mortality rates, compared to BSIs caused by F-SDD strains (30-day mortality rate 36.4%, 90-day mortality rate 43.8%). The mortality dynamics of FR isolates indicated a rapid rise in cumulative mortality from 7 to 90 days after BSI onset. This mortality dynamic was distinct from that of patients with F-SDD BSIs, who exhibited a steady curve after 60 days, consistent

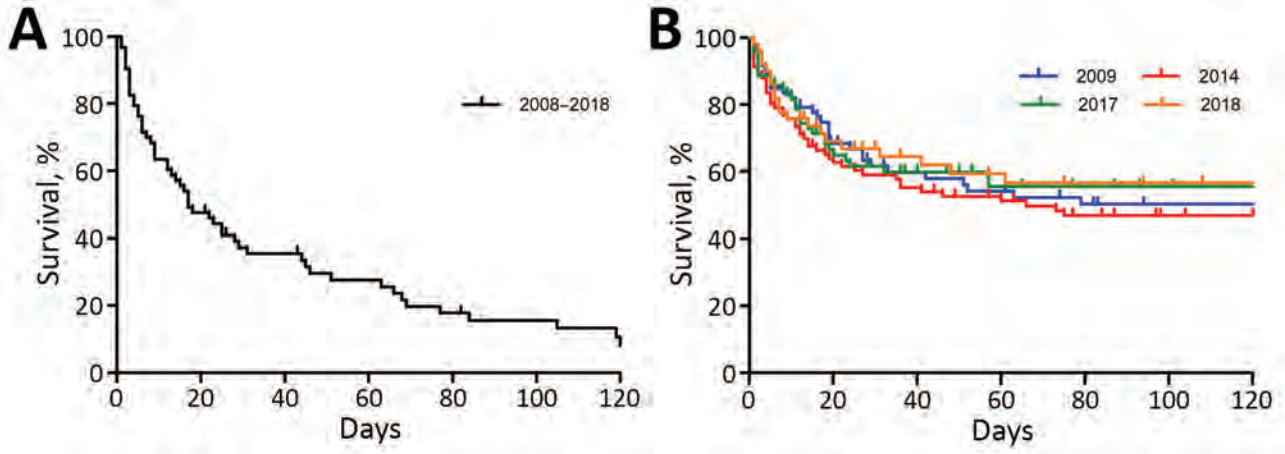

Figure. Kaplan–Meier and log-rank (Mantel–Cox) pairwise analyses of survival of patients with *Candida glabrata* candidemia, based on patient data and cultures collected during a multicenter surveillance study, South Korea, 2008–2018. A) Cumulative survival curves of 64 patients infected with fluconazole-resistant (FR) bloodstream infection (BSI) isolates. The cumulative mortality rates of 64 patients infected with FR *C. glabrata* BSIs increased over time (day 7 [29.7%], day 30 [60.9%], day 60 [68.8%], and day 90 [78.1%]). B) Cumulative survival curves of patients infected with fluconazole-susceptible dose-dependent (F-SDD) BSI isolates (297 patients total) in 2009 (75 patients in 6 hospitals), 2014 (97 patients in 7 hospitals), 2017 (75 patients in 9 hospitals), and 2018 (50 patients in 8 hospitals). The 30-day mortality rate of the F-SDD group was 34.7% in 2010, 39.2% in 2014, 37.3% in 2017, and 32.0% in 2018. The cumulative mortality rates of 297 patients infected with F-SDD BSI isolates of *C. glabrata* were found to be 18.5% at day 7 (p = 0.084), 36.4% at day 30 (p = 0.001), 41.8% at day 60 (p<0.001), and 43.8% at day 90 (p<0.001).

with previous reports of *C. glabrata* BSIs (*34*,*40*). The median survival of patients with FR *C. glabrata* BSIs (17 days) was also significantly shorter than that of patients with F-SDD *C. glabrata* BSIs (90 days). These findings are consistent with the results in a recent report regarding *C. glabrata* BSIs in South Korea, which showed that a high fluconazole MIC was associated with a poor outcome, although only 5 isolates in that study were FR (*37*).

In this study, MLST revealed that 56.1% of FR and 56.3% of echinocandin-resistant BSI isolates belonged to ST7, which accords with ST7 being the most common MLST genotype (47.8%) in South Korea (*21*). We found that 100% (6/6) of MDR isolates belonged to ST7, which harbored the V239L mutation in the mismatch repair gene (*MSH2*) associated with hypermutability (*21*,*25*). Given that the utility of *MSH2* gene mutations as antifungal-resistance markers remains controversial (*41*,*42*), further surveillance studies are needed. To date, few studies have been conducted on MLST genotype–specific differences in Pdr1p polymorphism among *C. glabrata* BSI isolates. We found that all 50 isolates of ST3 harbored the same Pdr1p AAS (P76S/P143T/D243N), all 7 isolates of ST55 harbored E259G, and all 4 isolates of ST59 harbored T745A, suggesting the presence of MLST genotype–specific Pdr1p AAS. P76S/P143T/D243N in Pdr1p was found to be common in China, Iran, and Australia (*13*,*14*,*43*,*44*), which accords with the high prevalence of ST3 in the study collections. Thus, the results of this study suggest that 5 Pdr1p AAS are MLST genotype–specific; because these AAS were found in both FR and F-SDD isolates, we confirmed that they cannot be responsible for azole resistance.

A single-point mutation in *PDR1* can contribute to azole resistance in *C. glabrata* (*7*,*8*). Our results show that, in FR isolates, AAS are scattered throughout the entire protein without distinct hotspots, as reported previously (*7*,*13*,*41*,*45*). Therefore, determining whether a certain Pdr1p AAS is a GOF mutation is difficult without data from gene editing experiments for all variable regions. A previous study identified 57 FR-specific AAS by comparing azole-susceptible and azole-resistant matched isolates recovered from different clinical specimens (*7*). Furthermore, 91% (74/81) of FR isolates from BSIs or vaginal infections contained a Pdr1 mutation, compared with 5.6%

Table 2. Pdr1 AAS in 66 FR isolates and 212 F-SDD BSI isolates of *Candida glabrata* and their MLST genotypes, based on cultures collected during a multicenter surveillance study, South Korea, 2008–2018*

MLST genotype	Fluconazole susceptibility	No. isolates tested	No. with echinocandin resistance	No. isolates with 5 Pdr1p AAS found in both FR and F-SDD isolates					No. isolates with additional Pdr1p AAS except for 5 Pdr1p AAS		
				P76S	P143T	D243N	E259G	T745A	1	2	Total
ST7	FR	37	6†						34	3	37
	F-SDD	98	3						0		0
ST3	FR	7	0	7	7	7			6	1	7
	F-SDD	43	1	43	43	43			0		0
ST26	FR	7	0						6		6
	F-SDD	10	1						0		0
ST22	FR	1	0						1		1
	F-SDD	16	1						0		0
ST10	FR	2	0						2		2
	F-SDD	9	0						0		0
ST55	FR	2	0				2		2		2
	F-SDD	6	1				6		1		1
ST2	FR	2	0						2		2
	F-SDD	3	0						0		0
ST6	FR	1	0						1		1
	F-SDD	5	2						0		0
ST59	FR	1	0					1	1		1
	F-SDD	3	1					3	0		0
ST1	FR	2	0						2		2
ST12	F-SDD	2	0						0		0
Other STs‡	FR	4	0				1		2	2	4
	F-SDD	17	0	2	2	2			1		1
Total, no. (%)	FR	66	6	7	7	7	3	1	59	6§	65 (98.5)
	F-SDD	212	10	45	45	45	6	3	2¶		2 (0.9)

*AAS, amino acid substitution; BSI, bloodstream infection; FR, fluconazole-resistant; F-SDD, fluconazole-susceptible dose-dependent; MLST, multilocus sequence typing; ST, sequence type.
†All 6 isolates showed multidrug resistance, defined as resistance to both fluconazole and echinocandins.
‡Includes 21 STs that were each unique to a single isolate.
§Each of 6 FR isolates harbored 2 additional Pdr1 AAS (E340G/D919Y [ST7], Y556C/F580I [ST7], N132S/G1099S [ST7], F832L/L833V [ST3], G189V/E340G [other ST], and L366P/E555D [other ST]).
¶Two F-SDD isolates harbored additional Pdr1 AAS (V502I [ST55] and R250K [other ST]).

Table 3. Pdr1 AAS in 59 FR isolates of *Candida glabrata* BSI isolates and their MLST genotypes, based on cultures collected during a multicenter surveillance study, South Korea, 2008–2018*

MLST genotype	No. isolates	Pdr1 AAS (no. isolates)†			
		Inhibition domain	Fungal-specific transcription factor domain	Activation domain	Other regions
ST7	34	P327L (2), G334V (1), **E340G** (1), E340K (1), G346S (1), **L347F** (1), L375P (1), **R376Q** (1), S391L (1)	**H576Y** (2), G583C (1)	**P927S** (1), **G943S** (1), S947L (1), D954N (1), G1088E (1), **Y1106N** (1)	S236N (1), **P258S** (1), **P258L** (1), V260A (1),L280S (1), Y556C (1), E714D (1), T752I (1), **N768D** (1), **R772K** (1), K776E (1), G788W (2), L825P (1), **T885A** (1)
ST26	6	K365E (1), **R376Q** (1), F377I (1), E388Q (1)		N1091D (1)	**S316I** (1)
ST3	6	**L347F** (1)	Y584D (1)	T1080N (1), **Y1106N** (1)	A731E (1), **N764D** (1)
ST1	2		**T607A** (2)		
ST2	2	G346S (2)			
ST10	2	S337F (1), I392M (1)			
ST55	2				F294S (1), **P258S** (1)
ST6	1			**G1079R** (1)	
ST22	1			Y932C (1)	
ST59	1	E369K (1)			
Others	2		L935F (1)		P696L (1)
No. (%) isolates	59	20 (33.9)	7 (11.9)	11 (18.6)	21 (35.6)
No. (%) Pdr1 AAS	49	15 (30.6)	5 (10.2)	10 (20.4)	19 (38.8)

*AAS, amino acid substitutions; BSI, bloodstream infection; FR, fluconazole-resistant; MLST, multilocus sequence typing; ST, sequence type.
†Previously reported Pdr1 AAS are shown in bold.

(1/18) of F-SDD isolates (*25*). In our study, we found that 98.5% (65/66) of FR BSI isolates and 0.9% (2/212) of F-SDD BSI isolates harbored an additional 1 or 2 Pdr1p AAS after exclusion of 5 genotype-specific AAS (P76S, P143T D243N, E259G, and T745A). After exclusion of 6 additional FR isolates that harbored 2 Pdr1p AAS (because determining which of the 2 AAS was critical for fluconazole resistance was difficult to determine), we found 49 Pdr1p AAS that were present alone in 59 FR isolates, strongly suggesting that these AAS were FR-specific. Of the 49 Pdr1p AAS, 16 have been described for FR isolates (*7*,*13*,*14*,*25*,*43*–*46*). In this study, FR isolates exhibited higher mean *CgCDR1*, *CgCDR2*, or *CgSNQ2* expression levels, compared with F-SDD isolates; all FR *C. glabrata* isolates were also resistant to voriconazole (MIC ≥0.5 mg/L), implying that fluconazole and voriconazole resistance are governed by the same mechanism (i.e., a GOF mutation in the transcription factor for Pdr1p) (*7*,*8*). Overall, our findings demonstrate that most FR BSI isolates of *C. glabrata* in South Korea harbor FR-specific Pdr1p AAS.

The cause of the high mortality rate associated with FR *C. glabrata* BSIs remains unclear. In this study, we focused on FR-specific Pdr1p AAS. *PDR1* mutations are associated with increased virulence of *C. glabrata*, expression of adhesins, and adherence to host epithelial cells (*7*,*12*,*47*,*48*). The fungal loads in the kidney, spleen, and liver were higher in mice infected with the FR Pdr1 mutant of *C. glabrata* than in mice infected with F-SDD isolates (*12*). *C. glabrata* might persist in the body by replicating inside phagocytes, eventually leading to cell lysis, rather than by active escape (the method used by *C. albicans*) (*47*,*49*). This process might partly explain the elevated cumulative mortality rate for patients with Pdr1 mutants. Appropriate antifungal therapy was the only independently associated protective factor, with respect to 30- and 90-day mortality rates, in patients infected with FR *C. glabrata* isolates. In patients who received inadequate antifungal therapy and azole monotherapy, the 30-day mortality rates were 90% (antifungal therapy) and 88.9% (azole monotherapy), which were significantly higher than those of the patients receiving combination therapy (36.4%) or appropriate antifungal therapy (47.7%). Previous antifungal exposure was not an independent risk factor for death among patients with FR isolates, although it was identified in 62.5% (40/64) of patients. Given that previous antifungal exposure is a risk factor for antifungal-resistant *Candida* BSI (*50*), further studies including F-SDD *C. glabrata* BSIs might elucidate the relationship between previous antifungal exposure and death. Taken together, these findings suggest that the high mortality rate associated with FR *C. glabrata* BSIs can be explained by the combination of FR and the virulence of Pdr1 mutants.

The first limitation of our study is that a *Candida* species might develop resistance within a patient during antifungal therapy; such resistance can be identified

through serial isolates, but we tested only the first isolate from each patient during 2016–2018. Second, our results did not show that FR, *PDR1* mutants, or previous antifungal exposure were independent risk factors for death in patients with *C. glabrata* BSIs. A total of 1,158 nonduplicate BSI isolates of *C. glabrata* from 19 university hospitals in South Korea were obtained during the 11-year study period, and the hospitals participating differed each year; therefore, we could not select an appropriate control group of F-SDD isolates. These limitations were partly overcome in a recent study involving 197 adult patients with *C. glabrata* BSI during January 2010–February 2016 at 7 university hospitals in South Korea. In that study, FR was shown to be associated with the 30-day mortality rate in a multivariate analysis (*37*). Third, only limited numbers of patients infected with F-SDD BSI isolates of *C. glabrata* were included in our mortality analysis. Nevertheless, we included a total of 297 patients infected with F-SDD BSI isolates of *C. glabrata,* which included all patients with *C. glabrata* from the participating hospitals in 2010, 2014, 2017, and 2018. The 30-day mortality rates of patients infected with F-SDD *C. glabrata* isolates were similar among those 4 years (32.0%–39.2%), despite differences in participating hospitals and collection periods; the 30-day mortality rate was similar to those reported in previous studies (*21*,*33*–*37*).

In conclusion, we demonstrated that nearly all FR BSI isolates of *C. glabrata* in South Korea harbored FR-specific Pdr1p mutations by excluding MLST genotype–specific Pdr1p AASs and that the isolates were associated with higher 30-day (60.9%) and 90-day (78.2%) mortality rates. These results suggest that Pdr1 mutants are associated with a risk for death in such patients. In addition, appropriate antifungal therapy was the only independent protective factor against death in patients with FR isolates. Because of the increasing prevalence of FR BSI isolates of *C. glabrata* worldwide, improved detection and appropriate antifungal treatments are critical.

This research was supported by the Basic Science Research Program through the National Research Foundation of South Korea funded by the Ministry of Education (grant no. NRF-2019R1A2C1004644).

About the Author

Dr. Won is an associate professor at Chonnam National University Hospital and Chonnam National University Medical School, Gwangju, South Korea. Her interests are the epidemiology, molecular identification, and resistance mechanisms of invasive fungal infections and medical parasitology. Dr. Choi works at the laboratory of medical mycology, focusing on invasive fungal infections, at Chonnam National University Hospital. She has conducted collaborative studies of the epidemiology of candidemia and related molecular resistance mechanisms.

References

1. Arendrup MC. Epidemiology of invasive candidiasis. Curr Opin Crit Care. 2010;16:445–52. https://doi.org/10.1097/MCC.0b013e32833e84d2
2. Arendrup MC, Patterson TF. Multidrug-resistant *Candida*: epidemiology, molecular mechanisms, and treatment. J Infect Dis. 2017;216(Suppl_3):S445–51. https://doi.org/10.1093/infdis/jix131
3. Jensen RH, Johansen HK, Søes LM, Lemming LE, Rosenvinge FS, Nielsen L, et al. Posttreatment antifungal resistance among colonizing *Candida* isolates in candidemia patients: results from a systematic multicenter study. Antimicrob Agents Chemother. 2015;60:1500–8. https://doi.org/10.1128/AAC.01763-15
4. Pfaller MA, Diekema DJ, Turnidge JD, Castanheira M, Jones RN. Twenty years of the SENTRY antifungal surveillance program: results for *Candida* species from 1997–2016. Open Forum Infect Dis. 2019;6(Suppl 1):S79–94. https://doi.org/10.1093/ofid/ofy358
5. Chapman B, Slavin M, Marriott D, Halliday C, Kidd S, Arthur I, et al.; Australian and New Zealand Mycoses Interest Group. Changing epidemiology of candidaemia in Australia. J Antimicrob Chemother. 2017;72:1103–8. https://doi.org/10.1093/jac/dkx047
6. Tan TY, Hsu LY, Alejandria MM, Chaiwarith R, Chinniah T, Chayakulkeeree M, et al. Antifungal susceptibility of invasive *Candida* bloodstream isolates from the Asia-Pacific region. Med Mycol. 2016;54:471–7. https://doi.org/10.1093/mmy/myv114
7. Ferrari S, Ischer F, Calabrese D, Posteraro B, Sanguinetti M, Fadda G, et al. Gain of function mutations in *CgPDR1* of *Candida glabrata* not only mediate antifungal resistance but also enhance virulence. PLoS Pathog. 2009;5:e1000268. https://doi.org/10.1371/journal.ppat.1000268
8. Tsai HF, Krol AA, Sarti KE, Bennett JE. *Candida glabrata PDR1*, a transcriptional regulator of a pleiotropic drug resistance network, mediates azole resistance in clinical isolates and petite mutants. Antimicrob Agents Chemother. 2006;50:1384–92. https://doi.org/10.1128/AAC.50.4.1384-1392.2006
9. Hull CM, Parker JE, Bader O, Weig M, Gross U, Warrilow AG, et al. Facultative sterol uptake in an ergosterol-deficient clinical isolate of *Candida glabrata* harboring a missense mutation in *ERG11* and exhibiting cross-resistance to azoles and amphotericin B. Antimicrob Agents Chemother. 2012;56:4223–32. https://doi.org/10.1128/AAC.06253-11
10. Abbes S, Mary C, Sellami H, Michel-Nguyen A, Ayadi A, Ranque S. Interactions between copy number and expression level of genes involved in fluconazole resistance in *Candida glabrata*. Front Cell Infect Microbiol. 2013;3:74. https://doi.org/10.3389/fcimb.2013.00074
11. Vu BG, Moye-Rowley WS. Construction and use of a recyclable marker to examine the role of major facilitator superfamily protein members in *Candida glabrata* drug resistance phenotypes. MSphere. 2018;3:e00099–18. https://doi.org/10.1128/mSphere.00099-18
12. Ferrari S, Sanguinetti M, Torelli R, Posteraro B, Sanglard D. Contribution of *CgPDR1*-regulated genes in enhanced

virulence of azole-resistant *Candida glabrata.* PLoS One. 2011;6:e17589. https://doi.org/10.1371/journal.pone.0017589
13. Hou X, Xiao M, Wang H, Yu SY, Zhang G, Zhao Y, et al. Profiling of *PDR1* and *MSH2* in *Candida glabrata* bloodstream isolates from a multicenter study in China. Antimicrob Agents Chemother. 2018;62:e00153–18. https://doi.org/10.1128/AAC.00153-18
14. Arastehfar A, Daneshnia F, Zomorodian K, Najafzadeh MJ, Khodavaisy S, Zarrinfar H, et al. Low level of antifungal resistance in Iranian isolates of *Candida glabrata* recovered from blood samples in a multicenter study from 2015 to 2018 and potential prognostic values of genotyping and sequencing of *PDR1.* Antimicrob Agents Chemother. 2019;63:e02503–18. https://doi.org/10.1128/AAC.02503-18
15. Hou X, Xiao M, Chen SC, Wang H, Yu SY, Fan X, et al. Identification and antifungal susceptibility profiles of *Candida nivariensis* and *Candida bracarensis* in a multi-center Chinese collection of yeasts. Front Microbiol. 2017;8:5. https://doi.org/10.3389/fmicb.2017.00005
16. Clinical and Laboratory Standards Institute. M27 reference method for broth dilution antifungal susceptibility testing of yeasts. 4th ed. Wayne (PA): Clinical and Laboratory Standards Institute; 2017.
17. Clinical and Laboratory Standards Institute. Performance standards for antifungal susceptibility testing of Yeasts. 1st ed. CLSI supplement M60. Wayne (PA): Clinical and Laboratory Standards Institute; 2017.
18. Clinical and Laboratory Standards Institute. Epidemiological cutoff values for antifungal susceptibility testing. 2nd ed. CLSI supplement M59. Wayne (PA): Clinical and Laboratory Standards Institute; 2018.
19. Rivero-Menendez O, Navarro-Rodriguez P, Bernal-Martinez L, Martin-Cano G, Lopez-Perez L, Sanchez-Romero I, et al. Clinical and laboratory development of echinocandin resistance in *Candida glabrata*: molecular characterization. Front Microbiol. 2019;10:1585. https://doi.org/10.3389/fmicb.2019.01585
20. Pappas PG, Kauffman CA, Andes DR, Clancy CJ, Marr KA, Ostrosky-Zeichner L, et al. Executive summary: clinical practice guideline for the management of candidiasis: 2016 update by the Infectious Diseases Society of America. Clin Infect Dis. 2016;62:409–17. https://doi.org/10.1093/cid/civ1194
21. Byun SA, Won EJ, Kim MN, Lee WG, Lee K, Lee HS, et al. Multilocus sequence typing (MLST) genotypes of *Candida glabrata* bloodstream isolates in Korea: association with antifungal resistance, mutations in mismatch repair gene (*Msh2*), and clinical outcomes. Front Microbiol. 2018;9:1523. https://doi.org/10.3389/fmicb.2018.01523
22. Kim MN, Shin JH, Sung H, Lee K, Kim EC, Ryoo N, et al. *Candida haemulonii* and closely related species at 5 university hospitals in Korea: identification, antifungal susceptibility, and clinical features. Clin Infect Dis. 2009;48:e57–61. https://doi.org/10.1086/597108
23. De Rosa FG, Trecarichi EM, Montrucchio C, Losito AR, Raviolo S, Posteraro B, et al. Mortality in patients with early- or late-onset candidaemia. J Antimicrob Chemother. 2013;68:927–35. https://doi.org/10.1093/jac/dks480
24. Nguyen MH, Clancy CJ, Yu VL, Yu YC, Morris AJ, Snydman DR, et al. Do in vitro susceptibility data predict the microbiologic response to amphotericin B? Results of a prospective study of patients with *Candida* fungemia. J Infect Dis. 1998;177:425–30. https://doi.org/10.1086/514193
25. Healey KR, Zhao Y, Perez WB, Lockhart SR, Sobel JD, Farmakiotis D, et al. Prevalent mutator genotype identified in fungal pathogen *Candida glabrata* promotes multi-drug resistance. Nat Commun. 2016;7:11128. https://doi.org/10.1038/ncomms11128
26. Niimi M, Nagai Y, Niimi K, Wada S, Cannon RD, Uehara Y, et al. Identification of two proteins induced by exposure of the pathogenic fungus *Candida glabrata* to fluconazole. J Chromatogr B Analyt Technol Biomed Life Sci. 2002;782:245–52. https://doi.org/10.1016/S1570-0232(02)00668-2
27. Sanguinetti M, Posteraro B, Fiori B, Ranno S, Torelli R, Fadda G. Mechanisms of azole resistance in clinical isolates of *Candida glabrata* collected during a hospital survey of antifungal resistance. Antimicrob Agents Chemother. 2005; 49:668–79. https://doi.org/10.1128/AAC.49.2.668-679.2005
28. Won EJ, Shin JH, Choi MJ, Lee WG, Park YJ, Uh Y, et al. Antifungal susceptibilities of bloodstream isolates of *Candida* species from nine hospitals in Korea: application of new antifungal breakpoints and relationship to antifungal usage. PLoS One. 2015;10:e0118770. https://doi.org/10.1371/journal.pone.0118770
29. Xiao M, Sun ZY, Kang M, Guo DW, Liao K, Chen SC, et al.; China Hospital Invasive Fungal Surveillance Net (CHIF-NET) Study Group. Five-year national surveillance of invasive candidiasis: species distribution and azole susceptibility from the China Hospital Invasive Fungal Surveillance Net (CHIF–NET) Study. J Clin Microbiol. 2018;56:e00577–18. https://doi.org/10.1128/JCM.00577-18
30. Hou X, Xiao M, Chen SC, Kong F, Wang H, Chu YZ, et al. Molecular epidemiology and antifungal susceptibility of *Candida glabrata* in China (August 2009 to July 2014): a multi-center study. Front Microbiol. 2017;8:880. https://doi.org/10.3389/fmicb.2017.00880
31. Ko JH, Jung DS, Lee JY, Kim HA, Ryu SY, Jung SI, et al. Changing epidemiology of non-*albicans* candidemia in Korea. J Infect Chemother. 2019;25:388–91. https://doi.org/10.1016/j.jiac.2018.09.016
32. Choi H, Kim JH, Seong H, Lee W, Jeong W, Ahn JY, et al. Changes in the utilization patterns of antifungal agents, medical cost and clinical outcomes of candidemia from the health-care benefit expansion to include newer antifungal agents. Int J Infect Dis. 2019;83:49–55. https://doi.org/10.1016/j.ijid.2019.03.039
33. Ruan SY, Huang YT, Chu CC, Yu CJ, Hsueh PR. *Candida glabrata* fungaemia in a tertiary centre in Taiwan: antifungal susceptibility and outcomes. Int J Antimicrob Agents. 2009;34:236–9. https://doi.org/10.1016/j.ijantimicag.2009.02.021
34. Horn DL, Neofytos D, Anaissie EJ, Fishman JA, Steinbach WJ, Olyaei AJ, et al. Epidemiology and outcomes of candidemia in 2019 patients: data from the prospective antifungal therapy alliance registry. Clin Infect Dis. 2009;48:1695–703. https://doi.org/10.1086/599039
35. Lee I, Morales KH, Zaoutis TE, Fishman NO, Nachamkin I, Lautenbach E. Clinical and economic outcomes of decreased fluconazole susceptibility in patients with *Candida glabrata* bloodstream infections. Am J Infect Control. 2010;38:740–5. https://doi.org/10.1016/j.ajic.2010.02.016
36. Eschenauer GA, Carver PL, Patel TS, Lin SW, Klinker KP, Pai MP, et al. Survival in patients with *Candida glabrata* bloodstream infection is associated with fluconazole dose. Antimicrob Agents Chemother. 2018;62:e02566–17. https://doi.org/10.1128/AAC.02566-17
37. Ko JH, Peck KR, Jung DS, Lee JY, Kim HA, Ryu SY, et al. Impact of high MIC of fluconazole on outcomes of *Candida glabrata* bloodstream infection: a retrospective multicenter cohort study. Diagn Microbiol Infect Dis. 2018;92:127–32. https://doi.org/10.1016/j.diagmicrobio.2018.05.001

38. Tortorano AM, Dho G, Prigitano A, Breda G, Grancini A, Emmi V, et al.; ECMM-FIMUA Study Group. Invasive fungal infections in the intensive care unit: a multicentre, prospective, observational study in Italy (2006–2008). Mycoses. 2012;55:73–9. https://doi.org/10.1111/j.1439-0507.2011.02044.x
39. Lortholary O, Renaudat C, Sitbon K, Madec Y, Denoeud-Ndam L, Wolff M, et al.; French Mycosis Study Group. Worrisome trends in incidence and mortality of candidemia in intensive care units (Paris area, 2002–2010). Intensive Care Med. 2014;40:1303–12. https://doi.org/10.1007/s00134-014-3408-3
40. Pfaller MA, Andes DR, Diekema DJ, Horn DL, Reboli AC, Rotstein C, et al. Epidemiology and outcomes of invasive candidiasis due to non-*albicans* species of *Candida* in 2,496 patients: data from the Prospective Antifungal Therapy (PATH) registry 2004-2008. PLoS One. 2014;9:e101510. https://doi.org/10.1371/journal.pone.0101510
41. Singh A, Healey KR, Yadav P, Upadhyaya G, Sachdeva N, Sarma S, et al. Absence of azole or echinocandin resistance in *Candida glabrata* isolates in India despite background prevalence of strains with defects in the DNA mismatch repair pathway. Antimicrob Agents Chemother. 2018;62:e00195–18. https://doi.org/10.1128/AAC.00195-18
42. Bordallo-Cardona MÁ, Agnelli C, Gómez-Nuñez A, Sánchez-Carrillo C, Bouza E, Muñoz P, et al. *MSH2* gene point mutations are not antifungal resistance markers in *Candida glabrata.* Antimicrob Agents Chemother. 2018;63:e01876–18. https://doi.org/10.1128/AAC.01876-18
43. Biswas C, Marcelino VR, Van Hal S, Halliday C, Martinez E, Wang Q, et al. Whole genome sequencing of Australian *Candida glabrata* isolates reveals genetic diversity and novel sequence types. Front Microbiol. 2018;9:2946. https://doi.org/10.3389/fmicb.2018.02946
44. Yao D, Chen J, Chen W, Li Z, Hu X. Mechanisms of azole resistance in clinical isolates of *Candida glabrata* from two hospitals in China. Infect Drug Resist. 2019;12:771–81. https://doi.org/10.2147/IDR.S202058
45. Whaley SG, Berkow EL, Rybak JM, Nishimoto AT, Barker KS, Rogers PD. Azole antifungal resistance in *Candida albicans* and emerging non–*albicans Candida* species. Front Microbiol. 2017;7:2173. https://doi.org/10.3389/fmicb.2016.02173
46. Tantivitayakul P, Lapirattanakul J, Kaypetch R, Muadcheingka T. Missense mutation in *CgPDR1* regulator associated with azole-resistant *Candida glabrata* recovered from Thai oral candidiasis patients. J Glob Antimicrob Resist. 2019;17:221–6. https://doi.org/10.1016/j.jgar.2019.01.006
47. Pais P, Galocha M, Viana R, Cavalheiro M, Pereira D, Teixeira MC. Microevolution of the pathogenic yeasts *Candida albicans* and *Candida glabrata* during antifungal therapy and host infection. Microb Cell. 2019;6:142–59. https://doi.org/10.15698/mic2019.03.670
48. Ni Q, Wang C, Tian Y, Dong D, Jiang C, Mao E, et al. *CgPDR1* gain-of-function mutations lead to azole-resistance and increased adhesion in clinical *Candida glabrata* strains. Mycoses. 2018;61:430–40. https://doi.org/10.1111/myc.12756
49. Brunke S, Hube B. Two unlike cousins: *Candida albicans* and *C. glabrata* infection strategies. Cell Microbiol. 2013;15:701–8. https://doi.org/10.1111/cmi.12091
50. Lortholary O, Desnos-Ollivier M, Sitbon K, Fontanet A, Bretagne S, Dromer F; French Mycosis Study Group. Recent exposure to caspofungin or fluconazole influences the epidemiology of candidemia: a prospective multicenter study involving 2,441 patients. Antimicrob Agents Chemother. 2011;55:532–8. https://doi.org/10.1128/AAC.01128-10

Address for correspondence: Jong Hee Shin, Department of Laboratory Medicine, Chonnam National University Medical School, 42 Jebong-ro, Dong-gu, Gwangju 61469, South Korea; email: shinjh@chonnam.ac.kr

Excess All-Cause Deaths during Coronavirus Disease Pandemic, Japan, January–May 2020[1]

Takayuki Kawashima,[2] Shuhei Nomura,[2] Yuta Tanoue, Daisuke Yoneoka, Akifumi Eguchi, Chris Fook Sheng Ng, Kentaro Matsuura, Shoi Shi, Koji Makiyama, Shinya Uryu, Yumi Kawamura, Shinichi Takayanagi, Stuart Gilmour, Hiroaki Miyata, Tomimasa Sunagawa, Takuri Takahashi, Yuuki Tsuchihashi, Yusuke Kobayashi, Yuzo Arima, Kazuhiko Kanou, Motoi Suzuki, Masahiro Hashizume

To provide insight into the mortality burden of coronavirus disease (COVID-19) in Japan, we estimated the excess all-cause deaths for each week during the pandemic, January–May 2020, by prefecture and age group. We applied quasi-Poisson regression models to vital statistics data. Excess deaths were expressed as the range of differences between the observed and expected number of all-cause deaths and the 95% upper bound of the 1-sided prediction interval. A total of 208–4,322 all-cause excess deaths at the national level indicated a 0.03%–0.72% excess in the observed number of deaths. Prefecture and age structure consistency between the reported COVID-19 deaths and our estimates was weak, suggesting the need to use cause-specific analyses to distinguish between direct and indirect consequences of COVID-19.

Severe acute respiratory syndrome coronavirus 2 (SARS-CoV-2) first appeared in December 2019 in Wuhan, China, and has rapidly led to a global pandemic (*1*). Globally, accurate figures on deaths caused by coronavirus disease (COVID-19) have been difficult to obtain because of limited availability and quality of virus testing (*2*,*3*) (Y. Yang et al., unpub. data, https://www.medrxiv.org/content/10.1101/2020.02.11.20021493v2); it is generally accepted that many deaths caused by COVID-19 have not yet been recorded (*4*). Lockdown measures are in place in many countries and regions around the world, but such measures can lead to reduced access to health services, exacerbating chronic diseases and delaying response to acute diseases (*5*). Access to hospitals for elective surgery may also be hampered by the collapsing medical system associated with the increased number of COVID-19 patients (*6*). The cause of death, especially among elderly persons in care homes or living alone, may not be adequately diagnosed or even recorded during a pandemic situation (*7*).

When comprehensive testing is lacking, the mortality burden of a new pandemic is commonly estimated by an increase in the number of deaths that is greater than would be expected under normal circumstances (e.g., in the absence of a pandemic)—the so-called excess-death approach (*8*,*9*). This approach can be applied to specific causes of death directly related to the pathogen, such as for pneumonia or other respiratory diseases, or to other categories of death that are directly or indirectly affected by a pandemic. For example, excess-death methods have been used to quantify formal underestimation of the mortality burden of COVID-19 in many heavily affected countries (*10*–*17*).

The early and comprehensive response to the COVID-19 pandemic in Japan probably enabled the

Author affiliations: Tokyo Institute of Technology, Tokyo, Japan (T. Kawashima); Keio University, Tokyo (T. Kawashima, S. Nomura, Y. Tanoue, D. Yoneoka, A. Eguchi, S. Shi, Y. Kawamura, H. Miyata); The University of Tokyo, Tokyo (S. Nomura, D. Yoneoka, S. Shi, M. Hashizume); Waseda University, Tokyo (Y. Tanoue); St. Luke's International University, Tokyo (D. Yoneoka, S. Gilmour); Chiba University, Chiba, Japan (A. Eguchi); Nagasaki University, Nagasaki, Japan (C.F.S. Ng); Tokyo University of Science, Tokyo (K. Matsuura); HOXO-M Inc., Tokyo (K. Matsuura, K. Makiyama, S. Takayanagi); RIKEN Center for Biosystems Dynamics Research, Osaka, Japan (S. Shi); National Institute for Environmental Studies, Tokyo (S. Uryu); RIKEN Center for Sustainable Resource Science, Saitama, Japan (Y. Kawamura); National Institute of Infectious Diseases, Tokyo (T. Sunagawa, T. Takahashi, Y. Tsuchihashi, Y. Kobayashi, Y. Arima, K. Kanou, M. Suzuki)

DOI: https://doi.org/10.3201/eid2703.203925

[1]A part of the estimates of excess all-cause deaths through May 2020, including those for all ages, reported in this article was also reported on the website of the National Institute of Infectious Diseases in Japan on August 31, 2020 (https://www.niid.go.jp/niid/ja/from-idsc/493-guidelines/9835-excess-mortality-20aug.html).

[2]These first authors contributed equally to this article.

country to avoid the severe epidemics experienced in Europe; as of September 2, 2020, a total of 68,392 COVID-19 cases and 1,296 related deaths had occurred in Japan (*18*). Nonetheless, despite an effective response, in early April as cases began to increase rapidly, the health system began to experience pressures similar to those in other countries, and the government declared a state of emergency (*19*). Perhaps uniquely among global movement restrictions, in Japan, these restrictions were completely voluntary, with no legal force; routine healthcare functions continued, including elective surgery and outpatient services for nonurgent health issues. Given the relatively limited spread of the epidemic in Japan and the voluntary nature of the lockdown, it is possible that the pattern of excess deaths in Japan differs from that in other countries. To provide insight into the mortality burden of COVID-19 in Japan, we estimated excess deaths from all causes during each week from the early COVID-19 outbreak in Japan, January–May 2020, by prefecture and patient age. Ethics approval was granted by the ethics committee of the National Institute of Infectious Diseases (authorization no. 1174).

Methods

Data

For this study, we used mortality data from the Vital Statistics System of Japan, which compiles the Vital Statistics Survey data prepared by each municipality under the Family Registration Law and the Provisions on the Notification of Stillbirths (*20*). Vital statistics are divided into 3 major types: annual vital statistics, monthly vital statistics, and prompt vital statistics. Annual vital statistics are compiled for 1 year (January–December) from the monthly vital statistics and are published around September each year. Monthly vital statistics are published ≈5 months after the month in which the survey forms are collected from the municipalities. Prompt vital statistics are published ≈2 months after the month of survey form collection.

According to the Family Registration Law, a notification of death must be submitted to a municipal office within 7 days of the day on which the person's death was confirmed. The notification must be submitted by a relative or a person who lived with the deceased or, in some cases, by landlords, house managers, or persons with similar roles. For the Prompt Vital Statistics report, data for a given month are based on death notifications reported to the municipality by the 14th of the following month. In other words, a death notification reported on or after the 15th with a death date of the previous month is placed in the dataset for the current month, not the previous month. For example, if a death notification is reported by February 14 with a death date of January 20, the data will be included in the January Prompt Vital Statistics report, but if the death is reported on February 15, it will be included in the February Prompt Vital Statistics report, referred to as a reporting delay. The delay in reporting deaths addressed in this study refers to any delays between the death confirmation process to submission of the death notifications to the municipal offices, perhaps depending on where the death occurs. The observed numbers of deaths in the Prompt Vital Statistics report were adjusted for this reporting delay up to 3 months to avoid a possible undercount of observed deaths. We used these adjusted data in our excess deaths analysis.

For this analysis, we used data from 2012 on (including the last few days of 2011 for weekly analysis purposes): Annual Vital Statistics report for 2011–2018, Monthly Vital Statistics report for 2019, and Prompt Vital Statistics report for January–May 2020. The target population was all persons who had resident cards and died in Japan, regardless of nationality. However, the analysis excluded those who died abroad, those who were staying in Japan for a short time (without a resident card), and those whose place of residence or date of birth was unknown. Our data did not include cause-of-death information; only age at death and place of residence (prefecture) were available for analysis.

Excess Deaths Analysis

To estimate excess deaths in Japan, we used the Farrington algorithm, which is commonly used to estimate excess deaths and is used by the US Centers for Disease Control and Prevention to estimate excess deaths associated with COVID-19 (*21*). The Farrington algorithm uses a quasi-Poisson regression (a generalized linear model accounting for overdispersion) to estimate the expected number of deaths per week. The algorithm is designed to limit the data used for estimation: the expected number of deaths at a certain week t is estimated by using only the data during $t - w$ and $t + w$ weeks of years $h - b$ and $h - 1$, where w and b are predetermined parameters and h is the year of t, referred to as the reference period. Data for a period of 1 year that is not included in the reference period are divided equally and included in the regression model as dummy variables, which enables the model to capture seasonality. Thus, the regression model is $\log(E(Y_t) = \alpha + \beta t + f^{\Gamma}(t)\gamma_{f(t)}$, where Y_t is the number of deaths at a certain week t, α and β are regression parameters, $\gamma_{f(t)}$ is a regression parameter vector representing seasonality, and $f(t)$ is a vector of

dummy variables that equally divides the time points outside the reference period.

In this study, we divided the data into 9 periods, as was done in a previous study (*21*). More details can be found elsewhere (*8*,*9*). In our study, we considered data up to 5 years ago ($b = 5$) and used data for 3 weeks ($w = 3$) before and after a certain point as the reference period, as was done in previous studies (*21*,*22*). We checked for overdispersion by comparing mean and variance of weekly deaths and used an overdispersed Poisson model where significant overdispersion was found after a regression-based (1-sided) test for overdispersion in the Poisson model (*23*). Also, as a sensitivity analysis, we changed the reference period to confirm the robustness of the results based on combinations of $b = 3$ or 4 and $w = 2$ or 4.

The model estimation was stratified by prefecture and age group (all ages, <25 years, 25–44 years, 45–64 years, 65–74 years, 75–84 years, ≥85 years). Age group was determined by considering the age structure and the number of persons sufficient for analysis. All age estimates (for all persons) do not add up to age group–specific estimates. The conversion from daily data to weekly data is based on the epidemiologic week of the National Institute of Infectious Diseases' Infectious Diseases Weekly Report (*24*).

Number of Excess All-Cause Deaths

On the basis of the model equation shown in the previous section, we estimated the expected number of all-cause deaths per week and the associated 95% upper bound of the 1-sided prediction interval, which is an indicator of uncertainty. We set these 2 thresholds (point estimate and upper bound) for excess death according to previous studies (*21*). We report the range of differences between the observed number of all-cause deaths and each of these thresholds as excess deaths.

To obtain the national level of excess all-cause deaths for each week, we summed the observed and the expected number of all-cause deaths separately across all prefectures in each week and computed the weekly differences for the country. The total (cumulative) number of excess all-cause deaths in each prefecture during the COVID-19 pandemic was calculated by summing the excess all-cause deaths (with negative values set to 0) in each week, from the beginning of 2020 (December 30, 2019–January 5, 2020) through May 2020 (May 25–31, 2020). We calculated the national cumulative number of excess all-cause deaths for the given period by summing the prefecture-specific excess deaths, a method consistent with US Centers for Disease Control and Prevention methods used (*8*). Last, we defined the percentage of excess deaths during the COVID-19 pandemic as the cumulative number of excess deaths divided by the observed cumulative number of deaths.

Adjusting for Reporting Delays

The observed number of deaths in the Prompt Vital Statistics report may differ from the actual number of deaths because of delays in reporting deaths (i.e., fewer deaths in the Prompt Vital Statistics report than in Monthly or Annual Vital Statistics reports published later). We took into account the reporting delay of up to 3 months by calculating the reporting delay rate (deaths reported 1, 2, and 3 months behind) for each prefecture and then adjusting the observed number of deaths in the latest 3 months (March–May 2020). Thus, the observed number of deaths in March was adjusted for a 3-month reporting delay (such as June deaths not available in our data; similarly, those in April were adjusted for 2- and 3-month reporting delays and those in May were adjusted for 1-, 2-, and 3-month reporting delays (Appendix, https://wwwnc.cdc.gov/EID/article/27/3/20-3925-App1.pdf).

To verify the validity of this adjustment method, we compared the weekly observed number of all-cause deaths in February, based on the Prompt Vital Statistics report through May with no adjustment for the reporting delay, and those in February, based on the Prompt Vital Statistics report through April with adjustment for reporting delays in May. The proportionate differences were then calculated for each week of February 2020. The largest difference was observed in Tokyo Prefecture (January 27–February 2, 2020) and Fukuoka Prefecture (January 27–February 2, 2020) at 5 deaths (Appendix Table 1), and the largest proportionate difference was observed in Tottori Prefecture (January 27–February 2, 2020) at 0.694%.

Results

We calculated mean and variance of the outcome (i.e., no. deaths/week among age- and prefecture-combined populations) to test the overdispersion; on the basis of the results ($p<0.01$), we used the quasi-Poisson regression for analysis. The cumulative number of excess all-cause deaths of the 47 prefectures was 208–4,322 (0.03%–0.72% excess) (Table). Weeks with observed all-cause deaths exceeding the 95% upper bound of the 1-sided interval of predicted deaths from the beginning of 2020 through May 2020 were detected in 13 prefectures. The cumulative numbers of excess all-cause deaths (percent excess) over the period for the 13 prefecture were as follows: Ibaraki, 1–87, 0.01%–0.60%; Tochigi, 13–137, 0.14%–1.42%; Gunma, 31–146, 0.30%–1.43%; Saitama, 14–334, 0.05%–1.10%; Chiba, 51–253,

0.19%–0.94%; Tokyo, 32–330, 0.06%–0.63%; Toyama, 18–120, 0.32%–2.11%; Shizuoka, 2–109, 0.01%–0.59%; Aichi, 7–214, 0.02%–0.70%; Osaka, 6–277, 0.01%–0.69%; Nara, 21–107, 0.32%–1.65%; Tokushima, 4–71, 0.09%–1.64%; and Kagawa, 8–135, 0.15%–2.51%.

Of the 32 prefectures in which COVID-19 deaths were confirmed through end of May 2020, the observed number of all-cause deaths for all ages exceeded the 95% upper bound in 11 prefectures (34.4%, 11 of 32) for some weeks and the point estimates in all prefectures. Of the remaining 15 prefectures in which no deaths from COVID-19 had been confirmed, the observed number of all-cause deaths for all ages exceeded the 95% upper bound in 2 (13.3%) of the 15 prefectures for some weeks and the point estimate in 14 (93.3%) of the 15 prefectures. Only in Niigata Prefecture did the observed number of all-cause deaths for all ages not exceed the point estimates for the period.

Sensitivity analyses in which the reference period was changed to confirm the robustness of the results

Table. Number of observed and excess all-cause deaths, and reported number of COVID-19 deaths, Japan, December 30, 2019–May 31, 2020*

Prefecture	No. all-cause deaths			No. COVID-19 deaths	No. tests
	Observed	Excess	Percentage		
Hokkaido	27,661	0–115	0.00–0.42	86	14,000
Aomori	7,713	0–36	0.00–0.47	1	850
Iwate	7,588	0–81	0.00–1.07	0	662
Miyagi	10,725	0–57	0.00–0.53	1	2,944
Akita	6,656	0–72	0.00–1.08	0	933
Yamagata	6,606	0–49	0.00–0.74	0	2,659
Fukushima	10,714	0–34	0.00–0.32	0	4,452
Ibaraki	14,443	1–87	0.01–0.60	10	4,628
Tochigi	9,623	13–137	0.14–1.42	0	3,871
Gunma	10,175	31–146	0.30–1.43	19	3,655
Saitama	30,426	14–334	0.05–1.10	48	20,735
Chiba	26,841	51–253	0.19–0.94	45	14,688
Tokyo	52,350	32–330	0.06–0.63	305	38,566
Kanagawa	36,174	0–89	0.00–0.25	82	9,446
Niigata	12,704	0–0	0.00–0.00	0	4,180
Toyama	5,689	18–120	0.32–2.11	22	3,144
Ishikawa	5,538	0–33	0.00–0.60	25	2,723
Fukui	4,045	0–47	0.00–1.16	8	2,631
Yamanashi	4,276	0–60	0.00–1.40	1	3,877
Nagano	11,148	0–29	0.00–0.26	0	2,714
Gifu	9,889	0–31	0.00–0.31	7	3,610
Shizuoka	18,554	2–109	0.01–0.59	1	3,521
Aichi	30,583	7–214	0.02–0.70	34	9,970
Mie	9,056	0–57	0.00–0.63	1	2,505
Shiga	5,606	0–65	0.00–1.16	1	1,856
Kyoto	11,814	0–84	0.00–0.71	17	7,933
Osaka	40,017	6–277	0.01–0.69	83	31,156
Hyogo	25,490	0–69	0.00–0.27	42	11,128
Nara	6,474	21–107	0.32–1.65	2	2,545
Wakayama	5,547	0–66	0.00–1.19	3	3,701
Tottori	3,156	0–44	0.00–1.39	0	1,338
Shimane	4,203	0–73	0.00–1.74	0	1,125
Okayama	9,493	0–75	0.00–0.79	0	1,705
Hiroshima	13,250	0–45	0.00–0.34	3	6,907
Yamaguchi	8,171	0–50	0.00–0.61	0	1,701
Tokushima	4,339	4–71	0.09–1.64	1	741
Kagawa	5,374	8–135	0.15–2.51	0	2,187
Ehime	7,913	0–50	0.00–0.63	4	2,074
Kochi	4,383	0–58	0.00–1.32	3	1,793
Fukuoka	23,346	0–77	0.00–0.33	26	12,634
Saga	4,412	0–53	0.00–1.20	0	1,417
Nagasaki	7,686	0–85	0.00–1.11	1	2,754
Kumamoto	9,340	0–43	0.00–0.46	3	3,924
Oita	6,279	0–52	0.00–0.83	1	3,988
Miyazaki	6,101	0–120	0.00–1.97	0	1,368
Kagoshima	9,309	0–59	0.00–0.63	0	1,859
Okinawa	5,334	0–44	0.00–0.82	6	2,863
Total	596,214	208–4,322	0.03–0.72	892	269,661

*The national-level cumulative number of excess all-cause deaths was calculated by summing the excess all-cause deaths of 47 prefectures (*25*).
COVID-19, coronavirus disease.

showed that, depending on the model parameter settings, weeks with observed all-cause deaths exceeding the 95% upper bound were also observed in additional prefectures, including Shiga, Shimane, Kochi, Fukuoka, Kumamoto, Oita, and Miyazaki (Appendix Table 2). As of the end of May 2020, deaths from COVID-19 had not been confirmed in Shimane and Miyazaki Prefectures.

The totals of excess all-cause deaths (percent excess) at the national level by age group were as follows: <25 years of age, 47–751 (1.61–25.76); 25–44 years, 66–1,302 (0.84–16.66); 45–64 years, 207–2,958 (0.47–6.67); 65–74 years, 143–2,959 (0.17–3.48); 75–84 years, 110–3,100 (0.07–1.86); and ≥85 years, 73–2,466 (0.03–0.85) (Appendix Table 3). Weeks with observed all-cause deaths exceeding the 95% upper bound for each age group were observed in 28, 23, 25, 25, 20, and 8 prefectures for these age groups, respectively. Weeks in which observed all-cause deaths exceeded point estimates were observed for all 47 prefectures and age groups.

Weekly observed and expected number of all-cause deaths in 4 prefectures reflect the large number of reported COVID19 deaths as of the end of May 2020 (Tokyo, Hokkaido, Osaka, and Kanagawa) for all ages and by age group (Appendix Figure 1). For all age groups, weeks of excess deaths occurred in previous years, not only during the COVID-19 pandemic. Data for the other 43 prefectures and national-level data are also shown (Appendix Figure 2).

Discussion

Excess-death monitoring has been used to track influenza epidemics worldwide and to identify the high potential mortality burden of COVID-19 in some hard-hit countries. We used a similar approach to capture the overall mortality burden of COVID-19. Monitoring changes and trends in all-cause deaths provides insight into the magnitude of the overall mortality burden caused by COVID-19, both directly and indirectly, which was overlooked in the official number of COVID-19 deaths. Given the variability in testing intensity among prefectures, this type of monitoring provides valuable information about the social effects of a pandemic and the extent to which virus testing may miss deaths caused by COVID-19. Useful indicators of the severity of the pandemic may include syndromic endpoints such as COVID-19 deaths, outpatient visits, and emergency department visits for fever or other COVID-19–associated symptoms (*26*). However, in the absence of comprehensive testing for COVID-19, estimates of the number of excess all-cause deaths may be more reliable than the reported number of COVID-19 deaths, especially in areas where testing is not widespread, so as to assess the progression of a pandemic and the effects of interventions.

During January–May 2020, the 208–4,322 excess deaths in all 47 prefectures represented just 0.03%–0.72% of all deaths observed in Japan through May 31, 2020. Although a complete country comparison is not possible, given the different methods for estimating excess deaths in each country (*2*,*3*) (Y. Yang et al., unpub. data, https://www.medrxiv.org/content/10.1101/2020.02.11.20021493v2), the number of deaths caused by COVID-19 in Japan, which was ≈0.7 deaths/100,000 population as of May 31 (and 1.3 deaths/100,000 population as of October 31), is 10 to 100 times lower than that for many countries in Europe and for the United States (*27*), indicating the relative low overall mortality burden from COVID-19 in Japan. This low overall mortality burden probably reflects the benefits of Japan's rapid and comprehensive response to the COVID-19 pandemic, which began with voluntary restrictions of public events in mid-February 2020 (*28*).

The excess all-cause deaths that we report can be interpreted as the sum of the following scenarios: 1) COVID-19 was the primary cause of death; 2) although other causes were diagnosed as the primary cause of death, the actual cause of death was COVID-19; 3) COVID-19 was not diagnosed as the primary cause of death, but because of the effects of the COVID-19 epidemic, death was caused by other diseases. For example, persons may hesitate to visit a hospital because of the declaration of an emergency or self-restraint in going out, or their chronic disease may worsen because of lifestyle changes, resulting in death (*21*). On the other hand, if deaths from causes other than COVID-19 decrease under the pandemic situation (as may have occurred with deaths from traffic accidents and suicide [*29*]), excess deaths directly caused by COVID-19 may be offset by the negative portion of those deaths. In fact, traffic accidents in Japan had decreased because of decreased traffic volume resulting from stay-at-home requests by central and local governments, and it is possible that the number of deaths from injuries had decreased (*29*).

Weeks with observed all-cause deaths exceeding the 95% upper bound of the 1-sided prediction interval were observed for 13 prefectures, of which COVID-19 deaths have been confirmed for 11. On the other hand, COVID-19 deaths have been observed in 22 other prefectures where no all-cause excess deaths were observed, suggesting that COVID-19 deaths in these prefectures were not high enough to overcome natural weekly variations in mortality rates, that there may be an offsetting

reduction in deaths because of the indirect effects of the pandemic in these communities, or both.

According to Ministry of Health, Labour and Welfare data as of May 27, 2020, proportions of COVID-19 deaths were higher for persons in older age groups: 55.8% at ≥80 years of age, followed by 27.3% at 70–79 years (*30*). Although the officially reported number of COVID-19 deaths may not be free of bias (e.g., different likelihood of testing by age group), these data indicate that prefecture and age structure of the reported COVID-19 deaths were not consistent with our estimates, suggesting the need to distinguish between direct and indirect consequences of COVID-19 by using cause-specific analyses. For the design of future broad-based infectious disease countermeasures such as lockdowns, knowing whether excess deaths in vulnerable age groups arises from direct COVID-19 deaths, indirect causes, or preventable deaths from unrelated causes would be useful.

The limitations of our analysis are the same as those for other excess-deaths studies (*15*,*31*). First, for this study, we did not take into account the cause of death, so the excess death estimates we present are not necessarily estimates of excess deaths caused by COVID-19. In addition, data from January–May 2020 are incomplete in the Prompt Vital Statistics report, especially in the most recent month. We have not considered the cause of the delay in reporting (e.g., delay mechanism) because we believe that adjusting for the delay by cause was impossible. Therefore, we selected a comprehensive adjustment method that does not depend on the cause of the delay by setting 3 assumptions (Appendix). We have also confirmed that validity is sufficient. Validity evaluation indicated that our adjustment for the reporting delay was reasonable to some extent, although this evaluation is within the scope of our 3 assumptions. Although waiting until Monthly Vital Statistics reports are published before analyzing the complete data would be ideal, during a public health emergency it is necessary to analyze the data in a timely manner and the limitations of data adjustment are a trade-off. Last, the method we used in this study is an algorithm for identifying excess deaths, which was not designed for assessing death reduction (*8*,*9*). If the expected number of deaths in a week was less than the actual number of deaths (negative value), the negative value was set to 0. However, as noted above, the effect of COVID-19 on mortality burden has not necessarily been positive (an increasing effect) but may be negative (a decreasing effect). For example, no deaths caused by COVID-19 were observed in Niigata Prefecture as of May 2020, and this study estimated 0–0 excess deaths in the prefecture during January–May 2020. In prefectures where the effect of COVID-19 is relatively small, an algorithm that identifies exiguous deaths might provide more suggestive data than an algorithm that identifies excess deaths. However, our aim with this study was to evaluate the increase in the mortality burden caused by COVID-19, using the methods of previous studies conducted in other countries; exiguous deaths will be evaluated in future analyses.

In conclusion, we found a much lower overall excess mortality burden from COVID-19 in Japan than in Europe and the United States. However, a weak prefecture and age structure consistency between the reported COVID-19 deaths and our estimates also suggest the need to distinguish between direct and indirect consequences of COVID-19 by cause-specific analyses, which can provide more information about the severity and progression of the COVID-19 pandemic. More detailed cause-specific analyses of excess deaths in Japan, especially among persons in older age groups, will enable better design of future interventions to protect vulnerable age groups and also offer lessons to other countries on proper management and implementation of movement restrictions. By paying careful attention to the excess death patterns in Japan, countries more heavily affected by COVID-19 can improve their own future response and better respond to the health needs of critically affected countries.

This study was supported in part by a grant from the Ministry of Health, Labour and Welfare of Japan (no. JPMH20HA2007 to M.S. and M.H.).

About the Authors

Dr. Kawashima is an assistant professor in the Department of Mathematical and Computing Science at Tokyo Institute of Technology, Tokyo, Japan. His research interests include mathematical statistics and its applications of related fields. Dr. Nomura is an associate professor working in the Department of Health Policy and Management, School of Medicine, Keio University, Tokyo; and an assistant professor of the Department of Global Health Policy, Graduate School of Medicine, The University of Tokyo, Tokyo. His research interests include global burden of disease, global health policy, biostatistics, and epidemiology.

References

1. World Health Organization. WHO Director-General's opening remarks at the media briefing on COVID-19 – 11 March 2020 [cited 2020 Aug 4]. https://www.who.int/dg/speeches/detail/who-director-general-s-opening-remarks-at-the-media-briefing-on-covid-19—11-march-2020
2. Lisboa Bastos M, Tavaziva G, Abidi SK, Campbell JR, Haraoui LP, Johnston JC, et al. Diagnostic accuracy of

serological tests for covid-19: systematic review and meta-analysis. BMJ. 2020;370:m2516. https://doi.org/10.1136/bmj.m2516
3. Kucirka LM, Lauer SA, Laeyendecker O, Boon D, Lessler J. Variation in false-negative rate of reverse transcriptase polymerase chain reaction-based SARS-CoV-2 tests by time since exposure. Ann Intern Med. 2020;173:262–7. https://doi.org/10.7326/M20-1495
4. Pulla P. What counts as a covid-19 death? BMJ. 2020;370:m2859. https://doi.org/10.1136/bmj.m2859
5. Kaufman HW, Chen Z, Niles J, Fesko Y. Changes in the number of US patients with newly identified cancer before and during the coronavirus disease 2019 (COVID-19) pandemic. JAMA Netw Open. 2020;3:e2017267. https://doi.org/10.1001/jamanetworkopen.2020.17267
6. Garcia S, Albaghdadi MS, Meraj PM, Schmidt C, Garberich R, Jaffer FA, et al. Reduction in ST-segment elevation cardiac catheterization laboratory activations in the United States during COVID-19 pandemic. J Am Coll Cardiol. 2020;75:2871–2. https://doi.org/10.1016/j.jacc.2020.04.011
7. BBC News. Coronavirus: older people being 'airbrushed' out of virus figures [cited 2020 Sep 3]. https://www.bbc.com/news/uk-52275823
8. Farrington CP, Andrews NJ, Beale AD, Catchpole MA. A statistical algorithm for the early detection of outbreaks of infectious disease. J R Stat Soc Ser A Stat Soc. 1996;159:547–63. https://doi.org/10.2307/2983331
9. Noufaily A, Enki DG, Farrington P, Garthwaite P, Andrews N, Charlett A. An improved algorithm for outbreak detection in multiple surveillance systems. Stat Med. 2013;32:1206–22. https://doi.org/10.1002/sim.5595
10. Michelozzi P, de'Donato F, Scortichini M, Pezzotti P, Stafoggia M, De Sario M, et al. Temporal dynamics in total excess mortality and COVID-19 deaths in Italian cities. BMC Public Health. 2020;20:1238. https://doi.org/10.1186/s12889-020-09335-8
11. Krieger N, Chen JT, Waterman PD. Excess mortality in men and women in Massachusetts during the COVID-19 pandemic. Lancet. 2020;395:1829. https://doi.org/10.1016/S0140-6736(20)31234-4
12. Banerjee A, Pasea L, Harris S, Gonzalez-Izquierdo A, Torralbo A, Shallcross L, et al. Estimating excess 1-year mortality associated with the COVID-19 pandemic according to underlying conditions and age: a population-based cohort study. Lancet. 2020;395:1715–25. https://doi.org/10.1016/S0140-6736(20)30854-0
13. Burki T. England and Wales see 20 000 excess deaths in care homes. Lancet. 2020;395:1602. https://doi.org/10.1016/S0140-6736(20)31199-5
14. Centers for Disease Control and Prevention. Preliminary estimate of excess mortality during the COVID-19 outbreak—New York City, March 11–May 2, 2020 [cited 2020 Aug 5]. https://www.cdc.gov/mmwr/volumes/69/wr/mm6919e5.htm
15. Vestergaard LS, Nielsen J, Richter L, Schmid D, Bustos N, Braeye T, et al.; ECDC Public Health Emergency Team for COVID-19. Excess all-cause mortality during the COVID-19 pandemic in Europe - preliminary pooled estimates from the EuroMOMO network, March to April 2020. Euro Surveill. 2020;25:2001214. https://doi.org/10.2807/1560-7917.ES.2020.25.26.2001214
16. Charu V, Simonsen L, Lustig R, Steiner C, Viboud C. Mortality burden of the 2009–10 influenza pandemic in the United States: improving the timeliness of influenza severity estimates using inpatient mortality records. Influenza Other Respir Viruses. 2013;7:863–71. https://doi.org/10.1111/irv.12096
17. Vestergaard LS, Nielsen J, Krause TG, Espenhain L, Tersago K, Bustos Sierra N, et al. Excess all-cause and influenza-attributable mortality in Europe, December 2016 to February 2017. Euro Surveill. 2017;22:30506. https://doi.org/10.2807/1560-7917.ES.2017.22.14.30506
18. Ministry of Health, Labour and Welfare. Press conference on COVID-19 on December 11, 2020 [cited 2020 Sep 3]. https://www.mhlw.go.jp/stf/seisakunitsuite/bunya/newpage_00032.html
19. Cabinet Secretariat. [COVID-19] press conference by the Prime Minister regarding the declaration of a state of emergency [cited 2020 Aug 4]. https://japan.kantei.go.jp/98_abe/statement/202004/_00001.html
20. Ministry of Health, Labour and Welfare. Outline of vital statistics in Japan [cited 2020 Aug 4]. https://www.mhlw.go.jp/english/database/db-hw/outline/index.html
21. Centers for Disease Control and Prevention. Excess deaths associated with COVID-19 [cited 2020 Aug 4]. https://www.cdc.gov/nchs/nvss/vsrr/covid19/excess_deaths.htm
22. Bédubourg G, Le Strat Y. Evaluation and comparison of statistical methods for early temporal detection of outbreaks: a simulation-based study. PLoS One. 2017;12:e0181227. https://doi.org/10.1371/journal.pone.0181227
23. Cameron AC, Trivedi PK. Regression-based tests for overdispersion in the Poisson model. Journal of Econometrics. 1990;46:347–64.
24. National Institute of Infectious Diseases. Report week correspondence table [in Japanese] [cited 2020 Aug 4]. https://www.niid.go.jp/niid/ja/calendar.html
25. Toyo Keizai Online. Coronavirus disease (COVID-19) situation report in Japan. 2020 [cited 2020 Aug 5]. https://toyokeizai.net/sp/visual/tko/covid19/en.html
26. Olson DR, Heffernan RT, Paladini M, Konty K, Weiss D, Mostashari F. Monitoring the impact of influenza by age: emergency department fever and respiratory complaint surveillance in New York City. PLoS Med. 2007;4:e247. https://doi.org/10.1371/journal.pmed.0040247
27. The Economist. Tracking covid-19 excess deaths across countries [cited 2020 Sep 3]. https://www.economist.com/graphic-detail/2020/07/15/tracking-covid-19-excess-deaths-across-countries
28. Ministry of Health, Labour and Welfare. Message to the public about holding events [in Japanese] [cited 2020 Sep 7]. https://www.mhlw.go.jp/stf/seisakunitsuite/newpage_00002.html#20
29. The Japan Times. Japan traffic accidents fall in first half amid pandemic [cited 2020 Aug 4]. https://www.japantimes.co.jp/news/2020/07/28/national/japan-traffic-accidents-fall-first-half-amid-pandemic/
30. Ministry of Health, Labour and Welfare. Domestic incidence of new coronavirus infections (at 18:00 pm on May 27, 2020) [in Japanese] [cited 2020 Sep 3]. https://www.mhlw.go.jp/content/10906000/000634824.pdf
31. Weinberger DM, Chen J, Cohen T, Crawford FW, Mostashari F, Olson D, et al. Estimation of excess deaths associated with the COVID-19 pandemic in the United States, March to May 2020. JAMA Intern Med. 2020;180:1336–44. https://doi.org/10.1001/jamainternmed.2020.3391

Address for correspondence: Masahiro Hashizume, Department of Global Health Policy, Graduate School of Medicine, The University of Tokyo, 7-3-1 Hongo, Bunkyo-ku, Tokyo 113-0033, Japan; email: hashizume@m.u-tokyo.ac.jp

Prevalence of SARS-CoV-2 Antibodies in First Responders and Public Safety Personnel, New York City, New York, USA, May–July 2020

Samira Sami, Lara J. Akinbami, Lyle R. Petersen, Addie Crawley, Susan L. Lukacs, Don Weiss, Rebecca A. Henseler, Nga Vuong, Lisa Mackey, Anita Patel, Lisa A. Grohskopf, Beth Maldin Morgenthau, Demetre Daskalakis, Preeti Pathela

We conducted a serologic survey in public service agencies in New York City, New York, USA, during May–July 2020 to determine prevalence of severe acute respiratory syndrome coronavirus 2 (SARS-CoV-2) infection among first responders. Of 22,647 participants, 22.5% tested positive for SARS-CoV-2–specific antibodies. Seroprevalence for police and firefighters was similar to overall seroprevalence; seroprevalence was highest in correctional staff (39.2%) and emergency medical technicians (38.3%) and lowest in laboratory technicians (10.1%) and medicolegal death investigators (10.8%). Adjusted analyses demonstrated association between seropositivity and exposure to SARS-CoV-2–positive household members (adjusted odds ratio [aOR] 3.52 [95% CI 3.19–3.87]), non-Hispanic Black race or ethnicity (aOR 1.50 [95% CI 1.33–1.68]), and severe obesity (aOR 1.31 [95% CI 1.05–1.65]). Consistent glove use (aOR 1.19 [95% CI 1.06–1.33]) increased likelihood of seropositivity; use of other personal protective equipment had no association. Infection control measures, including vaccination, should be prioritized for frontline workers.

Author affiliations: Centers for Disease Control and Prevention, Atlanta, Georgia, USA (S. Sami, A. Patel, L.A. Grohskopf); Centers for Disease Control and Prevention, Hyattsville, Maryland, USA (L.J. Akinbami, S.L. Lukacs); US Public Health Service, Rockville, Maryland, USA (L.J. Akinbami, S.L. Lukacs, L.A. Grohskopf); Centers for Disease Control and Prevention, Fort Collins, Colorado, USA (L.R. Petersen, N. Vuong, L. Mackey); New York City Department of Health and Mental Hygiene, Queens, New York, USA (A. Crawley, D. Weiss, R.A. Henseler, B. Maldin Morgenthau, D. Daskalakis, P. Pathela)

DOI: https://doi.org/10.3201/eid2703.204340

Coronavirus disease (COVID-19) was recognized in New York City (NYC), New York, USA, in late February 2020 and had spread throughout the community by March 2020 (*1*). First responders and public safety personnel have played a critical role in the COVID-19 pandemic response. Understanding the occupational risks for severe acute respiratory syndrome coronavirus 2 (SARS-CoV-2) infection is vital for designing workplace prevention protocols to reduce transmission. Serologic surveys can identify the prevalence of previous SARS-CoV-2 infection in the population.

We conducted a serologic survey to estimate SARS-CoV-2 infection prevalence among first responders, public safety personnel, and other public service workers in NYC. The study objectives were to determine the prevalence of IgG against SARS-CoV-2 and to examine associations between characteristics and occupational exposures and previous infection among workers in emergency response and public safety settings.

Methods

This cross-sectional survey was conducted during May 18–July 2, 2020, in the 5 NYC boroughs: Brooklyn, Manhattan, Queens, Staten Island, and the Bronx. The Institutional Review Board of the NYC Department of Health and Mental Hygiene and Centers for Disease Control and Prevention (CDC) human subjects research officials determined this activity to be public health surveillance as defined in 45 CFR 46.102(l) (*2*).

Adults ≥18 years of age working onsite in a public service agency were eligible to participate, including

employees of city departments of corrections, police, fire, medical examiner, and education, for a total of ≈60,000 persons. Educational settings were limited to Regional Enrichment Centers that served children of first responders and healthcare personnel. Persons who self-reported a positive result for SARS-CoV-2 or occurrence of COVID-19 symptoms ≤2 weeks before completing the questionnaire were ineligible.

A questionnaire assessed participant demographics and relevant household, occupation, and workplace risk factors for SARS-CoV-2 infection (Appendix Table 1, https://wwwnc.cdc.gov/EID/article/27/3/20-4030-App1.pdf). Participation was voluntary. Consenting participants completed the questionnaire online and provided a blood specimen at a collection site located at or near their workplace during May 18–July 2, 2020. Samples were tested for SARS-CoV-2 antibodies by using the VITROS Immunodiagnostic Products Anti-SARS-CoV-2 IgG Test (ORTHO Clinical Diagnostics Inc., https://www.orthoclinicaldiagnostics.com). Data for this test submitted to the Food and Drug Administration indicated a sensitivity of 90% and a specificity of 100% (*2*). Some tests were not performed because of lipemia or insufficient serum. CDC did not receive personal identifiers, and individual results were not shared with employers.

Participants self-reported their race or ethnicity. Reported height and weight were used to calculate body mass index (BMI); weight status categories were defined as underweight or normal (BMI <25), overweight (BMI ≥25 but <30), obese (BMI ≥30 but <40), and severely obese (BMI ≥40). Nonhospital healthcare workers (physicians, midlevel clinicians, nurse assistants, nurses, therapists, phlebotomists, imaging technicians, and dentists) were categorized as other direct patient care providers. Frequency of use of personal protective equipment (PPE) within 6 feet of a person with suspected or confirmed COVID-19 was categorized as all of the time, not all of the time (never or rarely, sometimes, and most of the time), and not applicable.

A total of 22,647 participants were included in our analysis (Appendix Figure 1). Percentage of SARS-CoV-2 IgG seropositivity and 95% CIs were calculated by selected characteristics and exposures. In subsequent analyses assessing seropositivity by frequency of aerosol-generating procedures and PPE use, we focused on occupations for which CDC-issued recommendations for PPE were in place: police (including traffic officers), medicolegal death investigators, firefighters, correctional staff, security guards, firefighters or medical first responders, paramedics, emergency medical technicians (EMTs), dispatchers (fire, emergency medical service [EMS], or police), and other direct patient-care providers (*3*–*6*). We performed multivariable logistic regression with seropositivity as the outcome variable. Covariates were chosen a priori and checked for collinearity. Participants with implausible weight or height (n = 15) or missing housing status (n = 6) were excluded. We used SAS version 9.4 (SAS Institute, https://www.sas.com) to perform statistical analyses. We considered 2-sided p values <0.05 to be statistically significant.

Results

A total of 5,091 (22.5% [95% CI 21.9%–23.0%]) participants tested positive for SARS-CoV-2 IgG (Table); however, only 10.1% (95% CI 9.8%–10.5%]) of participants reported previous positive results for SARS-CoV-2 by reverse transcription PCR. Seroprevalence was higher among women than men, higher among non-Hispanic Black persons than other racial or ethnic groups, higher among persons 18–24 years of age compared with older age groups, and higher among persons who were severely obese compared with those with a lower weight status (Table). Seropositivity was highest among those with exposure to a household member who tested positive for SARS-CoV-2 (48.3% [95% CI 46.3%–50.3%]). In addition, seropositivity was highest among persons who resided in the Bronx (28.8% [95% CI 26.8%–30.9%]) and lowest among those residing outside of NYC (18.3% [95% CI 17.5%–19.2%]). Participants who lived in multiunit housing had higher seropositivity than those who lived in single-family housing, as did participants in very large households (≥8 persons) compared with households of ≤7 persons (Appendix Figure 2).

Seroprevalence was higher among those who worked in correctional facilities (36.2% [95% CI 33.6%–39.0%]) and EMS agencies (35.2% [95% CI 33.3%–37.2%]) compared with those who worked in other workplaces (range 11.7%–21.3%) (Table). Seroprevalence also varied by occupation (Figure 1). We also observed differences in seroprevalence by workplace borough; prevalence was highest in the Bronx (26.8%) and lowest in Staten Island (17.4%) (Table).

The remainder of the analysis focused on first responders and public safety personnel (n = 19,909) (*3*–*6*). Seropositivity increased with increasing frequency of aerosol-generating procedures performed per shift (p = 0.002), ranging from 20.7% among persons who did not conduct these procedures to 31.6% among those who conducted procedures >25 times on average per shift (Figure 2). Seropositivity also varied by frequency of PPE use when within 6 feet of a person

with confirmed or suspected COVID-19, including stratification by occupation (Figure 2; Appendix Figure 3). Overall, for each PPE component, those who reported use all of the time had a significantly higher percent positivity than those who reported not all of the time ($p<0.05$).

In adjusted analyses, women and those exposed to a patient with suspected or confirmed COVID-19 were less likely to be seropositive than their counterparts (Figure 3; Appendix Table 2). Characteristics associated with increased odds of seropositivity were self-reported exposure to a household member who

Table. Percentage of respondents who were seropositive for SARS-CoV-2 IgG, by demographic and health characteristics, in a study of first responders and public safety personnel, New York City, New York, USA, May 18–July 2, 2020*

Characteristic	No. (%)	% Seropositive (95% CI)
Total	22,647 (100.0)	22.5 (21.9–23.0)
Sex		
M	17,118 (75.6)	21.9 (21.3–22.5)
F	5,529 (24.4)	24.2 (23.1–25.4)
Age group, y		
18–24	795 (3.5)	32.0 (28.7–35.3)
25–34	6,677 (29.5)	26.4 (25.3–27.5)
35–44	8,034 (35.5)	20.2 (19.4–21.1)
45–59	6,328 (27.9)	20.3 (19.4–21.4)
60–64	589 (2.6)	20.7 (17.5–24.2)
≥65	224 (1.0)	18.3 (13.5–24.0)
Race/ethnicity		
Non-Hispanic White	10,013 (44.2)	18.5 (17.7–19.2)
Non-Hispanic Black	3,292 (14.5)	30.1 (28.5–31.7)
Non-Hispanic Asian	1,647 (7.3)	21.3 (19.4–23.4)
Hispanic or Latino	5,460 (24.1)	26.9 (25.7–28.1)
Non-Hispanic other race†	548 (2.4)	20.3 (17.0–23.9)
Decline to answer	1,687 (7.5)	19.3 (17.4–21.2)
Weight status, n = 22,632‡		
Underweight or normal weight	4,048 (17.9)	21.4 (20.2–22.7)
Overweight	10,386 (45.9)	22.1 (21.3–22.9)
Obese	7,500 (33.1)	23.1 (22.1–24.1)
Severely obese	698 (3.1)	27.8 (24.5–31.3)
Housing, n = 22,641		
Single family	15,455 (68.3)	21.1 (20.5–21.8)
Multiunit	7,186 (31.7)	25.3 (24.3–26.4)
Residence borough		
Outside New York City	8,654 (38.2)	18.3 (17.5–19.2)
Bronx	1,948 (8.6)	28.8 (26.8–30.9)
Brooklyn	3,329 (14.7)	28.0 (26.5–29.5)
Manhattan	1,207 (5.3)	21.4 (19.1–23.8)
Queens	4,834 (21.3)	25.4 (24.2–26.6)
Staten Island	2,675 (11.8)	19.8 (18.3–21.3)
Workplace§		
Correctional facility	1,272 (5.6)	36.2 (33.6–39.0)
Emergency medical services	2,418 (10.7)	35.2 (33.3–37.2)
Childcare setting (Regional Enrichment Center)	677 (3.0)	21.3 (18.2–24.6)
Fire services	6,087 (26.9)	20.8 (19.8–21.9)
Police department	11,885 (52.5)	19.8 (19.1–20.5)
Medical examiner office	394 (1.7)	11.7 (8.7–15.3)
Workplace borough		
Bronx	3,524 (15.6)	26.8 (25.4–28.3)
Brooklyn	6,075 (26.8)	24.1 (23.1–25.2)
Manhattan	5,755 (25.4)	19.7 (18.6–20.7)
Queens	6,200 (27.4)	21.9 (20.9–23.0)
Staten Island	1,093 (4.8)	17.4 (15.2–19.8)
Exposure to persons who tested positive for SARS-CoV-2‡		
Household member	2,393 (10.6)	48.3 (46.3–50.3)
Coworker	14,912 (65.9)	23.7 (23.0–24.3)
Patient	6,502 (28.7)	26.9 (25.8–28.0)
Other person	7,721 (34.1)	26.8 (25.8–27.8)

*BMI, body mass index; SARS-CoV-2, severe acute respiratory syndrome coronavirus 2.
†Non-Hispanic other race includes Native Hawaiian and other Pacific Islander and American Indian and Alaska Native.
‡Weight status categories defined as underweight or normal weight (BMI <25), overweight (BMI ≥25 but <30), obese (BMI ≥30 but <40), and severely obese (BMI ≥40).
§Workplace and self-reported exposure to persons who tested positive for SARS-CoV-2 are not mutually exclusive.

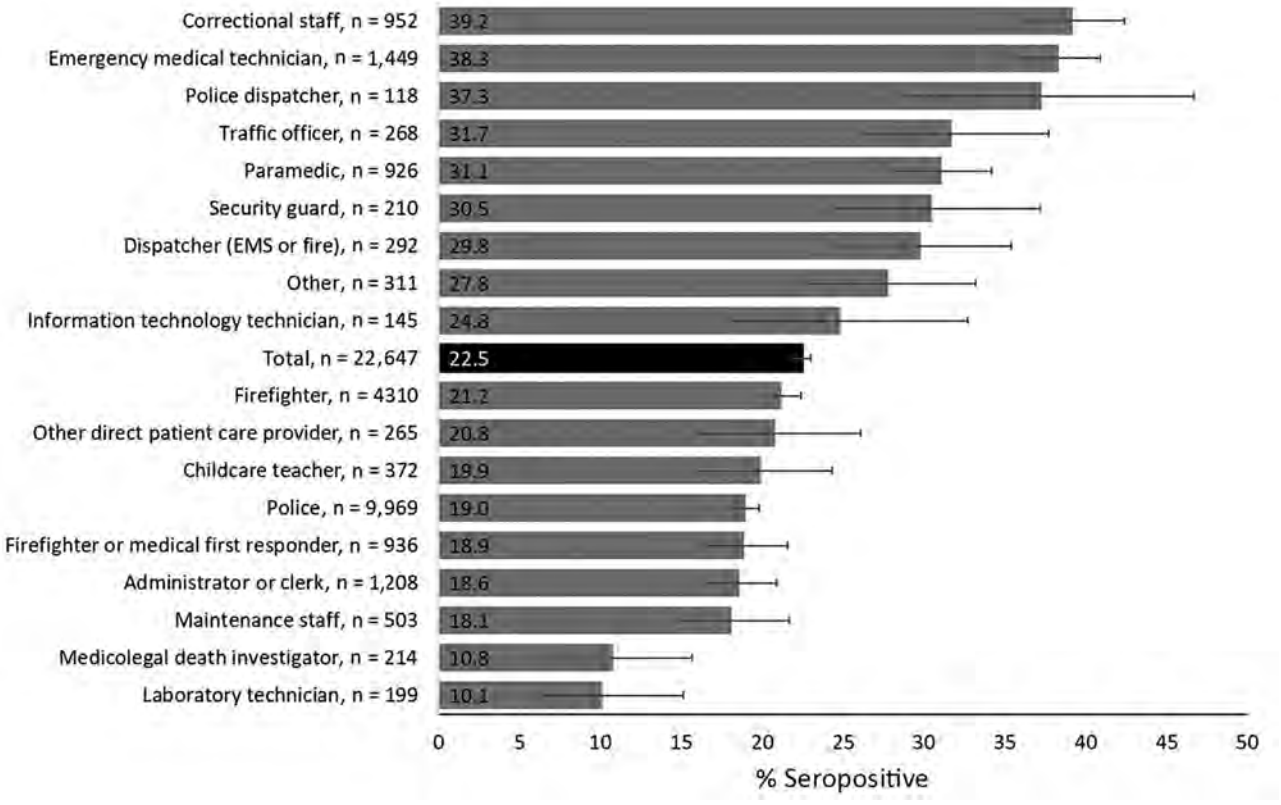

Figure 1. Percentage of respondents who were seropositive for severe acute respiratory syndrome coronavirus 2 IgG, by occupation, in a study of first responders and public safety personnel, New York City, New York, USA, May 18–July 2, 2020. Numbers within bars indicate percentage of seropositive respondents. Error bars indicate 95% CIs. Other includes students or trainees, pharmacists, medical registrars, orderlies, dietitians, medical assistants, counselors, social workers, dietary services staff, environmental services staff, and participants who selected this category and were not reassigned to an existing category. Firefighters includes fire inspectors and fire marshals. Other direct patient care providers include dentists, diagnostic imaging technicians, midlevel clinicians, nurses, nurse assistants, occupational therapists, speech therapists, physical therapists, phlebotomists, physicians, respiratory therapists, and therapy aides. EMS, emergency medical service.

tested positive for SARS-CoV-2, non-Hispanic Black versus non-Hispanic White race or ethnicity, severe obesity versus underweight or normal weight status, and residing or working in Brooklyn versus Staten Island. Correctional staff, EMTs, traffic officers, paramedics, security guards, dispatchers (EMS or fire and police), and firefighters were more likely than police to be seropositive; correctional staff had the highest likelihood of seropositivity (adjusted odds ratio [aOR] 2.55 [95% CI 2.18–2.99]). The aOR for seropositivity when using any PPE component all of the time was not significant. However, workers who reported using gloves all of the time were significantly more likely than those who used gloves not all of the time to be seropositive (aOR 1.19 [95% CI 1.06–1.33]).

Discussion

SARS-CoV-2 seroprevalence among public service agencies personnel (22.5%) was similar to the 19.5% seroprevalence estimate for NYC residents during comparative dates (*7*). However, seroprevalence varied nearly 4-fold by occupation, ranging from 10.1% in laboratory technicians to 39.2% in correctional staff. Similar to other studies, we found seroprevalence varied by nonoccupational factors such as race or ethnicity, age group, weight status, housing type, residence borough, and exposure to household members with COVID-19 (*8;* J.M. Baker, unpub. data, https://doi.org/10.1101/2020.10.30.20222877). However, even when controlling for these factors, we found that seroprevalence for police and firefighters was close to that of the general population; conversely, correctional staff and EMTs, the occupations with the highest seropositivity in our study, had a seroprevalence twice as high (*7*). These populations face unique challenges when working in congregate or uncontrolled settings and would be a critical population for vaccination and other public health efforts to reduce SARS-CoV-2 infection.

Correctional facility workers had the highest seroprevalence of SARS-CoV-2 antibodies, and the

odds of seropositivity were more than double for these workers compared with police, a group with a seroprevalence similar to the general population. COVID-19 in congregate settings has spread rapidly because of crowded living conditions and few options for isolation of exposed persons (*9*–*11*). Recent data from mass testing in correctional facilities found SARS-CoV-2 prevalence ranged from 0% to 87% (*12*). In New York state, 3,762 COVID-19 cases had been reported among staff of 28 correctional and detention facilities as of September 6, 2020 (*13*). Such recommendations as grouping persons with laboratory-confirmed infection are crucial to prevent COVID-19 outbreaks in correctional facilities, but additional

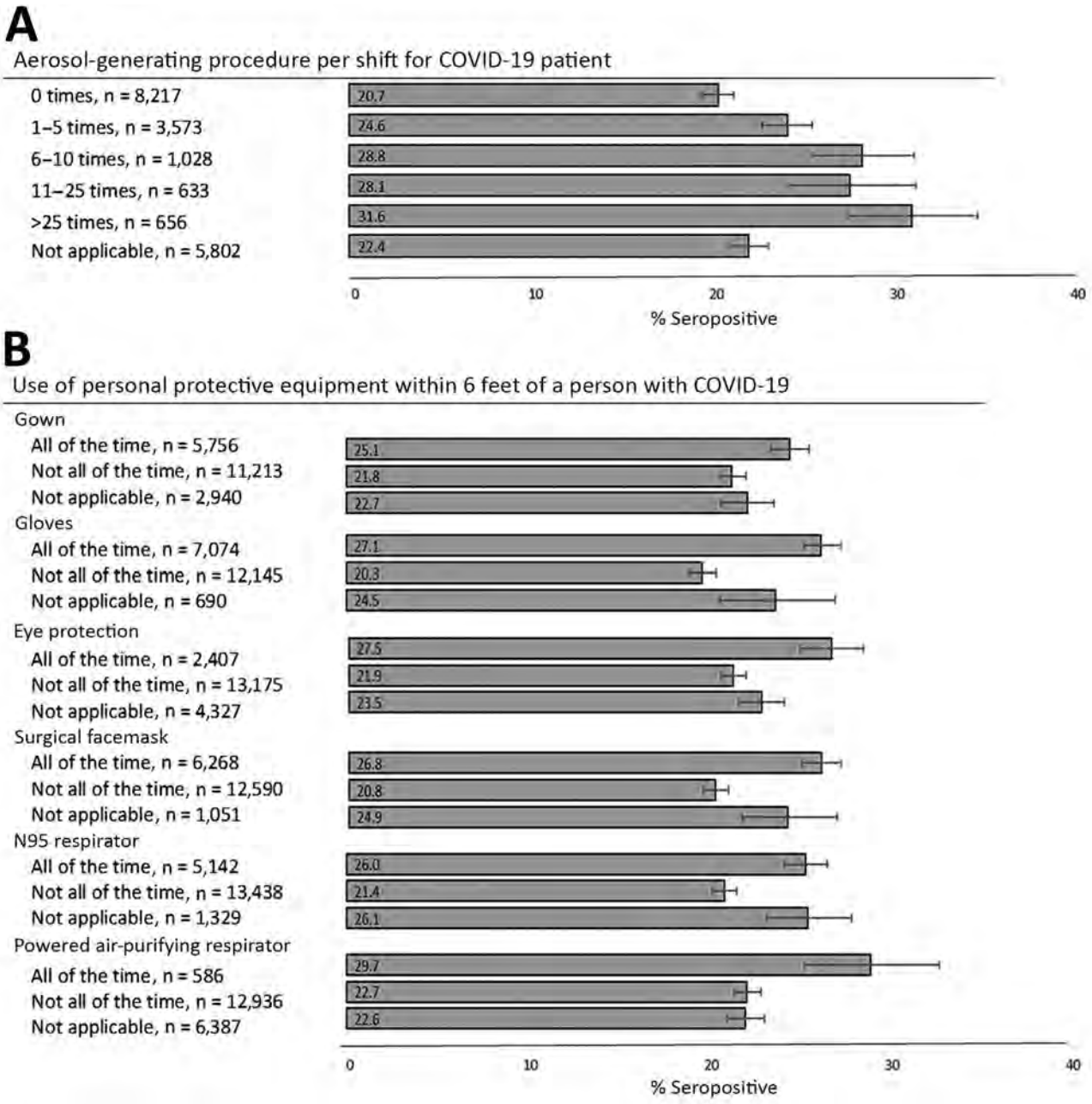

Figure 2. Unadjusted percentage of respondents who were seropositive for severe acute respiratory syndrome coronavirus 2 IgG, by aerosol-generating procedure frequency (A) and use of personal protective equipment (B), in a study of first responders and public safety personnel, New York City, New York, USA, May 18–July 2, 2020. Numbers within bars indicate percentage of seropositive respondents. Error bars indicate 95% CIs. First responders and public safety personnel include police, medicolegal death investigators, firefighters, correctional staff, security guards, traffic officers, police dispatchers, firefighters or medical first responders, paramedics, emergency medical technicians, dispatchers (emergency medical service or fire), and other direct patient-care providers. COVID-19, coronavirus disease.

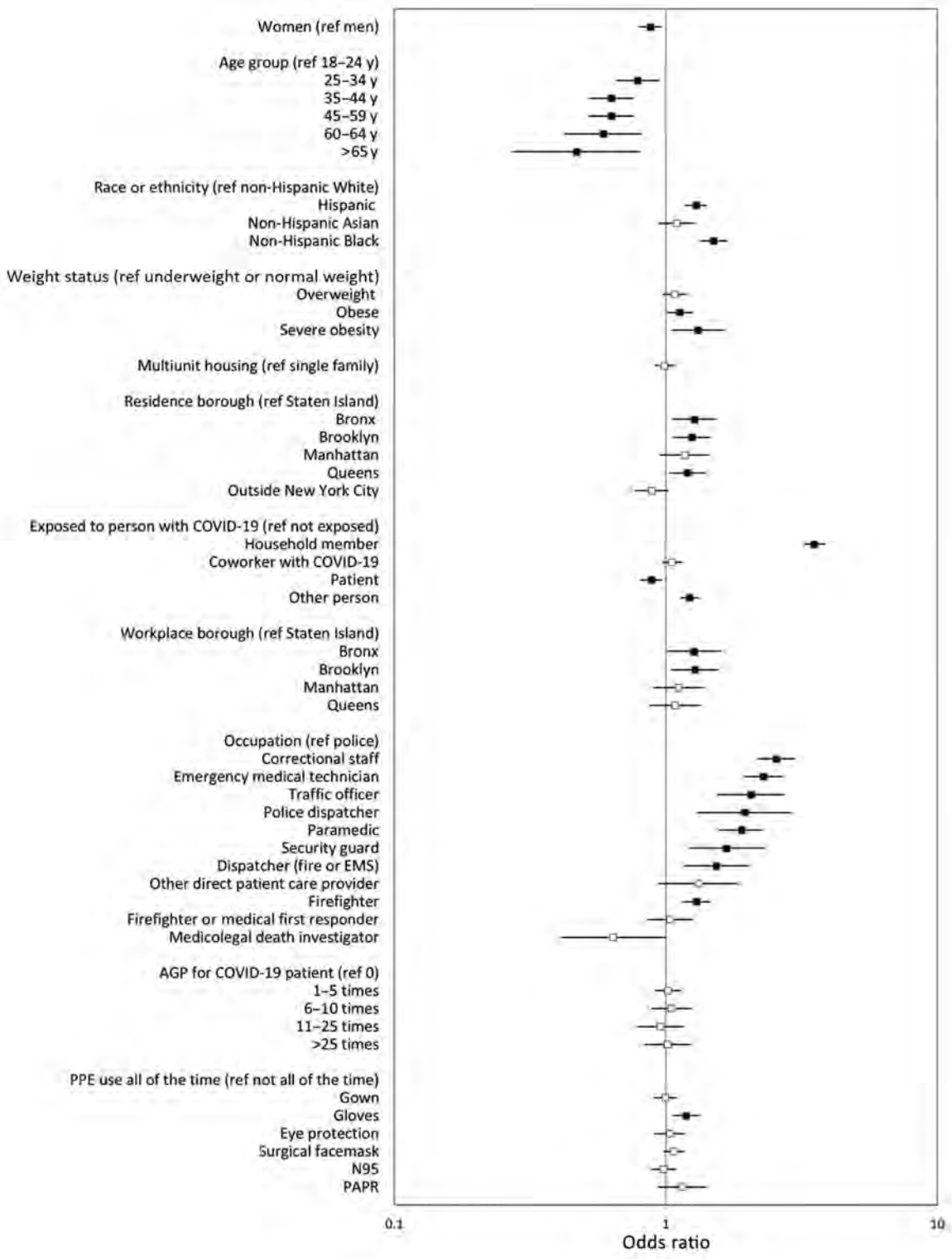

Figure 3. Adjusted odds ratios of seropositivity for severe acute respiratory syndrome coronavirus 2 IgG in a study of first responders and public safety personnel, New York City, New York, USA, May 18–July 2, 2020. Adjusted model includes all variables shown. Black boxes indicate statistically significant results; error bars indicate 95% CIs. Participants of other racial or ethnic groups or who declined to provide their race or ethnicity are included in the models but not shown as separate categories. Variables for exposure to person with COVID-19 are not mutually exclusive. AGP, aerosol-generating procedure; COVID-19, coronavirus disease; EMS, emergency medical service; ref, referent; PAPR, powered air-purifying respirator; PPE, personal protective equipment.

strategies are needed for settings in which isolating multiple persons infected with SARS-CoV-2 might not be possible (*5*,*14*).

Among healthcare workers, EMTs had a seroprevalence of 38.3% and the strongest association with seropositivity after adjustment. In contrast, other SARS-CoV-2 studies among NYC hospital-based healthcare workers found a seroprevalence ranging from 14% to 27% (*15*,*16*). EMS often occur in uncontrolled, unpredictable environments in which space is limited (e.g., ambulances) and require rapid decisions that might increase employee exposure risk. Although EMTs and paramedics both conduct procedures with a high risk for exposure (e.g., airway management), paramedics had a significantly lower seroprevalence than EMTs (*17*). Unmeasured factors, such as level of training, might account for the higher likelihood of seropositivity among EMTs compared with paramedics, who undergo an additional ≥1,000 training hours (*18*).

Other occupations with notably elevated seropositivity included traffic officers, security guards, and emergency dispatchers. Persons in these occupations have frequent and close interactions with the general public or work in environments in which space between coworkers is limited. Conversely, medicolegal death investigators and laboratory technicians, occupations with the lowest seroprevalence, might have less frequent close contact with other persons. Our findings also suggest that infection rates in the workplace might correlate with underlying community transmission, and not all observed associations are consistent with occupational risk. After adjustment, persons who worked or resided in the Bronx or Brooklyn had higher seropositivity compared with persons who worked or lived in Staten Island. This finding aligns with test results reported to the NYC Department of Health and Mental Hygiene, which found higher community seroprevalence in the Bronx (32.2%) and Brooklyn (27.0%) than in Staten Island (19.6%) (*1*).

Our finding that consistent use of gloves was associated with seropositivity was unexpected. However, among occupations without extensive training in glove use, a paradoxical association with infection has been previously observed: higher infection rates among consistent glove users was caused by cross-contamination and lack of hand hygiene after glove removal (*19*–*22*). PPE use has been demonstrated to be effective among healthcare workers in facility settings, but our study of first responders and public safety personnel in nonfacility settings demonstrates a different pattern, which warrants further investigation (*23*). Studies among healthcare workers found improper use of PPE, insufficient training, and perceived inadequacy of supplies increased transmission of other coronaviruses and might explain the higher seroprevalence documented in our study (*24*–*26*). Greater PPE use might be a surrogate for greater exposure to COVID-19 in the workplace. According to the hierarchy of controls, engineering and administrative controls (e.g., isolation and indoor ventilation) are preferred, and PPE should be the last line of defense to protect workers (*27*).

Public service personnel exposed to a SARS-CoV-2–positive household member also had higher seropositivity, a finding consistent with another study (*28*). This finding indicates the importance of managing exposure risk within households of frontline workers. Another factor to consider in NYC is the high density of living conditions, which was associated with greater likelihood of infection in our study. Even after controlling for occupation and housing type, racial and ethnic minority groups had higher seropositivity than non-Hispanic White workers. This pattern might be explained by unmeasured social disparities, such as lower income status, lack of paid sick leave, and mass transit use, which have been found to be associated with seropositivity among racial and ethnic minority groups in NYC (*29;* D. Carrion, unpub. data, https://doi.org/10.1101/2020.06.02.20120790; K.T.L Sy, unpub. data, https://doi.org/10.1101/2020.05.28.20115949). Mitigation measures should address persons working or residing in areas with high levels of SARS-CoV-2 transmission and racial or ethnic disparities.

Limitations of our study include that it was a convenience sample of public service agency personnel with limited numbers of healthcare professionals; participation ranged from an estimated 11% of ≈11,600 eligible correctional facility personnel to 81% of ≈10,300 fire services personnel. Participation might have been influenced by prior results of testing by reverse transcription PCR, expanded access to free antibody testing in the city, household exposure, and worker availability. Data collection occurred during May 18–July 2, 2020; recall bias could have affected responses for exposures 3 months before the survey. Study participants were also asked to recall PPE use during a wide period, and questions were not designed to measure adaptation to evolving PPE use. Temporality also limits our ability to know whether infection occurred before or after a potential exposure. Despite these limitations, our study provides seroprevalence estimates and factors associated with SARS-CoV-2 infection across a diverse set of occupations for which little data exist.

Nearly 25% of first responders and public safety personnel in our study were infected with SARS-CoV-2 before July 2020. Seroprevalence varied by nearly 4-fold among occupations; correctional staff and EMTs demonstrated highest levels of seropositivity. Other occupations with frequent close contact with the public also had elevated seroprevalence. We did not observe lower seroprevalence levels as expected from self-reported consistent PPE use, possibly because persons with consistent use had higher and more frequent exposure to SARS-CoV-2. Nevertheless, these results have identified high-risk occupations for which enhanced prevention measures including engineering and administrative controls and vaccination are required.

Acknowledgments

We thank members of CDC's National Institute for Occupational Safety and Health occupational data collection and coding support and consultation teams for their assistance with occupation and workplace classification: Pam Schumacher, Jennifer Cornell, Jeff Purdin, Matthew Groenewold, Sara Luckhaupt, Stacey Marovich, Matt Hirst, Liz Smith, Surprese Watts, Rebecca Purdin, Marie De Perio, Sherry Burrer, Laura Reynolds, and George (Reed) Grimes. We also thank members of CDC's Data Collation and Integration for Public Health Event Response (DCIPHER) team (National Center for Environmental Health, Center for Preparedness and Response) for their assistance in providing secure data transfer and storage: Stephen Sorokin, Nathan Golightly, Sachin Agnihotri, and Serena Burdyshaw. We thank members of Quest Diagnostics for their assistance with survey implementation: Vijay Paladugu, Walter Dusseldorp, Stephen Bonventre, Sahana Ramprasad, Rebecca Parsons, Brain Jaffa, Michael Kraky, Becky Hunt, Jody Reilly, Jeff Crawford, Kathryn Logan and Dianna Tate; we also thank David Prezant from the New York City Fire Department for input on questionnaire design. Finally, we are grateful to Brian Lein for assistance with survey planning and initial implementation.

Data and specimen collection activities and specimen testing were funded through a US Health and Human Services contract (no. 75P00120C00036).

About the Author

Dr. Sami is an epidemiologist in the Influenza Division, National Center for Immunization and Respiratory Diseases, Centers for Disease Control and Prevention, Atlanta, Georgia, USA. She and her colleagues have undertaken this research while deployed in support of the federal COVID-19 response.

References

1. NYC Health. COVID-19: data, antibody tests. 2020 Aug 23 [cited 2020 Aug 24]. https://www1.nyc.gov/site/doh/covid/covid-19-data-testing.page
2. US Food and Drug Administration. EUA authorized serology test performance. 2020 Aug 7 [cited 2020 Aug 11]. https://www.fda.gov/medical-devices/emergency-situations-medical-devices/eua-authorized-serology-test-performance
3. Centers for Disease Control and Prevention. COVID-19: using personal protective equipment (PPE). 2020 [cited 2020 Sep 8]. https://www.cdc.gov/coronavirus/2019-ncov/hcp/using-ppe.html
4. Centers for Disease Control and Prevention. COVID-19: FAQs for medicolegal death investigators. 2020 [cited 2020 Sep 8]. https://www.cdc.gov/coronavirus/2019-ncov/community/medicolegal-faq.html
5. Centers for Disease Control and Prevention. COVID-19: interim guidance on management of coronavirus disease 2019 (COVID-19) in correctional and detention facilities. 2020 Jul 22 [cited 2020 Aug 23]. https://www.cdc.gov/coronavirus/2019-ncov/community/correction-detention/guidance-correctional-detention.html
6. Centers for Disease Control and Prevention. COVID-19: interim recommendations for emergency medical services (EMS) systems and 911 public safety answering points/emergency communication centers (PSAP/ECCs) in the United States during the coronavirus disease (COVID-19) pandemic. 2020 [cited 2020 Sep 2]. https://www.cdc.gov/coronavirus/2019-ncov/hcp/guidance-for-ems.html
7. Centers for Disease Control and Prevention. CDC COVID data tracker: commercial laboratory seroprevalence survey data. 2020 [cited 2020 Sep 5]. https://covid.cdc.gov/covid-data-tracker/#serology-surveillance
8. Akinbami LJ, Vuong N, Petersen LR, Sami S, Patel A, Lukacs SL, et al. SARS-CoV-2 seroprevalence among healthcare, first response, and public safety personnel, Detroit metropolitan area, Michigan, USA, May–June 2020. Emerg Infect Dis. 2020;26:2863–71. https://doi.org/10.3201/eid2612.203764
9. Montoya-Barthelemy AG, Lee CD, Cundiff DR, Smith EB. COVID-19 and the correctional environment: the American prison as a focal point for public health. Am J Prev Med. 2020;58:888–91. https://doi.org/10.1016/j.amepre.2020.04.001
10. Wallace M, Marlow M, Simonson S, Walker M, Christophe N, Dominguez O, et al. Public health response to COVID-19 cases in correctional and detention facilities—Louisiana,March–April 2020. MMWR Morb Mortal Wkly Rep. 2020;69:594–8. https://doi.org/10.15585/mmwr.mm6919e3
11. Wallace M, Hagan L, Curran KG, Williams SP, Handanagic S, Bjork A, et al. COVID-19 in correctional and detention facilities—United States, February–April 2020. MMWR Morb Mortal Wkly Rep. 2020;69:587–90. https://doi.org/10.15585/mmwr.mm6919e1
12. Hagan LM, Williams SP, Spaulding AC, Toblin RL, Figlenski J, Ocampo J, et al. Mass testing for SARS-CoV-2 in 16 prisons and jails—six jurisdictions, United States, April–May 2020. MMWR Morb Mortal Wkly Rep. 2020;69:1139–43. https://doi.org/10.15585/mmwr.mm6933a3
13. Centers for Disease Control and Prevention. CDC COVID data tracker: confirmed COVID-19 cases and deaths in US correctional and detention facilities by state. 2020 [cited 2020 Sep 5]. https://covid.cdc.gov/covid-data-tracker/#correctional-facilities

14. Jiménez MC, Cowger TL, Simon LE, Behn M, Cassarino N, Bassett MT. Epidemiology of COVID-19 among incarcerated individuals and staff in Massachusetts jails and prisons. JAMA Netw Open. 2020;3:e2018851. https://doi.org/10.1001/jamanetworkopen.2020.18851
15. Moscola J, Sembajwe G, Jarrett M, Farber B, Chang T, McGinn T, et al.; Northwell Health COVID-19 Research Consortium. Prevalence of SARS-CoV-2 antibodies in health care personnel in the New York City area. JAMA. 2020;324:893–5. https://doi.org/10.1001/jama.2020.14765
16. Venugopal U, Jilani N, Rabah S, Shariff MA, Jawed M, Mendez Batres A, et al. SARS-CoV-2 seroprevalence among health care workers in a New York City hospital: a cross-sectional analysis during the COVID-19 pandemic. Int J Infect Dis. 2020;102:63–9. https://doi.org/10.1016/j.ijid.2020.10.036
17. Tran K, Cimon K, Severn M, Pessoa-Silva CL, Conly J. Aerosol generating procedures and risk of transmission of acute respiratory infections to healthcare workers: a systematic review. PLoS One. 2012;7:e35797. https://doi.org/10.1371/journal.pone.0035797
18. New York State Department of Health. Emergency medical technicians (EMTs) save lives! 2018 May [cited 2020 Sep 2]. https://health.ny.gov/professionals/ems
19. Blenkharn JI. Glove use by ancillary and support staff: a paradox of prevention? J Hosp Infect. 2006;62:519–20. https://doi.org/10.1016/j.jhin.2005.10.008
20. Lynch RAPM, Phillips ML, Elledge BL, Hanumanthaiah S, Boatright DT. A preliminary evaluation of the effect of glove use by food handlers in fast food restaurants. J Food Prot. 2005;68:187–90. https://doi.org/10.4315/0362-028X-68.1.187
21. Loveday HPLS, Lynam S, Singleton J, Wilson J. Clinical glove use: healthcare workers' actions and perceptions. J Hosp Infect. 2014;86:110–6. https://doi.org/10.1016/j.jhin.2013.11.003
22. Picheansanthian W, Chotibang J. Glove utilization in the prevention of cross transmission: a systematic review. JBI Database Syst Rev Implement Reports. 2015;13:188–230. https://doi.org/10.11124/01938924-201513040-00013
23. Chou R, Dana T, Buckley DI, Selph S, Fu R, Totten AM. Epidemiology of and risk factors for coronavirus infection in health care workers: a living rapid review. Ann Intern Med. 2020;173:120–36. https://doi.org/10.7326/M20-1632
24. Lau JTFK, Fung KS, Wong TW, Kim JH, Wong E, Chung S, et al. SARS transmission among hospital workers in Hong Kong. Emerg Infect Dis. 2004;10:280–6. https://doi.org/10.3201/eid1002.030534
25. Nishiyama A, Wakasugi N, Kirikae T, Quy T, Ha D, Ban VV, et al. Risk factors for SARS infection within hospitals in Hanoi, Vietnam. Jpn J Infect Dis. 2008;61:388–90.
26. Pei LYGZ, Gao ZC, Yang Z, Wei DG, Wang SX, Ji JM, et al. Investigation of the influencing factors on severe acute respiratory syndrome among health care workers. Beijing Da Xue Xue Bao Yi Xue Ban. 2006;38:271–5.
27. Centers for Disease Control and Prevention. The National Institute for Occupational Safety and Health (NIOSH): hierarchy of controls. 2015 [cited 2020 Sep 21]. https://www.cdc.gov/niosh/topics/hierarchy/default.html
28. Ran L, Chen X, Wang Y, Wu W, Zhang L, Tan X. Risk factors of healthcare workers with coronavirus disease 2019: a retrospective cohort study in a designated hospital of Wuhan in China. Clin Infect Dis. 2020;71:2218–21. https://doi.org/10.1093/cid/ciaa287
29. Maroko AR, Nash D, Pavilonis BT. COVID-19 and inequity: a comparative spatial analysis of New York City and Chicago hot spots. J Urban Health. 2020;97:461–70. https://doi.org/10.1007/s11524-020-00468-0

Address for correspondence: Samira Sami, Centers for Disease Control and Prevention, 1600 Clifton Rd NE, Atlanta, GA 30329-4027, USA; email: ssami@cdc.gov

Effectiveness of Preventive Therapy for Persons Exposed at Home to Drug-Resistant Tuberculosis, Karachi, Pakistan

Amyn A. Malik, Neel R. Gandhi, Timothy L. Lash, Lisa M. Cranmer, Saad B. Omer, Junaid F. Ahmed, Sara Siddiqui, Farhana Amanullah, Aamir J. Khan, Salmaan Keshavjee, Hamidah Hussain,[1] Mercedes C. Becerra[1]

Medscape EDUCATION ACTIVITY

In support of improving patient care, this activity has been planned and implemented by Medscape, LLC and Emerging Infectious Diseases. Medscape, LLC is jointly accredited by the Accreditation Council for Continuing Medical Education (ACCME), the Accreditation Council for Pharmacy Education (ACPE), and the American Nurses Credentialing Center (ANCC), to provide continuing education for the healthcare team.

Medscape, LLC designates this Journal-based CME activity for a maximum of 1.00 ***AMA PRA Category 1 Credit(s)™***. Physicians should claim only the credit commensurate with the extent of their participation in the activity.

Successful completion of this CME activity, which includes participation in the evaluation component, enables the participant to earn up to 1.0 MOC points in the American Board of Internal Medicine's (ABIM) Maintenance of Certification (MOC) program. Participants will earn MOC points equivalent to the amount of CME credits claimed for the activity. It is the CME activity provider's responsibility to submit participant completion information to ACCME for the purpose of granting ABIM MOC credit.

All other clinicians completing this activity will be issued a certificate of participation. To participate in this journal CME activity: (1) review the learning objectives and author disclosures; (2) study the education content; (3) take the post-test with a 75% minimum passing score and complete the evaluation at http://www.medscape.org/journal/eid; and (4) view/print certificate. For CME questions, see page 998.

Release date: February 22, 2021; Expiration date: February 22, 2022

Learning Objectives

Upon completion of this activity, participants will be able to:

- Evaluate the global effect of multidrug-resistant tuberculosis
- Assess risk factors for acquiring tuberculosis among household contacts of individuals with infection
- Analyze the efficacy of a 2-drug regimen to prevent infection with multidrug-resistant tuberculosis among household contacts.

CME Editor

Jill Russell, BA, Copyeditor, Emerging Infectious Diseases. *Disclosure: Jill Russell, BA, has disclosed no relevant financial relationships.*

CME Author

Charles P. Vega, MD, Health Sciences Clinical Professor of Family Medicine, University of California, Irvine School of Medicine, Irvine, California, USA. *Disclosure: Charles P. Vega, MD, has disclosed the following relevant financial relationships: served as an advisor or consultant for GlaxoSmithKline.*

Authors

Disclosures: ***Amyn A. Malik, MBBS, MPH, PhD; Neel R. Gandhi, MD; Timothy L. Lash, DSc, MPH; Lisa Marie Cranmer, MD, MPH; Saad B. Omer, MBBS, MPH, PhD, FIDSA; Junaid Fuad Ahmed, BSc; Sara Ahmed Siddiqui, BDS; Farhana Amanullah, MD, FAAP; Aamir J. Khan, PhD; Salmaan Keshavjee, MD, PhD; Hamidah Hussain, MBBS, MSc, PhD;*** *and* ***Mercedes C. Becerra, ScD,*** *have disclosed no relevant financial relationships.*

Author affiliations: Emory University Rollins School of Public Health, Atlanta, Georgia, USA (A.A. Malik, N.R. Gandhi, T.L. Lash); Yale University, New Haven, Connecticut, USA (A.A. Malik, S.B. Omer); Global Health Directorate, Indus Health Network, Karachi, Pakistan (A.A. Malik, J.F. Ahmed, S. Siddiqui); Interactive Research and Development, Singapore (A.A. Malik, A.J. Khan, H. Hussain); Emory University School of Medicine, Atlanta (N.R. Gandhi, L.M. Cranmer); Emory + Children's Pediatric Institute, Atlanta (L.M. Cranmer); The Indus Hospital, Karachi (F. Amanullah); Harvard University, Cambridge, Massachusetts, USA (A.J. Khan, S. Keshavjee, M.C. Becerra); Partners In Health, Boston, Massachusetts, USA (S. Keshavjee, M.C. Becerra); Brigham and Women's Hospital, Boston (S. Keshavjee, M.C. Becerra)

DOI: https://doi.org/10.3201/203916

[1]These authors contributed equally to this article.

In Karachi, Pakistan, a South Asian megacity with a high prevalence of tuberculosis (TB) and low HIV prevalence, we assessed the effectiveness of fluoroquinolone-based preventive therapy for drug-resistant (DR) TB exposure. During February 2016–March 2017, high-risk household contacts of DR TB patients began a 6-month course of preventive therapy with a fluoroquinolone-based, 2-drug regimen. We assessed effectiveness in this cohort by comparing the rate and risk for TB disease over 2 years to the rates and risks reported in the literature. Of 172 participants, TB occurred in 2 persons over 336 person-years of observation. TB disease incidence rate observed in the cohort was 6.0/1,000 person-years. The incidence rate ratio ranged from 0.29 (95% CI 0.04–1.3) to 0.50 (95% CI 0.06–2.8), with a pooled estimate of 0.35 (95% CI 0.14–0.87). Overall, fluoroquinolone-based preventive therapy for DR TB exposure reduced risk for TB disease by 65%.

Tuberculosis (TB) is the leading infectious cause of death globally and the 9th leading cause overall (*1*). TB causes ≈10 million new cases and 1.7 million deaths annually (*1*). Annually, ≈650,000 TB patients have multidrug-resistant (MDR) TB, defined as TB that is resistant to both isoniazid and rifampin (*1*). Treatment for MDR TB is toxic, complex, and prolonged, and it has a success rate of only 55% (*1*–*3*). Therefore, preventive interventions, including preventive therapy and future vaccines, are essential to reduce cases and deaths from MDR TB (*4*,*5*).

Delivering effective treatment for exposure to drug-resistant (DR) TB is central to the work of Zero TB Initiative coalitions, which aim to rapidly drive down TB rates worldwide (*6*). Household contacts of persons with DR TB are at high risk for TB (*7*) and are prime candidates for preventive interventions (*8*). Available standard preventive therapies are not expected to protect persons exposed to MDR TB because the infecting TB strain in the exposed person is highly likely to be resistant to isoniazid and rifampin. A meta-analysis of 33 studies found that >80% of household contacts of persons with DR TB in whom TB occurred also had isoniazid-resistant strains (*9*). Thus, household contacts of persons with DR TB should receive treatment under the assumption that they, too, are infected with a DR *Mycobacterium tuberculosis* strain (*9*).

Evidence is limited regarding effective preventive regimens for MDR TB, in contrast to the abundant evidence available for preventive therapy in isoniazid-sensitive TB (*10*). Although data from randomized controlled trials are not available to guide the approach to preventive therapy for MDR TB, observational studies from the Federated States of Micronesia, United States, United Kingdom, and South Africa have shown efficacy of fluoroquinolone-based preventive therapy in adults and children (*11*–*17*). The largest observational study with a comparison arm, from the Federated States of Micronesia, described 104 household contacts of persons with MDR TB who received preventive therapy with a fluoroquinolone-based regimen for 12 months. During 3 years of follow-up, TB did not occur in any of the contacts who received preventive therapy; in 3 (20%) of the 15 contacts who refused treatment, MDR TB occurred. A meta-analysis of observational studies determined MDR TB preventive therapy to be 90% effective, and a wide range of 9%–99% effectiveness was reported (*18*).

Most studies of preventive therapy for MDR TB have been conducted in either high-resource settings or settings with a high prevalence of HIV. Hence, evaluations of the effectiveness of MDR TB preventive therapy in other settings are needed. In Karachi, Pakistan, which has a high TB burden and low HIV prevalence setting (annual TB incidence of 265/100,000 and HIV prevalence [among persons 15–49 years of age] of 0.1%) (*1*,*19*), we examined the effectiveness of fluoroquinolone-based 2-drug preventive therapy for high-risk household contacts of persons with DR TB.

Methods

Setting, Study Design, and Population

During February 2016–March 2017, we prospectively enrolled household contacts of 100 consecutive (index) patients beginning treatment for culture-confirmed DR TB at the Indus Hospital in Karachi, Pakistan. Because this study was conducted in a programmatic setting, we identified index patients with any DR TB, not only the subset of patients with MDR TB. Household contacts of index patients whose isolates were shown in drug-susceptibility testing to be resistant to a fluoroquinolone in addition to other first-line drugs but not resistant to any of the second-line injectables were eligible for the study. Of the 100 index patients, 97 had documented resistance to rifampin; 15 also had documented resistance to a fluoroquinolone. Full details of the cohort are reported elsewhere (*20*,*21*).

The study cohort consisted of all children and adults residing with index patients at the time of the diagnosis of DR TB. At the baseline evaluation, all household contacts were evaluated for TB clinically, including chest radiograph and sputum testing if they were able to produce sputum. We conducted HIV testing if the person had HIV risk factors or if the index patient had HIV co-infection.

We excluded household members already receiving treatment for TB at the time of this evaluation (n = 8) or those in whom TB was diagnosed in the clinical evaluation (i.e., co-prevalent TB patients [n = 3]). We offered preventive therapy with a fluoroquinolone-based 2-drug regimen for 6 months to remaining household contacts who met these criteria: 0–4 years of age; 5–17 years of age with a positive tuberculin skin test (TST) result or evidence of immunocompromising condition, such as diabetes, HIV, or malnutrition (body mass index [BMI] <18.5 kg/m^2); or ≥18 years of age with evidence of an immunocompromising condition, such as diabetes, HIV, or malnutrition (BMI <18.5 kg/m^2). Persons who did not meet these criteria were not prescribed preventive therapy but were followed for the occurrence of active TB disease.

We provided 1 of 4 preventive regimens, each consisting of 2 drugs for a duration of 6 months (Table 1). Moxifloxacin-based regimens were given to household contacts of index patients with a levofloxacin-resistant TB strain. Ethambutol was the companion drug of choice unless it was not available in the correct dosing form; in that case, ethionamide was used.

A study physician clinically evaluated persons on preventive therapy every 2 months for 6 months. Between clinic visits, a study worker visited each household monthly to monitor for occurrence of TB symptoms or adverse events and to assess treatment adherence. Treatment adherence was self-reported and cross-checked through pill counts during home visits. We conducted follow-up on persons who completed the 6-month preventive regimen every 2 months at home or by telephone to monitor for occurrence of TB symptoms. We conducted follow-up symptom screening on persons who did not receive preventive therapy every 2 months at home or by telephone to monitor for occurrence of TB symptoms until the end of the study period. Any household contact experiencing TB symptoms was referred to The Indus Hospital clinic for further evaluation, including chest radiography and sputum testing if able to produce sputum.

Analysis

The primary outcome of interest was the effectiveness of preventive therapy in household contacts, defined as disease-free survival 2 years after the diagnosis of DR TB in the index patient. To establish an historical untreated group for comparison, we searched the published literature to find systematic reviews and meta-analyses of studies of the incidence of TB disease in close contacts after exposure to a person with TB. We found 2 such studies (*7*,*22*). We then searched for studies that were conducted after these meta-analyses were published. We did not restrict the search to studies that evaluated TB incidence only in persons exposed to drug-resistant TB disease, because no difference is expected in transmissibility or progression on the basis of drug-resistance profile (*7*,*23*). We used the definition of an incident case of TB disease and TST positivity as defined by each study.

From the identified studies, we extracted the incidence of TB disease among untreated household contacts by age, year postexposure, TST-positive results or high-risk classification, and preventive therapy status, if provided (*22*,*24*–*29*) (Table 2).

We calculated the observed incidence rate of TB disease in contacts who received preventive therapy by dividing the number of persons in whom TB occurred by the person-years accumulated by the cohort over 2 years. Cumulative incidence of TB over 2 years was calculated by dividing the number of persons in whom TB occurred by the total number of persons who received preventive therapy. We applied the incidence rates extracted from the literature (Table 2) to our cohort to calculate the expected number of persons in whom TB disease would have occurred within 2 years of exposure to a person with DR TB in the absence of preventive therapy. We calculated the expected incidence rate by dividing the expected number of persons in whom TB disease would have occurred by the total person-years accumulated in our cohort over 2 years. To assess the effectiveness of preventive therapy, we then compared the expected incidence rate and cumulative incidence of TB from the

Table 1. Preventive therapy regimens in study of persons exposed at home to drug-resistant tuberculosis, Karachi, Pakistan, February 2016–March 2017*

Regimen	Drug 1, dose	Drug 2, dose
Levofloxacin/ethambutol	Levofloxacin, ≤5 y: 15–20 mg/kg, >5 y: 7.5–10 mg/kg; max. dose 1,000 mg/d	Ethambutol, 15–25 mg/kg; max. dose 2,000 mg/kg
Levofloxacin/ethionamide	Levofloxacin, ≤5 y: 15–20 mg/kg, >5 y: 7.5–10 mg/kg; max. dose 1,000 mg/d	Ethionamide, 15–20 mg/kg; max. dose 750 mg/kg
Moxifloxacin/ethambutol	Moxifloxacin, 7.5–10 mg/kg; max. dose 400 mg/d	Ethambutol, 15–25 mg/kg; max. dose 2,000 mg/kg
Moxifloxacin/ethionamide	Moxifloxacin, 7.5–10 mg/kg; max. dose 400 mg/d	Ethionamide, 15–20 mg/kg; max. dose 750 mg/kg

*Max., maximum.

Table 2. Details of studies from which data were extracted for analysis in study of persons exposed at home to drug-resistant tuberculosis, Karachi, Pakistan, February 2016–March 2017*

Characteristic	Becerra et al. (*25*)	Fox et al. (*22*)	Reichler et al. (*26*)	Martin-Sanchez et al. (*27*)	Sloot et al. (*28*)	Saunders et al. (*29*)
Setting	Peru	Global	US and Canada	Spain	Netherlands	Peru
Year	2013	2013	2019	2019	2014	2017
HHC age group, y						
<15	1,299	N/A	879	77	1,489	NA
≥15	3,411	N/A	3,611	876	7,757	1,910
IR or risk	IR and risk	IR and risk	IR and risk	IR and risk	Risk	Risk
IR or risk by PT status	No PT for DR TB exposure	No	Yes	Yes	Yes	No
IR or risk by age and year of follow-up	Yes	Not by age but by year of follow-up	No	No cases in children	No	No
IR or risk by risk group	No	No	Yes	Yes	No	Yes
IR or risk reported	<15 y, Y 1: 2,079/100,000 p-y; <15 y, Y 2: 315/100,000 p-y; ≥15 y, Y 1: 2,610/100,000 p-y; ≥15 y, Y 2: 1,309/100,000 p-y; risk: 163/4,515 (3.6%)	Y 1: 1,478/100,000 p-y; Y 2: 831/100,000 p-y; risk: 898/65,935 (1.4%)	Rate: 951/100,000 p-y; 5 y risk for TST-positive contacts without PT: 49/446 (11.0%)	Rate: 1970/100,000 p-y; 5 y risk for TST-positive contacts not completing PT: 6/72 (8.3%)	2 y risk in TST-positive contacts without PT: 9/372 (2.4%)	2.5 y risk for medium- to high-risk contacts in validation cohort: 57/1,335 (4.3%)
Other limitations	Some children received isoniazid-based PT	NA	P-y accumulated over 5 y	No cases in children less than 15 y; p-y accumulated over 5.3 y	Definition of incidence >6 mo	HHCs >15 y

*DR TB, drug-resistant tuberculosis; HHC, household contacts; IR, incidence rate; PT, preventive therapy; p-y, person-years; TST, tuberculin skin test; Y, year of follow-up; NA, data not available.

studies in Table 2 with the observed incidence rate and cumulative incidence in our cohort. Incidence rate ratio (IRR), risk ratio (RR), incidence rate difference (IRD), and risk difference were used for comparison, depending on the available data. We calculated the number needed to treat to prevent 1 case of TB as the total number of persons receiving preventive therapy divided by the number of TB cases averted. Number of TB cases averted was calculated by subtracting the observed number of TB cases from the expected number of TB cases.

We generated pooled estimates of IRR and RR by using inverse-variance weighting with random effects for the effectiveness of preventive therapy that are robust to a range of different assumptions. We evaluated the validity of the pooled estimation method from the random effects model by a simulation study with 10,000 replications using a Poisson distribution for the incidence rate and a binomial distribution for risk for each study. Data were analyzed by using Stata version 15 (StataCorp, https://www.stata.com) and SAS software version 9.4 (SAS Institute, https://www.sas.com). This study was approved by the Institutional Review Boards of Interactive Research and Development, Harvard Medical School, and Emory University.

Results

Of the 800 household members enrolled in the study, 8 were receiving treatment for TB disease at the time of the baseline evaluation. Of the 792 remaining persons, we verbally asked 737 (93.1%) about symptoms; 402 (54.5%) met criteria for further evaluation, and we evaluated 326 (81.1%), none of which were infected with HIV. Active TB disease was diagnosed in 3 (0.9%) persons. Of the remaining 323 persons, 215 met the study criteria and were offered preventive therapy; within that cohort, median age was 7 years (interquartile range [IQR] 3–16) and median BMI was 14.8 kg/m^2 (IQR 13.4–16.9); 52% persons were male. Of the persons offered preventive therapy, 172 accepted and contributed 336 person-years of observation; 7 of these participants were household contacts of patients with rifampin-susceptible strains of TB. Preventive therapy was declined by 43 of 215 persons who were eligible for treatment, but they remained under observation. The 43 persons who did not start treatment were older (median age 16 years [IQR 3–22]) than those who started preventive treatment (median age 7 years [IQR 3–15]). The 2 groups had no other notable differences (Table 3). Of the whole cohort (91% [n=157] of those who began preventive therapy), 82% (n = 654) completed 2 years of

Table 3. Demographics and clinical characteristics of household contacts exposed to drug-resistant tuberculosis free of disease at baseline in study of preventive therapy in Karachi, Pakistan, February 2016–March 2017*

Characteristic	No. (%) or median [IQR]			
	Total, n = 789†	On PT, n = 172	Did not start PT, n = 43	Not eligible for PT, n = 574
Age group, y	19 [10–32]	7 [3–15]	16 [3–22]	24 [15–36]
<15	283 (36)	128 (74)	21 (49)	134 (23)
≥15	506 (64)	44 (26)	22 (51)	440 (77)
Sex				
M	423 (54)	91 (53)	20 (47)	312 (54)
F	366 (46)	81 (47)	23 (53)	262 (46)
BMI, kg/m^2	18.1 [14.8–24.0], n = 616	14.8 [13.4–16.9], n = 171	15.2 [13.4–16.9], n = 42	21.6 [17.1–26.0], n = 403
Presence of symptoms	n = 737	n = 172	n = 43	n = 522
Cough, duration	10 (1)	3 (2)	2 (5)	5 (1)
Fever	7 (1)	1 (1)	3 (7)	3 (1)
Weight loss	12 (2)	1 (1)	2 (5)	9 (2)
Additional TB risk factors	n = 737	n = 172	n = 43	n = 522
History of TB	9 (1)	0 (0)	0 (0)	9 (2)
TST >5 mm	6/136 (4)	6/64 (9)	0/11 (0)	0/61 (0)
Index patient resistant to FQ	138 (19)	16 (9)	11 (26)	111 (21)
Regimen given				
Levofloxacin/ethambutol	NA	102 (59)	NA	NA
Levofloxacin/ethionamide	NA	54 (31)	NA	NA
Moxifloxacin/ethambutol	NA	11 (6)	NA	NA
Moxifloxacin/ethionamide	NA	5 (3)	NA	NA
TB disease occurred during follow-up	2 (0.3)	2 (1)	0	0

*FQ, fluoroquinolone; NA, not applicable; PT, preventive therapy; TB, tuberculosis; TST, tuberculin skin test.
†Excluding 3 contacts found to have TB and 8 already on treatment for TB at time of screening.

observation, and 70% (n = 121) of those who started treatment completed it. There were no deaths during the follow-up period.

We calculated the expected incidence of TB disease in the group that received preventive therapy in Karachi by using incidence rates stratified by age and year of observation from a DR TB household cohort from Peru (*24*,*25*). Had no preventive therapy been given, we would have expected TB disease to occur in 4.7 patients, on the basis of the 336 person-years accumulated by our cohort (incidence rate 14/1,000 person-years). Only 2 patients in our study had TB over the 2 years of observation, resulting in a TB incidence rate of 6.0/1,000 person-years and cumulative incidence of 1.2%. Both case-patients had received preventive therapy (Appendix Table 1, https://wwwnc.cdc.gov/EID/article/27/3/20-3916-App1.pdf). IRR comparing observed and expected number of TB cases was 0.40 (95% CI 0.05–2.0) and IRD was −8.0/1,000 person-years (95% CI −23 to 7.1). Number needed to treat to avert 1 TB case was 64.

We performed the same exercise by using TB incidence rates from 2 other studies and a meta-analysis to demonstrate the potential range of IRR and IRD (*22*,*26*,*27*) (Table 4). Equivalent results were achieved by using rates from Reichler et al. (*26*) and Martin-Sanchez et al. (*27*); the expected number of TB cases was 6.6 and IRR was 0.29 (95% CI 0.04–1.3). By using rates of TB disease incidence in household contacts of TB patients as determined by Fox et al. (*22*), we calculated the IRR to be 0.50 (95% CI 0.06–2.8). The pooled estimate for IRR was 0.35 (95% CI 0.14–0.87) (Figure 1). Using the simulation study, the median IRR was 0.42 (2.5th–97.5th percentile 0.18–0.79).

We found 6 studies that estimated the risk for TB disease in household contacts exposed to a TB patient in the absence of preventive therapy, including the 4 studies we used for incidence rate calculations (*22*,*24*–*29*). By using risk figures from these 6 studies, we estimated the pooled RR to be 0.28 (95% CI 0.15–0.53) (Figure 2; Appendix Table 2). By using the simulation

Table 4. Incidence rate comparison of effectiveness of preventive therapy for tuberculosis in published studies in study of persons exposed at home to drug-resistant tuberculosis, Karachi, Pakistan*

Characteristic	Becerra et al. (*25*)	Fox et al. (*22*)	Reichler et al. (*26*)	Martin-Sanchez et al. (*27*)
No. expected cases	4.7	3.9	6.6	6.6
Expected IR per 1,000 p-y	15	12	20	20
IRR (95% CI)	0.40 (0.05–2.0)	0.50 (0.06–2.8)	0.29 (0.04–1.3)	0.29 (0.04–1.3)
IR difference per 1,000 p-y (95% CI)	−8.0 (–23.0 to 7.1)	−5.7 (–20.0 to 8.5)	−14 (–31.0 to 3.4)	−14 (–31.0 to 3.4)
NNT	64	91	37	37
Preventive fraction in exposed, %	57.5	48.7	69.5	69.7

*IR, incidence rate; IRR, incidence rate ratio; NNT, number needed to treat; p-y, person-years.

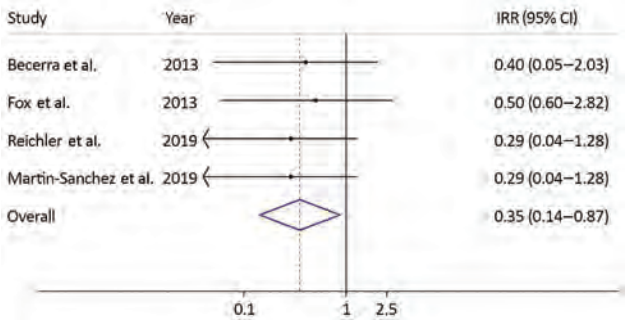

Figure 1. Incidence rate ratios for effectiveness of preventive therapy using data from published studies and a summary measure in study of preventive therapy for persons exposed at home to drug-resistant tuberculosis, Karachi, Pakistan, February 2016–March 2017. Solid line on y axis indicates null. Dotted line indicates pooled estimate of preventive therapy effectiveness. Blue diamond indicates 95% CI. Small diamonds indicate point estimates of preventive therapy effectiveness using data from each study with its CI. IRR, incident rate ratio.

study, we calculated the median RR to be 0.36 (2.5th–97.5th percentile 0.17–0.68).

When we applied an alternative definition of an incident TB case, in which diagnosis occurred earlier (>30 days as opposed to >180 days after diagnosis in the index patient), and used data from Sloot et al. (*28*) as a sensitivity analysis, the estimated RR for preventive therapy was 0.11 (95% CI 0.03–0.44). Using this figure in the pooled analysis resulted in an estimated pooled RR of 0.22 (95% CI 0.12–0.42).

Discussion

In our cohort of 172 DR TB household contacts who received fluoroquinolone-based preventive therapy, we observed 2 patients with TB disease over the course of 2 years. Applying the rates observed in a cohort of DR TB households from Lima, Peru (*25*), we would have expected to observe almost 5 TB cases over the same period. Thus, by providing preventive therapy, we averted almost 3 TB cases resulting in an effectiveness rate of 60%.

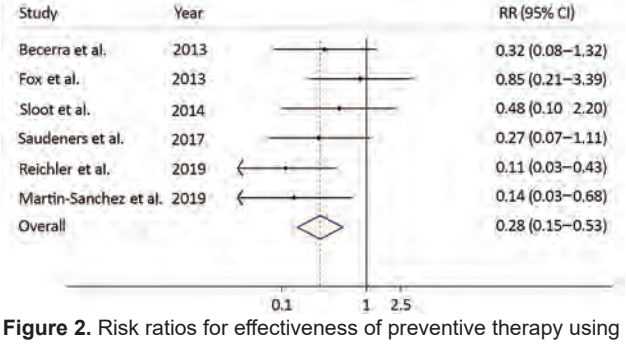

Figure 2. Risk ratios for effectiveness of preventive therapy using data from published studies and a summary measure in study of preventive therapy for persons exposed at home to drug-resistant tuberculosis, Karachi, Pakistan, February 2016–March 2017. Solid line on y axis indicates null. Dotted line indicates pooled estimate of preventive therapy effectiveness. Blue diamond indicates 95% CI. Small diamonds indicate point estimates of preventive therapy effectiveness using data from each study with its CI. RR, risk ratio.

Household contacts are a combination of several populations with different risk levels and biologic susceptibility. Saunders et al. (*29*), in a study from Peru, created a risk score to predict the persons in whom TB would occur after at-home exposure to TB; they demonstrated that 90% of TB cases occurred among persons at high or medium risk over 10 years. In that study, 2 of the risk factors for TB were low BMI and age; the score predicted the risk for TB independent of TB-infection status (*29*). Other studies have also documented increased risk for TB in children <5 years of age and persons with low BMI. We provided preventive therapy to household members at known high risk for TB on the basis of demographics and clinical manifestation; 35% of those started on preventive therapy were <5 years of age. Hence, the 60% effectiveness rate is likely an underestimate of its true effectiveness because the rates we used to calculate expected TB cases came from the whole household cohort and not only from persons at highest risk for incident TB. Some of the children in the comparison cohort also received isoniazid-based preventive therapy, which might have lowered their risk for TB.

By using TB incidence rates from 2 studies from the United States and Spain and a meta-analysis by Fox et al. (*22*), we calculated a range of 2–5 TB cases averted through this program and an effectiveness of 50%–71%. The meta-analysis also included persons who were prescribed preventive therapy, and it did not differentiate between those at higher and lower risk for incident TB disease, which probably resulted in lower overall incidence rate. The other 2 studies measured TB incidence rate over 5 years of follow-up, but the highest risk for incident TB disease is within the first 2 years after exposure. Thus, applying the rate measured over 5 years to a cohort followed for 2 years might result in underestimation of expected number of incident TB cases. The pooled estimate of effectiveness of the preventive therapy in this Karachi cohort compared with all 4 studies was 65%.

By using the pooled relative risk, we estimated the effectiveness of preventive therapy to be 72%. This estimate is comparable to the effectiveness that we found by using incidence rate data from other studies (*22*,*25*–*27*) and gives more confidence in interpretation of our results. Of note, these studies also had some of the limitations highlighted

previously. Our results are also consistent with the TB risk reduction reported with use of isoniazid-based preventive therapy for drug-susceptible TB (relative risk 0.40, 95% CI 0.31–0.52) (*30*). For MDR TB, Marks et al. (*18*), in their meta-analysis of published observational studies on preventive therapy for MDR TB exposure, estimated a risk reduction of 90% (range 9%–99%).

A key limitation of our study was reliance on at-home symptom screening for diagnosis of incident TB and on household members to report TB diagnoses or initiation of treatment for TB during the study period. The parent study was designed to evaluate operational feasibility of providing preventive therapy and was not designed as an effectiveness study, which explains these design features. This limitation could have led to an ascertainment bias. We do not, however, expect that our estimates would be substantially biased with this approach. In the same population during 2008–2011, Amanullah et al. (*31*) conducted a household cohort study by using a similar approach and found a high TB incidence of 5.4% among children in the first year after exposure to a person with DR TB. Our use of rates from countries with low to moderate TB burden, such as Peru, for comparison with the rates from this study in Pakistan, a country with a high burden of TB, might also have biased our results, potentially underestimating the protective effect of preventive therapy. Furthermore, the use of 5-year risks from some of the comparison studies might have overestimated the effectiveness of preventive therapy, given that in our study we calculated cumulative incidence at 2 years. This possibility is not very likely because, in those studies, most of the TB cases occurred within the first 2 years.

Strengths of our study include the prospective design, which resulted in >91% retention at 2 years and a high completion rate of preventive therapy. Our results were robust to a range of different assumptions and showed a similar decrease in TB incidence after provision of preventive therapy to that demonstrated in other observational studies.

In summary, in a setting with high TB burden and low HIV prevalence, we found that a fluoroquinolone-based, 2-drug preventive therapy reduced the risk for TB disease in high-risk persons exposed at home to DR TB by 65%. This study adds to the growing evidence base for effectiveness of preventive therapy for DR TB and MDR TB and is consistent with evidence that a fluoroquinolone-based 2-drug regimen can be used to protect children and adults exposed at home to DR *M. tuberculosis* strains.

Acknowledgments

We thank Rosa Sloot for providing access to her study dataset from Amsterdam and Mitchel Klein for helping with simulations to validate our study findings.

The study was supported through a grant from the Dubai Harvard Foundation for Medical Research to the Harvard Medical School Center for Global Health Delivery. It was also supported in part by grants from the US National Institutes of Health to NRG (no. K24AI114444), the Emory University Center for AIDS Research (no. P30AI050409), and TB Research Unit ASTRa (no. U19AI111211).

A.A.M., N.R.G., H.H., and M.C.B. conceptualized the study and wrote the protocol; A.A.M., J.F., and S.S. collected data under supervision from H.H., F.A., A.J.K., and S.K.; A.A.M., N.R.G., T.L.L., L.M.C., S.B.O., and M.C.B. performed and reviewed the analysis; and A.A.M., N.R.G., and M.C.B. wrote the initial draft of the manuscript. All authors helped interpret the findings and read and approved the final version of the manuscript.

About the Author

Dr. Malik is an infectious disease epidemiologist and postdoctoral associate at Yale Institute for Global Health. This work was undertaken as part of his PhD dissertation at Emory University. His research interests include drug-resistant tuberculosis and preventive treatment for tuberculosis.

References

1. World Health Organization. Global tuberculosis control report 2019. 2019 [cited 2020 Sep 1]. https://www.who.int/teams/global-tuberculosis-programme/tb-reports/global-report-2019
2. Cegielski JP, Nahid P, Sotgiu G. The continued hunt for the elusive standard short regimen for treatment of multidrug-resistant tuberculosis. Eur Respir J. 2020;55:2000224. https://doi.org/10.1183/13993003.00224-2020
3. Rodina O, Borisov SE, Ivanova D. Adverse events in patients with MDR TB, treated by three types of the chemotherapy regimens. Eur Respir J. 2019;54:PA5278.
4. Diel R, Loddenkemper R, Zellweger J-P, Sotgiu G, D'Ambrosio L, Centis R, et al.; European Forum for TB Innovation. Old ideas to innovate tuberculosis control: preventive treatment to achieve elimination. Eur Respir J. 2013;42:785–801. https://doi.org/10.1183/09031936.00205512
5. Gebreselassie N, Hutubessy R, Vekemans J, den Boon S, Kasaeva T, Zignol M. The case for assessing the full value of new tuberculosis vaccines. Eur Respir J. 2020;55:1902414. https://doi.org/10.1183/13993003.02414-2019
6. Keshavjee S, Nicholson T, Khan AJ, Ditiu L, Farmer PE, Becerra MC. Tuberculosis epidemic control: a comprehensive strategy to drive down tuberculosis. In: Friedman L, Dedicoat M, Davies PDO, editors. Clinical tuberculosis. 6th ed. Boca Raton (FL): CRC Press; 2020 p. 401–12.
7. Shah NS, Yuen CM, Heo M, Tolman AW, Becerra MC. Yield of contact investigations in households of patients with drug-

resistant tuberculosis: systematic review and meta-analysis. Clin Infect Dis. 2014;58:381–91. https://doi.org/10.1093/cid/cit643
8. Matteelli A, Lönnroth K, Getahun H, Falzon D, Migliori GB, Raviglione M. Numbers needed to treat to prevent tuberculosis. Eur Respir J. 2015;46:1838–9. https://doi.org/10.1183/13993003.01179-2015
9. Chiang SS, Brooks MB, Jenkins HE, Rubenstein D, Seddon JA, van de Water BJ, et al. Concordance of drug resistance profiles between persons with drug-resistant tuberculosis and their household contacts: a systematic review and meta-analysis. Clin Infect Dis. 2020 May 25 [Epub ahead of print].
10. World Health Organization. Latent tuberculosis infection: updated and consolidated guidelines for programmatic management. 2018 [cited 2020 Sep 1]. https://www.who.int/tb/publications/2018/latent-tuberculosis-infection
11. Adler-Shohet FC, Low J, Carson M, Girma H, Singh J. Management of latent tuberculosis infection in child contacts of multidrug-resistant tuberculosis. Pediatr Infect Dis J. 2014;33:664–6. https://doi.org/10.1097/INF.0000000000000260
12. Bamrah S, Brostrom R, Dorina F, Setik L, Song R, Kawamura LM, et al. Treatment for LTBI in contacts of MDR-TB patients, Federated States of Micronesia, 2009-2012. Int J Tuberc Lung Dis. 2014;18:912–8. https://doi.org/10.5588/ijtld.13.0028
13. Feja K, McNelley E, Tran CS, Burzynski J, Saiman L. Management of pediatric multidrug-resistant tuberculosis and latent tuberculosis infections in New York City from 1995 to 2003. Pediatr Infect Dis J. 2008;27:907–12. https://doi.org/10.1097/INF.0b013e3181783aca
14. Schaaf HS, Gie RP, Kennedy M, Beyers N, Hesseling PB, Donald PR. Evaluation of young children in contact with adult multidrug-resistant pulmonary tuberculosis: a 30-month follow-up. Pediatrics. 2002;109:765–71. https://doi.org/10.1542/peds.109.5.765
15. Seddon JA, Hesseling AC, Finlayson H, Fielding K, Cox H, Hughes J, et al. Preventive therapy for child contacts of multidrug-resistant tuberculosis: a prospective cohort study. Clin Infect Dis. 2013;57:1676–84. https://doi.org/10.1093/cid/cit655
16. Seddon JA, Fred D, Amanullah F, Schaaf HS, Starke JR, Keshavjee S, et al. Post-exposure management of multidrug-resistant tuberculosis contacts: evidence-based recommendations. Policy Brief No. 1. Dubai (United Arab Emirates): Harvard Medical School Center for Global Health Delivery–Dubai; 2015.
17. Trieu L, Proops DC, Ahuja SD. Moxifloxacin prophylaxis against MDR TB, New York, New York, USA. Emerg Infect Dis. 2015;21:500–3. https://doi.org/10.3201/eid2103.141313
18. Marks SM, Mase SR, Morris SB. Systematic review, meta-analysis, and cost-effectiveness of treatment of latent tuberculosis to reduce progression to multidrug-resistant tuberculosis. Clin Infect Dis. 2017;64:1670–7. https://doi.org/10.1093/cid/cix208
19. Joint United Nations Programme on HIV/AIDS. Pakistan. 2020 [cited 2020 Sep 1]. https://www.unaids.org/en/regionscountries/countries/pakistan
20. Malik AA, Fuad J, Siddiqui S, Amanullah F, Jaswal M, Barry Z, et al. Tuberculosis preventive therapy for individuals exposed to drug-resistant tuberculosis: feasibility and safety of a community-based delivery of fluoroquinolone-containing preventive regimen. Clin Infect Dis. 2020;70:1958–65. https://doi.org/10.1093/cid/ciz502
21. Malik AA, Becerra MC, Lash TL, Cranmer LM, Omer SB, Fuad J, et al. Risk factors for adverse events in household contacts prescribed preventive treatment for drug-resistant TB exposure. Clin Infect Dis. 2020 Apr 8 [Epub ahead of print].
22. Fox GJ, Barry SE, Britton WJ, Marks GB. Contact investigation for tuberculosis: a systematic review and meta-analysis. Eur Respir J. 2013;41:140–56. https://doi.org/10.1183/09031936.00070812
23. Becerra MC, Huang CC, Lecca L, Bayona J, Contreras C, Calderon R, et al. Transmissibility and potential for disease progression of drug resistant *Mycobacterium tuberculosis*: prospective cohort study. BMJ. 2019;367:l5894. https://doi.org/10.1136/bmj.l5894
24. Becerra MC, Appleton SC, Franke MF, Chalco K, Arteaga F, Bayona J, et al. Tuberculosis burden in households of patients with multidrug-resistant and extensively drug-resistant tuberculosis: a retrospective cohort study. Lancet. 2011;377:147–52. https://doi.org/10.1016/S0140-6736(10)61972-1
25. Becerra MC, Franke MF, Appleton SC, Joseph JK, Bayona J, Atwood SS, et al. Tuberculosis in children exposed at home to multidrug-resistant tuberculosis. Pediatr Infect Dis J. 2013;32:115–9. https://doi.org/10.1097/INF.0b013e31826f6063
26. Reichler MR, Khan A, Sterling TR, Zhao H, Chen B, Yuan Y, et al.; Tuberculosis Epidemiologic Studies Consortium Task Order 2 Team. Risk factors for tuberculosis and effect of preventive therapy among close contacts of persons with infectious tuberculosis. Clin Infect Dis. 2020;70:1562–72. https://doi.org/10.1093/cid/ciz438
27. Martin-Sanchez M, Brugueras S, de Andrés A, Simon P, Gorrindo P, Ros M, et al.; Contact Tracing Group of the Tuberculosis Investigation Unit of Barcelona. Tuberculosis incidence among infected contacts detected through contact tracing of smear-positive patients. PLoS One. 2019;14:e0215322. https://doi.org/10.1371/journal.pone.0215322
28. Sloot R, Schim van der Loeff MF, Kouw PM, Borgdorff MW. Risk of tuberculosis after recent exposure. A 10-year follow-up study of contacts in Amsterdam. Am J Respir Crit Care Med. 2014;190:1044–52. https://doi.org/10.1164/rccm.201406-1159OC
29. Saunders MJ, Wingfield T, Tovar MA, Baldwin MR, Datta S, Zevallos K, et al. A score to predict and stratify risk of tuberculosis in adult contacts of tuberculosis index cases: a prospective derivation and external validation cohort study. Lancet Infect Dis. 2017;17:1190–9. https://doi.org/10.1016/S1473-3099(17)30447-4
30. Smieja MJ, Marchetti CA, Cook DJ, Smaill FM. Isoniazid for preventing tuberculosis in non-HIV infected persons. Cochrane Database Syst Rev. 2000;1999(2):CD001363.
31. Amanullah F, Ashfaq M, Khowaja S, Parekh A, Salahuddin N, Lotia-Farrukh I, et al. High tuberculosis prevalence in children exposed at home to drug-resistant tuberculosis. Int J Tuberc Lung Dis. 2014;18:520–7. https://doi.org/10.5588/ijtld.13.0593

Address for correspondence: Amyn A. Malik, Yale Institute for Global Health, 1 Church St, Ste 340, New Haven, CT 06510, USA; email: amyn.malik@ird.global or amyn.malik@yale.edu

Clusters of Drug-Resistant *Mycobacterium tuberculosis* Detected by Whole-Genome Sequence Analysis of Nationwide Sample, Thailand, 2014–2017

Ditthawat Nonghanphithak, Angkana Chaiprasert, Saijai Smithtikarn, Phalin Kamolwat, Petchawan Pungrassami, Virasakdi Chongsuvivatwong, Surakameth Mahasirimongkol, Wipa Reechaipichitkul, Chaniya Leepiyasakulchai, Jody E. Phelan, David Blair, Taane G. Clark, Kiatichai Faksri

Multidrug-resistant tuberculosis (MDR TB), pre-extensively drug-resistant tuberculosis (pre-XDR TB), and extensively drug-resistant tuberculosis (XDR TB) complicate disease control. We analyzed whole-genome sequence data for 579 phenotypically drug-resistant *M. tuberculosis* isolates (28% of available MDR/pre-XDR and all culturable XDR TB isolates collected in Thailand during 2014–2017). Most isolates were from lineage 2 (n = 482; 83.2%). Cluster analysis revealed that 281/579 isolates (48.5%) formed 89 clusters, including 205 MDR TB, 46 pre-XDR TB, 19 XDR TB, and 11 poly–drug-resistant TB isolates based on genotypic drug resistance. Members of most clusters had the same subset of drug resistance-associated mutations, supporting potential primary resistance in MDR TB (n = 176/205; 85.9%), pre-XDR TB (n = 29/46; 63.0%), and XDR TB (n = 14/19; 73.7%). Thirteen major clades were significantly associated with geography (p<0.001). Clusters of clonal origin contribute greatly to the high prevalence of drug-resistant TB in Thailand.

Tuberculosis (TB), caused by *Mycobacterium tuberculosis*, is a major global public health issue. Southeast Asia contributes notably (44%) to global TB cases. Thailand is in the top 30 countries for drug-resistant (DR) TB incidence (*1*). DR TB, including rifampin-resistant TB and strains with additional resistance to isoniazid (multidrug-resistant [MDR] TB), remains a great challenge for TB control. In 2018, ≈500,000 new cases of rifampin-resistant TB were reported globally, of which 78% were MDR TB (*1*). More worrisome is extensively drug-resistant (XDR) TB, which further exhibits resistance to 1 fluoroquinolone and 1 injectable second-line drug. The average proportion of global MDR TB cases with XDR TB is 6.2% (*1*). In Thailand, despite the reducing incidence of TB, the reported number of MDR TB cases nearly doubled during 2014–2018 (*1*); some are likely to be XDR TB. Treatment for patients with DR TB is prolonged and expensive, and outcomes are poor.

Whole-genome sequencing (WGS) of *M. tuberculosis* provides insights into drug resistance, in which mechanisms almost exclusively involve mutations (mostly single-nucleotide polymorphisms [SNPs], but also insertion/deletions) in genes coding for drug targets or drug-converting enzymes. WGS data can also provide insights into transmission and the dating of clusters (*2*), in which strains with near-identical genetic variants are likely to be part of a transmission chain (*3*). Analysis of *M. tuberculosis* WGS data from isolates across Thailand could provide much-needed insights into MDR/XDR TB transmission. Previous studies of DR TB have used genotyping techniques (e.g., spoligotyping, mycobacterial interspersed repetitive unit–variable-number tandem-repeat, and restriction fragment length polymorphism) (*4*,*5*), but these methods have limited resolution for inferring transmission because they investigate <1% of the *M. tuberculosis*

Author affiliations: Khon Kaen University, Khon Kaen, Thailand (D. Nonghanphithak, W. Reechaipichitkul, K. Faksri); Mahidol University, Bangkok, Thailand (A. Chaiprasert, C. Leepiyasakulchai); Ministry of Public Health, Bangkok (S. Smithtikarn, P. Kamolwat, P. Pungrassami); Prince of Songkla University, Hat Yai, Songkhla, Thailand (V. Chongsuvivatwong); Ministry of Public Health, Nonthaburi, Thailand (S. Mahasirimongkol); London School of Hygiene and Tropical Medicine, London, UK (J.E. Phelan, T.G. Clark); James Cook University, Townsville, Queensland, Australia (D. Blair)

DOI: https://doi.org/10.3201/eid2703.204364

genome. A recent WGS analysis revealed possible clonal transmission of 4 MDR TB isolates in Kanchanaburi Province (*6*). However, the extent of MDR TB and XDR TB clusters across Thailand is unknown. Our aim was to investigate the clustering patterns and risk factors of possible MDR TB, pre-XDR TB, and XDR TB transmission clusters across Thailand using WGS data.

Methods

Study Population and Setting

During 2014–2017, a total of 2,071 *M. tuberculosis* culture-confirmed MDR TB, pre-XDR TB, and XDR TB cases were listed in the laboratory records of the National Tuberculosis Reference Laboratory (NTRL; Ministry of Public Health) and Siriraj Hospital, Mahidol University, Thailand. These 2 laboratories cover 230 hospitals handling most DR TB cases in Thailand (Appendix 1 Tables 1, 2, https://wwwnc.cdc.gov/EID/article/27/3/20-4364-App1.xlsx) (*7*). We randomly selected 547 *M. tuberculosis* isolates from MDR TB and pre-XDR TB cases across 6 regions and 71 of 77 provinces nationally. We also included all retrievable (n = 32) XDR TB isolates (Appendix 1 Table 3). For 11 cases, we used pairs of isolates collected at different times as internal controls for SNP distances. In each control pair, we included the isolate with the most mutations associated with drug resistance or the chronologically earlier isolate in the studied population (n = 579). We retrieved demographic data from laboratory records. The study protocol was approved by the Center for Ethics in Human Research, Khon Kaen University (approval no. HE601249).

Phenotypic Drug-Susceptibility Testing

We performed phenotypic drug-susceptibility testing (DST) using the standard agar proportional method in Lowenstein-Jensen medium (*8*). Drug concentrations used were 0.2 μg/mL for isoniazid; 40.0 μg/mL for rifampin, ethionamide, capreomycin, and cycloserine; 2.0 μg/mL for ethambutol, ofloxacin, and levofloxacin; 4.0 μg/mL for streptomycin; 30.0 μg/mL for kanamycin; and 0.5 μg/mL for *para*-aminosalicylic acid. We used *M. tuberculosis* H37Rv as the susceptible reference strain.

Whole-Genome Sequence Analysis

We used multiple loops of *M. tuberculosis* colonies for genomic DNA extraction (with the cetyl-trimethylammonium bromide-sodium chloride method) (*9*). WGS data for 590 *M. tuberculosis* isolates were produced by NovogeneAIT (https://en.novogene.com) using the HiSeq (Illumina, https://www.illumina.com) platform generating 150-bp paired-end reads. We checked the quality of sequence reads using FastQC version 0.11.7 (*10*). We mapped high-quality reads from each isolate onto the H37Rv reference genome (GenBank accession no. NC_000962.3) using BWA-MEM version 0.7.12 (Li H, unpub. data, https://arxiv.org/abs/1303.3997). The average depth of sequencing coverage was high (341.01 ± 61.98). We used SAMtools version 0.1.19 (*11*) and GATK version 3.4.0 (*12*) to call SNPs and insertion/deletions. We filtered variants on the basis of a minimum coverage depth of 10-fold and Q20 minimum base-call quality score, and the intersection set of GATK and SAMtools variants was retained. We used the online tool TB-Profiler version 2.8.6 (*13,14*) to infer drug resistance and *M. tuberculosis* lineage membership on the basis of SNPs from the WGS data. The WGS data are available in the ENA Sequence Read Archive (https://www.ebi.ac.uk/ena/browser/home) (accession nos. PRJNA598981 and PRJNA613706).

Phylogenetic Analysis

We constructed a phylogenetic tree based on 26,541 high-confidence SNPs among 590 isolates using the maximum-likelihood method with the selected general time-reversible with gamma-distribution model, implemented within MEGA version 10.1 (*15*). We excluded the 130 SNPs known to be associated with DR TB found in this study to ensure that they would not affect the phylogenetic analysis. We inferred a bootstrap consensus tree from 1,000 replicates. We produced the phylogenetic tree image using iTOL (*16*).

Data Analysis

Isolates forming monophyletic groups in which many or all pairs differed by ≤25 SNPs were placed in the same clade. Clusters included isolates differing by 0–11 SNPs. We regarded members of a single cluster as possibly descended from a single clone through recent transmission. Less-recently transmitted isolates within a clade differed by 12–25 SNPs. We calculated the clustering percentage as (no. clustering isolates/total no. isolates) × 100. We differentiated isolates with acquired DR TB from possible primary DR TB (MDR TB, pre-XDR TB, and XDR TB) isolates on the basis of acquisition of additional resistance-associated mutations, especially those associated with resistance to fluoroquinolones, kanamycin, or capreomycin, drugs that are used for DR TB classification. For clusters containing isolates with different types of DR TB (such as MDR TB and XDR TB), we used the acquisition of additional drug-resistance SNPs and

co-ancestral relationships to differentiate between 2 patterns of acquired resistance: chronological (ancestral strain had fewer mutations, lesser type of DR, or both) or nonchronological (ancestral strain had more mutations, stronger type of DR, or both). Although XDR TB and pre-XDR TB could be considered as subsets of MDR TB, we have treated all 3 as separate categories in our analyses.

We analyzed all data using R statistical software version 3.6.1 (https://www.r-project.org) and considered p values <0.05 to be statistically significant. We analyzed associations between clades/clusters and geography using χ^2 tests and visualized them with the R package vcd version 1.4–8. We calculated odds ratios (ORs) with 95% CIs using the R package epiR version 1.0–4. We tested factors associated with clustering isolates using the Student *t*-test (numerical data), χ^2 test, or Fisher exact test (categorical data), when applicable. We constructed graphs using the R package ggplot2 version 3.2.1 and built phylo-maps using the package phytools version 0.7–20.

Results

Study Population and Characteristics

Most (466; 80.5%) of the 579 culture-confirmed DR TB cases in the studied population were MDR TB, followed by 81 pre-XDR TB (14.0%) (Appendix 1 Table 2). We included all available XDR TB isolates (n = 32), constituting 5.5% of our samples but only 1.5% of the culture-confirmed 2,071 DR TB isolates collected nationally during 2014–2017. Central and

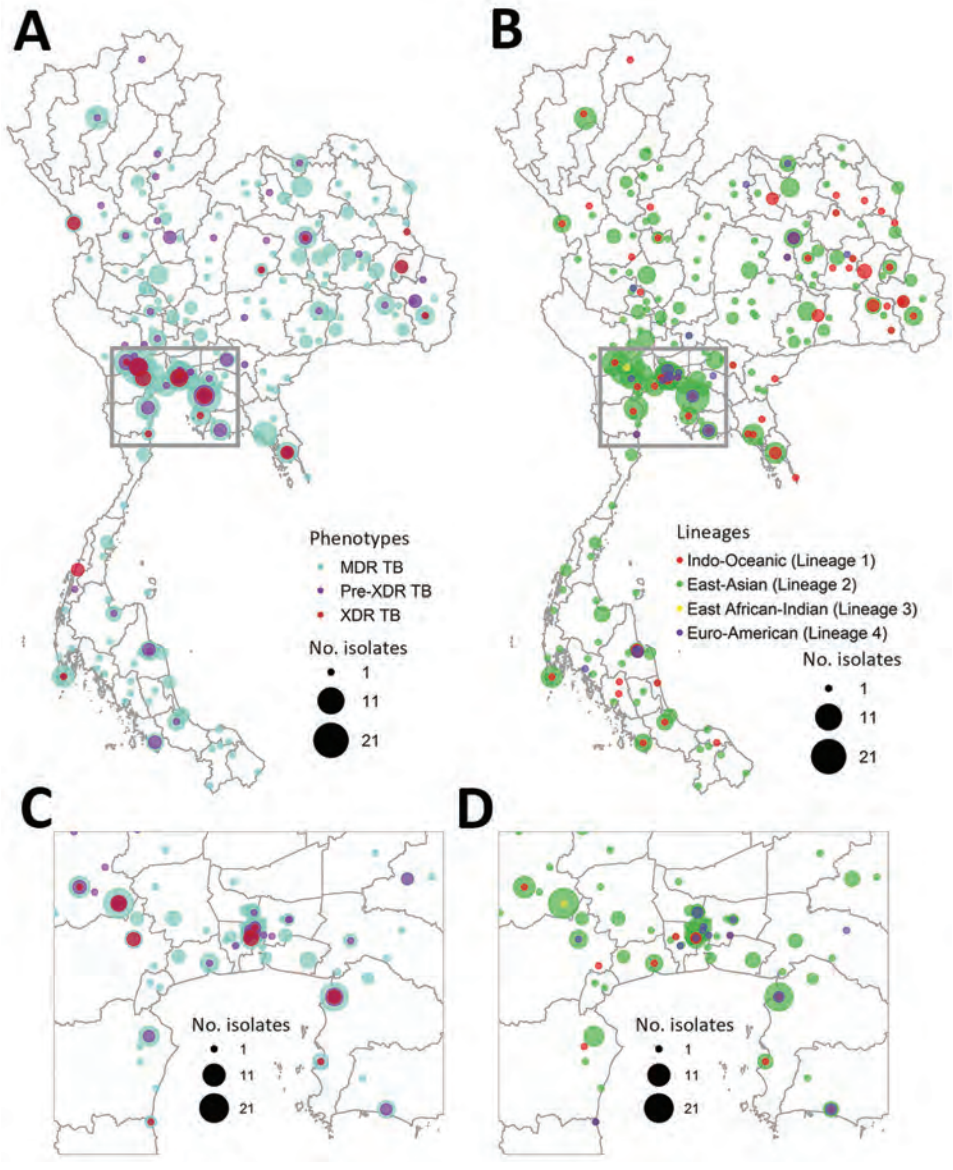

Figure 1. Geographic and lineage distribution of 579 drug-resistant *Mycobacterium tuberculosis* isolates in Thailand, 2014–2017. A) Geographic distribution of MDR TB, pre-XDR TB, and XDR TB. B) Lineage distribution of drug-resistant *M. tuberculosis*. C) Drug-resistant types, enlarged from panel A. D) Lineage distribution, enlarged from panel B. The size of each circle is proportional to the number of isolates. MDR, multidrug resistant; TB, tuberculosis; XDR, extensively drug-resistant.

northeast regions of Thailand had the highest DR TB proportions (Figure 1). The 3 provinces with the highest number of DR TB cases were Bangkok (n = 85; 14.7%), Kanchanaburi (n = 51; 8.8%), and Chonburi (n = 37; 6.4%) (Figure 1; Appendix 1 Table 3). Most patients were male (n = 419; 73.1%) and mean age was 43.5 (±14.7) years (Appendix 1 Table 4).

Phylogenetic Analysis

Most of the *M. tuberculosis* isolates belonged to the East-Asian lineage (lineage 2) (n = 482; 83.2%), followed by the Indo-Oceanic lineage (lineage 1) (n = 67; 11.6%), the Euro-American lineage (lineage 4) (n = 29; 5.0%), and the East African-Indian lineage (lineage 3) (n = 1; 0.2%) (Figure 2; Appendix 1 Table 5). Lineage 2.2.1 (n = 413; 71.3%) was the main sublineage among MDR, pre-XDR, and XDR TB.

Clustering and Possible Transmission Clusters

The phylogenetic tree (Figure 2) showed enormous diversity among the DR TB isolates from Thailand. Many isolates were distinct, differing from all others at a mean ±SD of 657 ± 626 SNPs. Most isolates (n = 319; 55.1%) grouped into 13 clades, each consisting of 5–86 isolates (Figure 3; Appendix 2 Figure 1, https://wwwnc.cdc.gov/EID/article/27/3/20-4364-App2.pdf). Clades 1, 6, 11, and 13 each consisted of a single small cluster of closely related isolates; the remaining clades included

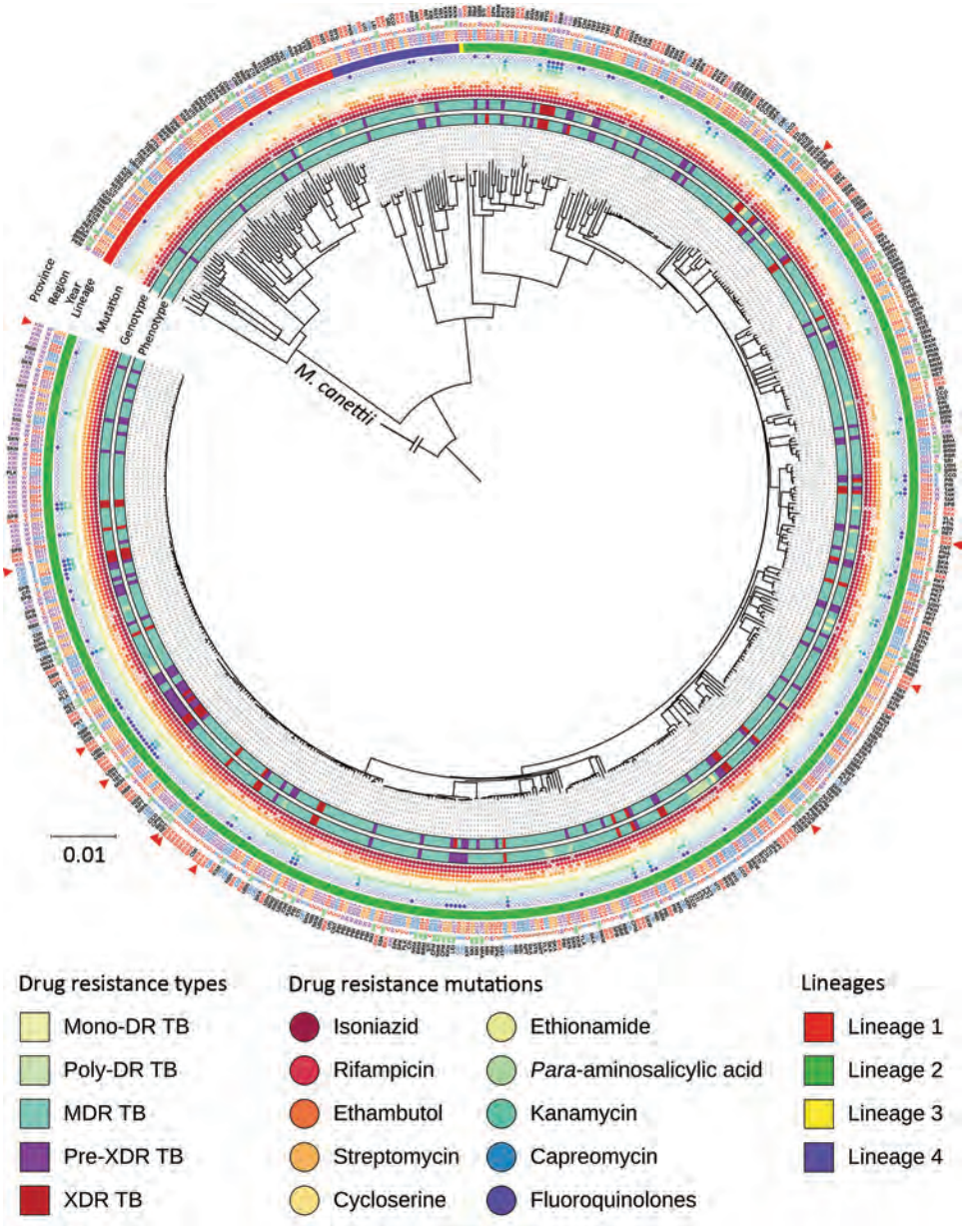

Figure 2. Phylogenetic tree for the 590 drug-resistant *Mycobaterium tuberculosis* isolates from Thailand, 2014–2017. From inner to the outer circles: culture-based phenotypic drug-susceptibility test, whole-genome sequencing–based drug-resistance profile (DR TB, MDR TB, pre-XDR TB, and XDR TB), drug-resistance mutations, lineage, year of collection, regions, and provinces. Red triangles indicate the paired isolates from the same patients (n = 11). Scale bar indicates the genetic distance proportional to the total number of single nucleotide polymorphisms. *M. canettii* was used as an outgroup. DR TB, drug-resistant tuberculosis; MDR, multidrug resistant; TB, tuberculosis; XDR, extensively drug-resistant.

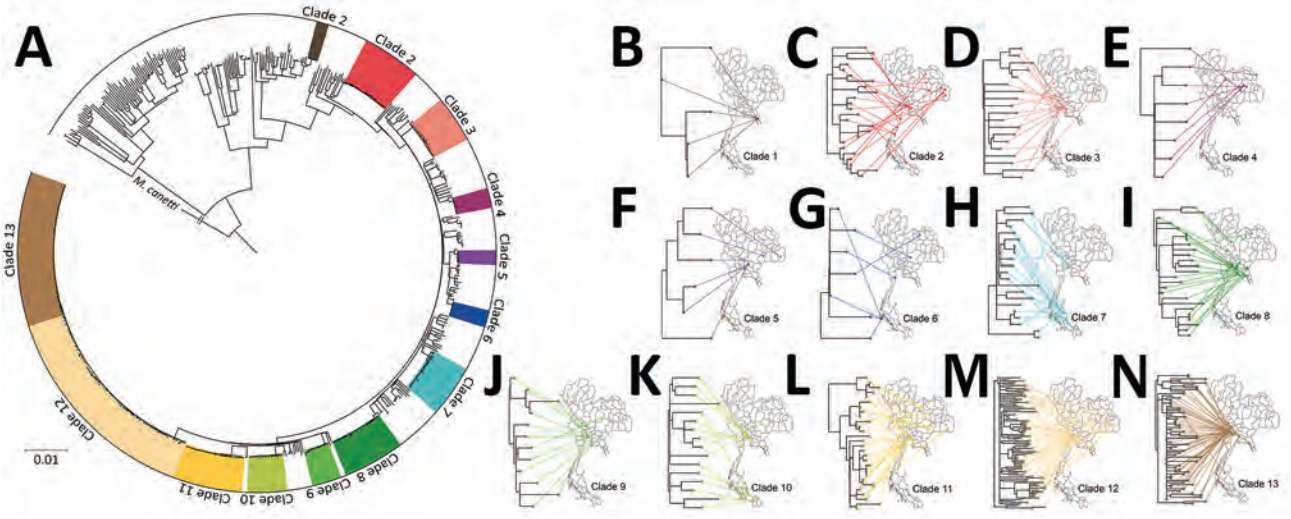

Figure 3. Geographic distribution of 13 major clades of drug-resistant tuberculosis in Thailand. A) The 13 clades are highlighted in the outer circle. Scale bar indicates the genetic distance proportional to the total number of single nucleotide polymorphisms. B–N) Each of the 13 major clades is associated with particular geographic regions, as shown. *Mycobacterium canettii* was used as an outgroup.

≥1 possible clusters (Appendix 2 Figure 2). The isolates grouped in each clade were significantly associated with a particular geographic region (p<0.001; Appendix 2 Figure 3, panel A). Clade 1 (Figure 3, panel B) was found only in Trat Province and clade 13 predominated in Kanchanaburi (Figure 3, panel N).

A total of 89 clusters contained 281 isolates (48.5%) (Appendix 1 Table 6). Sixty clusters (isolates differing by ≤11 SNPs), containing 2–34 isolates, fell within the major clades. A further 29 smaller clusters occurred elsewhere in the tree. Most isolates within a cluster shared geographic links (Figure 4, panels A–F; Appendix 1 Table 6). The percentages of MDR TB, pre-XDR TB, and XDR TB isolates (based on phenotypic DST) that fell into clusters were 46.1% (215/466) for MDR TB, 49.4% (40/81) for pre-XDR TB, and 81.3% (26/32) for XDR TB (Appendix 1 Table 6). Pairwise SNP distances within and between each of the 89 clusters are given summarized (Appendix 1 Table 7).

Some clusters included isolates with different types of DR TB. Nineteen of the 89 clusters (C2, C7, C10, C16, C22, C36, C37, C40, C43, C49, C59, C60, C63, C70, C72, C76, C80, C83, and C89) had a chronological pattern based on the progressive increase in numbers of DR mutations from base to tips in the phylogeny (Appendix 1 Table 8). The pattern of DR mutation changes was nonchronological in clusters C21, C23, C32, C35, C41, C55, C71, and C75. Among the 281 clustering isolates, 81.9% were classified as possible primary DR TB (n = 230), including MDR TB (n = 176/205; 85.9%), pre-XDR TB (n = 29/46; 63.0%), and XDR TB (n = 14/19; 73.7%). In addition, we identified 10 phenotypically MDR isolates and 1 phenotypically pre-XDR TB isolate as possible examples of primary isoniazid resistance (n = 11) based on genotypic DR. Other clustering isolates (n = 51/281, 18.1%) exhibited acquired DR TB (MDR TB [n = 29/205; 14.1%], pre-XDR TB [n = 17/46; 37.0%], and XDR TB [n = 5/19; 26.3%]) (Table 1).

Among clustered isolates, there was some discordance between phenotypic DST findings (MDR TB [n = 215], pre-XDR TB [n = 40], and XDR TB [n = 26]) and genotypic DST results (poly-DR TB [n = 11], MDR TB [n = 205], pre-XDR TB [n = 46], and XDR TB [n = 19]) (Appendix 1 Table 8). We identified 11 isolates of phenotypically MDR TB genotypically as poly-DR TB (resistant to >1 drug but not to both isoniazid and rifampicin). We identified 66 MDR TB, 9 pre-XDR TB, and 10 XDR TB clusters on the basis of phenotypic DST (Appendix 1 Table 9; Appendix 2 Figure 4, panels A–F). Most pre-XDR TB and XDR TB clusters had hospital-based links (Appendix 1 Table 9). All phenotypic DR TB clusters and resistance types, stratified by province, are shown (Appendix 1 Table 10).

Factors Associated with Possible DR TB Transmission Clusters

TB patients from whom clustering isolates were obtained had an average age of ≈42 years. Isolates falling within clusters were significantly associated with geographic regions (p = 0.001; Appendix 2 Figure 3, panel B). Patients with TB who lived in western provinces had a higher risk of being within possible DR

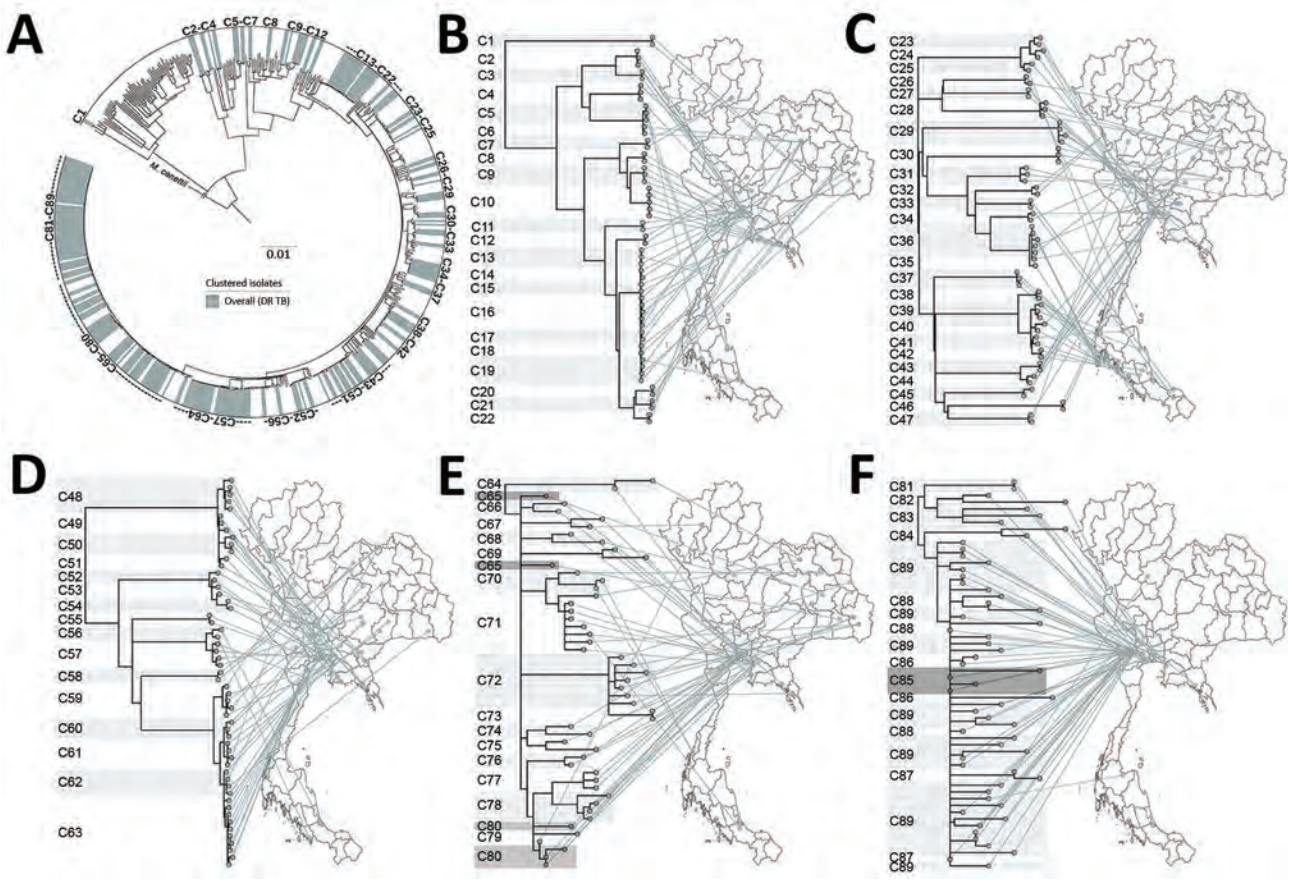

Figure 4. All clusters of DR TB isolates from Thailand. A) A total of 89 clusters are highlighted in the outer circle. Scale bar indicates the genetic distance proportional to the total number of single nucleotide polymorphisms. B–F) Phylogeographical links of each cluster are shown. For clarity, clusters are divided among 5 phylomaps. Some isolates in closely related clusters (C64–C65, C79–C80, and C85–C89) crossed localities. *Mycobacterium canettii* was used as an outgroup. DR TB, drug-resistant tuberculosis.

TB transmission clusters than those elsewhere (OR 2.44, 95% CI 1.53–3.89; Table 2). Lineage 2.2.1 (versus other lineages) was associated with a higher risk of possible DR TB transmission clusters (OR 3.59, 95% CI 2.42–5.32). Lineage 1 had the lowest risk of being represented in DR TB transmission clusters (OR 0.03, 95% CI 0.01–0.11). Clustering isolates had drug-resistance mutations such as *katG* S315T, *rpoB* S450L, and *embB* G406D (Table 2).

Discussion

MDR TB and XDR TB are serious global problems, but few studies have focused on their transmission at a nationwide resolution. Thailand has a high burden of MDR TB and increasing numbers of MDR TB cases (*1*). We sourced 579 DR TB isolates across 71 provinces during 2014–2017. Nearly half of these were in possible transmission clusters, mostly involving *M. tuberculosis* lineage 2.2.1. A total of 89 clusters, most distributed among 13 major clades, contributed to multiclonal MDR TB outbreaks associated with specific regions in Thailand. Bangkok, Kanchanaburi, and Chonburi were the provinces with the highest proportions of MDR TB, pre-XDR TB, and XDR TB clusters (i.e., groups of isolates differing by ≤11 SNPs). We used 2 criteria to select SNP cutoff values. First, the ≤11 SNP difference cutoff for a cluster was derived directly from the maximum number of differences between the 11 paired isolates used as an internal control. Second, we used an SNP cutoff concordant with, or more stringent than, those in previous studies (*17*–*20*). Our 11-SNP cutoff was proportionally 0.0004 of the 26,541 SNPs in our total set. This proportion was concordant with that in a previous study (*21*), and more stringent than those in other studies (*18*,*20*). A <12-SNP cutoff has been previously proposed as the upper boundary for possible cluster transmission events (*2*).

Phylogenetic analysis identified 13 major clades, each associated with a particular region(s). Pairwise

Table 1. Characteristics of isolates within 89 DR TB clusters, Thailand, 2014–2017*

	DR TB types, no. (%)†			
Clustered isolates, n = 281	INH-R, n = 11	MDR TB, n = 205	Pre-XDR TB, n = 46	XDR TB, n = 19
Possible primary DR TB,‡ n = 230, 81.85%	11 (100.0)	176 (85.85)	29 (63.04)	14 (73.68)
Possible acquired DR TB,‡ n = 51, 18.15%	0	29 (14.15)	17 (36.96)	5 (26.32)

*Using a pairwise-difference range of 0–11 single nucleotide polymorphisms, 89 clusters (minimum cluster size = 2 isolates) were recognized. DR, drug-resistant; INH-R, isoniazid resistant; MDR, multidrug-resistant; TB, tuberculosis; XDR, extensively drug-resistant.
†DR TB types based on genotypic drug susceptibility tests.
‡Possible primary DR TB isolates were differentiated from acquired DR TB isolates based on the acquisition of mutations associated with DR TB and from co-ancestral relationships.

SNP differences between isolates within clades ranged from >11 to ≈25, suggesting a range of divergence times from a common ancestor (Appendix 2 Figure 2). On the basis of the transmission time estimates (0.5 SNP/ge-nome/year) for *M. tuberculosis* (2), some of these major clades might have begun to circulate in Thailand ≈20–40 years ago, others more recently. Isolates differing by 12–25 SNPs nevertheless often shared geographic links. For example, 17 of 21 (81%) isolates in clade 7 (Figure 3, pan-el H), which had pairwise differences indicating a rela-tively nonrecent common ancestor, were located within neighboring provinces of southern Thailand. Clades 1, 6, 11, and 13 each consisted of isolates differing at very few SNPs, giving us confidence that these were likely examples of recent transmission. Nonetheless, isolates in clade 6 often occurred in different provinces.

The largest and most recent clade was clade 13 (Figure 3, panel N), comprising 62 cases (46 MDR TB, 11 pre-XDR TB, and 5 XDR TB based on pheno-typic DST) found in the western region, especially in Kanchanaburi. This finding suggests that clones of pre-XDR TB and XDR TB may emerge from recent

Table 2. Demographic and other factors associated with clustering (≤11 SNP difference) of TB isolates, Thailand, 2014–2017*

		Clustering isolates		
Characteristic	All isolates, n = 579	Isolates falling within clusters, n = 281	Nonclustering isolates, n = 298	Odds ratio (95% CI)
Sex, n = 573				
M	419 (73.12)	198 (70.71)	221 (75.43)	0.79 (0.54–1.14)
F	154 (26.88)	82 (29.29)	72 (24.57)	1.27 (0.88–1.84)
Age, y, n = 508				
Mean ± SD	43.51 ± 14.68	42.02 ± 15.23	44.94 ± 14.03	NA
Region				
Central	183 (31.61)	79 (28.11)	104 (34.90)	0.73 (0.51–1.04)
Eastern	88 (15.20)	47 (16.73)	41 (13.76)	1.26 (0.80–1.98)
Northeastern	125 (21.59)	56 (19.93)	69 (23.15)	0.83 (0.56–1.23)
Northern	17 (2.94)	4 (1.42)	13 (4.36)	0.32 (0.10–0.98)
Southern	73 (12.61)	33 (11.74)	40 (13.42)	0.86 (0.52–1.40)
Western	93 (16.06)	62 (22.06)	31 (10.40)	**2.44 (1.53–3.89)**
Lineage				
2.1	31 (5.35)	12 (4.27)	19 (6.38)	0.66 (0.31–1.38)
2.2.1	413 (71.33)	236 (83.99)	177 (59.40)	**3.59 (2.42–5.32)**
2.2.1.1	32 (5.53)	16 (5.69)	16 (5.37)	1.06 (0.52–2.17)
2.2.1.2 and 2.2.2	6 (1.04)	2 (0.71)	4 (1.34)	0.53 (0.05–3.71)
4	29 (5.01)	13 (4.64)	16 (5.35)	0.86 (0.41–1.82)
1	67 (11.57)	2 (0.71)	65 (21.81)	**0.03 (0.01–0.11)**
3	1 (0.17)	0 (0.00)	1 (0.34)	NA
Drug-resistance mutations				
Isoniazid, n = 565				
katG S315T	448 (79.29)	252 (89.68)	196 (69.01)	**3.90 (2.46–6.18)**
inhA −15c/t	52 (9.20)	7 (2.49)	45 (15.85)	**0.14 (0.06–0.31)**
Rifampin, n = 554				
rpoB S450L	279 (50.36)	176 (65.19)	103 (36.27)	**3.29 (2.32–4.66)**
Ethambutol, n = 335				
embB M306V	85 (25.37)	44 (20.75)	41 (33.33)	**0.52 (0.32–0.86)**
embB G406D	66 (19.70)	59 (27.83)	7 (5.69)	**6.39 (2.81–14.51)**
embB M306I	56 (16.72)	27 (12.74)	29 (23.58)	**0.47 (0.26–0.84)**
Streptomycin, n = 349				
rpsL K43R	295 (84.53)	188 (89.95)	107 (76.43)	**2.76 (1.52–5.01)**
Ethionamide, n = 268				
ethA 639–640del	143 (53.36)	105 (73.43)	38 (30.40)	**6.33 (3.72–10.77)**
inhA −15c/t	65 (24.25)	9 (6.29)	56 (44.80)	**0.08 (0.04–0.18)**
Para-aminosalicylic acid, n = 99				
folC S150G	39 (39.39)	32 (50.79)	7 (19.44)	**4.28 (1.63–11.19)**

*Values are no. (%) except as indicated. Bold type indicates statistical significance. NA, not applicable.

MDR TB ancestors. We confirmed a previous report (*22*) that there was a large MDR TB outbreak in Kanchanaburi. In addition, clade 13 is sister to clade 12, which consists of strains that spread in both central (especially Bangkok) and northeast Thailand and contain less recently transmitted strains. Therefore, the MDR TB outbreak clade in Kanchanaburi was derived from a less recently transmitted clade elsewhere in Thailand.

We identified 89 clusters (isolates in each differing by ≤11 SNPs) of DR TB in Thailand. The clustered isolates showed a strong association with geographic region. The largest cluster (C89), within clade 13 in Kanchanaburi, comprised 34 isolates (27 MDR TB and 7 pre-XDR TB based on phenotypic DST). In South Africa, WGS analysis of a large XDR TB cohort (>400 cases) from a single province showed that only 30% of participants had clear epidemiologic links (person–person or hospital link): 70% of transmission events may have resulted from casual contact between persons not known to one another (*23*). Another study in South Africa showed that 19% of XDR TB patients discharged from the hospital caused secondary XDR TB cases in the community (*24*). Here, we found 9 clusters of pre-XDR TB (the largest with 7 isolates) and 10 clusters (the largest with 4 isolates) of XDR TB in Thailand (Appendix 1 Table 9; Appendix 2 Figure 4).

To reflect the extent of the DR TB outbreak in Thailand, we calculated the proportion of isolates falling into the 89 DR TB clusters (Table 1). In some clusters, isolates exhibited different types of DR TB associated with chronology, revealing the progression of DR mutations in the phylogeny, moving from the ancestor toward the tips of the tree (Appendix 1 Table 8). Based on mutation-acquisition analysis within this phylogeny, we saw examples of possible primary resistance in 85.9% of MDR TB, 63.0% of pre-XDR TB, and 73.7% of XDR TB cases. Eight clusters included isolates with different types of DR and more resistance-associated mutations in the ancestral strain than in its descendants. This situation might be explained by different durations of the latency stage occurring after transmission events leading to the emergence of less troublesome DR TB cases (such as MDR TB) later than the more troublesome cases (such as XDR TB) (*25*). Because not all cases from the possible transmission chain could be included, undetected primary resistance might exist. Data from all DR TB cases in the community and information on treatment history and known exposure are needed to accurately and completely estimate the extent of primary DR TB. The proportion of primary DR TB cases could be higher because we reported numbers of MDR TB cases excluding pre-XDR TB and XDR TB (each of which was reported as a separate subset). In addition, some index cases might not have been included in the selected population.

Previously reported factors contributing to MDR TB transmission include illicit drug usage (*26*); delayed TB diagnosis and being >45 years of age (*18*); and being single, having low income, suffering frequent stress and other diseases, and lacking medical insurance (*27*). Lineage 2 predominated in previous studies of transmission of MDR TB (*18,26,28*). We found that infection with lineage 2.2.1 is the strongest predictor (3.6-fold) of DR TB clusters, whereas infection with lineage 1 had the lowest risk. Living in the western region of Thailand increased the risk of being in DR TB clusters by 2.4-fold. The western region, being close to the border with Myanmar, differs from other regions of the country in terms of both ethnicity and economic development. These differences might explain the increased risk there (*29*). Previously, clustering isolates were more likely to have mutations of *rpoB* S450L (*18,30*), *katG* S315T, or the *inhA* promoter (*31*). We also found a pattern of drug resistance-associated mutations (*katG* S315T, *rpoB* S450L, *embB* G406D, *rpsL* K43R, *ethA* 639–640del, and *folC* S150G) in clusters.

The DR TB situation in Thailand is a major concern and requires urgent implementation of control measures such as active case finding to disrupt the transmission chain and targeted intervention and contact tracing in hotspot regions. The mortality rate and cost of treatment of XDR TB is very high (*32*); therefore, these DR types should be the priority for intervention. The large size of some clusters might reflect their high transmissibility (*33*); thus, tracking clade 13 at Kanchanaburi should be a priority. Besides the 13 major clades, several small clusters of DR TB were found in many provinces. The potential for expansion of these small clusters is unknown. Here, we also identified the hotspot provinces to help prioritize locations for intervention.

Globally, few studies at the nationwide scale have used WGS analysis of MDR TB, pre-XDR TB, and XDR TB (*26,30,34–36*). Older studies have used blunt genotyping tools (e.g., IS*6110* restriction fragment length polymorphism, spoligotyping, and mycobacterial interspersed repetitive unit–variable-number tandem-repeat) with limited or convenient sample sizes. DR TB studies using WGS in Saudi Arabia and Portugal have revealed transmission clusters of MDR TB; however, they had small samples and provided limited data on epidemiologic links (*36,37*). Extrapolating from our

findings, primary-resistant TB strains may be the main contributors to the current global problem of high MDR TB and XDR TB prevalence.

The primary limitations of our study were that it was retrospective rather than prospective, lacked socioeconomic data for analysis and lacked fine-scale data of epidemiologic links: possible transmission clusters were presumed only from the genetic distances among isolates and each patient's hospital and province of residence. In addition, an accurate estimation of the exact time of the possible transmission cannot be made: clusters originating years ago may be continuing to spread. We also lacked information about treatment and exposure history and of the complete population to identify all index cases to differentiate between primary and acquired DR TB. In addition, the prevalence and clustering of MDR TB, pre-XDR TB, and XDR TB isolates in some provinces might be underestimated because of the low coverage of DST for the first-line drugs among TB cases (*1*).

In conclusion, we have demonstrated the usefulness of WGS for DR TB epidemiology. We have shown that close to half of MDR TB, pre-XDR TB, and XDR TB cases in Thailand might be caused by transmission clusters. Two thirds of pre-XDR TB and three quarters of MDR TB and XDR TB clustering isolates were possible examples of primary resistance. These results indicate that the emergence of MDR TB, pre-XDR TB, and XDR TB cases in Thailand might be from a narrow base of ancestral strains. The high prevalence of MDR/XDR TB in Thailand might be the result of multiclonal outbreaks. People living in the western region of Thailand had a 2.4-fold increased risk of DR TB clusters, and lineage 2.2.1 conferred a 3.6-fold increased risk of forming DR TB clusters relative to other lineages.

Acknowledgments

We thank the Research and Diagnostic Center for Emerging and Infectious Diseases (RCEID), Khon Kaen University, for laboratory and research facility support.

This work was supported by the National Research Council of Thailand and Health System Research Institute (HSRI) (grant nos. 60-057 and 62-003 to K.F.). D.N. is funded by Faculty of Medicine, Khon Kaen University. T.G.C. is funded by the Medical Research Council UK (grant nos. MR/M01360X/1, MR/N010469/1, MR/R025576/1, and MR/R020973/1) and Biotechnology and Biological Sciences Research Council UK (BB/R013063/1). A.C. is funded by the Medical Research Council and National Science and Technology Development Agency (MRC/NSTDA) (grant no. P-18-50228).

This work is dedicated to the late HRH Princess Galyanivadhana, the patroness of the Drug-Resistant Tuberculosis Fund.

About the Author

Mr. Nonghanphithak is a PhD student in the Medical Microbiology Program, Faculty of Medicine, Khon Kaen University, Khon Kaen, Thailand. His research interest is in the molecular epidemiology and prediction of drug resistance in tuberculosis using whole-genome sequencing techniques.

References

1. World Health Organization. Global tuberculosis report 2019. Geneva: The Organization; 2019.
2. Meehan CJ, Moris P, Kohl TA, Pečerska J, Akter S, Merker M, et al. The relationship between transmission time and clustering methods in *Mycobacterium tuberculosis* epidemiology. EBioMedicine. 2018;37:410–6. https://doi.org/10.1016/j.ebiom.2018.10.013
3. Guerra-Assunção JA, Crampin AC, Houben RM, Mzembe T, Mallard K, Coll F, et al. Large-scale whole genome sequencing of *M. tuberculosis* provides insights into transmission in a high prevalence area. eLife. 2015;4:e05166. https://doi.org/10.7554/eLife.05166
4. Disratthakit A, Meada S, Prammananan T, Thaipisuttikul I, Doi N, Chaiprasert A. Genotypic diversity of multidrug-, quinolone- and extensively drug-resistant *Mycobacterium tuberculosis isolates* in Thailand. Infect Genet Evol. 2015;32:432–9. https://doi.org/10.1016/j.meegid.2015.03.038
5. Rienthong D, Ajawatanawong P, Rienthong S, Smithtikarn S, Akarasewi P, Chaiprasert A, et al. Restriction fragment length polymorphism study of nationwide samples of *Mycobacterium tuberculosis* in Thailand, 1997–1998. Int J Tuberc Lung Dis. 2005;9:576–81.
6. Regmi SM, Chaiprasert A, Kulawonganunchai S, Tongsima S, Coker OO, Prammananan T, et al. Whole genome sequence analysis of multidrug-resistant *Mycobacterium tuberculosis* Beijing isolates from an outbreak in Thailand. Mol Genet Genomics. 2015;290:1933–41. https://doi.org/10.1007/s00438-015-1048-0
7. World Health Organization. Global tuberculosis report 2018. Geneva: The Organization; 2018.
8. Canetti G, Fox W, Khomenko A, Mahler HT, Menon NK, Mitchison DA, et al. Advances in techniques of testing mycobacterial drug sensitivity, and the use of sensitivity tests in tuberculosis control programmes. Bull World Health Organ. 1969;41:21–43.
9. Larsen MH, Biermann K, Tandberg S, Hsu T, Jacobs WR Jr. Genetic manipulation of *Mycobacterium tuberculosis*. Curr Protoc Microbiol. 2007;6:10A.2.1–21. https://doi.org/10.1002/9780471729259.mc10a02s6
10. Andrews S. FastQC: A quality control tool for high throughput sequence data. Cambridge (UK): Babraham Bioinformatics; 2010.
11. Li H, Handsaker B, Wysoker A, Fennell T, Ruan J, Homer N, et al.; 1000 Genome Project Data Processing Subgroup. The Sequence Alignment/Map format and SAMtools. Bioinformatics. 2009;25:2078–9. https://doi.org/10.1093/bioinformatics/btp352
12. McKenna A, Hanna M, Banks E, Sivachenko A, Cibulskis K, Kernytsky A, et al. The Genome Analysis Toolkit: a MapReduce framework for analyzing next-generation DNA

sequencing data. Genome Res. 2010;20:1297–303. https://doi.org/10.1101/gr.107524.110
13. Coll F, McNerney R, Preston MD, Guerra-Assunção JA, Warry A, Hill-Cawthorne G, et al. Rapid determination of anti-tuberculosis drug resistance from whole-genome sequences. Genome Med. 2015;7:51. https://doi.org/10.1186/s13073-015-0164-0
14. Phelan JE, O'Sullivan DM, Machado D, Ramos J, Oppong YEA, Campino S, et al. Integrating informatics tools and portable sequencing technology for rapid detection of resistance to anti-tuberculous drugs. Genome Med. 2019;11:41. https://doi.org/10.1186/s13073-019-0650-x
15. Kumar S, Stecher G, Li M, Knyaz C, Tamura K. MEGA X: Molecular Evolutionary Genetics Analysis across computing platforms. Mol Biol Evol. 2018;35:1547–9. https://doi.org/10.1093/molbev/msy096
16. Letunic I, Bork P. Interactive Tree Of Life (iTOL) v4: recent updates and new developments. Nucleic Acids Res. 2019;47(W1):W256–9. https://doi.org/10.1093/nar/gkz239
17. Walker TM, Ip CL, Harrell RH, Evans JT, Kapatai G, Dedicoat MJ, et al. Whole-genome sequencing to delineate *Mycobacterium tuberculosis* outbreaks: a retrospective observational study. Lancet Infect Dis. 2013;13:137–46. https://doi.org/10.1016/S1473-3099(12)70277-3
18. Yang C, Luo T, Shen X, Wu J, Gan M, Xu P, et al. Transmission of multidrug-resistant *Mycobacterium tuberculosis* in Shanghai, China: a retrospective observational study using whole-genome sequencing and epidemiological investigation. Lancet Infect Dis. 2017;17:275–84. https://doi.org/10.1016/S1473-3099(16)30418-2
19. Xu Y, Cancino-Muñoz I, Torres-Puente M, Villamayor LM, Borrás R, Borrás-Máñez M, et al. High-resolution mapping of tuberculosis transmission: whole genome sequencing and phylogenetic modelling of a cohort from Valencia region, Spain. PLoS Med. 2019;16:e1002961. https://doi.org/10.1371/journal.pmed.1002961
20. Shuaib YA, Khalil EAG, Wieler LH, Schaible UE, Bakheit MA, Mohamed-Noor SE, et al. *Mycobacterium tuberculosis* complex lineage 3 as causative agent of pulmonary tuberculosis, eastern Sudan. Emerg Infect Dis. 2020;26:427–36. https://doi.org/10.3201/eid2603.191145
21. Merker M, Nikolaevskaya E, Kohl TA, Molina-Moya B, Pavlovska O, Brännberg P, et al. Multidrug- and extensively drug-resistant *Mycobacterium tuberculosis* Beijing clades, Ukraine, 2015. Emerg Infect Dis. 2020;26:481–90. https://doi.org/10.3201/eid2603.190525
22. Boonthanapat N, Soontornmon K, Pungrassami P, Sukhasitwanichkul J, Mahasirimongkol S, Jiraphongsa C, et al. Use of network analysis multidrug-resistant tuberculosis contact investigation in Kanchanaburi, Thailand. Trop Med Int Health. 2019;24:320–7. https://doi.org/10.1111/tmi.13190
23. Auld SC, Shah NS, Mathema B, Brown TS, Ismail N, Omar SV, et al. Extensively drug-resistant tuberculosis in South Africa: genomic evidence supporting transmission in communities. Eur Respir J. 2018;52:1800246. https://doi.org/10.1183/13993003.00246-2018
24. Dheda K, Limberis JD, Pietersen E, Phelan J, Esmail A, Lesosky M, et al. Outcomes, infectiousness, and transmission dynamics of patients with extensively drug-resistant tuberculosis and home-discharged patients with programmatically incurable tuberculosis: a prospective cohort study. Lancet Respir Med. 2017;5:269–81. https://doi.org/10.1016/S2213-2600(16)30433-7
25. Knight GM, McQuaid CF, Dodd PJ, Houben RMGJ. Global burden of latent multidrug-resistant tuberculosis: trends and estimates based on mathematical modelling. Lancet Infect Dis. 2019;19:903–12. https://doi.org/10.1016/S1473-3099(19)30307-X
26. Anderson LF, Tamne S, Brown T, Watson JP, Mullarkey C, Zenner D, et al. Transmission of multidrug-resistant tuberculosis in the UK: a cross-sectional molecular and epidemiological study of clustering and contact tracing. Lancet Infect Dis. 2014;14:406–15. https://doi.org/10.1016/S1473-3099(14)70022-2
27. Li WB, Zhang YQ, Xing J, Ma ZY, Qu YH, Li XX. Factors associated with primary transmission of multidrug-resistant tuberculosis compared with healthy controls in Henan Province, China. Infect Dis Poverty. 2015;4:14. https://doi.org/10.1186/s40249-015-0045-1
28. Marais BJ, Mlambo CK, Rastogi N, Zozio T, Duse AG, Victor TC, et al. Epidemic spread of multidrug-resistant tuberculosis in Johannesburg, South Africa. J Clin Microbiol. 2013;51:1818–25. https://doi.org/10.1128/JCM.00200-13
29. Palittapongarnpim P, Ajawatanawong P, Viratyosin W, Smittipat N, Disratthakit A, Mahasirimongkol S, et al. Evidence for host-bacterial co-evolution via genome sequence analysis of 480 Thai *Mycobacterium tuberculosis* lineage 1 isolates. Sci Rep. 2018;8:11597. https://doi.org/10.1038/s41598-018-29986-3
30. Wang SF, Zhou Y, Pang Y, Zheng HW, Zhao YL. Prevalence and risk factors of primary drug-resistant tuberculosis in China. Biomed Environ Sci. 2016;29:91–8. https://doi.org/10.3967/bes2016.010
31. Gagneux S, Burgos MV, DeRiemer K, Enciso A, Muñoz S, Hopewell PC, et al. Impact of bacterial genetics on the transmission of isoniazid-resistant *Mycobacterium tuberculosis*. PLoS Pathog. 2006;2:e61. https://doi.org/10.1371/journal.ppat.0020061
32. Manjelievskaia J, Erck D, Piracha S, Schrager L. Drug-resistant TB: deadly, costly and in need of a vaccine. Trans R Soc Trop Med Hyg. 2016;110:186–91. https://doi.org/10.1093/trstmh/trw006
33. Sobkowiak B, Banda L, Mzembe T, Crampin AC, Glynn JR, Clark TG. Bayesian reconstruction of *Mycobacterium tuberculosis* transmission networks in a high incidence area over two decades in Malawi reveals associated risk factors and genomic variants. Microb Genom. 2020;6:e000361. https://doi.org/10.1099/mgen.0.000361
34. Jagielski T, Brzostek A, van Belkum A, Dziadek J, Augustynowicz-Kopeć E, Zwolska Z. A close-up on the epidemiology and transmission of multidrug-resistant tuberculosis in Poland. Eur J Clin Microbiol Infect Dis. 2015;34:41–53. https://doi.org/10.1007/s10096-014-2202-z
35. Somoskovi A, Helbling P, Deggim V, Hömke R, Ritter C, Böttger EC. Transmission of multidrug-resistant tuberculosis in a low-incidence setting, Switzerland, 2006 to 2012. Euro Surveill. 2014;19:20736. https://doi.org/10.2807/1560-7917.ES2014.19.11.20736
36. Oliveira O, Gaio R, Carvalho C, Correia-Neves M, Duarte R, Rito T. A nationwide study of multidrug-resistant tuberculosis in Portugal 2014–2017 using epidemiological and molecular clustering analyses. BMC Infect Dis. 2019;19:567. https://doi.org/10.1186/s12879-019-4189-7
37. Al-Ghafli H, Kohl TA, Merker M, Varghese B, Halees A, Niemann S, et al. Drug-resistance profiling and transmission dynamics of multidrug-resistant *Mycobacterium tuberculosis* in Saudi Arabia revealed by whole genome sequencing. Infect Drug Resist. 2018;11:2219–29. https://doi.org/10.2147/IDR.S181124

Address for correspondence: Kiatichai Faksri, Department of Microbiology, Faculty of Medicine, Khon Kaen University, Khon Kaen 40002, Thailand; email: kiatichai@kku.ac.th

Severe Acute Respiratory Syndrome Coronavirus 2 Seropositivity among Healthcare Personnel in Hospitals and Nursing Homes, Rhode Island, USA, July–August 2020

Lara J. Akinbami, Philip A. Chan, Nga Vuong, Samira Sami, Dawn Lewis, Philip E. Sheridan, Susan L. Lukacs, Lisa Mackey, Lisa A. Grohskopf, Anita Patel, Lyle R. Petersen

Healthcare personnel are recognized to be at higher risk for infection with severe acute respiratory syndrome coronavirus 2. We conducted a serologic survey in 15 hospitals and 56 nursing homes across Rhode Island, USA, during July 17–August 28, 2020. Overall seropositivity among 9,863 healthcare personnel was 4.6% (95% CI 4.2%–5.0%) but varied 4-fold between hospital personnel (3.1%, 95% CI 2.7%–3.5%) and nursing home personnel (13.1%, 95% CI 11.5%–14.9%). Within nursing homes, prevalence was highest among personnel working in coronavirus disease units (24.1%; 95% CI 20.6%–27.8%). Adjusted analysis showed that in hospitals, nurses and receptionists/medical assistants had a higher likelihood of seropositivity than physicians. In nursing homes, nursing assistants and social workers/case managers had higher likelihoods of seropositivity than occupational/physical/speech therapists. Nursing home personnel in all occupations had elevated seropositivity compared with hospital counterparts. Additional mitigation strategies are needed to protect nursing home personnel from infection, regardless of occupation.

Author affiliations: Centers for Disease Control and Prevention, Hyattsville, Maryland, USA (L. Akinbami, S.L. Lukacs); US Public Health Service, Rockville, Maryland, USA (L. Akinbami, S.L. Lukacs, L.A. Grohskopf); Rhode Island Department of Health, Providence, Rhode Island, USA (P.A. Chan, D. Lewis, P.E. Sheridan); Centers for Disease Control and Prevention, Fort Collins, Colorado, USA (N. Vuong, L. Mackey, L.R. Petersen); Centers for Disease Control and Prevention, Atlanta, Georgia, USA (S. Sami, L.A. Grohskopf, A. Patel)

DOI: https://doi.org/10.3201/eid2703.204508

Healthcare personnel face higher risk of infection during the coronavirus disease (COVID-19) pandemic because of their essential role in identifying and treating persons affected (*1*,*2*). Although essential workers in many occupations have higher risk of infection because of face-to-face interaction with the public, personnel in hospitals and nursing homes have more frequent and prolonged contact with persons known to be infected with severe acute respiratory syndrome coronavirus 2 (SARS-CoV-2).

Hospitals and nursing homes are potential hotspots of infection transmission. Hospital personnel conduct activities ranging from infection screening to administering advanced life support measures and may be exposed to patients with high viral loads (*3*). Infection risk can be exacerbated by shortages in personal protective equipment (PPE) and other resources, including staff (*4*,*5*). Nursing homes have been referred to as "ground zero" (*6*) of the pandemic because resident deaths have contributed disproportionately to overall COVID-19 mortality (*2*,*7*). Several factors may increase intrafacility transmission, including residents with risk factors for severe COVID-19 disease and prolonged viral shedding (e.g., advanced age, underlying conditions), a large proportion of asymptomatic infections, and new resource constraints alongside long-standing challenges (*8*–*11*). Assessing SARS-CoV-2 seropositivity among hospital and nursing home personnel may reveal risk factors that can be addressed through additional interventions. Community transmission has been identified as a primary determinant of transmission in both nursing homes and hospitals (*12*,*13*),

but the relative impact in each of these settings has not been simultaneously compared.

The Rhode Island Department of Health (RIDOH) and the US Centers for Disease Control and Prevention (CDC) collaborated on a serologic survey of personnel in hospitals, nursing homes, and first responder agencies (e.g., fire, law enforcement) across Rhode Island. As of July 17, 2020, when the survey was initiated, there were >17,700 persons positive for COVID-19 in Rhode Island, of whom 2,675 were nursing home residents and 1,210 nursing home staff, and just more than 1,000 deaths, most among nursing home residents (*14*). Because of the disproportionate impact on nursing homes, we made an added effort to include as many nursing home facilities as possible in the survey. This analysis compares SARS-CoV-2 seroprevalence among nursing homes and hospital personnel and assesses characteristics and factors related to seropositivity.

Methods

The serologic survey was conducted throughout Rhode Island during July 17–August 28, 2020. RIDOH performed outreach to all agencies to encourage participation. The protocol was reviewed by CDC human subjects research officials, who determined that the activity was public health surveillance as defined in 45 CFR 46 (*15*). Participation was voluntary, results were not shared with employers, and CDC did not have access to personally identifying information.

RIDOH provided participating agencies with study information and a link to the secure web-based survey to distribute to employees (Appendix Table 1, https://wwwnc.cdc.gov/EID/article/27/3/20-4508-App1.pdf). Upon completing the screening and questionnaire on a personal device, participants received information about blood collection events at their workplace or nearby facility. Each participant provided 10–15 mL of blood using standard venipuncture techniques. Centrifuged serum samples were transferred to a central laboratory for SARS-CoV-2 antibody testing using the ORTHO Clinical Diagnostics VITROS Immunodiagnostic Products Anti-SARS-CoV-2 IgG Test (https://www.orthoclinicaldiagnostics.com). The emergency use authorization data submitted to the US Food and Drug Administration indicated that this test measures IgG directed at the S1 domain of the spike protein with a sensitivity of 90% and a specificity of 100% (*16*). Results were reported to participants as negative (signal-to-cutoff ratio <1.0), positive (≥1.0), or lack of valid result.

A total of 11,987 participants ≥18 years of age consented to phlebotomy and reported no new symptoms of cough, shortness of breath, fever, change in sense of taste/smell, or positive test for SARS-CoV-2 by reverse transcription PCR (RT-PCR) in the 2 weeks before survey participation. Seven were excluded for lack of valid serologic test result because of lipemia or insufficient sample volume and 1,860 did not work in either a hospital (inpatient units and/or ambulatory clinics) or nursing home. Of the remaining 10,120 participants, 9,863 had occupations in direct patient care and support (Appendix Table 2) and were included in this analysis.

We calculated seropositivity (percent positive for SARS-CoV-2 antibodies) overall and for subgroups. We estimated exact Clopper-Pearson 95% CIs and assessed significant statistical differences by evaluating nonoverlapping 95% CI or χ^2 tests for categorical variables and Cochran-Armitage trend tests for ordinal variables (2-sided with $\alpha = 0.05$).

We classified participants who reported race/ethnicity as non-Hispanic Native Hawaiian or other Pacific Islander, non-Hispanic American Indian or Alaska Native, or other race as other race (n = 231, 2.3%) and those who declined to specify race/ethnicity as declined (n = 240, 2.4%). We stratified analyses by primary agency selected by participants: hospital or nursing home. Participants could then choose one or more specific workplaces from a precategorized list or free-text workplaces not listed. Hospital emergency department was inadvertently omitted from the response categories for specific workplace but was included in the analysis based on free-text responses. Some hospital and nursing home participants reported working in additional settings that were not the focus of the analysis (e.g., emergency medical services) or in the other agency type (e.g., 1% of hospital and 2% of nursing home personnel worked in both hospital and nursing home settings). These participants were retained in the analysis, but these other workplaces were reported infrequently and are not shown separately. A precategorized list and free-text option were also provided for occupation. Prespecified categories with low frequencies were combined (Appendix Table 2). Among nursing home occupations, 4 with low sample size were combined (other nursing home: engineer/maintenance staff, pharmacist, receptionist/medical assistant, and physician, n = 56). Analyzing workplace and occupation simultaneously resulted in small sample sizes. Only occupation/workplace groups with sample size >20 or with absolute 95% CI width >30% were shown to ensure estimate reliability (*17*). Each workplace was represented as a separate dichotomous variable to allow modeling of non–mutually exclusive categories.

Participants reported the frequency at which they performed aerosol-generating procedures; if they needed complete PPE, as defined by CDC recommendations by occupation and patient contact; if, since March 1, they ever used PPE shortage protocols (extended use, reuse, or both); if they lacked specific PPE components when in contact with a person with suspected/confirmed COVID-19 in the workplace; and if they received training in the previous year on PPE donning/doffing techniques. Participants also reported whether their work involved in-person interaction with the community, patients, or both and if they were exposed (spent >10 minutes within 6 feet) to any COVID-19 positive co-workers, household members, patients, or other persons.

We used generalized estimating equations to model likelihood of seropositivity, accounting for clustering by facility (15 hospitals and 56 nursing homes, using an independence correlation structure). PPE variables had a common category (never use PPE) and were thus collinear. Therefore, only PPE shortage protocol use was included in the model, given evidence that shortages may contribute to transmission (*12*). Similarly, questions assessing use of individual PPE components had a common category, not applicable. Of these, only use of an N95/powered air-purifying respirator (PAPR) was included in the model, because it had an unadjusted association with seroprevalence. For hospital occupations, physicians were the reference group for comparability to a previous study (*18*). There were not enough physicians in nursing homes to categorize separately, so occupational/physical/speech therapists were the reference group for nursing homes. No interaction terms were explored. We used SAS 9.4 software (SAS Institute, https://www.sas.com) for all analyses.

Results

Overall seropositivity for 9,863 participants was 4.6% (95% CI 4.2%–5.0%) but differed between hospital personnel (3.1%; 95% CI 2.7%–3.5%) and nursing home personnel (13.1%; 95% CI 11.5%–15.0%) (Table 1). Generally, we found higher facility-level seropositivity in nursing homes than in hospitals, as well as lower or 0% seropositivity in facilities in rural western Rhode Island (Figure 1). Demographic characteristics were similar between hospital and nursing home personnel, but some seropositivity patterns differed. Seropositivity was highest among hospital personnel 18–24 years of age, but there were no age differences among nursing home personnel ($p = 0.64$ by χ^2 test). For both groups, there were no differences by sex ($p>0.05$), and Hispanic and non-Hispanic Black personnel had higher seropositivity compared with non-Hispanic White personnel (pairwise $p<0.001$ for both groups). Among nursing home personnel, those who lived in multiunit housing had higher seroprevalence than those in single-family housing ($p = 0.001$).

Table 1. SARS-CoV-2 seropositivity among hospital and nursing home personnel, by demographic characteristics, Rhode Island, USA, July–August 2020*

	Hospital			Nursing home		
Characteristic	No. (%)	Seropositive, no.	Seropositive, % (95% CI)	No. (%)	Seropositive, no.	Seropositive, % (95% CI)
Total	8,370 (100)	256	3.1 (2.7–3.5)	1,494 (100)	196	13.1 (11.5–15.0)
Age group, y						
18–24	275 (3.3)	21	7.6 (4.8–11.4)	68 (4.6)	7	10.3 (4.2–20.1)
25–34	1,987 (23.7)	71	3.6 (2.8–4.5)	254 (17.0)	37	14.6 (10.5–19.5)
35–44	1,874 (22.4)	56	3.0 (2.3–3.9)	328 (22.0)	45	13.7 (10.2–17.9)
45–59	2,890 (34.5)	81	2.8 (2.2–3.5)	569 (38.1)	78	13.7 (11.0–16.8)
60–64	896 (10.7)	22	2.5 (1.6–3.7)	170 (11.4)	20	11.8 (7.3–17.6)
≥65	448 (5.4)	5	1.1 (0.4–2.6)	105 (7.0)	9	8.6 (4.0–15.7)
Sex						
M	1,582 (18.9)	44	2.8 (2.0–3.7)	227 (15.2)	39	17.2 (12.5–22.7)
F	6,788 (81.1)	212	3.1 (2.7–3.6)	1,267 (84.8)	157	12.4 (10.6–14.3)
Race/ethnicity						
Non-Hispanic White	6,829 (81.6)	182	2.7 (2.3–3.1)	1,165 (78.0)	119	10.2 (8.5–12.1)
Non-Hispanic Black	284 (3.4)	20	7.0 (4.4–10.7)	87 (5.8)	24	27.6 (18.5–38.2)
Non-Hispanic Asian	316 (3.8)	10	3.2 (1.5–5.7)	28 (1.9)	6	21.4 (8.3–41.0)
Hispanic	554 (6.6)	31	5.6 (3.8–7.9)	130 (8.7)	28	21.5 (14.8–29.6)
Other†	191 (2.3)	11	5.8 (2.9–10.1)	40 (2.7)	8	20.0 (9.1–36.7)
Decline	196 (2.3)	2	1.0 (0.1–3.6)	44 (2.9)	11	25.0 (13.2–40.3)
Housing						
Single family	6,924 (82.7)	204	3.0 (2.6–3.4)	1,136 (76.0)	131	11.5 (9.7–13.5)
Multiunit	1,446 (17.3)	52	3.6 (2.7–4.7)	358 (24.0)	65	18.2 (14.3–22.6)

*SARS-CoV-2, severe acute respiratory syndrome coronavirus 2.
†Other race/ethnicity includes non-Hispanic Native Hawaiian and other Pacific Islander, non-Hispanic American Indian and Alaska Native, and participants who indicated other non-Hispanic race.

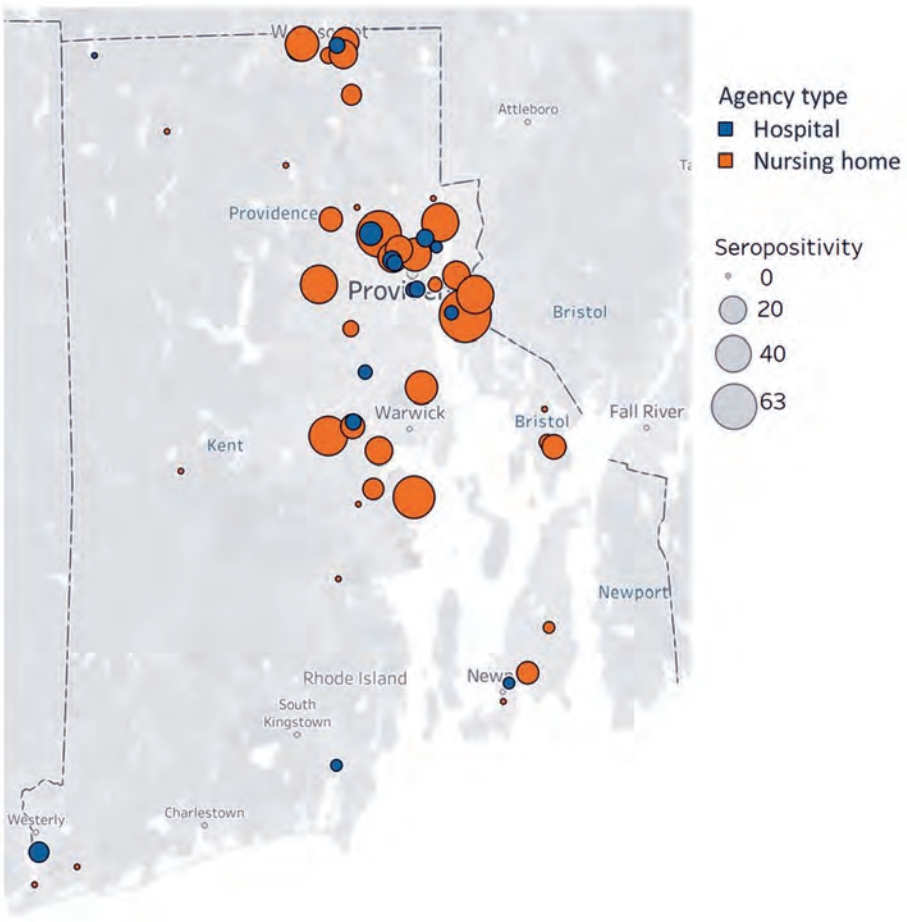

Figure 1. Seropositivity for severe acute respiratory syndrome coronavirus 2 among hospital and nursing home personnel, by facility, Rhode Island, USA, July–August 2020. Map based on average of longitude and average of latitude. Marker size is proportional to facility-level seroprevalence. Facilities with participant sample size <10 are not shown.

Among hospital personnel, nurse assistants had higher seropositivity (5.9%, 95% CI 3.8%–8.7%) than the overall hospital level of 3.1% (Table 2). Among nursing home personnel, nurse assistants had higher seropositivity (19.9%, 95% CI 15.5%–24.9%) than the overall nursing home level of 13.1%. Overall, 27.3% of participants reported working at >1 workplace. Among hospital personnel, seropositivity was higher among those working in hospital COVID-19 units (5.0%, 95% CI 4.0%–6.3%) than the overall hospital level. Among nursing home personnel, those working in nursing home COVID-19 units had higher seropositivity (24.1%, 95% CI 20.6%–27.8%) than the overall nursing home level. Figure 2 shows workplace and occupation together in non–mutually exclusive categories. Occupation/workplace groups with seroprevalence significantly elevated above the overall level of 4.6% included nurse assistants (31.4%, 95% CI 23.7%–39.9%), nurses (24.6%, 95% CI 18.7%–31.4%), and occupational therapists (13.4%, 95% CI 7.3%–21.8%) who worked in nursing home COVID-19 units; social workers/case managers (17.7%, 95% CI 6.8%–34.5%), nurse assistants (14.4%, 95% CI 10.0%–20.0%), and nurses (10.2%, 95% CI 7.1%–14.0%) who worked in nursing home non–COVID-19 units; and nurses (7.5%, 95% CI 5.5%–9.9%) who worked in hospital COVID-19 units. Across all occupational groups, seropositivity was higher for those who worked in nursing homes compared with those with the same occupation in hospitals.

Among hospital personnel, 27.2% of those exposed to a household member who tested positive for COVID-19 were seropositive versus 2.4% of those unexposed (Table 3). For nursing home personnel, 54.0% of those exposed to a household member with COVID-19 were seropositive versus 10.9% of those unexposed. For both hospital and nursing home personnel, exposure versus no exposure to a co-worker was associated with higher seropositivity, as was exposure to a patient (with or without PPE use) and exposure to some other person. Seropositivity was higher among personnel with community or patient interaction as part of work responsibilities compared with those without for both hospital (3.2% vs. 0.9%) and nursing home personnel (13.7% vs. 7.3%).

For both hospital and nursing home personnel, we found a significant linear trend of increasing

Table 2. SARS-CoV-2 seropositivity among hospital and nursing home personnel, by occupation and work location, Rhode Island, USA, July–August 2020*

	Hospital			Nursing home		
Category	No.	Seropositive, no.	Seropositive, % (95% CI)	No.	Seropositive, no.	Seropositive, % (95% CI)
Occupation						
Administrative/office staff/clerk	903	19	2.1 (1.3–3.3)	200	11	5.5 (2.8–9.6)
Diagnostic Imaging	369	11	3.0 (1.5–5.3)	0	NA	NA
Dietician/dietary services	135	3	2.2 (0.5–6.4)	114	10	8.8 (4.3–1.6)
Engineer/maintenance	108	2	1.9 (0.2–6.5)	26	6	23.1 (9.0–43.7)
Environmental services/cleaning	114	3	2.6 (0.6–7.5)	69	9	13.0 (6.1–23.3)
Laboratory technologist/technician	281	4	1.4 (0.4–3.6)	0	NA	NA
Nurse	2,733	114	4.2 (3.5–5.0)	413	63	15.3 (11.9–19.1)
Nurse assistant	392	23	5.9 (3.8–8.7)	296	59	19.9 (15.5–24.9)
Occupational/physical/speech therapist	283	8	2.8 (1.2–5.5)	163	16	9.8 (5.7–15.5)
Other healthcare	573	12	2.1 (1.1–3.6)	65	4	6.2 (1.7–15.0)
Pharmacist/pharmacist assistant	256	7	2.7 (1.1–5.6)	5	2	40.0 (5.3– 85.3)
Physician	1,001	22	2.2 (1.4–3.3)	10	0	0.0
Physician assistant	100	1	1.0 (0.0–5.5)	0	NA	NA
Receptionist/medical assistant	296	12	4.1 (2.1–7.0)	15	1	6.7 (0.2–32.0)
Social worker/case manager/counselor	432	7	1.6 (0.1–3.3)	46	10	21.7 (11.0–36.4)
Supervisor/manager	393	8	2.0 (0.9–4.0)	72	5	6.9 (2.3–15.5)
Workplace†						
Administrative office	1,132	21	1.9 (1.2–2.8)	218	12	5.5 (2.9–9.4)
Ambulatory healthcare/dental office	2,122	48	2.3 (1.7–3.0)	NA	NA	NA
Hospital COVID-19 unit	1,435	72	5.0 (4.0–6.3)	NA	NA	NA
Hospital general inpatient unit	3,752	138	3.7 (3.1–4.3)	NA	NA	NA
Hospital intensive care unit	1,250	37	3.0 (2.1–4.1)	NA	NA	NA
Hospital surgical unit	1,234	31	2.5 (1.7–3.6)	NA	NA	NA
Hospital emergency department	288	7	2.4 (1.0–4.9)	NA	NA	NA
Other hospital location	963	20	2.1 (1.3– 3.2)	NA	NA	NA
Nursing home COVID-19 unit	NA	NA	NA	565	136	24.1 (20.6–27.8)
Nursing home non–COVID-19 unit	NA	NA	NA	1,088	111	10.2 (8.5–12.2)

*Gray shading indicates nursing home occupation categories that had a sample size <30 and were combined into an other nursing home category, with a combined n = 56, percent seropositive 16.1% (7.6%–28.3%). COVID-19, coronavirus disease; NA, not applicable; SARS-CoV-2, severe acute respiratory syndrome coronavirus 2.

†Work location categories are not mutually exclusive: 27.3% of participants reported working in >1 workplace. Hospital and nursing home participants also reported working in other workplaces not shown in the table: corrections facilities (n = 16), Rhode Island Department of Health (n = 4), emergency medical services (n = 15), fire department (n = 6), law enforcement (n = 1), Rhode Island emergency management (n = 8), Rhode Island alternative hospital setup site (n = 14), Rhode Island remote COVID-19 testing site (n = 21), Rhode Island state warehouse (n = 1), or Rhode Island traffic and perimeter control (n = 1). Some worked in facilities in the other agency category; that is, 84 hospital personnel also worked in nursing home COVID-19 and non–COVID-19 units, and 34 nursing home personnel also worked in hospital COVID-19 units and general inpatient units.

seropositivity with greater procedure frequency of performing aerosol-generating procedures (Table 4). For both groups, seropositivity decreased with decreasing frequency of needing complete PPE. Among hospital personnel, those who reported no shortage of PPE had higher seropositivity than those who reused PPE (p = 0.006). Among nursing home personnel, there were no significant differences in seropositivity between those who reported no PPE shortages and those who reported extended use, reuse, or both. Among all personnel, there were no differences in seroprevalence between those who received PPE donning/doffing training versus those with no training (p>0.05 by χ^2 test). For each equipment type, there were no differences in seropositivity between those who reported having versus not having a specific PPE component, with one exception: hospital personnel who did not have an N95 respirator/PAPR were more likely to be seropositive than those who had this equipment (4.4% vs. 2.6%) (Figure 3).

In adjusted models (Figure 4; Appendix Table 3), both hospital personnel (Figure 4, panel A) and nursing home personnel (Figure 4, panel B) with exposure to a household member with COVID-19 had the highest odds of being seropositive. Otherwise, seropositivity patterns diverged by facility type. For hospital personnel, older age compared with 18–24 years of age was associated with lower seropositivity and non-Hispanic Black and Hispanic race/ethnicity were associated with higher seropositivity. Among nursing home personnel, there was no significant pattern of seropositivity by age or race/ethnicity. Personnel with work responsibilities including face-to-face interaction with members of the community or patients had a higher likelihood of seropositivity among hospital but not nursing home personnel. Among hospital personnel, nurses and receptionists or medical assistants had a higher likelihood of being seropositive compared with physicians. Among nursing home personnel, nurse assistants and social

workers or case managers had higher likelihood compared with occupational, physical, and speech therapists. Finally, hospital personnel working in surgical units had lower likelihood of being seropositive. There were no associations by frequency of aerosol-generating procedures, use of PPE shortage protocols, or not having or using an N95 respirator/PAPR among either hospital or nursing home personnel.

Discussion

In this study, we compared SARS-CoV-2 seroprevalence among nursing home personnel to hospital per-

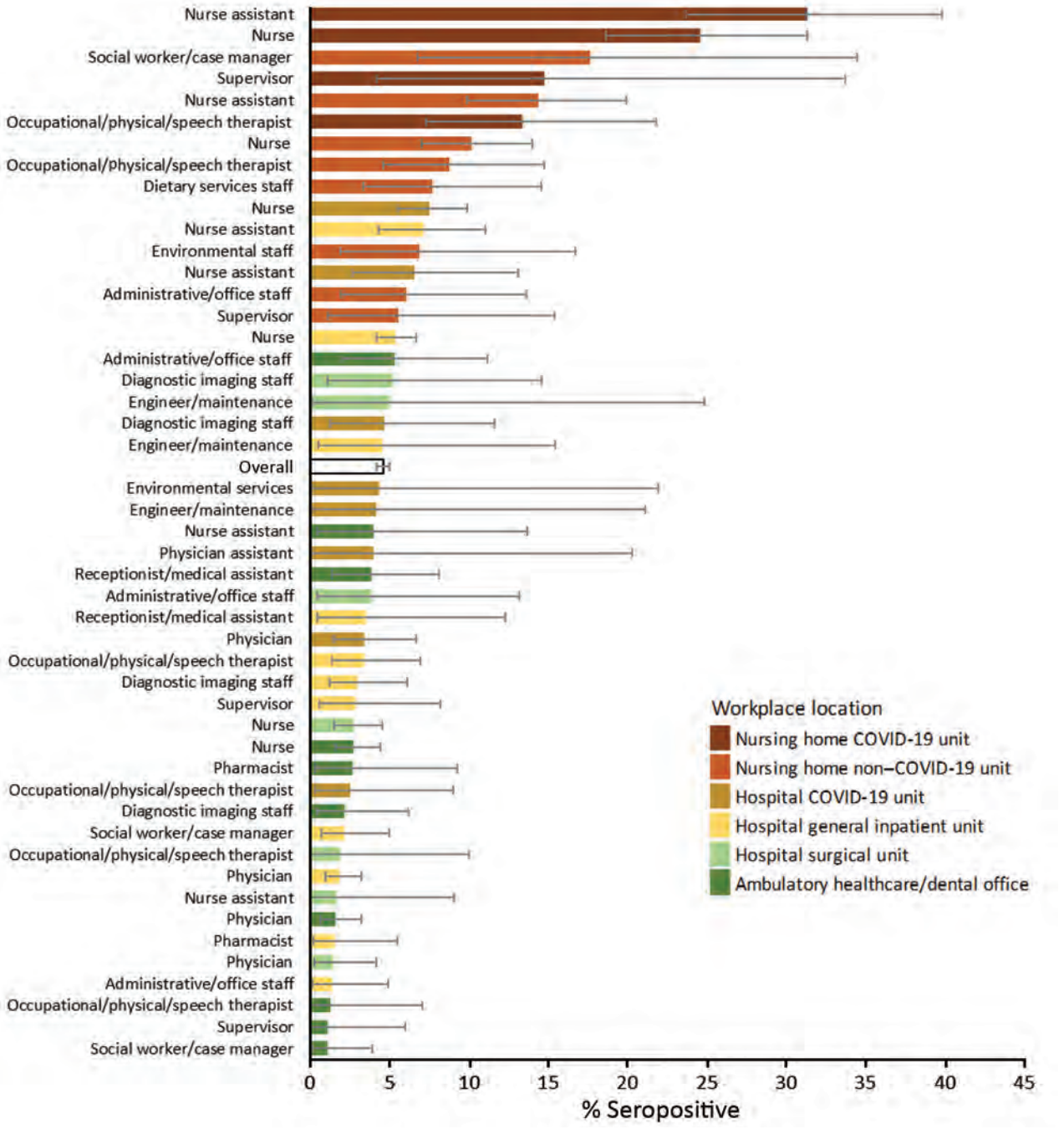

Figure 2. Seropositivity for severe acute respiratory syndrome coronavirus 2 among hospital and nursing home personnel, by selected workplace and occupation, Rhode Island, USA, July–August 2020. Error bars indicate 95% CIs. Workplace/occupation categories are not mutually exclusive: 27.3% of participants indicated >1 workplace. Occupations not included in the figure had 0% seroprevalence, sample size below n = 20, or absolute CI width >0.30 (unreliable estimate). Other healthcare category also not included. COVID-19, coronavirus disease.

Table 3. SARS-CoV-2 seropositivity among hospital and nursing home personnel, by exposure to persons testing positive for COVID-19 and in-person interaction in the workplace, Rhode Island, USA, July–August 2020*

	Hospital			Nursing home		
Question	No.	Seropositive, no.	Seropositive, % (95% CI)	No.	Seropositive, no.	Seropositive, % (95% CI)
Exposed to COVID-19–positive co-worker?						
Exposed	2,070	122	5.9 (4.9–7.0)	550	113	20.6 (17.2–24.2)
Not exposed/don't know	6,299	134	2.1 (1.8–2.5)	944	83	8.8 (7.1–10.8)
Exposed to COVID-19–positive household member?						
Exposed	213	58	27.2 (21.8–33.7)	76	41	54.0 (42.1–65.5)
Not exposed/don't know	8,156	198	2.4 (2.1–2.8)	1,418	155	10.9 (9.4–12.7)
Exposed to COVID-19–positive patient?						
Exposed while not wearing PPE	1,317	60	4.6 (3.5–5.8)	173	28	16.2 (11.0–22.5)
Exposed while wearing PPE	2,630	108	4.1 (3.4–4.9)	498	119	23.9 (20.2–27.9)
Not exposed/don't know	4,422	88	2.0 (1.6–2.5)	823	49	6.0 (4.4–7.8)
Exposed to other COVID-19–positive person?						
Exposed	827	67	8.1 (6.3–10.2)	163	54	33.1 (26.0–40.9)
Not exposed/don't know	7,542	189	2.5 (2.2–2.9)	1,331	142	10.7 (9.1–12.5)
In-person interaction with public/patients in the workplace?						
Work involves in-person interaction	7,795	251	3.2 (2.8–3.6)	1,370	187	13.7 (11.9–15.6)
No in-person interaction	574	5	0.9 (0.3–2.0)	124	9	7.3 (3.4–13.3)

*Exposure defined as being within 6 feet for at least 10 min. COVID-19, coronavirus disease; PPE, personal protective equipment; SARS-CoV-2, severe acute respiratory syndrome coronavirus 2.

sonnel within 1 state. Nursing home personnel had a significantly higher seroprevalence (13.1%) than hospital personnel (3.1%), who had levels comparable to statewide seroprevalence of 2.8% based on commercial laboratory data as of August 2020 (*19*). High prevalence among nursing home personnel was observed across all occupations studied. A study analyzing Centers for Medicare and Medicaid Services facility-level data found that community COVID-19 prevalence was the strongest predictor of COVID-19 cases and deaths in nursing homes (*12*). In this study, the association between facility and community seroprevalence may hold, but with exaggerated SARS-CoV-2 transmission in nursing homes versus hospitals. SARS-CoV-2 seropositivity among nursing home COVID-19 unit personnel was nearly 5 times higher than among hospital-based COVID-19 unit personnel. Nursing home non–COVID-19 unit personnel had seropositivity nearly 3 times higher than hospital general inpatient unit personnel. As of November 17,

Table 4. SARS-CoV-2 seropositivity among hospital and nursing home personnel, by frequency of conducting aerosol-generating procedures frequency and use of PPE, Rhode Island, USA, July–August 2020*

	Hospital			Nursing home		
Characteristic	No.	Seropositive, no.	Seropositive, % (95% CI)	No.	Seropositive, no.	Seropositive, % (95% CI)
Aerosol-generating procedure frequency						
0 times per shift per week	4,121	108	2.6 (2.2–3.2)	858	93	10.8 (8.8–13.1)
1–5 times	1,679	62	3.7 (2.8–4.7)	114	25	21.9 (14.7–30.7)
6–10 times	380	22	5.8 (3.7–8.6)	36	7	19.4 (8.2–36.0)
11–25 times	277	11	4.0 (2.0–7.0)	23	4	17.4 (5.0–38.8)
>25 times	366	19	5.2 (3.2–8.0)	41	12	29.3 (16.1–45.5)
NA	1,546	34	2.2 (1.5–3.1)	422	55	13.0 (10.0–16.6)
PPE use						
Never use PPE	2,939	64	2.2 (1.7–2.8)	322	19	5.9 (3.6–9.1)
Used PPE and reported frequency of needing complete PPE						
Daily	1,809	66	3.7 (2.8–4.6)	632	125	19.8 (16.7–23.1)
Few times a week	1,860	75	4.0 (3.2–5.0)	332	42	12.7 (9.3–16.7)
Less than once a week	1,761	51	2.9 (2.2–3.8)	208	10	4.8 (2.3–8.7)
Use of PPE shortage protocol						
No shortage	511	25	4.9 (3.2–7.1)	238	28	11.8 (8.0–16.6)
Reuse	934	21	2.3 (1.4–3.4)	186	21	11.3 (7.1–16.7)
Extended use	1,341	42	3.1 (2.3–4.2)	253	45	17.8 (13.3–23.1)
Extended and reuse	2,644	104	3.9 (3.2–4.8)	495	83	16.8 (13.6–20.4)
Donning/doffing training in past year						
Yes	5,140	184	3.6 (3.1–4.1)	1,135	170	15.0 (13.0–17.2)
No	199	5	2.5 (0.8–5.8)	15	3	20.0 (4.3–48.1)
Don't know	91	3	3.3 (0.7–9.3)	22	4	18.2 (5.2–40.3)

*Significant linear trend of seropositivity with rising frequency of aerosol-generating procedures and decreasing frequency of needing complete PPE for hospital and nursing home settings (p<0.001 for all). NA, not applicable; PPE, personal protective equipment; SARS-CoV-2, severe acute respiratory syndrome coronavirus 2.

2020, all 85 Rhode Island nursing homes had reported ≥1 COVID-19 cases; weekly counts of new cases were approximately equal for nursing home residents and staff, at ≈185 each as of November 25, 2020, according to RIDOH SARS-CoV-2 surveillance. Nursing homes have been deemed tinderboxes because of a constellation of factors that may perpetuate transmission, including resident populations with risk factors for severe COVID-19 and prolonged viral shedding, residents who may be asymptomatic or have nonspecific symptoms of infection (e.g., increased confusion), shared caretakers between patients, chronic staffing shortages that may be exacerbated by worker illness, and lack of testing and PPE (*10*,*12*,*20*–*22*). In addition, suboptimal infection control practices have been noted in direct observation studies of nursing home personnel (*23*).

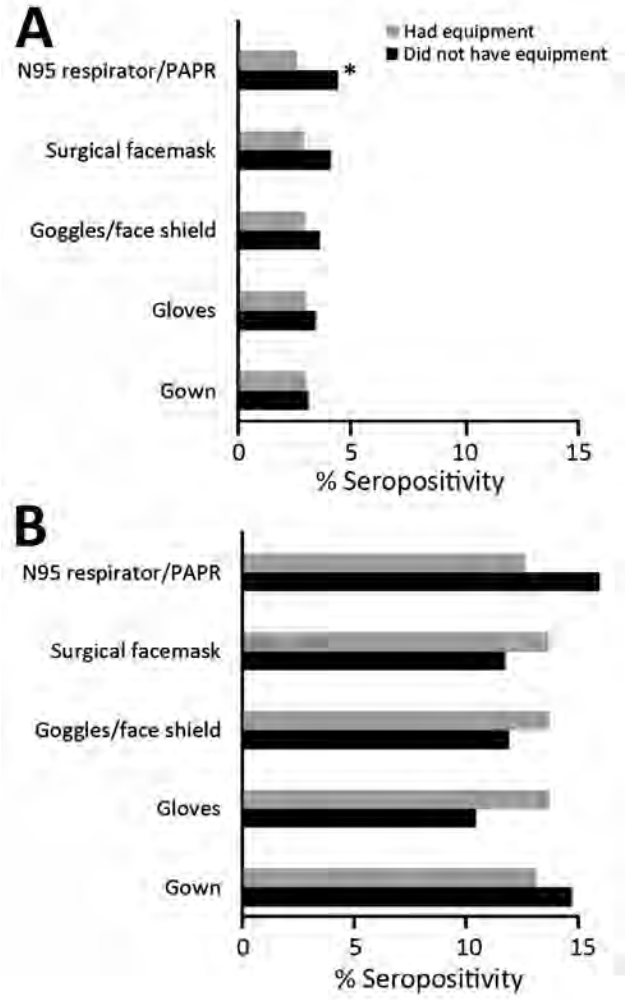

Figure 3. Seropositivity for severe acute respiratory syndrome coronavirus 2 among hospital and nursing home personnel, by having/not having specific PPE, Rhode Island, USA, July–August 2020. Excludes participants who reported no PPE use (19.6% of those in hospital settings, seropositivity 3.4%; 12.4% of those in nursing home settings, seropositivity 12.4%). Asterisk (*) indicates statistically significant difference ($p<0.05$ by χ^2 test). PPE, personal protective equipment.

We found patterns among hospital and nursing home personnel that suggest both community- and workplace-acquired infection. In both settings, contact with a COVID-19–positive household member was the strongest risk factor for seropositivity. Adjusted odds ratios for seropositivity by age group and race/ethnicity reflected community patterns (*24*–*26*) among hospital personnel but not among nursing home personnel. Other studies have found that seroprevalence was correlated with local cumulative COVID-19 incidence in general (*12*,*13*,*18*). Workplace transmission is suggested by higher likelihood of seropositivity among occupations with frequent and prolonged patient contact or working in common areas: nurses and receptionists/medical assistants in hospital settings and nurse assistants and social workers/case managers in nursing homes. Similar findings were noted in other studies (*2*,*18*,*27*). In hospitals, interaction with patients and community members was associated with higher seropositivity than was having no interaction as part of work responsibilities. Finally, in agreement with results from other hospital studies, our study found lower seropositivity among personnel in a controlled environment: hospital surgical units (*5*,*18*). However, in nursing homes, workplace factors appeared to dominate community factors given the elevated risk across occupation and seroprevalence >4 times greater than community levels (2.8%). Intrafacility transmission was found in a study of 2 skilled nursing facilities in which viral strains within each facility were genetically more similar than between the 2 facilities or the community; within 1 facility, there were 2 genetically distinct strains, which suggested community introduction into the facility followed by intrafacility transmission (*27*). That is, this group of studies suggest that community introduction into nursing homes may result in higher level of intrafacility transmission compared with hospital settings.

In at least 2 ways, the higher seroprevalence among nursing home COVID-19 unit personnel could have been partially driven by cohorting residents. First, even if the probability of transmission in facilities were equal, a higher percentage of infectious patients and residents in COVID-19 units would result in a greater number of transmitted infections. Second, if previously infected staff were assigned to COVID-19 units, seroprevalence among facility staff would be increased through staffing decisions rather than transmission. Without longitudinal or genotyping data, it is not possible to disentangle

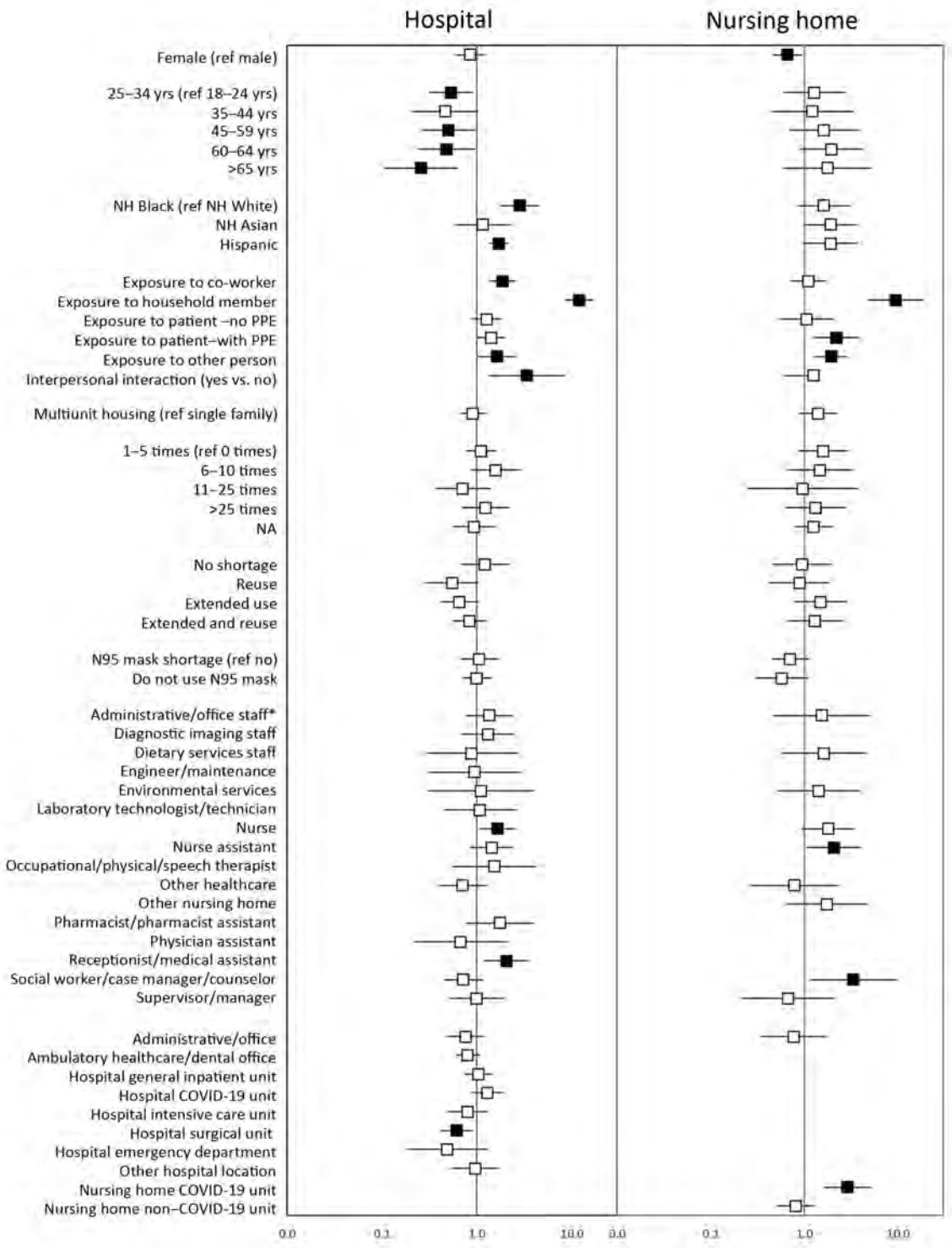

Figure 4. Adjusted odds ratios and 95% CIs for seropositivity, Rhode Island, USA, July–August 2020. The adjusted models were estimated using generalized estimating equations including all variables shown. Error bars indicate 95% CIs; black boxes denote adjusted odds ratios for which the 95% CI excludes 1.0. Workplace was represented by non–mutually exclusive dummy variables entered simultaneously into the model; the referent group for each workplace is not working in that specific workplace. Participants in workplaces with sample size <30 or with 0% seropositivity were included in the model but the workplace was not entered into the model. *For the hospital model, physicians were the referent occupation group. For the nursing home model, occupational/physical/speech therapists were the referent occupation group. Ref, referent; NH, non-Hispanic; PPE, personal protective equipment.

intrafacility transmission. Staff in Rhode Island were rarely transferred between facilities according to past infection status. Two facilities designated as COVID-19 facilities accepted infected residents, and the other 54 facilities cohorted patients within the facility or transferred residents to other facilities with COVID-19 units. No data were gathered on staff transfers within facilities between COVID-19 and non–COVID-19 units. Despite these gaps in fully understanding transmission, seroprevalence was still greatly elevated in nursing homes compared with hospitals among both COVID-19 and non–COVID-19 unit personnel.

Unadjusted analyses showed that those with daily requirements for complete PPE were more likely to be seropositive for both groups. However, there were no significant adjusted associations between seropositivity and frequency of requirement for complete PPE or PPE shortage protocol use. These findings suggest that PPE use was likely a marker for increased occupational risk (i.e., frequent close contact with infected patients or residents) and that personnel with the most frequent or intense patient contact may have received priority for PPE supplies or that PPE shortages did not have a major role in transmission in this study. More detailed studies are necessary to disentangle the complex factors surrounding PPE use.

Limitations include the cross-sectional study design. Patient or resident infection status was not ascertained. Infection timing relative to different exposures is unknown. For example, it is unknown whether participants who reported exposure to a COVID-19 positive household member were infected by that contact or introduced the infection into the household. Similarly, among seropositive participants who reported working in >1 workplace, it is not possible to ascertain their contribution, if any, to transmission between facilities. Furthermore, seroprevalence is a cumulative measure; antibody responses are reported to persist for ≥4 months (*28*). The extent to which seroprevalence was related to exposures early in the pandemic, when PPE shortages were more acute and infection control measures were still being developed, is unknown. Participation was voluntary among a convenience sample, so representativeness of the population is unknown. However, 56 of 85 nursing homes in Rhode Island were included and seropositivity among nursing home participants was related to resident and staff case counts in facilities, with higher seropositivity with rising quartile of case counts (Appendix Table 4). No information was collected about other possible exposures, such as travel and commuting (e.g., use of public transportation). In addition, there could be uncontrolled confounding, including factors related to other socioeconomic factors, such as less flexibility for household members to telework or otherwise reduce occupational exposures. Strengths included a large sample size that allowed stable estimates among subgroups.

This study highlights the increased risk among nursing home personnel for SARS-CoV-2 infection compared with hospital personnel. Although this study was not designed to pinpoint mechanisms underlying the higher seroprevalence among nursing home personnel, 2 patterns strongly suggest that additional workplace protections may mitigate risk in this setting: the elevated risk among all nursing home occupations compared with hospital counterparts and the weaker signals of community transmission among nursing home settings (i.e., no association between age group and race/ethnicity with seropositivity). Continued attention to adherence with current infection control recommendations (e.g., PPE use, handwashing) and ensuring adequate testing, equipment, training, and staffing are the foundations for bolstering the safety of nursing home personnel (*22*,*23*,*29*).

Acknowledgments

The authors thank members of the Quest Diagnostics team: Max Agbasi, Linda Dark, Travis Dick, Kris Irons, Rebecca Hunt, Brian Jaffa, Michael Kraky, Kathryn Logan, Rebecca Parsons, Amy Paolo, Sahana Ramprasad, Todd Raymond, Sean Spooner, Jeremy Stein, Dianna Tate, and Clare Wahl. The authors also thank Preetha Kutty and Matthey Stuckey for assistance with the study questionnaire and CDC's National Institute for Occupational Safety and Health Occupational Data Collection and Coding Support and Consultation Teams for their assistance with occupation and workplace classification: Pam Schumacher, Jennifer Cornell, Jeff Purdin, Matthew Groenewold, Sara Luckhaupt, Stacey Marovich, Matt Hirst, Liz Smith, Surprese Watts, Rebecca Purdin, Marie De Perio, Sherry Burrer, Laura Reynolds, and George (Reed) Grimes. The authors also thank members of the CDC Data Collation and Integration for Public Health Event Responses (DCIPHER) team (Center for Preparedness and Response, National Center for Environmental Health, CDC) for their assistance in providing secure data transfer and storage: Stephen Sorokin, Nathan Golightly, Sachin Agnihotri, and Serena Burdyshaw. Finally, the authors are grateful to Bonnie LaFleur for her statistical advice and Brian Lein for assistance with survey planning and initial implementation.

Data and specimen collection activities and specimen testing were funded by US Health and Human Services (contract no. 75P00120C00036).

About the Author

Dr. Akinbami is a pediatrician and epidemiologist with the Division of Health and Nutrition Examination Surveys National Center for Health Statistics, CDS. She and her colleagues have undertaken the current research while deployed to support the federal COVID-19 response.

References

1. Nguyen LH, Drew DA, Graham MS, Joshi AD, Guo C-G, Ma W, et al. Risk of COVID-19 among front-line health-care workers and the general community: a prospective cohort study. Lancet Public Health. 2020;5:e475–83. https://doi.org/10.1016/S2468-2667(20)30164-X
2. Hughes MM, Groenewold MR, Lessem SE, Xu K, Ussery EN, Wiegand RE, et al. Update: characteristics of health care personnel with COVID-19—United States, February 12–July 16, 2020. MMWR Morb Mortal Wkly Rep. 2020;69:1364–8. https://doi.org/10.15585/mmwr.mm6938a3
3. Chou R, Dana T, Buckley DI, Selph S, Fu R, Totten AM. Epidemiology of and risk factors for coronavirus infection in health care workers: a living rapid review. Ann Intern Med. 2020;173:120–36. https://doi.org/10.7326/M20-1632
4. Rebmann T, Vassallo A, Holdsworth JE. Availability of personal protective equipment and infection prevention supplies during the first month of the COVID-19 pandemic: a national study by the APIC COVID-19 task force. Am J Infect Control. 2020 Aug 26 [Epub ahead of print]. https://doi.org/10.1016/j.ajic.2020.08.029
5. Grant JJ, Wilmore SMS, McCann NS, Donnelly O, Lai RWL, Kinsella MJ, et al. Seroprevalence of SARS-CoV-2 antibodies in healthcare workers at a London NHS Trust. Infect Control Hosp Epidemiol. 2020 Aug 4 [Epub ahead of print]. https://doi.org/10.1017/ice.2020.402
6. Barnett ML, Grabowski DC. Nursing homes are ground zero for COVID-19 pandemic. JAMA Health Forum: JAMA, 2020: Insights: COVID-19 [cited 2020 Sep 30]. https://jamanetwork.com/channels/health-forum/fullarticle/2763666?utm_campaign=articlePDF%26utm_medium=articlePDFlink%26utm_source=articlePDF%26utm_content=jama.2020.10419
7. New York Times. About 40% of US coronavirus deaths are linked to nursing homes. 2020 July 8 [cited 2020 Oct 4]. https://www.nytimes.com/interactive/2020/us/coronavirus-nursing-homes.html
8. McGarry BE, Grabowski DC, Barnett ML. Severe staffing and personal protective equipment shortages faced by nursing homes during the COVID-19 pandemic. Health Aff (Millwood). 2020:39:1812–21. https://doi.org/10.1377/hlthaff.2020.01269
9. Lansbury LE, Brown CS, Nguyen-Van-Tam JS. Influenza in long-term care facilities. Influenza Other Respir Viruses. 2017;11:356–66. https://doi.org/10.1111/irv.12464
10. Kimball A, Hatfield KM, Arons M, James A, Taylor J, Spicer K, et al. Asymptomatic and presymptomatic SARS-CoV-2 infections in residents of a long-term care skilled nursing facility—King County, Washington, March 2020. MMWR Morb Mortal Wkly Rep. 2020;69:377–81. https://doi.org/10.15585/mmwr.mm6913e1
11. Li TZ, Cao ZH, Chen Y, Cai M-T, Zhang L-Y, Xu H, et al. Duration of SARS-CoV-2 RNA shedding and factors associated with prolonged viral shedding in patients with COVID-19. J Med Virol. 2020 Jul 9 [Epub ahead of print]. https://doi.org/10.1002/jmv.26280
12. Gorges RJ, Konetzka RT. Staffing levels and COVID-19 cases and outbreaks in U.S. nursing homes. J Am Geriatr Soc. 2020;68:2462–6. https://doi.org/10.1111/jgs.16787
13. Self WH, Tenforde MW, Stubblefield WB, Feldstein LR, Steingrub JS, Shapiro NI, et al. Seroprevalence of SARS-CoV-2 among frontline health care personnel in a multistate hospital network—13 academic medical centers, April–June 2020. MMWR Morb Mortal Wkly Rep. 2020;69:1221–6. https://doi.org/10.15585/mmwr.mm6935e2
14. Health RIDo. Rhode Island COVID-19 Response Data. 2020 [cited 2020 Nov 25]. https://ri-department-of-health-covid-19-data-rihealth.hub.arcgis.com
15. US Department of Health and Human Services. Title 45 Code of Federal Regulations 46, Protection of human subjects [cited 2020 Sep 30]. https://www.ecfr.gov/cgi-bin/text-idx?m=08&d=16&y=2020&cd=20200813&submit=GO&SID=83cd09e1c0f5c6937cd9d7513160fc3f&node=pt45.1.46&pd=20180719
16. US Food and Drug Administration. EUA authorized serology test performance [cited 2020 Jul 30]. https://www.fda.gov/medical-devices/emergency-situations-medical-devices/eua-authorized-serology-test-performance
17. Parker JD, Talih M, Malec DJ, Beresovsky V, Carroll M, Gonzalez JF, et al. Presentation standards for proportions. Washington (DC): Centers for Disease Control and Prevention, National Center for Health Statistics; 2017.
18. Akinbami LJ, Vuong N, Petersen LR, Sami S, Patel A, Lukacs SL, et al. SARS-CoV-2 seroprevalence among healthcare, first response, and public safety personnel, Detroit metropolitan area, Michigan, USA, May–June 2020. Emerg Infect Dis. 2020;26:2863–71. https://doi.org/10.3201/eid2612.203764
19. Centers for Disease Control and Prevention. CDC COVID Data Tracker: Nationwide Commercial Laboratory Seroprevalence Survey; 2020 [cited 2020 Oct 10]. https://covid.cdc.gov/covid-data-tracker/#national-lab
20. Ouslander JG, Grabowski DC. COVID-19 in nursing homes: calming the perfect storm. J Am Geriatr Soc. 2020;68:2153–62. https://doi.org/10.1111/jgs.16784
21. Arons MM, Hatfield KM, Reddy SC, Kimball A, James A, Jacobs JR, et al. Presymptomatic SARS-CoV-2 infections and transmission in a skilled nursing facility. N Engl J Med. 2020;382:2081–90. https://doi.org/10.1056/NEJMoa2008457
22. Kim JJ, Coffey KC, Morgan DJ, Roghmann MC. Lessons learned—outbreaks of COVID-19 in nursing homes. Am J Infect Control. 2020;48:1279–80. https://doi.org/10.1016/j.ajic.2020.07.028
23. Pineles L, Petruccelli C, Perencevich EN, Roghmann M-C, Gupta K, Cadena J, et al. The impact of isolation on healthcare worker contact and compliance with infection control practices in nursing homes. Infect Control Hosp Epidemiol. 2018;39:683–7. https://doi.org/10.1017/ice.2018.50
24. Boehmer TK, DeVies J, Caruso E, van Santen KL, Tang S, Black CL, et al. Changing age distribution of the COVID-19 pandemic—United States, May–August 2020. MMWR Morb Mortal Wkly Rep. 2020;69:1404–9. https://doi.org/10.15585/mmwr.mm6939e1
25. Centers for Disease Control and Prevention. COVID-19 hospitalization and death by race/ethnicity; 2020 [cited 2020 Oct 9]. https://www.cdc.gov/coronavirus/2019-ncov/

covid-data/investigations-discovery/hospitalization-death-by-race-ethnicity.html
26. Centers for Disease Control and Prevention. CDC COVID data tracker: United States COVID-19 casess and deaths by state; 2020 [cited 2020 Oct 4]. https://covid.cdc.gov/covid-data-tracker/#cases_casesper100k
27. Taylor J, Carter RJ, Lehnertz N, Kazazian L, Sullivan M, Wang X, et al. Serial testing for SARS-CoV-2 and virus whole genome sequencing inform infection risk at two skilled nursing facilities with COVID-19 outbreaks—Minnesota, April–June 2020. MMWR Morb Mortal Wkly Rep. 2020;69:1288–95. https://doi.org/10.15585/mmwr.mm6937a3
28. Gudbjartsson DF, Norddahl GL, Melsted P, Gunnarsdottir K, Holm H, Eythorsson E, et al. Humoral immuner to SARS-CoV-2 in Iceland. N Engl J Med. 2020;383:1724–34. https://doi.org/10.1056/NEJMoa2026116
29. Centers for Disease Control and Prevention. Healthcare workers: preparing for COVID-19 in nursing homes; 2020 [cited 2020 Oct 5]. https://www.cdc.gov/coronavirus/2019-ncov/hcp/long-term-care.htm.

Address for correspondence: Lara Akinbami, Centers for Disease Control and Prevention, 3311 Toledo Rd, Hyattsville, MD 20782, USA; email: lea8@cdc.gov

March 2020

Mycobacteria

- Clinical Characteristics of Disseminated Strongyloidiasis, Japan, 1975–2017
- Epidemiology of Cryptosporidiosis, New York City, New York, USA, 1995–2018
- Public Health Response to Tuberculosis Outbreak among Persons Experiencing Homelessness, Minneapolis, Minnesota, USA, 2017–2018
- *Mycobacterium tuberculosis* Complex Lineage 3 as Causative Agent of Pulmonary Tuberculosis, Eastern Sudan
- Norovirus Outbreak Surveillance, China, 2016–2018
- Methicillin-Resistant *Staphylococcus aureus* Bloodstream Infections and Injection Drug Use, Tennessee, USA, 2015–2017
- Randomized Trial of 2 Schedules of Meningococcal B Vaccine in Adolescents and Young Adults, Canada
- Human Immune Responses to Melioidosis and Cross-Reactivity to Low-Virulence Burkholderia Species, Thailand
- Multidrug- and Extensively Drug-Resistant *Mycobacterium tuberculosis* Beijing Clades, Ukraine, 2015
- Stable and Local Reservoirs of *Mycobacterium ulcerans* Inferred from the Nonrandom Distribution of Bacterial Genotypes, Benin
- US Tuberculosis Rates among Persons Born Outside the United States Compared with Rates in Their Countries of Birth, 2012–2016

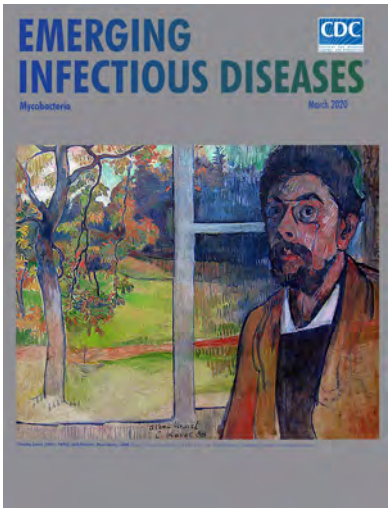

- Genomic and Phenotypic Variability in *Neisseria gonorrhoeae* Antimicrobial Susceptibility, England
- High Prevalence of and Risk Factors for Latent Tuberculosis Infection among Prisoners, Tianjin, China
- Whole-Genome Sequencing to Detect Numerous *Campylobacter jejuni* Outbreaks and Match Patient Isolates to Sources, Denmark, 2015–2017
- Pregnancy Outcomes among Women Receiving rVSVΔ-ZEBOV-GP Ebola Vaccine during the Sierra Leone Trial to Introduce a Vaccine against Ebola [
- Acquisition of Plasmid with Carbapenem-Resistance Gene bla_{KPC2} in Hypervirulent *Klebsiella pneumoniae*, Singapore
- Long-Term Rodent Surveillance after Outbreak of Hantavirus Infection, Yosemite National Park, California, USA, 2012
- *Mycobacterium tuberculosis* Beijing Lineage and Risk for Tuberculosis in Child Household Contacts, Peru
- Risk Factors for Complicated Lymphadenitis Caused by Nontuberculous Mycobacteria in Children
- Human Exposure to Hantaviruses Associated with Rodents of the Murinae Subfamily, Madagascar
- Avian Influenza Virus Detection Rates in Poultry and Environment at Live Poultry Markets, Guangdong, China
- Diphtheria Outbreaks in Schools in Central Highland Districts, Vietnam, 2015–2018
- Progressive Vaccinia Acquired through Zoonotic Transmission in a Patient with HIV/AIDS, Colombia
- Suspected Locally Acquired Coccidioidomycosis in Human, Spokane, Washington, USA
- *Mycobacterium senegalense* Infection after Implant-Based Breast Reconstruction, Spain
- Role of Live-Duck Movement Networks in Transmission of Avian Influenza, France, 2016–2017
- Low Prevalence of *Mycobacterium bovis* in Tuberculosis Patients, Ethiopia
- Metagenomics of Imported Multidrug-Resistant *Mycobacterium leprae*, Saudi Arabia, 2017

EMERGING INFECTIOUS DISEASES

To revisit the March 2020 issue, go to:
https://wwwnc.cdc.gov/eid/articles/issue/26/3/table-of-contents

Population-Based Geospatial and Molecular Epidemiologic Study of Tuberculosis Transmission Dynamics, Botswana, 2012–2016

Nicola M. Zetola, Patrick K. Moonan, Eleanor Click, John E. Oeltmann, Joyce Basotli, Xiao-Jun Wen, Rosanna Boyd, James L. Tobias, Alyssa Finlay,[1] Chawangwa Modongo[1]

Tuberculosis (TB) elimination requires interrupting transmission of *Mycobacterium tuberculosis*. We used a multidisciplinary approach to describe TB transmission in 2 sociodemographically distinct districts in Botswana (Kopanyo Study). During August 2012–March 2016, all patients who had TB were enrolled, their sputum samples were cultured, and *M. tuberculosis* isolates were genotyped by using 24-locus mycobacterial interspersed repetitive units–variable number of tandem repeats. Of 5,515 TB patients, 4,331 (79%) were enrolled. Annualized TB incidence varied by geography (range 66–1,140 TB patients/100,000 persons). A total of 1,796 patient isolates had valid genotyping results and residential geocoordinates; 780 (41%) patients were involved in a localized TB transmission event. Residence in areas with a high burden of TB, age <24 years, being a current smoker, and unemployment were factors associated with localized transmission events. Patients with known HIV-positive status had lower odds of being involved in localized transmission.

Tuberculosis (TB) was declared a public health emergency by the World Health Assembly in 2014, and the development of an ambitious global strategy to eliminate TB by 2035 soon followed (*1*,*2*). Five years later, progress toward elimination remains slow (*3*), in part because of the lack of effective interventions to interrupt the cycle of TB transmission (*4*). Ongoing transmission is the main driver of TB prevalence in high-burden communities (*5*,*6*). Historically, TB was believed to be the result of prolonged exposure to infectious TB patients, such as household contacts (*7*). More recently, molecular epidemiologic studies highlighted the possible role of casual exposures in the community (*8*,*9*). TB incidence and rates of TB transmission vary considerably across communities and might be dependent on high-risk behaviors, social determinates of disease (e.g., malnutrition, overcrowding, poverty), population dynamics, and transmission venues (*10*–*12*). Accordingly, interest has been renewed in increasing yield and cost-effectiveness of geographically targeted interventions.

Incremental progress toward elimination is possible with careful evidence-guided policy development, planning, and implementation. The design of effective, targeted TB interventions should be tailored to local epidemiology and program performance. In this population-based study, named the Kopanyo Study, we used a multidisciplinary approach combining classic epidemiologic approaches (i.e., relying on the behavioral, clinical, demographical, geospatial, social, and temporal characteristics of cases) with mycobacterial genetics to describe TB transmission in 2 large districts in Botswana.

Methods

Study Objective and Design

Kopanyo means "people gathering together" in the local Tswana language in Botswana. Consistent with this name, the overarching goal of the Kopanyo Study was to use geospatial analysis and patient interviews to define TB transmission networks and locations of TB transmission in 2 districts in Botswana, a country characterized by high rates of TB and HIV. More precisely, we aimed to describe and compare the clinical and microbiological characteristics of TB patients given a diagnosis in Gaborone and Ghanzi districts; describe and compare the spatial clustering and genotype clustering of patients and strains across and within districts; and determine the factors associated

Author affiliations: University of Pennsylvania Partnership, Philadelphia, Pennsylvania, USA (N.M. Zetola, C. Modongo); Centers for Disease Control and Prevention, Atlanta, Georgia, USA (P.K. Moonan, E. Click, J.E. Oeltmann, J. Basotli, X.-J. Wen, R. Boyd, J.L. Tobias, A. Finlay)

DOI: https://doi.org/10.3201/eid2703.203840

[1]These senior authors contributed equally to this article.

with genotype clustering, spatial clustering, as well as combined genotype and spatial clustering across and within districts. The design and procedures of this population-based, prospective study have been described in detail elsewhere (*8*,*13*).

Setting

Botswana is an economically and politically stable sub-Saharan country that has a universal healthcare system for its citizens. We recruited participants from 2 distinct geographic areas: the capital city and surrounding suburbs, Gaborone district; and the rural district of Ghanzi (Figure 1). The study sites were purposefully selected because they were believed to represent disparate populations in Botswana in terms of demographic, environmental, epidemiologic (i.e., HIV prevalence, TB prevalence) and socioeconomic characteristics. With a population of 354,380 persons, Gaborone is the largest and most crowded urban area in the country. In 2013, at the start of this study, 17% of the general population in Gaborone was estimated to be living with HIV (*14*). Annual TB rates in Gaborone ranged from 440 to 470 cases/100,000 population during the 5 years before study implementation; ≈70% of TB patients were co-infected with HIV (*15*).

In contrast, Ghanzi is a rural district in northwestern Botswana, and most of the 44,100 persons in this district live in congregate housing; the town of Ghanzi has

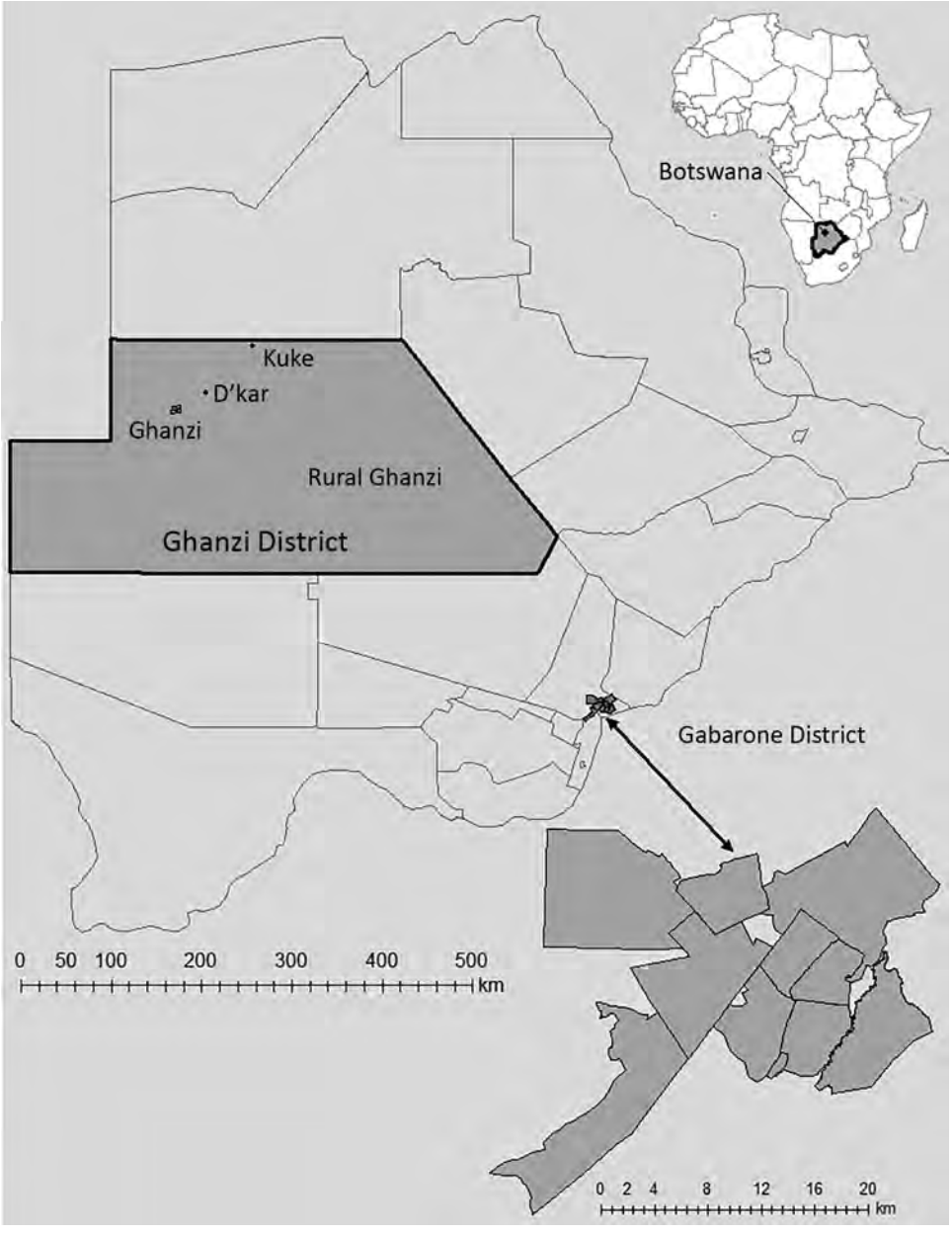

Figure 1. Catchment areas for population-based geospatial and molecular epidemiologic study of tuberculosis transmission dynamics, Botswana, 2012–2016 (Kopanyo Study). The 2 catchment areas are outlined in black. The neighborhoods within the Gaborone district (A–K, enlarged at bottom right) and Ghanzi district (W, DK, KU, and Y) are shown in gray. Inset map shows location of Botswana in Africa.

a population of 12,179 persons. Most of the population in the district is of San ethnicity. The San kept a traditionally hunter-gatherer lifestyle until early 1990s, when they were forced to transition to farming as a result of government-mandated modernization programs. Since then, most San live in large and crowded private freehold farms most of the year. For short periods during the year (ranging from days to several weeks), they transition through mid-size villages and the town of Ghanzi. Migration between farms and villages in the district is the norm and it is seasonal. However, because of cultural and geographic reasons there is little migration outside the district. Thus, despite major rotational migration between villages and farms, the community remains highly insular. Altogether, these unique cultural and social conditions contribute to the higher rates of TB transmission in Ghanzi. Over the past 2 decades, the TB notification rate in Ghanzi district has consistently been the highest in the country (722 cases/100,000 persons) (*14*,*15*). In 2013, the proportion of the general population in Ghanzi estimated to be living with HIV (17%) was similar to that for Gaborone; however, only 36% of TB patients are co-infected with HIV (*14*).

Recruitment

Participants were enrolled during August 2012–March 2016. All patients given a diagnosis of TB were eligible for enrollment. Participants were recruited from TB clinics and directly observed treatment centers in greater Gaborone (n = 24) and Ghanzi District (n = 6). Patients receiving TB treatment for ≥14 days before study screening, incarcerated persons, or those who did not consent were excluded from the study.

Data Sources, Measurements, and Variables

Behavioral, clinical, and demographic information were obtained by medical record abstraction and standardized interview at enrollment. Primary residential address, work place address at diagnosis, and address of social gathering venues of patients were obtained through patient interview. All addresses were verified by site visit geotagging, or through a reference layer created by manually relocating addresses in satellite imagery by using OpenStreetMap (http://www.openstreetmap.org) (*16*), Google Maps, and ArcGIS (Environmental System Research Institute, https://www.esri.com) online geocoding services. WGS 84 projection system latitude and longitude coordinates (with 1.1-m precision) were exported for each address. Botswana population and housing data was used to define geographic boundaries and enumerate localized populations necessary for TB incidence rates (*17*). We defined high-burden geographic areas if the estimated annualized TB incidence was >305 TB patients/100,000 persons, which is the estimated national TB incidence rate at the start of the study period.

HIV status was determined for all enrolled participants. Following national guidelines, we offered HIV testing to all participants who did not have documented HIV test results or had negative test results from >12 months before enrollment. Patients were asked to report the average number of alcoholic beverages consumed on the same occasion in the previous 30 days, the number of days consuming alcohol in the previous 30 days, and if they currently smoke tobacco. We defined excessive alcohol consumption as a self-report of >5 drinks on the same occasion or drinking on >5 days within the previous 30 days (*18*). Venues for social gathering were classified as alcohol-related (e.g., bars, liquor stores, pubs, shebeens), places of work, places of worship (e.g., churches, mosques, temples), and healthcare facilities.

Sputa Collection and Laboratory Methods

At least 1 expectorated sputum sample was obtained from each enrolled patient. Patients unable to produce enough sputum or high-quality sputum underwent inhaled nebulized hypertonic saline solution induction. Sputa were decontaminated by using the N-acetyl-L-cysteine and NaOH method with a final concentration of 1% NaOH, and then inoculated into 1 Mycobacterial Growth Indicator Tube (MGIT; Becton Dickinson, https://www.bd.com). MGIT cultures were incubated at 35°C–37°C in the MGIT960 instrument (Becton Dickinson) for ≤6 weeks. MGIT cultures scored as positive were examined by microscopy and Ziehl-Neelsen staining to identify acid-fast bacilli. SD. The Bioline TB Ag MPT64 Rapid Test (Abbott, https://www.globalpointofcare.abbott/en/product-details/sd-bioline-tb-ag-mpt64-rapid.html) was used to identify the *M. tuberculosis* complex. Cultures positive for acid-fast bacilli but with negative TB Ag MPT64 results were classified as nontuberculous mycobacteria. Cultures with evidence of both *Mycobacterium* species and other potential contaminating species were redecontaminated by using the standard method described above. Drug susceptibility testing (DST) for first-line anti-TB drugs was performed by using MGIT DST. Susceptibility was set at 0.1 μg/mL for isoniazid and 1.0 μg/mL for rifampin. We used DST with Lowenstein-Jensen medium in instances for which MGIT DST results were not available.

M. tuberculosis Genotyping

The first culture isolate per patient was genotyped (Genoscreen, https://www.genoscreen.fr) by using

24-locus mycobacterial interspersed repetitive units–variable number of tandem repeats (MIRU-VNTR) and standardized methods (*19*). MIRU-VNTR results with >1 copy number at ≥1 loci (i.e., double alleles) as seen with mixtures of different clonal subpopulations, or with missing or indeterminate copy number at any locus, were considered noninterpretable for cluster assignment and were excluded from analysis (*20*). Two or more patient isolates that had valid, complete, and matching MIRU results were classified as a genotype cluster.

Localized Transmission Events

We used SaTScan (https://www.satscan.org) to identify geographic areas with a larger-than-expected rate of unique genotype clusters. We also used data for all other culture-positive TB patients reported during the study as the background rate (*20*–*22*). In brief, all individual MIRU-VNTR results were assigned to the corresponding geocoordinates of the patient's residence. Each unique MIRU-VNTR result was then scanned separately, applying a purely spatial analysis, in which the number of events in an area was assumed to be Poisson distributed to generate circular zones of various sizes up to a maximum radius of 50 km. A log-likelihood ratio was calculated for each zone in comparison with all possible zones, with the maximum likelihood ratio representing the zone most likely to identify statistically significant spatial concentrations for each MIRU-VNTR result. Thus, by definition, localized transmission was characterized by genotypic and spatial clustering. A Monte Carlo simulation with 9,999 repetitions was used to determine the distribution of the scan statistic under the null hypothesis of spatial randomness; significant spatial clusters were chosen by using an α of $p<0.05$. No duplicative case counting occurred. The purpose of the spatial scan was to characterize each patient (based on residence) for a dichotomous outcome: member of a localized transmission event or not.

Statistical Methods

Annualized TB incidence per 100,000 persons and 95% CIs, assuming a Poisson distribution, were calculated for local geographies on the basis of the number of cases enrolled from each geography divided by the population estimates for each geography annualized to the duration of the study period. Estimates were assigned to the geographic centroid in ArcGIS. Isopleth cartographic images were produced by using a raster layer interpolated with inverse distance weighting (*21*). Differences in proportions between behavioral, clinical, and demographic variables by geographic location were assessed by using the χ^2 test. Multivariable logistic regression analysis was conducted to assess the association of involvement in a localized transmission event (coded as a binary yes/no variable) and select variables by using adjusted odds ratios (aORs) that were significant at the 95% CIs. All variables statistically associated with the main outcome in bivariable analyses ($p\leq0.1$) were included in the multivariate model.

Ethics

This study was approved by the Centers for Disease Control and Prevention Institutional Review Board; the Health Research and Development Committee, Ministry of Health and Wellness, Botswana; and the University of Pennsylvania Institutional Review Boards. Participants provided written informed consent.

Results

Patient Characteristics

A total of 5,515 patients were given a diagnosis of TB during the study period; 4,331 (79%) were enrolled (Figure 2). Primary residence was geocoded and validated for 3,736 (86%) participants. Of these participants, 2,659 (71%) resided in Gaborone District, 723 (19%) resided in Ghanzi District, and 354 (10%) resided in other locations outside Gaborone or Ghanzi Districts. There were no significant differences in proportions with regards to sex ($p = 0.116$) and having valid MIRU results ($p = 0.555$) between the 3 locations (Table 1). However, there were differences in proportions for Gaborone, Ghanzi District, and other locations, respectively, regarding age ($p<0.001$), residence in a high-burden neighborhood (14% vs. 73% vs. 0%; $p<0.001$), excessive alcohol use (25% vs. 32% vs. 14%; $p<0.001$), current smoking (20% vs. 43% vs. 13%; $p<0.001$), unemployment (30% vs. 67% vs. 58%; $p<0.001$) history of incarceration (5% vs. 8% vs. 5%; $p = 0.007$), positive HIV status (66% vs. 37% vs. 64%; $p<0.001$), culture-positive TB (68% vs. 78% vs. 48%; $p<0.001$), and MDR TB at baseline (1% vs. 2 vs. 6%; $p<0.001$) (Table 1).

Geographic Distribution of TB

The estimated annualized TB incidence for the overall study population was 306 TB patients/100,000 persons (95% CI 228–339) (Table 2). The incidence rate varied considerably by geography, ranging from 66 (95% CI 44–99) TB patients/100,000 persons in the suburban areas of Gaborone to 1,140 (95% 836–1,556) TB patients/100,000 persons in remote, rural villages of the Ghanzi District. The degree of heterogeneity was more pronounced in Gaborone than in Ghanzi District. For example, a 7.3-fold difference in annualized incidence

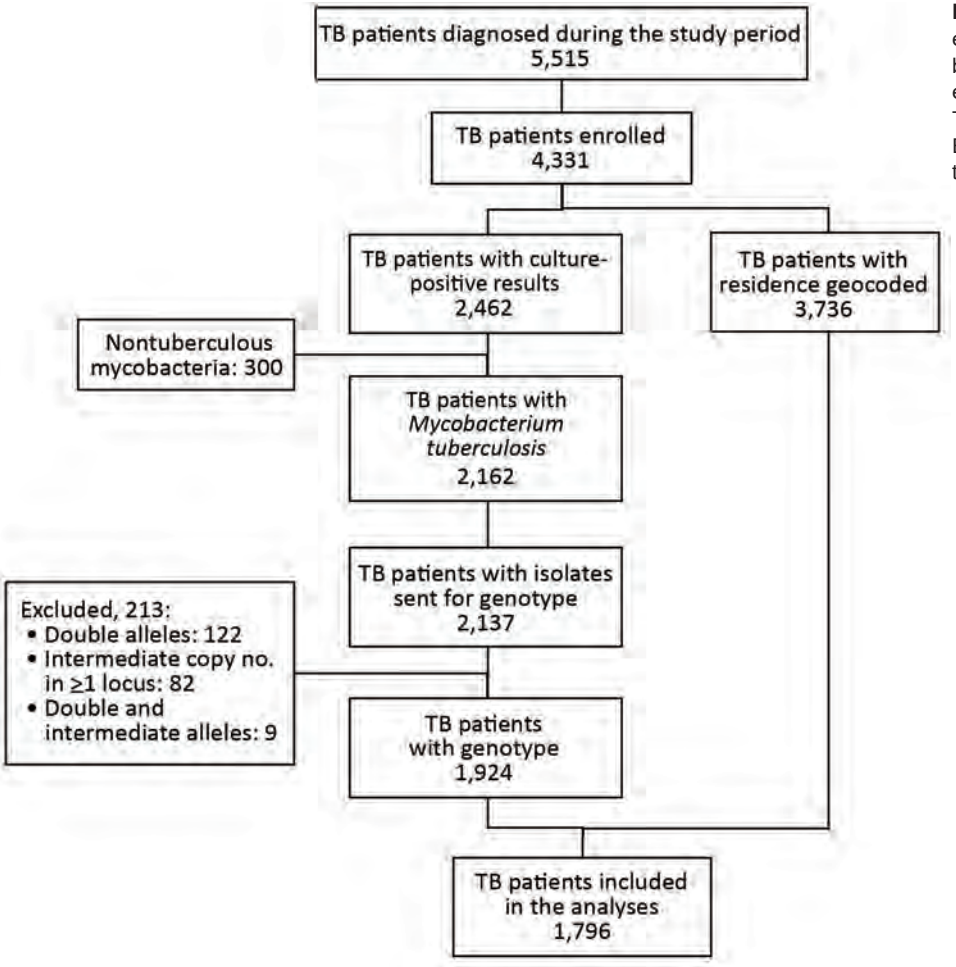

Figure 2. Flowchart of study enrollment for population-based geospatial and molecular epidemiologic study of TB transmission dynamics, Botswana, 2012–2016. TB, tuberculosis.

was found between the highest (location A) and lowest (location J) burden areas in Gaborone. This difference was 1.3 fold in Ghanzi District (highest location W and lowest location KU). In this context, we observed that certain neighborhoods contributed disproportionally to the district-level burden of TB. Some locations that had the lowest TB prevalence had the highest number and proportion of patients co-infected with HIV (Table 1).

Patient Isolate Characteristics

A total of 2,462 (56%) patients had ≥1 positive culture result; 2,162 (88%) were classified as *M. tuberculosis* complex, whereas 300 (12%) were classified as nontuberculous mycobacteria and were excluded. MIRU-VNTR results were available for 2,137 patient isolates. We excluded 213 (10%) patient isolates that had incomplete or noninterpretable genotyping results; this exclusion was described elsewhere (*23*,*24*). Thus, 1,924 patients were included in phylogenetic analysis. Among these patients, 128 had no residential geocoordinates, which resulted in 1,796 patients available for localized transmission analysis (Figure 2).

Localized Transmission

A total of 780 (43%) patients were members of localized transmission events. Among these patients, 537 (69%) resided in Gaborone, 241 (31%) resided in the Ghanzi District, and 2 (0.3%) resided elsewhere. Localized transmission was independently associated with younger age (<15 years of age, aOR 2.20, 95% CI 1.67–4.15; 16–24 years of age, aOR 1.41, 95% CI 1.05–1.89), residing in a high-burden neighborhood (aOR 2.75, 95 CI% 2.21–3.41), being a current smoker (aOR 1.71, 95% CI 1.38–2.11), and being unemployed (aOR 1.31, 95 CI% 1.08–1.59) (Table 3; Appendix Table, https://wwwnc.cdc.gov/EID/article/27/3/20-3840-App1.pdf). Patients who had a known HIV-positive status had lower odds of being a member of localized transmission (aOR 0.71, 95CI % 0.58–0.85). When we superimposed the SaTScan results over the interpolated with inverse distance-weighted TB incidence estimates, the spatial concentration for localized transmission coincided with higher TB incidence rates (Figure 3).

Table 1. Characteristics of enrolled patients by geography venues for population-based geospatial and molecular epidemiologic study of tuberculosis transmission dynamics, Botswana, 2012–2016*

Characteristic	No. (%) patients		
	Gaborone, n = 2,659	Ghanzi District, n = 723	Other, n = 354†
Sex			
M	1,501 (56.4)	403 (55.7)	181 (51.1)
F	1,158 (43.6)	320 (44.3)	173 (48.9)
Age, y			
≤15	111 (4.2)	91 (12.6)	47 (13.7)
16–24	329 (12.4)	126 (17.5)	32 (9.0)
25–40	1,388 (52.)	269 (37.3)	134 (37.9)
41–64	760 (28.6)	185 (25.6)	113 (31.9)
≥65	71 (2.7)	51 (7.1)	28 (7.9)
Income, Pula			
None	855 (32.3)	536 (74.4)	223 (63.4)
<800	186 (7.0)	89 (12.4)	17 (4.8)
801–1,500	646 (24.4)	53 (7.4)	21 (6.0)
1,501–2,999	479 (18.1)	23 (3.2)	39 (11.1)
3,000–4,999	225 (8.5)	9 (1.3)	21 (6.0)
5,000–9,999	184 (7.0)	8 (1.1)	18(5.1)
>10,000	68 (2.6)	2 (0.3)	13 (3.7)
Resided in high-burden geographic area‡	370 (13.9)	530 (73.3)	NA
Excessive alcohol use§	661 (24.9)	230 (31.8)	51 (14.4)
Current smoker	517 (19.5)	307 (42.5)	45 (12.7)
Unemployed	760 (29.8)	421 (66.6)	178 (58.0)
History of incarceration	143 (5.4)	61 (8.4)	18 (5.1)
HIV status			
Positive	1,706 (66.2)	259 (37.4)	221 (63.5)
Negative	872 (30.7)	434 (60.0)	127 (35.9)
Unknown	81 (3.1)	30 (2.6)	6 (0.6)
CD4+ cells/mm^3 at diagnosis, if HIV positive			
0–199	436 (44.7)	62 (30.8)	83 (54.2)
200–499	383 (39.2)	85 (42.3)	46 (30.1)
≥500	157 (16.1)	54 (26.9)	24 (15.7)
Previous TB episode	444 (16.7)	219 (30.3)	90 (25.4)
Culture positive	1,449 (68.1)	435 (78.0)	125 (47.9)
MDR TB at baseline	27 (1.1)	14 (2.1)	17 (5.8)

*Values are no. (%). MDR TB, multidrug-resistant tuberculosis; NA, not applicable; TB, tuberculosis.
†Includes patients with primary residence outside Gaborone and Ghanzi. Missing residential address, n = 595.
‡Residing in a geographic area with an estimated annualized TB incidence >305 patients/100,000 persons. Excludes 407 patients with culture results but no geocoded residence.
§Five or more drinks/session or drinking on ≥5 days/month.

Self-Reported Social Gathering Venues

The proportion matched by TB genotype was significantly larger in Ghanzi District (80%) than in Gaborone (64%) and other locations (4%; p<0.001) (Table 4). A total of 494 (22%) patients resided at the same address as another patient; among these, 29% matched by TB genotype. The proportion matched by TB genotype was significantly larger in the Ghanzi District (50%) than in Gaborone (18%; p<0.001). A total of 605 (32%) patients reported the same place of worship as another patient; among these, 11% matched by TB genotype. The proportion matched by TB genotype was significantly larger in Ghanzi District (24%) than in Gaborone (9%; p = 0.002). A total of 585 (30%) reported the same alcohol-related venue as another patient; among these, 28% matched by TB genotype. The proportion matched by TB genotype was significantly larger in Ghanzi District (57%) than in Gaborone (16%; p<0.001).

Discussion

Interrupting TB transmission is paramount for achieving TB elimination in high-burden settings. Accordingly, increasing interest exists on determining where, when, and among whom TB transmission occurs. Our study helps clarify factors fueling the TB epidemic in Botswana and highlights the necessity of understanding local epidemiology to design effective interventions aimed at interrupting TB transmission. We combined isolate genotype and spatial clustering as an indicator consistent with localized transmission. Although we acknowledge that some misclassification might occur with this approach, it enabled us to broadly consider geographic and individual characteristics that might be associated with localized transmission.

We found high incidence rates and substantial variation in TB incidence between neighborhoods and districts. Actual incidence rates are likely higher because we calculated estimates on the basis of numbers of enrolled patients, but not all persons with TB

were enrolled in this study. Residing in a high-burden geographic area was associated with localized transmission, likely reflecting more cumulative exposures leading to more infections, reinfections, and opportunities to progress to TB. In addition, the local differences in TB incidence likely overlaps with differences in the local distribution of social determinants of health (e.g., poverty, overcrowding, and housing conditions), which also influence TB epidemiology (*12*).

Our finding that localized transmission was associated with young age might be reflective of differences in the frequency and intensity of social activities across the course of life (*25*). Younger patients might have had more social connections and relationships with nonfamily members (*25*).

In addition, older patients might have progressed to having TB with non-genotype clustered strains from infections in the distant past (*26*). The large number of patients living in the same neighborhoods of another patient, and high proportion matching another patient by TB genotype, suggests targeted screening and treatment in high-burden neighborhoods might be cost-effective. Overall, a substantial proportion of patients (22%) resided at the same address as another patient; among these patients, 29% were matched by TB genotype. However, major differences occurred by geography. Among patients residing at the same address in Ghanzi, 50% were matched by genotyping, suggesting that household contact investigations in this district would be particularly effective at reducing transmission.

Social venue data suggested that community-based interventions might be effective for interrupting transmission. A substantial number of patients named the same places of worship (32%) or alcohol-related venues (30%) as another patient. Among persons naming the same alcohol-rated venue in Ghanzi, 57% were matched by TB genotype. These findings might help prioritize resources and guide effective strategies to interrupt *M. tuberculosis* transmission, such as intensified TB case finding in higher-burden geographic areas and targeted screening of frequently named social gathering venues.

Our results also highlight the need for using local data for local solutions. Comparative differences in spatial and genotypic clustering within and between communities reinforce the relative role of local factors that drive TB transmission and incidence. The proportion of patients attributed to localized transmission was higher in Ghanzi than in Gaborone. This finding suggests that, although TB transmission is a serious issue in both communities, a relatively higher proportion of TB cases might be caused by recent exposure to

Table 2. Demographic and clinical characteristics by geographic area venues for population-based geospatial and molec epidemiologic study of tuberculosis transmission dynamics, Botswana, 2012–2016*

Area	Population†	Size, km^2	Population density†	No. enrolled TB patients	No. who had TB (95% CI)‡	No. (%) enrolled HIV-positive patients	No. *M tul* ge
Gaborone							
A	19,143	1.4	13,973	370	483 (438–536)	245 (66.2)	
B	32,805	21.8	1,505	183	139 (121–161)	109 (59.6)	
C	59,100	16.0	3,694	591	250 (231–271)	379 (64.1)	
D	51,190	53.9	950	574	280 (259–305)	364 (63.4)	
E	34,262	39.5	867	249	182 (161–206)	165 (66.3)	
F	71,957	27.5	2,617	388	135 (122–149)	243 (62.6)	
G	28,639	17.9	1,600	139	121 (104–144)	79 (56.8)	
H	12,094	24.6	492	71	147 (117–185)	54 (76.1)	
I	7,677	77.7	99	28	91 (63–132)	17 (60.7)	
J	8,729	88.2	99	23	66 (44–99)	17 (73.9)	
K	14,104	72.4	195	43	76 (58–105)	34 (79.1)	
Ghanzi District							
W	12,179	45.8	266	419	860 (783–945)	158 (37.7)	
DK	1,668	9.7	172	73	1,094 (874–1,369)	17 (23.3)	
KU	833	7.5	111	38	1,140 (836–1,556)	16 (42.1)	
Y	2,203	1,607	1.3	193	NA	68 (35.2)	
Other location	354	NA	NA	354	NA	221 (62.4)	
Not geocoded	NA	NA	NA	595	NA	366 (61.5)	
Total	354,380	NA	NA	4,331	306 (228–339)	2,552 (58.9)	

*NA, not applicable; TB, tuberculosis.
†Persons residing/km^2. Based 2011 Population and Housing Census. Statistics Botswana.
‡TB incidence/100,000 persons; 95% CIs assume a Poisson distribution);based on no. cases enrolled from each geography divided by the estimates for each geography annualized to the duration of study period.
§Rows are not mutually exclusive; strains might be found in multiple locations.

Table 3. Characteristics associated with localized tuberculosis transmission venues for population-based geospatial and molecular epidemiologic study of tuberculosis transmission dynamics, Botswana, 2012–2016*

Characteristic	Member of localized TB transmission, n = 780	Not a member of localized TB transmission, n = 1,016	Adjusted odds ratio (95% CI)
Sex			
M	436 (55.9)	555 (54.6)	1.05 (0.87–1.27)
F	334 (44.1)	461 (45.4)	
Age, y			
≤15	26 (3.3)	18 (1.8)	**2.20 (1.67–4.15)**
16–24	157 (20.1)	170 (16.7)	**1.41 (1.05–1.89)**
25–40	418 (53.6)	558 (54.9)	1.14 (0.90–1.45)
41–64	158 (20.3)	241 (23.7)	Referent
≥65	21 (2.7)	29 (2.9)	1.11 (0.61–3.00)
Resided in high-burden geographic area†	291 (37.1)	181 (17.8)	**2.75 (2.21–3.41)**
Excessive alcohol use‡	160 (20.6)	205 (20.2)	1.03 (0.82–1.30)
Current smoker	250 (32.1)	220 (21.7)	**1.71 (1.38–2.11)**
Unemployed	314 (41.6)	352 (35.3)	1.31 (1.08–1.59)
History of incarceration	49 (6.3)	56 (5.5)	1.15 (0.78–1.71)
HIV positive	366 (48.5)	570 (57.2)	**0.71 (0.58–0.85)**
Previous TB episode	156 (20.0)	178 (17.5)	1.17 (0.93–1.49)

*Values are no. (%). Bold indicates statistical significance at α = 0.05. Localized transmission defined by SaTScan (https://www.satscan.org)–identified geographic areas with a larger-than-expected rate of unique genotype clustering compared with all other culture-positive TB patients as the background rate; excludes 128 patients with valid genotype results and no residential address. TB, tuberculosis.
†Residing in a geographic area with an estimated annualized TB incidence > 305 patients/100,000 persons.
‡Five or more drinks/session in the previous 30 d or drinking on ≥5 days in the previous 30 d.

an infectious TB case-patient in Ghanzi than in Gaborone. Differences in population density and behavioral factors, such as smoking, drinking, and social mixing, highlight the potential impact of targeting interventions for these vulnerable populations. However, in settings that have prevalent endemic strains, genotype clustering might not be caused by recent transmission; higher resolution molecular characterization, such as whole-genome sequencing, might help further distinguish recent transmission from reactivation of highly prevalent, closely related strains.

The trend toward an inverse population- and individual-level association between HIV and localized transmission is consistent with findings from previous TB molecular epidemiologic studies in Africa and highlights the complex time-dependent interactions between the TB and HIV epidemics (*27*–*32*). At the population-level, Gaborone neighborhoods, which had the highest proportion of HIV–co-infected TB patients also demonstrated the lowest TB incidence, and HIV infection was negatively associated with localized transmission. HIV–co-infected TB patients progress more rapidly to active disease after *M. tuberculosis* infection and are generally less infectious and have higher mortality rates (*33*). As HIV care improves and antiretroviral therapy becomes more widely available, TB incidence among the HIV-infected persons decreases, leading to decreasing the rates of progression to active disease (*34*). Furthermore, being infected with HIV often

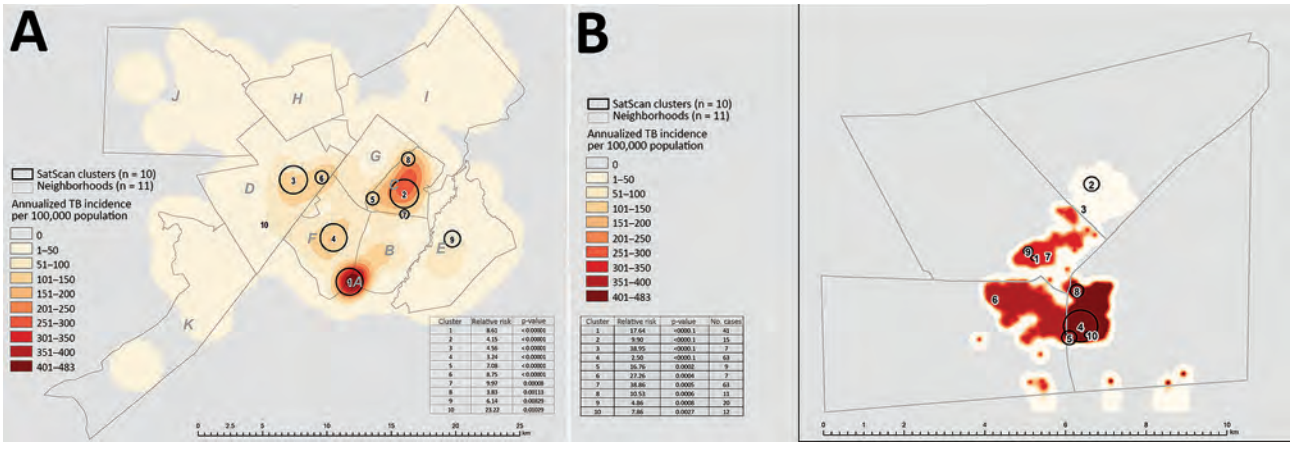

Figure 3. Annualized estimated TB incidence with the most probable localized transmission events superimposed, Botswana, 2012–2016. A) Gaborone; B) Ghanzi District. Shown are areas with most probable clusters identified by using spatial scan statistics (discrete Poisson) for 10 major clusters in Gaborone and Ghanzi (black circles). Data are superimposed on the inverse distance weighted map of annualized incidence of TB patients by neighborhood. TB, tuberculosis.

Table 4. Self-reported social gathering venues for population-based geospatial and molecular epidemiologic study of tuberculosis transmission dynamics, Botswana, 2012–2016*

	Total, n = 1,924		Gaborone, n = 1,524		Ghanzi District, n = 400	
Venue	Naming same venue	Naming same venue and same genotype result†	Naming same venue	Naming same venue and same genotype result†	Naming same venue	Naming same venue and same genotype result†
Alcohol-related‡	585 (30.4)	164 (28.0)	409 (26.8)	65 (4.3)	171 (42.8)	98 (24.5)
Place of worship‡	605 (31.4)	64 (10.6)	540 (35.4)	49 (3.2)	62 (15.5)	15 (3.8)
Same residence§	494 (29.4)	123 (28.8)	337 (22.1)	60 (3.9)	126 (31.5)	63 (15.8)

*Values are no. (%).
†Does not imply temporality.
‡Includes patients with residential location that is outside Gaborone or Ghanzi or that is unknown.
§Missing residential address, n = 128.

means more visits to healthcare facilities in which TB screening is part of routine visits.

Our population-based design and multidisciplinary approach enables a high degree of confidence in our results and conclusions. However, major limitations need to be considered. First, although our study was multiyear and covered a broad geographic area, it is possible that some members of the transmission networks were missed (e.g., given a diagnosis before the study period or resided in areas not covered by the study, or refused enrollment) leading to genotype clustering misclassification. Also, not all enrolled TB patients produced sputum samples, and not all samples led to *M. tuberculosis* isolation or valid genotype results. This limitation might result in missed transmission links. Second, our molecular techniques characterized only part of the *M. tuberculosis* genome (*17*). It possible that genetic heterogeneity in loci not covered by this method might have been missed, resulting in misclassification (*17*). Moreover, the use of 1 isolate/patient, exclusion of mixed infections, missing data, and recall bias for naming potential transmission venues should also be acknowledged as potential limitations.

The Kopanyo Study adds to understanding of TB transmission dynamics in settings hyperendemic for TB and HIV by providing empirical data demonstrating the role of localized TB transmission during district-level epidemics. Thus, interrupting TB transmission in Botswana might warrant local solutions tailored for community differences and based on local epidemiology.

Acknowledgments

We thank James Shepperd for providing substantial contributions during the early stages of this study; Ogopotse Masiri, Othusise Fane, and Mbashi Dima for coordinating field activities; Balladiah Kizito and Christopher Serumola for providing assistance with data cleaning and management; Sanghyuk S. Shin for providing insight and expertise to earlier versions of this manuscript; the Botswana Ministry of Health and Wellness, the Botswana National Tuberculosis Program, and the Botswana National Tuberculosis Reference Laboratory for providing constant support; and all study participants who contributed to the study.

This study was supported by the National Institutes of Health (grant R01AI097045) and the President's Emergency Plan for AIDS Relief through the Centers for Disease Control and Prevention.

About the Author

Dr. Zetola is an adjunct assistant professor at the University of Pennsylvania, Philadelphia, PA. His primary research interest is the interaction between HIV, tuberculosis infection, and global critical care medicines.

References

1. World Health Organization 67th World Health Assembly Global strategy and targets for tuberculosis prevention, care and control after 2015. A67/11. Geneva: World Health Organization, 2014.
2. Uplekar M, Weil D, Lonnroth K, Jaramillo E, Lienhardt C, Dias HM, et al.; for WHO's Global TB Programme. WHO's new end TB strategy. Lancet. 2015;385:1799–801. https://doi.org/10.1016/S0140-6736(15)60570-0
3. Floyd K, Glaziou P, Zumla A, Raviglione M. The global tuberculosis epidemic and progress in care, prevention, and research: an overview in year 3 of the end TB era. Lancet Respir Med. 2018;6:299–314. https://doi.org/10.1016/S2213-2600(18)30057-2
4. Matteelli A, Rendon A, Tiberi S, Al-Abri S, Voniatis C, Carvalho ACC, et al. Tuberculosis elimination: where are we now? Eur Respir Rev. 2018;27:180035. https://doi.org/10.1183/16000617.0035-2018
5. Mathema B, Andrews JR, Cohen T, Borgdorff MW, Behr M, Glynn JR, et al. Drivers of tuberculosis transmission. J Infect Dis. 2017;216(suppl_6):S644–53. https://doi.org/10.1093/infdis/jix354
6. Yates TA, Khan PY, Knight GM, Taylor JG, McHugh TD, Lipman M, et al. The transmission of *Mycobacterium tuberculosis* in high burden settings. Lancet Infect Dis. 2016;16:227–38. https://doi.org/10.1016/S1473-3099(15)00499-5
7. Donald PR, Diacon AH, Lange C, Demers AM, von Groote-Bidlingmaier F, Nardell E. Droplets, dust and guinea pigs: an historical review of tuberculosis transmission research, 1878–1940. Int J Tuberc Lung Dis. 2018;22:972–82. https://doi.org/10.5588/ijtld.18.0173
8. Surie D, Fane O, Finlay A, Ogopotse M, Tobias JL, Click ES, et al.; Kopanyo Study Group. Molecular, spatial, and field

epidemiology suggesting TB transmission in community, not hospital, Gaborone, Botswana. Emerg Infect Dis. 2017;23:487–90. https://doi.org/10.3201/eid2303.161183
9. Wang W, Mathema B, Hu Y, Zhao Q, Jiang W, Xu B. Role of casual contacts in the recent transmission of tuberculosis in settings with high disease burden. Clin Microbiol Infect. 2014;20:1140–5. https://doi.org/10.1111/1469- 691.12726
10. Murray M, Oxlade O, Lin HH. Modeling social, environmental and biological determinants of tuberculosis. Int J Tuberc Lung Dis. 2011;15(Suppl 2):64–70. https://doi.org/10.5588/ijtld.10.0535
11. Wanyeki I, Olson S, Brassard P, Menzies D, Ross N, Behr M, et al. Dwellings, crowding, and tuberculosis in Montreal. Soc Sci Med. 2006;63:501–11. https://doi.org/10.1016/j.socscimed.2005.12.015
12. Lönnroth K, Jaramillo E, Williams BG, Dye C, Raviglione M. Drivers of tuberculosis epidemics: the role of risk factors and social determinants. Soc Sci Med. 2009;68:2240–6. https://doi.org/10.1016/j.socscimed.2009.03.041
13. Zetola NM, Modongo C, Moonan PK, Click E, Oeltmann JE, Shepherd J, et al. Protocol for a population-based molecular epidemiology study of tuberculosis transmission in a high HIV-burden setting: the Botswana Kopanyo study. BMJ Open. 2016;6:e010046. https://doi.org/10.1136/bmjopen-2015-010046
14. Botswana Ministry of Health and Wellness. Botswana AIDS impact survey IV (BIAS IV), 2013. Government of Botswana, Gaborone, Botswana, 2014 [cited 2020 Dec 3]. http://www.statsbots.org.bw/latest-publications
15. Botswana National Tuberculosis Programme Annual Report. Government of Botswana, Gaborone, Botswana, 2014 [cited 2020 Dec 13]. https://www.who.int/hiv/pub/guidelines/botswana_tb.pdf
16. Faure E, Danjou AM, Clavel-Chapelon F, Boutron-Ruault MC, Dossus L, Fervers B. Accuracy of two geocoding methods for geographic information system-based exposure assessment in epidemiological studies. Environ Health. 2017;16:15. https://doi.org/10.1186/s12940-017-0217-5
17. Statistics Botswana. Population and housing census, 2011: analytical report [cited 2020 Dec 3]. http://www.statsbots.org.bw/latest-publications
18. Kalinowski A, Humphreys K. Governmental standard drink definitions and low-risk alcohol consumption guidelines in 37 countries. Addiction. 2016;111:1293–8. https://doi.org/10.1111/add.13341
19. Supply P, Allix C, Lesjean S, Cardoso-Oelemann M, Rüsch-Gerdes S, Willery E, et al. Proposal for standardization of optimized mycobacterial interspersed repetitive unit-variable-number tandem repeat typing of *Mycobacterium tuberculosis*. J Clin Microbiol. 2006;44:4498–510. https://doi.org/10.1128/JCM.01392-06
20. Mathema B, Kurepina NE, Bifani PJ, Kreiswirth BN. Molecular epidemiology of tuberculosis: current insights. Clin Microbiol Rev. 2006;19:658–85. https://doi.org/10.1128/CMR.00061-05
21. Kulldorff MA. A spatial scan statistic. Commun Stat Theory Methods. 1997;26:1481–96. https://doi.org/10.1080/03610929708831995
22. Moonan PK, Ghosh S, Oeltmann JE, Kammerer JS, Cowan LS, Navin TR. Using genotyping and geospatial scanning to estimate recent *Mycobacterium tuberculosis* transmission, United States. Emerg Infect Dis. 2012;18:458–65. https://doi.org/10.3201/eid1803.111107
23. Baik Y, Fane O, Wang Q, Modongo C, Caiphus C, Grover S, et al. Undetected tuberculosis at enrollment and after hospitalization in medical and oncology wards in Botswana. PLoS One. 2019;14:e0219678. https://doi.org/10.1371/journal.pone.0219678
24. Click ES, Finlay A, Oeltmann JE, Basotli J, Modongo C, Boyd R, et al. Phylogenetic diversity of *Mycobacterium tuberculosis* in two geographically distinct locations in Botswana: the Kopanyo Study. Infect Genet Evol. 2020;81:104232. https://doi.org/10.1016/j.meegid.2020.104232
25. Sander J, Schupp J, Richter D. Getting together: social contact frequency across the life span. Dev Psychol. 2017;53:1571–88. https://doi.org/10.1037/dev0000349
26. Yew WW, Yoshiyama T, Leung CC, Chan DP. Epidemiological, clinical and mechanistic perspectives of tuberculosis in older people. Respirology. 2018;23:567–75. https://doi.org/10.1111/resp.13303
27. Verver S, Warren RM, Munch Z, Vynnycky E, van Helden PD, Richardson M, et al. Transmission of tuberculosis in a high incidence urban community in South Africa. Int J Epidemiol. 2004;33:351–7. https://doi.org/10.1093/ije/dyh021
28. Lockman S, Sheppard JD, Braden CR, Mwasekaga MJ, Woodley CL, Kenyon TA, et al. Molecular and conventional epidemiology of *Mycobacterium tuberculosis* in Botswana: a population-based prospective study of 301 pulmonary tuberculosis patients. J Clin Microbiol. 2001;39:1042–7. https://doi.org/10.1128/JCM.39.3.1042-1047.2001
29. Glynn JR, Crampin AC, Yates MD, Traore H, Mwaungulu FD, Ngwira BM, et al. The importance of recent infection with *Mycobacterium tuberculosis* in an area with high HIV prevalence: a long-term molecular epidemiological study in northern Malawi. J Infect Dis. 2005;192:480–7. https://doi.org/10.1086/431517
30. Asiimwe BB, Joloba ML, Ghebremichael S, Koivula T, Kateete DP, Katabazi FA, et al. DNA restriction fragment length polymorphism analysis of *Mycobacterium tuberculosis* isolates from HIV-seropositive and HIV-seronegative patients in Kampala, Uganda. BMC Infect Dis. 2009;9:12. https://doi.org/10.1186/1471-2334-9-12
31. Muwonge A, Malama S, Johansen TB, Kankya C, Biffa D, Ssengooba W, et al. Molecular epidemiology, drug susceptibility and economic aspects of tuberculosis in Mubende district, Uganda. PLoS One. 2013;8:e64745. https://doi.org/10.1371/journal.pone.0064745
32. Tessema B, Beer J, Merker M, Emmrich F, Sack U, Rodloff AC, et al. Molecular epidemiology and transmission dynamics of *Mycobacterium tuberculosis* in northwest Ethiopia: new phylogenetic lineages found in northwest Ethiopia. BMC Infect Dis. 2013;13:131. https://doi.org/10.1186/1471-2334-13-131
33. Odone A, Amadasi S, White RG, Cohen T, Grant AD, Houben RM. The impact of antiretroviral therapy on mortality in HIV positive people during tuberculosis treatment: a systematic review and meta-analysis. PLoS One. 2014;9:e112017. https://doi.org/10.1371/journal.pone.0112017
34. Houben RM, Dowdy DW, Vassall A, Cohen T, Nicol MP, Granich RM, et al.; TB MAC TB-HIV meeting participants. How can mathematical models advance tuberculosis control in high HIV prevalence settings? Int J Tuberc Lung Dis. 2014;18:509–14. https://doi.org/10.5588/ijtld.13.0773

Address for correspondence: Nicola M. Zetola, University of Pennsylvania, Johnson Pavillion, Philadelphia, PA 19104-6243, USA; email: nzetola@gmail.com

Extrapulmonary Nontuberculous Mycobacteria Infections in Hospitalized Patients, United States, 2009–2014

Emily E. Ricotta, Jennifer Adjemian,[1] Rebekah A. Blakney, Yi Ling Lai, Sameer S. Kadri, D. Rebecca Prevots

Nontuberculous mycobacteria (NTM) cause pulmonary and extrapulmonary infections in susceptible persons. To characterize the epidemiology of skin and soft tissue (SST) and disseminated extrapulmonary infections caused by NTM in the United States, we used a large electronic health record database to examine clinical, demographic, and laboratory data for hospitalized patients with NTM isolated from extrapulmonary sources during 2009–2014. Using all unique inpatients as the denominator, we estimated prevalence and summarized cases by key characteristics. Of 9,196,147 inpatients, 831 had confirmed extrapulmonary NTM. The 6-year prevalence was 11 cases/100,000 inpatients; source-specific prevalence was 4.4 SST infections/100,000 inpatients and 3.7 disseminated infections/100,000 inpatients. NTM species varied across geographic region; rapidly growing NTM were most prevalent in southern states. Infection with *Mycobacterium avium* complex was more common among patients with concurrent HIV and fungal infection, a relevant finding because treatment is more effective for *M. avium* complex than for other NTM infections.

Nontuberculous mycobacteria (NTM) are opportunistic bacteria that are abundant in soil and water, including natural and plumbing-associated water sources (*1*,*2*). For a minority of susceptible persons, exposure to NTM can result in extrapulmonary infections (*3*), including skin, joint, lymph node, and disseminated infections. Extrapulmonary infections, especially disseminated disease, typically occur among persons with congenital or acquired immunodeficiencies (e.g., HIV infection) (*4*) but can also be associated with medical or cosmetic procedures that expose a wound to sources contaminated with mycobacteria (*5*,*6*). A recently described outbreak identified disseminated infections with *Mycobacterium chimaera* after open heart surgery, arising from contamination of heater–cooler units (*6*).

Few studies describe the epidemiology of extrapulmonary NTM in the United States at the national level. One recent study in Oregon evaluated the prevalence of extrapulmonary NTM by using statewide population-based laboratory surveillance data for 2007–2012, which included data for pulmonary and extrapulmonary NTM (*4*). The researchers estimated a stable annual incidence of extrapulmonary NTM infection of 1.5 cases/100,000 population. The average age of extrapulmonary NTM patients (median 51 years) was younger than that of pulmonary NTM patients. In addition, rapidly growing NTM species were identified at a much greater frequency in extrapulmonary than in pulmonary NTM patients and represented one third of all cases in Oregon (*4*). Epidemiologic studies of pulmonary NTM disease show tremendous geographic variation in prevalence and mycobacterial species (*7*,*8*), suggesting the possibility of differences for extrapulmonary NTM as well, given the environmental influences on NTM disease dynamics. To characterize the epidemiology of skin and soft tissue (SST) and disseminated NTM infections and evaluate regional differences in incidence and mycobacterial species distribution, we examined laboratory-confirmed cases from a large electronic health record (EHR)–based repository of inpatient encounters from a national sample of US hospitals.

Author affiliations: National Institutes of Health National Institute of Allergy and Infectious Diseases, Bethesda, Maryland, USA (E.E. Ricotta, J. Adjemian, R.A. Blakney, Y.L. Lai, D.R. Prevots); US Public Health Service Commissioned Corps, Rockville, Maryland, USA (J. Adjemian); National Institutes of Health Clinical Center, Bethesda (S.S. Kadri)

DOI: https://doi.org/10.3201/eid2703.201087

[1]Current affiliation: Centers for Disease Control and Prevention, Atlanta, Georgia, USA.

Methods

The nationally distributed, hospital-based Cerner Health Facts EHR database (https://sc-ctsi.org/resources/cerner-health-facts) includes linked demographic, clinical, and microbiological information for ≈9 million US inpatients. Using this database, we identified all US patients hospitalized during 2009–2014 with positive NTM cultures from extrapulmonary sources (excluding *M. gordonae* because it is considered an environmental contaminant) (Appendix Table 1, https://wwwnc.cdc.gov/EID/article/27/3/20-1087-App1.pdf). Patients were classified as having SST disease, disseminated disease (including those with infections in blood, central nervous system, and sterile bone and joint sources), or both; patients with infections from abdominal sites, urinary system, or other body sites were also identified and grouped as other sources (Table 1; Appendix Tables 2, 3). Sources were further classified as sterile or not sterile and whether they were associated with a device, prosthesis, or surgical procedure (Table 2). We excluded from analysis 142 patients with isolates from unknown sources and 4,385 patients with isolates from pulmonary sources.

Patients with extrapulmonary NTM were described by demographic factors (age, sex, race, and geographic region) and clinical factors (underlying conditions and procedural history via codes from the International Classification of Diseases, Ninth and Tenth Revisions, and Current Procedural Terminology). To compare demographics by infection type, we used the Pearson χ^2 test or analysis of variance, where appropriate. We calculated overall and annual inpatient prevalence estimates by determining the number of unique inpatients with ≥1 positive extrapulmonary NTM culture divided by the total number of unique inpatients identified during the study period among hospitals reporting ≥1 case of extrapulmonary NTM. Patients whose cultures grew multiple NTM species or had isolates cultured from multiple extrapulmonary sites were counted in each group unless specified. Statistical analyses were conducted by using R version 4.0.2 (https://www.R-project.org).

Table 1. Classification of extrapulmonary nontuberculous mycobacterial infection type, by body site, United States, 2009–2014*

Infection type	Site
Skin and soft tissue	Arm, boil, cheek, ear, foot, genital, groin, incision, leg, lymph node, mass, neck, node, nodule, skin, thigh, tissue, wound
Disseminated	
Blood	Blood, blood capillary, blood line, blood venous, blood whole, central line
Bone and joint (sterile)	Bone, bone marrow, wrist, synovial fluid, jaw, joint fluid, knee, hip
Central nervous system	Cerebrospinal fluid
Other	
Abdominal	Liver, ascites fluid, gastric tube, abdominal fluid, gastric fluid, nasogastric aspirate, peritoneal, peritoneal dialysis fluid, peritoneal fluid, gastric aspirate, perianal, colonic wash, feces, rectal, percutaneous endoscopic gastrostomy site
Urinary	Urine, urine catheterized, urine clean catch, urine midstream, urine voided
Other	Eye fluid, cervical, pericardial fluid, sternal, exit site, foreign body, pacemaker, plate, prosthesis, surgical, nasopharynx, throat, nonsterile bone and joint

*Data from in Cerner Health Facts database (https://sc-ctsi.org/resources/cerner-health-facts).

Results

Of 9,196,147 unique inpatients from 275 inpatient facilities reporting culture results throughout the United States, laboratory-confirmed extrapulmonary NTM was reported for 998 unique species/source isolates from 831 patients at 89 hospitals. Isolates represented 321 (39%) patients with SST infections, 269 (32%) with disseminated infections, and 337 (41%) with infection at other sites. Both disseminated and SST infections were reported for 23 (2.8%) patients. Most isolates identified to the species level were *Mycobacterium avium* complex (MAC) (50%), followed by *M. fortuitum* (10%), *M. abscessus* (9.4%), *M. chelonae* (5.3%), and *M. chelonae/abscessus* (4.3%). Other species were rapidly growing NTM (8.7%), non–rapidly growing NTM (3.7%), or not speciated (7.9%) (Table 3).

The overall 6-year prevalence of extrapulmonary NTM in hospitals reporting ≥1 inpatient with extrapulmonary NTM was 11 cases/100,000 inpatients. Site-specific infections were 4.4 SST infections/100,000 inpatients, 3.7 disseminated infections/100,000 inpatients, and 0.3 cases of both types of infection/100,000 inpatients. Annual prevalence of disseminated NTM remained stable over the study period, whereas SST infections increased 8.2% (95% CI 1%–15%) (Figure 1). Prevalence was highest in the Midwest (13 cases/100,000 inpatients), South (13 cases/100,000 inpatients), and Northeast (11 cases/100,000 inpatients) and lowest in the West (5.3 cases/100,000 inpatients).

Among patients, 49% were female, 58% were White, and 60% were >40 years of age; 32% were Black and 11% were <18 years of age. Relative to patients with SST infections, those with

Table 2. Sources of extrapulmonary nontuberculous mycobacterial infection, by site sterility and association with medical device, prosthetics, and surgery, United States, 2009–2014*

Source	Sterile, no. (%)	Not sterile, no. (%)	Device/prosthesis associated, no. (%)	Surgery-associated, no. (%)
Skin and soft tissue, n = 340	33 (10)	307 (90)	59 (17)	129 (38)
Disseminated, n = 290				
Blood, n = 259	259 (100)	NA	72 (28)	26 (10)
Bone and joint, n = 26	26 (100)	NA	7 (27)	7 (27)
Central nervous system, n = 5	5 (100)	NA	3 (60)	3 (60)
Other, n = 362				
Abdominal, n = 110	21 (19)	89 (81)	27 (24)	17 (15)
Urinary, n = 11	0	11 (100)	2 (18)	1 (9)
Other, n = 241	64 (27)	177 (73)	49 (20)	87 (36)

*Data from in Cerner Health Facts database (https://sc-ctsi.org/resources/cerner-health-facts). NA, not applicable.

disseminated cases were more frequently male (60% vs. 45%; p<0.001), younger (mean age 40 vs. 50 years; p<0.001), and Black (56% vs. 13%; p<0.001). Among patients with both SST and disseminated infection, 61% were female, most (52%) were White, and mean age was 52 years (Table 4). Among patients with SST infections, 15% had undergone a surgical procedure (e.g., invasive, minimally invasive, surgical biopsy) compared with 4% of patients with disseminated infection. Among all patients, 20% had ever taken an immunosuppressive drug (Table 4); among these, 19% had SST infection, 23% had disseminated infection, and 22% had both. Crude overall mortality rate was 5% (11% among those with disseminated and 2% among those with SST infections); 1 patient with both types of infection died.

MAC accounted for more than half of disseminated (54%) and SST infections (52%), and rapidly growing NTM accounted for 34% of SST infections and 37% of disseminated infections. Distribution of cases by source and species varied by region (Table 4). SST infections were more common in the Midwest (30% vs. 18%; p = 0.002) and Northeast (32% vs. 18%; p<0.001), and disseminated infections were more common in the South (60% vs. 32%; p<0.001). MAC was found at a higher proportion than rapidly growing NTM in the Northeast (30% vs. 13%; p<0.001), and rapidly growing NTM were found at a higher proportion in the Midwest (32% vs. 23%; p = 0.004) and South (52% vs .40%; p = 0.001). When infections were broken down further by species and infection type, a significantly higher proportion of MAC was found in the Northeast for disseminated (62% vs. 29%; p = 0.002) and SST infections (72% vs. 12%; p<0.001) and in the South for disseminated infections (54% vs. 36%; p<0.001). Compared with MAC, the proportion of rapidly growing NTM causing SST infections was higher in the South (51% vs. 33%; p = 0.009) (Figure 2).

Underlying conditions included fungal co-infections (11%), HIV infection (13%), cancer (4%), and other immunodeficiencies (2%); 14 (2%) NTM patients had a history of invasive cardiac procedures (Table 4). A higher proportion of patients with MAC than with rapidly growing NTM had HIV infection (21% vs. 1.5%; p<0.001) and fungal infections (16% vs. 6.7%; p<0.001), and a higher proportion of patients with rapidly growing NTM had cancer (6.7% vs. 1.4%; p<0.001). Co-infections (including pulmonary pathogens) identified during the same hospitalization as NTM isolation were common; ≥1 concomitant pathogen of interest grew for 42% of patients (Appendix Table 4).

By extrapulmonary NTM infection type, co-infection was found for 37% of patients with SST, 47% with disseminated, and 61% with both. Among all persons with co-infection, 13% had *Staphylococcus* spp., 10% had *Candida* spp., 9.0% had *Enterococcus* spp., 7.0% had *Streptococcus* spp., 6.6% had *Pseudomonas*

Table 3. Nontuberculous mycobacteria species distribution overall and by source, United States, 2009–2014*

Species	Total no. (%)	Disseminated, no. (%)	Skin and soft tissue, no. (%)	Other, no. (%)
Mycobacterium avium complex	501 (50)	157 (54)	177 (52)	167 (45)
M. abscessus	94 (9)	24 (8)	27 (8)	43 (12)
M. abscessus/chelonae	43 (4)	13 (4)	15 (4)	15 (4)
M. chelonae	53 (5)	14 (5)	21 (6)	18 (5)
M. fortuitum	104 (10)	20 (7)	36 (11)	48 (13)
M. kansasii	26 (3)	6 (2)	9 (3)	11 (3)
Mycobacterium spp.	79 (8)	17 (6)	20 (6)	42 (11)
Other non–rapidly growing NTM	37 (4)	3 (1)	20 (6)	14 (4)
Other rapidly growing NTM	61 (6)	36 (12)	15 (4)	10 (3)
Total	998 (100)	290 (29)	340 (34)	368 (37)

*Data from in Cerner Health Facts database (https://sc-ctsi.org/resources/cerner-health-facts).

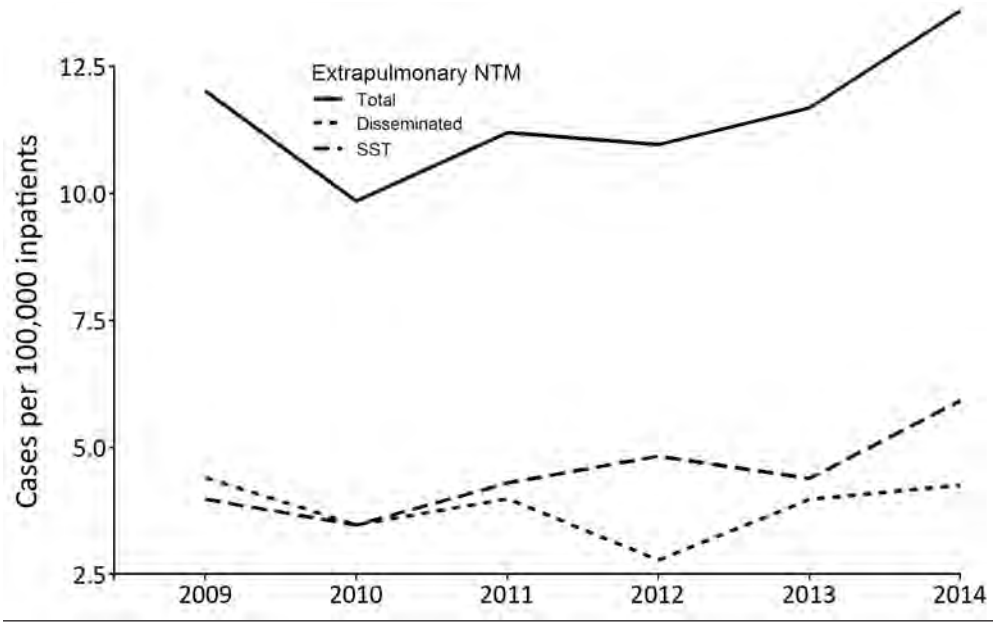

Figure 1. Annual prevalence of extrapulmonary nontuberculous mycobacteria cases by year and site of infection among hospitalized patients in the United States, 2009–2014. SST, skin and soft tissue.

spp., 5.2% had *Escherichia coli*, 3.8% had *Klebsiella* spp., and 8.2% had *M. tuberculosis* complex (MTBC) (Table 5). Of patients with both SST and disseminated NTM, 36% were co-infected with *Enterococcus* spp., 26% with MTBC, and 29% with *Staphylococcus* spp. (Figure 3). Patients with disseminated NTM had a higher proportion of *Acinetobacter* spp., *Bacillus* spp., *Candida* spp., *Clostridium* spp., *Coccidioides* spp., *Cryptococcus* spp., *Enterococcus* spp., *E. coli*, *Stenotrophomonas* spp., and *Streptococcus* spp. infection; patients with SST NTM infection had a higher proportion of *Aeromonas* spp., *Aspergillus* spp., *Corynebacterium* spp., *Enterobacter* spp., *Klebsiella* spp., MTBC, *Salmonella* spp., and *Staphylococcus* spp., although the differences were not significant (Table 5; Figure 3).

Discussion

Using the Cerner Health Facts EHR database, we found that the annual prevalence of extrapulmonary NTM overall was stable over time and that SST NTM infections increased significantly, which could result from the increased number of patients taking immunosuppressive drugs (20% of patients in this cohort) or increased cosmetic procedures (e.g., tattooing, pedicures) (*10*,*11*). Although population-based studies have found a lower and stable prevalence of extrapulmonary NTM, it is possible that the higher prevalence we found results from patients having more severe infections that necessitate testing, increasing the chances of diagnosing this disease (*4*,*11*).

NTM infections varied by geographic region in prevalence, infection type, and mycobacterial species. Specifically, prevalence of extrapulmonary NTM was higher among hospitalized patients in the South, Midwest, and Northeast than in the West, although these high rates resulted from disseminated infection in the South versus a more even distribution of SST infections in other regions. Recent studies of extrapulmonary NTM in the United States have focused on specific geographic locations. In Oregon, Shih et al. (*12*) and Henkle et al. (*4*) analyzed all extrapulmonary NTM cases identified via statewide laboratory-based active surveillance efforts and estimated incidence rates to be 1.1–1.5 cases/100,000 persons/year, with only one third of those patients hospitalized (*12*). These estimates are substantially lower than those reported in North Carolina (*13*), where a similar surveillance-based study estimated the prevalence among residents of 3 counties to be ≈3 cases/100,000 persons. The differences in prevalence estimates between Oregon and North Carolina similarly reflect the regional differences that we observed; prevalence was higher in southern than in western states. The geographic variations in prevalence of extrapulmonary NTM cases that we found are also similar to what has been shown in US population–level pulmonary NTM studies (*8*,*14*,*15*), that residents of southern states are at increased risk for NTM lung disease, particularly among high-risk groups such as persons with cystic fibrosis (*15*–*17*). Differences by geographic region are largely associated with environmental factors, such as greater amounts of water on land and in the lower level atmosphere (*14*–*16*), which probably contributes to increased environmental abundance

Table 4. Demographic and clinical characteristics of extrapulmonary nontuberculous mycobacteria cases among hospitalized patients from 82 hospitals, United States, 2009–2014*

Characteristics	Extrapulmonary NTM, no. (%), n = 831	Disseminated, no. (%), n = 246	SST, no. (%), n = 298	Other, no. (%), n = 264	Both, no. (%), n = 23
Patient characteristic					
Sex					
F	409 (49)	98 (40)	164 (55)	133 (50)	14 (61)
M	422 (51)	148 (60)	134 (45)	131 (50)	9 (39)
Race/ethnicity					
White	478 (58)	93 (38)	228 (77)	145 (55)	12 (52)
Black	269 (32)	138 (56)	38 (13)	83 (31)	10 (43)
Other	84 (10)	15 (6)	32 (11)	36 (14)	1 (4)
Age group, y					
≤18	91 (11)	13 (5)	43 (14)	35 (13)	0
>18–40	244 (29)	121 (49)	47 (16)	70 (27)	6 (26)
>40–60	266 (32)	86 (35)	93 (31)	78 (30)	9 (39)
>60	230 (28)	26 (11)	115 (39)	81 (31)	8 (35)
Ever had					
Fungal Infection	92 (11)	53 (22)	13 (4)	22 (8)	4 (17)
HIV infection	104 (13)	63 (26)	9 (3)	26 (10)	6 (26)
Invasive cardiac procedure	18 (2)	4 (2)	6 (2)	7 (3)	1 (4)
Cancer	31 (4)	11 (4)	9 (3)	11 (4)	0
Other immunologic disorder†	18 (2)	8 (3)	3 (1)	7 (3)	0
In-hospital death or discharged to hospice	47 (6)	29 (12)	5 (2)	12 (5)	1 (4)
Hospital characteristic					
Region					
South	375 (45)	147 (60)	94 (32)	125 (47)	9 (39)
Northeast	202 (24)	44 (18)	95 (32)	56 (21)	7 (30)
Midwest	200 (24)	44 (18)	88 (30)	64 (24)	4 (17)
West	54 (6)	11 (4)	21 (7)	19 (7)	3 (13)
Setting					
Urban	764 (92)	231 (94)	278 (93)	234 (89)	21 (91)
Rural	67 (8)	15 (6)	20 (7)	30 (11)	2 (9)
Teaching status‡					
Teaching facility	686 (83)	210(85)	247 (83)	209 (79)	20 (87)
Not teaching facility	112 (13)	30 (12)	35 (12)	209 (17)	3 (13)

*Data from in Cerner Health Facts database (https://sc-ctsi.org/resources/cerner-health-facts). Both, disseminated and SST infection; SST, skin and soft tissue.
†Antineoplastic and immunosuppressive drugs causing adverse effects in therapeutic use, autoimmune disease, not elsewhere classified, common variable immunodeficiency, encounter for antineoplastic immunotherapy, immunodeficiency with predominant T-cell defect, unspecified, other and unspecified nonspecific immunological findings, other specified disorders involving the immune mechanism, personal history of immunosuppression therapy, unspecified disorder of immune mechanism, unspecified immunity deficiency.
‡Status unknown for 33 patients.

of mycobacteria. In addition to higher levels of exposure to mycobacteria, studies have identified that these high-risk areas also tend to have a higher proportion of rapidly growing NTM species relative to MAC or other mycobacteria (*7*,*15*,*17*), which can result in more severe disease with limited effective treatment options (*3*).

Among extrapulmonary NTM cases, mycobacteria species also varied greatly by infection source and underlying condition. Although MAC infections were most frequent across all types of extrapulmonary NTM cases, in certain regions rapidly growing NTM play a substantial role in causing disease. Nearly all patients with HIV had MAC; those with a history of cancer were more likely to have rapidly growing NTM. Given that species of rapidly growing NTM, particularly *M. abscessus* and *M. fortuitum*, which were the most prevalent species in this study, are typically more challenging to treat than MAC, these findings have implications for the clinical management of these patients with complex infections and medical conditions. Co-infections were common among patients with extrapulmonary NTM, and ≥1 other pathogen was isolated from nearly half of all patients. Co-infections may complicate treatment-related decisions, particularly if mycobacteria, which are typically slow growing, are detected after other pathogens and are not treated with appropriate antimicrobial drug therapy.

Because we evaluated ≈9 million unique persons from 275 hospitals across the United States, we were able to identify key epidemiologic patterns for what is otherwise a very rare disease with limited population-level data. Because our analysis included only hospitalized patients, we probably overestimated the true incidence of extrapulmonary NTM disease

Table 5. Concomitant organisms isolated from hospitalized patients with extrapulmonary nontuberculous mycobacteria, overall and by source, United States, 2009–2014*

Genus	Total, no. (%)	Disseminated, no. (%)	SST, no. (%)	Both, no. (%)	Other, no. (%)
Acinetobacter	9 (3)	5 (5)	2 (2)	0	2 (2)
Aeromonas	3 (0.9)	0	1 (1)	0	2 (2)
Aspergillus	7 (2)	2 (2)	3 (3)	0	2 (2)
Bacillus	15 (4)	5 (5)	5 (5)	1 (7)	4 (3)
Candida	80 (23)	26 (25)	22 (20)	1 (7)	31 (26)
Clostridium	9 (3)	4 (4)	2 (2)	0	3 (3)
Coccidioides	2 (0.6)	1 (1)	0	0	1 (1)
Corynebacterium	31 (9)	8 (8)	13 (12)	0	10 (8)
Cryptococcus	6 (2)	4 (4)	1 (1)	0	1 (1)
Enterobacter	13 (4)	1 (1)	6 (5)	0	6 (5)
Enterococcus	75 (21)	27 (26)	25 (23)	5 (36)	18 (15)
Escherichia coli	43 (12)	11 (11)	11 (10)	1 (7)	20 (17)
Klebsiella	32 (9)	5 (5)	13 (12)	1 (7)	13 (11)
Mycobacterium tuberculosis	68 (19)	16 (15)	18 (16)	5 (36)	29 (24)
Pseudomonas	55 (16)	16 (15)	17 (15)	0	22 (18)
Salmonella	2 (0.6)	0	1 (1)	0	1 (1)
Staphylococcus	112 (32)	35 (33)	44 (40)	4 (29)	29 (24)
Stenotrophomonas	11 (3)	4 (4)	3 (3)	1 (7)	3 (3)
Streptococcus	58 (17)	21 (20)	13 (12)	0	24 (20)
Total patients with co-infection	350	105 (30)	111 (32)	14 (4)	120 (34)

*Data from in Cerner Health Facts database (https://sc-ctsi.org/resources/cerner-health-facts). Both, disseminated and SST infection; SST, skin and soft tissue.

in the general population by selecting for generally sicker patients with more severe underlying disease. We may have missed less severe SST infections that did not require extensive treatment or hospital intervention. Because the hospitals included here represent only those that use the Cerner Health Facts system, this study does not include patients at other facilities, which may also affect our incidence calculations. Similarly, not captured here were surgeries, procedures, or prior medical events that occurred in other facilities, which may be associated with risk, infection type, and outcome. However, these limitations would be applied systematically to the entire study population and therefore would probably not alter the geographic or temporal patterns that we found.

Overall, extrapulmonary NTM disease remains rare with relatively stable incidence rates for disseminated NTM infections and modestly increased rates for SST infections. In similar studies assessing pulmonary NTM, rates appear to be steadily increasing in the general population and among high-risk groups such as persons with cystic fibrosis (*8*,*17*). Patients with extrapulmonary NTM

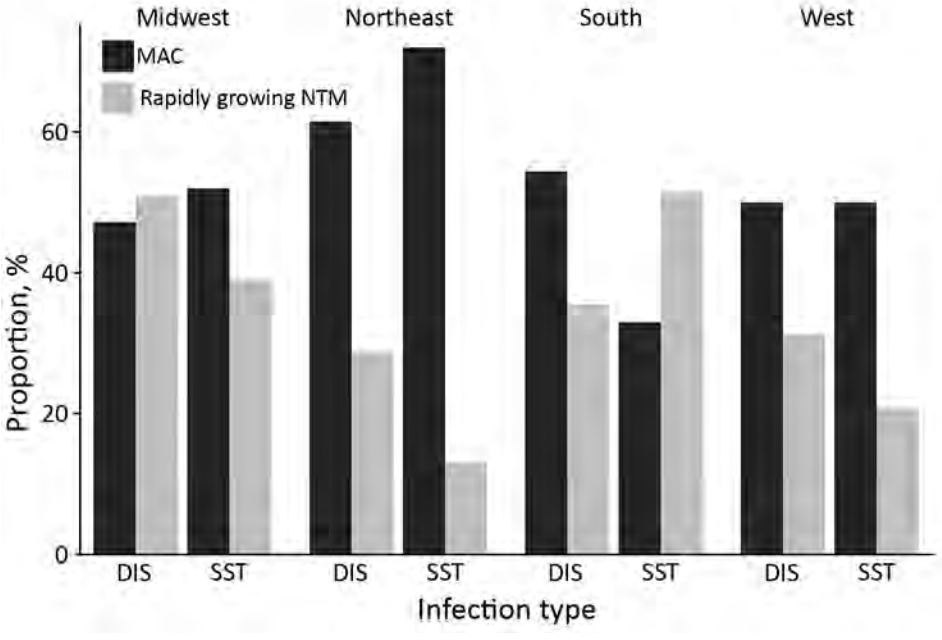

Figure 2. Distribution of extrapulmonary NTM cases by species and infection type across regions among hospitalized patients in the United States, 2009–2014. DIS, disseminated; NTM, nontuberculous mycobacteria; MAC, Mycobacterium avium complex; SST, skin and soft tissue.

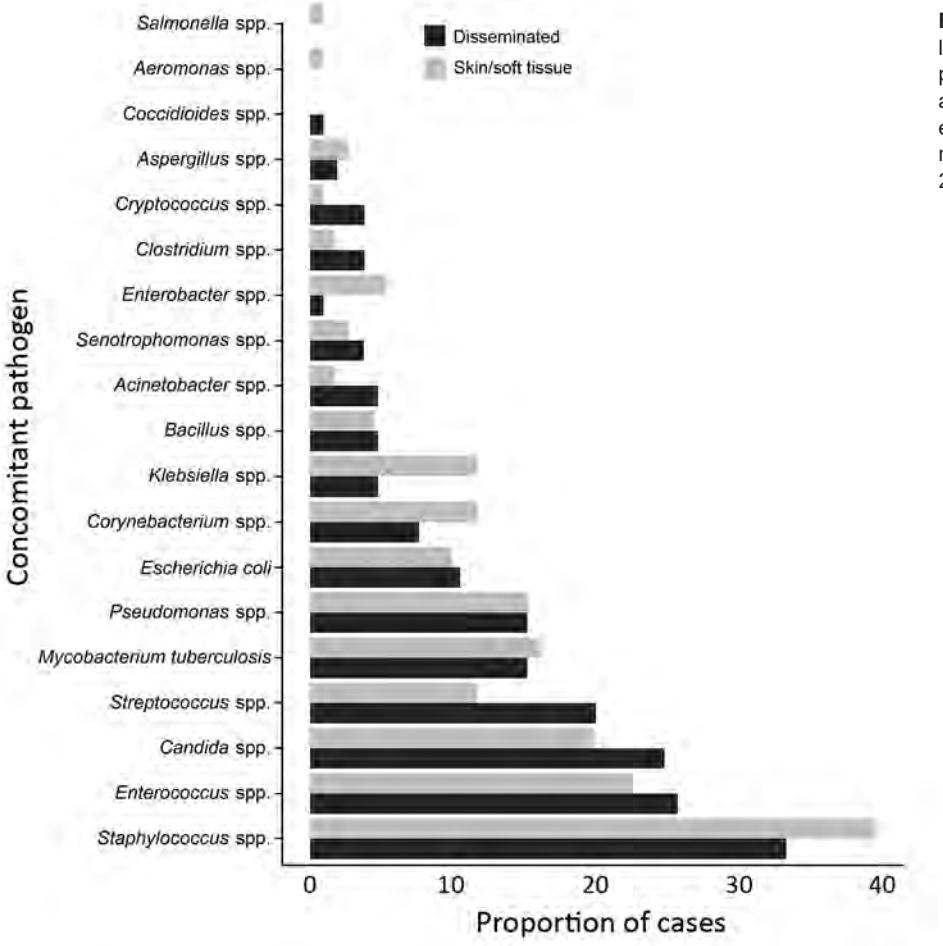

Figure 3. Distribution of laboratory-confirmed concomitant pathogens by infection type among hospitalized patients with extrapulmonary nontuberculous mycobacteria, United States, 2009–2014.

typically include persons with HIV, other underlying immunodeficiencies, histories of surgical procedures, or other unique exposures that increase the risk for infection. In addition, we found that species variability is associated with geographic region; rapidly growing NTM are more prevalent in the southern United States than in other regions. Given the added treatment challenges that exist for these patients with often-complex conditions, knowledge of key trends and risks by patient-level factors and geographic location is critical for improving clinical outcomes and determining sources of infections that may be common to patients with pulmonary and extrapulmonary NTM.

This work was supported by the Division of Intramural Research, National Institute of Allergy and Infectious Diseases, National Institutes of Health.

About the Author

Dr. Ricotta is a research fellow in the Epidemiology Unit, Division of Intramural Research, National Institute of Allergy and Infectious Diseases, National Institutes of Health. Her research focuses on studying the epidemiology of rare infectious diseases.

References

1. Falkinham JO III. Nontuberculous mycobacteria in the environment. Clin Chest Med. 2002;23:529–51. https://doi.org/10.1016/S0272-5231(02)00014-X
2. Falkinham JO III. Nontuberculous mycobacteria from household plumbing of patients with nontuberculous mycobacteria disease. Emerg Infect Dis. 2011;17:419–24. https://doi.org/10.3201/eid1703.101510
3. Griffith DE, Aksamit T, Brown-Elliott BA, Catanzaro A, Daley C, Gordin F, et al.; ATS Mycobacterial Diseases Subcommittee; American Thoracic Society; Infectious Disease Society of America. An official ATS/IDSA statement: diagnosis, treatment, and prevention of nontuberculous mycobacterial diseases. Am J Respir Crit Care Med. 2007;175:367–416. https://doi.org/10.1164/rccm.200604-571ST
4. Henkle E, Hedberg K, Schafer SD, Winthrop KL. Surveillance of extrapulmonary nontuberculous mycobacteria infections, Oregon, USA, 2007–2012. Emerg Infect Dis. 2017;23:1627–30. https://doi.org/10.3201/eid2310.170845
5. Piersimoni C, Scarparo C. Extrapulmonary infections associated with nontuberculous mycobacteria in

immunocompetent persons. Emerg Infect Dis. 2009;15:1351–8. https://doi.org/10.3201/eid1509.081259
6. Lyman MM, Grigg C, Kinsey CB, Keckler MS, Moulton-Meissner H, Cooper E, et al. Invasive nontuberculous mycobacterial infections among cardiothoracic surgical patients exposed to heater–cooler devices. Emerg Infect Dis. 2017;23:796–805. https://doi.org/10.3201/eid2305.161899
7. Spaulding AB, Lai YL, Zelazny AM, Olivier KN, Kadri SS, Prevots DR, et al. Geographic distribution of nontuberculous mycobacterial species identified among clinical isolates in the United States, 2009-2013. Ann Am Thorac Soc. 2017;14:1655–61. https://doi.org/10.1513/AnnalsATS.201611-860OC
8. Adjemian J, Olivier KN, Seitz A, Holland S, Prevots R. Prevalence of pulmonary nontuberculous mycobacterial infections among U.S. Medicare beneficiaries, 1997–2007. Am J Respir Crit Care Med. 2012;85:881–6.
10. Wi YM. Treatment of extrapulmonary nontuberculous mycobacterial diseases. Infect Chemother. 2019;51:245–55. https://doi.org/10.3947/ic.2019.51.3.245
11. Wentworth AB, Drage LA, Wengenack NL, Wilson JW, Lohse CM. Increased incidence of cutaneous nontuberculous mycobacterial infection, 1980 to 2009: a population-based study. Mayo Clin Proc. 2013;88:38–45. https://doi.org/10.1016/j.mayocp.2012.06.029
12. Shih DC, Cassidy PM, Perkins KM, Crist MB, Cieslak PR, Leman RL. Extrapulmonary nontuberculous mycobacterial disease surveillance—Oregon, 2014–2016. MMWR Morb Mortal Wkly Rep. 2018;67:854–7. https://doi.org/10.15585/mmwr.mm6731a3
13. Smith GS, Ghio AJ, Stout JE, Messier KP, Hudgens EE, Murphy MS, et al. Epidemiology of nontuberculous mycobacteria isolations among central North Carolina residents, 2006–2010. J Infect. 2016;72:678–86. https://doi.org/10.1016/j.jinf.2016.03.008
14. Adjemian J, Olivier KN, Seitz AE, Falkinham JO III, Holland SM, Prevots DR. Spatial clusters of nontuberculous mycobacterial lung disease in the United States. Am J Respir Crit Care Med. 2012;186:553–8. https://doi.org/10.1164/rccm.201205-0913OC
15. Adjemian J, Olivier K, Prevots DR. Nontuberculous mycobacteria among cystic fibrosis patients in the United States: screening practices and environmental risk. Am J Respir Crit Care Med. 2014;190:581–6. https://doi.org/10.1164/rccm.201405-0884OC
16. Bouso JM, Burns JJ, Amin R, Livingston FR, Elidemir O. Household proximity to water and nontuberculous mycobacteria in children with cystic fibrosis. Pediatr Pulmonol. 2017;52:324–30. https://doi.org/10.1002/ppul.23646
17. Adjemian J, Olivier KN, Prevots DR. Epidemiology of pulmonary nontuberculous mycobacterial sputum positivity in patients with cystic fibrosis in the United States, 2010–2014. Ann Am Thorac Soc. 2018;15:817–26. https://doi.org/10.1513/AnnalsATS.201709-727OC

Address for correspondence: Emily Ricotta, National Institute of Allergy and Infectious Diseases, National Institutes of Health, 5601 Fishers Ln, 7D18, Rockville, MD 20852, USA; email: emily.ricotta@nih.gov

Genomic Characterization of *hlyF*-positive Shiga Toxin–Producing *Escherichia coli*, Italy and the Netherlands, 2000–2019

Federica Gigliucci, Angela H.A.M. van Hoek, Paola Chiani, Arnold Knijn, Fabio Minelli, Gaia Scavia, Eelco Franz, Stefano Morabito, Valeria Michelacci

Shiga toxin–producing *Escherichia coli* (STEC) O80:H2 has emerged in Europe as a cause of hemolytic uremic syndrome associated with bacteremia. STEC O80:H2 harbors the mosaic plasmid pR444_A, which combines several virulence genes, including *hlyF* and antimicrobial resistance genes. pR444_A is found in some extraintestinal pathogenic *E. coli* (ExPEC) strains. We identified and characterized 53 STEC strains with ExPEC-associated virulence genes isolated in Italy and the Netherlands during 2000–2019. The isolates belong to 2 major populations: 1 belongs to sequence type 301 and harbors diverse stx_2 subtypes, the intimin variant *eae*-ξ, and pO157-like and pR444_A plasmids; 1 consists of strains belonging to various sequence types, some of which lack the pO157 plasmid, the locus of enterocyte effacement, and the antimicrobial resistance–encoding region. Our results showed that STEC strains harboring ExPEC-associated virulence genes can include multiple serotypes and that the pR444_A plasmid can be acquired and mobilized by STEC strains.

Shiga toxin–producing *Escherichia coli* (STEC) is a group of enteric pathogens that cause foodborne disease ranging from uncomplicated diarrhea to hemorrhagic colitis (HC) or hemolytic uremic syndrome (HUS) (*1*). The most serious complication of STEC infection is HUS, which can be fatal.

STEC strains produce Shiga toxins (Stx), a family composed of 2 main types of cytotoxins: Stx1 and Stx2 (*2*). Stx1 is classified into subtypes a, c, and d; Stx2 is classified into subtypes a–k (*3*–*6*). Lysogenic bacteriophages harbor the genes for different types of Stx; infected bacteria then produce the protein (*7*). Although the production of Stx plays a central role in the pathogenesis of STEC-associated illness, the development of HC and HUS requires an efficient host colonization by the infecting STEC. Many HUS-associated STEC strains possess a chromosomal pathogenicity island, defined as the locus of enterocyte effacement (LEE), which is associated with the attaching and effacing lesions (*8*) described in enteropathogenic *E. coli* (*9*), or possess the genetic machinery conferring the enteroaggregative pattern of adhesion to the enterocyte described in enteroaggregative *E. coli* (*10*,*11*). Other STEC strains harbor colonization factors of enterotoxigenic *E. coli* (*12*,*13*) and genes encoding virulence features associated with extraintestinal pathogenic *E. coli* (ExPEC) (*14*,*15*). The ExPEC-associated virulence genes code for aerobactin (encoded by *iucC*), salmochelin (*iroN*), serum resistance protein (*iss*), a putative secretion system I (*etsABC*), omptin (*ompT*), hemolysin (*hlyF*), and bacteriocins (*cia* and *cva*) (*14*,*15*).

STEC strains belonging to the O157, O26, O103, O111, and O145 serogroups are considered critical public health concerns. Nevertheless, since 2015, other STEC serogroups have been increasingly associated with HUS and other infections in humans (*16*). Among these, O80 is emerging in Europe (*17*–*21*); since 2015, it has become a predominant serogroup associated with HUS in children in France (*22*). In addition to the typical clinical features of a STEC infection, bacteremia can develop in patients with STEC O80 (*19*,*23*).

Virulence genes increase the pathogenicity of STEC strains. For example, the strains associated with HUS are characterized by specific subtypes of the stx_2 gene, mainly stx_{2a}, stx_{2c}, and stx_{2d} (*24*). In 2020, experts proposed a new approach to categorizing STEC

Author affiliations: Istituto Superiore di Sanità, Rome, Italy (F. Gigliucci, P. Chiani, A. Knijn, F. Minelli, G. Scavia, S. Morabito, V. Michelacci); National Institute for Public Health and the Environment, Bilthoven, the Netherlands (A.H.A.M. van Hoek, E. Franz)

DOI: https://doi.org/10.3201/eid2703.203110

infections on the basis of virulence genes (*24*). STEC O80 strains possess virulence genes carried by mobile genetic elements associated with intestinal and extraintestinal pathogenic *E. coli* (*14*). Such strains harbor the LEE locus, the stx_2 gene, and a plasmid resembling the pO157 first described in STEC O157 serogroup carrying virulence genes including the enterohemolysin encoding gene (*ehxA*) (*25*,*26*). In addition, these strains often possess a peculiar mosaic plasmid called pR444_A. This pS88-like plasmid was first described in a STEC O80 strain isolated from a HUS patient with bacteremia in France (*14*). The pR444_A plasmid combines virulence genes of ExPEC strain S88, including the *hlyF*, *iro(BCDEN)*, *iss*, and *ompT* genes, with multiple antimicrobial resistance (AMR) determinants (*14*,*27*–*31*). The *hlyF* gene is associated with an increased production of outer membrane vesicles, possibly contributing to the release of cytolethal distending toxin and other chemicals involved in ExPEC pathogenesis (*32*).

Little data exist on the circulation of STEC strains harboring ExPEC-associated virulence traits. Infections from such pathogens rarely have been described outside France, except for 1 report about severe HUS caused by an O80:H2 strain in the Netherlands (*18*). We characterized the genomes of STEC strains with ExPEC-associated virulence traits isolated from infected patients and contaminated food in Italy and the Netherlands. We accessed these genomes through the Istituto Superiore di Sanità (Rome, Italy) and the National Institute for Public Health and the Environment (Bilthoven, the Netherlands). To infer population structure, we conducted a phylogenetic comparison of an additional 50 genomes of STEC strains with ExPEC-associated features from GenBank and RefSeq (https://www.ncbi.nlm.nih.gov/RefSeq).

Material and Methods

Bacterial Strains

For this study, we used STEC strains from the culture collections at the Istituto Superiore di Sanità and the National Institute for Public Health and the Environment. We investigated 500 STEC strains isolated in Italy during 2000–2019 by the National Reference Laboratory for *E. coli* as part of the national surveillance program for HUS and samples isolated from animal and food products in the framework of the official control activity. We also investigated 884 STEC strains isolated in the Netherlands from clinical samples collected during 2017–2019 as part of the surveillance for human STEC infections in the Netherlands.

Whole-Genome Sequencing

We extracted the total DNA of the STEC strains from Italy from 2 mL of overnight culture of each strain grown in TSB at 37°C with the E.Z.N.A. Bacterial DNA kit (Omega Bio-tek, Inc., https://www.omegabiotek.com). We prepared sequencing libraries of ≈400 bp from 100 ng of total DNA using the NEBNext Fast DNA Fragmentation & Library Prep Set for Ion Torrent (New England BioLabs, https://www.neb.com). We amplified and enriched the libraries through emulsion PCR using the Ion OneTouch 2 System (Thermo Fisher Scientific, https://www.thermofisher.com) and sequenced on an Ion Torrent S5 platform (Thermo Fisher Scientific, https://www.thermofisher.com) using the ION 520/530 KIT-OT2 (Thermo Fisher Scientific) according to the manufacturer's instructions for 400 bp DNA libraries on ION 530 chips.

We generated cell pellets of the STEC strains from the Netherlands using 1.8 mL of overnight culture of each strain grown in brain heart infusion broth (Thermo Fisher Scientific) at 37°C. We resuspended the pellets in DNA/RNA Shield (Zymo Research, https://www.zymoresearch.com) and sent them to BaseClear (https://www.baseclear.com) for DNA isolation and whole-genome sequencing. The BaseClear service generated paired-end 2 × 150 bp short-reads using a Nextera XT library preparation (Illumina, Inc., https://www.illumina.com) and sequenced the libraries on the HiSeq 2500 or NovaSeq 6000 systems (Illumina, Inc.). All the genomic sequences are available at the European Nucleotide Archive at the European Molecular Biology Laboratory (accession nos. PRJEB38068 and PRJEB38651).

Bioinformatic Analysis

We conducted the bioinformatic analyses for the characterization of the genomes using the tools on the Galaxy public server ARIES (Istituto Superiore di Sanità, https://www.iss.it/site/aries) (A. Knijn, unpub. data, https://www.biorxiv.org/content/10.1101/2020.05.14.095901v1). We assembled the single-end reads from the Ion Torrent S5 platform using SPADES version 3.12.0 with default parameters (*33*) and filtered with the Filter SPAdes repeats tool (https://github.com/phac-nml/galaxy_tools) with default parameters to remove the contigs that were repeated or <1,000 bases. We trimmed the paired-end reads, filtered them with the Extended Randomized Numerical alignEr–filter (*34*), and assembled them de novo by using SPAdes version 3.10.0 (*33*).

Basic Characterization of STEC Strains

We conducted multilocus sequence typing by using the MentaLiST tool version 0.2.3 (*35*), applying the scheme developed by Wirth et al. (*36*). We determined the virulence gene content of the STEC genomes and then identified the intimin gene (*eae*) subtype with the Patho_typing tool (https://github.com/B-UMMI/patho_typing) developed by the INNUENDO project (*37*) using the *E. coli* virulence genes database (*38*). We analyzed the assembled contigs with BLAST (http://blast.ncbi.nlm.nih.gov/Blast.cgi) and the blastn algorithm version 2.7.1. We determined the serotype by aligning the contigs with the reference sequences for the O and H antigen genes (*39*). We also used BLAST to identify the Stx subtype with the Statens Serum Institut Shiga toxin subtypes database (https://bitbucket.org/genomicepidemiology/virulencefinder_db/src/master/stx.fsa). We conducted phylogrouping using a blastn search of the specific genes (*40*) on the contigs.

Characterization of STEC Strains Harboring ExPEC Virulence Genes

We used the *hlyF* gene as a putative marker for the pR444_A plasmid (*14*). We searched the assembled genomes for the *hlyF* gene (RefSeq accession no. NC_011980.1). We screened the *hlyF*-positive strains for antimicrobial and virulence genes associated with pR444_A using the ABRicate tool (https://github.com/tseemann/abricate).

We used PCR to confirm the presence of the *hlyF* gene in the strains from Italy, as described by Dissanayake et al. (*41*). We also investigated the presence of the pR444_A plasmid using the BRIG tool version 0.95 (http://brig.sourceforge.net) by aligning the contigs on the reference sequence from pR444_A (RefSeq accession no. NZ_QBDM01000004.1). In addition, we conducted the conjugation experiment among donor ED1284 and recipient CSH26Nal strains. We used streptomycin (10 μg/mL) as a selective agent for the pR444_A plasmid and nalidixic acid (10 μg/mL) for the recipient strain. We confirmed the colonies to be transconjugants with PCR selective for the *hlyF*, *traT*, *iroN*, *cvaC*, *iss*, and *ompT* genes. We also plated the colonies on Müller-Hinton agar plates containing trimethoprim (2 μg/mL), MacConkey plates to differentiate donor (*lac*+) and recipient (*lac*–) strains, and LB plates containing ampicillin (100 μg/mL), kanamycin (40 μg/mL), tetracycline (100 μg/mL), or sulfonamide (100 μg/mL).

Cluster Analysis

To identify additional STEC strains with ExPEC-associated virulence features, we conducted a blastn search in GenBank and RefSeq for genomes positive for either *stx* (using the *stx*-subtypes sequence database) or *hlyF* (accession no. NC_011980.1) genes. We included these genomes in a cluster analysis along with the *hlyF*-positive STEC genomes produced in the current study. We carried out the analysis with core genome multilocus sequence typing (cgMLST) using the chewBBACA tool and the scheme developed by the INNUENDO project, which comprises 2,360 loci in total (*37*,*42*).

We considered the pairwise comparison to be reliable when ≥80% of loci were assigned to an allele. We calculated the distances between strains by pairwise comparison of the allelic profiles using the chewTree tool available on ARIES webserver (A. Knijn, unpub. data, https://www.biorxiv.org/content/10.1101/2020.05.14.095901v1). For each pair of samples, we excluded the alleles not found, only partially found, or not correctly assigned to any locus. We visualized the resulting dendrogram with FigTree version 1.4.4 (https://github.com/rambaut/figtree/releases).

Results

Circulating STEC Strains with ExPEC-Associated Virulence Genes

The analyzed sequences had an average coverage of 118× and the assembled contigs an N50 average of 94,346 bp (Appendix 1 Table 1, https://wwwnc.cdc.gov/EID/article/27/3/20-3110-App1.pdf). Screening for the *hlyF* gene suggested the presence of the pR444_A plasmid in 53 (3.8%) of 1,384 STEC genomes (Appendix 1 Table 2). Of the 53 *hlyF*-positive strains, 30 had been isolated in Italy, mostly from patients with HUS or severe HC. Two were from food products of bovine origin in Italy (Appendix 1 Table 2). The remaining 23 STEC strains had been isolated from patients in the Netherlands, some of whom had diarrhea or bloody diarrhea and some of whom were hospitalized (Appendix 1 Table 2).

Genomic Characterization of *hlyF*-Positive STEC Strains

The genomic analysis revealed that the 53 *hlyF*-positive STEC strains belonged to 10 different serotypes; O80:H2 was the most common (Appendix 1 Table 2). Most of the strains harbored the genes encoding the flagellar antigen H2, including 33 O80:H2 strains, 3 O186:H2 strains, and 4 O45:H2 strains (Appendix 1 Table 2). Two *hlyF*-positive STEC strains belonged to serotype O26:H11, one of the most common causes of HUS in Italy (*43*).

In silico MLST showed that ST301 was the most abundant sequence type (ST) (41/53; 77.4%) (Appendix 1 Table 2). Strains of 4 different serotypes belonged to ST301: 33 O80:H2 strains, 4 O45:H2 strains, 3 O186:H2 strains, and 1 O55:H9 strain. Two STEC O26:H11 strains belonged to ST21; the 10 remaining strains belonged to 6 other STs (Appendix 1 Table 2). All the strains belonged to the B1 phylogroup, except for 1 strain belonging to the B2 phylogroup and 3 strains whose phylogroup could not be identified (Appendix 1 Table 2).

In total, 49 strains tested positive for the stx_2 gene and 4 for stx_1 (Appendix 1 Table 2). The stx_2 gene subtyping revealed stx_{2a}, stx_{2b}, stx_{2d}, stx_{2e}, and stx_{2f} subtypes: stx_{2a} was the most common. All stx_1 genes were stx_{1a} (Appendix 1 Table 2).

The 41 ST301 and 2 O26:H11 ST21 strains also harbored genes such as *ehxA* that are commonly found on pO157-like plasmids. In addition, they also tested positive for the intimin-coding *eae* gene, which indicates the presence of the LEE locus (Appendix 1 Table 2). All 41 ST301 genomes, regardless of serotype, carried the rare *eae-ξ* variant (Appendix 1 Table 2). The remaining 10 *hlyF*-positive strains tested negative for pO157-like plasmid genes and the LEE locus, except for strain NL1701358, which had the LEE locus with the *eae-λ3* variant. The NL1700566, NL1701474, NL1800025, and NL1800037 strains also carried the *hlyA* gene (data not shown), which encodes α-hemolysin (HlyA), a pore-forming toxin found in ExPEC strains that cause urinary tract infection (*44*,*45*).

In addition to *hlyF*, the pR444_A plasmid also contains other virulence-associated genes such as *ompT*, *iss*, the *iroBCDEN* gene cluster, and a gene cassette that encodes determinants of AMR (*14*). The *hlyF*- positive STEC strains identified in this study carried many of these virulence determinants (Appendix 1 Table 2), suggesting the presence of a similar plasmid. Most *hlyF*-positive strains also had an AMR-encoding region (Appendix 1 Table 3). The alignment of the contigs on the pR444_A sequence further confirmed the presence of pR444_A–like plasmids in most *hlyF*-positive strains, regardless of country of isolation (Figures 1, 2). In most strains, we could not identify the regions of the pR444_A plasmid that harbor the *iucABCD* and *etsABC* genes. We conducted conjugation experiments to confirm the presence of

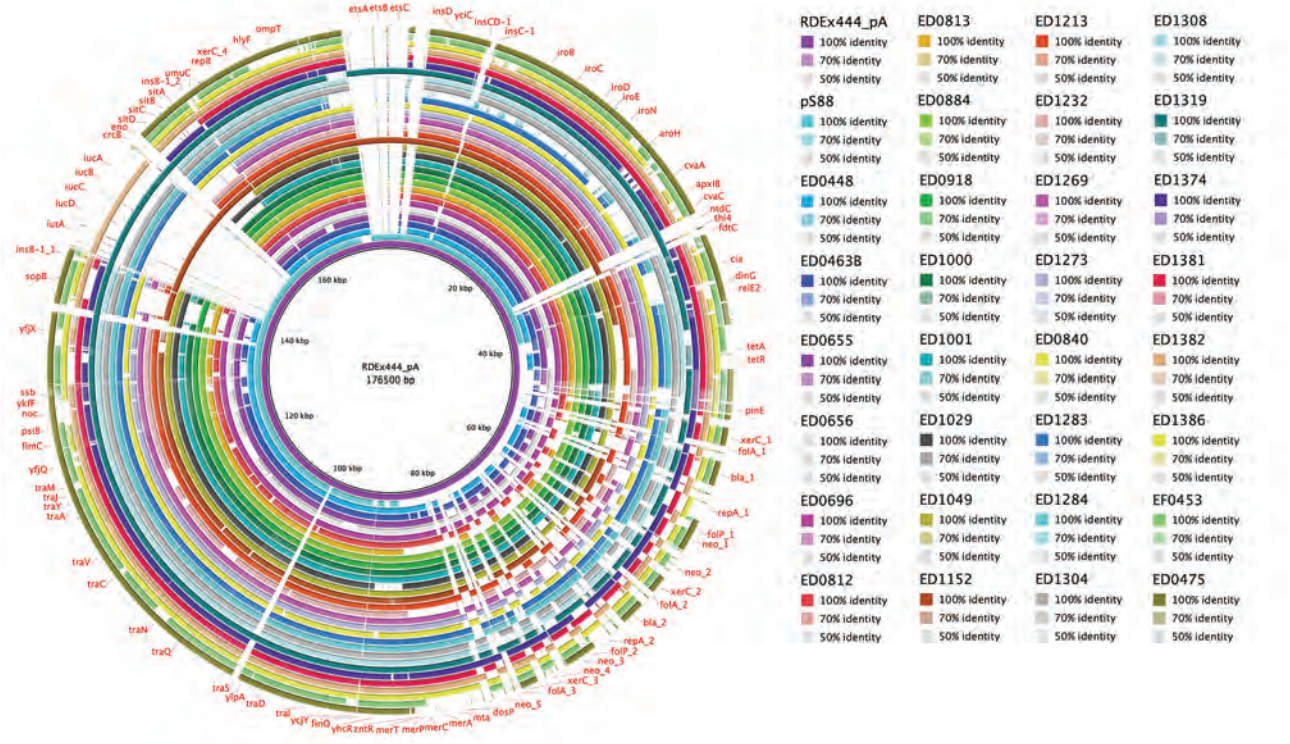

Figure 1. Whole-genome comparison of pR444_A–like plasmids in Shiga toxin–producing *Escherichia coli* strains harboring extraintestinal pathogenic *E. coli* (ExPEC)–associated virulence genes, Italy, 2000–2019. The pR444_A plasmid from RDEx444 strain was used as reference for alignment and gene annotation. Genomic annotation was performed by using the Prokka tool 1.14.5 (https://github.com/tseemann/prokka) and a multi-fasta file of trusted proteins related to ExPEC-associated genes on pR444_A. The comparative analysis also included the pS88 plasmid (GenBank accession no. CU928146.1) commonly found in ExPEC strains.

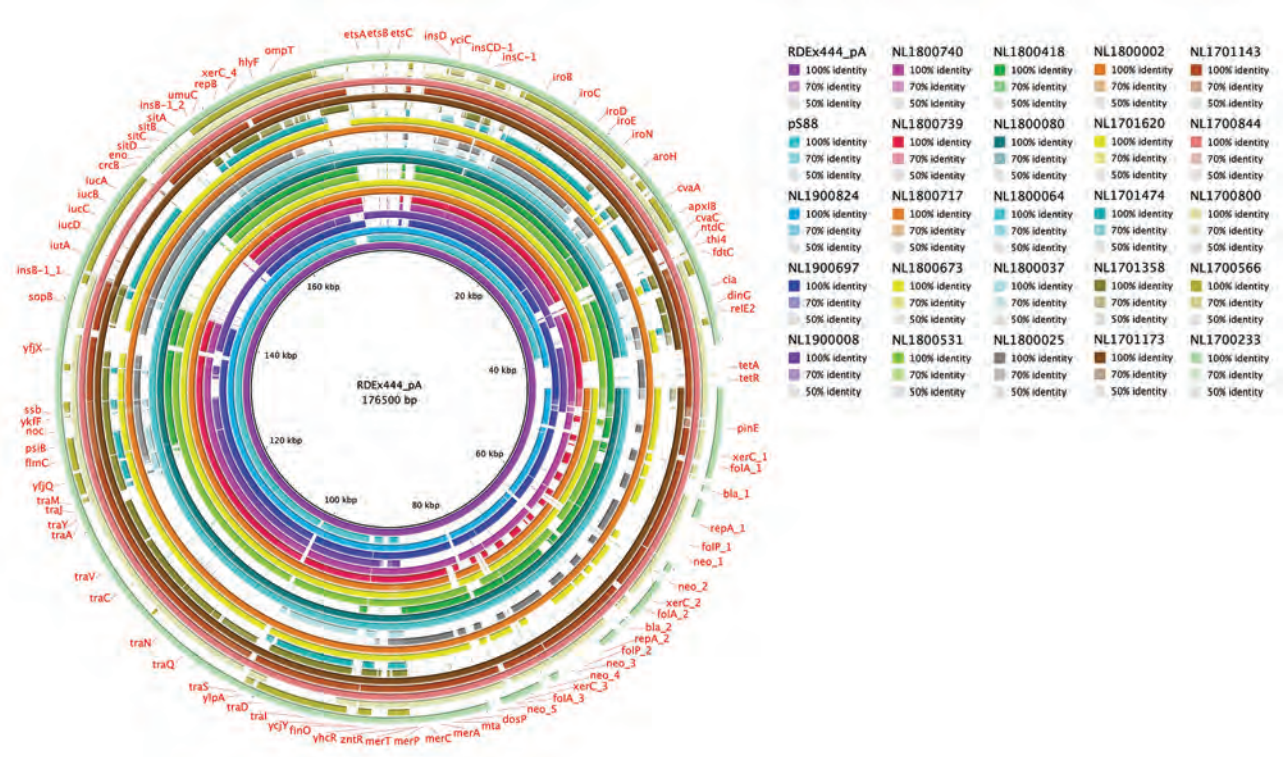

Figure 2. Whole-genome comparison of pR444_A–like plasmids in Shiga toxin–producing *Escherichia coli* strains harboring extraintestinal pathogenic *E. coli* (ExPEC)–associated virulence genes, the Netherlands, 2017–2019. The pR444_A plasmid from the RDEx444 strain was used as reference for alignment and gene annotation. Genomic annotation was performed with the Prokka tool 1.14.5 (https://github.com/tseemann/prokka) and a multi-fasta file of trusted proteins related to ExPEC-associated genes on pR444_A. The comparative analysis also included the pS88 plasmid (accession no. CU928146.1) commonly found in ExPEC strains.

a transferable pR444_A–like plasmid in the O26:H11 strain ED1284. After the mating, we observed that the *hlyF*, *iroN*, *cvaC*, *iss*, *traT*, and *ompT* genes were successfully transferred to the recipient K12 strain along with the cassette conferring resistance to streptomycin, ampicillin, sulfonamide, and trimethoprim.

Phylogenetic Analysis of STEC Strains with ExPEC-Associated Virulence Genes

We conducted a whole-genome comparison; we included the STEC O80:H2 strain RDEx444 isolated in France (*14*) as reference strain, and 2 *hlyF*-negative STEC O80:H2 strains, ED0867 and ED1301, which were isolated in Italy, for comparative purposes. To more broadly analyze the population structure, we also included 50 *hlyF*-positive STEC strains retrieved from GenBank and RefSeq (Appendix 1 Tables 4, 5). Then, we computed the number of allelic differences between strains (Appendix 2 Table, https://wwwnc.cdc.gov/EID/article/27/3/20-3110-App2.xlsx).

The results of the cluster analysis clearly distinguished the strains belonging to ST301 (Figure 3). The strains belonging to serotype O80:H2 were related, showing a range of 2–210 allelic differences (Appendix 2 Table). The strains harboring the stx_{2d} subtype, regardless of country origin, also were related (Figure 3). The branch containing the ST301 strains was divided into subclades corresponding to serotype (Figure 3). Among the ST301 strains, the O55:H9 EF0475 and O45:H2 strains were located close to the O80:H2 population, with a range of 58–219 allelic differences (Appendix 2 Table). The remaining genomes displayed >1,400 allelic differences from the ST301 strains (Appendix 2 Table).

Discussion

E. coli bacteria continually acquire and lose genomic information carried by mobile genetic elements through horizontal gene transfer. This process contributes to the emergence of pathogenic *E. coli* variants. Horizontal gene transfer also can occur between pathogenic *E. coli* variants, producing hybrid pathogenic strains. Some STEC hybrid strains are highly virulent, such as enteroaggregative STEC serotype O104:H4, which caused one of the most severe STEC outbreaks ever reported (*46*).

Extraintestinal STEC serotype O80:H2 is a serious threat to public health. This hybrid clone was described in France in 2005 (*19*). Since then, extraintestinal STEC O80 strains have caused cases of severe HUS associated with bacteremia (*19*,*22*,*23*). In 2017, an O80:H2 strain caused a severe case of HUS with multiorgan failure in the Netherlands (*18*). Other cases of STEC O80:H2 infection have occurred in Switzerland and Belgium (*20*,*21*).

In this study, we demonstrated that genetic features associated with STEC and ExPEC strains are not restricted to the O80:H2 serotype. The STEC strains presenting ExPEC-associated virulence genes investigated in this study belonged to 10 different serotypes, with a high prevalence of O80:H2. We also identified 5 additional serotypes from the genomes available in GenBank and RefSeq. Most of the strains in

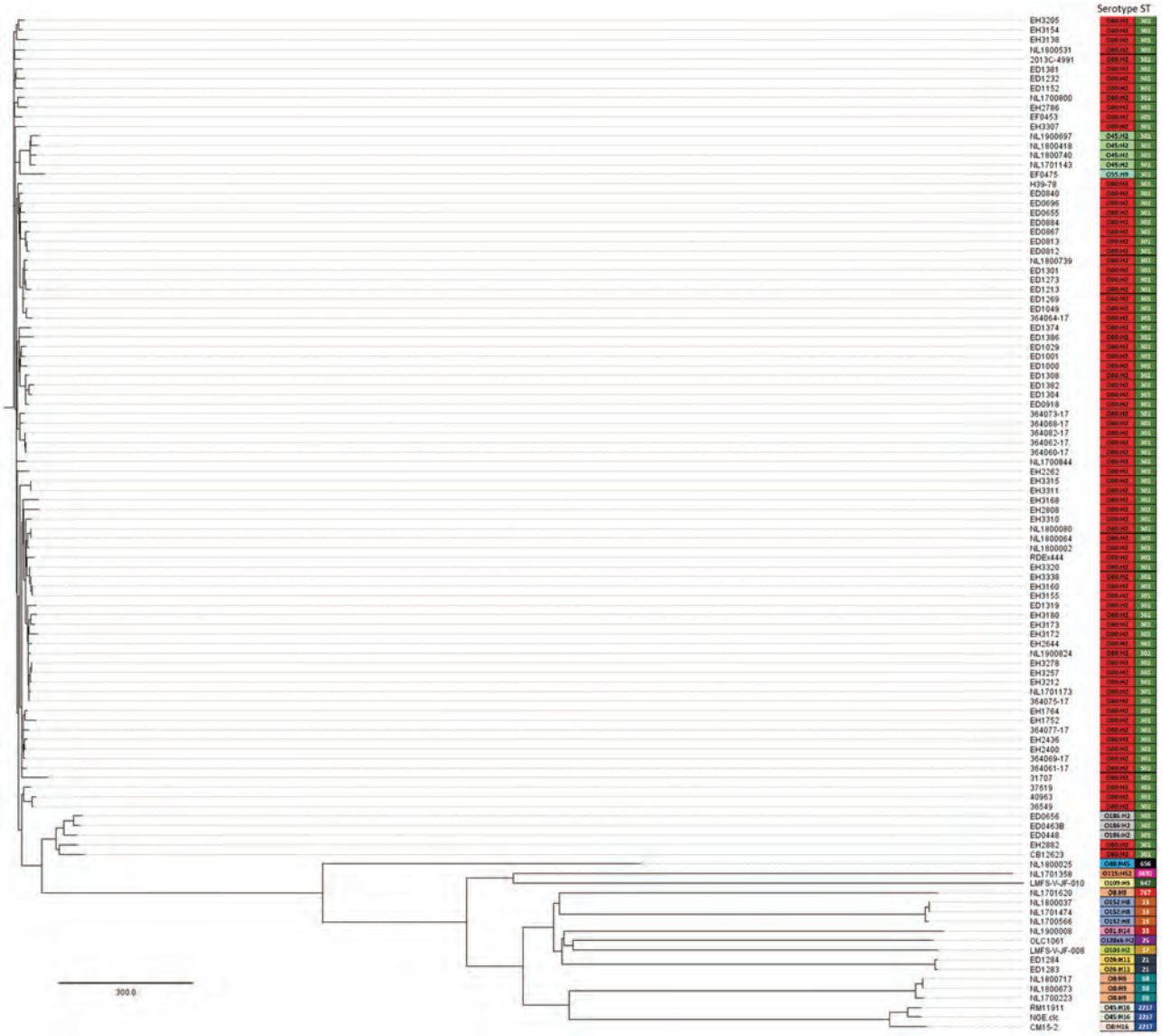

Figure 3. Cluster analysis by core genome multilocus sequence typing of Shiga toxin–producing *Escherichia coli* strains harboring extraintestinal pathogenic *E. coli*–associated virulence genes. The analysis also included the RDEx444 strain from France; 2 Shiga toxin–producing *E. coli* O80:H2 strains negative for the pR444_A plasmid (i.e., ED0867 and ED1301); and the set of 50 *E. coli* genomes positive either for *stx* or *hlyF* genes, downloaded from GenBank or RefSeq (www.ncbi.nlm.nih.gov/RefSeq). Each entry on the phylogenetic tree indicates the strain name, corresponding serotype, and sequence type. Colors indicates serotype and sequence type. Scale bar indicates the number of allelic differences.

this study, regardless of serogroup, were of ST301; had the flagellar antigen H2; and harbored the stx_2, *eae-ξ*, and *ehxA* genes (Appendix 1 Table 2). This genetic homogeneity seems to extend beyond the presence of these genes; cgMLST showed that the ST301 genomes were related. The ST301 strains formed subclades corresponding to serotype and *stx* subtype (Figure 3). The stx_{2d}–positive RDEx444 strain isolated in France in 2016 clustered with strains of the same *stx* subtype isolated in Italy and the Netherlands during 2016–2019, and in Belgium and Switzerland during 2015–2019, suggesting a spatiotemporal persistence of this clade in the last decade.

The phylogenetic analysis highlighted that the O80:H2, O45:H2, and O55:H9 genomes were closely related (Appendix 2 Table). These genomes also shared a clade with the 2 STEC O80:H2 strains that tested negative for pR444_A. This finding suggests that the pR444_A plasmid was acquired before these different serotypes diverged from a common ancestor of ST301. It is also possible that this plasmid was acquired in multiple events during the evolution of these serotypes; however, the presence of the rare *eae-ξ* gene in all these serotypes suggests that the plasmid was probably acquired in a single event.

The genomic analysis also revealed that the *hlyF*-positive STEC O26:H11 strains were distantly related to the other *hlyF*-positive STEC ST301 strains (Figure 3). These isolates resembled typical STEC O26:H11 strains because they possessed the *eae-β1* variant (Appendix 1 Table 2) and a pO157-like plasmid harboring the *katP* gene (not shown), which is not found on the pO157-like plasmid found in ST301 strains (*14*). STEC O26:H11 strain ED1284 successfully transferred the pR444_A plasmid through conjugation, indicating that STEC O26:H11 can acquire and maintain an additional large virulence plasmid conferring supplementary pathogenic potential while retaining the ability to spread this mobile genetic element to other *E. coli*. In Italy, we observed some HUS patients with STEC O80:H2 and enteropathogenic *E. coli* O26:H11 coinfection (S. Morabito, G. Scavia, unpub. data). Other O80:H2–O26:H11 coinfections were described during an outbreak linked to unpasteurized cheese (*47*), possibly explaining the presence of the pR444_A plasmid in STEC O26 strains.

In this study, 2 strains from Italy (Appendix 1 Table 2) and 1 strain from the GenBank and RefSeq databases were isolated from food products of bovine origin, suggesting the potential for zoonotic transmission. Since 1987, several studies have reported the isolation of STEC and atypical enteropathogenic *E. coli* with ExPEC-associated virulence genes from cattle (*21*,*48*). On the other hand, human infections caused by similar strains have been described only since 2008, mainly in the form of rare and mild disease (*21*). We showed that since 2001, STEC strains with ExPEC-associated virulence genes, especially those belonging to ST301, have caused many severe diseases including HUS, HC, and HC associated with severe diarrhea (Appendix 1 Table 2); these findings reinforce the high pathogenic potential of such hybrid strains.

Of the 53 *hlyF*-positive strains analyzed in this study, 4 also tested positive for the *hlyA* gene, which encodes an α-hemolysin typically produced by ExPEC strains that cause urinary tract infection (*44*,*45*). Such strains formed a distinct population of STEC strains; these strains lacked the pO157-like plasmid and the LEE locus and harbored a pR444_A plasmid without the AMR-encoding region (Figure 2; Appendix 1 Table 3). Accordingly, all their genomes grouped together in the cgMLST analysis and far from the bigger group of the ST301 strains (Figure 3; Appendix 2 Table).

In conclusion, STEC strains with ExPEC-associated virulence genes have circulated in Europe and caused human severe infections since 2001 or earlier. Moreover, we showed that this group of pathogenic *E. coli* includes multiple serotypes and sequence types. We propose that these strains belong to ≥2 different lineages that might have emerged after the dissemination of the ExPEC plasmid pR444_A into a heterogeneous population of STEC strains.

Acknowledgments

We thank the entire network of the Istituto Zooprofilattico Sperimentale (IZS) laboratories, especially Lucia Decastelli and Valle d'Aosta for providing the strain isolated from raw bovine milk. We also thank Massimo Fabbi and Emilia-Romagna for providing the strain isolated from beef liver and Bianca Colonna for providing the CSH26Nal strain. We thank the Italian Registry of Hemolytic Uremic Syndrome and the Italian Society for Pediatric Nephrology for the surveillance data on hemolytic uremic syndrome. We also thank Marco Crescenzi, Manuela Marra, Fiorella Ciaffoni, and Maria Carollo from the Core Facilities Technical—Scientific Service Team at Istituto Superiore di Sanità for the whole-genome sequencing of the strains isolated in Italy.

About the Author

Dr. Gigliucci is a researcher at the European Reference Laboratory for *Escherichia coli*, located at the Istituto Superiore di Sanità, Rome. Her research interests include the use of whole-genome sequencing for the surveillance and monitoring of STEC infections.

References

1. Karmali MA. Host and pathogen determinants of verocytotoxin-producing *Escherichia coli*–associated hemolytic uremic syndrome. Kidney Int Suppl. 2009;75:S4–7. https://doi.org/10.1038/ki.2008.608
2. O'Brien AD, Tesh VL, Donohue-Rolfe A, Jackson MP, Olsnes S, Sandvig K, et al. Shiga toxin: biochemistry, genetics, mode of action, and role in pathogenesis. Curr Top Microbiol Immunol. 1992;180:65–94. https://doi.org/10.1007/978-3-642-77238-2_4
3. Scheutz F, Teel LD, Beutin L, Piérard D, Buvens G, Karch H, et al. Multicenter evaluation of a sequence-based protocol for subtyping Shiga toxins and standardizing Stx nomenclature. J Clin Microbiol. 2012;50:2951–63. https://doi.org/10.1128/JCM.00860-12
4. Bai X, Fu S, Zhang J, Fan R, Xu Y, Sun H, et al. Identification and pathogenomic analysis of an *Escherichia coli* strain producing a novel Shiga toxin 2 subtype. Sci Rep. 2018;8:6756. https://doi.org/10.1038/s41598-018-25233-x
5. Lacher DW, Gangiredla J, Patel I, Elkins CA, Feng PC. Use of the *Escherichia coli* identification microarray for characterizing the health risks of Shiga toxin–producing *Escherichia coli* isolated from foods. J Food Prot. 2016;79:1656–62. https://doi.org/10.4315/0362-028X.JFP-16-176
6. Yang X, Bai X, Zhang J, Sun H, Fu S, Fan R, et al. *Escherichia coli* strains producing a novel Shiga toxin 2 subtype circulate in China. Int J Med Microbiol. 2020;310:151377. https://doi.org/10.1016/j.ijmm.2019.151377
7. O'Brien AD, Newland JW, Miller SF, Holmes RK, Smith HW, Formal SB. Shiga-like toxin–converting phages from *Escherichia coli* strains that cause hemorrhagic colitis or infantile diarrhea. Science. 1984;226:694–6. https://doi.org/10.1126/science.6387911
8. Jerse AE, Yu J, Tall BD, Kaper JB. A genetic locus of enteropathogenic *Escherichia coli* necessary for the production of attaching and effacing lesions on tissue culture cells. Proc Natl Acad Sci U S A. 1990;87:7839–43. https://doi.org/10.1073/pnas.87.20.7839
9. Nataro JP, Kaper JB. Diarrheagenic *Escherichia coli*. [Erratum in: Clin Microbiol Rev. 1998; 11:403]. Clin Microbiol Rev. 1998;11:142–201. https://doi.org/10.1128/CMR.11.1.142
10. Navarro-Garcia F. *Escherichia coli* O104:H4 pathogenesis: an enteroaggregative *E. coli*/Shiga toxin–producing *E. coli* explosive cocktail of high virulence. Microbiol Spectr. 2014;2. https://doi.org/10.1128/microbiolspec.EHEC-0008-2013
11. Morabito S, Karch H, Mariani-Kurkdjian P, Schmidt H, Minelli F, Bingen E, et al. Enteroaggregative, Shiga toxin–producing *Escherichia coli* O111:H2 associated with an outbreak of hemolytic-uremic syndrome. J Clin Microbiol. 1998;36:840–2. https://doi.org/10.1128/JCM.36.3.840-842.1998
12. Michelacci V, Maugliani A, Tozzoli R, Corteselli G, Chiani P, Minelli F, et al. Characterization of a novel plasmid encoding F4-like fimbriae present in a Shiga-toxin producing enterotoxigenic *Escherichia coli* isolated during the investigation on a case of hemolytic-uremic syndrome. Int J Med Microbiol. 2018;308:947–55. https://doi.org/10.1016/j.ijmm.2018.07.002
13. Nyholm O, Halkilahti J, Wiklund G, Okeke U, Paulin L, Auvinen P, et al. Comparative genomics and characterization of hybrid Shigatoxigenic and enterotoxigenic *Escherichia coli* (STEC/ETEC) strains. PLoS One. 2015;10:e0135936. https://doi.org/10.1371/journal.pone.0135936
14. Cointe A, Birgy A, Mariani-Kurkdjian P, Liguori S, Courroux C, Blanco J, et al. Emerging multidrug-resistant hybrid pathotype Shiga toxin–producing *Escherichia coli* O80 and related strains of clonal complex 165, Europe. Emerg Infect Dis. 2018;24:2262–9. https://doi.org/10.3201/eid2412.180272
15. Malberg Tetzschner AM, Johnson JR, Johnston BD, Lund O, Scheutz F. *In silico* genotyping of *Escherichia coli* isolates for extraintestinal virulence genes by use of whole-genome sequencing data. J Clin Microbiol. 2020;58:e01269–20. https://doi.org/10.1128/JCM.01269-20
16. European Food Safety Authority and European Centre for Disease Prevention and Control. The European Union summary report on trends and sources of zoonoses, zoonotic agents and food-borne outbreaks in 2017. EFSA J. 2018;16:5500.
17. Nüesch-Inderbinen M, Cernela N, Wüthrich D, Egli A, Stephan R. Genetic characterization of Shiga toxin producing *Escherichia coli* belonging to the emerging hybrid pathotype O80:H2 isolated from humans 2010–2017 in Switzerland. Int J Med Microbiol. 2018;308:534–8. https://doi.org/10.1016/j.ijmm.2018.05.007
18. Wijnsma KL, Schijvens AM, Rossen JWA, Kooistra-Smid AMDM, Schreuder MF, van de Kar NCAJ. Unusual severe case of hemolytic uremic syndrome due to Shiga toxin 2d-producing *E. coli* O80:H2. Pediatr Nephrol. 2017;32:1263–8. https://doi.org/10.1007/s00467-017-3642-3
19. Soysal N, Mariani-Kurkdjian P, Smail Y, Liguori S, Gouali M, Loukiadis E, et al. Enterohemorrhagic *Escherichia coli* hybrid pathotype O80:H2 as a new therapeutic challenge. Emerg Infect Dis. 2016;22:1604–12. https://doi.org/10.3201/eid2209.160304
20. Fierz L, Cernela N, Hauser E, Nüesch-Inderbinen M, Stephan R. Characteristics of Shigatoxin–producing *Escherichia coli* strains isolated during 2010–2014 from human infections in Switzerland. Front Microbiol. 2017;8:1471. https://doi.org/10.3389/fmicb.2017.01471
21. De Rauw K, Thiry D, Caljon B, Saulmont M, Mainil J, Pierard D. Characteristics of Shiga toxin producing– and enteropathogenic *Escherichia coli* of the emerging serotype O80:H2 isolated from humans and diarrhoeic calves in Belgium. Clin Microbiol Infect. 2019;25:111.e5–111.e8.
22. Ingelbeen B, Bruyand M, Mariani-Kurkjian P, Le Hello S, Danis K, Sommen C, et al. Emerging Shiga-toxin–producing *Escherichia coli* serogroup O80 associated hemolytic and uremic syndrome in France, 2013–2016: differences with other serogroups. PLoS One. 2018;13:e0207492. https://doi.org/10.1371/journal.pone.0207492
23. Mariani-Kurkdjian P, Lemaître C, Bidet P, Perez D, Boggini L, Kwon T, et al. Haemolytic-uraemic syndrome with bacteraemia caused by a new hybrid *Escherichia coli* pathotype. New Microbes New Infect. 2014;2:127–31. https://doi.org/10.1002/nmi2.49
24. Koutsoumanis K, Allende A, Alvarez-Ordonez A, Bover-Cid S, Chemaly M, et al.; EFSA BIOHAZ Panel. Scientific Opinion on the pathogenicity assessment of Shiga toxin–producing *Escherichia coli* (STEC) and the public health risk posed by contamination of food with STEC. EFSA Journal. 2020;18:5967.
25. Karch H, Heesemann J, Laufs R, O'Brien AD, Tacket CO, Levine MM. A plasmid of enterohemorrhagic *Escherichia coli* O157:H7 is required for expression of a new fimbrial antigen and for adhesion to epithelial cells. Infect Immun. 1987;55:455–61. https://doi.org/10.1128/IAI.55.2.455-461.1987
26. Beutin L, Prada J, Zimmermann S, Stephan R, Orskov I, Orskov F. Enterohemolysin, a new type of hemolysin produced by some strains of enteropathogenic *E. coli* (EPEC).

Zentralbl Bakteriol Mikrobiol Hyg A. 1988;267:576–88. https://doi.org/10.1016/S0176-6724(88)80042-7
27. Peigne C, Bidet P, Mahjoub-Messai F, Plainvert C, Barbe V, Médigue C, et al. The plasmid of *Escherichia coli* strain S88 (O45:K1:H7) that causes neonatal meningitis is closely related to avian pathogenic *E. coli* plasmids and is associated with high-level bacteremia in a neonatal rat meningitis model. Infect Immun. 2009;77:2272–84. https://doi.org/10.1128/IAI.01333-08
28. Morales C, Lee MD, Hofacre C, Maurer JJ. Detection of a novel virulence gene and a *Salmonella* virulence homologue among *Escherichia coli* isolated from broiler chickens. Foodborne Pathog Dis. 2004;1:160–5. https://doi.org/10.1089/fpd.2004.1.160
29. Dozois CM, Daigle F, Curtiss R III. Identification of pathogen-specific and conserved genes expressed in vivo by an avian pathogenic *Escherichia coli* strain. Proc Natl Acad Sci U S A. 2003;100:247–52. https://doi.org/10.1073/pnas.232686799
30. Chuba PJ, Leon MA, Banerjee A, Palchaudhuri S. Cloning and DNA sequence of plasmid determinant *iss*, coding for increased serum survival and surface exclusion, which has homology with lambda DNA. Mol Gen Genet. 1989;216:287–92. https://doi.org/10.1007/BF00334367
31. Haiko J, Laakkonen L, Juuti K, Kalkkinen N, Korhonen TK. The omptins of *Yersinia pestis* and *Salmonella enterica* cleave the reactive center loop of plasminogen activator inhibitor 1. J Bacteriol. 2010;192:4553–61. https://doi.org/10.1128/JB.00458-10
32. Murase K, Martin P, Porcheron G, Houle S, Helloin E, Pénary M, et al. HlyF produced by extraintestinal pathogenic *Escherichia coli* is a virulence factor that regulates outer membrane vesicle biogenesis. J Infect Dis. 2016;213:856–65. https://doi.org/10.1093/infdis/jiv506
33. Bankevich A, Nurk S, Antipov D, Gurevich AA, Dvorkin M, Kulikov AS, et al. SPAdes: a new genome assembly algorithm and its applications to single-cell sequencing. J Comput Biol. 2012;19:455–77. https://doi.org/10.1089/cmb.2012.0021
34. Del Fabbro C, Scalabrin S, Morgante M, Giorgi FM. An extensive evaluation of read trimming effects on Illumina NGS data analysis. PLoS One. 2013;8:e85024. https://doi.org/10.1371/journal.pone.0085024
35. Feijao P, Yao HT, Fornika D, Gardy J, Hsiao W, Chauve C, et al. MentaLiST—a fast MLST caller for large MLST schemes. Microb Genom. 2018;4. https://doi.org/10.1099/mgen.0.000146
36. Wirth T, Falush D, Lan R, Colles F, Mensa P, Wieler LH, et al. Sex and virulence in *Escherichia coli*: an evolutionary perspective. Mol Microbiol. 2006;60:1136–51. https://doi.org/10.1111/j.1365-2958.2006.05172.x
37. Llarena AK, Ribeiro-Gonçalves BF, Nuno Silva D, Halkilahti J, Machado MP, Da Silva MS, et al. INNUENDO: A cross-sectoral platform for the integration of genomics in the surveillance of food-borne pathogens. EFSA Supporting Publication. 2018;15:EN-1498.
38. Joensen KG, Scheutz F, Lund O, Hasman H, Kaas RS, Nielsen EM, et al. Real-time whole-genome sequencing for routine typing, surveillance, and outbreak detection of verotoxigenic *Escherichia coli*. J Clin Microbiol. 2014;52:1501–10. https://doi.org/10.1128/JCM.03617-13
39. Joensen KG, Tetzschner AM, Iguchi A, Aarestrup FM, Scheutz F. Rapid and easy in silico serotyping of *Escherichia coli* isolates by use of whole-genome sequencing data. J Clin Microbiol. 2015;53:2410–26. https://doi.org/10.1128/JCM.00008-15
40. Clermont O, Christenson JK, Denamur E, Gordon DM. The Clermont *Escherichia coli* phylo-typing method revisited: improvement of specificity and detection of new phylo-groups. Environ Microbiol Rep. 2013;5:58–65. https://doi.org/10.1111/1758-2229.12019
41. Dissanayake DR, Octavia S, Lan R. Population structure and virulence content of avian pathogenic *Escherichia coli* isolated from outbreaks in Sri Lanka. Vet Microbiol. 2014;168:403–12. https://doi.org/10.1016/j.vetmic.2013.11.028
42. Silva M, Machado MP, Silva DN, Rossi M, Moran-Gilad J, Santos S, et al. chewBBACA: A complete suite for gene-by-gene schema creation and strain identification. Microb Genom. 2018;4. https://doi.org/10.1099/mgen.0.000166
43. Scavia G, Gianviti A, Labriola V, Chiani P, Maugliani A, Michelacci V, et al. A case of haemolytic uraemic syndrome (HUS) revealed an outbreak of Shiga toxin-2–producing *Escherichia coli* O26:H11 infection in a nursery, with long-lasting shedders and person-to-person transmission, Italy 2015. J Med Microbiol. 2018;67:775–82. https://doi.org/10.1099/jmm.0.000738
44. Goebel W, Hedgpeth J. Cloning and functional characterization of the plasmid-encoded hemolysin determinant of *Escherichia coli*. J Bacteriol. 1982;151:1290–8. https://doi.org/10.1128/JB.151.3.1290-1298.1982
45. Dhakal BK, Mulvey MA. The UPEC pore-forming toxin α-hemolysin triggers proteolysis of host proteins to disrupt cell adhesion, inflammatory, and survival pathways. Cell Host Microbe. 2012;11:58–69. https://doi.org/10.1016/j.chom.2011.12.003
46. Frank C, Werber D, Cramer JP, Askar M, Faber M, an der Heiden M, et al.; HUS Investigation Team. Epidemic profile of Shiga-toxin–producing *Escherichia coli* O104:H4 outbreak in Germany. N Engl J Med. 2011;365:1771–80. https://doi.org/10.1056/NEJMoa1106483
47. Espié E, Grimont F, Mariani-Kurkdjian P, Bouvet P, Haeghebaert S, Filliol I, et al. Surveillance of hemolytic uremic syndrome in children less than 15 years of age, a system to monitor O157 and non-O157 Shiga toxin–producing *Escherichia coli* infections in France, 1996–2006. Pediatr Infect Dis J. 2008;27:595–601. https://doi.org/10.1097/INF.0b013e31816a062f
48. Blanco M, Blanco JE, Mora A, Dahbi G, Alonso MP, González EA, et al. Serotypes, virulence genes, and intimin types of Shiga toxin (verotoxin)–producing *Escherichia coli* isolates from cattle in Spain and identification of a new intimin variant gene (*eae*-xi). J Clin Microbiol. 2004;42:645–51. https://doi.org/10.1128/JCM.42.2.645-651.2004

Address for correspondence: Federica Gigliucci, Department of Food Safety, Nutrition and Veterinary Public Health, Istituto Superiore di Sanità, viale Regina Elena, 299, Rome, Italy; email: federica.gigliucci@iss.it

Isolate-Based Surveillance of *Bordetella pertussis*, Austria, 2018–2020

Adriana Cabal, Daniela Schmid, Markus Hell, Ali Chakeri, Elisabeth Mustafa-Korninger, Alexandra Wojna, Anna Stöger, Johannes Möst, Eva Leitner, Patrick Hyden, Thomas Rattei, Adele Habington, Ursula Wiedermann, Franz Allerberger, Werner Ruppitsch

Pertussis is a vaccine-preventable disease, and its recent resurgence might be attributable to the emergence of strains that differ genetically from the vaccine strain. We describe a novel pertussis isolate-based surveillance system and a core genome multilocus sequence typing scheme to assess *Bordetella pertussis* genetic variability and investigate the increased incidence of pertussis in Austria. During 2018–2020, we obtained 123 *B. pertussis* isolates and typed them with the new scheme (2,983 targets and preliminary cluster threshold of ≤6 alleles). *B. pertussis* isolates in Austria differed genetically from the vaccine strain, both in their core genomes and in their vaccine antigen genes; 31.7% of the isolates were pertactin-deficient. We detected 8 clusters, 1 of them with pertactin-deficient isolates and possibly part of a local outbreak. National expansion of the isolate-based surveillance system is needed to implement pertussis-control strategies.

Bordetella pertussis is the main causative agent of the reemerging respiratory disease commonly known as whooping cough (*1*). *B. pertussis* infection usually affects infants, toddlers, and children of school age, although adolescents and adults also can get infected and have symptoms. In addition, because transmission of pertussis can go unnoticed, asymptomatic carriers are considered an important source of infection (*2*). Despite its low sensitivity, culturing pertussis from nasopharyngeal swabs remains the standard diagnostic technique, although today it is scarcely performed (*3*).

To some extent, pertussis can be prevented by vaccination with either cellular or acellular vaccines (*4*). In Austria, cellular pertussis vaccines were replaced in 1998 by acellular vaccines (ACVs), and ever since, either 2 (filamentous hemagglutinin [FHA] and pertussis toxin [PTX]) or 3 (FHA, PTX, and pertactin) component vaccines have been used for primary vaccination. Booster immunizations have been recommended since 2003 for children of school age and adolescents. These vaccines include either 3 (FHA, PTX, and pertactin) or 5 (FHA, PTX, pertactin, FIM2, and FIM3) components.

Despite vaccinations, the incidence of pertussis has been increasing in the past few decades (*5*–*7*). In Austria, 579 pertussis cases were reported in 2015; the number increased to 1,274 in 2016, 1,411 in 2017, 2,198 in 2018, and 2,246 in 2019. The increase in the incidence of pertussis worldwide can be explained partially by the loss of the protective effect after immunity wanes; this loss is strongly associated with ACV use (*8*). Another factor that contributes to the resurgence of pertussis is the emergence of vaccine-evasive *B. pertussis* strains that differ genetically from the vaccine strains (*9*,*10*).

A molecular study conducted on pertussis cases from 3 different cities in Austria assessed the genetic variability of *B. pertussis* nationwide (*5*). However, the study used respiratory samples to perform PCR, followed by Sanger sequencing; therefore, typing was not based on whole-genome sequencing (WGS) of *B. pertussis* isolates.

Author affiliations: Institute for Medical Microbiology and Hygiene, Austrian Agency for Health and Food Safety, Vienna, Austria (A. Cabal, D. Schmid, A. Chakeri, A. Stöger, F. Allerberger, W. Ruppitsch); MEDILAB, Teaching Laboratory of the Paracelsus Medical University, Salzburg, Austria (M. Hell, E. Mustafa-Korninger, A. Wojna); Centre for Public Health, Medical University Vienna, Vienna (A. Chakeri); MB-LAB Clinical Microbiology Laboratory, Innsbruck, Austria (J. Möst); Consultant Laboratory for Bordetella of the Robert Koch Institute, Medical University of Graz, Graz, Austria (E. Leitner); Centre for Microbiology and Environmental Systems Science, University of Vienna, Vienna (P. Hyden, T. Rattei); Children's Health Ireland at Crumlin, Dublin, Ireland (A. Habington); Institute of Specific Prophylaxis and Tropical Medicine, Medical University of Vienna, Vienna (U. Wiedermann)

DOI: https://doi.org/10.3201/eid2703.202314

Because of the rise in the incidence of pertussis in Austria in recent years, we investigated pertussis cases from 3 states in Austria to assess the genetic variability of their *B. pertussis* isolates through WGS-based typing. The first objective was to set up a national isolate-based surveillance system, complementary to the case-based surveillance system in Austria, for collecting isolates from patients with suspected pertussis. Second, we aimed to characterize and to compare *B. pertussis* isolates with the vaccine strain Tohama I and other isolates from different geographic regions outside Austria.

Methods

Setup of the Surveillance System and Sequencing

For 2 years (May 2018–May 2020), hospitals, general practitioners, and pediatricians using clinical laboratories located in 3 states in Austria (Salzburg, Tyrol, and Styria) were asked to collect ≥1 nasopharyngeal swab containing transport medium (ESwab; Copan, https://www.copangroup.com) from patients with suspected *B. pertussis* infection (Figure 1). When possible, a second nasopharyngeal swab containing charcoal-based medium (Transystem Amies medium with charcoal; Copan) was collected.The swabs were then sent to the clinical laboratory of each state participating in the study. For each suspected case, PCR was performed using the swab containing the transport medium with a commercial kit (BD MAX, Becton Dickinson, http://bd.com; or BORDETELLA R-gene, bioMérieux, https://www.biomerieux.com). When PCR results were positive, either the same swab used for PCR or, if available, the charcoal swab was stroked on Oxoid *Bordetella*–selective medium (Thermo Fisher Scientific, https://www.thermofisher.com) or Bordet Gengou agar with 15% sheep blood (Becton Dickinson), followed by cultivation at 37°C under aerobic and humid conditions for 48–120 hours. Colonies compatible with *B. pertussis* were tested by MALDI Biotyper software version 3.0 (Bruker, https://www.bruker.com) or VitekMS software version 3.2 (bioMérieux). Colonies indentified as *B. pertussis* were sent to the Austrian Agency for Health and Food Safety in Vienna for further DNA extraction and 300-bp paired-end WGS using an Illumina Miseq device (https://www.illumina.com), as described in Appendix 1 (https://wwwnc.cdc.gov/EID/article/27/3/20-2314-App1.pdf). Additional information on the sequencing process, de novo assembly, and sequence quality checks also are found in Appendix 1. The Illumina reads of the 123 isolates in Austria have been deposited in the National Center for Biotechnology Information (NCBI) Sequence Read Archive repository under project number PRJNA642701.

Generation of a *B. pertussis* cgMLST Scheme

A stable, ad hoc, core-genome multilocus sequence typing (cgMLST) scheme and accessory genome scheme were created by using Ridom SeqSphere + version 4.1.9 (Ridom, https://www.ridom.de; Appendix 1). In brief, 15 genomes (Appendix 2 Table 1, https://wwwnc.cdc.gov/EID/article/27/3/20-2314-App2.xlsx) were used as query genomes and the Tohama I vaccine strain genome (GenBank accession no. NC_002929.2) as a seed genome. Afterwards, 263 taxonomic and quality outliers were discarded, leaving a total of 2,983 core genome targets (Appendix 2 Table 2) and 179 accessory genome targets (Appendix 2 Table 3). We considered as core genes only those targets (i.e., genes) that were present in 100% of the genomes. Further validation of the scheme was based on a selection of *B. pertussis* genomes available in NCBI (n = 391), many of which were associated with outbreaks (Appendix 2 Table 4), and an old collection of clinical *Bordetella* sp. strains from Austria (Appendix 2 Table 5).

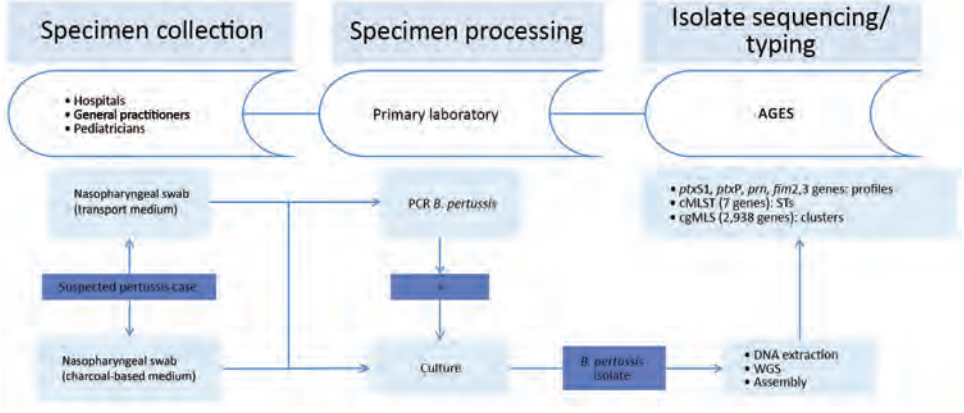

Figure 1. Flow chart of the *Bordetella pertussis* isolate–based surveillance system, Austria, May 2018–May 2020. AGES, Agentur für Gesundheit und Ernährungssicherheit (Austrian Agency for Health and Food Safety); cgMLST, core-genome multilocus sequence typing; ST, sequence type.

Typing of *B. pertussis* Isolates and Comparative Analysis

During the 2-year study period, all the clinical isolates collected within the isolate-based surveillance system were typed with our newly implemented cgMLST scheme. Allelic differences among the isolates from Austria and the vaccine strain Tohama I were visualized by generating minimum spanning trees with a preliminary cluster threshold established at ≤6 alleles (Appendix 1). We extracted the sequence types (STs) from the WGS data corresponding to the classical multilocus sequence typing (*11*), the variants and mutations present in each of the genes used as vaccine antigens (*ptx*S1, *ptx*P, *prn*, *fim*2, *fim*3), and their combination (genetic profiles).

To be certain that our scheme could be applied beyond our set of *B. pertussis* isolates from Austria, we used a selection (n = 106) of *B. pertussis* genomes, including outbreak strains used in the validation of the cgMLST scheme, to perform a genomic comparative analysis (Appendix 1; Appendix 2 Table 4). We compared the gene content obtained for our cgMLST scheme with the cgMLST scheme developed by the Pasteur Institute (Paris, France) (*12*). In addition, we compared the results obtained when applying our cgMLST with those derived from a single-nucleotide polymorphism (SNP)–based analysis on the 123 isolates from Austria (Appendix 1).

Table 1. Demographic characteristics of the 123 pertussis case-patients in the *Bordetella pertussis* isolate–based surveillance system, Austria, May 2018–May 2020

Characteristic	No.
Age group, y	
<1	8
1–4	15
5–9	31
10–14	31
15–19	7
20–29	3
30–39	7
40–49	11
50–59	3
≥60	7
Sex	
F	69
M	54
State	
Salzburg	86
Tyrol	21
Styria	12
Upper Austria	4
Clinical symptoms	
Coughing fits	66
Cough >4 weeks	64
Medical whooping cough diagnosis	37
Missing data	7
Post-coughing vomiting	7
Inspiratory whooping	5
Asymptomatic	2
Vaccination status	
Vaccinated	53
1st booster	1
2nd booster	22
3rd booster	16
4th booster	7
Unknown doses	7
Not vaccinated	39
Unknown	31

Statistical Analysis

Personal information and vaccination status were obtained for each pertussis culture-positive case-patient from the national electronic reporting system. We calculated odds ratios with Stata software version 13 (StataCorp, https://www.stata.com) to measure for associations between pertactin deficiency and vaccination status. In the analysis, we included all case-patients who had received ≥1 dose of pertussis vaccine and those reported as unvaccinated. Case-patients with an unknown vaccination status (n = 31) were excluded from the analysis. Statistical significance was defined as $p<0.05$ by using the Pearson χ^2 test or Fisher exact test.

Results

Culture-Positive Cases

At the Austrian Agency for Health and Food Safety, we received 123 *B. pertussis* isolates, collected from 123 pertussis case-patients (Table 1), through our newly implemented isolate-based pertussis surveillance system during May 2018–May 2020. Fewer than 20% of the total pertussis cases reported in Salzburg state (n = 310) in 2018 were estimated to be culture-positive, and no information on the proportion of cases with a positive pertussis culture was available for the other 8 states in Austria.

A total of 119 *B. pertussis* isolates belonged to patients with PCR-positive confirmed pertussis from Salzburg, Tyrol, and Styria (Figure 2), and 4 isolates belonged to pertussis case-patients identified in the state of Upper Austria, provided by a clinical microbiology laboratory located in Salzburg (MB-LAB Clinical Microbiology Laboratory). Overall, 15 *B. pertussis* isolates belonged to culture-positive pertussis case-patients who lived in the same household with ≥1 other culture-positive case-patient. Additional metadata for the 123 pertussis cases are presented in Appendix 2 Table 6.

Sequence Types and Typing of Vaccine Target Genes

The *B. pertussis* isolates obtained from the 123 pertussis patients in Austria differed in sequence type and in the vaccine antigen genes from the vaccine strain Tohama I (Table 2). We detected ST2 for all but 1

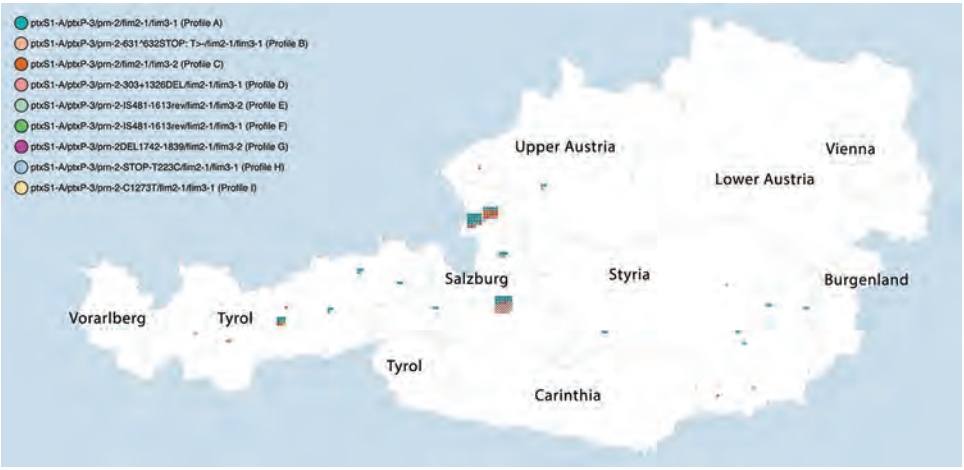

Figure 2. Pertussis cases by district of residence of case-patient and genetic profile of the corresponding *Bordetella pertussis* isolate identified in a *B. pertussis* isolate–based surveillance study, Austria, May 2018–May 2020. Each dot represents 1 case. Cases grouping next to each other belong to the same district. To protect patient confidentiality, only states and not districts are labeled.

isolate, which was of ST83. We found 9 different genetic profiles (A–I), 1 of which was new (profile G) (Table 2; Figure 3; Appendix 2 Table 7).

We found 7 pertactin-deficient profiles (B and D–I), representing 31.7% (n = 39) of the isolates, and 6 different known pertactin inactivation mechanisms (*13*–*16*; Table 2; Appendix 2 Table 7). Pertactin-deficient isolates were mostly of profile B (n = 23 [18.7%]). Twenty case-patients (51.3%) with pertactin-deficient isolates had been vaccinated, 11 (28.2%) case-patients were unvaccinated, and for 8 (20.5%) case-patients, vaccination status was unknown. Case-patients having received ≥1 dose of pertussis ACV were 1.5 times more likely to have a pertactin-deficient *B. pertussis* isolate (of any genetic profile) compared with unvaccinated case-patients, although this relationship was not statistically significant (unadjusted odds ratio 1.5, 95% CI 0.6–3.8). Persons living in the district of St. Johann in Pongau (Salzburg state) were 21.17 (95% CI 6.7–81.1) times more likely to have profile B, and this association was significant (p<0.001). Stratifying by vaccination status, vaccinated persons from St. Johann in Pongau were 13.3 (95% C: 2.9–99.1; p<0.001) times more likely to present profile B, whereas unvaccinated ones had 58.5 (95% CI 5.6–1876; p<0.001) times more chances to present profile B. No association was seen between the different age groups or having a pertactin-deficient profile and having profile B.

cgMLST and Comparative Analysis

The 123 *B. pertussis* isolates were closely related, differing by a maximum of 38 alleles (≤44 alleles when including the accessory genome), and they seemed to cluster in groups (Figure 3). We observed that we could separate *fim*3-1 and *fim*3-1 isolates into 2 branches (Figure 4) and that pertactin-deficient isolates of genetic profile B grouped together. Isolates of profile B (n = 23) differed by a maximum of 9 alleles when including the only isolate from Tyrol of that profile, and by ≤6 alleles, excluding the isolate from Tyrol. All other isolates were from Salzburg (n = 20), Styria (n = 1), and Upper Austria (n = 1). Isolates from profile D also clustered together (≤6 alleles), differing by ≥8 alleles with isolates of profiles A and B.

With the preliminary cluster threshold of ≤6 alleles, we distinguished 8 clusters (Figure 3; Appendix

Table 2. Genetic profiles of the 123 *Bordetella pertussis* isolates obtained through the *B. pertussis* isolate–based surveillance system, Austria, May 2018–May 2020*

		B. pertussis vaccine antigen genes					
Profile	No. (%)	*ptx*S1	*ptx*P	*prn*	*fim*2	*fim*3	Reference
Profile vaccine strain Tohama I	0	*ptx*S1-D	*ptx*P-1	*prn*-1	*fim*2-1	*fim*3-1	NA
Profile A	64 (52.3)	*ptx*S1-A	*ptx*P-3	*prn*-2	*fim*2-1	*fim*3-1	(*13*,*14*)
Profile B	23 (18.7)	*ptx*S1-A	*ptx*P-3	*prn*-2–631^632STOP:T>-	*fim*2-1	*fim*3-1	(*15*)
Profile C	20 (16.2)	*ptx*S1-A	*ptx*P-3	*prn*-2	*fim*2-1	*fim*3-2	(*13*,*14*)
Profile D	8 (6.50)	*ptx*S1-A	*ptx*P-3	*prn*-2–303+1326DEL	*fim*2-1	*fim*3-1	(*16*)
Profile E	3† (2.44)	*ptx*S1-A	*ptx*P-3	*prn*-2-IS481–1613rev	*fim*2-1	*fim*3-2	(*13*,*14*)
Profile F	2 (1.62)	*ptx*S1-A	*ptx*P-3	*prn*-2-IS481–1613rev	*fim*2-1	*fim*3-1	(*14*)
Profile G	1 (0.8)	*ptx*S1-A	*ptx*P-3	*prn*-2- DEL1742–1839‡	*fim*2-1	*fim*3-2	This study
Profile H	1 (0.8)	*ptx*S1-A	*ptx*P-3	*prn*-2-STOP-T223C	*fim*2-1	*fim*3-1	(*14*)
Profile I	1 (0.8)	*ptx*S1-A	*ptx*P-3	*prn*-2-C1273T	*fim*2-1	*fim*3-1	(*13*,*14*)

*NA, not applicable.
†One isolate was sequence type 83.
‡This isolate showed an insertion longer than 200 bp in the *prn* gene combined with a partial deletion at positions nt 1742–1839.

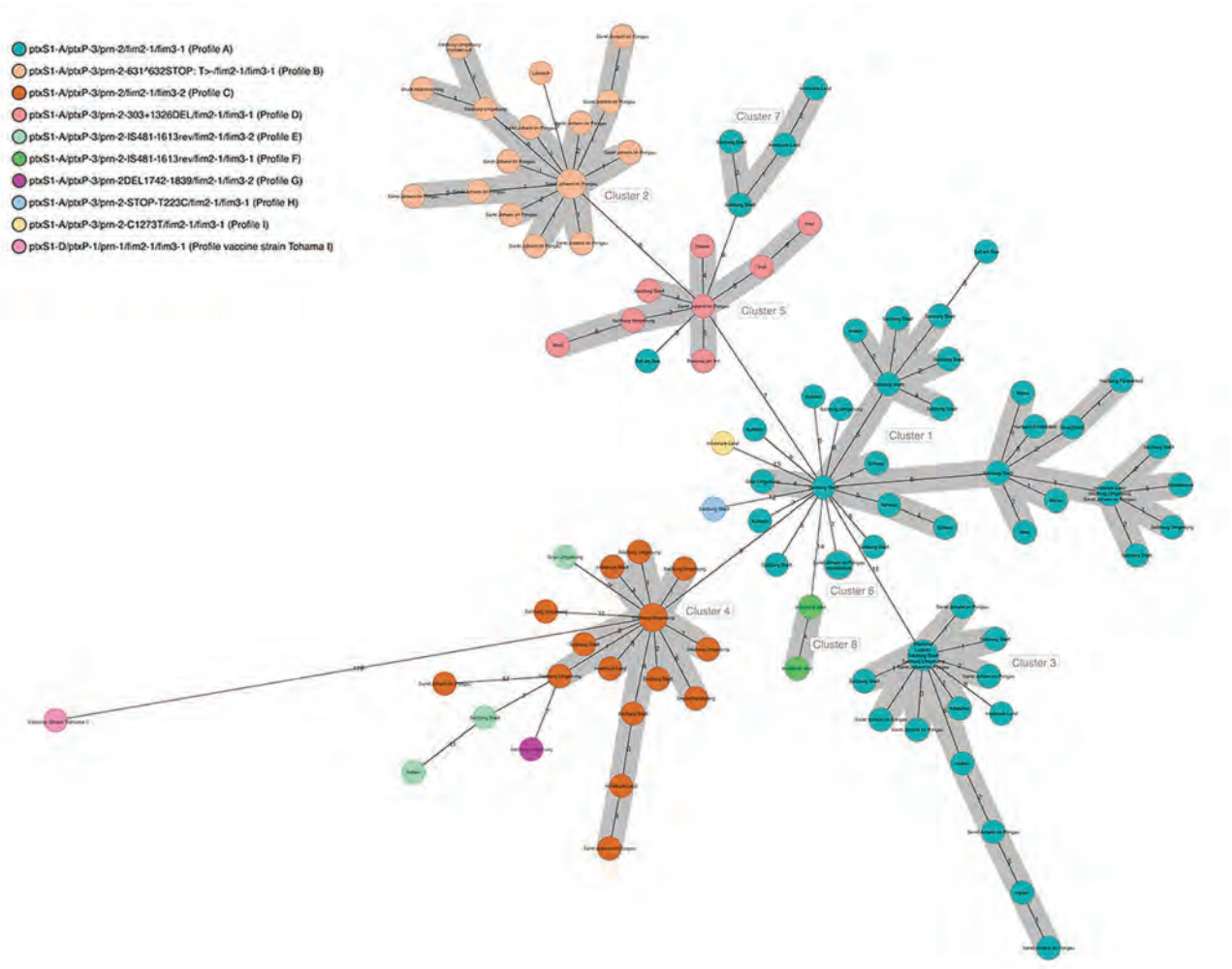

Figure 3. Minimum spanning tree of 123 *Bordetella pertussis* isolates and their clusters by genetic profile based on core-genome multilocus sequence typing in a *B. pertussis* isolate–based surveillance study, Austria, May 2018–May 2020. Numbers on connection lines represent the number of allelic differences among the isolates.

1). Cluster 1 integrated only profile A isolates (n = 26) from all states. Isolates in cluster 2 (n = 22) were of profile B. Most of the isolates in this cluster (n = 20) originated from case-patients living in Salzburg state. Eighteen of them resided in the district of St. Johann in Pongau. Of the 2 case-patients who did not live in Salzburg state, 1 had a confirmed epidemiologic link with a pertussis-positive relative in Salzburg. A trend compatible with a local outbreak of genetic profile B *B. pertussis* was distinguished (Appendix 1 Figure 1) for this cluster when we compared the number of profile B cases with the total number of reported cases (culture positive and nonculture positive) in the same period for St. Johann in Pongau (n = 160). In addition, a peak of cases in November 2018 corresponded to a small peak of cases with genetic profile B isolates. Cluster 3 had 19 isolates of profile A that were obtained from case-patients living in Salzburg, Tyrol, and Styria. Cluster 4 had 18 isolates of profile C from Salzburg, Tyrol, and Styria. Cluster 5 consisted of 9 profile D isolates from Salzburg, Styria, Tyrol, and Upper Austria. Cluster 6 included 5 profile A isolates from Salzburg and Upper Austria, and cluster 7 combined 4 profile A isolates from Salzburg and Tyrol. Cluster 8 had only 2 isolates, both of profile F, which originated from case-patients from Tyrol. Isolates from profiles E, G, H, and I did not cluster with any other isolate. The ST83 isolate did not cluster with any other isolate and differed from isolates in cluster 4 by ≥9 alleles.

In 6 households (A–E and G) (Appendix 2 Table 8), we confirmed the transmission of the same *B. pertussis* strain between 2 or 3 household members with a maximum of 4 allelic differences and an identical

genetic profile. In 1 household (F), transmission of *B. pertussis* was ruled out when cgMLST revealed 18 allelic differences between 2 isolates obtained from 2 case-patients living together, each of them with a *B. pertussis* strain of a different genetic profile (A and I).

We developed a comparative analysis between our 123 *B. pertussis* isolates and 106 *B. pertussis* genomes from NCBI, including mostly isolates from the United States and United Kingdom (Appendix 2 Table 4) from the 2010 and 2012 epidemics (*13*,*14*,*16*) (Figure 4). All *fim*3-1 isolates were clearly separated from *fim*3-2 isolates, but we could also differentiate isolates from the same country in different branches. On the basis of the *prn* type, which comprised the *prn* wild type alleles or mutations in this gene (i.e., insertions, deletions, and truncations), we distinguished isolates grouping closely to each other, sometimes originating from different countries. Genetic profiles A, C, H, and I were also represented in strains from outside Austria.

We compared target content between the Pasteur Institute's cgMLST scheme and ours (Appendix 2 Table 9). A total of 1,749 genes were common to both schemes; 1,239 genes were only present in our scheme, and 294 genes were only present in Pasteur Institute's scheme. The SNP analysis revealed isolates grouping in clusters in a similar way to that resulting from the cgMLST analysis (Appendix 1 Figure 2).

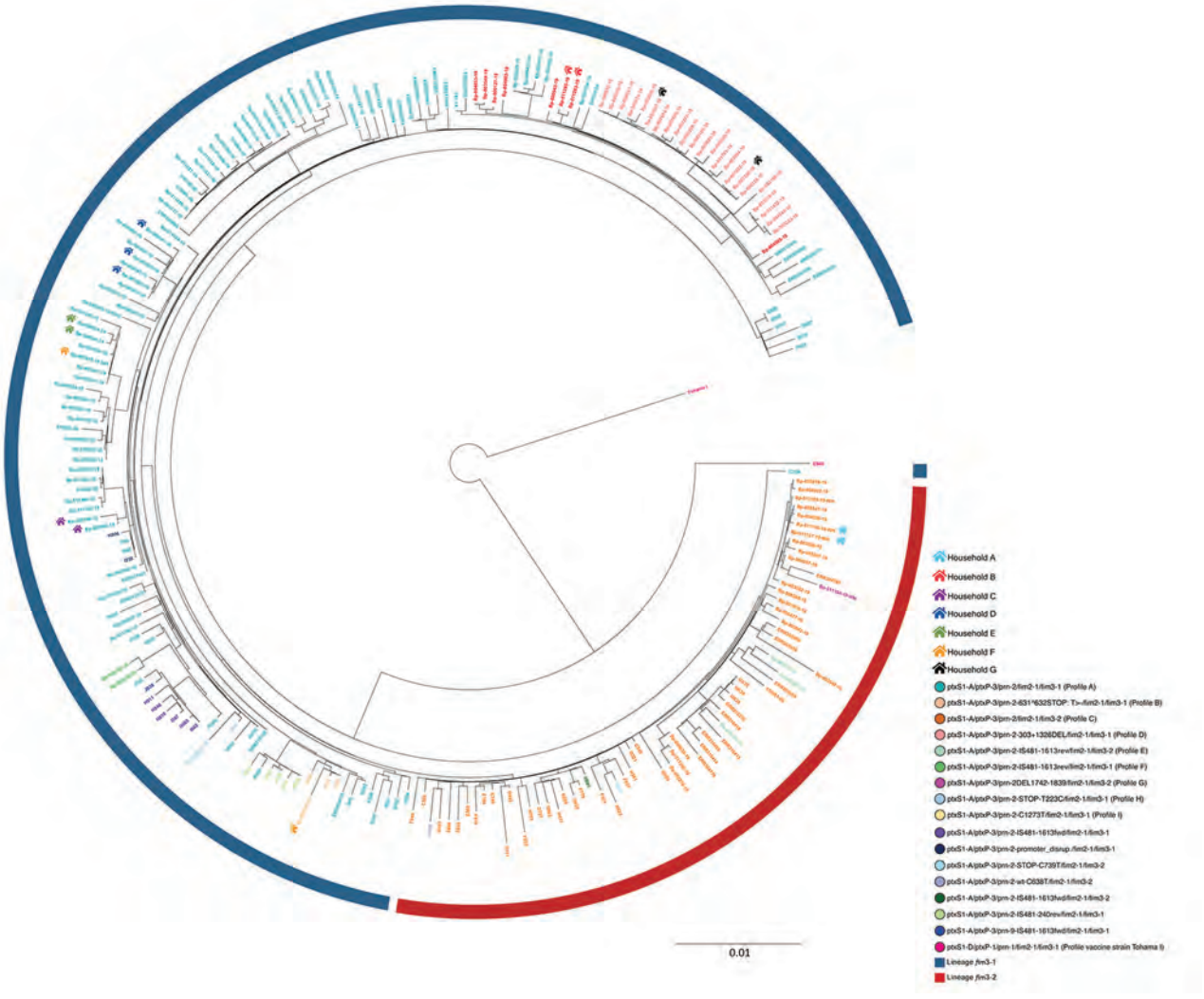

Figure 4. Maximum-likelihood phylogenetic tree generated using core-genome multilocus sequence typing data from 106 outbreak genome sequences from the United States and the United Kingdom and the 123 *Bordetella pertussis* isolates identified in an isolate-based surveillance study, Austria, May 2018–May 2020. Isolate identifiers are colored by genetic profile. These genetic profiles include profiles A–I, defined in this study, and other genetic profiles described outside of Austria. The circular blue line represents isolates of *fim*3-1 lineage; the circular red line represents *fim*3-1 isolates. A color-coded house-like symbol indicates isolates obtained from case-patients living in the same household. Scale bar indicates nucleotide substitutions per site.

Discussion

Our newly implemented *B. pertussis* isolate–based surveillance system has contributed to a better understanding of the molecular epidemiology of pertussis in Austria. No relationship existed between the pertussis incidence in the 3 states in Austria and the number of isolates collected, which depended mainly on the expertise of the respective laboratories in obtaining *B. pertussis* cultures. The estimated proportion (≈20%) of culture-positive pertussis cases found in relation to the total number of pertussis cases reported in Salzburg state was consistent with previous reports (*17*), whereas other authors reported up to 30% (*18*).

Results retrieved from the typing of the 123 *B. pertussis* isolates revealed the presence of the *ptxP*-3 allele in all isolates tested, consistent with other studies (*19*–*21*), thereby clearly indicating a divergence from the vaccine strain in Austria and a substitution among currently circulating *B. pertussis* strains of the *ptx*P-1 allele by the *ptxP*-3 allele. In comparison, during 2002–2008, a previous study in Austria still detected the *ptxP*-1 allele in 7% of the samples (*5*). Previous data also showed most of *B. pertussis* isolates (≈80%) grouping in the *fim*3-1 clade, which is more ancestral than *fim*3-2 (*22*). Therefore, not surprisingly, the genetic profile A (*fim3*-1 clade) was one of the most frequently detected genetic profiles globally (*22*–*24*), consistent with the findings of our study.

As for the proportion of pertactin-deficient isolates detected (31.7%), this finding was similar to the frequency reported during 2012–2015 in Norway, where ACVs were also introduced in 1998 and booster doses recommended after 2001 (*15*). In contrast, up to 98% of pertactin-deficient isolates were reported outside the European Union (*25*). In general, the proportion of *B. pertussis* isolates with pertactin deficiency seemed to be vary among countries depending on the vaccination schedule and vaccine type used (*26*). Those countries still using cellular pertussis vaccines have never or rarely reported pertactin-deficient isolates (*27*,*28*), whereas countries using ACVs have seen a direct association between the year of introduction of ACVs in the country and the appearance of pertactin-deficient isolates (*15*). Moreover, ACV-vaccinated persons seem more susceptible to pertactin-deficient strains than to pertactin-producing strains, given that pertactin-deficient strains are better able to colonize the respiratory tract (*29*). According to some authors, immunization with 2-component ACVs (instead of an ACV with 4 or 5 components) might affect immunogenicity (*30*–*32*). However, more time is needed to evaluate whether the lack of the pertactin component of 1 of the ACVs affects the incidence of pertussis in Austria in the coming years. Nevertheless, the higher likelihood of profile B strains found in the St. Johann in Pongau district seems not to have been influenced by vaccination.

Regarding the mechanisms causing pertactin deficiency, we reported a mutation at the 632 nt of the *prn* gene for our profile B isolates, previously described for isolates collected in Italy, Sweden, and Denmark during 2012–2015 (*15*). Likewise, this deletion was reported in Ireland in 2016 in an isolate (GenBank accession no. KX462969.1) differing from the isolates of cluster 2 in Austria by only 8 alleles. On the contrary, the mutation T223C in profile H had been previously reported during 2012–2015 in Australia, the Netherlands, Norway, Sweden, the United Kingdom, and the United States (*33*–*35*). The mutation in the *prn* gene at nt 1326 was reported in the United Kingdom (*16*) in 2012. Similar mutations at nt 1325 and 1340 of the *prn* gene were also detected in isolates from Australia (*35*) and the United States (*36*). Likewise, the mutation at nt 1273 had been previously found in Canada (*37*) and the United States as well (*13*,*14*). Last, the insertion of the *IS*481 at nt 1613 in reverse direction was also reported in Canada and the United States (*13*,*14*).

The preliminary cluster threshold proposed in this study has served to delineate clusters and can be adjusted when more epidemiologic data derived from contact tracing are available. Establishing a fixed cluster threshold for *B. pertussis* is challenging also because of its homogeneous core genome. Also, because the bacterium undergoes large genomic rearrangements that are only detectable with advanced bioinformatics (*14*), this diversity might not be captured by cgMLST alone. A possibility to increase the typing resolution obtained with cgMLST for detecting pertussis outbreaks might be to investigate the distribution of *IS*481 within the *B. pertussis* genome, as proposed elsewhere (*14*). In either case, cgMLST allowed the identification of a cluster (cluster 2) of pertactin-deficient isolates from case-patients living in St. Johann in Pongau, possibly indicating the presence of a local pertussis outbreak. We could not determine whether all cases occurring within the period of detection of the genetic profile B belonged to that profile or to another genetic profile because we did not receive *B. pertussis* cultures for each pertussis case. Except for cluster 2, we could neither confirm nor refute that all clusters identified in our study represented single outbreaks. However, we demonstrated the direct transmission of the same pertussis strain by cgMLST among members of the same household. We hypothesize that the 2 case-patients in the household where 2 different genetic

profiles and cgMLST (18 alleles of difference) were detected might have acquired pertussis from different sources.

Our results of the comparative genomic analysis using global strains were concordant with other studies, in which diverse *B. pertussis* genetic profiles are shown to be distributed across countries (*12*–*14*,*16*). The pertactin-deficient strains seemed not to belong to the same clone and the mutations observed in each country might consist of independent mutations, as previously described (*38*). In the absence of more sequences to compare with our isolates in Austria, profile B isolates seemed to be found only in Austria, although the mutation *prn*-2–631^632STOP:T>- had already been reported (*15*). In addition, the number of allelic differences between isolates not geographically nor temporally related to the isolates in Austria was sometimes as low as 2, matching recently reported findings (*12*).

The small differences observed between the SNP-based analysis and the cgMLST-based analysis might be attributable to the slightly higher discriminatory power of SNP-based analysis (*39*). Conversely, the differences in gene content between the Pasteur Institute's cgMLST scheme and ours indicate that our cgMLST was more discriminatory and therefore more suitable for cluster detection in Austria. The uneven number of loci composing each cgMLST might be partially attributable to the different algorithms used by Seqsphere and BIGSdb (*40*) but also to the fact that only targets that were present in all query genomes were included as targets of our cgMLST scheme. In contrast, the Pasteur Institute's scheme included targets present in ≥95% of all query genomes. Bouchez et al. (*12*) did not define a threshold for their cgMLST scheme, and hence both schemes might not be comparable in terms of isolate clustering.

The main limitation of our study was the incomplete information on the vaccination status of the case-patients and other epidemiologic data, which prevented better assessment of the effects of these genetic shifts on pertussis incidence. Because of the reduced sample size, whether detecting pertactin-deficient strains is linked to an increase in pertussis incidence is unclear; therefore, expanding the isolate-based surveillance system at the national level is advisable.

In summary, we found that *B. pertussis* strains in Austria differ genetically from the vaccine strain, both in their core genomes and their vaccine antigen genes. Furthermore, our cgMLST method has proven to be stable enough to be applied beyond our set of 123 *B. pertussis* isolates and proven useful to confirm transmission chains among household members and to detect 8 clusters, 1 of which indicated a possible local outbreak. To detect pertussis outbreaks and target pertussis-control strategies, we recommend performing genomic surveillance of *B. pertussis* using the proposed cgMLST scheme with a preliminary cluster threshold of ≤6 alleles, typing data on the vaccine antigen genes, and completing epidemiologic information on pertussis cases.

About the Author

Dr. Cabal Rosel is a postdoctoral researcher working as a public health microbiologist at the Austrian Agency for Health and Food Safety in Vienna, Austria. Her research interests include microbial genomics, One Health, antimicrobial resistance, and epidemiology.

References

1. Kilgore PE, Salim AM, Zervos MJ, Schmitt HJ. Pertussis: microbiology, disease, treatment, and prevention. Clin Microbiol Rev. 2016;29:449–86. https://doi.org/10.1128/CMR.00083-15
2. Paisley RD, Blaylock J, Hartzell JD. Whooping cough in adults: an update on a reemerging infection. Am J Med. 2012;125:141–3. https://doi.org/10.1016/j.amjmed.2011.05.008
3. Lee AD, Cassiday PK, Pawloski LC, Tatti KM, Martin MD, Briere EC, et al.; Clinical Validation Study Group. Clinical evaluation and validation of laboratory methods for the diagnosis of *Bordetella pertussis* infection: culture, polymerase chain reaction (PCR) and anti-pertussis toxin IgG serology (IgG-PT). PLoS One. 2018;13:e0195979. https://doi.org/10.1371/journal.pone.0195979
4. Mir-Cros A, Moreno-Mingorance A, Martín-Gómez MT, Codina G, Cornejo-Sánchez T, Rajadell M, et al. Population dynamics and antigenic drift of *Bordetella pertussis* following whole cell vaccine replacement, Barcelona, Spain, 1986–2015. Emerg Microbes Infect. 2019;8:1711–20. https://doi.org/10.1080/22221751.2019.1694395
5. Wagner B, Melzer H, Freymüller G, Stumvoll S, Rendi-Wagner P, Paulke-Korinek M, et al. Genetic variation of *Bordetella pertussis* in Austria. PLoS One. 2015;10:e013262.
6. Latasa P, García-Comas L, Gil de Miguel A, Barranco MD, Rodero I, Sanz JC, et al. Effectiveness of acellular pertussis vaccine and evolution of pertussis incidence in the community of Madrid from 1998 to 2015. Vaccine. 2018;36:1643–9. https://doi.org/10.1016/j.vaccine.2018.01.070
7. Esposito S, Stefanelli P, Fry NK, Fedele G, He Q, Paterson P, et al.; World Association of Infectious Diseases and Immunological Disorders (WAidid) and the Vaccine Study Group of the European Society of Clinical Microbiology and Infectious Diseases (EVASG). Pertussis prevention: reasons for resurgence, and differences in the current acellular pertussis vaccines. Front Immunol. 2019;10:1344. https://doi.org/10.3389/fimmu.2019.01344
8. Burdin N, Handy LK, Plotkin SA. What is wrong with pertussis vaccine immunity? The problem of waning effectiveness of pertussis vaccines. Cold Spring Harb Perspect Biol. 2017;9:a029454. https://doi.org/10.1101/cshperspect.a029454

9. Chiappini E, Stival A, Galli L, de Martino M. Pertussis re-emergence in the post-vaccination era. BMC Infect Dis. 2013;13:151. https://doi.org/10.1186/1471-2334-13-151
10. Mooi FR, van Oirschot H, Heuvelman K, van der Heide HGJ, Gaastra W, Willems RJL. Polymorphism in the *Bordetella pertussis* virulence factors P.69/pertactin and pertussis toxin in the Netherlands: temporal trends and evidence for vaccine-driven evolution. Infect Immun. 1998;66:670–5. https://doi.org/10.1128/IAI.66.2.670-675.1998
11. Diavatopoulos DA, Cummings CA, Schouls LM, Brinig MM, Relman DA, Mooi FR. *Bordetella pertussis*, the causative agent of whooping cough, evolved from a distinct, human-associated lineage of *B. bronchiseptica*. PLoS Pathog. 2005;1:e45. https://doi.org/10.1371/journal.ppat.0010045
12. Bouchez V, Guglielmini J, Dazas M, Landier A, Toubiana J, Guillot S, et al. Genomic sequencing of *Bordetella pertussis* for epidemiology and global surveillance of whooping cough. Emerg Infect Dis. 2018;24:988–94. https://doi.org/10.3201/eid2406.171464
13. Bowden KE, Weigand MR, Peng Y, Cassiday PK, Sammons S, Knipe K, et al. Genome structural diversity among 31 *Bordetella pertussis* isolates from two recent U.S. whooping cough statewide epidemics. MSphere. 2016; 1:e00036–16. https://doi.org/10.1128/mSphere.00036-16
14. Weigand MR, Peng Y, Loparev V, Batra D, Bowden KE, Burroughs M, et al. The history of *Bordetella pertussis* genome evolution includes structural rearrangement. J Bacteriol. 2017;199:199. https://doi.org/10.1128/JB.00806-16
15. Barkoff A-M, Mertsola J, Pierard D, Dalby T, Hoegh SV, Guillot S, et al. Pertactin-deficient *Bordetella pertussis* isolates: evidence of increased circulation in Europe, 1998 to 2015. Euro Surveill. 2019;24:1700832. https://doi.org/10.2807/1560-7917.ES.2019.24.7.1700832
16. Sealey KL, Harris SR, Fry NK, Hurst LD, Gorringe AR, Parkhill J, et al. Genomic analysis of isolates from the United Kingdom 2012 pertussis outbreak reveals that vaccine antigen genes are unusually fast evolving. J Infect Dis. 2015;212:294–301. https://doi.org/10.1093/infdis/jiu665
17. Vestrheim DF, Steinbakk M, Bjørnstad ML, Moghaddam A, Reinton N, Dahl ML, et al. Recovery of *Bordetella pertussis* from PCR-positive nasopharyngeal samples is dependent on bacterial load. J Clin Microbiol. 2012;50:4114–5. https://doi.org/10.1128/JCM.01553-12
18. Martini H, Rodeghiero C, VAN DEN Poel C, Vincent M, Pierard D, Huygen K. Pertussis diagnosis in Belgium: results of the National Reference Centre for *Bordetella anno* 2015. Epidemiol Infect. 2017;145:2366–73. https://doi.org/10.1017/S0950268817001108
19. Lam C, Octavia S, Bahrame Z, Sintchenko V, Gilbert GL, Lan R. Selection and emergence of pertussis toxin promoter *ptxP3* allele in the evolution of *Bordetella pertussis*. Infect Genet Evol. 2012;12:492–5. https://doi.org/10.1016/j.meegid.2012.01.001
20. Bowden KE, Williams MM, Cassiday PK, Milton A, Pawloski L, Harrison M, et al. Molecular epidemiology of the pertussis epidemic in Washington State in 2012. J Clin Microbiol. 2014;52:3549–57. https://doi.org/10.1128/JCM.01189-14
21. van Gent M, Heuvelman CJ, van der Heide HG, Hallander HO, Advani A, Guiso N, et al. Analysis of *Bordetella pertussis* clinical isolates circulating in European countries during the period 1998–2012. Eur J Clin Microbiol Infect Dis. 2015;34:821–30. https://doi.org/10.1007/s10096-014-2297-2
22. Bart MJ, Harris SR, Advani A, Arakawa Y, Bottero D, Bouchez V, et al. Global population structure and evolution of *Bordetella pertussis* and their relationship with vaccination. MBio. 2014;5:e01074–14. https://doi.org/10.1128/mBio.01074-14
23. Moriuchi T, Vichit O, Vutthikol Y, Hossain MS, Samnang C, Toda K, et al. Molecular epidemiology of *Bordetella pertussis* in Cambodia determined by direct genotyping of clinical specimens. Int J Infect Dis. 2017;62:56–8. https://doi.org/10.1016/j.ijid.2017.07.015
24. Miyaji Y, Otsuka N, Toyoizumi-Ajisaka H, Shibayama K, Kamachi K. Genetic analysis of *Bordetella pertussis* isolates from the 2008–2010 pertussis epidemic in Japan. PLoS One. 2013;8:e77165. https://doi.org/10.1371/journal.pone.0077165
25. Breakwell L, Kelso P, Finley C, Schoenfeld S, Goode B, Misegades LK, et al. Pertussis vaccine effectiveness in the setting of pertactin-deficient pertussis. Pediatrics. 2016;137:e20153973. https://doi.org/10.1542/peds.2015-3973
26. Etskovitz H, Anastasio N, Green E, May M. Role of evolutionary selection scting on vaccine antigens in the re-emergence of *Bordetella pertussis*. Diseases. 2019;7:35. https://doi.org/10.3390/diseases7020035
27. Safarchi A, Octavia S, Nikbin VS, Lotfi MN, Zahraei SM, Tay CY, et al. Genomic epidemiology of Iranian *Bordetella pertussis*: 50 years after the implementation of whole cell vaccine. Emerg Microbes Infect. 2019;8:1416–27. https://doi.org/10.1080/22221751.2019.1665479
28. Carriquiriborde F, Regidor V, Aispuro PM, Magali G, Bartel E, Bottero D, et al. Rare detection of *Bordetella pertussis* pertactin-deficient strains in Argentina. Emerg Infect Dis. 2019;25:2048–54. https://doi.org/10.3201/eid2511.190329
29. Safarchi A, Octavia S, Luu LD, Tay CY, Sintchenko V, Wood N, et al. Pertactin negative *Bordetella pertussis* demonstrates higher fitness under vaccine selection pressure in a mixed infection model. Vaccine. 2015;33:6277–81. https://doi.org/10.1016/j.vaccine.2015.09.064
30. Carvalho CFA, Andrews N, Dabrera G, Ribeiro S, Stowe J, Ramsay M, et al. National Outbreak of Pertussis in England, 2011–2012: a case-control study comparing 3-component and 5-component acellular vaccines with whole-cell pertussis vaccines. Clin Infect Dis. 2020;70:200–7. https://doi.org/10.1093/cid/ciz199
31. van Twillert I, Bonačić Marinović AA, Kuipers B, van Gaans-van den Brink JAM, Sanders EAM, van Els CACM. Impact of age and vaccination history on long-term serological responses after symptomatic *B. pertussis* infection, a high dimensional data analysis. Sci Rep. 2017;7:40328. https://doi.org/10.1038/srep40328
32. Olin P, Rasmussen F, Gustafsson L, Hallander HO, Heijbel H; Ad Hoc Group for the Study of Pertussis Vaccines. Randomised controlled trial of two-component, three-component, and five-component acellular pertussis vaccines compared with whole-cell pertussis vaccine. Lancet. 1997;350:1569–77. https://doi.org/10.1016/S0140-6736(97)06508-2
33. Zeddeman A, van Gent M, Heuvelman CJ, van der Heide HG, Bart MJ, Advani A, et al. Investigations into the emergence of pertactin-deficient *Bordetella pertussis* isolates in six European countries, 1996 to 2012. Euro Surveill. 2014;19:20881. https://doi.org/10.2807/1560-7917.ES2014.19.33.20881
34. Weigand MR, Williams MM, Peng Y, Kania D, Pawloski LC, Tondella ML; CDC Pertussis Working Group. Genomic survey of *Bordetella pertussis* diversity, United States, 2000–2013. Emerg Infect Dis. 2019;25:780–3. https://doi.org/10.3201/eid2504.180812

35. Xu Z, Octavia S, Luu LDW, Payne M, Timms V, Tay CY, et al. Pertactin-negative and filamentous hemagglutinin-negative *Bordetella pertussis*, Australia, 2013–2017. Emerg Infect Dis. 2019;25:1196–9. PubMed https://doi.org/10.3201/eid2506.180240
36. Weigand MR, Peng Y, Cassiday PK, Loparev VN, Johnson T, Juieng P, et al. Complete genome sequences of *Bordetella pertussis* isolates with novel pertactin-deficient deletions. Genome Announc. 2017;5:e00973–17. https://doi.org/10.1128/genomeA.00973-17
37. Tsang RS, Shuel M, Jamieson FB, Drews S, Hoang L, Horsman G, et al. Pertactin-negative *Bordetella pertussis* strains in Canada: characterization of a dozen isolates based on a survey of 224 samples collected in different parts of the country over the last 20 years. Int J Infect Dis. 2014;28:65–9. https://doi.org/10.1016/j.ijid.2014.08.002
38. Lam C, Octavia S, Ricafort L, Sintchenko V, Gilbert GL, Wood N, et al. Rapid increase in pertactin-deficient *Bordetella pertussis* isolates, Australia. Emerg Infect Dis. 2014;20:626–33. https://doi.org/10.3201/eid2004.131478
39. Uelze L, Grützke J, Borowiak M, Hammerl JA, Juraschek K, Deneke C, et al. Typing methods based on whole genome sequencing data. One Health Outlook. 2020;2:3. https://doi.org/10.1186/s42522-020-0010-1
40. Jolley KA, Bray JE, Maiden MCJ. Open-access bacterial population genomics: BIGSdb software, the PubMLST.org website and their applications. Wellcome Open Res. 2018;3:124. https://doi.org/10.12688/wellcomeopenres.14826.1

Address for correspondence: Adriana Cabal Rosel, Austrian Agency for Health and Food Safety, Währingerstraße 25a, 1096 Vienna, Austria; email: adriana@cabalrosel.com

Emerging Infectious Diseases

Spotlight Topics

Antimicrobial resistance • Ebola
Etymologia • Food safety • HIV-AIDS
Influenza • Lyme disease • Malaria
MERS • Pneumonia • Rabies • Ticks
Tuberculosis • Coronavirus • Zika

EID's spotlight topics highlight the latest articles and information on emerging infectious disease topics in our global community

https://wwwnc.cdc.gov/eid/page/spotlight-topics

Decline of Tuberculosis Burden in Vietnam Measured by Consecutive National Surveys, 2007–2017

Hai Viet Nguyen, Hoa Binh Nguyen, Nhung Viet Nguyen, Frank Cobelens, Alyssa Finlay, Cu Huy Dao, Veriko Mirtskhulava, Philippe Glaziou, Huyen T.T. Pham, Petra de Haas, Edine Tiemersma

Vietnam, a high tuberculosis (TB) burden country, conducted national TB prevalence surveys in 2007 and 2017. In both surveys participants were screened by using a questionnaire and chest radiograph; sputum samples were then collected to test for *Mycobacterium tuberculosis* by smear microscopy and Löwenstein-Jensen culture. Culture-positive, smear-positive, and smear-negative TB cases were defined by laboratory results, and the prevalence of tuberculosis was compared between the 2 surveys. The results showed prevalence of culture-positive TB decreased by 37% (95% CI 11.5%–55.4%), from 199 (95% CI 160–248) cases/100,000 adults in 2007 to 125 (95% CI 98–159) cases/100,000 adults in 2017. Prevalence of smear-positive TB dropped by 53% (95% CI 27.0%–69.7%), from 99 (95% CI 78–125) cases/100,000 adults to 46 (95% CI 32–68) cases/100,000 adults; smear-negative TB showed no substantial decrease. Replacing microscopy with molecular methods for primary diagnostics might enhance diagnosis of pulmonary TB cases and further lower TB burden.

Despite global progress in preventing and controlling tuberculosis (TB), reducing worldwide burden has fallen short of the World Health Organization's (WHO) End-TB elimination target (*1*). However, in most high-burden countries, estimates of burden and its trend over time are derived indirectly (*1*). One main factor that impedes global efforts to estimate the effects of and eliminate TB is the gap in case detection. In most high-burden lower-middle income countries, an unknown proportion of incident TB remains undiagnosed and unreported (*2*). To estimate TB incidence, WHO has applied the results of nationwide prevalence surveys to a model of disease duration distribution, among other estimation methods (*3*). These surveys were administered to determine a country's gaps in detecting TB cases, help plan interventions, and estimate the resources required (*4*). Prevalence surveys measure TB burden directly; surveys that are repeated have particular strategic importance. Comparing TB prevalence over time enables public health authorities to assess the trend in burden and therefore to evaluate the effect of TB control interventions between surveys and develop policies to guide future actions (*5*).

Vietnam is among the 30 countries with the highest burden of TB in the world (*6*). In 2006–2007, the Vietnam National TB Program (NTP) conducted the first national TB prevalence survey, which identified 307 (95% CI 249–366) pulmonary TB cases/100,000 adult participants (*7*). Since then, to reduce the TB burden in Vietnam NTP has applied a broad package of TB control interventions (*8*). In addition to strengthening routine TB care and treatment, NTP has introduced new TB diagnostics, TB drugs, and treatment regimens for multidrug-resistant TB patients, preventive treatment for children ≤5 years of age living with ≥1 additional TB patients, household contact tracing, and active case finding (*9*,*10*). Although after 2007 the TB notification rate in Vietnam declined (*11*), it remained unknown to what extent this represented a decrease in TB burden.

In 2017–2018, NTP administered a second national TB prevalence survey in Vietnam, which showed 322 (260–399) TB cases/100,000 adults (*12*). These findings suggested no change in burden over the 10-year period. However, to be in line with WHO recommendations, the second survey used TB screening procedures and diagnostics that were state-of-the-art in 2017–2018 but not available in 2006–2007 (*13*).

Author affiliations: National Tuberculosis Programme, Hanoi, Vietnam (H.V. Nguyen, H.B. Nguyen, N.V. Nguyen, C.H. Dao, H.T.T. Pham); Amsterdam University Medical Centers, Amsterdam, the Netherlands (H.V. Nguyen, F. Cobelens); US Centers for Disease Control and Prevention, Vietnam Office, Hanoi (A. Finlay); KNCV Tuberculosis Foundation, Den Haag, the Netherlands (V. Mirtskhulava, P. de Hass, E. Tiemersma); World Health Organization, Geneva, Switzerland (P. Glaziou).

DOI: https://doi.org/10.3201/eid2703.204253

These methods differed from those used in the first survey, potentially affecting estimates of trends in prevalence. To enable direct comparisons, we also analyzed data from the second survey using screening and diagnostic methods similar to those used in the first survey. To directly measure the change in TB burden over time and the effect of control interventions in Vietnam, as much as possible we compared the results of the 2 surveys based on the same methods with regard to sampling, screening, laboratory testing, case definitions, and statistical adjustments. Our primary comparison considered the adjusted prevalence of culture-positive TB; secondary comparisons included adjusted and unadjusted prevalence of smear-positive TB and smear-negative TB.

This study was given scientific and ethics approval by the Institutional Review Board of the Vietnam National Lung Hospital, under approval letter number 62/17/CTHĐKH-ĐĐ. The risks and benefits of the study were explained to participants and each signed a written informed consent. All of those with >1 positive test result for TB were referred for TB treatment; we followed up to verify that they received adequate health care and treatment.

Methods

Study Design and Population

Both the first and second surveys were cross-sectional studies using multistage cluster sampling. The sample size of both surveys was based on the estimated prevalence of TB in the country at the time of study design (*3*). Also, a frequentist approach was applied in the second survey (*14*) to ensure a large enough sample for finding a difference in TB prevalence between the 2 surveys of >25%, with a power of 80%.

Sampling methods were similar between the 2 surveys, except for small details in the sampling frames, enumeration, and inclusion criteria (Appendix Table 1, https://wwwnc.cdc.gov/EID/article/27/3/20-4253-App1.pdf). The sampling frame used in the second survey did not include stratification, whereas the sampling frame in the first survey was stratified by urban, rural, and remote areas. Enumeration criteria differed slightly; the first survey included all adult residents (≥15 years old) who had lived in households of the selected clusters for >3 months, but the duration used in the second survey was ≥2 weeks. All enumerated persons who met the inclusion criteria were considered eligible for the second survey, but for the first survey, they also had to indicate that they planned to attend the survey site for screening.

Screening and Diagnostic Procedures

For both surveys, all participants were screened for TB based on self-reported symptoms and chest radiograph results. Those who reported TB symptoms, had TB treatment history <2 years before the respective survey, or had chest radiograph abnormalities consistent with TB were considered screen-positive and were eligible for sputum collection and examination. For the second survey, all chest radiographs were digital, whereas in the first survey, only two thirds of the clusters used digital chest radiographs (Appendix Table 2). The criteria for defining screen-positive participants based on symptoms differed slightly between the 2 surveys. In the first survey only those reporting productive cough for >2 weeks were considered positive on their symptom screens. In the second survey, all participants reporting any cough lasting >2 weeks, as well as pregnant women reporting any cough of any duration, were considered to have a positive symptom screen. To compare the 2 surveys, we only considered participants screen-positive if they reported productive cough for >2 weeks or had a history of TB treatment <2 years before the survey (Appendix Table 3).

Recommended laboratory methods for prevalence survey estimates were followed in each survey, but guidelines have changed over time (*14*). The first survey used sputum smear microscopy and Löwenstein-Jensen (LJ) solid culture assays; the second survey used the molecular assay Xpert MTB/RIF (Cepheid, https://www.cepheid.com) and BD MGIT BACTEC 960 liquid culture (https://www.bd.com). To ensure comparable laboratory results between the surveys, for the second survey we also conducted sputum smear microscopy and LJ solid culture on sputum samples (Appendix Table 2). Sputum sample processing was slightly different between surveys. For the first survey we used 4% NALC-NaOH to decontaminate the specimen before LJ culture; for the second survey we used the modified Petrov method with 3% NALC-NaOH for decontamination.

Case Definition

TB case definitions used for comparison purposes were based solely on laboratory results in which each screen-positive participant had 1 early morning sputum sample tested for TB by sputum smear microscopy and LJ culture in designated survey laboratories. Screen-positive participants whose result from sputum smear was positive for acid-fast bacilli and whose LJ culture grew *Mycobacterium tuberculosis* were defined as smear-positive TB cases, whereas those who had a negative sputum smear result and LJ

culture grew *M. tuberculosis* were defined as smear-negative. Culture-positive TB cases had either smear-negative or smear-positive TB.

Data Analysis

We combined data from the 2 surveys into 1 database, assigning a unique personal identification code for each observation, and adapted the variables needed to compare the 2 surveys. Similar to what we reported for the second survey, data analysis was conducted on the combined database, with updated inclusion criteria and case definitions, as stated (*12*). The adjusted analysis involved multiple imputation by chained equation for missing data, including sputum smear and LJ culture results, and inverse probability weighting as recommended by WHO (*13*). To ensure the comparability of the 2 surveys and adjust for the relative sampling probability of each participant in both surveys, we applied poststratification using population data for Vietnam estimated by the General Statistics Office of Vietnam in 2007 and 2017 (*16*).

We assessed statistical differences in characteristics between the 2 surveys by $\chi 2$ test and logistic regression. We calculated point estimates and 95% CIs for TB prevalence in Stata version 14.0 (StataCorp, https://www.stata.com) using the mim and svy commands with pweights specified to adjust for design effect. We derived 95% CIs and p values using Rubin's rules (*17*). To assess whether TB prevalence had changed between the 2 surveys, we calculated a prevalence difference on the combined dataset using Stata's epitab module (StataCorp), including the outcome "TB case Yes/No" as the dependent variable and first or second survey as the explanatory variable.

Results

There were 94,156 participants (90.7% of the eligible survey population) in the first survey and 61,763 (70.8% of the eligible survey population) in the second. Among participants in the first survey, 99.9% were screened for TB symptoms and had chest radiographs; in the second survey, 93.1% were screened and had radiographs. Among all survey participants, in the first survey 7,529/94,156 (8.0%) tested screen-positive; in the second, 4,595/61,763 (7.3%) tested screen-positive (Figure 1; Table 1).

Among screen-positive participants in the first survey, 6,780/7,529 (90.1%) had available sputum smear microscopy results; 121 (0.13% of 94,156 total participants) were smear-positive (Table 2). This proportion was similar in the second survey with positive sputum smear results in 77 (0.12% of 61,763 total participants; p = 0.835). There were 218 (0.23%) participants culture-positive for *M. tuberculosis* in the first survey and 125 (0.20%) in the second (p = 0.230). The proportion of LJ cultures growing nontuberculous mycobacteria or being contaminated was significantly higher in the second survey than in the first survey (p<0.001; Table 2).

Overall, the crude prevalence of culture-positive TB decreased 26.1% (95% CI 7.5%–44.7%) between the 2 surveys (p = 0.007; Appendix Table 5), from 191 (95% CI 167–218) cases/100,000 adults in the first survey to 142 cases/100,000 adults (95% CI 113–169) in the second survey. The crude prevalence of smear-positive TB decreased by 53.0% (95% CI 28.7%–77.2%; Appendix Table 6), from 92 (95% CI 78–125) cases/100,000 adults in 2006–2007 to 43 (95% CI 31–59) cases/100,000 adults in 2017–2018. The crude prevalence of smear-negative TB was 99 (95% CI 82–119) cases/100,000 adults in the first survey and 99 (95% CI 80–122) cases/100,000 adults (p = 0.938) in the second survey (Appendix Table 7).

Sputum smear results, LJ culture results, or both, were missing for 805/7,529 (10.7%) screen-positive participants in the first survey and for 881/4,595 (19.2%) in the second survey. Imputation and adjustment by inverse probability weighting and poststratification resulted in increased adjusted prevalence rates for culture- or smear-positive TB and for smear-negative TB by an average of 11.3% for the first survey and by an average of 20.0% for the second survey. The adjusted prevalence of culture-positive TB declined by 37.1% (95% CI 11.5%–55.4%), from 199 (95% CI 160–248) cases/100,000 adults in 2006–2007 to 125 (95% CI 98–159) cases/100,000 adults in 2017–2018 (p = 0.008; Figure 2; Appendix Table 5). This decline was 53.1% (95% CI 27.0–69.7) for smear-positive, from 99 cases/100,000 adults (95% CI 78–125) to 46 cases/100,000 adults (95% CI 32–68) (p = 0.001; Figure 2; Appendix Table 6). We observed no significant reduction in smear-negative TB prevalence (21.3%, 95% CI: −22.0% to 49.7%; p = 0.679) (Appendix Table 7).

When we stratified results by age and sex, we found a significant reduction (64.0%, 95% CI 40.1%–78.4%; p<0.001) in the prevalence of smear-positive TB among men: 71% (95% CI 32.9%–87.6%; p = 0.026) among men in the 35–44 year age group and 73.8% (95% CI 22.5%–91.1%; p = 0.019) among men ≥65 years of age (Appendix Table 6). The adjusted prevalence of smear-positive TB significantly decreased from the first survey to the second in rural areas (73.5%, 95% CI 35.1%–89.2%; p = 0.017), and in the southern (53.5%, 95% CI 8.3%–76.5%; p = 0.047) and northern (65.2%, 95% CI 20.6%–84.7%; p = 0.022) regions of Vietnam (Appendix Table 6); a significant decline in

culture-positive TB (33.3%, 95% CI 7.4%–65.0%; p = 0.023) occurred only in rural areas (Appendix Table 5). In-depth interviews in the 2 surveys showed no difference between the symptoms reported by the screen-positive participants and TB cases found in the 2 surveys, except for self-reported weight loss, which was lower in the second survey (Figure 3; Appendix Table 4).

Discussion

Our analyses show a 37% decline in the adjusted prevalence of culture-positive TB in Vietnam over a 10-year period between 2006–2007 and 2017–2018, equating to an average annual decline of 4.5%. This decline was mainly due to the 53% reduction in smear-positive TB, particularly because of substantial reductions among men, persons living in rural areas, and persons in the northern and southern parts of the country. We found no reduction in the adjusted prevalence of smear-negative TB. These results are in line with a 57% decline in smear-positive TB prevalence observed from 2000 to 2010 in China (*18*) and declines in culture-positive TB of 45% and smear-positive TB of 38% in Cambodia from 2002 to 2011 (*19*).

The second survey's participation rate was much lower than that for the first survey (Figure 1), which could be explained by the difference between the household enumeration inclusion criteria of the 2 surveys; in the first survey, only those who confirmed availability to participate in the survey

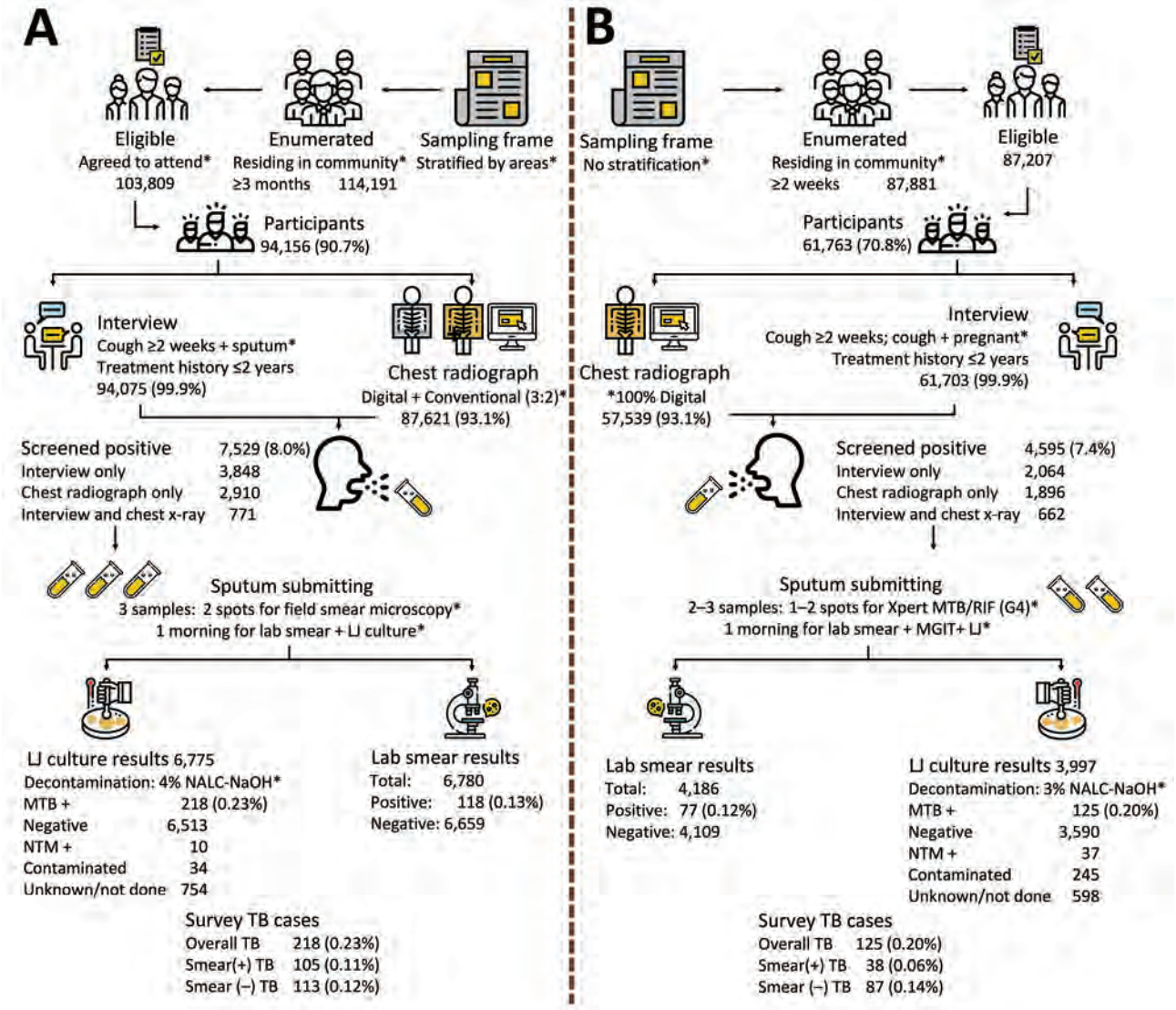

Figure 1. Summary results and comparison between the first (A) and second (B) national TB prevalence surveys in Vietnam, 2007 and 2017. Asterisk (*) indicates differences in methods between the 2 surveys. MTB, *Mycobacterium tuberculosis*; NTM, nontuberculosis mycobacteria; TB, tuberculosis; +, positive; –, negative.

Table 1. Comparison of characteristics of participants eligible for sputum collection during 2 national TB prevalence surveys in Vietnam, 2007 and 2017

Characteristic	First survey, 2007			Second survey, 2017			p value†
	Participants	Screened positive*	% Positive	Participants	Screened positive*	% Positive	
Total	94,156	7,529	8.0	61,763	4,595	7.4	<0.001
Sex							
M	42,596	4,580	10.8	27,150	2,794	10.3	0.053
F	51,560	2,949	5.7	34,613	1,801	5.2	0.001
Age group, y							
15–24	20,934	620	3.0	6,542	120	1.8	<0.001
25–34	18,681	950	5.1	10,191	349	3.4	<0.001
35–44	19,790	1,429	7.2	11,508	548	4.8	<0.001
45–54	16,285	1,587	9.8	13,289	1,056	8.0	<0.001
55–64	8,138	1,055	13.0	11,143	1,162	10.4	<0.001
≥65	10,328	1,888	18.3	9,090	1,360	15.0	<0.001
Area							
Urban	26,353	2,058	7.8	18,656	1,383	7.4	0.119
Remote	27,532	2,406	8.7	15,882	1,179	7.4	<0.001
Rural	40,271	3,065	7.6	27,225	2,033	7.5	0.489
Region							
North	45,669	3,913	8.6	25,575	1,849	7.2	<0.001
Central	14,646	1,062	7.3	13,525	1,195	8.8	<0.001
South	33,841	2,554	7.6	22,663	1,551	6.8	0.002

*Screened positive if participants had ≥1 of self-reported cough for ≥2 wk, TB treatment <2 y preceding the survey, or abnormal chest radiography images.
†By Pearson χ^2 test to compare characteristics between the first and the second surveys.

during fieldwork days were recorded as eligible. Also, recent economic growth in Vietnam has enabled more people to access out-of-pocket healthcare services, making attending a TB prevalence survey to receive free health checkups less attractive. The types of symptoms and proportion of participants with any symptoms suggestive of TB among screen-positive participants and culture-positive TB cases in the 2 surveys were similar, except that weight loss was more frequently reported in the first survey. This difference could be attributable to differences in training interviewers; for the first survey the interviewers were explicitly trained to ask carefully about weight loss to help ascertain the prevalence of chronic obstructive pulmonary disease, a secondary objective in the first survey only (H.B. Nguyen, unpub. data).

Over the decade between surveys, smear-positive TB prevalence declined, but smear-negative TB prevalence remained static. Vietnam, as a low-middle income country, has used sputum smear microscopy

Table 2. Results of laboratory testing and TB cases during 2 national TB prevalence surveys in Vietnam, 2007 and 2017*

	First survey, 2007		Second survey, 2017		p value†
	No. participants	% Participants	No. participants	% Participants	
Total participants	94,156	100.0	61,763	100.0	NA
Participants screened positive	7,529	8.0	4,595	7.4	<0.001
DSSM‡					
Negative	6,659	7.07	4,109	6.65	0.001
Any positive	118	0.13	77	0.12	0.835
Positive scanty	35	0.04	36	0.06	0.056
Positive 1+	47	0.05	26	0.04	0.485
Positive 2+	21	0.02	7	0.01	0.114
Positive 3+	15	0.02	8	0.01	0.636
Not reported§	752	0.80	409	0.66	0.003
LJ culture					
MTB growth	218	0.23	125	0.20	0.230
NTM growth	10	0.01	37	0.06	<0.001
No growth	6,513	6.92	3,590	5.81	<0.001
Contaminated	34	0.04	245	0.40	<0.001
Not reported§	754	0.80	598	0.97	<0.001
TB case	218	0.23	125	0.20	0.204
DSSM(+) – LJ(+)	105	0.11	38	0.06	0.001
DSSM(–) – LJ(+)	113	0.12	87	0.14	0.298

*DSSM, direct smear microscopy; LJ, Lowenstein-Jensen; MTB, *Mycobacterium tuberculosis*; NA, not applicable; NTM, nontuberculosis mycobacteria; TB, tuberculosis; +, positive; –, negative..
†Pearson χ^2 test to compare characteristics between the first and the second surveys.
‡Direct smear microscopy of the morning sample only.
§Test result was unknown or no sample available.

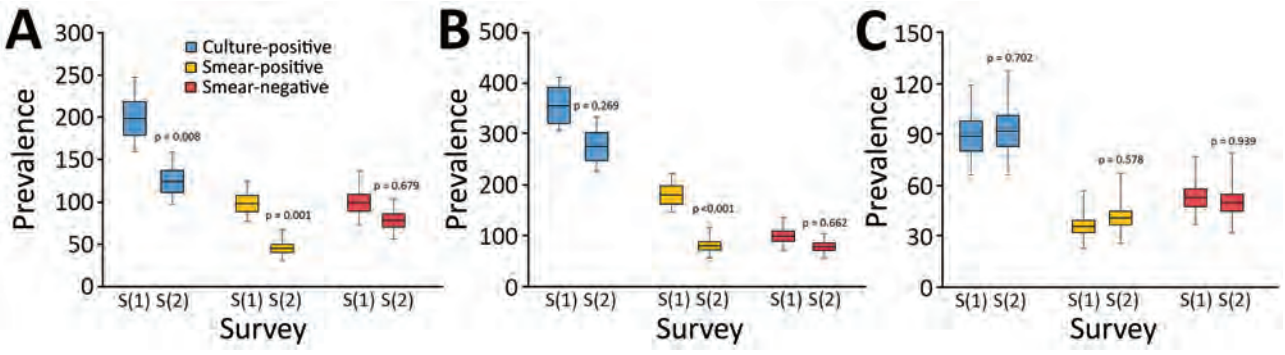

Figure 2 Comparison of the prevalence (cases/100,000 adults) of culture-positive TB, smear-positive TB and smear-negative TB between the first and second national TB prevalence surveys in Vietnam, 2007 and 2017. (A) Overall prevalence; (B) prevalence among male participants; (C) prevalence among female participants. Box tops and bottoms indicate the standard errors of the prevalence; horizontal lines within boxes indicate the point estimates of the prevalence; error bars indicate 95% CIs. S(1), first TB prevalence survey (2007); S(2), second TB prevalence survey (2017).

as a key method to diagnose TB nationwide (*20*). Microscopy cannot detect smear-negative TB, which might explain why the recorded prevalence of smear-negative TB did not change after the first survey. Of note, whereas the prevalence of smear-positive TB decreased by 64% among men, it did not change among women. This difference may be because for decades women in Vietnam have sought healthcare more often than men and experienced shorter delays (*21*). TB case finding among women, with the support of the Women's Union, has been instrumental in reducing TB prevalence (*22*). Thus, it may be that, compared with men, women already had relatively shorter TB duration, and so prevalence was less affected by TB control interventions during the decade. In addition, the Global Adult Tobacco Survey conducted in Vietnam in 2015 found that smoking, a well-known risk factor for TB, was more frequent among men (47.4%) than among women (1.4%), although the smoking prevalence among men had declined slightly compared with a similar survey in 2010 (*23*).

The difference in TB prevalence between men and women was also reflected in the decline of the male-to-female ratio in the prevalence of culture-positive TB found in the 2 surveys by using similar methods, from 4.0:1 in 2006–2007 to 3.0:1 in 2017–2018. This ratio is still high compared with the average found in 56 previous TB prevalence surveys in low-middle income countries (2.2:1) (*24*). The consistently high male-to-female ratios in both studies suggest that the difference by sex in recorded TB prevalence reflects an actual difference in disease occurrence, warranting further research.

We cannot be conclusive about the causes of the reduction in TB prevalence in our study because confounding factors may have affected the trend in TB burden in Vietnam. One factor is economic growth in Vietnam during 2007–2017; steady annual GDP growth rates ranged from 5.2% to 7.1% (*25*). When the economy grows, TB burden tends to decline because nutritional, housing, and working conditions improve (*26*). A decline solely due to economic growth would likely have affected smear-positive and smear-negative TB equally. However, many interventions employed by NTP in the 10 years between surveys relied on sputum smear microscopy, which cannot detect smear-negative TB, possibly explaining these divergent trends. The decline in smear-positive TB suggests that the interventions were effective and are at least partially responsible for the observed decline. Nevertheless, estimates of the burden of TB in Vietnam remained high when newer, more advanced, recommended diagnostics were applied to measure prevalence. Data based only on sputum smear microscopy and LJ culture underestimated prevalence by 60%–62% compared with prevalence estimated by using Xpert MTB/RIF rapid molecular assays (Cepheid) and the more sensitive MGIT BACTEC960 liquid culture method (BD) (*12*). It is reasonable to believe that the first survey underestimated the TB prevalence to a similar extent, which may be true for many prevalence surveys using less sensitive methods. This likelihood also underscores the need to replace microscopy with Xpert MTB/RIF as the primary TB diagnostic method for TB care nationwide.

Our study's first limitation was that we could not address all of the analytic differences in screening and diagnostic technologies used in the 2 surveys. This difference may have affected the comparability of screening and diagnostic results, contributing to uncertainties surrounding the true TB burden in both surveys. For screening, digital chest radiograph was applied in all clusters in the second survey, whereas

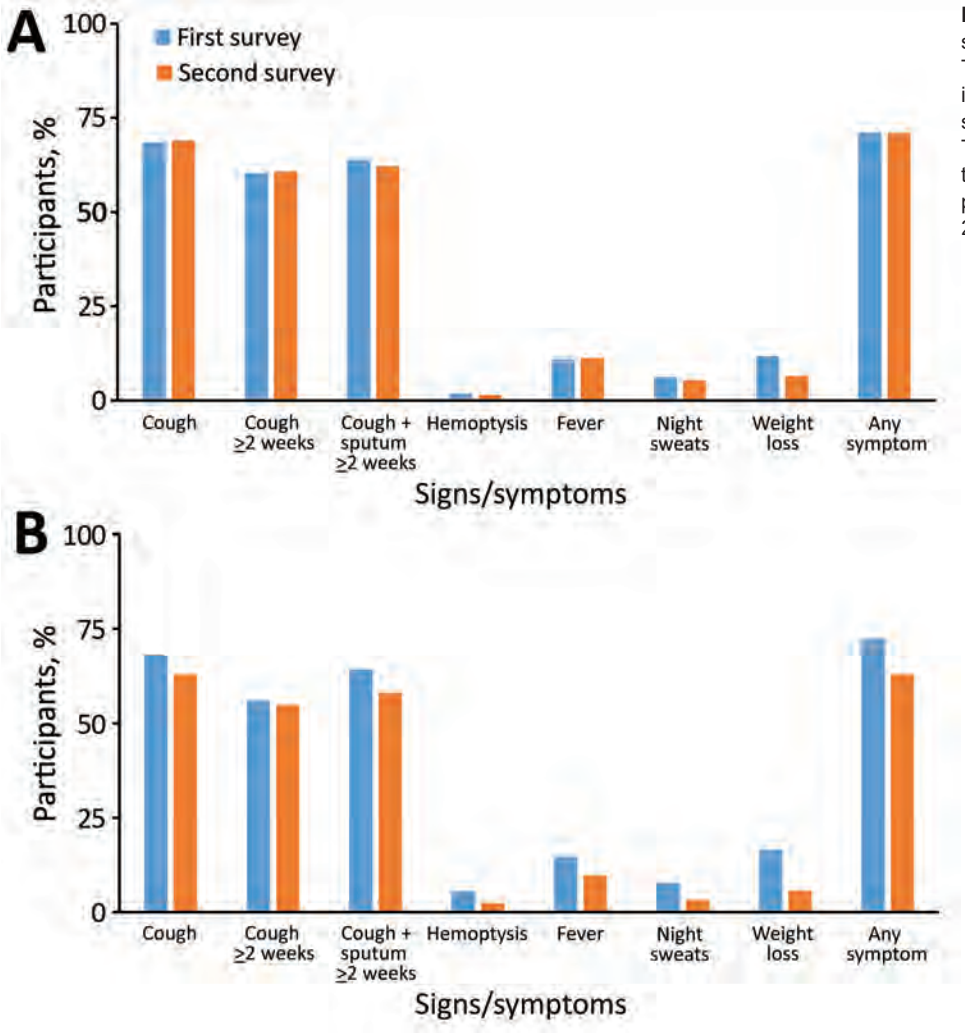

Figure 3. Comparison of symptoms suggestive of TB reported during in-depth interviews of participants who screened positive (A) and survey TB cases (B) identified during the first and second national TB prevalence surveys in Vietnam, 2007 and 2017.

participants in only two thirds of the clusters in the first survey had digital chest radiograph, which probably resulted in lower sensitivity of TB screening in the first survey (Appendix Table 2). For diagnosis, sputum processing using harsher decontamination methods during the first survey might have resulted in more false-negative culture results compared with the second survey. The difference in sputum processing could also explain the higher rate of contamination in the second survey. Second, the comparison of TB prevalence between surveys among participants in the youngest age group (15–24 years of age) was not available because no culture-positive TB case was found in the second survey among this age group. This lack of results might be due to undersampling in this age group because the time they needed to go to school or work interfered with the timing of fieldwork, as described elsewhere (*12*). We attempted to correct for this lack of data using multiple imputation and poststratification as recommended (*13*).

In summary, our study shows a statistically significant reduction in prevalence of smear-positive TB in Vietnam between 2007 and 2017 but no statistically significant reduction in prevalence of smear-negative TB. These results should be used by the NTP to direct efforts and resources to support TB prevention and control nationwide. In particular, our results suggest that replacing microscopy with rapid molecular diagnostic methods, such as Xpert MTB/RIF, and screening for TB using digital chest radiograph to enhance rapid case finding and treatment could further reduce the TB burden in Vietnam.

Acknowledgment

We thank the Vietnam National Tuberculosis Program board of directors, all tuberculosis staff, and the study participants involved in both surveys. Also, we thank the WHO Tuberculosis Monitoring & Evaluation team in Geneva for technical support with data analysis.

This study was funded by the Vietnam Ministry of Health; The Global Fund to Fight AIDS, Tuberculosis and Malaria; the US Agency for International Development; the US Centers for Disease Control and Prevention (CDC), Vietnam Office; the KNCV Tuberculosis Foundation; and the World Health Organization (WHO). CDC, KNCV, and WHO provided assistance in study design, data collection supervision, data analysis, and manuscript preparation.

About the Author

Dr. Nguyen is a medical doctor and researcher at the Vietnam Integrated Centre for Tuberculosis and Respirology Research, Vietnam National Tuberculosis Program. He is pursuing his PhD at the University of Amsterdam using the findings from the second national TB prevalence survey in Vietnam. He is interested in research on TB epidemiology and whole-genome sequencing technology.

References

1. Glaziou P, Floyd K, Raviglione MC. Global epidemiology of tuberculosis. Semin Respir Crit Care Med. 2018;39:271–85. https://doi.org/10.1055/s-0038-1651492
2. Satyanarayana S, Nair SA, Chadha SS, Shivashankar R, Sharma G, Yadav S, et al. From where are tuberculosis patients accessing treatment in India? Results from a cross-sectional community based survey of 30 districts. PLoS One. 2011;6:e24160. https://doi.org/10.1371/journal.pone.0024160
3. Glaziou P, Charalambos S, Carel P, Floyd F. Methods used by WHO to estimate the global burden of TB disease. 2016 Mar 1 [cited 2020 Oct 10]. https://arxiv.org/abs/1603.00278
4. Jenkins HE. Global burden of childhood tuberculosis. Pneumonia (Nathan). 2016;8:24. https://doi.org/10.1186/s41479-016-0018-6
5. World Health Organization. Repeat prevalence surveys in Asia: design and analysis. Workshop on repeat prevalence surveys in Asia. Phnom Penh, Cambodia. February 8–11, 2012 [cited 2020 Oct 10]. https://www.who.int/tb/advisory_bodies/impact_measurement_taskforce/meetings/prevalence_survey/feb2012cambodia_meetingreport.pdf
6. World Health Organisation. Global tuberculosis report 2018. Geneva: The Organization. 2018 [cited 2020 Oct 10]. https://reliefweb.int/sites/reliefweb.int/files/resources/9789241565646-eng.pdf
7. Hoa NB, Sy DN, Nhung NV, Tiemersma EW, Borgdorff MW, Cobelens FGJ. National survey of tuberculosis prevalence in Viet Nam. Bull World Health Organ. 2010;88:273–80. https://doi.org/10.2471/BLT.09.067801
8. Vietnam National Tuberculosis Program. Vietnam tuberculosis national strategic plan 2015–2020. Hanoi (Vietnam): Ministry of Health; 2014.
9. Fox GJ, Nhung NV, Sy DN, Lien LT, Cuong NK, Britton WJ, et al. Contact investigation in households of patients with tuberculosis in Hanoi, Vietnam: a prospective cohort study. PLoS One. 2012;7:e49880. https://doi.org/10.1371/journal.pone.0049880
10. Fox GJ, Nhung NV, Sy DN, Britton WJ, Marks GB. Household contact investigation for tuberculosis in Vietnam: study protocol for a cluster randomized controlled trial. [PubMed]. Trials. 2013;14:342. https://doi.org/10.1186/1745-6215-14-342
11. Nhung NV, Hoa NB, Khanh PH, Hennig C. Tuberculosis case notification data in Viet Nam, 2007 to 2012. Western Pac Surveill Response J. 2015;6:7–14. https://doi.org/10.5365/wpsar.2014.5.2.005
12. Nguyen HV, Tiemersma EW, Nguyen HB, Cobelens FGJ, Finlay A, Glaziou P, et al. The second national tuberculosis prevalence survey in Vietnam. PLoS One. 2020;15:e0232142. https://doi.org/10.1371/journal.pone.0232142
13. Floyd S, Sismanidis C, Yamada N, Daniel R, Lagahid J, Mecatti F,et al. Analysis of tuberculosis prevalence surveys: new guidance on best-practice methods. Emerg Themes Epidemiol. 2013;10:10. https://doi.org/10.1186/1742-7622-10-10
14. World Health Organization. Tuberculosis prevalence surveys: a handbook. Geneva: The Organization; 2011.
15. World Health Organization. Assessing tuberculosis prevalence through population-based surveys. Geneva: The Organization; 2007.
16. Kulas JT, Robinson DH, Smith JA, Kellar DZ. Post-stratification weighting in organizational surveys: a cross-disciplinary tutorial. Hum Resour Manage. 2018;57:419–36. https://doi.org/10.1002/hrm.21796
17. Rubin DB. Multiple imputation for nonresponse in surveys. New York: John Wiley & Sons, Inc.; 1987.
18. Wang L, Zhang H, Ruan Y, Chin DP, Xia Y, Cheng S, et al. Tuberculosis prevalence in China, 1990-2010; a longitudinal analysis of national survey data. Lancet. 2014;383:2057–64. https://doi.org/10.1016/S0140-6736(13)62639-2
19. National Center for Tuberculosis and Leprosy Control. Second national tuberculosis prevalence survey Cambodia, 2011. Cambodia Ministry of Health. 2012 [cited 2020 Oct 11]. https://openjicareport.jica.go.jp/pdf/12120325.pdf
20. Huong NT, Duong BD, Linh NN, Van LN, Co NV, Broekmans JF, et al. Evaluation of sputum smear microscopy in the National Tuberculosis Control Programme in the north of Vietnam. Int J Tuberc Lung Dis. 2006;10:277–82.
21. Hoa NB, Tiemersma EW, Sy DN, Nhung NV, Vree M, Borgdorff MW, et al. Health-seeking behaviour among adults with prolonged cough in Vietnam. Trop Med Int Health. 2011;16:1260–7. https://doi.org/10.1111/j.1365-3156.2011.02823.x
22. World Health Organization and Stop TB Partnership. Partnering and public health practice: experience of national TB partnerships. Geneva: The Organization; 2013 [cited 2020 Oct 11]. https://apps.who.int/iris/handle/10665/85315
23. Vietnam Ministry of Health. Global adult tobacco survey (GATS) Viet Nam 2015. Hanoi (Vietnam): The Ministry; 2016 [cited 2020 Oct 12]. https://www.who.int/tobacco/surveillance/survey/gats/vietnam-country-report-2015.pdf
24. Horton KC, MacPherson P, Houben RMGJ, White RG, Corbett EL. Sex differences in tuberculosis burden and notifications in low- and middle-income countries: a systematic review and meta-analysis. PLoS Med. 2016;13:e1002119. https://doi.org/10.1371/journal.pmed.1002119
25. The World Bank. DataBank: world development indicators. 2020 [cited 2020 Oct 13] https://databank.worldbank.org/reports.aspx?source=2&series=NY.GDP.MKTP.KD.ZG&country=VNM
26. van Helden PD. The economic divide and tuberculosis. Tuberculosis is not just a medical problem, but also a problem of social inequality and poverty. EMBO Rep. 2003;4(S1):S24–8. https://doi.org/10.1038/sj.embor.embor842

Address for correspondence: Hoa Binh Nguyen, National Tuberculosis Programme, 463 Hoang Hoa Tham St, Hanoi, Vietnam; email: nguyenbinhhoatb@yahoo.com

Foodborne Origin and Local and Global Spread of *Staphylococcus saprophyticus* Causing Human Urinary Tract Infections

Opeyemi U. Lawal, Maria J. Fraqueza, Ons Bouchami, Peder Worning, Mette D. Bartels, Maria L. Gonçalves, Paulo Paixão, Elsa Gonçalves, Cristina Toscano, Joanna Empel, Małgorzata Urbaś, M. Angeles Domínguez, Henrik Westh, Hermínia de Lencastre, Maria Miragaia

Staphylococcus saprophyticus is a primary cause of community-acquired urinary tract infections (UTIs) in young women. *S. saprophyticus* colonizes humans and animals but basic features of its molecular epidemiology are undetermined. We conducted a phylogenomic analysis of 321 *S. saprophyticus* isolates collected from human UTIs worldwide during 1997–2017 and 232 isolates from human UTIs and the pig-processing chain in a confined region during 2016–2017. We found epidemiologic and genomic evidence that the meat-production chain is a major source of *S. saprophyticus* causing human UTIs; human microbiota is another possible origin. Pathogenic *S. saprophyticus* belonged to 2 lineages with distinctive generic features that are globally and locally disseminated. Pangenome-wide approaches identified a strong association between pathogenicity and antimicrobial resistance, phages, platelet binding proteins, and an increased recombination rate. Our study provides insight into the origin, transmission, and population structure of pathogenic *S. saprophyticus* and identifies putative new virulence factors.

Staphylococcus saprophyticus is the cause of uncomplicated urinary tract infection (UTI) in 10%–20% of young women (*1*). Despite a greater successful treatment rate, *S. saprophyticus* UTI has a higher recurrent infection frequency than *Escherichia coli* UTI (*2*). Rare complications of *S. saprophyticus* UTI include acute pyelonephritis, nephrolithiasis, and endocarditis (*3*).

S. saprophyticus frequently colonizes humans and can be found in the gastrointestinal tract, vagina, and perineum (*4*). *S. saprophyticus* also is part of the gut and rectal flora of livestock, including pigs and cattle, and a frequent contaminant of meat and fermented food products (*1*). *S. saprophyticus* also has been recovered from polluted aquatic environments (*5*).

The reservoirs of *S. saprophyticus* causing UTI in humans are believed to be endogenous, but evidence is lacking. Moreover, given the frequent bacterial contamination of meat through the meat-processing chain, meat and food are speculated to be sources of human gut colonization and human *S. saprophyticus* infection (*6*). Some studies have reported high genetic diversity among isolates from human infections, food products, and other sources (*5*,*7*,*8*). However, previous studies were performed with a limited number of isolates, which prevented the description of the global and local molecular epidemiology of *S. saprophyticus*.

We used phenotypic, genomic, and pangenome-wide association study (pan-GWAS) approaches to characterize *S. saprophyticus* both globally and locally. In addition, we identified adaptive features that drive *S. saprophyticus* evolution, defined the *S. saprophyticus* population structure, investigated dissemination routes, and identified new pathogenicity factors.

Methods

Ethics Considerations

The human isolates used in our study were recovered as part of routine clinical diagnostic testing; thus,

Author affiliations: Universidade Nova de Lisboa, Oeiras, Portugal (O.U. Lawal, O. Bouchami, H. de Lencastre, M. Miragaia); Centre for Interdisciplinary Research in Animal Health (CIISA), Universidade de Lisboa, Lisbon, Portugal (M.J., Fraqueza); Hvidovre University Hospital, Hvidovre, Denmark (P. Worning, M.D. Bartels, H. Westh); SAMS Hospital, Lisbon (M.L. Gonçalves); Hospital da Luz, Lisbon (P. Paixão); Hospital Egas Moniz, Lisbon (E. Gonçalves, C. Toscano); Narodowy Instytut Leków, Warsaw, Poland (J. Empel, M. Urbaś); Hospital Universitari de Bellvitge, Barcelona, Spain (M.A. Domínguez); University of Copenhagen, Copenhagen, Denmark (H. Westh); The Rockefeller University, New York, New York, USA (H. de Lencastre)

DOI: https://doi.org/10.3201/eid2703.200852

ethics approval and informed consent were not required. All data were handled anonymously. Sample collection was in accordance with the European Parliament and Council decision for the epidemiologic surveillance and control of communicable disease through the European Antimicrobial Resistance Surveillance Network (http://www.ecdc.europa.eu/en/activities/surveillance/EARS-Net/Pages/index.aspx). Slaughterhouse samples were part of the routine control practices for evaluation of good hygiene practices and programs to assure meat safety (European Parliament and Council regulation no. 853/2004).

Bacterial Isolates

The global *S. saprophyticus* collection we used included 299 isolates from humans collected in 7 countries during 1997–2017: 286 from UTIs, 12 from invasive disease, and 1 from colonization (Appendix 1 Table 1, https://wwwnc.cdc.gov/EID/article/27/3/20-0852-App1.xlsx). We also analyzed the genomes of *S. saprophyticus* for 38 isolates from 5 other countries: 35 isolates from human UTIs (*8*), 2 from human hand swabs (*8*), an isolate from Byzantine Troy (*8*), and ATCC 15305 (*9*), a previously investigated human UTI-causing isolate.

The local collection included isolates collected in Lisbon, Portugal, during 2016–2017: 128 human UTI isolates collected in 3 hospitals and 104 slaughterhouse isolates collected from equipment, pork samples, workers' hands, and a pig's rectum. In addition, we included 5 isolates from animals and 12 isolates from food used in other studies (*8*) (Appendix 2, https://wwwnc.cdc.gov/EID/article/27/3/20-0852-App2.pdf).

Whole-Genome Sequencing and Assembly

Phylogenetic Analysis

We performed whole-genome sequencing (WGS) on MiSeq (Illumina, https://www.illumina.com) and MinIon nanopore (Oxford Nanopore, https://nanoporetech.com) platforms, as described (*10*) (Appendix 2). We separately analyzed global population and local epidemiology of *S. saprophyticus* and their phylogeny by using single-nucleotide polymorphisms (SNPs). We identified SNPs by mapping the draft genomes to a reference genome, *S. saprophyticus* ATCC 15305 (GenBank accession no. AP008934.1) by using the web-based CSI phylogeny version 1.4 (*11*) with the default parameter, but we disabled the minimum distance between SNPs in the parameter. We used Gubbins version 2.3.4 (*12*) with default parameters to concatenate SNPs and remove recombination regions. We reconstructed the phylogenies by using RAxML version 8.2.4 (https://github.com/stamatak/standard-RAxML) and generalized time-reversible nucleotide substitution with gamma correction model with 100 bootstrap value. We visualized the maximum-likelihood trees by using Interactive Tree of Life (ihttps://itol.embl.de) (Figures 1–3; Appendix 2 Figure 3). Recombination to mutation (r/m) ratios detected by using Gubbins were calculated as the average r/m of isolates in the entire collection and separately for each lineage by using as reference closed genomes of KS40 for lineage G and KS160 for lineage S, both obtained on the MinIon platform (Oxford Nanopore).

Pan-GWAS

We used Prokka version 1.13 (https://vicbioinformatics.com/software.prokka.shtml) to annotate genomes and defined the pangenome by using 85% blastp (https://blast.ncbi.nlm.nih.gov/Blast.cgi) identity in Roary version 3.12 (http://sanger-pathogens.github.io/Roary). We performed GWAS by using Scoary version 1.6.16 (*13*) to identify genes associated with lineages and considered Bonferroni corrected $p<0.05$ (odds ratio [OR] >1) statistically significant; we identified genes associated with epidemiologic groups and considered Benjamini Hochberg corrected and pairwise comparison $p<0.05$ statistically significant. Sequence data from this study are available in GenBank (accession no. PRJNA604222).

Resistome and Virulome Analyses

We screened genomes for resistance and virulence genes by using ResFinder version 2.3 (http://cge.cbs.dtu.dk/services/ResFinder), an in-house virulence genes database, and the virulence factor database (*14*), integrated into ABRicate version 0.5 (https://github.com/tseemann/abricate). We considered genes with a threshold $\geq$90% nucleotide identity and $\geq$60% coverage to be present.

Statistical Analyses

We used Prism 6.0 (GraphPad, https://www.graphpad.com) to compare the means of 2 groups. We used a 2-tailed unpaired Mann-Whitney test or χ^2 test for comparison and considered $p<0.05$ statistically significant.

Results

Lineages of *S. saprophyticus* Causing UTIs

Among study isolates, we first analyzed the diversity of *S. saprophyticus* causing UTIs by using genomic data of 321 human UTI isolates collected from 8 countries

on 4 continents during 1997–2017. From the SNPs initially detected, 42% arose from recombination events in the population, corresponding to a mean genome-wide r/m of 1.5:1, meaning that high accumulation of SNPs was due to recombination rather than mutation in UTI strains. The maximum-likelihood tree constructed from the 9,134 SNPs without recombination defined 2 lineages, which we called G and S (Figure 1). Most (74%, 236/321) UTI isolates were from lineage G and differed by 0–4,318 SNPs with an average nucleotide identity (ANI) of 98.5%–99.999%, whereas S isolates (26%, n = 85/321) were slightly less distantly

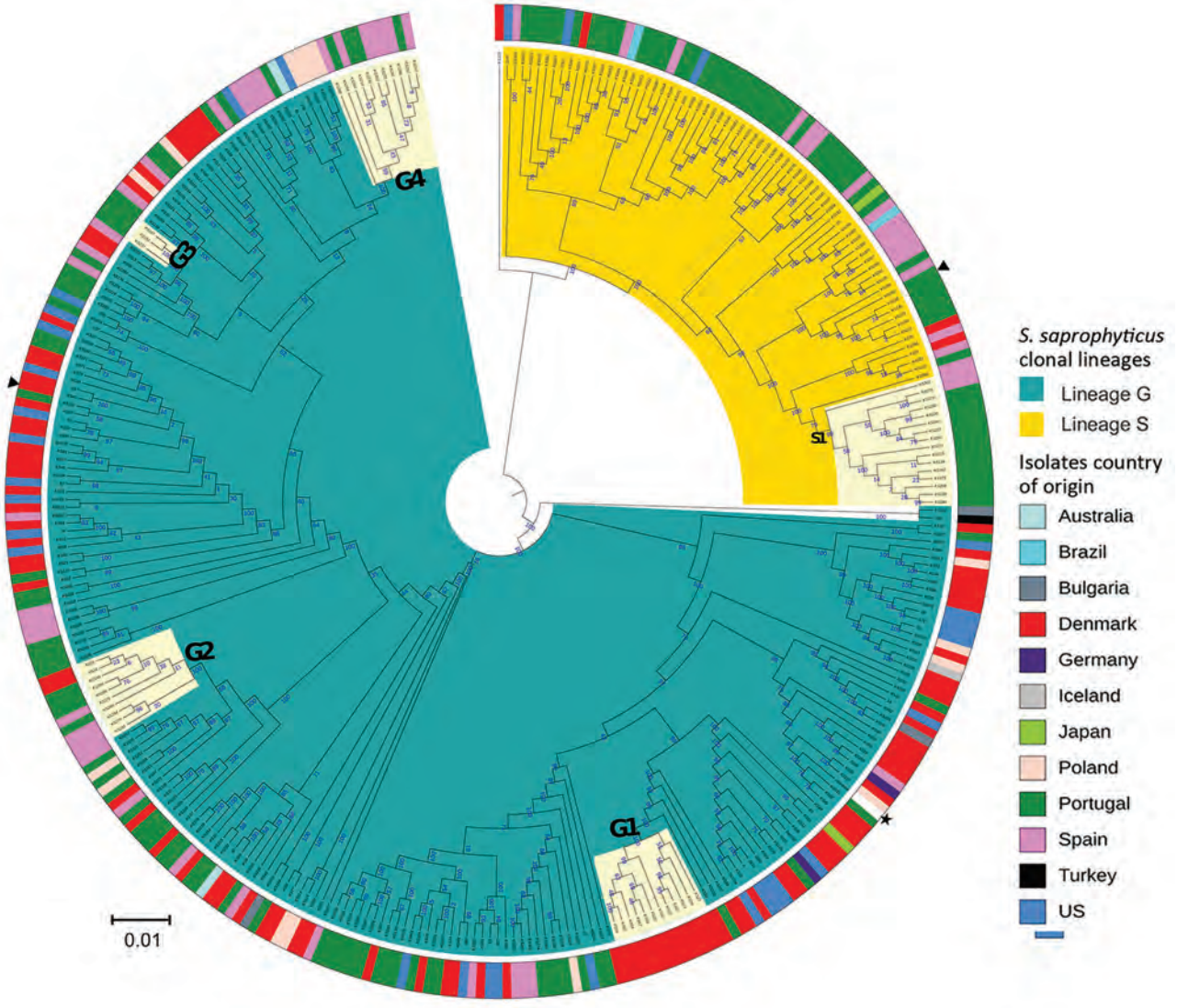

Figure 1. Maximum-likelihood tree of *Staphylococcus saprophyticus* isolates recovered from human infections and colonization globally, 1997–2017. The tree was constructed by using 9,134 SNPs without recombination. Among analyzed isolates, 321 were recovered from UTIs, 12 from blood, and 4 from colonization. Each node represents a strain; nodes with identical color belong to the same lineage. The assembled contigs were mapped to the reference genome *S. saprophyticus* ATCC 15305 (GenBank accession no. AP008934.1; black star). Polymorphic sites resulting from recombination events in the single-nucleotide polymorphism (SNP) alignments were filtered out by using Gubbins version 2.3.4 (*12*). Maximum likelihood tree was reconstructed by using RAxML version 8.2.4 (https://github.com/stamatak/standard-RAxML). We performed generalized time-reversible nucleotide substitution model with gamma correction with 100 bootstraps random resampling for support. We visualized the tree by using Interactive Tree of Life (iTOL; https://itol.embl.de). Black triangles represent isolates fully sequenced by using the long-read nanopore technologies and used as reference to estimate r/m in the respective lineage. Cream color represents clusters G1, G2, G3, G4, and S1, which had dissemination and transmission in same country and in different countries. The outer ring represents isolates' country of origin; blocks with identical color represent isolates from the same country. Of note, cluster G4 contains a pair of isolates collected in 2016 that had only 10 SNPs difference; one is a blood isolate from Barcelona, Spain (KS266) and the other is a UTI isolate recovered in Lisbon, Portugal (KS135). Scale bar indicates number of substitutions per site. UTI, urinary tract infection; r/m, recombination to mutation ratio.

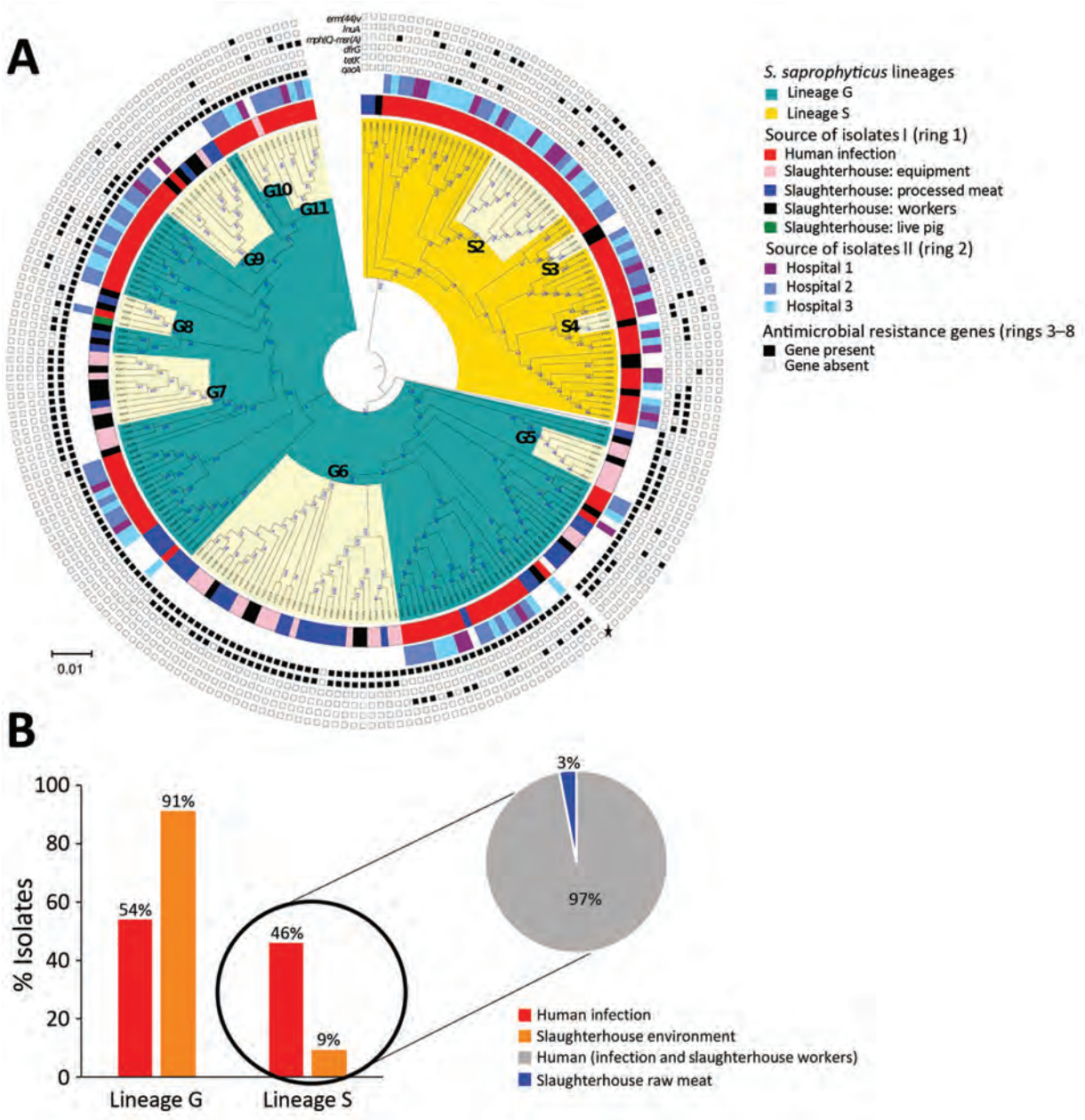

Figure 2. Phylogenomic analysis and distribution of *Staphylococcus saprophyticus* isolates collected from human infections and a slaughterhouse, Portugal, 2016–2017. A) Maximum-likelihood tree of 232 isolates from human infections or slaughterhouse contamination. The tree was constructed by using 14,110 single-nucleotide polymorphisms (SNPs) without recombination. Each node represents a strain; nodes with identical color belong to the same lineage. The assembled contigs were mapped to the reference genome *S. saprophyticus* ATCC 15305 (GenBank accession no. AP008934.1; black star). SNPs generated from each genome were concatenated to single alignment corresponding to position of the reference genome. Polymorphic sites resulting from recombination events in the SNP alignments were filtered out by using out by using Gubbins version 2.3.4 (*12*). Tree was reconstructed by using RAxML version 8.2.4 (https://github.com/stamatak/standard-RAxML). The generalized time-reversible nucleotide substitution model with gamma correction was performed with 100 bootstrap random re-samplings for support. The tree was visualized by using Interactive Tree of Life (iTOL; https://itol.embl.de). The clusters highlighted in cream represent admixture of isolates recovered from different sources that are closely related by SNPs in clusters G5–G11 and S2–S4. The inner ring (ring 1) represents genetic relatedness of isolates recovered from different sites inside the slaughterhouses and those recovered from infection in the community. The center ring (ring 2) identifies the isolates recovered from different hospitals. The outer rings (rings 3–8) represent the distribution of 6 genes that convey antimicrobial resistance. Scale bar indicates nucleotide substitutions per site. B) Source-based distribution of *S. saprophyticus* isolates in the lineage G and lineage S. Lineage G consisted isolates from infections, colonization, and contamination. Almost all (97%) isolates in lineage S are from human colonization and infection.

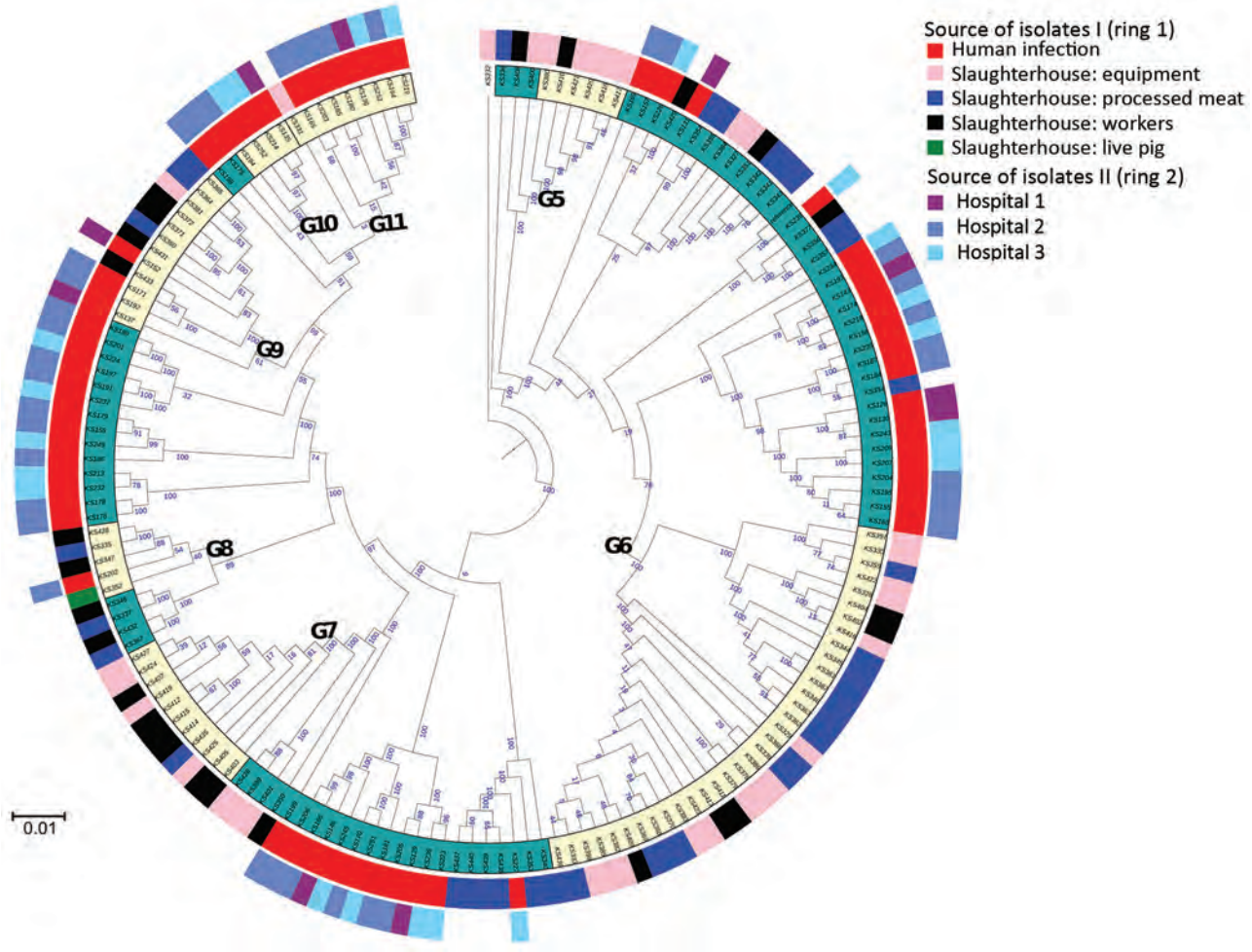

Figure 3. Maximum-likelihood tree depicting the genetic relatedness of *Staphylococcus saprophyticus* isolates belonging to clonal lineage G recovered from human infections or slaughterhouse contamination, Portugal, 2016–2017. Each node represents a strain. The tree was visualized by using Interactive Tree of Life (iTOL; https://itol.embl.de). Clusters highlighted in cream in the innermost ring represent admixture of isolates in clusters G5–G11, which were recovered from different sources and are closely related by single-nucleotide polymorphism. Ring 1 represents genetic relatedness of isolates recovered from different sites in the slaughterhouses and those recovered from infection in the community. Ring 2 depicts the isolates recovered from different hospitals. Scale bar indicates nucleotide substitutions per site.

related, differing by 0–3,540 SNPs with an ANI of 99.3%–99.991% (Appendix 2 Figure 1).

S. saprophyticus lineages we identified among UTI isolates worldwide had distinctive features indicative of 2 evolutionary histories. Although strains of both lineages had similar genome size as determined by their closed genomes (lineage G was 2.5 Mb and S 2.6 Mb), isolates from lineage S (n = 6) grew significantly faster in tryptic soy broth incubated at 37°C ($\mu_{average}$ = 0.34 h^{-1}) than G strains (n = 8) ($\mu_{average}$ = 0.22 h^{-1}; p = 0.0007) (Figure 4; Appendix 2). Moreover, we separately analyzed r/m of both lineages by using the respective closed genome of strains from each lineage as a reference and found that the mean estimated r/m was 9 times higher in S isolates (r/m = 4.4:1) than G isolates (r/m = 0.5:1). We did not detect a temporal signal when performing regression analysis (r) of tip-to-root distance versus isolation date, either in the entire collection (r = −0.2423) or for separate lineages (for G, r = −0.1314; for S, r = 0.1889) (Appendix). Hence, we could not determine when the 2 lineages diverged. The lack of temporal signal probably results from the limited number of isolates in each time point.

To further compare the 2 lineages, we constructed the pangenome of the 338 human *S. saprophyticus* genomes and identified 10,222 genes with 85% blastp clustering by using Roary. Among these, 8,351 genes,

present in <99% of the genomes, constituted the accessory genome. A gene accumulation plot of all the genes against the genomes sequenced showed that *S. saprophyticus* has an open pangenome (Appendix 2 Figure 2, panels A, B). The pan-GWAS analysis of the accessory genome indicated that G and S isolates have different genomic content (Bonferroni p<0.05, OR >1). A total of 128 genes were specific/enriched in the G lineage, including those encoding a type I restriction subunit (*group_383*), a defense mechanism against genetic transfer (*15*); metabolism of melibiose (*ebgA*, *melB*) (*16*) and inositol (*iolE*) (*17*), compounds that are excreted in urine; toxin–antitoxin systems (*group_4685*, *group_5665*), involved in stress response (*18*); and antimicrobial resistance (*qacA*) (*19*) (Table 1; Figure 5, panel A; Appendix 2 Table 1).

For S lineage, 237 genes were specific/enriched, some of which are involved in metabolism

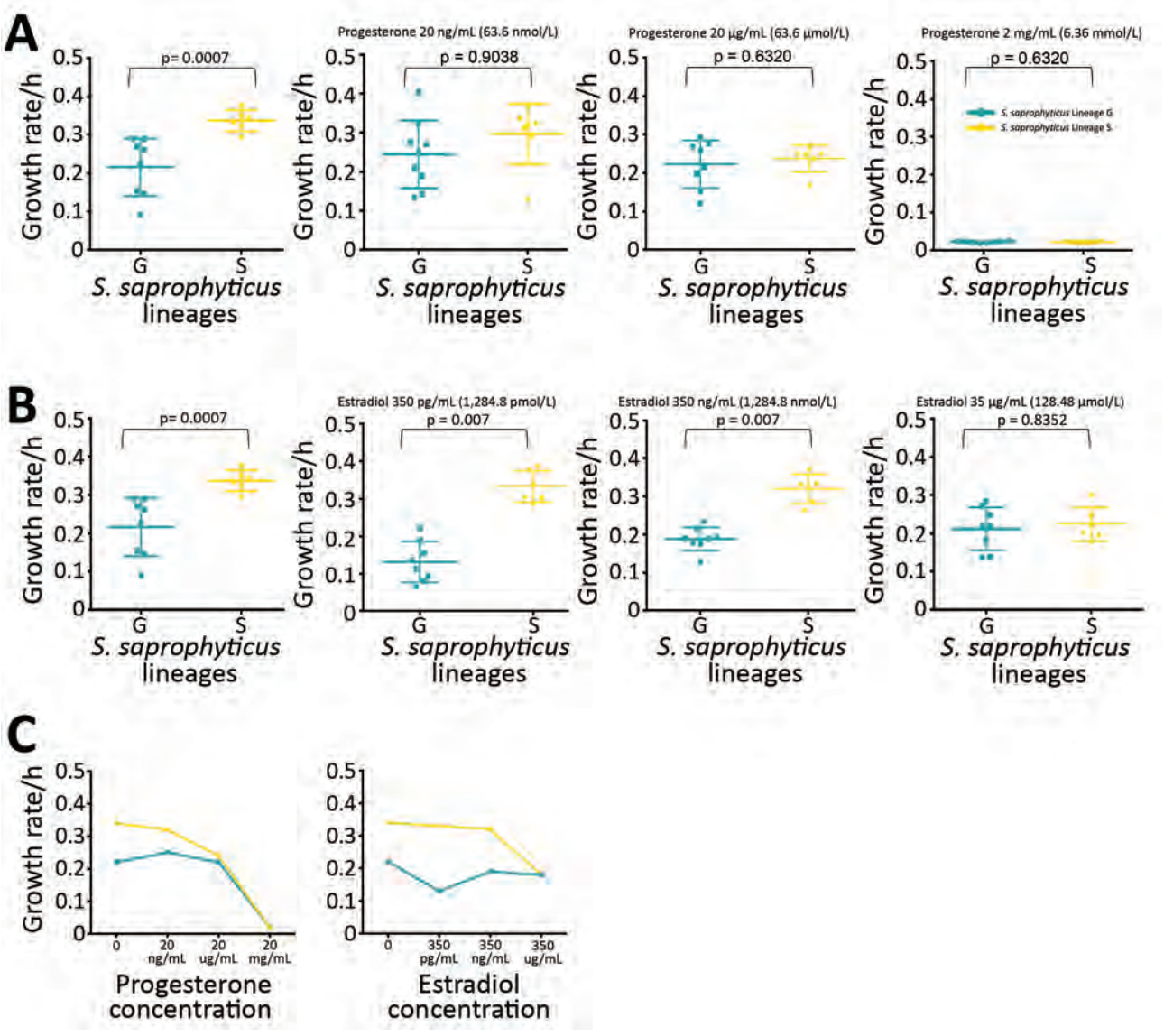

Figure 4. Growth rate of *Staphylococcus saprophyticus* clonal lineages in tryptic soy broth (TSB) and in different concentrations of female sex hormones. All assays were performed in triplicate and each experiment was repeated 3 times. A) Growth rate of *S. saprophyticus* strains in different concentrations of progesterone. First panel represents growth rate in TSB at 37°C; isolates belonging to lineage S grew significantly faster (p = 0.0007) than isolates in lineage G in TSB without hormones. However, no statistically significant difference in the growth rate of either lineage was noted in physiologic (2.0–200 ng/mL) and higher concentrations of progesterone. B) Growth rate of *S. saprophyticus* strains in TSB (first panel) and different concentrations of estradiol. Lineage S isolates grew faster in physiologic concentrations (350 pg/mL–350 ng/mL) and higher of estradiol, suggesting that this lineage is better adapted to the hormone-rich environment of the urine and the vagina than lineage G. Error bars indicate 95% CIs; horizontal lines indicate medians. C) Growth rate mean values of *S. saprophyticus* strains in progesterone and estradiol.

Table 1. List of genes exclusively associated with lineage G *Staphylococcus saprophyticus* strains in study of foodborne origin and local and global spread of *S. saprophyticus* causing human urinary tract infections*

Genes	Gene predicted function	Biologic function group	Frequency, %	Reference no.
group_383	Type I site-specific deoxyribonuclease restriction subunit	Endonuclease	96	(*15*)
icaR	Ica operon HTH-type negative transcription regulator	Transcription	95	NA
licT	Transcription antiterminator LicT	Transcription	80	NA
iolE	Inosose dehydratase	Inositol metabolism	86	(*17*)
group_4976	Phage infection protein	Phage-related protein	46	NA
group_869	Bacteriophage integrase	Phage-related protein	42	NA
tnpC_1	Transposase for transposon Tn*554*	Mobile genetic element	17	NA
group_744	Putative glucarate transporter	Transporter	29	NA
group_4685	Addiction module toxin Txe/YoeB family protein	Stress response (Type II toxin–antitoxin system)	20	(*18*)
group_5665	Addiction module antitoxin Axe family protein	Stress response (Type II toxin–antitoxin system)	19	(*18*)
yhjQ	Putative cysteine-rich protein YhjQ	Putative function	17	NA

*List of genes also include 53 hypothetical proteins. Bonferroni adjusted p≤0.032. NA, not applicable.

of ascorbate (*ulaA*) and thiamine (*tenI*) (*20*); induction of phosphate starvation (*psiE*), which was previously linked to switch on virulence in other uropathogens (*21*); platelet binding (*splE*, *sdrE*) associated with virulence (*22*); steroid metabolism (*group_7190*); and resistance to trimethoprim (*dfrG*) and biocides (*qacC*) (Table 2; Figure 5, panel A; Appendix 2 Table 1). Additional genes associated with S lineage that could explain its increased growth rate include those linked to lactose and cellobiose metabolism (*group_5572* gene) (*23*) and cell wall hydrolysis (*lytN*) (*24*), whereas the prevalence of transposases (*group_3547* and *group_1828*) (*25*) and phage genes (*recT* and *yueB*) (*27*) could justify its increased recombination rate.

Local and Global Spread of *S. saprophyticus* Clones Causing UTIs

We observed no time-based clustering of *S. saprophyticus* UTI isolates in the phylogeny, but we noted some geographic clustering. In particular, 89% (n = 78) of S isolates were found in Portugal and Spain (Figure 1). In addition, we identified clusters containing isolates from a single country. For instance, cluster G3 (1–8 SNPs) contained only isolates from Portugal and cluster G1 (0–63 SNPs) only isolates from Denmark (Figure 1).

We noted a high degree of isolate admixture in the maximum-likelihood tree of our global collection, suggesting that *S. saprophyticus* isolates of both lineages are disseminated geographically. G strains were distributed most widely, in 11 countries on 4 continents, whereas we found S isolates in only 6 countries. Despite the genetic diversity described, we still found isolates from different countries that differed by only a few SNPs. One pair in cluster G4 that had only 10 SNPs difference was a blood isolate from Barcelona, Spain (KS266), and a UTI isolate from Lisbon (KS135), collected in 2016 (Figure 1).

Although a relatedness cutoff is not defined yet for *S. saprophyticus*, the low number of SNPs observed between strains from the same and different countries is below the relatedness cutoff of 10–40 SNPs for most bacterial species (*28*). The apparent relatedness we noted implies that UTI isolates from different patients in the same country and in different countries are highly related and could belong to a cross-border chain of transmission. This finding challenges the assumption that *S. saprophyticus* causing UTIs were mainly endogenous (*29*).

Genetic Relatedness of *S. saprophyticus* from Slaughterhouses and UTIs

Pork is the most frequently consumed red meat in Europe (*30*) and is often contaminated with *S. saprophyticus* (*1*). We found that 35% of slaughterhouse samples (from meat, equipment, workers' hands, and a live pig) were contaminated with *S. saprophyticus*.

To understand whether *S. saprophyticus* causing UTIs could be related to *S. saprophyticus* in pork, we compared 104 isolates collected from a slaughterhouse against 128 isolates collected from human UTIs in Lisbon during 2016–2017. Among the 104 isolates from the slaughterhouse, 39 (37.5%) were collected from meat, 32 (30.8%) from equipment, 32 (30.8%) from workers' hands, and 1 (≈ 1%) from a live pig. SNP-based phylogenetic analysis with a tree-rooted at the midpoint showed that most (91%; 95/104) slaughterhouse isolates belonged to lineage G (Figure 2, panels A, B) and that a strain from slaughterhouse equipment was at the base of this lineage (bootstrap 100). In addition, the phylogenetic reconstruction including isolates from this study and other isolates

from production and companion animals (including 2 pigs, 2 bovine, and 1 canine) and food (*8*) showed that most (3/5) animal isolates clustered together at a basal clade of lineage G (bootstrap 100) (Appendix 2 Figure 2). Some clusters in the phylogenetic tree (e.g., G9) had slaughterhouse isolates at the base and UTI isolates at the tip. However, we also observed the opposite (e.g., G11), tree clusters with slaughterhouse isolates at the tip and UTI isolates at the base (Figure 2, panel A).Moreover, 41% of G strains included the antimicrobial resistance gene *tetK* ($p<0.0001$) (Figure 2, panel A), which is associated with resistance to tetracycline, an antimicrobial drug extensively used in animal production (*31*).

Phylogenetic reconstruction of all isolates from Lisbon based on SNPs provided additional examples of admixture of isolates recovered from different sampling sites in the slaughterhouse and from the slaughterhouse and humans. Isolates from meat were frequently intermixed with isolates from equipment and colonized workers as observed in cluster G6 wherein strains differed by only 1–65 SNPs (Figure 2, panel A; Figure 3). Likewise, cluster G9 included isolates from the slaughterhouse that were intermixed with human UTI isolates. Isolates collected from slaughterhouse equipment differed by only 19 SNPs from human UTI isolates. Likewise, human UTI isolates differed from meat isolates by 25 SNPs and from isolates of colonized workers by 26 SNPs. In addition, slaughterhouse and human UTI isolates had the same antimicrobial resistance profile, exhibiting resistance to fosfomycin, fusidic acid, and tetracycline (Appendix

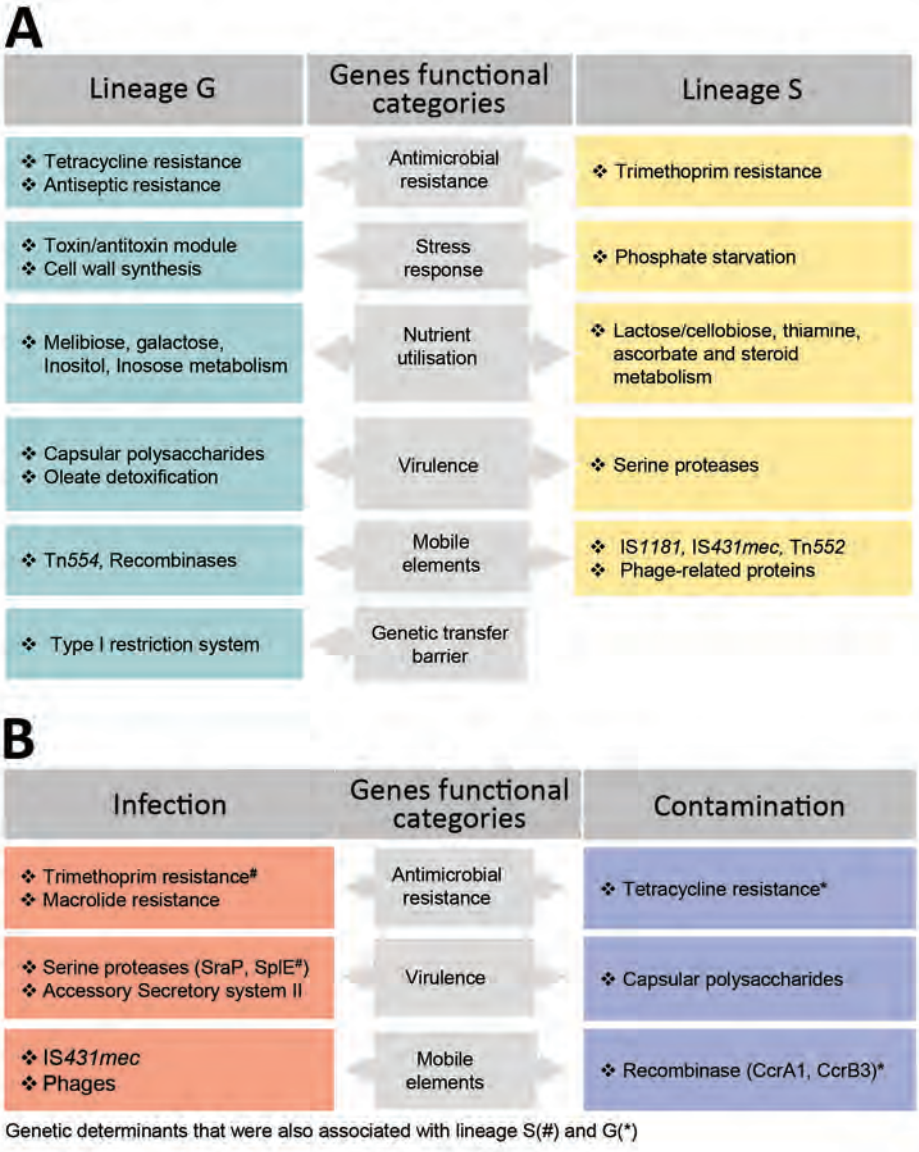

Figure 5. Genetic determinants that contribute to the distinction of clonal lineages and lifestyle of *Staphylococcus saprophyticus*. The graph displays determinants that contribute (A) and mediate (B) adaptation of *S. saprophyticus* to either infection or contamination. We used the genome-wide association study (GWAS) method to identify genetic factors by using 2 association comparisons: lineage G versus lineage S and human infection versus surface contamination. We used the pairwise comparison and included a core-SNP phylogenetic tree without recombination to remove the lineage effect in the analysis. Hits with Benjamini Hochberg corrected $p \leq 0.05$ and odds ratio >1 were considered statistically significant. We grouped the identified genes into biologic functions based on gene annotation predicted by Prokka (https://vicbioinformatics.com/software.prokka.shtml). Some genetic factors that were associated with infections and contamination also were associated with the lineages despite subjecting the GWAS to lineage correction.

Table 2. List of lineage S genes exclusively associated with *Staphylococcus saprophyticus* strains in study of foodborne origin and local and global spread of *S. saprophyticus* causing human urinary tract infections*

Genes	Gene predicted function	Biologic function group	Frequency, %	Reference no.
group_5572	Phosphotransferase system, lactose/ cellobiose-specific IIB subunit	Sugar metabolism	99	(*23*)
ulaA	PTS system ascorbate-specific IIC component	Sugar metabolism	99	(*20*)
group_5955	Sugar phosphate isomerase/epimerase	Sugar metabolism	26	(*23*)
lytN	C51 family D-Ala-D-Gly carboxypeptidase	Cell wall hydrolase	85	(*24*)
psiE	Protein PsiE	Phosphate starvation	22	(*21*)
group_1438	Arsenite methyltransferase	Arsenite resistance	25	NA
dfrG	Trimethoprim-resistance dihydrofolate reductase	Antimicrobial resistance	18	NA
group_7190	3-β hydroxysteroid dehydrogenase/isomerase	Steroid metabolism	17	(*26*)
group_273	Recombinase/resolvase	Mobile genetic element	69	(*25*)
group_2198	Putative ATPase/transposase	Mobile genetic element	26	(*25*)
group_275	Recombinase/resolvase	Mobile genetic element	21	(*25*)
group_355	Transposase for IS*431mec*	Mobile genetic element	17	(*25*)
group_7470	Putative replication-associated protein	Mobile genetic element	10	NA
group_3363	putative DoxX family membrane protein	Putative functions	85	NA
mviM	NADH-dependent dehydrogenase	Putative functions	26	NA
nmrA	Putative nmrA negative transcriptional regulator family protein	Transcription	17	NA
group_7195	Amidohydrolase	Hydrolase	17	NA
group_6430	Putative restriction enzyme	Restriction enzyme	17	NA

*List of genes also include 84 hypothetical proteins. Bonferroni p≤0.031. NA, not applicable.

1 Table 1). We could not ascertain any epidemiologic link between the workers in the slaughterhouse and UTI patients, due to data protection limitations, but contact with meat production previously has been identified as a risk factor for UTI (*6*).

The only live-pig isolate was intermixed in cluster G8 with isolates from meat, slaughterhouse workers, and UTI patients (Figure 3), having 307–658 SNPs difference. The admixture of strains in the tree suggests the existence of frequent cross-transmission within the slaughterhouse and between the slaughterhouse and humans.

Insufficient disinfection procedures probably contributed to the high transmission rate of *S. saprophyticus* within the slaughterhouse, as demonstrated by the highly related strains (<11 SNPs) on dirty and clean equipment surfaces and similar strains (<16 SNPs) isolated 12 months apart. Carriage of the antimicrobial resistance gene, *qacA*, by all G strains could justify the observed unsuccessful cleaning procedures (Figure 2, panel A).

The accumulation of substitutions and genetic distance evidenced by the phylogenetic analysis suggest that isolates from slaughterhouses and food probably are the primary sources of *S. saprophyticus* G strains (Figure 3). Transmission probably occurs more frequently from the slaughterhouse and food to humans; however, we cannot ascertain directionality due to the lack of temporal signal.

Evidence Supporting the Human Origin of Lineage S

In contrast to isolates belonging to lineage G, which were mostly from UTIs and the slaughterhouse, S isolates were almost exclusively of human origin (97%; n = 66/68), either from UTIs (n = 59) or human colonization (n = 7) (Figure 2, panels A, B). When we reconstructed the phylogeny of all isolates in this and other studies (*8*) (Appendix 2 Figure 3), a human isolate was at the base of the S lineage. The only 2 S isolates seen in animals were from nonhuman primates. Furthermore, a resistance determinant for trimethoprim (*dfrG*), which routinely is used to treat human UTIs, was associated with this lineage (18%; p<0.05) (Figure 2, panel A; Table 2).

To determine whether S isolates could have originated in humans, we grew isolates from both lineages in the absence and presence of human physiologic concentrations (15–350 pg/mL) of estradiol (*32*), a female hormone commonly found in urine and the vagina, and in different pH values mimicking the stomach (pH 2.5), vagina (pH ≤4.5) (*33*), skin (pH 5.5), and urine (pH 4.5–8.0) (*34*). The growth rate of S isolates did not change significantly at the highest physiologic concentration of estradiol specific to humans (0.34 h^{-1} vs. 0.33 h^{-1}), but the growth rate for G strains decreased by 59% at this concentration (0.22 h^{-1} vs. 0.13 h^{-1}; p = 0.0007) (Figure 4, panels A–C; Appendix 2). All isolates grew at all pH levels assayed, except for pH 2.5. At pH 4.5 and 5.5, isolates of both lineages had similar growth rates, but S isolates had a higher growth rate than G isolates at pH 8, although this difference was not statistically significant (p = 0.133). These results suggest that lineage S isolates are more adapted than lineage G strains to high estradiol concentrations found in women, but not found in other female animal hosts, such as pigs, bovine, or canines (*35*). GWAS also identified a gene involved in

steroid metabolism, 3-β hydroxysteroid dehydrogenase (HSD), associated with lineage S (Table 2; Figure 5, panels A, B). Steroids such as estradiol are primary signaling molecules for host–microbe interactions (*26*) and involved in the interconversion of active and inactive steroid hormones (*26*). Presence of HSD could be an adaptive evolution to colonization of the bladder, a hormone-rich environment. Evidence supports a human (primate) origin for lineage S, but studies sampling a wider range of ecologic sites and geographic regions are needed.

UTIs and *S. saprophyticus* Dissemination among Humans in the Community

To explore dissemination of *S. saprophyticus* causing UTIs in the community through human-to-human contact, we analyzed genomic data of the 128 UTI isolates from outpatients of 3 hospitals in the Lisbon area. Transmission of *S. saprophyticus* from lineage G and S between persons in the community was apparent, as demonstrated by the high relatedness of strains from UTI patients at different hospitals. In the G cluster, G10 isolates had 9–24 SNPs difference, and in the S cluster, S2, differed by 6–64 SNPs (Figure 2, panel A). However, due to data protection regulations, we could not ascertain whether the patients were epidemiologically linked. Results suggest that patients might have acquired these strains from the same reservoir or that direct and indirect cross-transmission could have occurred in the community.

Disease Signatures among *S. saprophyticus* Populations

Several virulence factors, including urease, have been described in *S. saprophyticus* (*36*), but the basis of pathogenicity in this species is mainly unknown. We used a pan-GWAS approach to compare the genetic content of 128 isolates from human infections to 104 isolates recovered from a slaughterhouse, all collected in Lisbon during 2016–2017. We identified 6 genes that appear to be associated with an increased pathogenic potential in *S. saprophyticus* (Figure 5, panel A; Appendix 2 Tables 2–5). These genes included those encoding an SplE-like protein and a gene cluster encoding a complete accessory secretory system associated with a serine-rich adhesion, similar to SraP. Previous studies have described highly homologous secretory system (>97% nucleotide identity) associated to serine-rich proteins that bind platelets, including SraP in *S. aureus* (*37*) and UafB in *S. saprophyticus* (*38*).

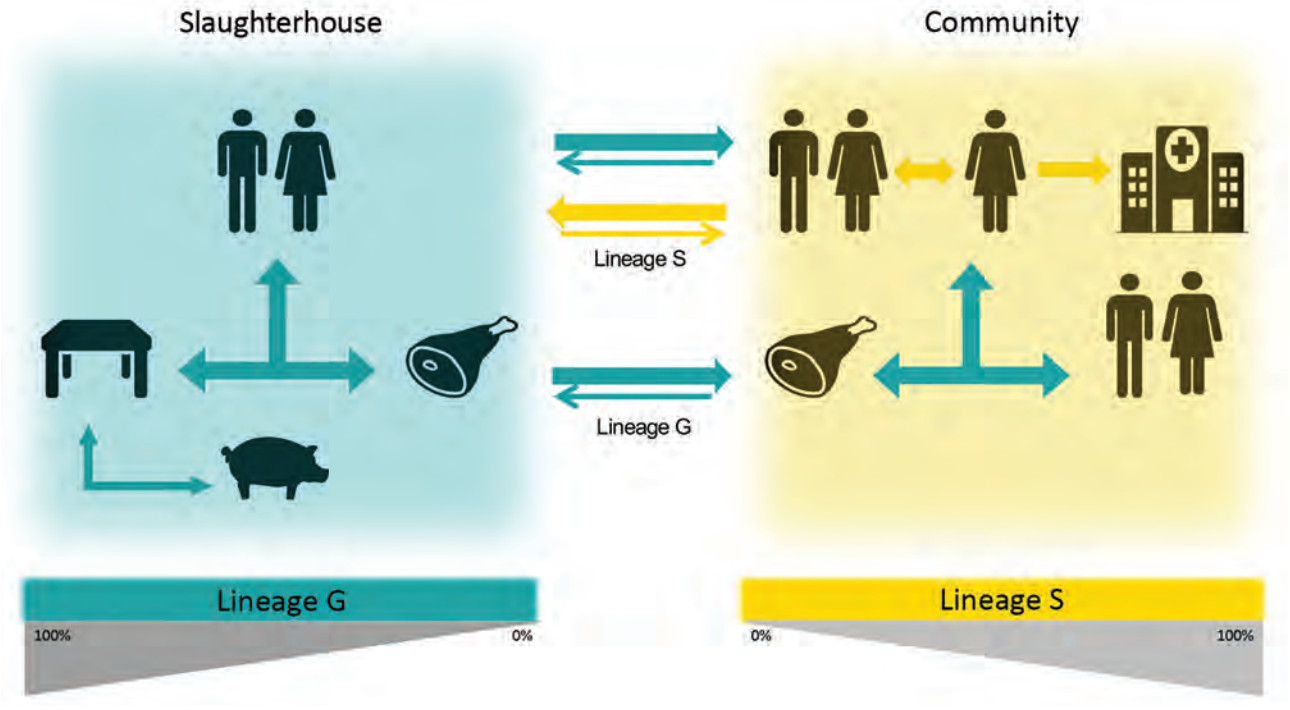

Figure 6. A proposed model for the dissemination and transmission of *Staphylococcus saprophyticus* in the community. The arrows represent the dissemination and transmission of *S. saprophyticus* isolates that belonged to lineage G (green) and lineage S (yellow). Lineage G *S. saprophyticus* strains are of animal origin and enter the slaughterhouse through production animals, such as pigs, persist on the equipment, and contaminate the meat in processing chain. Lineage G strains could enter the community through contaminated meat and workers colonized in the slaughterhouse. Lineage S strains most likely are of humans and primate origin and probably are disseminated by person-to-person contact within the community.

We also found other genes associated with infection that encoded phage proteins. An analysis on 128 UTI isolates using PHASTER (*39*) identified 5 phages in 48 (38%) strains. The phages were 38–125 Kb and had <50% identity with any known phage. The genomic vicinity of the identified phages varied in the chromosome, suggesting that lysogenic conversion was not the mechanism involved in pathogenicity of these strains; instead, hypothetical phage genes could be crucial for pathogenicity. In addition, genes encoding resistance to the antimicrobial drugs trimethoprim (*dfrG*), lincosamide (*lnuA*), streptogramin B (*erm44v*), or to macrolides (*mphC-msrA*) also were associated with strains from human infections (Figure 2; Figure 5, panel B; Appendix 2 Tables 2–5).

Another factor highly associated with human infections was the occurrence of recombination, which was 6 times higher in isolates from UTIs (r/m 1.7:1) than from isolates associated with colonization or contamination (r/m 0.3:1). This finding suggests recombination might be a strategy of *S. saprophyticus* to evade the host immune system, as described elsewhere (*40*).

Discussion

We identified 2 *S. saprophyticus* lineages, G and S, associated with human UTIs that appeared to have different evolutionary histories. Our data support a foodborne origin for lineage G and its transmission through food products to humans. We also found evidence of a human origin for lineage S and additional proof for the occurrence of direct or indirect human-to-human dissemination in the community, which could explain not only the local dissemination of both lineages but also the wide geographic dissemination, as described for *S. aureus* (*41*) and *E. coli* (*42*).

Our conclusions were limited by the characteristics of the sample collection analyzed. In particular, the lack of temporal signal did not enable inference of the direction of transmission between the sampling sites. We could establish obvious genomic relatedness between the meat production chain and human UTIs and UTIs from different persons in the community. However, lack of samples from other animal hosts, environments, or different ecologic niches in humans, did not enable us to establish pig meat and humans as the unique sources of the 2 lineages nor identify the preferred ecologic niche of *S. saprophyticus* in humans.

Our observed *S. saprophyticus* colonization rate among pigs was extremely low (1%) compared with previous studies (*43*), which could be explained by possible cross-inhibitory bacterial interactions (*44*); however, contamination within the slaughterhouse environment sometimes reached 35%. Amplification of *S. saprophyticus* in the slaughterhouse environment was probably potentiated by resistance to biocides. We found that slaughterhouse workers' washed hands were colonized with strains that were highly related to slaughterhouse environmental isolates and to strains causing UTIs, suggesting exposure of workers to the slaughterhouse environment as a risk factor for human colonization (Figure 6).

The transmission chain of S lineage isolates appears to be different and to have no link to meat production. S lineage UTIs might originate from human gut or vaginal colonization; both have been reported as possible human niches (*2*,*4*). Evidence for the human origin of S lineage included the almost exclusive (97%) identification in humans, where S lineage was better adapted to the physiologic high concentration of human female sex hormones; grew at vagina, skin, and urine pH values; and harbored 2 serine-proteases that presumably can bind to human platelets, as described for SraP (*37*). The distinct genetic content and phenotypic features of lineages G and S further reflected the diverse selective pressures of the human and animal, slaughterhouse, and food environments and suggest different evolutionary strategies toward pathogenicity. In particular, we found that tetracycline and antimicrobial resistance genes associated with colonization-contamination also were associated with isolates of the G lineage. Furthermore, genes encoding sugar metabolism, serine proteases, and a trimethoprim resistance associated with infection were also associated with isolates of the S lineage, implying distinctive specialization of the 2 lineages.

Our results also indicate a key role of setting-associated antimicrobial drug usage, especially for trimethoprim, macrolides, and tetracycline, in resistance development and pathogenicity. Subinhibitory concentrations of these drugs have been shown to promote virulence in bacteria through the induction of biofilm production (*45*), quorum-sensing (*45*), or phages (*46*) and might also increase *S. saprophyticus* pathogenicity.

We found a high r/m rate in isolates of the S lineage and in strains from UTIs, comparable to naturally transformable bacterial species like *Klebsiella pneumoniae* and *Streptococcus pyogenes* (*47*). A similar phenomenon was observed for *S. epidermidis* (*48*); variation in cell surface proteins was shown to contribute to evasion of human immunity (*48*), and a similar strategy might be advantageous for *S. saprophyticus* in infection. The recombination might have resulted from defects in repair of double stranded DNA breaks from

oxidative stress induced by leukocytes during infection, as previously described (*48*). However, the mechanism linking infection and recombination in *S. saprophyticus* remains elusive.

Last, we identified factors associated with infection that could represent new *S. saprophyticus* virulence factors, including 2 serine-proteases, *sraP*-like and *splE*-like, and phages SraP and SplE, which previously were connected to pathogenicity in *S. aureus* (*22*,*37*). In addition, phages have been described to transport pathogenicity islands in staphylococci (*49*). Our study constitutes a deep-structured analysis of *S. saprophyticus* population structure and genomic epidemiology, providing groundwork for future studies on the pathogenicity and population genetics of this bacterium.

O.U.L. was supported by PhD grants from the Fundação para a Ciência e Tecnologia (FCT) (grant no. PD/BD/113992/2015). This work was partially supported by FCT (project no. PTDC/CVT-CVT/29510/2017), Microbiologia Molecular, Estrutural e Celular (project nos. LISBOA-01-0145-FEDER-007660 and UID/Multi/04378/2019) and by the COMPETE2020 Programa Operacional Competitividade e Internacionalização; ONEIDA (project no. LISBOA-01-0145-FEDER-016417), and co-funded by Fundos Europeus Estruturais e de Investimento from Programa Operacional Regional Lisboa2020 and by national funds through FCT.

O.U.L. and O.B. cultured the isolates. O.U.L. performed the phenotypic experiments and bioinformatics analysis. O.U.L., H.W., P.W., M.D.B. performed the sequencing of the isolates. O.U.L. and M.M. carried out the data analysis and interpretation and wrote the manuscript. M.J.F., M.L.G., P.P., E.G., C.T., J.E., M.U., H.M.L., H.W., M.D.B. provided the isolates. M.J.F., M.L.G., P.P., E.G., C.T., J.E., M.U., H.M.L., H.W., P.W., M.D.B. were involved in manuscript revision. All authors read and approved the final manuscript.

About the Author

Dr. Lawal is a postdoctoral researcher at the Instituto de Tecnologia Quimica e Biologica, Universidade Nova de Lisboa (ITQB-NOVA), Oeiras, Portugal. His primary research interests include antimicrobial resistance, bacterial evolution and transmission dynamics of *Staphylococcus saprophyticus*.

References

1. Becker K, Heilmann C, Peters G. Coagulase-negative staphylococci. Clin Microbiol Rev. 2014;27:870–926. https://doi.org/10.1128/CMR.00109-13
2. Latham RH, Running K, Stamm WE. Urinary tract infections in young adult women caused by *Staphylococcus saprophyticus*. JAMA. 1983;250:3063–6. https://doi.org/10.1001/jama.1983.03340220031028
3. Garduño E, Márquez I, Beteta A, Said I, Blanco J, Pineda T. *Staphylococcus saprophyticus* causing native valve endocarditis. Scand J Infect Dis. 2005;37:690–1. https://doi.org/10.1080/00365540510027200
4. Rupp ME, Soper DE, Archer GL. Colonization of the female genital tract with *Staphylococcus saprophyticus*. J Clin Microbiol. 1992;30:2975–9. https://doi.org/10.1128/JCM.30.11.2975-2979.1992
5. de Sousa VS, da-Silva APS, Sorenson L, Paschoal RP, Rabello RF, Campana EH, et al. *Staphylococcus saprophyticus* recovered from humans, food, and recreational waters in Rio de Janeiro, Brazil. Int J Microbiol. 2017;2017:4287547. https://doi.org/10.1155/2017/4287547
6. Hedman P, Ringertz O, Eriksson B, Kvarnfors P, Andersson M, Bengtsson L, et al. *Staphylococcus saprophyticus* found to be a common contaminant of food. J Infect. 1990;21:11–9. https://doi.org/10.1016/0163-4453(90)90554-L
7. Lee B, Jeong D-W, Lee J-H. Genetic diversity and antibiotic resistance of *Staphylococcus saprophyticus* isolates from fermented foods and clinical samples. J Korean Soc Appl Biol Chem. 2015;58:659–68. https://doi.org/10.1007/s13765-015-0091-1
8. Mortimer TD, Annis DS, O'Neill MB, Bohr LL, Smith TM, Poinar HN, et al. Adaptation in a fibronectin binding autolysin of *Staphylococcus saprophyticus*. MSphere. 2017;2:e00511–17. https://doi.org/10.1128/mSphere.00511-17
9. Kuroda M, Yamashita A, Hirakawa H, Kumano M, Morikawa K, Higashide M, et al. Whole genome sequence of *Staphylococcus saprophyticus* reveals the pathogenesis of uncomplicated urinary tract infection. Proc Natl Acad Sci U S A. 2005;102:13272–7. PubMed https://doi.org/10.1073/pnas.0502950102
10. Hansen KH, Andreasen MR, Pedersen MS, Westh H, Jelsbak L, Schønning K. Resistance to piperacillin/tazobactam in *Escherichia coli* resulting from extensive IS*26*-associated gene amplification of *blaTEM-1*. J Antimicrob Chemother. 2019;74:3179–83. https://doi.org/10.1093/jac/dkz349
11. Kaas RS, Leekitcharoenphon P, Aarestrup FM, Lund O. Solving the problem of comparing whole bacterial genomes across different sequencing platforms. PLoS One. 2014;9:e104984. https://doi.org/10.1371/journal.pone.0104984
12. Croucher NJ, Page AJ, Connor TR, Delaney AJ, Keane JA, Bentley SD, et al. Rapid phylogenetic analysis of large samples of recombinant bacterial whole genome sequences using Gubbins. Nucleic Acids Res. 2015;43:e15. https://doi.org/10.1093/nar/gku1196
13. Brynildsrud O, Bohlin J, Scheffer L, Eldholm V. Erratum to: Rapid scoring of genes in microbial pan-genome-wide association studies with Scoary. Genome Biol. 2016;17:1–9. https://doi.org/10.1186/s13059-016-1108-8
14. Chen L, Zheng D, Liu B, Yang J, Jin Q. VFDB 2016: hierarchical and refined dataset for big data analysis—10 years on. Nucleic Acids Res. 2016;44(D1):D694–7. https://doi.org/10.1093/nar/gkv1239
15. Monk IR, Foster TJ. Genetic manipulation of Staphylococci-breaking through the barrier. Front Cell Infect Microbiol. 2012;2:49. https://doi.org/10.3389/fcimb.2012.00049
16. Tomita K, Nagura T, Okuhara Y, Nakajima-Adachi H, Shigematsu N, Aritsuka T, et al. Dietary melibiose regulates the cell response and enhances the induction of oral

tolerance. Biosci Biotechnol Biochem. 2007;71:2774–80. https://doi.org/10.1271/bbb.70372
17. Dinicola S, Minini M, Unfer V, Verna R, Cucina A, Bizzarri M. Nutritional and acquired deficiencies in inositol bioavailability. Correlations with metabolic disorders. Int J Mol Sci. 2017;18:E2187. https://doi.org/10.3390/ijms18102187
18. Gómez FA, Cárdenas C, Henríquez V, Marshall SH. Characterization of a functional toxin-antitoxin module in the genome of the fish pathogen *Piscirickettsia salmonis*. FEMS Microbiol Lett. 2011;317:83–92. https://doi.org/10.1111/j.1574-6968.2011.02218.x
19. Conceição T, Coelho C, de Lencastre H, Aires-de-Sousa M. High prevalence of biocide resistance determinants in *Staphylococcus aureus* isolates from three African countries. Antimicrob Agents Chemother. 2015;60:678–81. https://doi.org/10.1128/AAC.02140-15
20. Costliow ZA, Degnan PH. Thiamine acquisition strategies impact metabolism and competition in the gut microbe *Bacteroides thetaiotaomicron*. mSystems. 2017;2:1–17. https://doi.org/10.1128/mSystems.00116-17
21. Chekabab SM, Harel J, Dozois CM. Interplay between genetic regulation of phosphate homeostasis and bacterial virulence. Virulence. 2014;5:786–93. https://doi.org/10.4161/viru.29307
22. Sharp JA, Echague CG, Hair PS, Ward MD, Nyalwidhe JO, Geoghegan JA, et al. Staphylococcus aureus surface protein SdrE binds complement regulator factor H as an immune evasion tactic. PLoS One. 2012;7:e38407. https://doi.org/10.1371/journal.pone.0038407
23. Ghali I, Sofyan A, Ohmori H, Shinkai T, Mitsumori M. Diauxic growth of *Fibrobacter succinogenes* S85 on cellobiose and lactose. FEMS Microbiol Lett. 2017;364:1–9. https://doi.org/10.1093/femsle/fnx150
24. Frankel MB, Hendrickx APA, Missiakas DM, Schneewind O. LytN, a murein hydrolase in the cross-wall compartment of *Staphylococcus aureus*, is involved in proper bacterial growth and envelope assembly. J Biol Chem. 2011;286:32593–605. https://doi.org/10.1074/jbc.M111.258863
25. Hallet B, Sherratt DJ. Transposition and site-specific recombination: adapting DNA cut-and-paste mechanisms to a variety of genetic rearrangements. FEMS Microbiol Rev. 1997;21:157–78. https://doi.org/10.1111/j.1574-6976.1997.tb00349.x
26. García-Gómez E, González-Pedrajo B, Camacho-Arroyo I. Role of sex steroid hormones in bacterial-host interactions. BioMed Res Int. 2013;2013:928290. https://doi.org/10.1155/2013/928290
27. Datta S, Costantino N, Zhou X, Court DL. Identification and analysis of recombineering functions from Gram-negative and Gram-positive bacteria and their phages. Proc Natl Acad Sci U S A. 2008;105:1626–31. https://doi.org/10.1073/pnas.0709089105
28. Schürch AC, Arredondo-Alonso S, Willems RJL, Goering RV. Whole genome sequencing options for bacterial strain typing and epidemiologic analysis based on single nucleotide polymorphism versus gene-by-gene-based approaches. Clin Microbiol Infect. 2018;24:350–4. https://doi.org/10.1016/j.cmi.2017.12.016
29. Ronald A. The etiology of urinary tract infection: traditional and emerging pathogens. Dis Mon. 2003;49:71–82. https://doi.org/10.1067/mda.2003.8
30. González-García S, Belo S, Dias AC, Rodrigues JV, Da Costa RR, Ferreira A, et al. Life cycle assessment of pigmeat production: Portuguese case study and proposal of improvement options. J Clean Prod. 2015;100:126–39. https://doi.org/10.1016/j.jclepro.2015.03.048
31. Chopra I, Roberts M. Tetracycline antibiotics: mode of action, applications, molecular biology, and epidemiology of bacterial resistance. Microbiol Mol Biol Rev. 2001;65:232–60. https://doi.org/10.1128/MMBR.65.2.232-260.2001
32. Walker SW. Laboratory reference ranges. In: Endocrine self-assessment program. Washington, D.C.: Endocrine Society; 2015. p. 1–5 [cited 2019 Apr 29]. https://education.endocrine.org/system/files/ESAP%202015%20Laboratory%20Reference%20Ranges.pdf
33. Linhares IM, Minis E, Robial R, Witkin SS. The human vaginal microbiome. In: Faintuch J, Faintuch S, editors. Microbiome and metabolome in diagnosis, therapy, and other strategic applications. London: Elsevier, Inc.; 2019. p. 109–14. https://doi.org/10.1016/B978-0-12-815249-2.00011-7
34. Clarkson MR, Magee CN, Brenner BM. Chapter 2: Laboratory assessment of kidney disease. In: Clarkson MR, Magee CN, Brenner BM eds. Pocket companion to Brenner and Rector's the Kidney 8th edition. London: Elsevier; 2011. p. 21–41 [cited 2019 Apr 29]. https://www.sciencedirect.com/science/article/pii/B9781416066408000026
35. Frank LA, Mullins R, Rohrbach BW. Variability of estradiol concentration in normal dogs. Vet Dermatol. 2010;21:490–3. https://doi.org/10.1111/j.1365-3164.2010.00896.x
36. Flores-Mireles AL, Walker JN, Caparon M, Hultgren SJ. Urinary tract infections: epidemiology, mechanisms of infection and treatment options. Nat Rev Microbiol. 2015;13:269–84. https://doi.org/10.1038/nrmicro3432
37. Siboo IR, Chaffin DO, Rubens CE, Sullam PM. Characterization of the accessory *Sec* system of *Staphylococcus aureus*. J Bacteriol. 2008;190:6188–96. https://doi.org/10.1128/JB.00300-08
38. King NP, Beatson SA, Totsika M, Ulett GC, Alm RA, Manning PA, et al. UafB is a serine-rich repeat adhesin of *Staphylococcus saprophyticus* that mediates binding to fibronectin, fibrinogen and human uroepithelial cells. Microbiology (Reading). 2011;157:1161–75. https://doi.org/10.1099/mic.0.047639-0
39. Arndt D, Grant JR, Marcu A, Sajed T, Pon A, Liang Y, et al. PHASTER: a better, faster version of the PHAST phage search tool. Nucleic Acids Res. 2016;44:W16–21. https://doi.org/10.1093/nar/gkw387
40. Yahara K, Didelot X, Jolley KA, Kobayashi I, Maiden MCJ, Sheppard SK, et al. The landscape of realized homologous recombination in pathogenic bacteria. Mol Biol Evol. 2016;33:456–71. https://doi.org/10.1093/molbev/msv237
41. Tristan A, Bes M, Meugnier H, Lina G, Bozdogan B, Courvalin P, et al. Global distribution of Panton-Valentine leukocidin—positive methicillin-resistant *Staphylococcus aureus*, 2006. Emerg Infect Dis. 2007;13:594–600. https://doi.org/10.3201/eid1304.061316
42. Vincent C, Boerlin P, Daignault D, Dozois CM, Dutil L, Galanakis C, et al. Food reservoir for *Escherichia coli* causing urinary tract infections. Emerg Infect Dis. 2010;16:88–95. https://doi.org/10.3201/eid1601.091118
43. Hedman P, Ringertz O, Lindström M, Olsson K. The origin of *Staphylococcus saprophyticus* from cattle and pigs. Scand J Infect Dis. 1993;25:57–60. https://doi.org/10.1080/00365549309169670
44. Verstappen KM, Willems E, Fluit AC, Duim B, Martens M, Wagenaar JA. *Staphylococcus aureus* nasal colonization differs among pig lineages and is associated with the presence of other staphylococcal species. Front Vet Sci. 2017;4:97. https://doi.org/10.3389/fvets.2017.00097
45. Imperi F, Leoni L, Visca P. Antivirulence activity of azithromycin in *Pseudomonas aeruginosa*. Front Microbiol. 2014;5:178. https://doi.org/10.3389/fmicb.2014.00178

46. Goerke C, Köller J, Wolz C. Ciprofloxacin and trimethoprim cause phage induction and virulence modulation in *Staphylococcus aureus*. Antimicrob Agents Chemother. 2006; 50:171–7. https://doi.org/10.1128/AAC.50.1.171-177.2006
47. Davies MR, McIntyre L, Mutreja A, Lacey JA, Lees JA, Towers RJ, et al. Atlas of group A streptococcal vaccine candidates compiled using large-scale comparative genomics. Nat Genet. 2019;51:1035–43. https://doi.org/10.1038/s41588-019-0417-8
48. Méric G, Mageiros L, Pensar J, Laabei M, Yahara K, Pascoe B, et al. Disease-associated genotypes of the commensal skin bacterium *Staphylococcus epidermidis*. Nat Commun. 2018;9:5034. https://doi.org/10.1038/s41467-018-07368-7
49. Dearborn AD, Dokland T. Mobilization of pathogenicity islands by *Staphylococcus aureus* strain Newman bacteriophages. Bacteriophage. 2012;2:70–8. https://doi.org/10.4161/bact.20632

Address for correspondence: Maria Miragaia, Laboratory of Bacterial Evolution and Molecular Epidemiology, Instituto de Tecnologia Química e Biológica, Universidade Nova de Lisboa (ITQB-NOVA), Avenida da República, 2780-157, Oeiras, Portugal; email: miragaia@itqb.unl.pt

April 2020

Vectorborne Infections

- Stemming the Rising Tide of Human-Biting Ticks and Tickborne Diseases, United States
- Ecology and Epidemiology of Tickborne Pathogens, Washington, USA, 2011–2016
- Imported Arbovirus Infections in Spain, 2009–2018
- Decreased Susceptibility to Azithromycin in Clinical *Shigella* Isolates Associated with HIV and Sexually Transmitted Bacterial Diseases, Minnesota, USA, 2012–2015
- High Incidence of Active Tuberculosis in Asylum Seekers from Eritrea and Somalia in the First 5 Years after Arrival in the Netherlands
- Severe Dengue Epidemic, Sri Lanka, 2017
- Severe Fever with Thrombocytopenia Syndrome, Japan, 2013–2017
- Comprehensive Profiling of Zika Virus Risk with Natural and Artificial Mitigating Strategies, United States
- Genomic Insight into the Spread of Meropenem-Resistant *Streptococcus pneumoniae* Spain-ST81, Taiwan
- Isolation of Drug-Resistant *Gallibacterium anatis* from Calves with Unresponsive Bronchopneumonia, Belgium
- Guaroa Virus and *Plasmodium vivax* Co-Infections, Peruvian Amazon
- Intensified Short Symptom Screening Program for Dengue Infection during Pregnancy, India

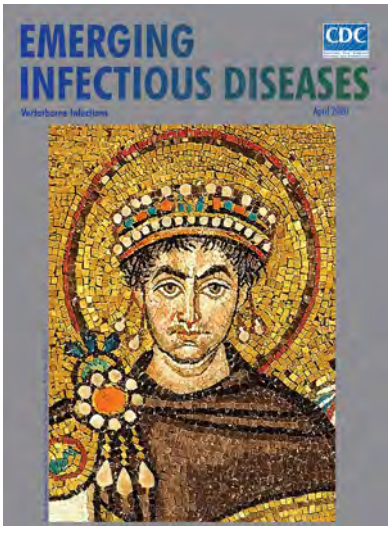

- Prevalence of Antibodies to Crimean-Congo Hemorrhagic Fever Virus in Ruminants, Nigeria, 2015
- Recurrent Herpes Simplex Virus 2 Lymphocytic Meningitis in Patient with IgG Subclass 2 Deficiency
- Health-Related Quality of Life after Dengue Fever, Morelos, Mexico, 2016–2017
- Person-to-Person Transmission of Andes Virus in Hantavirus Pulmonary Syndrome, Argentina, 2014
- Ebola Virus Neutralizing Antibodies in Dogs from Sierra Leone, 2017
- Outbreak of *Dirkmeia churashimaensis* Fungemia in a Neonatal Intensive Care Unit, India
- Rift Valley Fever Outbreak, Mayotte, France, 2018–2019
- Crimean-Congo Hemorrhagic Fever Virus in Humans and Livestock, Pakistan, 2015–2017
- Detection of Zoonotic Bartonella Pathogens in Rabbit Fleas, Colorado, USA
- Human-to-Human Transmission of Monkeypox Virus, United Kingdom, October 2018
- Whole-Genome Analysis of *Salmonella enterica* Serovar Enteritidis Isolates in Outbreak Linked to Online Food Delivery, Shenzhen, China, 2018
- Pruritic Cutaneous Nematodiasis Caused by Avian Eyeworm *Oxyspirura* Larvae, Vietnam
- Novel Rapid Test for Detecting Carbapenemase
- Arthritis Caused by MRSA CC398 in a Patient without Animal Contact, Japan
- Detection of Rocio Virus SPH 34675 during Dengue Epidemics, Brazil, 2011–2013
- Epidemiology of Lassa Fever and Factors Associated with Deaths, Bauchi State, Nigeria, 2015–2018
- Plague Epizootic Dynamics in Chipmunk Fleas, Sierra Nevada Mountains, California, USA, 2013–2015
- Knowledge of Infectious Disease Specialists Regarding Aspergillosis Complicating Influenza, United States

EMERGING INFECTIOUS DISEASES®

To revisit the April 2020 issue, go to:
https://wwwnc.cdc.gov/eid/articles/issue/26/4/table-of-contents

Mycoplasma genitalium and Other Reproductive Tract Infections in Pregnant Women, Papua New Guinea, 2015–2017

Michelle J.L. Scoullar, Philippe Boeuf, Elizabeth Peach, Ruth Fidelis, Kerryanne Tokmun, Pele Melepia, Arthur Elijah, Catriona S. Bradshaw, Glenda Fehler, Peter M. Siba, Simon Erskine, Elisa Mokany, Elissa Kennedy, Alexandra J. Umbers, Stanley Luchters, Leanne J. Robinson, Nicholas C. Wong, Andrew J. Vallely, Steven G. Badman, Lisa M. Vallely, Freya J.I. Fowkes, Christopher Morgan, William Pomat, Brendan S. Crabb, James G. Beeson, Healthy Mothers Healthy Babies Study Team[1]

Much about the range of pathogens, frequency of coinfection, and clinical effects of reproductive tract infections (RTIs) among pregnant women remains unknown. We report on RTIs (*Mycoplasma genitalium*, *Chlamydia trachomatis*, *Neisseria gonorrhoeae*, *Trichomonas vaginalis*, *Treponema pallidum* subspecies *pallidum*, bacterial vaginosis, and vulvovaginal candidiasis) and other reproductive health indicators in 699 pregnant women in Papua New Guinea during 2015–2017. We found *M. genitalium*, an emerging pathogen in Papua New Guinea, in 12.5% of participants. These infections showed no evidence of macrolide resistance. In total, 74.1% of pregnant women had ≥1 RTI; most of these infections were treatable. We detected sexually transmitted infections (excluding syphilis) in 37.7% of women. Our findings showed that syndromic management of infections is greatly inadequate. In total, 98.4% of women had never used barrier contraception. These findings will inform efforts to improve reproductive healthcare in Papua New Guinea.

Reproductive tract infections (RTIs), including sexually transmitted infections (STIs), are preventable and often curable health conditions. Public health officials consider *Chlamydia trachomatis*, *Neisseria gonorrhoeae*, *Trichomonas vaginalis*, and *Treponema pallidum* subspecies *pallidum* infections to be curable diseases. An estimated 376.4 million new cases of these 4 infections occur globally in adults each year; the World Health Organization Western Pacific Region has the highest number of annual new cases, estimated at 142 million (*1*–*3*). Other RTIs, such as bacterial vaginosis (BV) and vulvovaginal candidiasis (VVC) caused by *Candida albicans*, are also common. However, global estimates for these diseases are less certain because of differing diagnostic methodologies for BV (*4*) and prevalence of commensal *C. albicans*. Current estimates suggest that 8%–51% of pregnant women have BV (*5*); 20%–30% of asymptomatic and 40% of symptomatic women have vaginal *C. albicans* infections (*6*). RTIs can cause substantial pain and discomfort and some patients might experience debilitating stigma from their families and communities (*7*). Possible complications include pelvic inflammatory disease, infertility, and increased risk for other STIs. In

Author affiliations: Burnet Institute, Melbourne, Victoria, Australia (M.J.L. Scoullar, P. Boeuf, E. Peach, R. Fidelis, K. Tokmun, P. Melepia, E. Kennedy, A.J. Umbers, S. Luchters, L.J. Robinson, F.J.I. Fowkes, C. Morgan, B.S. Crabb, J.G. Beeson); Burnet Institute, Kokopo, Papua New Guinea (M.J.L. Scoullar, P. Boeuf, E. Peach, R. Fidelis, K. Tokmun, P. Melepia, E. Kennedy, A.J. Umbers, S. Luchters, L.J. Robinson, F.J.I. Fowkes, C. Morgan, B.S. Crabb, J.G. Beeson); University of Melbourne, Melbourne (M.J.L Scoullar, P. Boeuf, C.S. Bradshaw, L.J. Robinson, F.J.I. Fowkes, C. Morgan, B.S. Crabb, J.G. Beeson); University of Papua New Guinea, Port Moresby, Papua New Guinea (A. Elijah); Melbourne Sexual Health Centre, Melbourne (C.S. Bradshaw, G. Fehler); Monash University, Melbourne (C.S. Bradshaw, S. Luchters, L.J. Robinson, N.C. Wong, F.J.I. Fowkes, C. Morgan, B.S. Crabb, J.G. Beeson); Papua New Guinea Institute of Medical Research, Goroka, Papua New Guinea (P.M. Siba, L.J. Robinson, A. Vallely, L.M. Vallely, W. Pomat); SpeeDx Pty Ltd, Sydney, New South Wales, Australia (S. Erskine, E. Mokany); Aga Khan University, Nairobi, Kenya (S. Luchters); Ghent University, Ghent, Belgium (S. Luchters); University of New South Wales, Sydney (A. Vallely, S.G. Badman, L.M. Vallely); James Cook University, Townsville, Queensland, Australia (L.M. Vallely)

DOI: https://doi.org/10.3201/eid2703.201783

[1]Members of this group are listed at the end of this article.

pregnant women, RTIs can cause miscarriage, stillbirth, preterm birth, or neonatal death, as well as serious neonatal conditions such as blindness, congenital malformations, and lifelong disability (*1*,*8*,*9*).

Mycoplasma genitalium is increasingly understood to be a major cause of poor sexual health and is associated with pelvic inflammatory disease, cervicitis, miscarriage, and preterm birth (*10*,*11*). Limited data exists on *M. genitalium* prevalence, although estimates range from <1.0% in the general adult population to 15.9% in groups at high risk, such as female commercial sex workers (*12*,*13*). In pregnant women, estimates range from 0.7% in the United Kingdom (*14*) to 11.9% in the Solomon Islands (*15*). During 2010–2019, global macrolide resistance to *M. genitalium* increased from 10% to >50% (*16*). In many regions, the prevalence of *M. genitalium* and its susceptibility to antimicrobial drugs is unknown.

Papua New Guinea is a country in the southwestern Pacific Ocean with >8.5 million persons (*17*). Poor pregnancy outcomes are common in this country. Estimates are imprecise because of weaknesses in vital registry systems, but <50% of women give birth with a skilled birth attendant (*18*). Ultrasound machines for gestational age assessment are largely inaccessible because of scarcity, cost, and location. The estimated prevalence of low birthweight (weight <2.5 kg) ranges from 10%–24% and preterm birth from 7%–18% (*19*). Papua New Guinea has a high perinatal death rate of 17 deaths/1,000 pregnancies (*19*). Curable STIs are common; rates of *C. trachomatis*, *N. gonorrhoeae*, *T. vaginalis*, and *T. pallidum* infections exceed those of other high-prevalence regions such as sub-Saharan Africa (*1*,*20*). However, little to no data exists on the prevalence of *M. genitalium* in Papua New Guinea. We evaluated the prevalence of *M. genitalium* and other RTIs among pregnant women attending antenatal clinics in the East New Britain (ENB) province of Papua New Guinea. We also investigated molecular markers of resistance in clinical samples from these patients. We investigated the relationships between different RTIs, factors associated with infection, and analyzed the diagnostic accuracy of syndromic management guidelines.

Materials and Methods

Study Site and Population

We studied cross-sectional baseline data from 699 pregnant women attending their first antenatal clinic. Study participants were enrolled in Healthy Mothers Healthy Babies, a prospective cohort study undertaken at 5 health facilities in 3 of the 4 districts of ENB. The study sites included the hospitals in the 2 major urban areas and the 3 largest rural health centers of ENB. Members of the largest ethnic group, the Tolai, access all facilities; members of the second largest ethnic group, the Baining, predominantly access Kerevat Rural Hospital, the government-operated rural facility. Enrollment in the Healthy Mothers Healthy Babies cohort, and thus this study, occurred during March 2015–June 2017. Women ≥16 years of age who were living in the facilities' catchment area and attending clinic for the first time in the current pregnancy, regardless of gestational age, were eligible to participate. At each site, women were randomly selected through a dice roll. After the women underwent eligibility screening and provided informed consent, they completed a questionnaire administered by a trained research officer. We collected sociodemographic and clinical information through the questionnaire and patient-held medical records. We obtained urine, capillary finger prick blood, self-collected vaginal swab, and venous blood samples. We communicated all abnormal results available at the point of care, such as results of the urine dipstick and syphilis, malaria, and hemoglobin assays, to the participant and the healthcare provider.

Study Procedures

Health facility staff provided routine antenatal care, including intermittent preventive treatment in pregnancy for malaria, syndromic management for vaginal discharge (Appendix, https://wwwnc.cdc.gov/EID/article/27/3/20-1783-App1.pdf), iron and folate supplementation, voluntary counselling and testing for HIV using Alere Determine HIV-1/2 (Abbott, https://www.abbott.com), and point-of-care syphilis testing using Alere Determine Syphilis TP (Abbott), in accordance with national guidelines (*21*,*22*). At the beginning of the study period, the participating healthcare facilities conducted syphilis testing. However, interruptions in stock supply nationally led to fewer women being tested for syphilis. The research team subsequently supplied and conducted testing for study participants. Stock interruptions of HIV testing materials also occurred; however, our research team was not qualified for voluntary counselling and testing and did not have ethics approval to conduct HIV testing.

Each participant provided 2 self-collected vaginal swab samples: 1 GeneXpert vaginal/endocervical swab (Cepheid, https://www.cepheid.com), which was placed directly into its transport medium, and 1 Copan flocked swab (Copan Diagnostics, Inc., https://www.copanusa.com), which was first used

Table 2. Prevalence of reproductive tract infections among pregnant women in East New Britain, Papua New Guinea, 2015–2017*

Reproductive tract infection	Tested	Frequency	Prevalence, % (95% CI)
No current RTI†	467	121	25.9 (22–30.1)
No current STI‡	485	302	62.3 (57.8–66.6)
Mycoplasma genitalium	625	78	12.5 (10–15.3)
Chlamydia trachomatis	640	122	19.1 (16.1–22.3)
Neisseria gonorrhoeae	640	35	5.5 (3.8–7.5)
Trichomonas vaginalis	581	117	20.1 (16.9–23.6)
Syphilis§	437	79	18.1 (14.6–22)
Bacterial vaginosis	653	170	26 (22.7–29.6)
Vulvovaginal candidiasis	653	245	37.5 (33.8–41.4)
Co-infections			
≥1 Current RTI	467	346	74.1 (69.9–78)
≥1 Current STI	485	183	37.7 (33.4–42.2)
≥1 MG, CT, NG, TV, or syphilis infection	302	144	47.7 (41.9–53.5)
≥1 MG, CT, NG, TV, or BV infection	467	250	53.5 (48.9–58.1)
≥1 Infection diagnosed by GeneXpert¶	546	175	32.1 (28.2–36.1)
≥1 Vaginal infection#	542	362	66.8 (62.6–70.7)
≥1 BV or VVC infection	653	376	57.6 (53.7–61.4)
Multiple current STIs			
2	661	75	11.3 (9–14)
3	536	15	2.8 (1.6–4.6)

*Participants result included only if they had all tests done for each of the infections within group of RTIs. BV, bacterial vaginosis; CT, *Chlamydia trachomatis*; MG, *Mycoplasma genitalium*; NG, *Neisseria gonorrhoeae*; RTI, reproductive tract infection; STI, sexually transmitted infection; TV, *Trichomonas vaginalis*; VVC, vulvovaginal candidiasis.
†RTIs include MG, CT, NG, TV, BC, and VVC (syphilis not included).
‡STIs include MG, CT, NG, TV (syphilis not included).
§Diagnosed with Alere Determine Syphilis TP (Abbott, https://www.abbott.com).
¶CT, NG, and TV infections diagnosed with GeneXpert (Cepheid, https://www.cepheid.com).
#Vaginal infections include BV, TV, and VVC.

to prepare a vaginal smear on a slide for microscopy, and then placed in 1.0 mL Copan Universal Transport Medium (Copan Diagnostics, Inc.) specific for bacterial STIs. The number of vaginal swabs and smears available for diagnosis varied because of occasional reluctance to provide a swab, quality of vaginal smear, and availability of GeneXpert testing cartridges. Each woman self-collected a urine sample in a sterile container. All specimens were stored in a chilled box at 2°C–7°C for the remainder of clinic day, then stored at 2°C–7°C or −20°C until tested.

Laboratory Methods

We used the GeneXpert molecular platform (Cepheid) to test vaginal and urine specimens for *C. trachomatis*, *N. gonorrhoeae*, and *T. vaginalis* at the Burnet Institute/Papua New Guinea Institute of Medical Research laboratory at St. Mary's Hospital Vunapope (Kokopo, Papua New Guinea). *M. genitalilum* and resistance mutations were detected by quantitative PCR (ResistancePlus MG kit, SpeeDx Pty Ltd, https://plexpcr.com). Gram-stained vaginal smears were read by an experienced microscopist at the Melbourne Sexual Health Centre (Melbourne, Victoria, Australia) (Appendix).

Data Management and Statistical Analysis

Researchers interviewed participants and documented their responses using electronic tablets. We employed stringent data management protocols (Appendix).

The questionnaire included details about the enrollment clinic, participant characteristics at enrollment, and relevant obstetric history (Appendix). This study produced prevalence estimates of *M. genitalium*, *C. trachomatis*, *N. gonorrhoeae*, *T. vaginalis*, *T. pallidum*, BV, and VVC among pregnant women in Papua New Guinea. We used logistic regression to assess the association between patient characteristics and STIs, including *C. trachomatis*, *N. gonorrhoeae*, *T. vaginalis*, and *M. genitalium*. We included all variables of interest in the univariable analysis. The multivariable model retained variables associated with the outcome at $p<0.10$ in the univariable analysis. We also analyzed the effectiveness of syndromic management guidelines using the standard question about current symptoms compared with an alternative question about symptoms experienced during the current pregnancy.

Ethics Considerations

All participants provided individual written, informed consent. Ethics approval was provided from the Medical Research Advisory Committee of the Papua New Guinea National Department of Health (approval no. 14.27), the Papua New Guinea Institute of Medical Research Institutional Review Board (approval no. 1114), and the Human Research Ethics Committee of the Alfred Hospital in Australia (approval no. 348/14). Provincial approval was obtained

from the East New Britain Provincial Executive Committee and participating facilities. A series of community engagement meetings provided broader community support and assent for the study.

Results

We enrolled 699 pregnant women at 5 antenatal clinics in ENB. The median maternal age was 26 years (interquartile range [IQR] 22–30 years), 25.3% (177/699) of women were primigravida, 95.1% (663/697) were married or lived with a partner, and 46.5% (325/698) had only completed primary school (Table 1, https://wwwnc.cdc.gov/EID/article/27/3/20-1783-T1.htm). In total, 82.5% (569/690) of women had never used a modern method of contraception; only 11 (1.6%) women had ever used a condom for men or women.

High Burden of RTIs During Pregnancy

The total number of women tested for each pathogen varied as detailed in Methods. Of the 699 women enrolled, 12.5% (78/625; 95% CI 10.0%–15.3%) had *M. genitalium* infections. We found no evidence of macrolide-resistant mutations (Table 2). Among the samples tested, 19.1% (122/640; 95% CI 16.1%–22.3%) of women had *C. trachomatis* infections, 5.5% (35/640; 95% CI 3.8%–7.5%) had *N. gonorrhoeae* infections; and 20.1% (117/581; 95% CI 17.0%–23.7%) of tested samples were positive for *T. vaginalis*. Lifetime exposure to syphilis was extremely high: 18.1% (79/437; 95% CI 14.6%–22.0%) of samples were positive by *T. pallidum* serologic testing. Among the 653 vaginal smears available for microscopy, BV prevalence was 26.0% (170/653; 95% CI 22.7%–29.6%) and VVC prevalence was 37.5% (245/653; 95% CI 33.8%–41.4%). Facility-based HIV rapid test results were available for 205 women, of whom 2 (0.98%) were HIV-positive.

Among women for whom all results were available, most (74.1%; 346/467) had ≥1 RTI (i.e., BV, VVC, *M. genitalium*, *C. trachomatis*, *N. gonorrhoeae*, or *T. vaginalis*) at the time of screening; 37.7% (183/485) had ≥1 curable STI (i.e., *M. genitalium*, *C. trachomatis*, *N. gonorrhoeae*, or *T. vaginalis*) at the time of screening. Among the women who were tested, 32.1% (175/546) had an STI diagnosed using GeneXpert (*C. trachomatis*, *N. gonorrhoeae*, or *T. vaginalis*), 11.3% (75/661) had ≥2 concurrent STIs, 2.8% (15/536) of women had ≥3 coinfections, and 1 woman had 4 STIs.

Associations between Infections

Of the 78 women with *M. genitalium* infections, 28 (35.9%) had ≥1 concurrent STI detected: 20 (25.6%) had *C. trachomatis* infections, 13 (16.7%) had *T. vaginalis* infections, and 6 (7.7%) had *N. gonorrhoeae* infections (Figure 1; Appendix Table 2). Co-infections were most frequent among women with *N. gonorrhoeae* infections (80%; 28/35); most women with *N. gonorrhoeae* infections also had *C. trachomatis* infections (71.4%; 25/35), *T. vaginalis* infections (22.8%; 8/35), or *M. genitalium* infections (17.1%; 6/35). We did not consider syphilis in estimates of coinfections because the syphilis test did not distinguish between current or previous infection. Of 170 women with BV, 40.6% (69/170) had a co-infection; the most common were *C. trachomatis* (24.1%; 41/170), *T. vaginalis* (12.3%; 21/170), *M. genitalium* (12.3%; 21/170), and *N. gonorrhoeae* (7.6%; 13/170) (Appendix Table 3).

Relationship between Abnormal Vaginal Discharge and Infection

We compared the infections of women with current abnormal vaginal discharge (as defined by national treatment guidelines) with those who had abnormal vaginal discharge currently or at any time in pregnancy before their first antenatal clinic visit (Table 3). A total of 98 women (14.1%; 98/697) had current symptoms (i.e., abnormal vaginal discharge) that would have prompted treatment according to syndromic management guidelines (2 women did not answer this question). An additional 37 women did not have

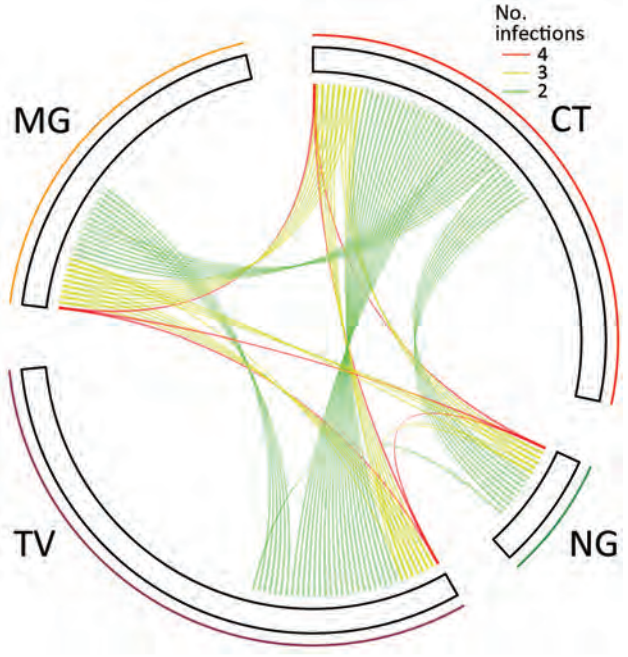

Figure 1. Relationships among sexually transmitted infections in pregnant women, East New Britain, Papua New Guinea, 2015–2017. Each line indicates ≥2 concurrent infections in 1 participant. The length of each sector corresponds to the number of monoinfections. MG, *Mycoplasma genitalium*; CT, *Chlamydia trachomatis*; NG, *Neisseria gonorrhoeae*; TV, *Trichomonas vaginalis*.

Table 3. Screening question for RTIs in pregnant women, East New Britain, Papua New Guinea, 2015–2017*

Category (*22*)	Screening question as per syndromic management guidelines: Do you currently have any abnormal vaginal discharge?			Alternative question: Have you experienced any abnormal vaginal discharge earlier in the pregnancy or now?		
	No	Yes	Total	No	Yes	Total
Total	599 (85.9)	98 (14.1)	697	563 (80.7)	135 (19.3)	698
Reproductive tract infection						
No current RTI†	112 (93.3)	8 (6.7)	120	108 (89.3)	13 (10.7)	121
No current STI‡	265 (88.0)	36 (12.0)	301	249 (82.5)	53 (17.5)	302
Mycoplasma genitalium	66 (84.6)	12 (15.4)	78	61 (78.2)	17 (21.8)	78
Chlamydia trachomatis	98 (80.3)	24 (19.7)	122	90 (73.8)	32 (26.2)	122
Neisseria gonorrhoeae	28 (80.0)	7 (20.0)	35	26 (74.3)	9 (25.7)	35
Trichomonas vaginalis	94 (80.3)	23 (19.7)	117	83 (70.9)	34 (29.1)	117
Syphilis§	68 (86.1)	11 (13.9)	79	65 (82.3)	14 (17.7)	79
Bacterial vaginosis	146 (85.9)	24 (14.1)	170	136 (80.0)	34 (20.0)	170
Vulvovaginal candidiasis	199 (81.2)	46 (18.8)	245	182 (74.3)	63 (25.7)	245
Co-infections						
≥1 Current RTI	292 (84.4)	54 (15.6)	346	268 (77.5)	78 (22.5)	346
≥1 Current STI	154 (84.2)	29 (15.8)	183	141 (77.0)	42 (23.0)	183
≥1 Infection diagnosed by GeneXpert¶	141 (80.6)	34 (19.4)	175	127 (72.6)	48 (27.4)	175
≥1 Vaginal infection#	298 (82.3)	64 (17.7)	362	271 (74.9)	91 (25.1)	362
≥1 BV or VVC infection	314 (83.5)	62 (16.5)	376	290 (77.1)	86 (22.9)	376
Any 2 current STIs	58 (77.3)	17 (22.7)	75	53 (70.7)	22 (29.3)	75

*Values are frequency, no. (%). Missing data for 1 woman who responded yes to the alternative question had a missing response to the standard question. BV, bacterial vaginosis; CT, *Chlamydia trachomatis*; MG, *Mycoplasma genitalium*; NG, *Neisseria gonorrhoeae*; RTI, reproductive tract infection; STI, sexually transmitted infection; TV, *Trichomonas vaginalis*; VVC, vulvovaginal candidiasis.
†RTIs include MG, CT, NG, TV, BC, and VVC (syphilis not included).
‡STIs include MG, CT, NG, TV (syphilis not included).
§Diagnosed with Alere Determine Syphilis TP (Abbott, https://www.abbott.com).
¶CT, NG, and TV infections diagnosed with GeneXpert (Cepheid, https://www.cepheid.com).
#Vaginal infections include BV, TV, and VVC.

abnormal vaginal discharge at the time of the screening but had experienced it earlier in the pregnancy. According to the national treatment guidelines, these women would not normally receive treatment.

Most STIs were asymptomatic and neither criteria (current abnormal vaginal discharge vs. current or previous abnormal vaginal discharge during this pregnancy) performed well as a marker of infection. Of those women with a detected STI, 84.1% (154/183) had no current symptoms and 77.0% (141/183) had not experienced symptoms during their current pregnancy. Conversely, 12.0% (36/301) of uninfected women had current symptoms and 17.6% (53/302) had experienced symptoms during their current pregnancy. Of those with *M. genitalium* infection, only 12 women (15.4%;12/78) would have been treated according to syndromic management guidelines used by Papua New Guinea.

Asking whether women had any symptoms during their current pregnancy was consistently more sensitive than asking about current symptoms as per the standard diagnostic question (Figure 2); however, the sensitivity of both questions was <30% for all individual or collective pathogens. The alternative question was less specific for ≥1 current STI (82.5% [p = 0.15] vs. 88% [p = 0.22]; Appendix Table 4). The alternative question was best able to identify women with *T. vaginalis* infection (p<0.01) and VVC (p<0.01) (Appendix Table 4); however, this question still missed most infections.

Factors Associated with Curable STIs

We did not identify any factors in the univariable (Appendix Table 5) or multivariable (Table 4) analysis that were associated with an increased odds of *M. genitalium* infection. The univariable analysis showed that women who were younger, in their first pregnancy, employed, single or separated, had never used a modern method of contraception, or had abnormal vaginal discharge at any time in their current pregnancy were at increased risk for certain STIs, to varying degrees of statistical significance. In the multivariable analysis, primigravida women and those 16–24 years of age had higher odds for *C. trachomatis* infection (adjusted odds ratio [aOR] 2.17, 95% CI 1.29–3.64 [p<0.01], and aOR 3.39, 95% CI 1.24–9.28 [p = 0.02], respectively). Primigravida women also had higher odds for *N. gonorrhoeae* infection (aOR 4.33, 95% CI 1.74–10.75; p<0.01). Women 16–24 years of age had increased odds for testing positive for ≥1 STI compared with women in other age groups (aOR 2.45, 95% CI 1.17–5.16; p = 0.02).

Discussion

We confirmed that *M. genitalium* is widespread among pregnant women in Papua New Guinea, which has

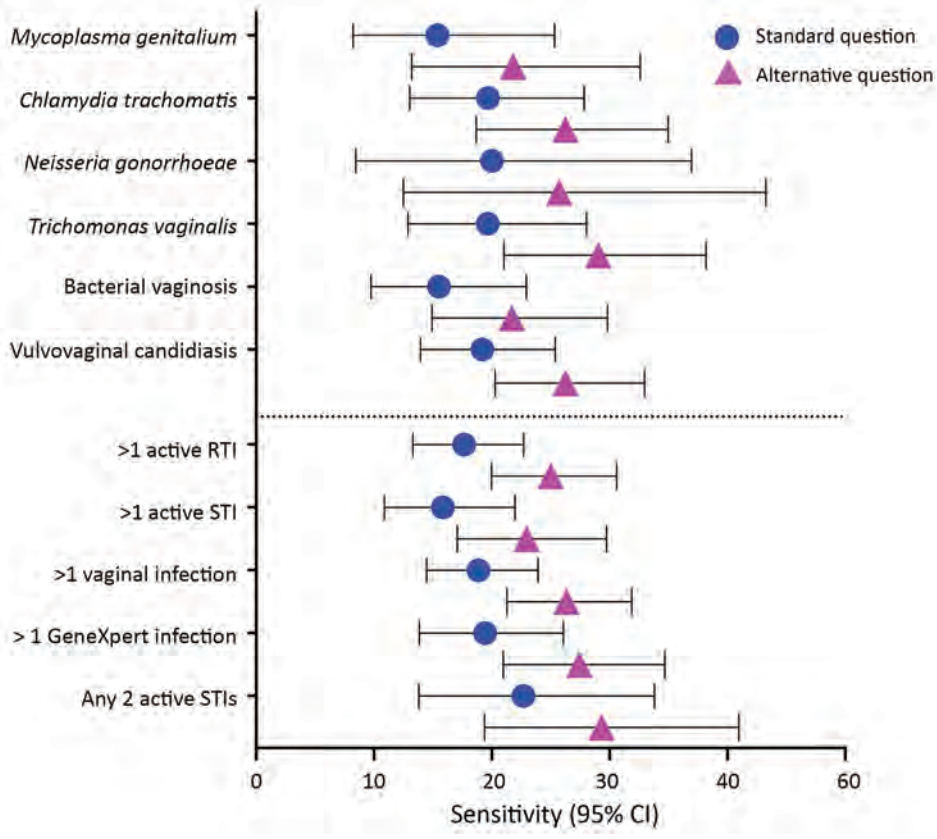

Figure 2. Sensitivity of syndromic management for sexually transmitted infections in pregnant women, East New Britain, Papua New Guinea, 2015–2017. Participants answered the standard question according to Papua New Guinea national guidelines "Do you currently have any abnormal vaginal discharge?" or the alternative question "Have you experienced any abnormal vaginal discharge earlier in the pregnancy or now?" (*22*). *Chlamydia trachomatis*, *Neisseria gonorrhoeae*, and *Trichomonas vaginalis* infections diagnosed with GeneXpert (Cepheid, https://www.cepheid.com). RTI, reproductive tract infection; STI, sexually transmitted infection.

one of the highest prevalence rates of this infection globally. We did not find evidence of macrolide resistance. The high prevalence of *M. genitalium* (12.5%) among pregnant women suggests an estimated 13,000 (95% CI 10,342–15,823) current cases among women of reproductive age in the province (Appendix). In addition, we provide contemporary data on RTIs in pregnant women from the New Guinea Islands region of Papua New Guinea; the most recent report on the subject is >20 years old (*23*). Our study indicates that ≥1 in 2 (53.5%) pregnant women in ENB have a treatable RTI (including BV, STI, or both) known to cause harmful sexual and reproductive health outcomes. These RTIs are not usually detectable by the syndromic management practices described in the national health guidelines of PNG. This high prevalence of poor sexual and reproductive health has major national and regional public health significance.

No global surveillance system for *M. genitalium* currently exists (*24*). Different detection methods have varying levels of sensitivity, limiting scientific understanding of its epidemiology. High-income countries report rates of *M. genitalium* infection ranging from 0.3%–3.3% (*11*,*13*,*25*) in the general population, with higher estimates in certain populations (*26*,*27*). Fewer data are available from low- and middle-income countries (LMICs) but prevalence appears to be higher, ranging from 3% in the general population in Tanzania (*13*) to 8%–9% in Honduras and South Africa (*13*,*28*). The highest prevalence has been reported among sex workers: 16% in Kenya (*29*) and 26% in Uganda (*30*). Data on *M. genitalium* infection among pregnant women remains limited despite the disease's association with adverse pregnancy outcomes (*26*); available estimates range from 0.7%–0.9% in the United Kingdom and France (*14*,*31*) to 6.2% in Guinea-Bissau (*32*) and 11.9% in the Solomon Islands (*15*). More data on the prevalence and consequences of *M. genitalium* infection among pregnant women are needed.

Regional data on *M. genitalium* in LMICs are limited. One study from the Solomon Islands examined the effects of mass drug administration (MDA) using 1 g of oral azithromycin for eliminating ocular *C. trachomatis* on *M. genitalium* infection rates (*15*). Before MDA, the study found an 11.9% (95% CI 8.3%–16.6%; n = 236) prevalence of *M. genitalium* among pregnant women. After MDA, the prevalence remained high at 10.9% with no evidence of macrolide resistance. However, only 5 of the 28 *M. genitalium*–positive women in the post-MDA group had received azithromycin (*15*).

In this study, the lack of macrolide resistance among *M. genitalium* infections in pregnant women warrants further exploration. Macrolide susceptibility might reflect a population's lack of exposure to this class of antimicrobial drugs. However, macrolides are used widely in Papua New Guinea (*22*,*33*) and are available without prescription (although over-the-counter macrolides are more expensive than their prescribed counterparts).

We observed a prevalence of curable STIs substantially greater than in most settings included in the 2016 global estimates of curable STIs (*3*). The 32.1% observed prevalence of ≥1 current STI diagnosable by GeneXpert is less than the 42.7% reported in a study of antenatal clinics from 3 mainland provinces of Papua New Guinea in 2014 (*20*), but similar to the 33.7% prevalence among pregnant women in Madang Province in 2012 (*34*). We found a 19.1% prevalence of *C. trachomatis* infection among pregnant women, consistent with reports from other provinces (22.9% in the Eastern Highlands, Hela, and Central provinces [*20*] and 20.0% in the Milne Bay province [*35*]) and the neighboring Solomon Islands (20.3%) (*36*). Similarly, Papua New Guinea and Solomon Islands have the highest reported rates of *N. gonorrhoeae* among pregnant women (5.1%–

Table 4. Multivariable analysis of factors associated with current sexually transmitted infections in pregnant women, East New Britain, Papua New Guinea, 2015–2017*

Characteristic	Sexually transmitted infection, aOR (95% CI); p value				
	Mycoplasma genitalium	*Chlamydia trachomatis*	*Neisseria gonorrhoeae*	*Trichomonas vaginalis*	≥1 infection
Clinic					
Vunapope	Referent	Referent	Referent	Referent	Referent
Nonga	0.68 (0.28–1.62); 0.38	0.88 (0.43–1.78); 0.72	2.35 (0.76–7.32); 0.14	0.91 (0.42–1.97); 0.82	0.84 (0.43–1.63); 0.61
Kerevat	0.9 (0.43–1.88); 0.77	0.55 (0.28–1.09); 0.09	1.03 (0.3–3.5); 0.97	0.84 (0.41–1.72); 0.62	0.58 (0.31–1.11); 0.10
Napapar	0.76 (0.37–1.57); 0.46	0.9 (0.5–1.62); 0.73	0.99 (0.31–3.15); 0.98	1.09 (0.6–1.99); 0.77	0.64 (0.36–1.13); 0.12
Paparatava	0.86 (0.43–1.73); 0.68	0.86 (0.47–1.57); 0.62	2.04 (0.7–5.95); 0.19	1.08 (0.59–1.99); 0.79	1.01 (0.58–1.75); 0.97
Age, y					
≥35	Referent	Referent	Referent	Referent	Referent
25–34	0.76 (0.34–1.69); 0.50	2.47 (0.94–6.52); 0.07	1.01 (0.2–4.98); 0.99	1.85 (0.78–4.37); 0.16	1.7 (0.85–3.38); 0.13
16–24	1.21 (0.52–2.82); 0.66	3.39 (1.24–9.28); 0.02	1.86 (0.36–9.63); 0.46	2.31 (0.93–5.7); 0.07	2.45 (1.17–5.16); 0.02
Gravidity					
Multigravida	Referent	Referent	Referent	Referent	Referent
Primigravida	0.87 (0.46–1.65); 0.67	2.17 (1.29–3.64); <0.01	4.33 (1.74–10.75); <0.01	1.09 (0.62–1.92); 0.75	1.45 (0.87–2.42); 0.15
Marital status					
Married/cohabiting	Referent	Referent	Referent	Referent	Referent
Single/separated	1.06 (0.34–3.3); 0.92	1.31 (0.54–3.13); 0.55	0.44 (0.09–2.23); 0.32	4.48 (1.9–10.55); <0.01	1.6 (0.61–4.21); 0.34
Vaginal discharge					
No symptoms	Referent	Referent	Referent	Referent	Referent
Abnormal discharge (current or before first antenatal clinic)	1.17 (0.63–2.15); 0.62	1.29 (0.78–2.14); 0.33	1.45 (0.6–3.53); 0.41	1.56 (0.94–2.59); 0.09	1.29 (0.79–2.11); 0.31
Has used modern contraception					
Yes	Referent	Referent	Referent	Referent	Referent
No	1.82 (0.82–4.08); 0.14	1.04 (0.56–1.95); 0.90	0.77 (0.23–2.59); 0.67	1.27 (0.66–2.43); 0.47	1.17 (0.67–2.05); 0.57
Employment status					
Unemployed	Referent	Referent	Referent	Referent	Referent
Employed	0.89 (0.49–1.62); 0.71	1.27 (0.79–2.05); 0.32	2.66 (1.24–5.71); 0.01	0.96 (0.57–1.62); 0.89	1.29 (0.81–2.06); 0.28
Urine nitrite					
Trace	0.49 (0.11–2.12); 0.34	0.78 (0.25–2.43); 0.667	0.68 (0.08–5.55); 0.72	0.34 (0.07–1.61); 0.17	0.35 (0.11–1.11); 0.08
Positive	1.32 (0.58–3); 0.50	1.88 (0.94–3.74); 0.07	1.6 (0.5–5.09); 0.43	1.29 (0.6–2.76); 0.51	1.26 (0.62–2.58); 0.53
Fever during pregnancy					
No	Referent	Referent	Referent	Referent	Referent
Yes (before first antenatal clinic)	1.15 (0.66–1.99); 0.63	0.75 (0.46–1.24); 0.26	0.69 (0.29–1.65); 0.41	1.58 (0.99–2.53); 0.05	1 (0.63–1.57); 0.99

*aOR, adjusted odds ratio.

14.2%) (*34*,*36*–*38*) in the world. In addition, 2 studies from South Africa also report very high rates of *N. gonorrhoeae*: 10.1% among patients in a primary care setting (*39*) and 6.4% among pregnant women (*40*).

Risk factors for different STIs identified in this study (e.g., primigravida, age 16–24 years, employment, being single or separated) could have several explanations. Younger women in their first pregnancy might have had less interaction with reproductive health services. Also, employed women might have more mobility, which increases risk for STI acquisition. We did not identify any risk factors for *M. genitalium* infection, although younger women (16–24 years of age) were at increased risk for ≥1 of the curable current STIs. Risk factors for STIs in pregnancy reported elsewhere in Papua New Guinea include having >1 lifetime sexual partner, low education level of the woman or her partner, rural location, history of miscarriage or stillbirth, and low socioeconomic status (*20*,*34*).

This study also provides data on BV and VVC; 57.6% of participants had ≥1 of these infections. VVC can cause extreme discomfort and increase a woman's risk for postpartum breast candidiasis, which can affect breastfeeding, but VVC is treatable with antimicrobial drugs (*41*). We found a 37.5% prevalence of VVC, higher than the 23% prevalence reported in Papua New Guinea in 1991 (*42*). Comparisons with other LMICs are difficult because of the limited amount of contemporary data (*41*,*43*). We found a 1-in-4 prevalence of BV among pregnant women, higher than the 17.6% prevalence previously reported in Papua New Guinea (*35*), but in keeping with recent global estimates of 23%–29% (*5*). However, our results might underestimate the true prevalence because diagnosis was limited to only women with a Nugent score of 7–10.

In Papua New Guinea, syndromic management of RTIs is common because access to diagnostic services is limited. We confirm previous reports from Papua New Guinea and elsewhere (*28*,*37*) that syndromic management is an inadequate tool to effectively treat RTIs. This approach missed 78.2% of *M. genitalium* infections and 3 of 4 RTIs. Alternative approaches are essential to effectively prevent, detect, and treat RTIs in a cost-effective, feasible manner in resource-constrained settings. Although condoms are available, their use is limited by gender disparities, stigma, and financial barriers (*23*). Improved access to affordable, accurate point-of-care diagnostics would lead to more accessible and appropriate treatment, resulting in improved sexual and reproductive health; the widespread implementation of GeneXpert for tuberculosis diagnosis (*44*) might also increase access to STI diagnosis in Papua New Guinea.

The main limitation of this study is the facility-based recruitment of participants because results might not represent women who do not attend any antenatal clinic. However, routinely collected provincial data for 2015–2017 estimated that 73%–85% of pregnant women attended ≥1 appointment at an antenatal clinic (*45*,*46*). The number of women who had a point-of-care syphilis test was lower than other tests. These results did not differentiate between active or latent infection; we also were unable to exclude exposure to yaws, which is endemic to Papua New Guinea (*47*). Yaws and syphilis are caused by different subspecies of *T. pallidum* and cannot be distinguished by this test alone. Prevalence of yaws varies widely within Papua New Guinea; estimates for ENB are unavailable, although neighboring New Ireland Province has a 1.8% prevalence of active yaws according to a population-wide survey (*48*).

In conclusion, we provide data on *M. genitalium* prevalence and antimicrobial resistance markers in Papua New Guinea, revealing a high prevalence of infection underrecognized by syndromic management guidelines. This data contributes to the understanding of the global prevalence of this infection among pregnant women. We found that STIs were common among pregnant women; 37.7% of participants had ≥1 STI at the time of the study. This study also highlights the high prevalence of BV and VVC and confirms that current antenatal screening practices with syndromic management is inadequate. This high prevalence of disease negatively affects sexual and reproductive health. Urgent action towards ensuring access to affordable prevention, diagnosis, and treatment of RTIs in communities in Papua New Guinea and similar settings is essential. This action will be crucial to achieving the sustainable development goal of ensuring universal access to sexual and reproductive healthcare services by 2030 (*49*). Expanding treatment access will contribute to improved sexual and reproductive health outcomes for women in Papua New Guinea.

The Healthy Mothers Healthy Babies Study Team also includes: Hadlee Supsup, Dukduk Kabiu, Priscah Hezeri, Primrose Homiehombo, Rose Suruka, Benishar Kombut, Thalia Wat, Noelyne Taraba, Chris Sohenaloe, Dorish Palangat, Zoe Saulep, Elizabeth Walep, Lucy Au, Irene Daniels, Gabriella Kalimet-Tade, Noreen Tamtilik, Ellen Kavang, Wilson Philip, Wilson Kondo, Allan Tirang, Michael Palauva, Ioni Pidian, Teddy Wanahau, and Eremas Amos.

Acknowledgments

We extend our heartfelt thanks to the women and infants who participated in this study, as well as the families and communities who supported them to do so. Our special thanks to the National Department of Health, the East New Britain Provincial Administration, the Provincial Health Authority, Catholic Health Services, and participating health facilities (Nonga General Hospital, St Mary's Hospital Vunapope, Kerevat Rural Hospital, Napapar Health Centre, Paparatava Health Centre) for enthusiastically facilitating this research. Specific thanks to Levi Mano, Nicholas Larme, Ako Yap, Moses Bogandri, Benedict Mode, Pinip Wapi, Felix Diaku, Tanmay Bagade, Delly Babona, Placidia Nohan, Theonila Wat, and Rebecca Penaia who have provided invaluable support and advice throughout the planning and implementation of this work in East New Britain. We gratefully acknowledge the dedication and contribution by our Burnet Institute Kokopo staff who worked tirelessly to support the research team to implement this study, especially Stenard Hiasihri, Essie Koniel, Bettie Matonge, Elice Adimain, Thelma Punion, and Lucy Palom. We thank Burnet Institute Melbourne for invaluable project support, especially Kellie Woiwod, James Lawson, Lisa Davidson, Vivian Newton, Lisa Vitasovich, and Rodney Stewart. We thank our many collaborators, including Louis Samiak, Lahui Geita (deceased), Jack Richards, Suman Majumdar, Lisa Natoli, and especially John Kaldor and Rebecca Guy for advice on STIs. We also thank Michael Toole, Margaret Hellard, and Caroline Homer for their vision, overall leadership, and technical guidance to the Healthy Mothers Healthy Babies program.

This work was funded by the Burnet Institute with philanthropic support provided by numerous private and business donors in Australia andPapau New Guinea, including the Bank South Pacific PNG Community Grant, the Gras Foundation, the Finkel Foundation, the June Canavan Foundation, the Naylor Steward Ancillary Fund, and the Chrysalis Foundation. Several authors receive funding from the National Health and Medical Research Council of Australia: Senior Research Fellowship to J.G.B., Program Grant to J.G.B. and B.S.C., Career Development Fellowships to F.J.I.F. and L.J.R., Postgraduate Research Scholarship to C.M. M.J.L.S. received a Basser Research Entry Scholarship from the Royal Australasian College of Physicians Foundation (2018 and 2020). The Burnet Institute is supported by an Operational Infrastructure Grant from the State Government of Victoria, Australia, and the Independent Research Institutes Infrastructure Support Scheme of the National Health and Medical Research Council of Australia.

About the Author

Dr. Scoullar is a senior research officer at the Burnet Institute, Melbourne. Her primary research interests include infection and nutrition in pregnancy, and their subsequent effects on neonatal and infant health, especially birthweight and growth through infancy.

References

1. Newman L, Rowley J, Vander Hoorn S, Wijesooriya NS, Unemo M, Low N, et al. Global estimates of the prevalence and incidence of four curable sexually transmitted infections in 2012 based on systematic review and global reporting. PLoS One. 2015;10:e0143304. https://doi.org/10.1371/journal.pone.0143304
2. World Health Organization. Report on global sexually transmitted infection surveillance, 2018. 2018 [cited 2019 Dec 9]. https://www.who.int/reproductivehealth/publications/stis-surveillance-2018
3. Rowley J, Vander Hoorn S, Korenromp E, Low N, Unemo M, Abu-Raddad LJ, et al. Chlamydia, gonorrhoea, trichomoniasis and syphilis: global prevalence and incidence estimates, 2016. Bulletin of the World Health Organization. 2019;97:548–62, 62A–62P. https://doi.org/10.2471/BLT.18.228486
4. van de Wijgert JHHM, Jespers V. The global health impact of vaginal dysbiosis. Res Microbiol. 2017;168:859–64. https://doi.org/10.1016/j.resmic.2017.02.003
5. Peebles K, Velloza J, Balkus JE, McClelland RS, Barnabas RV. High global burden and costs of bacterial vaginosis: a systematic review and meta-analysis. Sex Transm Dis. 2019;46:304–11. https://doi.org/10.1097/OLQ.0000000000000972
6. Cauchie M, Desmet S, Lagrou K. Candida and its dual lifestyle as a commensal and a pathogen. Res Microbiol. 2017;168:802–10. https://doi.org/10.1016/j.resmic.2017.02.005
7. Donovan B. Sexually transmissible infections other than HIV. Lancet. 2004;363:545–56. https://doi.org/10.1016/S0140-6736(04)15543-8
8. Arol OA, Over M, Manhard L, Holmes KK. Sexually transmitted infections. In: Jamison DT, Breman JG, Measham AR, Alleyne G, Claeson M, Evans DB, et al., editors. Disease control priorities in developing countries. 2nd ed. New York: Oxford University Press; 2006. p. 315
9. Thwaites A, Flanagan K, Datta S. Non-HIV sexually transmitted infections in pregnancy. Obstet Gynaecol Reprod Med. 2019;29:151–7. https://doi.org/10.1016/j.ogrm.2019.03.001
10. Martin DH, Manhart LE, Workowski KA. *Mycoplasma genitalium* from basic science to public health: summary of the results from a National Institute of Allergy and Infectious Diseases Technical Consultation and Consensus Recommendations for Future Research Priorities. J Infect Dis. 2017;216:S427–30. https://doi.org/10.1093/infdis/jix147
11. Lis R, Rowhani-Rahbar A, Manhart LE. *Mycoplasma genitalium* infection and female reproductive tract disease: a meta-analysis. Clin Infect Dis. 2015;61:418–26. https://doi.org/10.1093/cid/civ312
12. Sonnenberg P, Ison CA, Clifton S, Field N, Tanton C, Soldan K, et al. Epidemiology of *Mycoplasma genitalium* in British men and women aged 16–44 years: evidence from the third National Survey of Sexual Attitudes and Lifestyles (Natsal-3). Int J Epidemiol. 2015;44:1982–94. https://doi.org/10.1093/ije/dyv194

13. Baumann L, Cina M, Egli-Gany D, Goutaki M, Halbeisen FS, Lohrer G-R, et al. Prevalence of *Mycoplasma genitalium* in different population groups: systematic review and meta-analysis. Sex Transm Infect. 2018;94:255–62. https://doi.org/10.1136/sextrans-2017-053384
14. Oakeshott P, Hay P, Taylor-Robinson D, Hay S, Dohn B, Kerry S, et al. Prevalence of *Mycoplasma genitalium* in early pregnancy and relationship between its presence and pregnancy outcome. BJOG. 2004;111:1464–7. https://doi.org/10.1111/j.1471-0528.2004.00276.x
15. Harrison MA, Harding-Esch EM, Marks M, Pond MJ, Butcher R, Solomon AW, et al. Impact of mass drug administration of azithromycin for trachoma elimination on prevalence and azithromycin resistance of genital *Mycoplasma genitalium* infection. Sex Transm Infect. 2019;95:522–8. https://doi.org/10.1136/sextrans-2018-053938
16. Machalek DA, Tao Y, Shilling H, Jensen JS, Unemo M, Murray G, et al. Prevalence of mutations associated with resistance to macrolides and fluoroquinolones in *Mycoplasma genitalium*: a systematic review and meta-analysis. Lancet Infect Dis. 2020;20:1302–14. https://doi.org/10.1016/S1473-3099(20)30154-7
17. The World Bank Group. Papua New Guinea. 2019 [cited 2020 Feb 25]. https://data.worldbank.org/country/papua-new-guinea
18. National Statistical Office of Papua New Guinea; ICF International, Inc. Papua New Guinea demographic and health survey 2016–18. 2019 [cited 2020 Aug 10]. https://www.nso.gov.pg/census-surveys/demographic-and-health-survey
19. Robbers G, Vogel JP, Mola G, Bolgna J, Homer CSE. Maternal and newborn health indicators in Papua New Guinea—2008–2018. Sex Reprod Health Matters. 2019;27:52. https://doi.org/10.1080/26410397.2019.1686199
20. Vallely LM, Toliman P, Ryan C, Rai G, Wapling J, Tomado C, et al. Prevalence and risk factors of *Chlamydia trachomatis*, *Neisseria gonorrhoeae*, *Trichomonas vaginalis* and other sexually transmissible infections among women attending antenatal clinics in three provinces in Papua New Guinea: a cross-sectional survey. Sex Health. 2016;13:420–7. https://doi.org/10.1071/SH15227
21. Mola G, Amoa A, Bagita M, Augerea L, Geita L, O'Connor M. Manual of standard managements in obstetrics and gynaecology for doctors, HEOs and nurses in Papua New Guinea. 7th ed. Port Moresby (Papua New Guinea): World Health Organization; 2016. p. 10, 94.
22. National Department of Health. Standard treatment guidelines for common illness of adults in Papua New Guinea. 6th ed. Port Moresby (Papua New Guinea): World Health Organization; 2012. p. 41–2.
23. Vallely A, Page A, Dias S, Siba P, Lupiwa T, Law G, et al. The prevalence of sexually transmitted infections in Papua New Guinea: a systematic review and meta-analysis. PLoS One. 2010;5:e15586. https://doi.org/10.1371/journal.pone.0015586
24. Golden MR, Workowski KA, Bolan G. Developing a public health response to *Mycoplasma genitalium*. J Infect Dis. 2017;216:S420–6. https://doi.org/10.1093/infdis/jix200
25. Jensen JS, Cusini M, Gomberg M, Moi H. 2016 European guideline on *Mycoplasma genitalium* infections. J Eur Acad Dermatol Venereol. 2016;30:1650–6. https://doi.org/10.1111/jdv.13849
26. Donders GGG, Ruban K, Bellen G, Petricevic L. Mycoplasma/ureaplasma infection in pregnancy: to screen or not to screen. J Perinat Med. 2017;45:505–15. https://doi.org/10.1515/jpm-2016-0111
27. Deborde M, Pereyre S, Puges M, Bébéar C, Desclaux A, Hessamfar M, et al. High prevalence of *Mycoplasma genitalium* infection and macrolide resistance in patients enrolled in HIV pre-exposure prophylaxis program. Med Mal Infect. 2019;49:347–9. https://doi.org/10.1016/j.medmal.2019.03.007
28. Hoffman CM, Mbambazela N, Sithole P, Morré SA, Dubbink JH, Railton J, et al. Provision of sexually transmitted infection services in a mobile clinic reveals high unmet need in remote areas of South Africa: a cross-sectional study. Sex Transm Dis. 2019;46:206–12. https://doi.org/10.1097/OLQ.0000000000000931
29. Cohen CR, Nosek M, Meier A, Astete SG, Iverson-Cabral S, Mugo NR, et al. *Mycoplasma genitalium* infection and persistence in a cohort of female sex workers in Nairobi, Kenya. Sex Transm Dis. 2007;34:274–9. https://doi.org/10.1097/01.olq.0000237860.61298.54
30. Vandepitte J, Muller E, Bukenya J, Nakubulwa S, Kyakuwa N, Buvé A, et al. Prevalence and correlates of *Mycoplasma genitalium* infection among female sex workers in Kampala, Uganda. J Infect Dis. 2012;205:289–96. https://doi.org/10.1093/infdis/jir733
31. Peuchant O, Le Roy C, Desveaux C, Paris A, Asselineau J, Maldonado C, et al. Screening for *Chlamydia trachomatis*, *Neisseria gonorrhoeae*, and *Mycoplasma genitalium* should it be integrated into routine pregnancy care in French young pregnant women? Diagn Microbiol Infect Dis. 2015;82:14–9. https://doi.org/10.1016/j.diagmicrobio.2015.01.014
32. Labbé AC, Frost E, Deslandes S, Mendonça AP, Alves AC, Pépin J. *Mycoplasma genitalium* is not associated with adverse outcomes of pregnancy in Guinea-Bissau. Sex Transm Infect. 2002;78:289–91. https://doi.org/10.1136/sti.78.4.289
33. Joshua IB, Passmore PR, Sunderland BV. An evaluation of the Essential Medicines List, Standard Treatment Guidelines and prescribing restrictions, as an integrated strategy to enhance quality, efficacy and safety of and improve access to essential medicines in Papua New Guinea. Health Policy Plan. 2016;31:538–46. https://doi.org/10.1093/heapol/czv083
34. Wangnapi RA, Soso S, Unger HW, Sawera C, Ome M, Umbers AJ, et al. Prevalence and risk factors for *Chlamydia trachomatis*, *Neisseria gonorrhoeae* and *Trichomonas vaginalis* infection in pregnant women in Papua New Guinea. Sex Transm Infect. 2015;91:194–200. https://doi.org/10.1136/sextrans-2014-051670
35. Badman SG, Vallely LM, Toliman P, Kariwiga G, Lote B, Pomat W, et al. A novel point-of-care testing strategy for sexually transmitted infections among pregnant women in high-burden settings: results of a feasibility study in Papua New Guinea. BMC Infect Dis. 2016;16:250. https://doi.org/10.1186/s12879-016-1573-4
36. Marks M, Kako H, Butcher R, Lauri B, Puiahi E, Pitakaka R, et al. Prevalence of sexually transmitted infections in female clinic attendees in Honiara, Solomon Islands. BMJ Open. 2015;5:e007276. https://doi.org/10.1136/bmjopen-2014-007276
37. Vallely LM, Toliman P, Ryan C, Rai G, Wapling J, Gabuzzi J, et al. Performance of syndromic management for the detection and treatment of genital *Chlamydia trachomatis*, *Neisseria gonorrhoeae* and *Trichomonas vaginalis* among women attending antenatal, well woman and sexual health clinics in Papua New Guinea: a cross-sectional study. BMJ Open. 2017;7:e018630. https://doi.org/10.1136/bmjopen-2017-018630
38. Unger HW, Ome-Kaius M, Wangnapi RA, Umbers AJ, Hanieh S, Suen CSNLW, et al. Sulphadoxine-pyrimethamine

plus azithromycin for the prevention of low birthweight in Papua New Guinea: a randomised controlled trial. BMC Med. 2015;13:9. https://doi.org/10.1186/s12916-014-0258-3
39. Peters RPH, Dubbink JH, van der Eem L, Verweij SP, Bos MLA, Ouburg S, et al. Cross-sectional study of genital, rectal, and pharyngeal chlamydia and gonorrhea in women in rural South Africa. Sex Transm Dis. 2014;41:564–9. https://doi.org/10.1097/OLQ.0000000000000175
40. Moodley D, Moodley P, Sebitloane M, Soowamber D, McNaughton-Reyes HL, Groves AK, et al. High prevalence and incidence of asymptomatic sexually transmitted infections during pregnancy and postdelivery in KwaZulu Natal, South Africa. Sex Transm Dis. 2015;42:43–7. https://doi.org/10.1097/OLQ.0000000000000219
41. Pappas PG, Kauffman CA, Andes D, Benjamin DK Jr, Calandra TF, Edwards JE Jr, et al.; Infectious Diseases Society of America. Clinical practice guidelines for the management of candidiasis: 2009 update by the Infectious Diseases Society of America. Clin Infect Dis. 2009;48:503–35. https://doi.org/10.1086/596757
42. Klufio CA, Amoa AB, Delamare O, Hombhanje M, Kariwiga G, Igo J. Prevalence of vaginal infections with bacterial vaginosis, *Trichomonas vaginalis* and *Candida albicans* among pregnant women at the Port Moresby General Hospital Antenatal Clinic. P N G Med J. 1995;38:163–71.
43. Sobel JD. Vulvovaginal candidosis. Lancet. 2007;369:1961–71. https://doi.org/10.1016/S0140-6736(07)60917-9
44. Lavu EK, Johnson K, Banamu J, Pandey S, Carter R, Coulter C, et al. Drug-resistant tuberculosis diagnosis since Xpert MTB/RIF introduction in Papua New Guinea, 2012–2017. Public Health Action. 2019;9:S12–8. https://doi.org/10.5588/pha.19.0005
45. Papua New Guinea National Department of Health. Sector performance annual review. Port Moresby (Papua New Guinea): Ministry of Health; 2018.
46. Papua New Guinea National Department of Health. Sector performance annual review. Port Moresby (Papua New Guinea): Ministry of Health; 2016.
47. Mitjà O, Marks M, Konan DJP, Ayelo G, Gonzalez-Beiras C, Boua B, et al. Global epidemiology of yaws: a systematic review. Lancet Glob Health. 2015;3:e324–31. https://doi.org/10.1016/S2214-109X(15)00011-X
48. Mitjà O, Godornes C, Houinei W, Kapa A, Paru R, Abel H, et al. Re-emergence of yaws after single mass azithromycin treatment followed by targeted treatment: a longitudinal study. Lancet. 2018;391:1599–607. https://doi.org/10.1016/S0140-6736(18)30204-6
49. United Nations. SDG indicators: global indicator framework for the Sustainable Development Goals and targets of the 2030 Agenda for Sustainable Development. 2021 [cited 2021 Jan 14]. https://unstats.un.org/sdgs/indicators/indicators-list

Address for correspondence: Michelle Scoullar or James Beeson, Burnet Institute, 85 Commercial Road, Melbourne, VIC 3004, Australia; email: michelle.scoullar@burnet.edu.au or beeson@burnet.edu.au

Local and Travel-Associated Transmission of Tuberculosis at Central Western Border of Brazil, 2014–2017

Katharine S. Walter,[1] Mariana Bento Tatara,[1] Kesia Esther da Silva, Flora Martinez Figueira Moreira, Paulo Cesar Pereira dos Santos, Dândrea Driely de Melo Ferrari, Eunice Atsuko Cunha, Jason R. Andrews,[2] Julio Croda[2]

International migrants are at heightened risk for tuberculosis (TB) disease. Intensified incarceration at international borders may compound population-wide TB risk. However, few studies have investigated the contributions of migration, local transmission, or prisons in driving incident TB at international borders. We conducted prospective population-based genomic surveillance in 3 cities along Brazil's central western border from 2014–2017. Although most isolates (89/132; 67%) fell within genomic transmission clusters, genetically unique isolates disproportionately occurred among participants with recent international travel (17/42; 40.5%), suggesting that both local transmission and migration contribute to incident TB. Isolates from 40 participants with and 76 without an incarceration history clustered together throughout a maximum-likelihood phylogeny, indicating the close interrelatedness of prison and community epidemics. Our findings highlight the need for ongoing surveillance to control continued introductions of TB and reduce the disproportionate burden of TB in prisons at Brazil's international borders.

The global expansion and local spread of tuberculosis (TB) have been shaped by patterns of human migration (*1*–*4*). The 258 million international migrants who live outside their country of birth are frequently put at high risk for TB disease and death because of the many health risks associated with migration including limited access to healthcare (*5*,*6*). Further, in countries with low- or medium-incidence of TB, a substantial proportion of TB is frequently found among recent immigrants (*7*,*8*). Understanding the contribution of local transmission and importation of *Mycobacterium tuberculosis* acquired elsewhere to incident TB cases can inform public health responses. However, few studies have explored the drivers of incident TB along international borders.

Brazil's national borders, settings characterized by frequent population movement and often overburdened health systems, have higher TB incidence than do nonborder areas (*9*–*11*). In Mato Grosso do Sul state in the Central West region of Brazil, TB notification rates, mortality rates, and rates of treatment abandonment are higher in counties at the borders with Bolivia and Paraguay, compared with counties in the state's interior (*11*). Similarly, rates of drug resistance and multidrug resistance are higher at the state's border than elsewhere in the state (*12*). However, the drivers of the increased incidence of TB here remain unknown. The long and variable latency period of TB makes it difficult to identify where transmission occurred.

To reduce the burden of local transmission, identifying congregate settings that play a disproportionate role in transmission is an urgent priority. TB notification rates have rapidly increased within prisons in Brazil (*13*), and TB is increasingly concentrated among incarcerated populations. In Mato Grosso do Sul, the state with the highest incarceration rate in Brazil (618/100,000 population) (*14*), 28.9% of notified TB

Author affiliations: Stanford University School of Medicine, Stanford, California, USA (K.S. Walter, K.E. da Silva, J.R. Andrews); Federal University of Grande Dourados, Dourados, Brazil (M.B. Tatara, F.M.F. Moreira, P.C.P. dos Santos, D.D. de Melo Ferrari); Central Laboratory of Public Health, Campo Grande, Brazil (E.A. Cunha); Federal University of Mato Grosso do Sul, Campo Grande, Brazil (J. Croda); Oswaldo Cruz Foundation, Mato Grosso do Sul, Brazil (J. Croda); Yale School of Public Health, New Haven, Connecticut, USA (J. Croda)

DOI: https://doi.org/10.3201/eid2703.203839

[1]These authors contributed equally to this article.

[2]These authors contributed equally to this article.

cases occurred among incarcerated persons in 2017. Prisons are not isolated institutions, and frequent movement of persons inside and outside prisons means that the heightened TB risk created by prison environments may extend to nearby communities (*15*). Furthermore, prisons are frequently high-transmission environments for drug-resistant TB (*16*,*17*). Although extremely drug-resistant TB (XDR TB) is thus far less prevalent in prisons in Brazil than those in Eastern Europe, pre-XDR TB has been associated with prisons in the southern state of Rio Grande do Sul, Brazil (*18*). Whether prisons similarly amplify drug-resistant TB in border cities is not known.

To investigate the drivers of TB transmission along Brazil's borders, we conducted a prospective genomic epidemiology study of *M. tuberculosis* in the 3 largest international border cities in Mato Grosso do Sul, Brazil. We assessed the phylogenetic structure and predicted transmission clusters to characterize the contribution of local transmission and migration-associated importation to incident TB cases and the role of prisons in driving local transmission.

Methods

Study Population and Data Collection

We conducted a population-based prospective study of newly diagnosed and retreated pulmonary TB cases in 3 cities at Brazil's borders with Paraguay and Bolivia during January 2014–April 2017. Patients with clinical suspicion of TB sought care at primary care providers or hospitals in Ponta Porã, Corumbá, and Ladário, Brazil. Diagnostic tests were done at Hospital Regional Dr. José de Simone Neto in Ponta Porã and the Laboratório Municipal de Corumbá, a public health diagnostic laboratory. Patients with nontuberculous mycobacteria or without positive cultures for *M. tuberculosis* were excluded. There was no incentive for study participation. After a positive culture, a team of researchers carried out a home or prison visit to recruit participants and administer the study questionnaire. Participants answered structured questions about their birthplace; residential address and residential history; previous history of TB diagnosis, treatment, and treatment outcomes; potential contact with patients who had pulmonary TB; incarceration history (incarcerated at the time of diagnosis, formerly incarcerated, any contact with those incarcerated, or no contact with incarcerated persons); and travel history. Recent immigrants were defined as participants with residency in Brazil for <2 years; recent travel was defined as international travel of any duration in the previous 5 years. We obtained additional sociodemographic and clinical data from the National Reporting System on Notifiable Diseases (SINAN). We stored and managed data in an electronic database (REDCap, https://projectredcap.org). We used a 3-sample proportion test to determine whether study participants were representative of all notified TB cases with respect to incarceration status reported in SINAN; we compared the proportion incarcerated, not incarcerated, and with no information about incarceration status at the time of TB notification among study participants and all notified TB cases. We were not able to do a similar comparison for immigration history or recent travel, which were collected in questionnaires.

All participants provided written consent. We obtained approval from the Research Ethics Committee of the Federal University of Grande Dourados (no. CAE 12676613.3.1001.5160) and Stanford University Institutional Review Board (IRB-40285).

Laboratory Diagnosis and Drug Susceptibility Testing

All sputum specimens collected in the participating laboratories were examined by microscopy or GeneXpert MTB/RIF (Cepheid, https://www.cepheid.com), processed with sodium hydroxide (NaOH), and inoculated in Ogawa-Kudoh culture medium. We incubated cultures at 37°C for ≤8 weeks and checked weekly for visible colonies at the participating laboratories. We determined microbial species using the MPT64 protein detection-based immunochromatographic rapid test (SD Bioline Kit; Standard Diagnostics, Inc., (http://www.standardia.com). We performed phenotypic susceptibility testing of *M. tuberculosis* isolates using the BACTEC MGIT 960 system (Becton Dickinson, https://www.bd.com)

Whole-Genome Sequencing

We extracted DNA from cultured isolates with the manual CTAB (cetyl trimethylammonium bromide) method and sequenced the whole genome on an Illumina NextSeq (2 × 151-bp) (https://illumina.com). Sequence data are available on the Sequence Read Archive (accession no. PRJNA671770). We trimmed low-quality bases (Phred-scaled base quality <20) and removed adapters with Trim Galore (stringency = 3) (*19*). We used CutAdapt to further filter reads (–nextseq-trim = 20 – minimum-length = 20 – pair-filter = any) (*20*). To exclude potential contamination, we used Kraken2 (*21*) to taxonomically classify reads and removed reads that were not assigned to the *Mycobacterium* genus or that were assigned to a *Mycobacterium* species other than *M. tuberculosis*.

We applied variant calling methods closely following those described in Menardo et al. (*22*) to be consistent with the methods used for molecular clock estimation. We mapped reads with bwa version 0.7.15 (*23*) (bwa mem) to the H37Rv reference genome (NCBI accession no. NC_000962.3) and performed local read realignment with the RealignerTargetCreator and IndelRealigner modules of GATK version 3.8. We created read pileups with Samtools version 1.9 and called variants for individual samples with varscan version 2.4.4. As described by Menardo et al (*22*), we called variants at positions with a minimum mapping quality of 20; minimum base quality of 20; minimum read depth of 7×; minimum percentage of reads supporting the call 90%; and ≤90%, or <10% of reads supporting a call in the same orientation (varscan strand bias filter).

We excluded single-nucleotide polymorphisms (SNPs) in previously defined repetitive regions (PPE and PE-PGRS genes, phages, insertion sequences, and repeats longer than 50 bp) (*24*). We excluded all isolates with mean coverage <15× and isolates with >50% of SNPs failing the strand bias filter, and genomes with >50% of SNPs that had a variant allele frequency of 10%–90%. We also excluded isolates that were assigned to multiple lineages with TBProfiler version 2.8.6 (*25*). We measured drug-resistance associated mutations with MykrobePredict version 0.8.0 (*26*), using the 201901 database of genomic predictors of resistance (*27*). We identified lineage with TBProfiler version 2.8.6 (*25*).

Phylogenetic and Bayesian Evolutionary Analysis

We constructed full-length consensus sequences from VCF files and used SNP sites to extract a multiple alignment of internal variant sites (*28*). We used the R package ape version 5.4 to measure the number of pairwise site differences between samples (*29*). We fit maximum likelihood trees with RAxML-ng 0.9.0 (*30*). We used a general time-reversible substitution model and a Stamatakis ascertainment bias correction for invariant sites in our alignment. We divided the number of invariant sites by 1,000 to avoid issues created by small branch lengths. We defined nucleotide stationary frequencies as frequencies in the reference genome. We clustered isolates using a common 12-SNP threshold (*31*) for relatedness of isolates from epidemiologically related hosts. We constructed haplotype networks with the R package pegas version 0.13 (*32*).

We fit a Bayesian tree to the sequences from the multidrug resistance (MDR)-associated transmission cluster with BEAST 2.6.2 (*33*). We applied a strict clock and constant coalescent population size model and used TB notification dates to calibrate tips. We used an HKY substitution rate model and estimated base frequencies. Because it would not be possible to estimate substitution rates from a small tree, we specified a narrow log-normal prior distribution on substitution rate (mean −16.1, SD 0.16), consistent with previous estimates of *M. tuberculosis* lineage 4 substitution rate estimates (mean 5.8×10^{-8}, SD 2.0×10^{-8}) (*22*). We ran sampling chains for 100 million iterations or until effective sample size estimates were >200 (Tracer version 1.7.1 [*34*]), indicating good convergence, and discarded 10% of samples as burn-in. We corrected for ascertainment bias by specifying the number of invariant sites in the alignment.

Results

Study Population

A total of 400 patients had notified TB in 3 cities at Brazil's central western border with Paraguay and Bolivia, Ponta Porã, Corumbá, and Ladário, during January 2014–April 2017 (Figure 1). Of these, 243 were cultured and 215 were culture positive. We enrolled 142 participants, and we generated high-quality sequences for 132 (61.4% of culture-positive notifications). Twenty-seven percent of participants reported international travel within the past 5 years (38/142). Fifty-one percent (74/142) of the study population did not have an incarceration history; 18.8% (27/142) were formerly incarcerated; 9.0% were incarcerated at the time of notification (13/142); 7.6% (11/142) reported contact with incarcerated population; and 13.2% (19/142) did not provide information about incarceration history. The proportion of study participants with an incarceration history did not differ significantly from that of the population with notified TB during the study period (p = 0.1585, as determined by 3-sample test for equality of proportions) (Table).

All of the 132 whole genome sequences were assigned to the European-American lineage and specifically to sublineages 4.1 (47), 4.3 (71), 4.4 (9), 4.8 (3), and 4.9 (2) with TBProfiler (*25*). Genomic (*19*) and phenotypic predictions of drug resistance were largely concordant: >93% concordance for ethambutol, isoniazid, and rifampin and 75% for streptomycin. For clarity, we refer to the genomic resistance predictions, for which we had information about additional drugs. Whereas most samples (80.3%; 106/132) were susceptible to all drugs, the remaining samples were resistant to ≥1 drug. A total of 22 (16.7%) isolates were isoniazid resistant, and 3 isolates (2.2%) were multidrug resistant, resistant to both isoniazid and rifampin. Five of the 14 isoniazid monoresistant case-

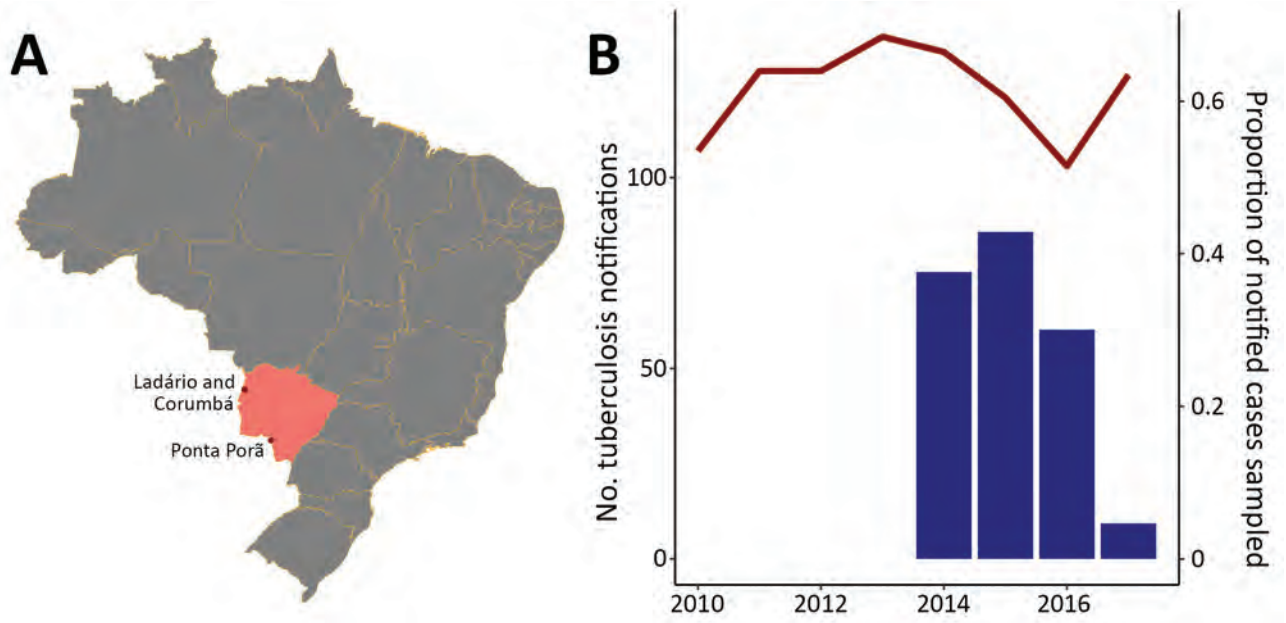

Figure 1. Tuberculosis case notifications in border cities in Mato Grosso do Sul state, Brazil. A) Location of Mato Grosso do Sul state (pink); dots indicate the 3 largest border cities, Ponta Porã, Corumbá, and Ladário, which is surrounded by Corumbá. B) Tuberculosis notifications in the 3 border cities reported in the state tuberculosis registry, SINAN, from 2010–2018 (red line), and the proportion of yearly notified cases sampled (blue bars) in this study, January 2014–April 2017.

patients and 3 of the 5 isolates resistant to both isoniazid and streptomycin had been previously treated; the 3 MDR isolates were from newly notified cases.

Phylogenetic Structure

A maximum-likelihood tree constructed from a multiple alignment of 6,590 SNPs shows a pattern of extensive co-circulating *M. tuberculosis* diversity with several genetically distinct clades of closely related isolates (Figure 2). Isolates from patients with an incarceration history (incarcerated at the time of diagnosis or formerly incarcerated) are dispersed throughout the tree and do not form a monophyletic clade. Neither do isolates from community members reporting no incarceration history, indicating a lack of distinct epidemics within and outside prisons. Four isolates were from recent immigrants to Mato Grosso do Sul state; these isolates were similarly distributed throughout the tree and differed by 165–274 SNPs.

We observed evidence of limited geographic structure. Isolates from Ponta Porã often form monophyletic clades dispersed throughout isolates sampled from the other 2 cities, indicating that both local transmission and between-city migration contribute to the spread of *M. tuberculosis* strains (Figure 2).

Transmission Clusters

To investigate potential recent transmission, we applied a commonly used 12-SNP threshold (*31*) to genetically cluster isolates. We identified 20 clusters, including 89 isolates, and 43 unique isolates. We predicted that if prison and community-associated epidemics were distinct, isolates from the community would be most closely related to and cluster with other isolates from the community. Conversely, if transmission frequently occurred between incarcerated and nonincarcerated persons, we would expect no clear genetic differentiation between isolates from the community and prisons. Of the 20 clusters, 9 included participants both with and without a reported incarceration history, 10 included only participants with no reported incarceration history, and 1 included only persons who were currently or formerly incarcerated (Figure 3).

To test for assortative clustering between participants with an incarceration history and without an incarceration history, under which participants disproportionately cluster with others with the same incarceration status, we applied a permutation test. We randomly reassigned reported incarceration histories to the observed clusters 1,000 times, holding the number and size of clusters constant. The observed number of clusters containing members with and without an incarceration history does not significantly differ from clustering under proportionate, or random, mixing ($p = 0.19$). Similarly, the observed number of clusters including only members currently or formerly incarcerated does not differ from what would

be expected under proportionate mixing (p = 0.76). The observed patterns of clustering indicate that transmission networks inside and outside prisons are closely related.

To further investigate genetic structure among sampled isolates, we identified the most closely related isolate to each study isolate, including multiple isolates when there were multiple nearest genetic neighbors. Many isolates from participants reporting no incarceration history were most closely related to isolates from participants who were currently or previously incarcerated (15/62; 24.2%) or participants reporting contact with those incarcerated (7/62; 11.3%) (Figure 3). Similarly, isolates from participants with an incarceration history were most closely related to isolates from participants reporting no incarceration history (18/38; 47.4%). The close relatedness between many isolates from participants within and outside prisons again suggests potential transmission between those with an incarceration history and those outside of prison. TB transmission rates are elevated in prisons compared with rates outside of prisons (*13*,*35*); although we cannot infer the direction of transmission from genomic clusters alone, the close interrelatedness of prison and community epidemics indicates that prison epidemics can affect the community.

Patients with a recent history of travel, defined as travel within the previous 5 years, were significantly more likely to be infected with an unclustered or unique isolate (17/36) than patients with no history of travel (25/92) (p = 0.03 by Fisher exact test; odds ratio = 2.38), potential evidence that they were infected outside of Brazil. These participants reported travel to Bolivia (9), Spain (1), Paraguay (5), Paraguay and Argentina (1) and Paraguay and Bolivia (1). All 4 isolates from recent immigrants to Brazil were unique and fell outside of predicted transmission clusters; again, possibly indicating they were infected outside of Brazil. However, limited sampling constrains our ability to predict whether genetically unique isolates represent imported lineages or locally circulating but unsampled lineages.

We then examined the distribution of drug resistance across predicted transmission clusters. The 22 isoniazid-resistant isolates occurred within 4 distinct transmission clusters; 1 isolate fell outside of the clusters, suggesting that isoniazid resistance has emerged or been introduced several times within the sampled isolates. The genetic clustering of resistance indicates that the majority of isoniazid resistance in this study was transmitted rather than acquired de novo. Similarly, streptomycin-resistant isolates occurred in 2 predicted transmission clusters, each including 1 person incarcerated at the time of TB diagnosis and a single unique isolate, which was evidence of transmitted resistance. In contrast, the 2 pyrazinamide-resistant isolates were unique.

MDR-Containing Cluster

The 3 MDR isolates fell within a single predicted transmission cluster of 14 isolates from a single city,

Table. Characteristics of study participants with notified tuberculosis, Central West region, Brazil, 2014–2017*

Characteristic	Participants, N = 142
City	
Corumbá	114/142 (80.3)
Ladário	3/142 (2.1)
Ponta Porã	25/142 (17.6)
Sex	
M	92/142 (64.8)
F	50/142 (35.2)
Age, y	
Median (IQR)	37 (27–53)
0–14	1/142 (0.7)
15–20	7/142 (4.9)
21–40	74/142 (52.1)
41–60	44/142 (31.0)
>60	16/142 (11.3)
Race, self-reported	
White	30/141 (21.3)
Mixed	66/141 (46.8)
Black	38/141 (26.9)
Indigenous	7/141 (5.0)
Asian	0/141 (0.0)
Education level, y	
<1	11/133 (8.3)
1–4	47/133 (35.3)
5–8	44/133 (33.1)
9–11	29/133 (21.8)
>11	2/133 (1.5)
Marital status, married	61/134 (45.5)
Monthly individual income <$100 US	104/119 (87.4)
Recipient of a cash transfer program	46/142 (32.4)
International travel within the past 5 y	38/142 (26.8)
Vulnerable population	
Currently incarcerated	16/142 (11.3)
Formerly incarcerated	27/142 (19.0)
Contact with someone with incarceration history	13/142 (9.1)
Homeless	3/142 (2.1)
Immigrant: <2 y resident in Brazil	5/133 (3.7)
Comorbidities	
Alcoholism	33/134 (24.6)
Diabetes	7/134 (5.2)
HIV	8/138 (5.8)
Mental illness	2/134 (1.5)
Hypertension	36/131 (27.5)
Renal failure	31/133 (23.3)
Hepatic failure	34/132 (25.7)
Smoking history	80/140 (57.1)
Drug use	35/134 (26.1)
TB history	
Previous TB	29/141 (20.6)
History of contact with TB case	69/132 (52.3)
BCG scar	104/133 (78.2)
Supervised treatment	41/135 (30.4)

*Values are no. (%) except as indicated. BCG, Bacillus Calmett-Guérin.

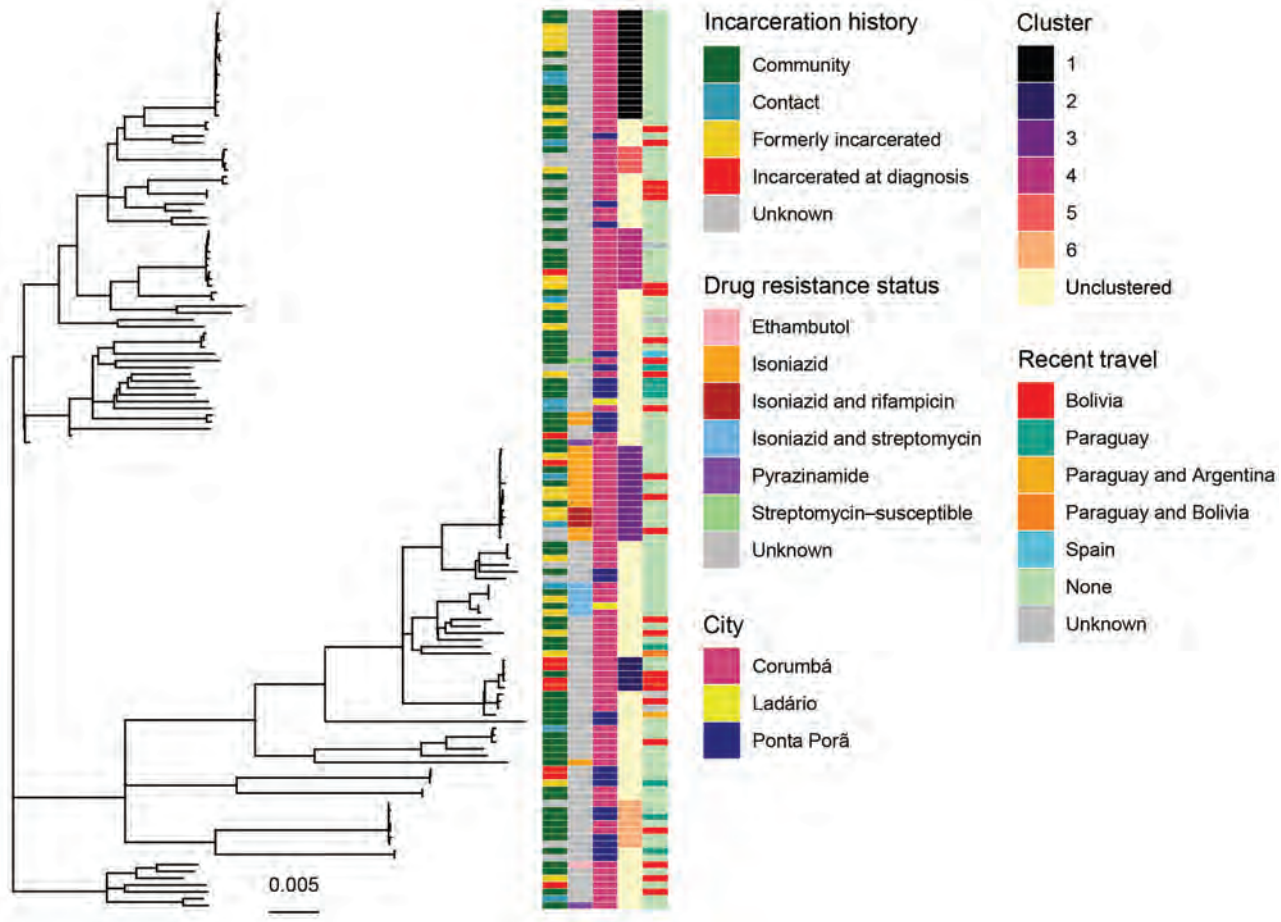

Figure 2. Unrooted maximum-likelihood phylogeny of 132 *Mycobacterium tuberculosis* isolates from Central West Brazil, 2014–2017, inferred from a multiple alignment of 6,590 single-nucleotide polymorphisms. From left, columns are colored by patient's incarceration history, drug-resistance status, city, predicted transmission cluster, and recent travel history. Incarceration history is defined by responses to the study questionnaire and incarceration information in the tuberculosis registry; community includes patients who have not been incarcerated at the time of tuberculosis notification; contact indicates any reported contact with incarcerated persons; formerly incarcerated includes patients who report incarceration prior to their tuberculosis notification; and incarcerated at diagnosis includes patients notified at time of incarceration. Transmission cluster membership is shown for clusters with ≥4 isolates; all other isolates are labeled as unclustered. Scale bar indicates substitutions per site.

Corumbá (Figure 3, cluster 3). All isolates within the cluster were isoniazid resistant and shared the *inhA* S94A mutation. In addition, the 3 MDR isolates all shared the *rpoB* S450L, rifampin-conferring mutation. Two of the MDR isolates occurred among persons who were previously incarcerated, and one was from a participant with an incarcerated family member. The mean pairwise distance between MDR isolates was 4 SNPs (range 3–5 SNPs), suggesting that MDR was transmitted (primary MDR) rather than acquired de novo.

We more closely examined the MDR-containing cluster by fitting a Bayesian timed tree (Figure 4). The most recent common ancestor (MRCA) of the cluster occurred in 2005 (95% CI 1998–2010). The MDR isolates fall within a well-supported monophyletic clade, with MRCA in 2011 (95% CI 2008–2014), evidence that MDR evolved a single time among sampled isolates and that MDR TB has been circulating locally for ≥6 years (the time between the MRCA of the MDR clade and the most recent date of sampling).

Discussion

In recent years, while TB incidence declined nationally in Brazil, TB notifications have increased in its Central West region border cities. We found evidence that both local transmission and travel-associated introductions contribute to incident cases. In addition, we found that many genomic clusters involved persons with and without an incarceration history,

evidence that prison and community epidemics of TB are closely interrelated in cities at Brazil's Central West border. During 2005–2017, the state's incarcerated population more than doubled (increasing from 8,273 to 16,634) (*36*). Dramatic rises in incarceration rates, combined with the elevated TB incidence rate within prisons, are likely contributing to ongoing local transmission at the border.

The prevalence of primary isoniazid resistance and MDR TB have increased across Brazil over the past 20 years (*37*). In this border setting, most drug-resistant isolates fell within predicted transmission clusters, indicating that interventions are needed to prevent the ongoing local transmission of drug-resistant strains. Whereas the prevalence of drug resistance in Central West Brazil has not yet reached the levels found in Rio de Janeiro, for example, we found evidence of ongoing local transmission of an isoniazid-resistant clone for >10 years. We additionally identified the emergence of an MDR *M. tuberculosis* clone associated with prisons that circulated locally for ≥6 years. Our findings highlight the critical need for the early detection of drug-resistant TB to prevent ongoing transmission.

Our investigation of TB transmission at Brazil's Central Western international borders has several limitations. In a setting characterized by frequent population movement, it is possible that many persons are not linked to healthcare, and TB may be undiagnosed, unnotified, or notified elsewhere. Further, more complete sampling among notified cases would enable a more complete portrait of transmission in border cities. For example, additional sampling could reveal that isolates we identified as genetically distinct do indeed fall within local transmission clusters; our estimates of the contribution of ongoing local transmission are likely conservative. In addition, selection bias could have been introduced if enrolled culture-positive participants were demographically different from the total population with TB. Although we did not find a difference in the proportion of incarcerated patients among study participants and all notified TB patients during the study period, we were unable to compare other characteristics such as recent travel history or migration history. It is possible that recent immigrants may have limited access to healthcare and therefore were undersampled; if so, the result would be underestimation of the role of travel-associated importation in incident TB. More complete information about study participants' residential and travel histories could inform inferences of where transmission occurred. By contextualizing the *M. tuberculosis* diversity observed within this study with a larger sample of genomes sampled from across Mato Grosso do Sul state, Paraguay, and Bolivia, we could better characterize the contributions of local transmission and importation of lineages into Brazil's border cities. Finally, because of incomplete epidemic sampling and within-host diversity, phylogenetic trees constructed from consensus genomes do not represent actual transmission histories, but instead, the evolutionary histories of sampled *M. tuberculosis*. Phylogenetic trees

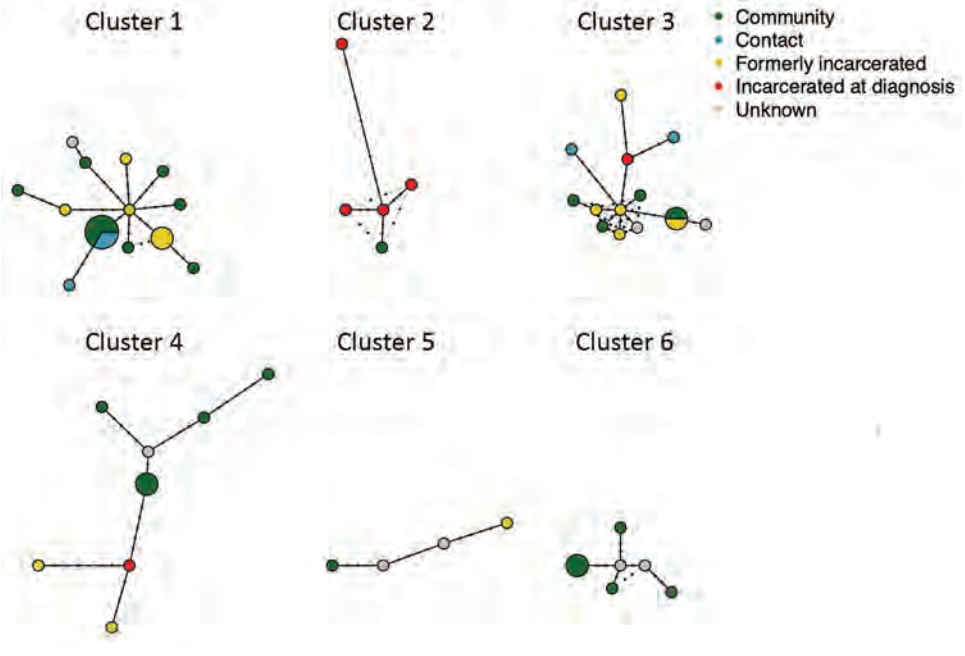

Figure 3. Haplotype networks of the 6 predicted tuberculosis transmission clusters with ≥4 members from Central West Brazil, 2014–2017. Nodes represent unique haplotypes and are scaled to size. Points along branches indicate single-nucleotide polymorphism distances between isolates. Node color indicates incarceration status at the time of diagnosis. Light gray lines indicate possible alternative links between haplotypes.

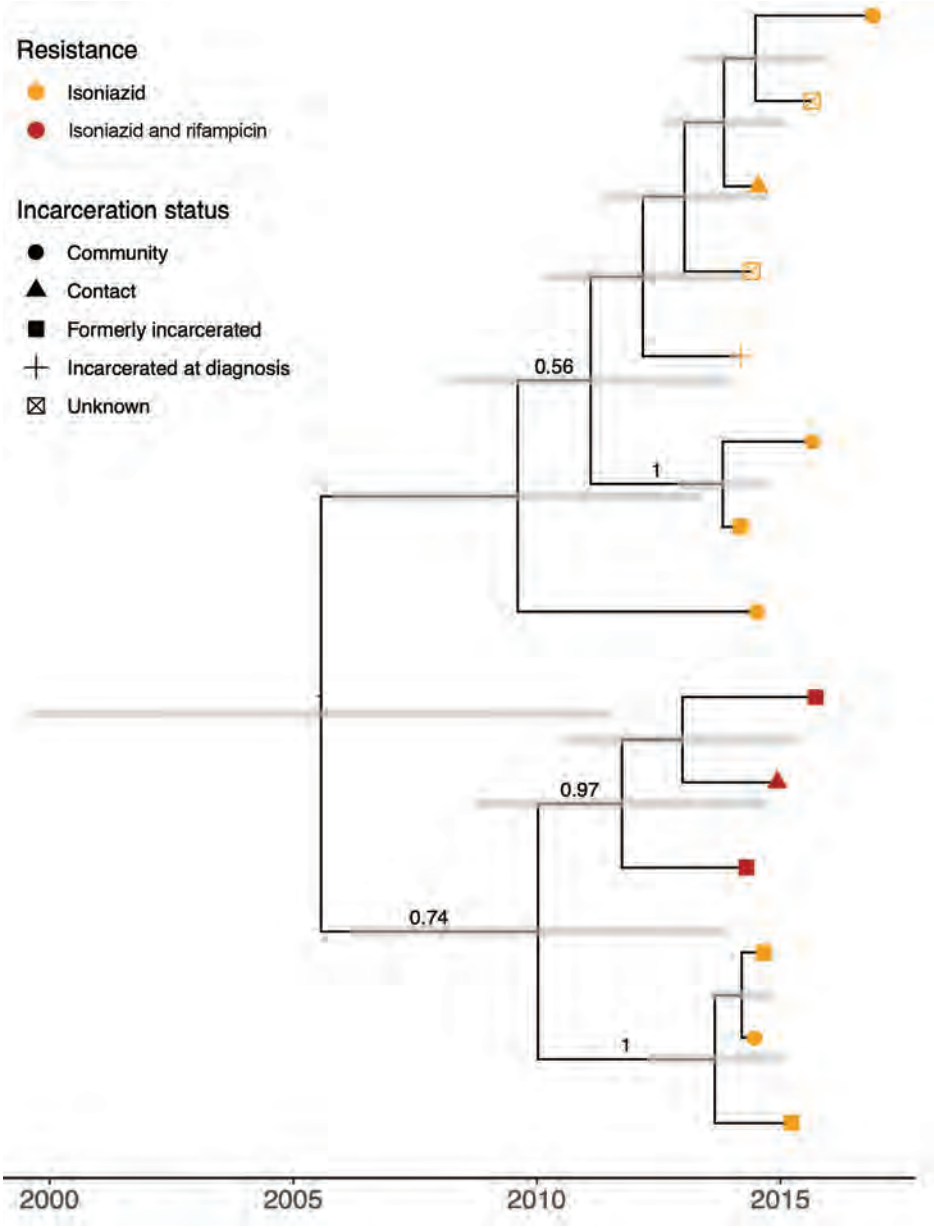

Figure 4. Bayesian timed tree of 14 isoniazid-resistant isolates that circulated for 11 years, from 2005 (95% CI 1998–2010) to November 2016, the most recent sampling date, in Central West region, Brazil. Tip points are colored by genotypic drug resistance; point shape indicates incarceration status. Gray error bars indicate 95% Bayesian highest posterior density intervals for node date. Clade posterior support values are shown on the middle of branches for clades with posterior support >0.5.

enable us to characterize genetic structure in our study sample yet cannot be used to directly assess the probability of individual transmission events nor to quantify the role of high-transmission environments in driving the local epidemic.

Our findings indicate that both local transmission and long-distance importation of TB drive local TB incidence in Brazil's Central Western border cities. Prison and community TB epidemics are interrelated, and prisons are associated with ongoing transmission of drug-resistant strains. The conditions for transmission and spread of TB in these border communities and congregate settings may undermine the broader national progress in TB control. Our study highlights the need for heightened surveillance and transmission-blocking interventions to prevent continued transmission of drug-sensitive and drug-resistant TB strains.

About the Authors

Dr. Walter is a postdoctoral fellow at Stanford University. Her research leverages pathogen evolution to investigate the transmission and geographic spread of infectious diseases with the goal of informing public health responses. Ms. Tatara is a biologist at the Federal University of Grande Dourados, Dourados, Brazil. Her research focuses on the genomic epidemiology of tuberculosis with the goal of informing public health.

References

1. Stucki D, Brites D, Jeljeli L, Coscolla M, Liu Q, Trauner A, et al. *Mycobacterium tuberculosis* lineage 4 comprises globally distributed and geographically restricted sublineages. Nat Genet. 2016;48:1535–43 https://doi.org/10.1038/ng.3704
2. Yang C, Lu L, Warren JL, Wu J, Jiang Q, Zuo T, et al. Internal migration and transmission dynamics of tuberculosis in Shanghai, China: an epidemiological, spatial, genomic analysis. Lancet Infect Dis. 2018;18:788–95. https://doi.org/10.1016/S1473-3099(18)30218-4
3. O'Neill MB, Shockey A, Zarley A, Aylward W, Eldholm V, Kitchen A, et al. Lineage-specific histories of *Mycobacterium tuberculosis* dispersal in Africa and Eurasia. Mol Ecol. 2019;28:3241–56. https://doi.org/10.1111/mec.15120
4. Ayabina D, Ronning JO, Alfsnes K, Debech N, Brynildsrud OB, Arnesen T, et al. Genome-based transmission modelling separates imported tuberculosis from recent transmission within an immigrant population. Microb Genomics. 2018;4:e000219. https://doi.org/10.1099/mgen.0.000219
5. Dhavan P, Dias HM, Creswell J, Weil D. An overview of tuberculosis and migration. Int J Tuberc Lung Dis. 2017;21:610–23.
6. Aldridge RW, Nellums LB, Bartlett S, Barr AL, Patel P, Burns R, et al. Global patterns of mortality in international migrants: a systematic review and meta-analysis. Lancet. 2018;392:2553–66. https://doi.org/10.1016/S0140-6736(18)32781-8
7. Menzies NA, Hill AN, Cohen T, Salomon JA. The impact of migration on tuberculosis in the United States. Int J Tuberc Lung Dis. 2018;22:1392–403. https://doi.org/10.5588/ijtld.17.0185
8. Lönnroth K, Mor Z, Erkens C, Bruchfeld J, Nathavitharana RR, van der Werf MJ, et al. Tuberculosis in migrants in low-incidence countries: epidemiology and intervention entry points. Int J Tuberc Lung Dis. 2017;21:624–36. https://doi.org/10.5588/ijtld.16.0845
9. Silva-Sobrinho RA, Ponce MAZ, Andrade RL, Beraldo AA, Pinto ÉSG, Scatena LM, et al. Effectiveness in the diagnosis of tuberculosis in Foz do Iguaçu, the triple-border area of Brazil, Paraguay and Argentina [in Portuguese]. Rev Esc Enferm USP. 2013;47:1373–80. https://doi.org/10.1590/S0080-623420130000600018
10. Souza DCS, Oliveira KS, Andrade RLP, Scatena LM, Silva-Sobrinho RA. Aspects related to the outcomes of the treatment, in international borders, of cases of tuberculosis as associated to comorbidities. Rev Gaúcha Enferm. 2019;40:e20190050. https://doi.org/10.1590/1983-1447.2019.20190050
11. Marques M, Ruffino-Netto A, Marques AMC, Andrade SM, Silva BA, Pontes ERJC. Pulmonary tuberculosis among residents of municipalities in Mato Grosso do Sul state, Brazil, bordering on Paraguay and Bolivia. Cad Saude Publica. 2014;30:2631–42. https://doi.org/10.1590/0102-311x00191513
12. Marques M, Cunha EAT, Evangelista MSN, Basta PC, Marques AMC, Croda J, et al. Antituberculosis-drug resistance in the border of Brazil with Paraguay and Bolivia. Rev Panam Salud Publica. 2017;41:e9. https://doi.org/10.26633/RPSP.2017.9
13. Bourdillon PM, Gonçalves CCM, Pelissari DM, Arakaki-Sanchez D, Ko AI, Croda J, et al. Increase in tuberculosis cases among prisoners, Brazil, 2009–2014. Emerg Infect Dis. 2017;23:496–9. https://doi.org/10.3201/eid2303.161006
14. Ministério da Justiça e Segurança Pública. Levantamento Nacional de informações penitenciárias. 2017 [cited 2021 Jan 6]. http://www.justica.gov.br/news/ha-726-712-pessoas-presas-no-brasil/relatorio_2016_junho.pdf
15. Mabud TS, de Lourdes Delgado Alves M, Ko AI, Basu S, Walter KS, Cohen T, et al. Evaluating strategies for control of tuberculosis in prisons and prevention of spillover into communities: an observational and modeling study from Brazil. PLoS Med. 2019;16:e1002737. http://dx.plos.org/10.1371/journal.pmed.1002737
16. Portaels F, Rigouts L, Bastian I. Addressing multidrug-resistant tuberculosis in penitentiary hospitals and in the general population of the former Soviet Union. Int J Tuberc Lung Dis. 1999;3:582–588
17. Zumla A, Grange JM. Multidrug-resistant tuberculosis—can the tide be turned? Lancet. 2001;1:199–202.
18. Salvato RS, Costa ERD, Reis AJ, Schiefelbein SH, Halon ML, Barcellos RB, et al. First insights into circulating XDR and pre-XDR *Mycobacterium tuberculosis* in southern Brazil. Infect Genet Evol. 2020;78:104127. https://doi.org/10.1016/j.meegid.2019.104127
19. Krueger F; Babraham Bioinformatics. Trim galore. Github. 2019 [cited 2021 Jan 6]. https://github.com/FelixKrueger/TrimGalore
20. Martin M. Cutadapt removes adapter sequences from high-throughput sequencing reads. EMBnet J. 2011;17:10–12. https://doi.org/10.14806/ej.17.1.200
21. Wood DE, Salzberg SL. Kraken: ultrafast metagenomic sequence classification using exact alignments. Genome Biol. 2014;15:R46. https://doi.org/10.1186/gb-2014-15-3-r46
22. Menardo F, Duchêne S, Brites D, Gagneux S. The molecular clock of *Mycobacterium tuberculosis*. PLoS Pathog. 2019;15:e1008067. https://doi.org/10.1371/journal.ppat.1008067
23. Li H, Durbin R. Fast and accurate short read alignment with Burrows-Wheeler transform. Bioinformatics. 2009;25:1754–60. https://doi.org/10.1093/bioinformatics/btp324
24. Brites D, Loiseau C, Menardo F, Borrell S, Boniotti MB, Warren R, et al. A new phylogenetic framework for the animal-adapted *Mycobacterium tuberculosis* complex. Front Microbiol. 2018;9:2820. https://doi.org/10.3389/fmicb.2018.02820
25. Phelan JE, O'Sullivan DM, Machado D, Ramos J, Oppong YEA, Campino S, et al. Integrating informatics tools and portable sequencing technology for rapid detection of resistance to anti-tuberculous drugs. Genome Med. 2019;11:41. https://doi.org/10.1186/s13073-019-0650-x
26. Bradley P, Gordon NC, Walker TM, Dunn L, Heys S, Huang B, et al. Rapid antibiotic-resistance predictions from genome sequence data for *Staphylococcus aureus* and *Mycobacterium tuberculosis*. Nat Commun. 2015;6:10063. https://doi.org/10.1038/ncomms10063
27. Allix-Béguec C, Arandjelovic I, Bi L, Beckert P, Bonnet M, Bradley P, et al.; CRyPTIC Consortium and the 100,000 Genomes Project. Prediction of susceptibility to first-line tuberculosis drugs by DNA sequencing. N Engl J Med. 2018;379:1403–15. PubMed https://doi.org/10.1056/NEJMoa1800474
28. Page AJ, Taylor B, Delaney AJ, Soares J, Seemann T, Keane JA, et al. SNP-sites: rapid efficient extraction of SNPs from multi-FASTA alignments. Microb Genom. 2016;2:e000056. https://doi.org/10.1099/mgen.0.000056
29. Paradis E, Schliep K. ape 5.0: an environment for modern phylogenetics and evolutionary analyses in R. Bioinformatics. 2019;35:526–8. https://doi.org/10.1093/bioinformatics/bty633
30. Kozlov AM, Darriba D, Flouri T, Morel B, Stamatakis A. RAxML-NG: A fast, scalable, and user-friendly tool for

maximum likelihood phylogenetic inference. Bioinformatics. 2019;35:4453–55. https://doi.org/10.1093/bioinformatics/btz305
31. Walker TM, Kohl TA, Omar SV, Hedge J, Del Ojo Elias C, Bradley P, et al.; Modernizing Medical Microbiology (MMM) Informatics Group. Whole-genome sequencing for prediction of *Mycobacterium tuberculosis* drug susceptibility and resistance: a retrospective cohort study. Lancet Infect Dis. 2015;15:1193–202. https://doi.org/10.1016/S1473-3099(15)00062-6
32. Paradis E. pegas: an R package for population genetics with an integrated-modular approach. Bioinformatics. 2010;26:419–20. https://doi.org/10.1093/bioinformatics/btp696
33. Bouckaert R, Vaughan TG, Barido-Sottani J, Duchêne S, Fourment M, Gavryushkina A, et al. BEAST 2.5: an advanced software platform for Bayesian evolutionary analysis. PLOS Comput Biol. 2019;15:e1006650. https://doi.org/10.1371/journal.pcbi.1006650
34. Rambaut A, Drummond AJ, Xie D, Baele G, Suchard MA. Posterior summarization in Bayesian phylogenetics using Tracer 1.7. Syst Biol. 2018;67:901–4 https://academic.oup.com/sysbio/article-abstract/67/5/901/4989127. https://doi.org/10.1093/sysbio/syy032
35. Santos AS, de Oliveira RD, Lemos EF, Lima F, Cohen T, Cords O, et al. Yield, efficiency, and costs of mass screening algorithms for tuberculosis in Brazilian prisons. Clin Infect Dis. 2020 [cited 2020 Oct 3]. https://doi.org/10.1093/cid/ciaa135
36. Ministério da Justiça. Sistema Integrado de Informações Penitenciárias—InfoPen. Brasília, BR; 2017 [cited 2021 Jan 22]. http://antigo.depen.gov.br/DEPEN/depen/sisdepen/infopen
37. Rabahi MF, Da Silva Júnior JLR, Conde MB. Evaluation of the impact that the changes in tuberculosis treatment implemented in Brazil in 2009 have had on disease control in the country. J Bras Pneumol. 2017;43:437–44. https://doi.org/10.1590/s1806-37562017000000004

Address for correspondence: Katharine S. Walter, Stanford University School of Medicine, 300 Pasteur Dr, L-134, Stanford, CA 94305 USA; kwalter@stanford.edu

EID Podcast:
Unusual Outbreak of Rift Valley Fever in Sudan

Rift Valley Fever is a devastating disease that can cause bleeding from the eyes and gums, blindness, and death. In 2019, an outbreak of this vectorborne disease erupted among people and animals in a politically volatile region of Sudan. This outbreak broke traditional patterns of Rift Valley Fever, sending scientists scrambling to figure out what was going on and how they could stop it.

In this EID podcast, Dr. Ayman Ahmed, a scientist at the University of Texas Medical Branch and a lecturer at the Institute of Endemic Diseases in Sudan, discusses the intersection of political unrest and public health.

Visit our website to listen: http://go.usa.gov/xAC5H

EMERGING INFECTIOUS DISEASES

Familial Clusters of Coronavirus Disease in 10 Prefectures, Japan, February–May 2020

Reiko Miyahara, Naho Tsuchiya, Ikkoh Yasuda, Yura K. Ko, Yuki Furuse, Eiichiro Sando, Shohei Nagata, Tadatsugu Imamura, Mayuko Saito, Konosuke Morimoto, Takeaki Imamura, Yugo Shobugawa, Hiroshi Nishiura, Motoi Suzuki, Hitoshi Oshitani

The overall coronavirus disease secondary attack rate (SAR) in family members was 19.0% in 10 prefectures of Japan during February 22–May 31, 2020. The SAR was lower for primary cases diagnosed early, within 2 days after symptom onset. The SAR of asymptomatic primary cases was 11.8%.

As of May 31, 2020, Japan had reported >16,800 confirmed coronavirus disease (COVID-19) cases and 890 related deaths. The cluster-based approach is one of the pillars of control measures in Japan (*1*). Sixty-one clusters were documented in healthcare facilities, restaurants, workplaces, and music venues during January–April 2020 (*2*). However, the transmission within households, one of the highest-risk settings, has not been fully investigated.

A meta-analysis of 43 studies showed that the pooled household secondary attack rate (SAR) was 18.1%, and heterogeneity ranged from 3.9% to 54.9% (*3*). Heterogeneity of SAR could occur because of variations in susceptibility to infection (*3*), variations in exposure (*4*), and variations in infectiousness. The primary cases of infectiousness defined by age, sex, and symptoms were less studied in the different settings. Furthermore, there were few reports of SAR among asymptomatic primary cases (*3*,*5*,*6*). Therefore, we estimated the SAR of COVID-19 and assessed the effects of age and sex of primary cases, symptoms of primary cases, and the time between diagnosis and symptom onset for primary cases on infectiousness in familial clusters.

Author affiliations: National Center for Global Health and Medicine, Tokyo, Japan (R. Miyahara); National Institute of Infectious Diseases, Tokyo (R. Miyahara, M. Suzuki); Tohoku University, Miyagi, Japan (N. Tsuchiya, Y.K. Ko, S. Nagata, T. Imamura, M. Saito, H. Oshitani); Nagasaki University, Nagasaki, Japan (I. Yasuda, E. Sando, K. Morimoto); Kyoto University, Kyoto, Japan (Y. Furuse, H. Nishiura); Japan International Cooperation Agency, Tokyo (T. Imamura); National Center for Child Health and Development, Tokyo (T. Imamura); Niigata University Graduate School of Medical and Dental Sciences, Niigata, Japan (Y. Shobugawa); Hokkaido University, Hokkaido, Japan (H. Nishiura)

DOI: https://doi.org/10.3201/eid2703.203882

The Study

Among 47 prefectures in Japan, 10 prefectures (Aomori, Akita, Gunma, Tochigi, Toyama, Shiga, Okayama, Kochi, Saga, and Kagoshima) (Appendix Figure 1, https://wwwnc.cdc.gov/EID/article/27/3/20-3882-App1.pdf) that showed a relatively low COVID-19 prevalence posted laboratory-confirmed cases and contact-tracing results on their websites (Appendix Table 1). In this study, we collected basic characteristics of cases from the reports issued during February 22–May 31, 2020, on those websites. The websites did not provide characteristics of uninfected close contacts or details of residence of family members. During the study period in Japan, doctors provided diagnoses of COVID-19 by using real-time PCR and reported cases to healthcare centers. These centers listed close contacts according to whether they spent >15 min in face-to-face contact and conducted follow-up by telephone for ≥14 days to monitor their symptoms.

Persons who had any COVID-19–related signs/symptoms, such as fever, cough, and fatigue, were categorized as having symptomatic cases. Asymptomatic cases were those without any symptoms at diagnosis. During this study period, all confirmed case-patients were hospitalized after they were given a diagnosis. Suspected case-patients and asymptomatic close contacts self-quarantined at home. Healthcare centers in 8 prefectures performed PCRs for close contacts regardless of their symptoms. One prefecture did not show the strategy of PCR testing for asymptomatic contacts, and 1 prefecture performed PCRs for symptomatic contacts, such as persons who had fever and respiratory symptoms.

In this study, we defined a primary case as the first case to show development of symptoms and to be diagnosed in a family or the first diagnosed asymptomatic case in a family who had an apparent history of contact with a nonfamilial COVID-19 case-patient. We defined secondary cases as laboratory-confirmed cases from the list of close family contacts of primary case-patients. Because websites provided only symptoms at diagnosis, we could not identify presymptomatic cases. We calculated SAR as the proportion of secondary cases of family close contacts among the total number of family close contacts and determined the SAR, risk ratio, and 95% CI, stratified by the characteristics of the primary case-patients. We compared the SAR before and after the declaration of the state of emergency on April 16. All statistical analyses were conducted by using Stata version 14.0 (StataCorp, https://www.stata.com).

During February 22–May 31, 2020, the 10 prefectures reported 306 primary cases and 775 family close contacts from 306 families. Eighty-seven primary cases were associated with 147 family secondary cases (Table 1; Appendix Figure 2). The overall SAR was 19.0%. Among 28 asymptomatic primary cases, 7 caused family clusters (Table 2; Appendix Table 2), and the SAR was 11.8%. Eight prefectures that tested for asymptomatic contacts showed an SAR that was 1.77 times higher than the SAR for 2 prefectures that used a nontesting strategy. The age-stratified SAR was higher for persons 60–69 years of age (36.5%) and persons <20 years of age (23.8%) than for persons 20–29 years of age (13.3%), persons 30–39 years of age (20.4%), persons 40–49 years of age (10.1%), and persons 50–59 years of age (16.1%) (Table 2).

With increasing time from symptom onset to diagnosis, the SARs in households increased from 11.6% (≥2 days) to 40.0% (≥14 days) (Table 2). When the data were stratified for analysis by the number of household contacts, 4 household contacts showed the highest SAR (25.7%). After a quarantine at home was requested from the government on April 16, the SAR increased from 17.4% to 21.0%, but the risk ratio did not reach statistical significance.

Conclusions

This family cluster analysis in the 10 prefectures of Japan showed that the overall SAR of the family cluster was estimated to be 19.0% in Japan. Meta-analysis from 43 household transmission studies estimated a SAR of 18.1% (*3*): 3.9% in Singapore (*7*), 4.6% in Taiwan (*8*), 10.3%–54.9% in China (*9*–*12*), and ≈30% in

Table 1. Characteristics of primary and secondary case-patients in households of familial clusters of coronavirus disease in 10 prefectures, Japan, February−May, 2020*

Characteristic	Primary	Secondary
No. case-patients	306	147
Sex		
F	152 (49.7)	82 (55.8)
M	153 (50.0)	64 (43.5)
Unknown	1 (0.3)	1 (0.7)
Age, y		
0–19	11 (3.5)	28 (19.0)
20–29	48 (15.7)	14 (9.5)
30–39	36 (11.8)	16 (10.9)
40–49	58 (19.0)	8 (5.4)
50–59	57 (18.6)	24 (16.3)
60–69	43 (14.1)	29 (19.7)
70–79	31 (10.1)	14 (9.5)
>80	22 (7.2)	14 (9.5)
Unknown	0 (0)	1 (0.7)
Contact history to COVID-19 nonfamilial cases		
No	146 (47.7)	147 (100)
Yes	159 (52)	0
Unknown	1 (0.3)	0
Symptom		
Symptomatic	271 (88.6)	103 (70.1)
Asymptomatic	28 (9.2)	39 (26.5)
Unknown	7 (2.3)	5 (3.4)
Median time from symptom onset to diagnosis, d (IQR)	6 (4–9)	5 (2.5–9)
Confirmed date of primary case		
On or before April 16	179 (58.5)	NA
After April 16	127 (41.5)	NA
Policy of testing for asymptomatic contacts		
No testing, 2 prefectures	54 (17.6)	16 (10.9)
Testing for asymptomatic contacts, 8 prefectures	252 (82.4)	131 (89.1)

*Values are no. (%) unless otherwise indicated. COVID-19, coronavirus disease; IQR, interquartile range; NA, not applicable.

Table 2. Characteristics of primary cases in households and SAR categorized for households of familial clusters of coronavirus disease in 10 prefectures, Japan, February−May, 2020*

Variable	No. (%) primary cases	No. family contacts	No. secondary infected cases	No. symptomatic secondary infected cases	No. asymptomatic secondary infected cases	SAR, % (95% CI)	Risk ratio (95% CI)
Overall	306 (100)	775	147	103	39	19.0 (16.3–21.9)	
Sex							
F	152 (49.7)	408	68	50	14	16.7 (13.2–20.6)	Referent
M	153 (50.0)	366	79	53	25	21.6 (17.5–26.2)	1.29 (0.97–1.73)
Unknown	1 (0.3)	1	1	0	1	NA	NA
Age, y							
<1–19	10 (3.6)	42	10	7	3	23.8 (12.1–39.5)	Referent
20–29	48 (15.7)	135	18	15	2	13.3 (8.1–20.3)	0.56 (0.28–1.12)
30–39	36 (11.8)	103	21	15	6	20.4 (13.1–29.5)	0.85 (0.44–1.66)
40–49	58 (19.0)	139	14	9	5	10.1 (5.6–16.3)	0.42 (0.20–0.88)
50–59	57 (18.6)	155	25	13	9	16.1 (10.7–22.9)	0.68 (0.35–1.30)
60–69	43 (14.1)	85	31	20	10	36.5 (26.3–47.6)	1.53 (0.83–2.81)
70–79	31 (10.1)	53	11	10	1	20.8 (10.8–34.1)	0.87 (0.41–1.85)
≥80	22 (7.2)	63	17	14	3	29.4 (23.2–36.2)	1.13 (0.58–2.23)
Contact history with nonfamilial COVID-19 cases							
No	146 (47.7)	357	91	64	24	25.4 (21.0–30.3)	1.90 (1.4–2.57)
Yes	159 (52.0)	417	56	39	15	13.4 (10.3–17.1)	Referent
Unknown	1 (0.3)	1	0	0	0	NA	NA
No. household contacts per primary case							
1	88 (28.8)	88	17	15	2	19.3 (11.7–29.1)	Referent
2	75 (24.5)	150	26	16	8	17.3 (11.6–24.4)	0.90 (0.52–1.56)
3	82 (26.8)	246	47	32	13	19.1 (14.4–24.6)	0.90 (0.60–1.63)
4	35 (11.4)	140	36	27	8	25.7 (18.7–33.8)	1.33 (0.80–2.22)
≥5	26 (8.5)	151	21	13	8	13.9 (8.8–20.5)	0.72 (0.40–1.29)
Symptoms							
Symptomatic	271 (88.6)	661	136	98	33	20.6 (17.6–23.9)	Referent
Asymptomatic	28 (9.2)	93	11	5	6	11.8 (6.1–20.2)	0.57 (0.32–1.02)
Unknown	7 (3.6)	21	0	0	0	NA	NA
Time from symptom onset to diagnosis, d, n = 271							
0–2	30 (11.1)	65	4	3	1	11.6 (5.1–21.6)	Referent
3–7	130 (48.0)	319	63	42	21	19.8 (15.5–24.5)	3.21 (1.21–8.51)
8–14	94 (34.7)	230	51	40	8	22.2 (17.0–28.1)	3.60 (1.35–9.6)
>14	17 (6.3)	45	18	9	9	40.0 (25.7–55.7)	6.50 (2.36–17.93)
Confirmed date of primary case							
Feb 22–Apr 16	179 (58.5)	448	78	57	16	17.4 (14.0–21.3)	Referent
Apr 17–May 31	127 (41.5)	328	69	46	23	21.0 (16.8–25.9)	1.21 (0.90–1.61)
Policy of testing for asymptomatic contacts							
No testing, 2 prefectures	54 (17.6)	138	16	12	1	11.6 (6.8–18.1)	Referent
Testing for asymptomatic contacts, 8 prefectures	252 (82.4)	637	131	91	38	20.6 (17.5–23.9)	1.77 (1.09–2.88)

*COVID-19, coronavirus disease; NA, not applicable; SAR, secondary attack rate.

the United States (*13*) and Norway (*14*). In addition, the SAR of asymptomatic primary cases was 11.8% in our study, which was higher than the 0%–4.4% reported in a limited number of previous studies (*6*,*15*). The SAR heterogeneity might have been dependent on the surveillance protocol for asymptomatic contacts. The studies in the United States (*13*) and Norway (*14*), which had high SARs, detected secondary cases by using serologic tests. Our study also indicated that 8 prefectures that tested for asymptomatic contacts showed a 1.8 times higher SAR than did 2 prefectures that tested only for symptomatic contacts. A low proportion of diagnoses of asymptomatic cases might underestimate the SAR.

We showed that SAR was higher for persons <1–19 years of age and ≥60 years of age than for other age groups. High infectivity for the younger age group (*6*) and the older age group (*4*) was reported from South Korea and China, as in our study, but most other studies did not show significant differences in SAR by age of primary case-patients (*9*,*13*). Age-dependent infectivity might be associated with household lifestyles, family structure, and clinical conditions (*9*). Meta-analysis showed that the sex of the primary case-patient was not associated with transmission (*5*).

If primary cases were detected ≤2 days of symptom onset, the SAR was lower than that for primary cases detected >2 days after symptom onset. This

finding was related to the low SAR for case-patients who had a contact history because they could receive PCRs, as close contacts did earlier, and might have had a short time of exposure to family members. Our results were concordant with previous studies showing an increased risk for transmission as the contact duration was prolonged (*4*), as well as the effect of quarantining index case-patients when symptoms were reported (*10*).

The first limitation of our study is that symptomatic cases diagnosed during the presymptomatic period might have been classified as asymptomatic cases. Second, the number of asymptomatic cases might have been underreported because of different testing protocols among prefectures. Third, we might have misclassified the primary cases if a coprimary case existed or the direction of transmission between asymptomatic cases and symptomatic cases was not clear.

In summary, our study results provide us with useful implications of the high SAR of asymptomatic primary case-patients and contacts with long exposure times to primary case-patients. Self-quarantine and rapid isolation of confirmed case-patients from households after symptom onset might be needed to reduce transmission in families.

Acknowledgments

We thank local health care centers and prefectural offices in Aomori, Akita, Gunma, Tochigi, Toyama, Shiga, Okayama, Kochi, Saga, and Kagoshima Prefectures for providing COVID-19 public health responses and making data publicly available on their websites.

This work was supported by the Ministry of Health, Labour, and Welfare CA Program (grant no. JPMH20CA2024).

About the Author

Dr. Miyahara is a project researcher at the National Center for Global Health and Medicine, Tokyo, Japan. Her primary research interest is the clinical and genetic epidemiology of infectious diseases.

References

1. Oshitani H. Experts Members of The National COVID-19 Cluster Taskforce at Ministry of Health, Labour and Welfare, Japan. Cluster-based approach to coronavirus disease 2019 (COVID-19) response in Japan, from February to April 2020. Jpn J Infect Dis. 2020;73:491–3. https://doi.org/10.7883/yoken.JJID.2020.363
2. Furuse Y, Sando E, Tsuchiya N, Miyahara R, Yasuda I, Ko YK, et al. Clusters of coronavirus disease in communities, Japan, January–April 2020. Emerg Infect Dis. 2020;26: 2176–9. https://doi.org/10.3201/eid2609.202272
3. Koh WC, Naing L, Chaw L, Rosledzana MA, Alikhan MF, Jamaludin SA, et al. What do we know about SARS-CoV-2 transmission? A systematic review and meta-analysis of the secondary attack rate and associated risk factors. PLoS One. 2020;15:e0240205. https://doi.org/10.1371/journal.pone.0240205
4. Xin H, Jiang F, Xue A, Liang J, Zhang J, Yang F, et al. Risk factors associated with occurrence of COVID-19 among household persons exposed to patients with confirmed COVID-19 in Qingdao Municipal, China. Transbound Emerg Dis. 2020;Jul 20 [Epub ahead of print]. https://doi.org/10.1111/tbed.13743
5. Madewell ZJ, Yang Y, Longini IM Jr, Halloran ME, Dean NE. Household transmission of SARS-CoV-2: a systematic review and meta-analysis. JAMA Netw Open. 2020;3:e2031756. https://doi.org/10.1001/jamanetworkopen.2020.31756
6. Park SY, Kim Y-M, Yi S, Lee S, Na B-J, Kim CB, et al. Coronavirus disease outbreak in call center, South Korea. Emerg Infect Dis. 2020;26:1666–70. https://doi.org/10.3201/eid2608.201274
7. Pung R, Park M, Cook AR, Lee VJ. Age-related risk of household transmission of COVID-19 in Singapore. I nfluenza Other Respir Viruses. 2020;Sep 29:10.1111/irv.12809. https://doi.org/10.1111/irv.12809
8. Cheng HY, Jian SW, Liu DP, Ng TC, Huang WT, Lin HH; Taiwan COVID-19 Outbreak Investigation Team. Contact tracing assessment of COVID-19 transmission dynamics in Taiwan and risk at different exposure periods before and after symptom onset. JAMA Intern Med. 2020;180:1156–63. https://doi.org/10.1001/jamainternmed.2020.2020
9. Jing Q-L, Liu M-J, Zhang Z-B, Fang L-Q, Yuan J, Zhang A-R, et al. Household secondary attack rate of COVID-19 and associated determinants in Guangzhou, China: a retrospective cohort study. Lancet Infect Dis. 2020;20:1141–50. https://doi.org/10.1016/S1473-3099(20)30471-0
10. Li W, Zhang B, Lu J, Liu S, Chang Z, Peng C, et al. The characteristics of household transmission of COVID-19. Clin Infect Dis. 2020;71:1943–6. https://doi.org/10.1093/cid/ciaa450
11. Luo L, Liu D, Liao X, Wu X, Jing Q, Zheng J, et al. Contact settings and risk for transmission in 3,410 close contacts of patients with COVID-19 in Guangzhou, China: a prospective cohort study. Ann Intern Med. 2020;173:879–87. https://doi.org/10.7326/M20-2671
12. Zhang J, Litvinova M, Liang Y, Wang Y, Wang W, Zhao S, et al. Changes in contact patterns shape the dynamics of the COVID-19 outbreak in China. Science. 2020;368:1481–6. https://doi.org/10.1126/science.abb8001
13. Lewis NM, Chu VT, Ye D, Conners EE, Gharpure R, Laws RL, et al. Household transmission of SARS-CoV-2 in the United States. Clin Infect Dis. 2020;ciaa1166. https://doi.org/10.1093/cid/ciaa1166
14. Cox RJ, Brokstad KA, Krammer F, Langeland N, Blomberg B, Kuwelker K, et al.; Bergen COVID-19 Research Group. Seroconversion in household members of COVID-19 outpatients. Lancet Infect Dis. 2020;S1473-3099(20)30466-7. https://doi.org/10.1016/S1473-3099(20)30466-7
15. Chaw L, Koh WC, Jamaludin SA, Naing L, Alikhan MF, Wong J. Analysis of SARS-CoV-2 transmission in different settings, Brunei. Emerg Infect Dis. 2020;26:2598–606. https://doi.org/10.3201/eid2611.202263

Address for correspondence: Reiko Miyahara, National Center for Global Health and Medicine, 1-21-1 Toyama, Shinjuku-ku, Tokyo, 162-8655 Japan; email: rmiyahara@ri.ncgm.go.jp

Lung Pathology of Mutually Exclusive Co-infection with SARS-CoV-2 and *Streptococcus pneumoniae*

Tetsuya Tsukamoto,[1] Noriko Nakajima,[1] Aki Sakurai,[1] Masayuki Nakajima, Eiko Sakurai, Yuko Sato, Kenta Takahashi, Takayuki Kanno, Michiko Kataoka, Harutaka Katano, Mitsunaga Iwata, Yohei Doi, Tadaki Suzuki

Postmortem lung pathology of a patient in Japan with severe acute respiratory syndrome coronavirus 2 infection showed diffuse alveolar damage as well as bronchopneumonia caused by *Streptococcus pneumoniae* infection. The distribution of each pathogen and the accompanying histopathology suggested the infections progressed in a mutually exclusive manner within the lung, resulting in fatal respiratory failure.

Coronavirus disease (COVID-19), caused by severe acute respiratory syndrome coronavirus 2 (SARS-CoV-2) (*1*), has claimed >1 million lives worldwide (*2*). Respiratory failure is the leading cause of death from COVID-19; however, the pathogenic process of the combined infection of SARS-CoV-2 and other respiratory pathogens is not fully understood.

We describe the clinical course and postmortem pathologic findings of a patient in Japan who died from SARS-CoV-2 and *Streptococcus pneumoniae* co-infection. Extensive histopathologic and molecular analyses of the lungs and other organs provided insights into the pathogenesis of severe lung disease caused by the co-infection.

Case Report

In March 2020, an 84-year-old man was brought to the emergency department at Fujita Health University Hospital (Toyoake, Japan) in cardiopulmonary arrest; his death was confirmed 20 minutes after he arrived at the hospital. He was found to have been in close contact with persons with confirmed SARS-CoV-2 cases at the adult day care center he attended and had been in self-isolation at home for 5 days before his death. He had been in generally good health until 8 days before his arrival at the hospital, when he developed sore throat and fatigue. Four days later, he developed a cough and lost his appetite. A whole-body computed tomography scan performed at the hospital showed bilateral diffuse consolidation with ground-glass opacities in the lungs and no gross abnormality in the other organs (Appendix Figure 1, https://wwwnc.cdc.gov/EID/article/27/3/20-4024-App1.pdf). SARS-CoV-2 infection was diagnosed after his death by real-time reverse transcription PCR (rRT-PCR) of a nasopharyngeal swab specimen. The family gave consent for an autopsy to be performed.

The autopsy was conducted 45 hours after the patient's death. Macroscopically, the lungs (left, 680 g; right, 800 g) were mostly colored red and consolidated with only remnant airspaces accompanied by a small pleural effusion. The heart (450 g) exhibited no macroscopic intravascular thrombosis. There were no remarkable changes in other organs, including the liver (1120 g), kidneys (left, 140 g; right, 100 g), and spleen (110 g). Microscopically, the epithelial cells of the trachea, bronchi, and bronchioles were mostly denuded, with submucosal inflammatory cell infiltration, edema, and congestion (Appendix Figure 2, panel A). Histological analysis of 42 lung sections (Figure 1) showed the acute exudative phase and early organizing phase of diffuse alveolar damage (DAD) with hyaline membrane formation (Figure 2, panels A, B; Appendix Figure 2, panel B). We observed edema with fibrin deposits,

Author affiliations: Fujita Health University School of Medicine, Toyoake, Japan (T. Tsukamoto, A. Sakurai, M. Nakajima, E. Sakurai, M. Iwata, Y. Doi); National Institute of Infectious Diseases, Tokyo, Japan (N. Nakajima, Y. Sato, K. Takahashi, T. Kanno, M. Kataoka, H. Katano, T. Suzuki)

DOI: https://doi.org/10.3201/eid2703.204024

[1]These authors contributed equally to this article.

desquamated alveolar epithelial cells, mononuclear cell infiltrates, and multinucleated syncytial cells in the alveolar air spaces (Appendix Figure 2, panel C), and various degrees of inflammatory cell infiltration and edema in the interstitium. In addition, we observed neutrophil infiltration in the alveolar spaces scattered throughout the lower lobes, suggestive of acute bronchopneumonia (Figure 2, panels A, C; Appendix Figure 2, panel D). We noted a limited number of gram-positive cocci in the intracellular and extracellular regions (Appendix Figure 2, panel E). Vascular congestion was present in several lung sections with prominent fibrin microthrombi in blood vessels of various sizes (Appendix Figure 2, panel F). We did not see either endotheliitis or vasculitis with fibrinoid necrosis.

We determined the copy numbers of SARS-CoV-2 RNA and human glyceraldehyde 3-phosphate dehydrogenase mRNA in formalin-fixed paraffin-embedded tissue specimens by rRT-PCR, as previously described (*3*). We detected moderate or higher copy numbers of SARS-CoV-2 RNA in all lung sections. The ratios of SARS-CoV-2 RNA to glyceraldehyde 3-phosphate dehydrogenase mRNA in the upper lobes were significantly greater than those in the lower lobes (Mann-Whitney test: right lung, $p<0.05$; left lung, $p<0.0001$) (Table; Appendix Figure 3, panel A). We screened the microbial DNA in the formalin-fixed paraffin-embedded lung specimens using a multimicrobial rRT-PCR system that simultaneously detects 68 bacterial species and 9 fungal species (*4*). This screening yielded a positive result for *S. pneumoniae*, which was confirmed by rRT-PCR (*5*). The ratio of *S. pneumoniae* DNA to β-actin DNA (*6*) in the lower lobes was significantly greater than that in the upper lobes (Mann-Whitney test: right lung, $p<0.005$; left lung, $p<0.0001$) (Table; Appendix Figure 3, panel B). *S. pneumoniae* DNA was not detected in several lung sections in the upper lobes and the extrapulmonary tissues except for the pharynx and trachea, suggesting absence of bacteremia.

We performed immunohistochemistry (IHC) using a rabbit polyclonal antibody against SARS-CoV-2 antigens (*7*). We detected a large number of viral antigen-positive cells in lung sections with high SARS-CoV-2 RNA scores (Figure 2, panel D; Appendix Figure 2, panels G, H). The distribution of SARS-CoV-2 spike RNA detected by in situ hybridization (*8*) was similar to that of the viral antigen (Appendix Figure 2, panel I). Double fluorescence staining for in situ hybridization and IHC detected both the viral RNA and viral antigen in the same cells (Appendix Figure 4, panels A–C). Double immunofluorescence staining revealed that SARS-CoV-2 antigens were present in epithelial membrane antigen–positive bronchiolar and

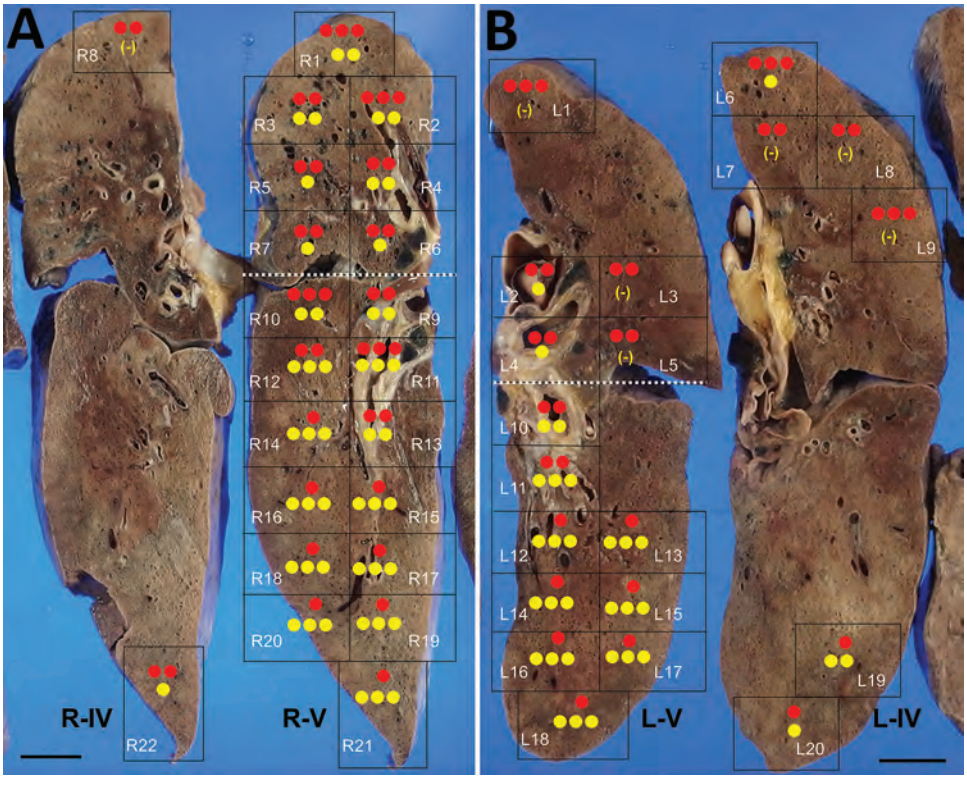

Figure 1. Molecular detection of SARS-CoV-2 and *Streptococcus pneumoniae* in the lungs of a patient in Japan co-infected with both pathogens. The 42 lung sections were analyzed and the amount of SARS-CoV-2 RNA and *S. pneumoniae* DNA in each section was evaluated. A) The right lung was cut into 6 (R–I to R–VI); B) the left lung was cut into 7 (L–I to L–VII) coronal slices, from ventral to dorsal. Twenty-two right sections (R1–R22) in R–IV and R–V and 20 left sections (L1–L20) in L–V and L–IV are shown in black boxes. The dotted white line is the boundary between the upper and lower lobes. The SARS-CoV-2 RNA score is indicated by the number of red circles and the *S. pneumoniae* DNA score is indicated by the number of yellow circles. (-) indicates results under the detection limit. Scale bars indicate 2 cm. SARS-CoV-2, severe acute respiratory syndrome coronavirus 2.

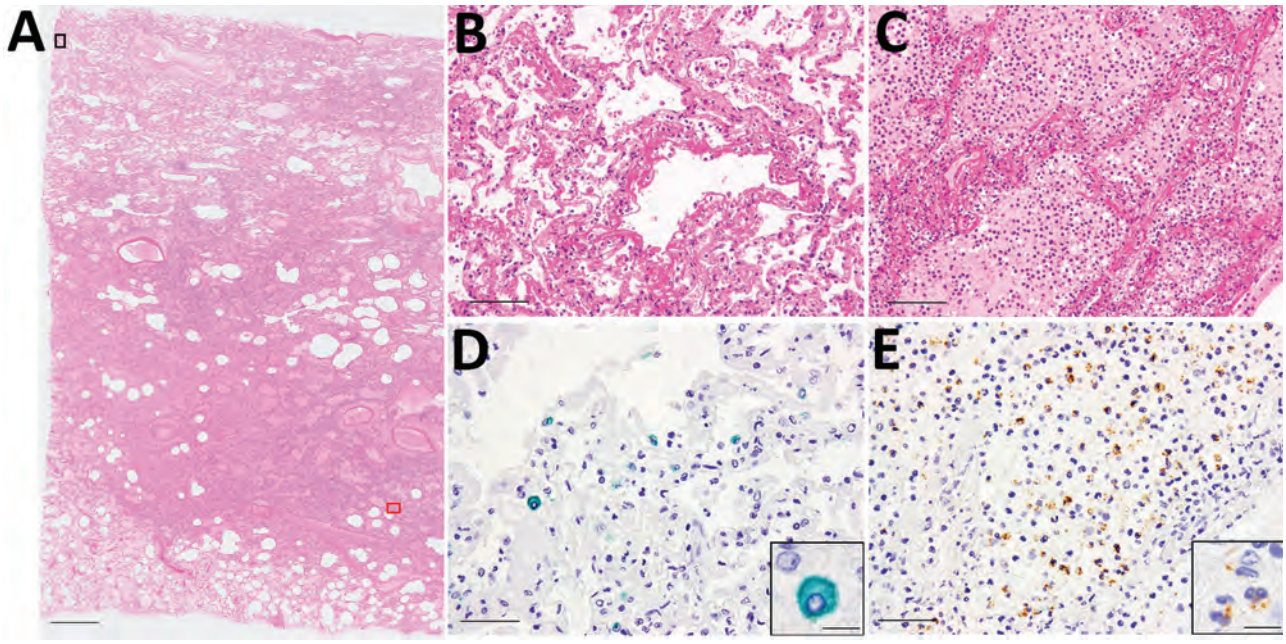

Figure 2. Microscopic findings of the lungs of a patient in Japan co-infected with SARS-CoV-2 and *Streptococcus pneumoniae*. A) Histopathology of lung section R12 (shown in Figure 1). Scale bar indicates 2 mm. B) Magnified image of the black square (top left) in panel A: exudative phase of diffuse alveolar damage (DAD) with hyaline membranes. Scale bar indicates 100 μm. C) Magnified image of the red square (bottom right) in panel A: edema and bronchopneumonia with massive infiltration of neutrophils in the alveolar spaces. Scale bar indicates 100 μm. D, E) Magnified images of the same areas of consecutive sections as B and C, respectively, showing SARS-CoV-2 antigen stained green (Vina green) and *S. pneumoniae* antigen stained brown (3,3′-diaminobenzidine) by enzyme-labeled double immunohistochemistry. The SARS-CoV-2 antigens were detected predominantly in the DAD area (D; scale bar indicates 50 μm). The *S. pneumoniae* antigens were detected predominantly in the bronchopneumonia area (E; scale bar indicates 50 μm). Insets show magnified images of the staining cells (scale bars indicate 10 μm).

alveolar epithelial cells and CD68-positive macrophages/monocytes (Appendix Figure 4, panels D–I). We found multiple fibrin microthrombi in several lung vessels, but we detected no viral antigen in CD34-positive vascular endothelial cells (data not shown). IHC using an antibody against *S. pneumoniae* spp. (NB100–64502; Novus Biologicals, https://www.novusbio.com) showed both intact streptococci and granular antigens staining in neutrophils, macrophages, or both, particularly in the lesion with bronchopneumonia (Figure 2, panel E).

Of note, the copy numbers of viral RNA and bacterial DNA in each lung section were found to be inversely correlated, suggesting that the viral and bacterial infections occurred in a mutually exclusive manner in the lung tissues (Figure 1; Appendix Figure 5). Enzyme-labeled double IHC detected only viral antigens in areas of DAD and only bacterial antigens in bronchopneumonia lesions, similar to the findings in the whole lungs (Figure 2, panels D, E). Although it is unknown whether SARS-CoV-2 infection preceded, coincided with, or followed *S. pneumoniae* infection, it can be assumed that the patient developed acute respiratory distress syndrome induced by COVID-19 pneumonia and had concomitant bronchopneumonia caused by *S. pneumoniae* infection.

We found no notable changes in the extrapulmonary tissues related to COVID-19, including thrombosis. Although low copy numbers of SARS-CoV-2 RNA were detected in the pharynx, trachea, and intestines, we detected no viral antigens.

Conclusions

The patient, who died on the eighth day of illness, had mostly acute-phase DAD with overwhelming viral infection, as demonstrated by detection of high titers of viral RNA and antigens in the lung sections. These results indicate a relatively early phase of SARS-CoV-2 infection, which implies that bacterial co-infection may have contributed to an abrupt deterioration of respiratory function in the patient. Bacterial co-infection of the respiratory tract has been well characterized in influenza, with a reported co-infection rate exceeding 30% in hospitalized patients (*9*,*10*). Co-infection with *S. pneumoniae* and *Staphylococcus aureus* has been linked to excess illness and death (*9*). In contrast, recent studies have suggested

that bacterial co-infection is relatively uncommon in patients with COVID-19, with a prevalence of 3.5% in patients who were newly admitted to the hospital (*11*,*12*). However, given the serious and potentially lethal complications resulting from bacterial infections, the possibility of co-infection with other microbial pathogens should be also considered in patients with COVID-19, especially in elderly patients with severe disease, and it is difficult to identify bacterial co-infection on computed tomography images alone after the development of acute respiratory distress syndrome (*13*).

In conclusion, in-depth postmortem examination revealed that SARS-CoV-2 and *S. pneumoniae* had differential intrapulmonary distribution in this patient, independently causing DAD and bronchopneumonia

Table. Quantification of SARS-CoV-2 RNA and *Streptococcus pneumoniae* DNA in 42 lung sections from a patient in Japan co-infecte with both pathogens*

Lung lobe	Lung section	SARS-CoV-2 RNA, copies/μL	GAPDH mRNA, copies/μL	SARS-CoV-2 RNA/GAPDH mRNA ratio	SARS-CoV-2 RNA score†	*S. pneumoniae* DNA, copies/μL	ACTB DNA, copies/μL	*S. pneumoniae* DNA/ACTB DNA ratio × 10^5	*S. pneumonia* DNA score
RUL	R1§	2.01×10^6	1.31×10^3	1,534	3	1.67×10^2	5.66×10^4	295	2
	R2	1.71×10^6	1.03×10^3	1,660	3	2.01×10^2	8.24×10^4	244	2
	R3	6.66×10^5	1.66×10^3	401	2	4.17×10^1	3.40×10^4	123	2
	R4	6.93×10^5	1.70×10^3	408	2	5.36×10^1	4.58×10^4	117	2
	R5	6.87×10^5	1.80×10^3	382	2	2.48×10^1	7.39×10^4	34	1
	R6	1.98×10^5	1.21×10^3	164	2	9.07×10^1	1.33×10^5	68	1
	R7	8.98×10^5	1.65×10^3	544	2	5.24×10^1	1.02×10^5	51	1
	R8	5.48×10^5	8.66×10^2	633	2	UDL	1.07×10^5	UDL	0
RLL	R9	7.50×10^5	8.82×10^2	850	2	2.10×10^2	7.33×10^4	286	2
	R10	1.71×10^6	1.31×10^3	1,305	3	4.50×10^2	1.02×10^5	441	2
	R11	1.15×10^6	1.08×10^3	1,065	3	8.94×10^2	6.72×10^4	1,330	3
	R12	1.39×10^5	8.85×10^2	157	2	4.70×10^3	6.33×10^4	7,425	3
	R13	3.45×10^5	9.42×10^2	366	2	9.44×10^1	8.59×10^4	110	2
	R14	6.62×10^3	5.55×10^2	12	1	5.37×10^3	6.98×10^4	7,693	3
	R15	1.85×10^4	9.14×10^2	20	1	1.74×10^3	9.09×10^4	1,914	3
	R16	1.40×10^4	8.20×10^2	17	1	4.14×10^3	1.03×10^5	4,019	3
	R17	2.92×10^4	8.58×10^2	34	1	2.67×10^3	6.54×10^4	4,083	3
	R18	1.93×10^4	8.04×10^2	24	1	3.18×10^3	8.22×10^4	3,869	3
	R19	3.05×10^4	6.46×10^2	47	1	2.56×10^3	6.00×10^4	4,267	3
	R20	5.16×10^4	6.81×10^2	76	1	2.92×10^3	5.92×10^4	4,932	3
	R21	1.50×10^4	5.82×10^2	26	1	3.18×10^3	8.53×10^4	3,728	3
	R22	5.27×10^5	5.88×10^2	896	2	2.12×10^1	4.57×10^4	46	1
LUL	L1	5.44×10^6	1.52×10^3	3,579	3	UDL	7.39×10^4	UDL	0
	L2	1.34×10^6	1.91×10^3	702	2	6.85×10^1	1.20×10^5	57	1
	L3	6.73×10^5	1.78×10^3	378	2	UDL	6.16×10^4	UDL	0
	L4	1.52×10^5	1.36×10^3	112	2	2.00×10^1	8.92×10^4	22	1
	L5	9.59×10^5	1.83×10^3	524	2	UDL	4.99×10^4	UDL	0
	L6	3.85×10^6	1.94×10^3	1,985	3	1.50×10^1	6.69×10^4	22	1
	L7	1.77×10^6	2.36×10^3	750	2	UDL	5.40×10^4	UDL	0
	L8	1.02×10^6	1.37×10^3	745	2	UDL	4.96×10^4	UDL	0
	L9	3.11×10^6	2.22×10^3	1,401	3	UDL	6.25×10^4	UDL	0
	L10	1.59×10^5	1.33×10^3	120	2	3.13×10^2	4.26×10^4	735	2
	L11	1.27×10^5	1.07×10^3	119	2	5.54×10^2	4.49×10^4	1,234	3
LLL	L12	3.80×10^4	8.48×10^2	45	1	6.42×10^3	1.12×10^5	5,732	3
	L13	2.16×10^4	7.91×10^2	27	1	5.91×10^3	8.87×10^4	6,663	3
	L14	4.87×10^4	8.73×10^2	56	1	2.85×10^3	7.76×10^4	3,673	3
	L15	4.65×10^4	1.22×10^3	38	1	4.08×10^3	6.36×10^4	6,415	3
	L16	2.86×10^4	8.88×10^2	32	1	5.68×10^3	6.80×10^4	8,353	3
	L17	3.42×10^4	9.42×10^2	36	1	3.58×10^3	6.45×10^4	5,550	3
	L18	3.89×10^4	9.47×10^2	41	1	4.64×10^3	6.87×10^4	6,754	3
	L19	4.25×10^3	5.81×10^2	7	1	5.82×10^2	1.02×10^5	571	2
	L20	1.56×10^4	8.09×10^2	19	1	6.10×10^1	9.11×10^4	67	1
	L20	1.56×10^4	8.09×10^2	19	1	6.10×10^1	9.11×10^4	67	1

*ACTB, β-actin; GAPDH, glyceraldehyde 3-phosphate dehydrogenase; LLL, left lower lobe; LUL, left upper lobe; RLL, right lower lobe; RUL, right upper lobe; SARS-CoV-2, severe acute respiratory syndrome coronavirus 2; UDL, under detection limit.
†SARS-CoV-2-RNA score is as follows: score 1, SARS-CoV-2 RNA/GAPDH mRNA ratio<100; score 2, 100–1,000; score 3, 1,000–10,000.
‡*S. pneumoniae* DNA score is as follows: score 1, *S. pneumoniae* DNA/ ACTB DNA ratio × 10^5 <100; score 2, 100–1,000; score 3, 1,000–10,000.
§Lung sections R1–R22 and L1–L20) are shown in Figure 1.

pathology. Patients with COVID-19 should be evaluated carefully for co-infection with other pathogens to fully understand the effect of co-infection on COVID-19 pathology.

Acknowledgments

We thank the patient's family for sharing their story and for allowing the data to be published. We also thank the staff of Fujita Health University Hospital for their dedication to patient care during the coronavirus pandemic.

This study was supported in part by grants-in-aid from the Japan Agency for Medical Research and Development to T.S. (grant nos. JP20fk0108104, JP19fk0108110, and JP20fk0108082), and N.N. (grant no. JP20fk0108082).

About the Author

Dr. Tsukamoto is a professor in the Department of Diagnostic Pathology, Fujita Health University School of Medicine, Toyoake, Aichi, Japan. His primary research interests include oncological and experimental pathology and artificial intelligence in diagnostic pathology.

References

1. Coronaviridae Study Group of the International Committee on Taxonomy of Viruses. The species *Severe acute respiratory syndrome-related coronavirus*: classifying 2019-nCoV and naming it SARS-CoV-2. Nat Microbiol. 2020;5:536–44. https://doi.org/10.1038/s41564-020-0695-z
2. World Health Organization. Coronavirus disease (COVID-19) dashboard; 2020 [cited 2020 Sep 11]. https://covid19.who.int
3. Adachi T, Chong JM, Nakajima N, Sano M, Yamazaki J, Miyamoto I, et al. Clinicopathologic and immunohistochemical findings from autopsy of patient with COVID-19, Japan. Emerg Infect Dis. 2020;26:2157–61. https://doi.org/10.3201/eid2609.201353
4. Fukumoto H, Sato Y, Hasegawa H, Saeki H, Katano H. Development of a new real-time PCR system for simultaneous detection of bacteria and fungi in pathological samples. Int J Clin Exp Pathol. 2015;8:15479–88.
5. Carvalho MGS, Tondella ML, McCaustland K, Weidlich L, McGee L, Mayer LW, et al. Evaluation and improvement of real-time PCR assays targeting *lytA*, *ply*, and *psaA* genes for detection of pneumococcal DNA. J Clin Microbiol. 2007;45:2460–6. https://doi.org/10.1128/JCM.02498-06
6. Kuramochi H, Hayashi K, Uchida K, Miyakura S, Shimizu D, Vallböhmer D, et al. Vascular endothelial growth factor messenger RNA expression level is preserved in liver metastases compared with corresponding primary colorectal cancer. Clin Cancer Res. 2006;12:29–33. https://doi.org/10.1158/1078-0432.CCR-05-1275
7. Fukushi S, Mizutani T, Saijo M, Matsuyama S, Miyajima N, Taguchi F, et al. Vesicular stomatitis virus pseudotyped with severe acute respiratory syndrome coronavirus spike protein. J Gen Virol. 2005;86:2269–74. https://doi.org/10.1099/vir.0.80955-0
8. Schaefer IM, Padera RF, Solomon IH, Kanjilal S, Hammer MM, Hornick JL, et al. In situ detection of SARS-CoV-2 in lungs and airways of patients with COVID-19. Mod Pathol. 2020;33:2104–14. https://doi.org/10.1038/s41379-020-0595-z
9. Chertow DS, Memoli MJ. Bacterial coinfection in influenza: a grand rounds review. JAMA. 2013;309:275–82. https://doi.org/10.1001/jama.2012.194139
10. Klein EY, Monteforte B, Gupta A, Jiang W, May L, Hsieh YH, et al. The frequency of influenza and bacterial coinfection: a systematic review and meta-analysis. Influenza Other Respir Viruses. 2016;10:394–403. https://doi.org/10.1111/irv.12398
11. Hughes S, Troise O, Donaldson H, Mughal N, Moore LSP. Bacterial and fungal coinfection among hospitalized patients with COVID-19: a retrospective cohort study in a UK secondary-care setting. Clin Microbiol Infect. 2020;26:1395–9. https://doi.org/10.1016/j.cmi.2020.06.025
12. Langford BJ, So M, Raybardhan S, Leung V, Westwood D, MacFadden DR, et al. Bacterial co-infection and secondary infection in patients with COVID-19: a living rapid review and meta-analysis. Clin Microbiol Infect. 2020;26:1622–9. https://doi.org/10.1016/j.cmi.2020.07.016
13. Zhou J, Liao X, Cao J, Ling G, Ding X, Long Q. Differential diagnosis between the coronavirus disease 2019 and *Streptococcus pneumoniae* pneumonia by thin-slice CT features. Clin Imaging. 2021;69:318–23. https://doi.org/10.1016/j.clinimag.2020.09.012

Address for correspondence: Tadaki Suzuki, Department of Pathology, National Institute of Infectious Diseases, 1-23-1, Toyama, Shinjuku-ku, Tokyo 162-8640, Japan; email: tksuzuki@nih.go.jp

COVID-19 Outbreak in a Large Penitentiary Complex, April–June 2020, Brazil

Fernando A. Gouvea-Reis, Patrícia D. Oliveira, Danniely C.S. Silva, Lairton S. Borja, Jadher Percio, Fábio S. Souza, Cássio Peterka, Claudia Feres, Janaína de Oliveira, Giselle Sodré, Wallace dos Santos, Camile de Moraes

An outbreak of coronavirus disease began in a large penitentiary complex in Brazil on April 1, 2020. By June 12, there were 1,057 confirmed cases among inmates and staff. Nine patients were hospitalized, and 3 died. Mean serial interval was ≈2.5 days; reproduction number range was 1.0–2.3.

Detention facilities constitute an environment optimal for the introduction and spread of respiratory infectious diseases. Living conditions of inmates are frequently overcrowded and poorly ventilated, might provide limited access to running water, and lack adequate sanitary facilities. These conditions increase risk factors for and background prevalence of infection (*1*,*2*). Furthermore, prisons commonly must deal with understaffing and lack of resources, presenting additional challenges to triaging and treating higher-risk patients in a timely manner (*3*).

The first case of coronavirus disease (COVID-19) in Brazil was reported on February 26, 2020. The introduction of severe acute respiratory syndrome coronavirus 2 (SARS-CoV-2), the causative agent of COVID-19, into prisons adds an extra burden into an already overwhelmed environment. COVID-19 could be introduced through staff, visitors, or inmates under a semi-open regime, in which they spend the day outside the penitentiary complex and return in the evening. In addition, a new disease for which there is no existing immunity increases the health risk. Therefore, control of COVID-19 in prisons must be considered an essential part of a public health response (*4*).

In Brazil, ≈750,000 people are imprisoned in a system built to hold just over 442,000 (*5*). By June 12, Brazil had reported 828,810 COVID-19 cases nationwide, with >2,200 of those within prison settings (*6*,*7*). Testing in Brasília, located in Brazil's Federal District, accounted for 65.5% of all COVID-19 tests performed among imprisoned persons; ≈48% of the total national cases in prisons were reported in a maximum-security penitentiary complex in Brasília. The complex includes 4 prison units: Unit I houses persons under pretrial detention, Unit II houses inmates under a semi-open regime, and Units III and IV house convicted inmates. Overall, the prison is one of the largest penitentiary complexes in Brazil, housing >13,000 male inmates, as of June 2020.

In this report, we provide a descriptive analysis of the outbreak and estimate the disease transmissibility in its early stages. Data were collected from secondary sources, including the penitentiary monitoring dataset for COVID-19 notifications, the penitentiary administration system, and the monitoring resources of the healthcare system. The public health response was a joint effort from the state health and security departments, local health and security teams, and the Brazil Ministry of Health's Brazilian Field Epidemiology Training Program. Ethics approval was obtained under CONEP (Comissão Nacional de Ética em Pesquisa [National Research Ethics Commission], protocol number 37007220.1.0000.0008).

The Study

The first COVID-19 case in Brasília was reported on March 5; on April 1, the first case in the penitentiary complex, in a prison guard, was confirmed. The earliest infections occurred among security officers; the first inmate with COVID-19 was reported on April 7 in Unit I, the pretrial detention area. Six cases were

Author affiliations: Ministério da Saúde, Brasília, Brazil (F.A. Gouvea-Reis, P.D. Oliveira, D.C.S. Silva, L.S. Borja, J. Percio, C. de Moraes); Secretaria de Estado de Administração Penitenciária, Brasília (F.S. Souza); Secretaria de Estado da Saúde do Distrito Federal, Brasília (C. Peterka, C. Feres, J. de Oliveira, G. Sodré, W. dos Santos)

DOI: https://doi.org/10.3201/eid2703.204079

reported on April 10 in 2 different wings from the same block in that unit. The location of the first cases in the other prison units indicated that COVID-19 had dispersed across the penitentiary complex. In Unit II, 13 cases were reported on April 9–10 in 3 different blocks. In Unit III, 5 cases were confirmed on April 17 in 2 different blocks. In Unit IV, 6 cases were confirmed on April 15–17 in 3 different blocks. Although the virus was not introduced inside the penitentiary complex until ≈1 month after the first reported case in Brasilia, the complex rapidly attained the highest incidence in the region. By May 1, whereas the incidence rate was 47 cases/100,000 persons in the city, it was 1,832 cases/100,000 persons among inmates (*8*).

During April 1–June 12, there were 1,057 reported cases at the prison: 859 (81.3%) in inmates, 180 (17.1%) in prison guards, 9 (0.8%) in contracted staff, and 9 (0.8%) in health professionals. Distribution of the symptomatic cases over time is shown in Figure 1. Nine patients were hospitalized, and 3 deaths were reported: 1 prison guard and 2 inmates.

Among infected inmates, mean age was 38 years (SD 14.1 years); 296 (34.5%) were 18–29 years of age, 245 (28.5%) 30–39 years, 124 (14.4%) 40–49 years, 61 (7.1%) 50–59 years, and 133 (15.5%) ≥60 years. Information about ethnicity was available for 783 patients; 407 (52.0%) were mixed race, 214 (27.3%) White, 93 (11.9%) Asian, 67 (8.5%) Black, and 2 (0.3%) Indigenous. Underlying medical conditions were reported in 160 (18.6%) patients; the most prevalent were cardiovascular diseases (11.8%), diabetes (5.1%), and pneumopathies (2.8%). We were able to evaluate the presence of symptoms on medical records from 401 patients with confirmed COVID-19 cases. The most prevalent symptoms were headache (34.9%), cough (30.2%), and fever (28.9%) (Table).

We applied the EpiEstim R package (https://cran.r-project.org) to estimate the reproduction number over time (R_t), the number of secondary PCR-confirmed cases resulting from a single initial case, for the penitentiary complex. We estimated the serial interval by computing the difference between the dates of symptom onset for pairs of primary and secondary infected inmates in 144 cases confirmed by reverse transcription PCR (RT-PCR) recorded in April, during the early stages of the outbreak, within all 4 prison units. We identified the primary infected inmate as the person in a cell having the first RT-PCR–confirmed case; we identified secondary infected inmates as anyone sharing a cell with a primary case patient who tested positive for COVID-19 by RT-PCR ≤14 days after symptom onset in the cellmate. Local health teams identified suspected cases through daily active case finding; patients with confirmed cases were isolated as separate cohorts.

We estimated the mean serial interval at 2.51 days (SD 1.21). We found high transmissibility at the start of the outbreak, when the overall R_t was 2.28 in the prison complex (Figure 2). April was the

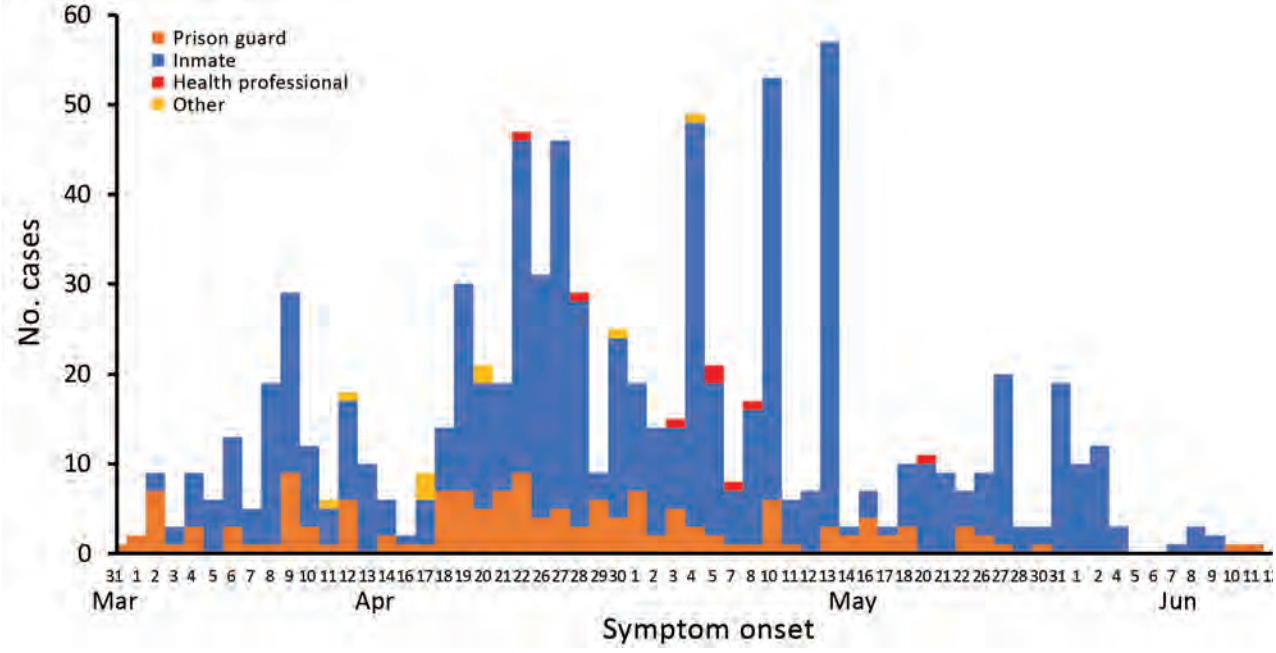

Figure 1. Distribution of symptomatic coronavirus disease cases over time by symptom onset date in a penitentiary complex, Brasília, Brazil, March–June 2020.

Table. Characteristics of coronavirus disease cases within the penitentiary complex, Brasília, Brazil, April–June 2020

Characteristic	No.	% Total
Age, y		
18–29	296	34.5
30–39	245	28.5
40–49	124	14.4
50–59	61	7.1
≥60	133	15.5
Ethnicity*		
Asian	93	11.9
White	214	27.3
Indigenous	2	0.3
Mixed race	407	52.0
Black	67	8.5
Symptoms†		
Headache	140	34.9
Cough	121	30.2
Fever	116	28.9
Ageusia/anosmia	79	19.7
Dyspnea	67	16.7
Myalgia	42	10.5
Sore throat	32	8.0
Nasal congestion	23	5.7
Diarrhea	16	4.0
Underlying health conditions		
Cardiovascular disease	101	11.8
Diabetes	44	5.1
Pneumopathies	24	2.8
Others‡	8	0.9

*Data available for 783 cases.
†Data available for 401 cases.
‡Includes metabolic disorders, immunosuppression, psychiatric disease, and chronic hepatitis.

month with the most intense transmission; Units III and IV reported 149 cases during April 20–30, which is reflected in the R_t peaks in those units (Appendix Figure, https://wwwnc.cdc.gov/EID/article/27/3/20-4079-App1.pdf). R_t decreased over time, to ≈1.0 during most of May.

Conclusions

We found a shorter serial interval for COVID-19 in this prison than that estimated for Brazil overall

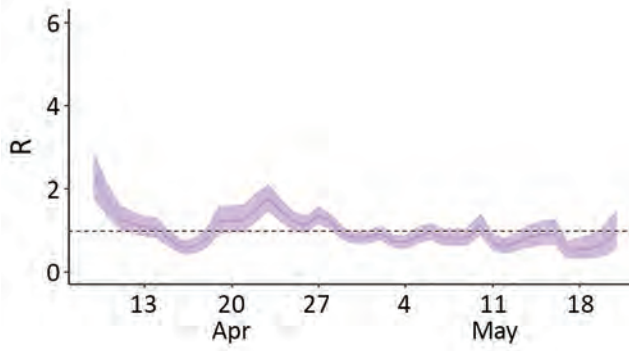

Figure 2. R_t for severe acute respiratory syndrome coronavirus 2 transmission in a penitentiary complex, Brasília, Brazil, April–May 2020. Blue line indicates median R_t; blue shading indicates 95% CI. Dashed line indicates R_t = 1.

(*9*). This finding supports the idea of a faster viral spread in overcrowded settings, and considering that the estimated serial interval was lower than the mean incubation period, the likely transmission of presymptomatic cases might have played an important role in viral spread inside the prison complex (*10*,*11*). Asymptomatic or presymptomatic cases, other sources of infection, or inmates failing to report symptoms might have affected accurately identifying primary infected inmates, resulting in our possibly underestimating the serial interval, R_t, or both. Considering the overcrowded conditions in the penitentiary complex and the impossibility of mandating effective social distancing, implementing broad testing strategies is fundamental for accurately measuring viral spread and planning better interventions.

The opinions expressed by authors do not necessarily reflect the opinions of the Ministry of Health of Brazil or the institutions with which the authors are affiliated.

About the Author

Dr. Gouvea-Reis is a fellow at the Field Epidemiology Training Program, Ministry of Health, Brazil. His research interests include global health, infectious diseases, and epidemiology.

References

1. Sánchez A, Simas L, Diuana V, Larouze B. COVID-19 in prisons: an impossible challenge for public health? [in Portuguese]. Cad Saude Publica. 2020;36:e00083520. https://doi.org/10.1590/0102-311x00083520
2. Dolan K, Wirtz AL, Moazen B, Ndeffo-Mbah M, Galvani A, Kinner SA, et al. Global burden of HIV, viral hepatitis, and tuberculosis in prisoners and detainees. Lancet. 2016;388:1089–102. https://doi.org/10.1016/S0140-6736(16)30466-4
3. Burki T. Prisons are "in no way equipped" to deal with COVID-19. Lancet. 2020;395:1411–2. https://doi.org/10.1016/S0140-6736(20)30984-3
4. Kinner SA, Young JT, Snow K, Southalan L, Lopez-Acuña D, Ferreira-Borges C, et al. Prisons and custodial settings are part of a comprehensive response to COVID-19. Lancet Public Health. 2020;5:e188–9. https://doi.org/10.1016/S2468-2667(20)30058-X
5. Departamento Penitenciário Nacional. National survey of penitentiary information [in Portuguese] [cited 2020 Sep 21]. https://www.gov.br/depen/pt-br/sisdepen
6. Ministério da Saúde. Coronavirus panel [in Portuguese] [cited 2020 Sep 21]. https://covid.saude.gov.br
7. Conselho Nacional De Justiça [Internet]. CNJ renews Recommendation no. 62 for another 90 days and releases new data [in Portuguese] [cited 2020 Sep 21]. https://www.cnj.jus.br/cnj-renova-recomendacao-n-62-por-mais-90-dias-e-divulga-novos-dados
8. Secretaria de Saúde do Distrito Federal. Epidemiologic bulletin for 01.05.2020: public health emergency COVID-19

within the Federal District [in Portuguese] [cited 2020 Sep 21]. http://www.saude.df.gov.br/wp-conteudo/uploads/2020/03/Boletim-COVID_DF-01-05-2020.pdf
9. Prete CA, Buss L, Dighe A, Porto VB, Candido DS, Ghilardi F. et al. Serial interval distribution of SARS-CoV-2 infection in Brazil. J Travel Med. 2020:taaa115. https://doi.org/10.1093/jtm/taaa115
10. Lauer SA, Grantz KH, Bi Q, Jones FK, Zheng Q, Meredith HR, et al. The incubation period of coronavirus disease 2019 (COVID-19) from publicly reported confirmed cases: estimation and application. Ann Intern Med. 2020;172:577–82. https://doi.org/10.7326/M20-0504
11. Backer JA, Klinkenberg D, Wallinga J. Incubation period of 2019 novel coronavirus (2019-nCoV) infections among travellers from Wuhan, China, 20–28 January 2020. Euro Surveill. 2020;25:2000062. https://doi.org/10.2807/1560-7917.ES.2020.25.5.2000062

Address for correspondence: Fernando Gouvea Reis, EpiSUS–Programa de Epidemiologia de Campo Aplicada aos Serviços do SUS, Secretaria de Vigilância em Saúde, Ministério da Saúde. Edifício PO700, 6 andar, SRTV 702, Via W 5 Norte, Brasília, DF, Brazil; email: fernando.reis@saude.gov.br

February 2020

Coronaviruses

- Middle East Respiratory Syndrome Coronavirus Transmission
- Acute Toxoplasmosis among Canadian Deer Hunters Associated with Consumption of Undercooked Deer
- Public Health Program for Decreasing Risk for Ebola Virus Disease Resurgence from Survivors of the 2013–2016 Outbreak, Guinea
- Characteristics of Patients with Acute Flaccid Myelitis, United States, 2015–2018
- Illness Severity in Hospitalized Influenza Patients by Virus Type and Subtype, Spain, 2010–2017
- Exposure to Ebola Virus and Risk for Infection with Malaria Parasites, Rural Gabon
- Cost-effectiveness of Screening Program for Chronic Q Fever, the Netherlands
- Unique Clindamycin-Resistant *Clostridioides difficile* Strain Related to Fluoroquinolone-Resistant Epidemic BI/RT027 Strain
- Porcine Deltacoronavirus Infection and Transmission in Poultry, United States
- Chronic Human Pegivirus 2 without Hepatitis C Virus Co-infection
- Interspecies Transmission of Reassortant Swine Influenza A Virus Containing Genes from Swine Influenza A(H1N1)pdm09 and A(H1N2) Viruses
- Influence of Rainfall on *Leptospira* Infection and Disease in a Tropical Urban Setting, Brazil

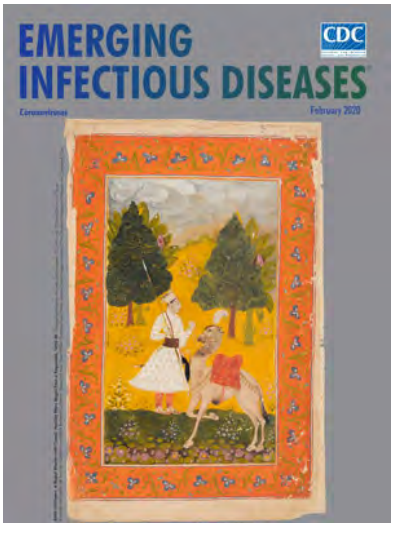

- Multiplex Mediator Displacement Loop-Mediated Isothermal Amplification for Detection of *Treponema pallidum* and *Haemophilus ducreyi*
- Novel Subclone of Carbapenem-Resistant *Klebsiella pneumoniae* Sequence Type 11 with Enhanced Virulence and Transmissibility, China
- Neutralizing Antibodies against Enteroviruses in Patients with Hand, Foot and Mouth Disease
- Systematic Hospital-Based Travel Screening to Assess Exposure to Zika Virus
- Rapid Nanopore Whole-Genome Sequencing for Anthrax Emergency Preparedness

- *Elizabethkingia anophelis* Infection in Infants, Cambodia, 2012–2018
- Global Expansion of Pacific Northwest Vibrio parahaemolyticus Sequence Type 36
- Surge in Anaplasmosis Cases in Maine, USA, 2013–2017
- Emergence of Chikungunya Virus, Pakistan, 2016–2017
- *Mycoplasma genitalium* Antimicrobial Resistance in Community and Sexual Health Clinic Patients, Auckland, New Zealand
- Early Detection of Public Health Emergencies of International Concern through Undiagnosed Disease Reports in ProMED-Mail
- Ocular *Spiroplasma ixodetis* in Newborns, France
- Use of Surveillance Outbreak Response Management and Analysis System for Human Monkeypox Outbreak, Nigeria, 2017–2019
- Human Norovirus Infection in Dogs, Thailand
- Hepatitis E Virus in Pigs from Slaughterhouses, United States, 2017–2019
- *Rickettsia mongolitimonae* Encephalitis, Southern France, 2018
- Human Alveolar Echinococcosis, Croatia
- Two Cases of Newly Characterized Neisseria Species, Brazil
- Hepatitis A Virus Genotype IB Outbreak among Internally Displaced Persons, Syria

EMERGING INFECTIOUS DISEASES®

To revisit the February 2020 issue, go to:
https://wwwnc.cdc.gov/eid/articles/issue/26/2/table-of-contents

Antibody Responses 8 Months after Asymptomatic or Mild SARS-CoV-2 Infection

Pyoeng Gyun Choe,[1] Kye-Hyung Kim,[1] Chang Kyung Kang, Hyeon Jeong Suh, EunKyo Kang, Sun Young Lee, Nam Joong Kim, Jongyoun Yi, Wan Beom Park, Myoung-don Oh

Waning humoral immunity in coronavirus disease patients has raised concern over usefulness of serologic testing. We investigated antibody responses of 58 persons 8 months after asymptomatic or mildly symptomatic infection with severe acute respiratory syndrome coronavirus 2. For 3 of 4 immunoassays used, seropositivity rates were high (69.0%–91.4%).

Infection with severe acute respiratory syndrome coronavirus 2 (SARS-CoV-2) leads to an antibody response, even in those who are completely asymptomatic. However, the initial immune response is not as strong as in patients with more severe disease, and concerns about waning immunity have been raised (*1*,*2*). We evaluated the antibody responses of 58 persons in South Korea 8 months after asymptomatic or mildly symptomatic SARS-CoV-2 infection.

The Study

The eligible participants for this cross-sectional survey were persons with reverse transcription PCR–confirmed coronavirus disease (COVID-19) who had been isolated in a community treatment center (CTC) operated by Seoul National University Hospital during March 5–April 9, 2020. Isolation was in response to the COVID-19 outbreak in Daegu, South Korea (population 2.4 million), the first large outbreak outside of China, which resulted in 6,620 confirmed cases during February 18–March 24, 2020 (*3*). CTC admission criteria were as follows: alert, age <65 years, no underlying disease or well-controlled underlying disease, body temperature <38.0°C with or without antipyretics, and no dyspnea. During participants' CTC stay, physicians and nurses comprehensively evaluated them twice daily via video consultation. Asymptomatic persons were defined as those with body temperature <37.5°C and no signs or symptoms (e.g., no subjective fever, myalgia, rhinorrhea, sore throat, cough, sputum, or chest discomfort) during the entire CTC stay; others were classified as mildly symptomatic patients (*4*). From all participants who provided informed consent, we collected serum samples at 8 months after infection.

We measured SARS-CoV-2–specific antibodies by using 4 commercial immunoassays: an antinucleocapsid (anti-N) panimmunoglobulin (pan-Ig) electrochemiluminescence immunoassay (ECLIA) (Elecsys Anti-SARS-CoV-2; Roche Diagnostics, https://diagnostics.roche.com), an anti-N IgG ELISA (EDI Novel Coronavirus COVID-19 ELISA Kit; Epitope Diagnostics, https://www.epitopediagnostics.com), an antispike (anti-S) IgG ELISA (SCoV-2 Detect IgG ELISA; InBios International, https://www.inbios.com), and an anti-S1 spike subunit IgG ELISA [Anti-SARS-CoV-2 ELISA (IgG); Euroimmun, https://www.euroimmune.com]. Except for the anti-N IgG ELISA, these immunoassays were granted Emergency Use Authorization by the US Food and Drug Administration. Measurement and interpretation of results were made according to each manufacturer's instructions. For the anti-N and anti-S1 IgG ELISAs, borderline results were regarded as negative. To evaluate neutralizing activity targeting the spike receptor–binding domain, we used a surrogate virus neutralization test (sVNT) (SARS-CoV-2 Surrogate Virus Neutralization Test; GenScript, https://www.genscript.com) (*5*). The Institutional Review Boards of Seoul National University Hospital and the Pusan National University Hospital approved the study (IRB nos. H-2009-168-1160 and H-2010-013-096).

Author affiliations: Seoul National University College of Medicine, Seoul, South Korea (P.G. Choe, C.K. Kang, H.J. Suh, E. Kang, S.Y. Lee, N.J. Kim, W.B. Park, M.-d. Oh); Pusan National University School of Medicine, Busan, South Korea (K.-H. Kim, J. Yi)

DOI: https://doi.org/10.3201/eid2703.204543

[1]These first authors equally contributed to this article.

We analyzed data from 7 participants with asymptomatic SARS-CoV-2 infection and 51 patients with mildly symptomatic COVID-19 (Table 1). Eight months after their infections, we detected anti-N pan-Ig in 53 (91.4%), anti-N IgG in 15 (25.9%), anti-S IgG in 50 (86.2%), and anti-S1 IgG in 40 (69.0%) (p<0.01) (Table 2). The sVNT found positive neutralizing activity for 31 (53.4%). For female participants, positivity was significantly higher for anti-N IgG (40.0% female vs. 4.3% male; p<0.01), anti-S IgG (94.3% vs. 73.9%; p<0.05), anti-S1 IgG (82.9% vs. 47.8%; p<0.01), and sVNT (68.6% vs. 30.4%; p<0.01). Positivity by PCR for ≤14 days was associated with a lower rate of positivity for anti-N pan-Ig (50.0% for ≤14 d vs. 96.0% for >14 d; p<0.01) (Table 2). Logistic regression analysis, for which anti-N IgG ELISA results were excluded because of exceptionally low positivity, indicated that negative results from ≥2 commercial immunoassays were significantly associated with positivity by PCR for ≤14 days after adjustment for sex (adjusted odds ratio 11.49; 95% CI 1.45–90.79; p = 0.02) (Appendix, https://wwwnc.cdc.gov/EID/article/27/3/20-4543-App1.pdf).

Conclusions

Knowledge of the longevity of humoral immunity to SARS-CoV-2 is essential for predicting herd immunity and interpreting seroepidemiologic data. Recent studies showed that the antibody titers of patients with mild SARS-CoV-2 infection declined more quickly than those reported for SARS-CoV patients (*6*), and waning immunity was confirmed 5 months after infection (*7*). Concern about the usefulness of population-based seroprevalence studies has been raised because rapidly waning immunity may lead to a substantial number of false-negative immunoassay results (*2*). However, in this study, we confirmed that rates of antibody positivity according to 3 commercial kits was still high at 8 months after infection, even in asymptomatic or mildly symptomatic participants (69.0%–91.4%). Rates differed according to immunoassay methods or manufacturers, thereby explaining differences in rates between the studies (*2*,*8*). A previous study argued that among asymptomatic persons who had been antibody positive early in the infection, 40% became antibody negative in 2–3 months, even when tested by chemiluminescence immunoassay (CLIA) (*2*); however, their results are in stark contrast to ours, which may have resulted from variations in the characteristics of CLIA products from different manufacturers. In a systematic review and meta-analysis, pooled sensitivity was 97.8% with CLIA in contrast to 84.3% with ELISA (*9*). In a head-to-head benchmark comparison study, anti-N pan-Ig ECLIA showed 97.2% sensitivity and 99.8% specificity (*10*). In the previous studies, CLIA showed high sensitivity and specificity for recent or past SARS-CoV-2 infection. Therefore, our results show that a serosurvey is useful even 8 months after an outbreak if an appropriate binding immuno-

Table 1. Clinical characteristics of 58 persons with asymptomatic or mildly symptomatic severe acute respiratory syndrome coronavirus 2 infection, South Korea*

Characteristic	Asymptomatic	Mildly symptomatic
Total no. persons	7	51
Sex, no. (%)		
M	5 (71.4)	18 (35.3)
F	2 (28.6)	33 (64.7)
Age, y, median (IQR)	25 (21–26)	26 (22–40)
Underlying disease, no. (%)†	0	3 (5.9)
Smoking status		
Smoker	0	0
Ex-smoker	1 (14.3)	2 (3.9)
Nonsmoker	6 (85.7)	49 (96.1)
Signs/symptoms, no. (%)		
Febrile/chilling sense	NA	8 (15.7)
Myalgia	NA	5 (9.8)
Headache	NA	13 (25.5)
Cough	NA	20 (39.2)
Sputum	NA	33 (64.7)
Rhinorrhea	NA	25 (49.0)
Sore throat	NA	3 (5.9)
Chest discomfort/dyspnea	NA	4 (7.8)
Duration of PCR positivity, d, median (IQR)	29 (25–34)	24 (19–34)
Days from symptom onset to blood sampling, median (IQR)‡	231 (231–233)	234 (231–234)

*IQR, interquartile range; NA, not applicable.
†One each: hypertension, diabetes mellitus, asthma.
‡For asymptomatic patients, time from the first PCR-positive result to blood sampling.

Table 2. Positivity of antibodies to severe acute respiratory syndrome coronavirus 2 in 58 asymptomatic or mildly symptomatic patients at 8 mo after infection, South Korea*

Characteristic	Anti-N pan-Ig ECLIA, no. (%)†	Anti-N IgG ELISA, no. (%)‡	Anti-S IgG ELISA, no. (%)§	Anti-S1 IgG ELISA, no. (%)¶	sVNT, no. (%)#
Total	53/58 (91.4)	15/58 (25.9)	50/58 (86.2)	40/58 (69.0)	31/58 (53.4)
Sex					
M	21/23 (91.3)	1/23 (4.3)	17/23 (73.9)	11/23 (47.8)	7/23 (30.4)
F	32/35 (91.4)	14/35 (40.0)**	33/35 (94.3)††	29/35 (82.9)**	24/35 (68.6)**
Age, y					
≤30	35/38 (92.1)	5/38 (13.2)	33/38 (86.8)	25/38 (65.8)	19/38 (50.0)
>30	18/20 (90.0)	10/20 (50.0)**	17/20 (85.0)	15/20 (75.0)	12/20 (60.0)
Duration of PCR positivity					
≤14 d	3/6 (50.0)	3/6 (50.0)	4/6 (66.7)	3/6 (50.0)	2/6 (33.3)
>14 d	48/50 (96.0)**	10/50 (20.0)	44/50 (88.0)	36/50 (72.0)	27/50 (54.0)
Disease severity					
Asymptomatic	7/7 (100)	0/7 (0)	5/7 (71.4)	4/7 (57.1)	4/7 (57.1)
Mildly symptomatic	46/51 (90.2)	15/51 (29.4)	45/51 (88.2)	36/51 (70.6)	27/51 (52.9)

*Anti-N, antinucleocapsid; anti-S, antispike; anti-S1, antispike subunit; ECLIA, electrochemiluminescence immunoassay; pan-Ig, panimmunoglobulin; sVNT, surrogate virus neutralization test.
†Roche Diagnostics, https://diagnostics.roche.com.
‡Epitope Diagnostics, https://www.epitopediagnostics.com.
§InBios International, https://www.inbios.com.
¶Euroimmun, https://www.euroimmune.com.
#GenScript, https://www.genscript.com.
**p<0.01.
††p<0.05.

assay format like an anti-N pan-Ig ECLIA is used. A serosurvey that uses a binding immunoassay can determine the infected proportion of the population and also the proportion of infections detected by PCR, thus enabling inference of the infection-fatality ratio rather than just the case-fatality ratio; however, it cannot accurately assess population immunity because it is not a functional immunoassay for detecting neutralizing activity.

Neutralizing activity, a functional aspect of antibodies, is essential for protection from reinfection and screening potential convalescent plasma therapy donors (*8*). In our study, neutralizing activity was detected in 53.4% of asymptomatic or mildly symptomatic participants after 8 months of infection, which was considerably lower than the rate of positivity detected by binding immunoassays such as ECLIA or ELISAs. This finding is not surprising because neutralizing activity is affected by various factors, including the antigen specificity and the amount of existing antibody. However, confirming sVNT results by conventional VNT might be needed, although the reported specificity (100%) and sensitivity (98%–98.9%) of sVNT showed good correlation with conventional VNT (*5*). A recently published study of convalescent plasma therapy found detectable neutralizing antibodies in 63.6% persons a median of 41 days after PCR-confirmed diagnosis of mild COVID-19 (*11*).

According to our study, prolonged duration of virus shedding is associated with long-term antibody positivity in patients with mild COVID-19, which aligns with previous findings of higher IgG levels during weeks 4–8 in those in the prolonged virus shedding group (*12*). Factors associated with prolonged virus shedding include male sex, old age, severe illness at admission, and invasive mechanical ventilation (*13*). Our findings suggest that the duration of virus shedding reflects the amount of humoral immune stimulation, even in asymptomatic or mildly symptomatic persons with COVID-19.

One limitation of our study was the relatively small sample size and the predominantly young population, which lessen generalization of the results. Also, because of the cross-sectional design, we could not obtain baseline or longitudinal serum samples. For the 7 asymptomatic participants in our study, we evaluated antibody responses at 2 and 5 months after infection; 5/7 (71%) had positive ELISA results at 2 months after infection, 4/7 (57.1%) had positive ELISA results at 5 months after infection, and all had neutralizing antibodies at 2 and 5 months after infection (*1*,*7*). Last, we could not assess the individual possibilities of reexposure or reinfection. However, it is unlikely that humoral immunity was boosted because in Daegu, where the study participants reside, during April–October 2020, the daily incidence rate for COVID-19 was <0.5 cases/100,000 population (*14*). In conclusion, despite concerns of waning immunity, appropriate immunoassays can detect antibodies against SARS-CoV-2 at 8 months after infection in most asymptomatic or mildly symptomatic persons.

Acknowledgments

We thank Kyung Sook Ahn for administrative support and Areum Jo, Su Jin Choi, and Mee Kyung Ko for technical support.

This work was supported by a 2-year research grant from Pusan National University. The funding agencies had no role in the design and conduct of the study; collection, management, analysis, and interpretation of the data; preparation, review, or approval of the manuscript; and decision to submit the manuscript for publication.

About the Author

Dr. Choe is a clinical scientist at Seoul National University Hospital. His research interests focus on preventing healthcare-associated infection and responding to emerging infectious diseases.

References

1. Choe PG, Kang CK, Suh HJ, Jung J, Kang E, Lee SY, et al. Antibody responses to SARS-CoV-2 at 8 weeks postinfection in asymptomatic patients. Emerg Infect Dis. 2020;26:2484–7. https://doi.org/10.3201/eid2610.202211
2. Long QX, Tang XJ, Shi QL, Li Q, Deng HJ, Yuan J, et al. Clinical and immunological assessment of asymptomatic SARS-CoV-2 infections. Nat Med. 2020;26:1200–4. https://doi.org/10.1038/s41591-020-0965-6
3. Kang E, Lee SY, Jung H, Kim MS, Cho B, Kim YS. Operating protocols of a community treatment center for isolation of patients with coronavirus disease, South Korea. Emerg Infect Dis. 2020;26:2329–37. https://doi.org/10.3201/eid2610.201460
4. Choe PG, Kang EK, Lee SY, Oh B, Im D, Lee HY, et al. Selecting coronavirus disease 2019 patients with negligible risk of progression: early experience from non-hospital isolation facility in Korea. Korean J Intern Med. 2020;35:765–70. https://doi.org/10.3904/kjim.2020.159
5. Tan CW, Chia WN, Qin X, Liu P, Chen MI, Tiu C, et al. A SARS-CoV-2 surrogate virus neutralization test based on antibody-mediated blockage of ACE2-spike protein-protein interaction. Nat Biotechnol. 2020;38:1073–8. https://doi.org/10.1038/s41587-020-0631-z
6. Ibarrondo FJ, Fulcher JA, Goodman-Meza D, Elliott J, Hofmann C, Hausner MA, et al. Rapid decay of anti-SARS-CoV-2 antibodies in persons with mild Covid-19. N Engl J Med. 2020;383:1085–7. https://doi.org/10.1056/NEJMc2025179
7. Choe PG, Kang CK, Suh HJ, Jung J, Song KH, Bang JH, et al. Waning antibody responses in asymptomatic and symptomatic SARS-CoV-2 infection. Emerg Infect Dis. 2020;27. Epub 2020 Oct 13.
8. Wajnberg A, Amanat F, Firpo A, Altman DR, Bailey MJ, Mansour M, et al. Robust neutralizing antibodies to SARS-CoV-2 infection persist for months. Science. 2020;370:1227–30. https://doi.org/10.1126/science.abd7728
9. Lisboa Bastos M, Tavaziva G, Abidi SK, Campbell JR, Haraoui LP, Johnston JC, et al. Diagnostic accuracy of s erological tests for covid-19: systematic review and meta-analysis. BMJ. 2020;370:m2516. https://doi.org/10.1136/bmj.m2516
10. Ainsworth M, Andersson M, Auckland K, Baillie JK, Barnes E, Beer S, et al.; National SARS-CoV-2 Serology Assay Evaluation Group. Performance characteristics of five immunoassays for SARS-CoV-2: a head-to-head benchmark comparison. Lancet Infect Dis. 2020;20:1390–400. https://doi.org/10.1016/S1473-3099(20)30634-4
11. Agarwal A, Mukherjee A, Kumar G, Chatterjee P, Bhatnagar T, Malhotra P; PLACID Trial Collaborators. Convalescent plasma in the management of moderate covid-19 in adults in India: open label phase II multicentre randomised controlled trial (PLACID Trial). BMJ. 2020;371:m3939. https://doi.org/10.1136/bmj.m3939
12. Jin CC, Zhu L, Gao C, Zhang S. Correlation between viral RNA shedding and serum antibodies in individuals with coronavirus disease 2019. Clin Microbiol Infect. 2020; S1198-743X(20)30299-8.
13. Xu K, Chen Y, Yuan J, Yi P, Ding C, Wu W, et al. Factors associated with prolonged viral RNA shedding in patients with coronavirus disease 2019 (COVID-19). Clin Infect Dis. 2020;71:799–806. https://doi.org/10.1093/cid/ciaa351
14. Ministry of Health and Welfare. Coronavirus disease–19, Republic of Korea [cited 2020 Nov 5]. http://ncov.mohw.go.kr/en

Address for correspondence: Jongyoun Yi, Department of Laboratory Medicine, Pusan National University School of Medicine, 179 Gudeok-ro, Seo-gu, Busan, 49241, South Korea; email: socioliberal@yahoo.co.kr; Wan Beom Park, Department of Internal Medicine, Seoul National University College of Medicine, 103 Daehak-ro, Jongro-gu, Seoul, 03080, South Korea; email: wbpark1@snu.ac.kr

Tropheryma whipplei in Feces of Patients with Diarrhea in 3 Locations on Different Continents

Gerhard E. Feurle, Verena Moos, Olfert Landt, Craig Corcoran, Udo Reischl, Matthias Maiwald

We examined fecal specimens of patients with diarrhea from 3 continents for *Tropheryma whipplei* and enteropathogens. *T. whipplei* was most common in South Africa, followed by Singapore and Germany. Its presence was associated with the presence of other pathogens. An independent causative role in diarrhea appears unlikely.

Tropheryma whipplei is the causative agent of Whipple disease (*1*). The organism has also been detected in the feces of healthy or asymptomatic persons (*2*,*3*) and in the feces of patients with diarrhea (*4*–*6*). A causative role in gastroenteritis has been proposed.

To investigate the role of enteric *T. whipplei*, we examined fecal specimens of patients with diarrhea using conventional methods and PCR to detect enteric pathogens and *T. whipplei*. Our aim was to collect epidemiologic evidence regarding a causative role of *T. whipplei* in diarrhea.

The Study

The 3 participating sites were the Molecular Biology Laboratory, AMPATH (Centurion, South Africa); the Department of Pathology and Laboratory Medicine at KK Women's and Children's Hospital (Singapore); and the Institute of Microbiology and Hygiene at the University Hospital Regensburg (Regensburg, Germany). We examined fecal samples from patients with diarrhea that were submitted for microbiological laboratory diagnosis; we used a combination of conventional tests and multiplex PCRs covering the pathogens shown in Table 1, with differences owing to local arrangements (Appendix, https://wwwnc.cdc.gov/EID/article/27/3/20-0182-App1.pdf).

We investigated a total of 590 fecal samples. In South Africa, 97 of 100 targeted samples were usable. In Singapore, 193 of 200 targeted specimens contained sufficient material; of these, 19 were originally submitted for bacterial culture, 77 for rotavirus antigen testing, and 97 for both. In Germany, we tested samples from 300 patients. In South Africa and Singapore, patients were mainly children, both outpatients and inpatients. In Singapore, the total included 13 immunocompromised children with hematologic/oncologic diseases and 1 with a short bowel syndrome. In Germany, all were inpatients and mostly elderly, about one quarter from the hematologic/oncologic ward (Figure).

Overall, 56 patients had positive test results for *T. whipplei* in the feces: 17 (17.5%) in South Africa, 29 (15%) in Singapore, and 10 (3.3%) in Germany. The frequency distribution of the organisms detected is shown in Table 1. In South Africa, *T. whipplei* was the most common fecal organism, followed by *Shigella*, rotavirus, and adenovirus. In Singapore, rotavirus was the most frequently detected organism, followed by norovirus, *T. whipplei*, and *Salmonella*. In Germany, *Clostridioides difficile* was the most frequently detected organism, followed by *T. whipplei* and *Blastocystis hominis*; viruses were not sought in Germany. The frequency of *C. difficile* likely reflects the high proportion of elderly inpatients.

Fecal specimens testing positive for *T. whipplei* averaged 0.91 other pathogens per specimen, in contrast to only 0.46 per specimen in those testing negative for *T. whipplei* ($p = 0.0001$; Table 2). Similarly, of the fecal specimens testing positive for *T. whipplei*, 69.6% contained other pathogens, in contrast to only 34.5% of the specimens testing negative for *T. whipplei* ($p<0.0001$; Appendix Table 1). Thus, specimens con-

Author affiliations: DRK Krankenhaus, Neuwied, Germany (G.E. Feurle); Charité–Universitätsmedizin Berlin, Berlin, Germany (V. Moos); TIB MOLBIOL Syntheselabor GmbH, Berlin, Germany (O. Landt); National Reference Laboratory AMPATH, Centurion, South Africa (C. Corcoran); Institute of Clinical Microbiology and Hygiene, University Hospital Regensburg, Regensburg, Germany (U. Reischl); KK Women's and Children's Hospital, Singapore (M. Maiwald); National University of Singapore, Singapore (M. Maiwald); Duke-National University of Singapore Graduate Medical School, Singapore (M. Maiwald)

DOI: https://doi.org/10.3201/eid2703.200182

taining *T. whipplei* contained other pathogens about twice as frequently as specimens without *T. whipplei*. In Singapore, 1 specimen contained 4 pathogens: *T. whipplei*, *Blastocystis*, astrovirus, and *Dientamoeba*.

Data on watery consistency and the presence of blood in feces were available for South Africa and Singapore, and microscopy data (e.g., erythrocytes, mucus, yeast cells) were available for South Africa (Appendix Table 2). There was no apparent relationship between these parameters and the presence of *T. whipplei*. Thus, an independent diarrheagenic role of *T. whipplei* was not apparent from these macroscopic and microscopic findings.

An association between the presence of *Campylobacter* and *T. whipplei* (Appendix Table 3) became apparent. Of 534 *T. whipplei*–negative fecal samples, 21 (3.9%) were positive for *Campylobacter* across all sites, whereas 8 (14.3%) of 56 *T. whipplei*–positive samples were positive for *Campylobacter*. This difference was statistically significant (p = 0.0035). In relative terms, specimens carrying *T. whipplei* contained *Campylobacter* 3 times more commonly than those without *T. whipplei*. When looking at the frequency ranking for all pathogens, *Campylobacter* rose from seventh position in *T. whipplei*–negative samples to being the fourth most common enteropathogen in *T. whipplei*–positive samples in South Africa and from fourth to second position in Singapore, whereas the position in Germany remained unchanged (Appendix Table 4).

The mechanisms underlying the *Campylobacter*–*Tropheryma* association remain unclear, but may include similar modes of acquisition. *T. whipplei* can be transmitted by the fecal–oral route (*7*,*8*). *Campylobacter* spp. are commensals in the gut of a variety of animals, especially poultry; the main infection routes for *Campylobacter* species are foodborne and fecal–oral transmission (*9*). Both *T. whipplei* and *Campylobacter* can be found in sewage (*9*–*11*).

Our study's first limitation was that it was done in real-life settings of diagnostic laboratories where the routine investigations were supplemented by additional PCR tests (Appendix). Pathogens tested and diagnostic techniques differed among the 3 laboratories but were identical within each laboratory between the specimens with and without *T. whipplei*. However, this diversity may even increase the robustness of data. The proportions of fecal samples with no pathogen detected were 81% in Germany, 57% in South Africa, and 29% in Singapore. These findings reflect not only the absence of pathogens but also the pathogen spectrum investigated; a higher number of different pathogens investigated will lead to more positive results, and Singapore had the most comprehensive tests. A high rate of negative findings limits the analyses concerning co-infections of *T. whipplei* with other pathogens.

Second, our study did not include asymptomatic controls, as did the Global Enteric Multicenter Study (*12*,*13*). In South Africa, *T. whipplei* was the most frequent fecal microorganism, followed by *Shigella*, rotavirus, and adenovirus, in descending order, the last

Table 1. Frequency distribution of fecal pathogens in South Africa, Singapore, and Germany*

Location	No. (%)
Centurion, South Africa, 97 specimens	
Tropheryma whipplei	17 (17.53)
Shigella spp.	15 (15.46)
Rotavirus A	7 (7.22)
Adenovirus type F, 40, 41	5 (5.15)
Salmonella spp.	4 (4.12)
Campylobacter spp.	4 (4.12)
Blastocystis hominis	4 (4.12)
Cryptosporidium spp.	4 (4.12)
Giardia lamblia	4 (4.12)
Yersinia enterocolitica	1 (1.03)
Escherichia coli, EPEC, EHEC	1 (1.03)
Aeromonas hydrophila	1 (1.03)
Plesiomonas shigelloides	0
No infective agent detected	55 (56.70)
T. whipplei solo	8 (8.25)
Singapore, 193 specimens	
Rotavirus A	73 (37.82)
Norovirus GG1/2	35 (18.13)
T. whipplei	29 (15.03)
Salmonella spp.	24 (12.44)
Campylobacter spp.	17 (8.81)
A. hydrophila	10 (5.18)
Sapovirus	9 (4.66)
Astrovirus	8 (4.15)
Adenovirus type F, 40, 41	5 (2.59)
G. lamblia	2 (1.04)
Dientamoeba fragilis	2 (1.04)
Shigella spp.	1 (0.52)
B. hominis	1 (0.52)
Vibrio spp.	0
Entamoeba histolytica	0
Y. enterocolitica	0
Cryptosporidium spp.	0
No infective agent detected	55 (28.50)
T. whipplei solo	2 (1.04)
Regensburg, Germany, 300 specimens	
Clostridioides difficile	28 (9.33)
T. whipplei	10 (3.33)
B. hominis	10 (3.33)
Campylobacter spp.	8 (2.66)
G. lamblia	8 (2.66)
Salmonella spp.	3 (1.00)
Y. enterocolitica	2 (0.66)
A. hydrophila	2 (0.66)
Shigella spp.	1 (0.33)
D. fragilis	1 (0.33)
Cryptosporidium spp.	0)
E. histolytica	0
No infective agent detected	242 (80.66)
T. whipplei solo	7 (2.33)

*More than 1 pathogen was detected in some fecal specimens. *T. whipplei* solo indicates that *T. whipplei* was the sole organism detected. EPEC, enteropathogenic *Escherichia coli*; EHEC, enterohemorrhagic *Escherichia coli*.

Table 2. Numbers of enteropathogens in fecal specimens with and without *Tropheryma whipplei* in South Africa, Singapore, and Germany*

Location	Specimens without *T. whipplei*		Specimens with *T. whipplei*	
	No. specimens	No. (rate) of enteropathogens	No. specimens	No. (rate) of enteropathogens
Centurion, South Africa	80	40 (0.50)	17	10 (0.59)
Singapore	164	145 (0.88)	29	38 (1.31)
Regensburg, Germany	290	60 (0.21)	10	3 (0.30)
Total†	534	245 (0.46)	56	51 (0.91)

*Total numbers and rates per specimen of all enteropathogens across all specimens collected at each site; multiple pathogens in a single specimen were counted as multiple entries.
†Incidence rate χ^2, p<0.0001.

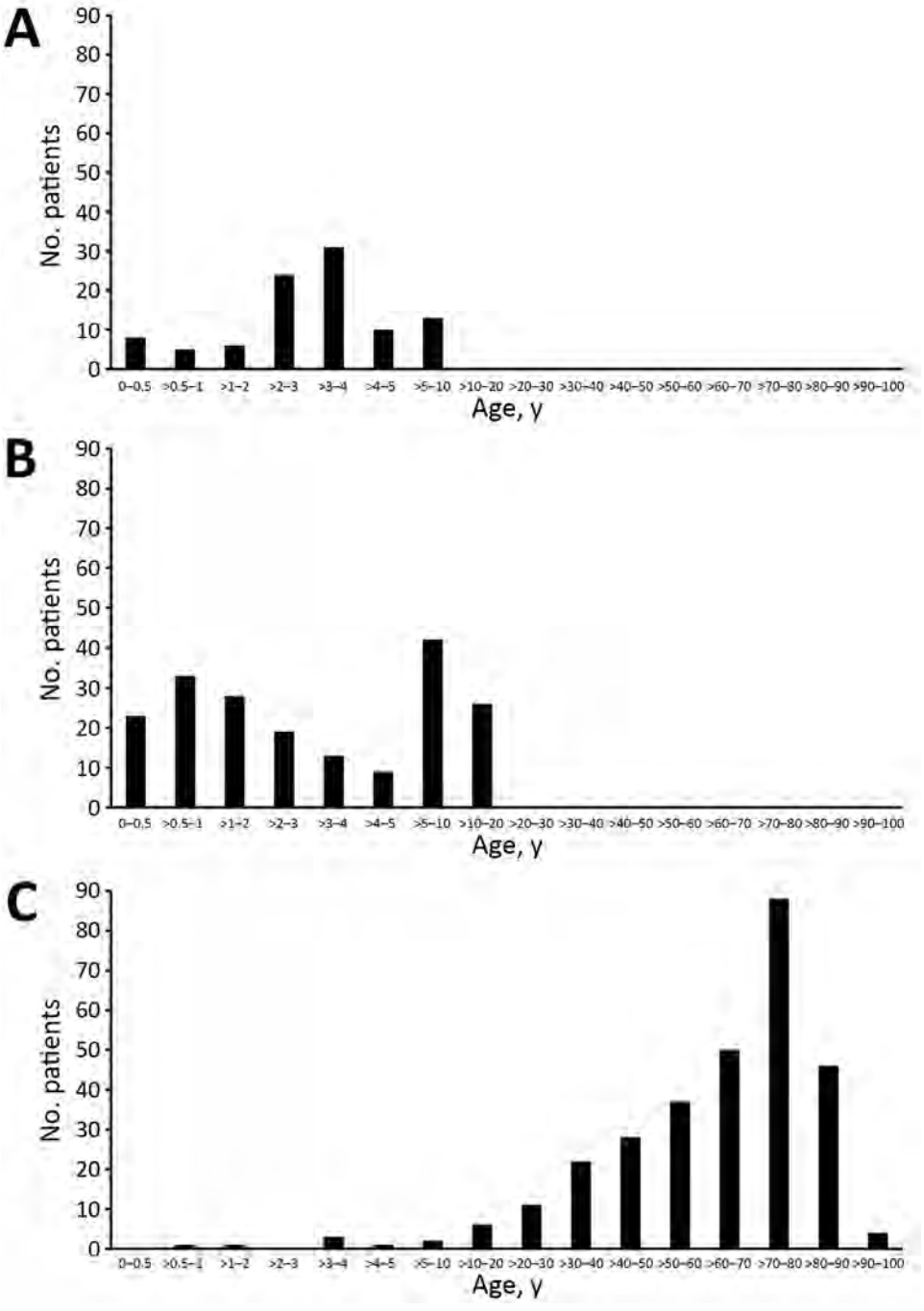

Figure. Age distribution of patients at 3 sites in study of *Tropheryma whipplei* in feces of patients with diarrhea: A) Centurion, South Africa; B) Singapore; and C) Regensburg, Germany.

3 exactly as in the Global Enteric Multicenter Study. In Singapore, *T. whipplei* was third after rotavirus and norovirus, but the ranking of rotavirus may be an artifact because rotavirus antigen was the most frequent ordered laboratory test.

We postulate that the different prevalence of pathogens at the 3 locations (Table 1) is related not just to the different diagnostic strategies but probably also to different climate, development, and hygiene. The Sustainable Development Goals indices for water, sanitation, and hygiene were 68, 66, and 90 in South Africa; 98, 99, and 97 in Singapore; and 100, 100, and 100 in Germany (*14*). These data reflect the order of prevalence of *T. whipplei* in feces in the 3 locations, which is in accordance with a prevalence approaching 50% in children in Laos (*15*).

Conclusions

Using diagnostic specimens from microbiology laboratories on 3 continents, we were able to confirm that *T. whipplei* can be found frequently in the feces of patients with diarrhea (*4*,*5*). Across the 3 locations, the numbers of traditional enteropathogens were significantly increased in specimens also containing *T. whipplei*, and we found an association between the presence of *T. whipplei* and *Campylobacter*. Our findings support the hypothesis that enteric *T. whipplei* may not be causative for diarrhea but may possibly be a result of different sanitary and climatic conditions.

Acknowledgments

We thank Annette Moter and Thomas Schneider for their contributions to the process of conceiving the study protocol. We also thank the staff of the Microbiology Laboratory at KK Women's and Children's Hospital, Singapore, in particular, Liat Hui Loo and Han Yang Soong, for their contributions to conducting the Singapore part of the study. We thank John C. Allen for help with statistical analyses.

About the Author

Dr. Feurle is an emeritus professor of internal medicine and gastroenterology at the DRK Krankenhaus Neuwied, a teaching hospital of the University of Bonn, Germany. His primary research interest is Whipple disease.

References

1. Schneider T, Moos V, Loddenkemper C, Marth T, Fenollar F, Raoult D. Whipple's disease: new aspects of pathogenesis and treatment. Lancet Infect Dis. 2008;8:179–90. https://doi.org/10.1016/S1473-3099(08)70042-2
2. Fenollar F, Trani M, Davoust B, Salle B, Birg ML, Rolain JM, et al. Prevalence of asymptomatic *Tropheryma whipplei* carriage among humans and nonhuman primates. J Infect Dis. 2008;197:880–7. https://doi.org/10.1086/528693
3. García-Álvarez L, Pérez-Matute P, Blanco JR, Ibarra V, Oteo JA. High prevalence of asymptomatic carriers of *Tropheryma whipplei* in different populations from the north of Spain. Enferm Infecc Microbiol Clin. 2016;34:340–5. https://doi.org/10.1016/j.eimc.2015.09.006
4. Raoult D, Fenollar F, Rolain JM, Minodier P, Bosdure E, Li W, et al. *Tropheryma whipplei* in children with gastroenteritis. Emerg Infect Dis. 2010;16:776–82. https://doi.org/10.3201/eid1605.091801
5. Fenollar F, Minodier P, Boutin A, Laporte R, Brémond V, Noël G, et al. *Tropheryma whipplei* associated with diarrhoea in young children. Clin Microbiol Infect. 2016;22:869–74. https://doi.org/10.1016/j.cmi.2016.07.005
6. Vinnemeier CD, Klupp EM, Krumkamp R, Rolling T, Fischer N, Owusu-Dabo E, et al. *Tropheryma whipplei* in children with diarrhoea in rural Ghana. Clin Microbiol Infect. 2016;22:65.e1–3. https://doi.org/10.1016/j.cmi.2015.09.022
7. Keita AK, Brouqui P, Badiaga S, Benkouiten S, Ratmanov P, Raoult D, et al. *Tropheryma whipplei* prevalence strongly suggests human transmission in homeless shelters. Int J Infect Dis. 2013;17:e67–8. https://doi.org/10.1016/j.ijid.2012.05.1033
8. Ramharter M, Harrison N, Bühler T, Herold B, Lagler H, Lötsch F, et al. Prevalence and risk factor assessment of *Tropheryma whipplei* in a rural community in Gabon: a community-based cross-sectional study. Clin Microbiol Infect. 2014;20:1189–94. https://doi.org/10.1111/1469-0691.12724
9. Pitkanen T, Hanninen ML. Members of the family Campylobacteraceae: *Campylobacter jejuni*, *Campylobacter coli*. In: Rose JB, Jiménez-Cisneros B, editors. Global Water Pathogen Project. East Lansing (MI): Michigan State University and UNESCO; 2017. https://doi.org/10.14321/waterpathogens.23
10. Maiwald M, Schuhmacher F, Ditton HJ, von Herbay A. Environmental occurrence of the Whipple's disease bacterium (*Tropheryma whippelii*). Appl Environ Microbiol. 1998;64:760–2. https://doi.org/10.1128/AEM.64.2.760-762.1998
11. Schöniger-Hekele M, Petermann D, Weber B, Müller C. *Tropheryma whipplei* in the environment: survey of sewage plant influxes and sewage plant workers. Appl Environ Microbiol. 2007;73:2033–5. https://doi.org/10.1128/AEM.02335-06
12. Kotloff KL, Nataro JP, Blackwelder WC, Nasrin D, Farag TH, Panchalingam S, et al. Burden and aetiology of diarrhoeal disease in infants and young children in developing countries (the Global Enteric Multicenter Study, GEMS): a prospective, case-control study. Lancet. 2013;382:209–22. https://doi.org/10.1016/S0140-6736(13)60844-2
13. Liu J, Platts-Mills JA, Juma J, Kabir F, Nkeze J, Okoi C, et al. Use of quantitative molecular diagnostic methods to identify causes of diarrhoea in children: a reanalysis of the GEMS case-control study. Lancet. 2016;388:1291–301. https://doi.org/10.1016/S0140-6736(16)31529-X
14. Lozano R, Fullman N, Abate D, Abay SM, Abbafati C, Abbasi N, et al.; GBD 2017 SDG Collaborators. Measuring progress from 1990 to 2017 and projecting attainment to 2030 of the health-related Sustainable Development Goals for 195 countries and territories: a systematic analysis for the Global Burden of Disease Study 2017. Lancet. 2018;392:2091–138. https://doi.org/10.1016/S0140-6736(18)32281-5
15. Keita AK, Dubot-Pérès A, Phommasone K, Sibounheuang B, Vongsouvath M, Mayxay M, et al. High prevalence of *Tropheryma whipplei* in Lao kindergarten children. PLoS Negl Trop Dis. 2015;9:e0003538. https://doi.org/10.1371/journal.pntd.0003538

Address for correspondence: Gerhard E. Feurle, DRK Krankenhaus Neuwied, Innere Medizin I, Marktstrasse 104, 56564 Neuwied, Germany; email: g.e.feurle@t-online.de

Extraintestinal Seeding of *Salmonella enterica* Serotype Typhi, Pakistan

Seema Irfan, Mohammad Zeeshan, Salima Rattani, Joveria Farooqi, Sadia Shakoor, Rumina Hasan, Afia Zafar

We evaluated *Salmonella enterica* serotype Typhi strains isolated from all body sites in Pakistan during 2013–2018. Despite an increase in overall number of localized, extensively drug-resistant *Salmonella* Typhi in organ infections during 2018, there was no increase in the proportion of such isolates in comparison with non–extensively drug-resistant isolates.

Salmonella enterica serotype Typhi is a major pathogen affecting populations from low- and middle-income countries that generally lack clean, potable water and good sanitary disposal systems (*1*). The global incidence of enteric fever is ≈21 million cases annually, and there are ≈200,000 typhoid-related deaths/year (*2*). Pakistan is among the high-burden countries that has reported annual incidence of 493.5 case/100,000 persons (*3*–*5*). Seeding of deep-seated organs by *Salmonella* Typhi, resulting in bone and soft tissue infections and splenic and hepatic abscesses, has been reported (*6*–*9*). Extensively drug-resistant (XDR) *Salmonella* Typhi, a strain resistant to 5 groups of antimicrobial drugs, including third-generation cephalosporins (*10*,*11*), has emerged in 2 cities in the southern part of Sindh Province and further disseminated to other parts of Pakistan, raising concern for persistence of the organism in hosts because of delays in appropriate therapy.

During 2018, a sudden increase in isolation frequency of XDR *Salmonella* Typhi from clinical samples other than blood, stool, and urine in Pakistan was observed. We conducted a study to determine if there was a true increase in the proportion of extraintestinal XDR *Salmonella* Typhi infections compared with non-XDR infections.

The Study

This study was conducted at the clinical microbiology laboratory at Aga Khan Hospital (Karachi, Pakistan). After approval was obtained from the Ethical Review Committee at Aga Khan Hospital, all reports of clinical specimens that showed growth of *Salmonella* Typhi during January 2013–December 2018 were extracted from the laboratory database and included in the study. The frequency of isolation of the organism from extraintestinal organ infections was compared with that of blood/bone marrow, stool, and urine. In addition, informed consent and detailed history were obtained by telephone from patients who had XDR *Salmonella* Typhi isolated from sites other than blood/bone marrow, stool, and urine during 2018.

Salmonella Typhi were identified by using conventional biochemical reactions and API 20E (bioMérieux, https://www.biomerieux.com) and then confirmed by serotyping with *Salmonella* antisera (Becton Dickinson, https://www.bd.com). Susceptibility testing was performed by using the disk diffusion Kirby-Bauer method and recent Clinical and Laboratory Standards Institute (https://clsi.org) performance standards. For XDR *Salmonella* Typhi strains, susceptibility was confirmed by using the Vitek2 System (bioMérieux), except for azithromycin, which was reported by using the disk diffusion method. The Pearson χ^2 test was applied to calculate the statistical significance by using Stata SE 12.1 software (https://www.stata.com).

During the 6-year study period, 8,736 isolates of *Salmonella* Typhi were reported from blood, bone marrow, stool, and urine, and 62 isolates were reported from other body sites (Table 1). Yearly isolation of *Salmonella* Typhi from different body sites gradually decreased during 2013–2017, but during 2018, there was a slight increase. In addition, although XDR *Salmonella* Typhi isolation from blood, feces, and urine had been consistently increasing since the beginning of outbreak, its isolation from other body sites was not observed until 2017. During 2018, these strains emerged from other sterile body tissues and fluids. However, their isolation

Author affiliation: Aga Khan University, Karachi, Pakistan

DOI: https://doi.org/10.3201/eid2703.200464

Table 1. *Salmonella enterica* serotype Typhi isolates from blood, feces, and urine versus other body sites, Pakistan 2013–2018

Characteristic		No. (%, 95% CI) in blood, feces, or urine	No. (%, 95% CI) in other body sites	Total cases	p value
No. ceftriaxone sensitive		5,858 (99.1, 98.9–99.4)	51 (0.86, 0.63–1.10)	5,909	0.011
No. ceftriaxone resistant		2,878 (99.6, 99.4–99.8)	11 (0.38, 0.16–0.61)	2,889	
Total		8,736 (99.3, 99.1–99.5)	62 (0.70, 0.53–0.88)	8,798	
Year	Ceftriaoxne susceptibility				
2013	Sensitive	662 (98.5, 97.6–99.4)	10 (1.49, 0.57–2.41)	672	0.902
	Resistant	0	0	0	
2014	Sensitive	701 (98.7, 97.9–99.6)	9 (1.27, 0.45–2.10)	710	0.873
	Resistant	0	0	0	
2015	Sensitive	881(98.9, 98.3–99.6)	9 (1.01, 0.36–1.68)	890	0.839
	Resistant	0	0	0	
2016	Sensitive	1,167 (99.5, 99.2–99.9)	5 (0.42, 0.05–0.80)	1,172	0.764
	Resistant	21 (100)*	0	21	
2017	Sensitive	1,299 (99.3, 98.9–99.8)	9 (0.69) 24–1.14)	1,308	0.057
	Resistant	526 (100)*	0	526	
2018†	Sensitive	1,155 (99.2, 98.7–99.7)	9 (0.77, 0.27–1.28)	1,164	0.264
	Resistant	2,324 (99.5, 99.3–99.8)	11 (0.47, 0.19–0.75)	2,335	

*Because 100% of extensively drug-resistant *Salmonella* Typhi were obtained from blood, stool, or urine, there was no 95% CI.
†A total of 20 (0.57%) of 3,499 *Salmonella* Typhi were isolated from other body sites during 2018.

proportion was not significant compared with non-XDR isolates (Table 1).

Most (7/11, 63.6%) cases showing growth of XDR *Salmonella* Typhi from other body sites were in children, but 4 (36.4%) were in adults. The average duration from fever onset until care was sought was ≈2 weeks. For 9 (81.8%) of 11 case-patients, complications came in the form of deep abscesses at body sites such as gluteal muscles, deltoid muscles, spleen, subdiaphragmatic recess, pleural cavity, breast, and fractured site of a limb. One case-patient who had no concurrent conditions had acute meningitis, and another case-patient had acute abdominal pain secondary to intestinal perforation and leading to pneumoperitoneum.

Antimicrobial drugs such as clindamycin, ciprofloxacin, amoxicillin/clavulanic acid, ceftriaxone, and cefepime showed inappropriate coverage and treatment duration against XDR *Salmonella* Typhi and were used for 8/11 (72.7%) patients during the course of illness. One patient was lost to follow up, but 10/11 (90.9%) patients showed marked improvement after appropriate antimicrobial drug treatment (intramuscular meropenem or oral azithromycin) and survived (Table 2, https://wwwnc.cdc.gov/EID/article/27/3/20-0464-T2.htm).

Conclusions

Our study was a comparison of isolation rates of XDR and non-XDR *Salmonella* Typhi from extraintestinal organ infections after the recognition of an XDR *Salmonella* Typhi outbreak in Pakistan. Our laboratory data highlights that, although isolation of XDR *Salmonella* Typhi from blood cultures has been performed since 2016, emergence and detection of XDR *Salmonella* Typhi from other body sites started during 2018, indicating a lag period of 14 months between the outbreak and extraintestinal organ infections. Except for 1 case of postileal perforation and collection of intraabdominal material, most of these manifestations were probably secondary to bacteremic seeding at various body sites. According to disease pathogenesis, different factors can contribute toward typhoid complication, including host-related factors, such as defects in innate immunity, any existing scar in soft tissue, inappropriate use of antimicrobial drugs, and organism-related virulence factors (*12*).

In this study, apparent immune dysfunction was found in only 2 patients: a 45-year-old woman who had a breast abscess and diabetes mellitus, and a 15-year-old boy who had splenic abscess and autoimmune hepatitis. A 55-year-old patient had a history of splenic injury and later showed development of a splenic abscess. Inappropriate antimicrobial drug use (Table 2), a common finding for most uncomplicated enteric fever cases, could be another contributing factor for uncontrolled disease process, leading to complications. However, this factor cannot solely be identified as a risk factor for these complicated cases. Another finding was that 4 of 11 extraintestinal organ infections were in adults, despite enteric fever being a disease with highest occurrence among children. We suggest future cohort studies to determine the reason for this delay in appearance and distribution of complicated cases.

Our data showed that during 2013–2018, irrespective of susceptibility pattern, the proportion of complicated enteric fever cases in Pakistan decreased (Table 1). Nonetheless, this finding could be a false impression and might be caused by an extraordinary increase in number of blood cultures requested during recent years. In Pakistan, laboratory diagnosis of enteric

fever is commonly made on the basis of either positive serologic test results or blood culture. In view of low sensitivity and specificity of available serologic tests, our clinical laboratory purposely removed these isolates from its test procedure during 2015. Thus, blood culture is currently used as the main tool for diagnosis of enteric fever. During 2017, the number of XDR *Salmonella* Typhi cases increased from 21 during 2016 to 526 during 2017, but there was no similar emergence of XDR *Salmonella* Typhi in deep-seated infections.

Whole-genome sequencing of initial outbreak XDR isolates identified plasmid encoding resistance elements, including the $bla_{\text{CTX-M-15}}$ extended-spectrum β-lactamase carrying the *qnrS* fluoroquinolone resistance gene. This IncY plasmid exhibited high sequence identity to plasmids found in other enteric bacteria isolated from widely distributed geographic locations (*13*). However, in our study, molecular analysis was not performed, which is a limitation. In addition, our study was retrospective and single-laboratory based. Therefore, our study does not reflect the experience from other centers.

There was no increase in the proportion of XDR *Salmonella* Typhi extraintestinal isolates compared with non-XDR isolates. Because of the high endemicity of XDR *Salmonella* Typhi in Pakistan, general practitioners in outpatient clinics usually start empirical treatment for enteric fever on the basis of clinical judgment and serologic investigations. Enteric fever clinical practice guidelines specific to Pakistan are available (*14*) and should be followed to avoid complications of the disease. Lack of physician awareness regarding extraintestinal seeding of *Salmonella* Typhi can lead to inappropriate treatment. Thus, culturing of organisms is recommended before starting treatment.

Acknowledgments

We thank Yusra Shafqat for collecting clinical information, Faisal Malik for collecting laboratory data, and Ghazala Jabeen and Samia Tariq for providing technical support.

About the Author

Dr. Irfan is a clinical microbiologist and associate professor in the department of pathology and Laboratory Medicine at Aga Khan University, Karachi, Pakistan. Her primary research interests are antimicrobial drug resistance, its laboratory detection methods, testing newer drug options, and infection prevention and control.

References

1. Mogasale V, Maskery B, Ochiai RL, Lee JS, Mogasale VV, Ramani E, et al. Burden of typhoid fever in low-income and middle-income countries: a systematic, literature-based update with risk-factor adjustment. Lancet Glob Health. 2014;2:e570–80. https://doi.org/10.1016/S2214-109X(14)70301-8
2. Matono T, Morita M, Yahara K, Lee K-i, Izumiya H, Kaku M, et al. Emergence of resistance mutations in *Salmonells enterica* serovar Typhi against fluoroquinolones. Open Forum Infect Dis. 2017;4:eofx230.
3. Malik A, Yasar A, Tabinda A, Abubakar M. Water-borne diseases, cost of illness and willingness to pay for diseases interventions in rural communities of developing countries. Iran J Public Health. 2012;41:39–49.
4. Daud MK, Nafees M, Ali S, Rizwan M, Bajwa RA, Shakoor MB, et al. Drinking water quality status and contamination in Pakistan. BioMed Res Int. 2017; 2017:7908183. https://doi.org/10.1155/2017/7908183
5. Das JK, Hasan R, Zafar A, Ahmed I, Ikram A, Nizamuddin S, et al. Trends, associations, and antimicrobial resistance of *Salmonella typhi* and *paratyphi* in Pakistan. Am J Trop Med Hyg. 2018;99(Suppl):48–54. https://doi.org/10.4269/ajtmh.18-0145
6. Huang DB, DuPont HL. Problem pathogens: extra-intestinal complications of *Salmonella enterica* serotype Typhi infection. Lancet Infect Dis. 2005;5:341–8. https://doi.org/10.1016/S1473-3099(05)70138-9
7. Rohilla R, Bhatia M, Gupta P, Singh A, Shankar R, Omar BJ. *Salmonella* osteomyelitis: a rare extraintestinal manifestation of an endemic pathogen. J Lab Physicians. 2019;11:164–70. https://doi.org/10.4103/JLP.JLP_165_18
8. Villablanca P, Mohananey D, Meier G, Yap JE, Chouksey S, Abegunde AT. *Salmonella* Berta myocarditis: case report and systematic review of non-typhoid *Salmonella* myocarditis. World J Cardiol. 2015;7:931–7. https://doi.org/10.4330/wjc.v7.i12.931
9. Meyyur Aravamudan V, Kee Fong P, Singh P, Sze Chin J, Sam YS, Tambyah PA. Extraintestinal salmonellosis in the immunocompromised: an unusual case of pyomyositis. Case Rep Med. 2017;2017:5030961. https://doi.org/10.1155/2017/5030961
10. Mushtaq MA. What after ciprofloxacin and ceftriaxone in treatment of *Salmonella* Typhi. Pak J Med Sci. 2006;22:51–4.
11. Qamar FN, Azmatullah A, Kazi AM, Khan E, Zaidi AK. A three-year review of antimicrobial resistance of *Salmonella enterica* serovars Typhi and Paratyphi A in Pakistan. J Infect Dev Ctries. 2014;8:981–6. https://doi.org/10.3855/jidc.3817
12. Crump JA, Sjölund-Karlsson M, Gordon MA, Parry CM. Epidemiology, clinical presentation, laboratory diagnosis, antimicrobial resistance, and antimicrobial management of invasive *Salmonella infections*. Clin Microbiol Rev. 2015;28:901–37. https://doi.org/10.1128/CMR.00002-15
13. Klemm EJ, Shakoor S, Page AJ, Qamar FN, Judge K, Saeed DK, et al. Emergence of an extensively drug-resistant *Salmonella enterica* serovar Typhi clone harboring a promiscuous plasmid encoding resistance to fluoroquinolones and third-generation cephalosporins. MBio. 2018;9:e00105-18. https://doi.org/10.1128/mBio.00105-18
14. National Institute of Health. Advisory for prevention and treatment of typhoid fever including XDR typhoid, July 2020 [cited 2020 Nov 27]. https://www.nih.org.pk/wp-content/uploads/2020/07/Advisory-for-Prevention-and-Treatment-of-Typhoid-Fever-including-XDR-Typhoid.pdf

Address for correspondence: Seema Irfan, Section of Microbiology, Department of Pathology and Laboratory Medicine, Aga Khan University, PO Box 3500, Stadium R, Karachi 74800, Pakistan; email: seema.irfan@aku.edu

Human Infection with Eurasian Avian-Like Swine Influenza A(H1N1) Virus, the Netherlands, September 2019

Anna Parys, Elien Vandoorn, Jacqueline King, Annika Graaf, Anne Pohlmann, Martin Beer, Timm Harder, Kristien Van Reeth

We report a zoonotic infection of a pig farmer in the Netherlands with a Eurasian avian-like swine influenza A(H1N1) virus that was also detected in the farmed pigs. Both viruses were antigenically and genetically characterized. Continued surveillance of swine influenza A viruses is needed for risk assessment in humans and swine.

Eurasian avian-like swine influenza A(H1N1) viruses (IAVs) are entirely derived from a precursor virus of avian origin (*1*) and have been enzootic in the swine population in Europe since 1979 and in Asia since 1993. Zoonotic infections with such viruses, which are then termed H1N1 variant (H1N1v) viruses, occur sporadically. Most cases occur in humans who have direct exposure to pigs. Since 1986, several human cases of Eurasian avian-like H1N1 swine IAV have been reported in Europe (*2*–*4*) and China (*3*,*5*).

These events reflect the possibility of Eurasian avian-like H1N1 swine IAV transmission from swine to humans. In this study, we report an infection with a Eurasian avian-like H1N1 swine IAV in a pig farmer and his pigs in a herd in the Netherlands. We also conducted whole-genome characterization of viruses from the man and the pigs.

The Study

On September 18, 2019, acute respiratory disease was observed in a 43-year-old man (farmer) and his 14-week-old fattening pigs and gilts. The pigs of this closed farm showed coughing, anorexia, tachypnea, dyspnea, and lethargy. Two days earlier, a 44-year-old man (animal caretaker) had reported similar symptoms. The sows of this herd (n = 420) were vaccinated against swine IAVs with Respiporc FLU3 vaccine (Ceva, https://www.ceva.com), but the farmer and animal caretaker were not recently vaccinated against human seasonal influenza viruses. Both humans and the pigs recovered completely within 10 days after the first appearance of signs or symptoms. Family members and close contacts of the men did not show development of influenza-like symptoms.

Six days after onset of disease, nasal swab samples were collected from the farmer, the animal caretaker, and 6 symptomatic pigs. Human samples were collected by self-sampling, and informed consent was obtained from the farmer and the animal caretaker. Subsequently, samples were shipped to the Laboratory of Virology, Faculty of Veterinary Medicine, Ghent University (Merelbeke, Belgium).

Upon inoculation into MDCK cells, IAV was isolated from the sample of the farmer and from a pooled sample of the pigs; no virus was isolated from the animal caretaker. Public health authorities in the Netherlands were notified about the H1N1v infection. The human H1N1v isolate was named A/Netherlands/Gent-193/2019, and the swine H1N1 isolate was named A/swine/Netherlands/Gent-193/2019.

Virus neutralization tests with swine antiserum against swine IAVs of the H1N1, H1N2, and H3N2 subtypes showed an antigenic relationship between both newly discovered isolates and Eurasian avian-like H1N1 swine IAVs from 1998 and 2010, as well as the prototype influenza A(H1N1)pdm09 (pH1N1) A/California/04/2009 virus. Serologic cross-reactivity with H1N2 or H3N2 swine IAVs was not observed (Table 1).

Initial analyses by multiplex real-time reverse transcription PCRs (*6*) and whole-genome next-generation

Author affiliation: Ghent University, Merelbeke, Belgium (A. Parys, E. Vandoorn, K. Van Reeth); Friedrich-Loeffler-Institut, Greifswald Insel-Riems, Germany (J. King, A. Graaf, A. Pohlmann, M. Beer, T. Harder)

DOI: https://doi.org/10.3201/eid2703.201863

Table 1. Cross-reactivity in virus neutralization tests between isolates from a pig farmer and his pigs and reference swine H1N1, pH1N1, H1N2 and H3N2 viruses*

			Virus neutralization titer for swine antiserum†						
Virus	Subtype	H1 clade	swBe98	swG10	Ca09	swG99	swG12	swFl98	swG08
swBe98	H1N1	1C.2	**4,096**	256	96	32	<4	<4	<4
swG10	H1N1	1C.2.1	48	**768**	12	<4	<4	<4	<4
Ca09	pH1N1	1A.3.3.2	12	96	**1,536**	<4	<4	<4	<4
swG99	H1N2	1B.1.2.1	6	<4	4	**1,024**	768	<4	<4
swG12	H1N2	1B.1.2.1	<4	<4	6	768	**1,536**	<4	<4
swFl98	H3N2	NA	<4	<4	4	<4	<4	**8,129**	512
swG08	H3N2	NA	<4	<4	<4	<4	<4	3,072	**768**
Ne19	H1N1v	1C.2.2	128	64	8	<4	<4	<4	<4
swNe19	H1N1	1C.2.2	256	384	1,536	8	<4	<4	<4

*Ne19 indicates isolate from the farmer; swNe19 indicates the isolate from the pigs. Homologous titers are indicated in bold. H1N1v, H1N1 variant; NA, not applicable; pH1N1, influenza A(H1N1)pdm09; swBe98, A/swine/Belgium/1/98; swG10, A/swine/Gent/28/2010; Ca09, A/California/04/2009; swG99, A/swine/Gent/7625/99; swG12, A/swine/Gent/26/2012; swFl98, A/swine/Flanders/1/98; swG08, A/swine/Gent/172/2008; Ne19, A/Netherlands/Gent-193/2019; swNe19, A/swine/Netherlands/Gent-193/2019.
†Swine antiserum was obtained by a double vaccination with whole inactivated virus vaccines.

sequencing (*7*) of both isolates confirmed that all genome segments were closely related to those of Eurasian avian-like H1N1 swine IAVs. A BLAST homology search (http://www.fludb.org) with both whole genomes showed highest nucleotide identities (96%) for hemagglutinin (HA) and neuraminidase with clade 1C.2.2 Eurasian avian-like H1N1 swine IAVs isolated in Germany and the Netherlands during 2011–2012. These databases contain limited numbers of sequences of this swine IAV clade, which explains the lack of similar recent viruses. A phylogenetic tree of Eurasian avian-like H1N1 swine IAVs isolated in Europe and Asia was constructed by using MEGA7 software (https://www.megasoftware.net). Phylogenetic analysis confirmed the genetic relationship of the HA1 genes of both isolates with Eurasian

Table 2. Influenza virus sequences downloaded from GenBank, GISAID, or unpublished data and used in phylogenetic analysis*

Isolate	Country	Collection date	Date of download	Accession no.
A/swine/Finistere/2899/82	France	1982	2019 Nov 16	AJ344015
A/Netherlands/386/86	Netherlands	1986	2019 Nov 16	AF320065
A/Netherlands/477/93	Netherlands	1993	2019 Nov 16	AF320066
A/swine/Denmark/19126/93	Denmark	1993	2019 Nov 16	KC900289
A/swine/Netherlands/609/96	Netherlands	1996	2019 Nov 16	AF320064
A/swine/Belgium/1/98	Belgium	1998	2019 Nov 17	AY590824
A/swine/Italy/1513–1/98	Italy	1998	2019 Nov 16	CY116458
A/Switzerland/8808/2002	Switzerland	2002	2019 Nov 16	AJ517815
A/swine/Spain/50047/2003	Spain	2003	2019 Nov 7	CY009892
A/swine/Spain/53207/2004	Spain	2004	2019 Nov 17	KR700597
A/swine/Zhejiang/1/2007	China	2007 Nov 15	2019 Nov 7	FJ415610
A/swine/Germany/SIV04/2008	Germany	2008 Jun	2019 Nov 16	FN429078
A/swine/France/CotesdArmor-0388/2009	France	2009 Jul 28	2019 Nov 17	KC881265
A/swine/Gent/28/2010	Belgium	2010 Jan 13	2019 Jul 29	KP406525
A/Jiangsu/1/2011	China	2011 Jan 4	2019 Nov 23	KF057112
A/swine/Jiangsu/40/2011	China	2011 Jan 9	2019 Nov 23	JQ319648
A/swine/Germany/Wunnenberg-IDT13220/2011	Germany	2011 Mar 31	2019 Dec 16	KR699726
A/swine/Germany/Reinberg-IDT14457–1/2012	Germany	2012 Jan 2	2019 Dec 16	KR700366
A/swine/Netherlands/Dalfsen-12/2012	Netherlands	2012 Jan 10	2019 Dec 16	KR700020
A/swine/Germany/Ellerbrock-IDT14696/2012	Germany	2012 Jan 18	2019 Dec 16	KR700389
A/swine/Gent/62/2015	Netherlands	2015 Mar 19	NA	Unpub. data†
A/Hunan/42443/2015	China	2015 Jul 2	2020 Jun 15	EPI206573‡
A/swine/Gent/173/2015	Belgium	2015 Sep 4	NA	Unpub.data†
A/Pavia/65/2016	Italy	2016 Oct	2020 Mar 27	KY368150
A/Netherlands/3315/2016	Netherlands	2016 Oct	2020 Mar 27	KY250319
A/swine/Gent/150/2016	Belgium	2016 Nov 18	NA	Unpub. data†
A/swine/Gent/196/2018	Belgium	2018 Oct 12	NA	Unpub. data†
A/swine/Gent/241/2018	Belgium	2018 Nov 4	NA	Unpub. data†
A/swine/Gent/05/2019	Belgium	2019 Jan 9	NA	Unpub. data†
A/swine/Gent/54/2019	Belgium	2019 Mar 13	NA	Unpub. data†
A/swine/Netherlands/Gent-193/2019	Netherlands	2019 Sep 24	2020 Apr 29	MT395373
A/Netherlands/Gent-193/2019	Netherlands	2019 Sep 24	2020 Apr 29	MT395365
A/swine/Gent/203/2019	Belgium	2019 Oct 9	NA	Unpub. data†

*Accession numbers are from GenBank except as indicated. NA, not applicable.
†Ghent University (Merelbeke, Belgium).
‡GISAID, https://www.gisaid.org.

avian-like H1N1 swine IAVs of clade 1C.2.2 (Table 2; Figure).

The human H1N1v and swine H1N1 isolates differed in several positions in the genes coding for the 3 polymerase proteins (polymerase basic [PB] 2, PB1, and polymerase acidic), the HA gene, and the nonstructural protein gene. The other 3 gene segments (neuraminidase, nucleoprotein, and matrix) were 100% identical. HA gene sequences of the swine H1N1 and the human H1N1v isolates showed amino acid substitutions K142N, N195S, and V215I (H1 numbering). Position 142 is located in antigenic site Ca2 142 and position 195 in antigenic site Sb (*8*). In human seasonal influenza A(H1N1) viruses, a substitution at position 142 was reported to cause antigenic change (*9*). This substitution might explain the loss of reactivity with pH1N1 antiserum for the human H1N1v isolate versus the swine H1N1 isolate (Table 1). In addition, in H5 IAVs this substitution decreased the pH at which the HA underwent fusion (*10*).

Because human-adapted viruses undergo fusion at a lower pH (5.0–5.5) than swine-adapted and avian-adapted viruses (pH 5.6–6.0), such mutations might contribute to human adaptation of zoonotic viruses. We found multiple substitutions in the polymerase genes of the human H1N1v isolate: R739Q in PB2, L108I and T652A in PB1, and D682N in polymerase acidic. Based on analyses in the FluSurver database (http://flusurver.bii.a-star.edu.sg/), the R739Q

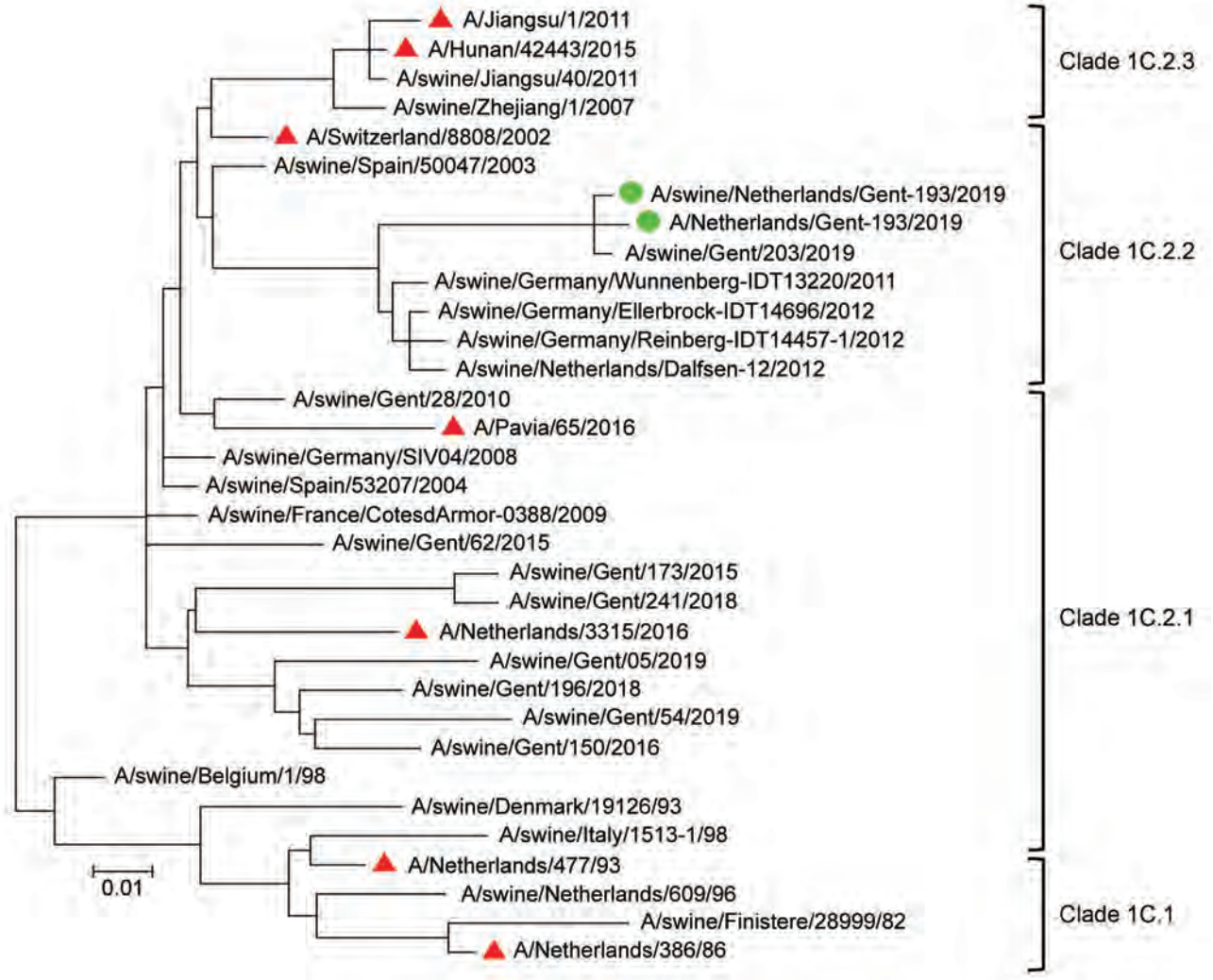

Figure. Phylogenetic tree based on amino acid sequences of the hemagglutinin 1 of Eurasian avian-like swine influenza A(H1N1) virus isolates from a pig farmer and his pigs (green circles), the Netherlands, and reference sequences (see Table 2). Red triangles indicate reference sequences from humans. Phylogenetic relationships were estimated by using the maximum-likelihood method in MEGA7 software (https://www.megasoftware.net) and the Jones-Taylor-Thornton substitution model with a gamma distribution of among-site rate. Branch length is proportional to genetic distance. Scale bar indicates amino acid substitutions per site.

substitution in the PB2 gene might influence the binding of PB2 to host protein(s). We also found 2 substitutions in the nonstructural protein gene: V18I and G227R. Sequences were made publicly available in GenBank (accession nos. MT395362–77), and GISAID (https://www.gisaid.org; accession nos. EPI_ISL_430866 [A/swine/Netherlands/Gent-193/2019] and EPI_ISL_0865 [A/Netherlands/Gent-193/2019]).

Conclusions

We report another zoonotic infection with a Eurasian avian-like H1N1 swine IAV in Europe since the emergence of the virus in 1979 (*2*–*4*). No further human-to-human transmission was reported, although it cannot be excluded that the farmer was infected by the animal caretaker. The nasal swab sample from the caretaker might have tested negative because it was collected as late as 8 days after he reported influenza-like symptoms.

The swine antiserum against the pH1N1 virus cross-reacted with the swine H1N1 isolate from this investigation (Table 1) but had a 192-fold lower virus neutralization titer against the human H1N1v isolate. Therefore, it is unlikely that current human seasonal vaccines would provide cross-protection against the human H1N1v isolate. This finding is consistent with our recent investigations of human serum samples for antibodies against 8 H1 swine IAVs representing 7 predominant H1 clades of swine IAVs; only 55 (10%) of 549 human serum samples had hemagglutination inhibition titers ≥40 against a European avian-like H1N1 swine IAV of clade 1C.2.1, which is predominant in swine in Europe (*11*), compared with 24%–54% against 5 other clades (*12*). These data point toward a relatively greater zoonotic risk for avian-like H1N1 swine IAVs from Europe and are consistent with previous studies about Eurasian avian-like H1N1 swine IAVs from China (*5*,*13*). Our data further support the notion that Eurasian avian-like H1N1 swine IAVs need to be monitored closely.

We found several amino acid substitutions between the H1N1 swine isolate and the H1N1v human isolate, but their role remains obscure. The past 2 decades have seen an unprecedented increase of data for putative mammalian-adaptive mutations of avian influenza viruses. The known genetic markers are mainly based on studies with wholly avian viruses of various HA subtypes in mammalian cell culture or in ferrets. Knowledge of amino acid substitutions that might enable adaptation of swine-adapted influenza viruses to humans, in contrast, is almost nonexistent (*14*). This finding is true for Eurasian avian-like H1N1 swine IAVs, as well as for the pH1N1 virus, which is the only known swine-origin virus with the ability to spread efficiently between humans. Our study highlights the need for experimental research on this topic and for continued surveillance of swine IAVs because of the risk for human infection or zoonotic spread.

Acknowledgments

We thank the farmer, animal caretaker, and veterinarian for their cooperation and Nele Dennequin and Melanie Bauwens for providing technical assistance.

This study was supported by the University of Ghent Research Fund Bijzonder OnderzoeksFonds (grant no. 01J102017) and the European Union Horizon 2020 Research and Innovation Programme (grant no. 727922 DELTA-FLU).

About the Author

Ms. Parys is a PhD student in the Laboratory of Virology, Faculty of Veterinary Medicine, Ghent University, Merelbeke, Belgium. Her primary research interests are the pig as a model for development of broadly protective influenza A vaccines and public health implications of swine influenza.

References

1. Pensaert M, Ottis K, Vandeputte J, Kaplan MM, Bachmann PA. Evidence for the natural transmission of influenza A virus from wild ducks to swine and its potential importance for man. Bull World Health Organ. 1981;59:75–8.
2. Freidl GS, Meijer A, de Bruin E, de Nardi M, Munoz O, Capua I, et al.; FLURISK Consortium. Influenza at the animal-human interface: a review of the literature for virological evidence of human infection with swine or avian influenza viruses other than A(H5N1). Euro Surveill. 2014;19:20793. https://doi.org/10.2807/1560-7917.ES2014.19.18.20793
3. World Health Organization. Antigenic and genetic characteristics of zoonotic influenza viruses and development of candidate vaccine viruses for pandemic preparedness [cited 2020 Jun 18]. https://www.who.int/influenza/vaccines/virus/202009_zoonotic_vaccinevirusupdate.pdf
4. European Centre for Disease Prevention and Control. Update: swine-origin triple reassortant influenza A(H3N2) variant viruses in North America, 2012. Stockholm: The Centre [cited 2020 Dec 9]. https://www.ecdc.europa.eu/sites/default/files/media/en/publications/publications/1208-ter-rapid-risk-assessment-influenza-ah3n2-us.pdf
5. Sun H, Xiao Y, Liu J, Wang D, Li F, Wang C, et al. Prevalent Eurasian avian-like H1N1 swine influenza virus with 2009 pandemic viral genes facilitating human infection. Proc Natl Acad Sci U S A. 2020;117:17204–10. https://doi.org/10.1073/pnas.1921186117
6. Henritzi D, Zhao N, Starick E, Simon G, Krog JS, Larsen LE, et al. Rapid detection and subtyping of European swine influenza viruses in porcine clinical samples by haemagglutinin- and neuraminidase-specific tetra- and triplex real-time RT-PCRs. Influenza Other Respir Viruses. 2016;10:504–17. https://doi.org/10.1111/irv.12407

7. King J, Schulze C, Engelhardt A, Hlinak A, Lennermann SL, Rigbers K, et al. Novel HPAIV H5N8 reassortant (Clade 2.3.4.4b) detected in Germany. Viruses. 2020;12:1–7. https://doi.org/10.3390/v12030281
8. Brownlee GG, Fodor E. The predicted antigenicity of the haemagglutinin of the 1918 Spanish influenza pandemic suggests an avian origin. Philos Trans R Soc Lond B Biol Sci. 2001;356:1871–6. https://doi.org/10.1098/rstb.2001.1001
9. Harvey WT, Benton DJ, Gregory V, Hall JPJ, Daniels RS, Bedford T, et al. Identification of low- and high-impact hemagglutinin amino acid substitutions that drive antigenic drift of influenza A (H1N1) viruses. PLoS Pathog. 2016;12:e1005526. https://doi.org/10.1371/journal.ppat.1005526
10. Rudneva IA, Timofeeva TA, Ignatieva AV, Shilov AA, Krylov PS, Ilyushina NA, et al. Pleiotropic effects of hemagglutinin amino acid substitutions of H5 influenza escape mutants. Virology. 2013;447:233–9. https://doi.org/10.1016/j.virol.2013.09.013
11. Anderson TK, Macken CA, Lewis NS, Scheuermann RH, Van Reeth K, Brown IH, et al. A phylogeny-based global nomenclature system and automated annotation tool for H1 hemagglutinin genes from swine influenza A viruses. MSphere. 2016;1:e00275–16. https://doi.org/10.1128/mSphere.00275-16
12. Vandoorn E, Leroux-Roels I, Leroux-Roels G, Parys A, Vincent A, Van Reeth K. Detection of H1 swine influenza A virus antibodies in human serum samples by age group. Emerg Infect Dis. 2020;26:2118–28. https://doi.org/10.3201/eid2609.191796
13. Yang H, Chen Y, Qiao C, He X, Zhou H, Sun Y, et al. Prevalence, genetics, and transmissibility in ferrets of Eurasian avian-like H1N1 swine influenza viruses. Proc Natl Acad Sci U S A. 2016;113:392–7. https://doi.org/10.1073/pnas.1522643113
14. Pulit-Penaloza JA, Belser JA, Tumpey TM, Maines TR. Sowing the seeds of a pandemic? Mammalian pathogenicity and transmissibility of H1 variant influenza viruses from the swine reservoir. Trop Med Infect Dis. 2019;4:1–21. https://doi.org/10.3390/tropicalmed4010041

Address for correspondence: Kristien Van Reeth, Laboratory of Virology, Faculty of Veterinary Medicine, Ghent University, Salisburylaan 133, 9820 Merelbeke, Belgium; email: kristien.vanreeth@ugent.be

EID Podcast:
Two Ways of Tracking *C. difficile* in Switzerland

Science wields many different tools in the pursuit of public health. These tools can work together to capture a detailed picture of disease. However, many tools accomplish similar tasks, often leaving policymakers wondering, when it comes to disease surveillance, what is the best tool for the job?

Different tests are currently used to diagnose *Clostridioides difficile*, a dangerous bacterium found in hospitals around the world. As rates of this infection surge globally, researchers need to be able to compare statistics from different hospitals, regions, and countries.

In this EID podcast, Sarah Tschudin-Sutter, a professor of infectious disease epidemiology at the University Hospital - Basel in Switzerland, discusses using 2 tests for *C. difficile* infection in Europe.

Visit our website to listen:
https://go.usa.gov/xGEuz

EMERGING INFECTIOUS DISEASES

Bedaquiline as Treatment for Disseminated Nontuberculous *Mycobacteria* Infection in 2 Patients Co-Infected with HIV

Eliza Gil, Nicola Sweeney, Veronica Barrett, Stephen Morris-Jones, Robert F. Miller, Victoria J. Johnston, Michael Brown

Nontuberculous mycobacteria can cause disseminated infections in immunocompromised patients and are challenging to treat because of antimicrobial resistance and adverse effects of prolonged multidrug treatment. We report successful treatment with bedaquiline, a novel antimycobacterial drug, as part of combination therapy for 2 patients with disseminated nontuberculous mycobacteria co-infected with HIV.

Nontuberculous mycobacteria (NTM) cause a broad spectrum of disease, most commonly pulmonary infection, but also cause disseminated infection in immunocompromised patients, posing a major risk for illness and death (*1*). Treatment involves immune function optimization and prolonged use of combinations of species-specific antimycobacterial drugs but is often complicated by the intrinsic or acquired drug resistance of NTM (*2*) and adverse effects of the drug combinations; treatment failure is common. Therefore, there is considerable interest in the use of novel drugs (*3*).

Bedaquiline, a novel, oral, diarylquinolone antimycobacterial drug, is used in treatment of infections with multidrug-resistant *Mycobacterium tuberculosis* (*4*). However, its role in treatment of disseminated NTM infections remains unclear. We report the successful use of bedaquiline in treatment for 2 HIV-infected patients in London, UK, who had disseminated NTM infections.

Author affiliations: University College London Hospitals, National Health Service Foundation Trust, London, UK (E. Gil, N. Sweeney, V. Barrett, S. Morris-Jones, V.J. Johnston, M. Brown); Central and North West London National Health Service Foundation Trust, London (R.F. Miller); University College London, London (R.F. Miller); London School of Hygiene and Tropical Medicine, London (R.F. Miller, V.J. Johnston, M. Brown)

DOI: https://doi.org/10.3201/eid2703.202359

The Study

Case-patient 1 was a 54-year-old HIV-infected man who had colonic perforation secondary to rectal trauma. He underwent an emergency Hartmann's procedure and showed an uncomplicated immediate recovery. Two months later, he showed development of fevers, breathlessness, and a purulent exudate at the abdominal wound site, which did not improve after receiving antimicrobial drug therapy. Imaging showed pleural effusions and perihepatic collections; mycobacterial liquid culture of effusions, collections, and wound exudate contained *M. abscessus*, presumed secondary to fecal abdominal cavity contamination. Mycobacterial blood cultures were negative.

At diagnosis of his disseminated NTM infection, HIV viral load was undetectable (CD4 count >900 cells/μL). Empirical treatment was begun and then refined after speciation as *M. abscessus* (Figure 1, panel A). Susceptibility testing subsequently demonstrated extensive drug resistance (Table 1). MIC estimations for bedaquiline showed in vitro susceptibility (MIC ≤0.0625 mg/L). There was no information on Clinical and Laboratory Standards Institute/European Committee on Antimicrobial Susceptibility Testing for *M. abscessus*. The MIC breakpoint for this drug with *M. tuberculosis* was 0.25 mg/L (T. McHugh, University College London, pers. comm., 2020 Jun 29). Compassionate access to bedaquiline was obtained from Janssen-Cilag (https://www.janssen.com). Treatment was initiated (400 mg/d for 2 wks, followed by 200 mg 3×/wk), as per treatment for tuberculosis. Bedaquiline was well tolerated and treatment continued for a year; there was a brief interruption because of a delay in reapproval.

During his treatment for NTM, the patient showed adverse effects caused by intravenous amikacin (1 g/d) and mild renal impairment. Therefore,

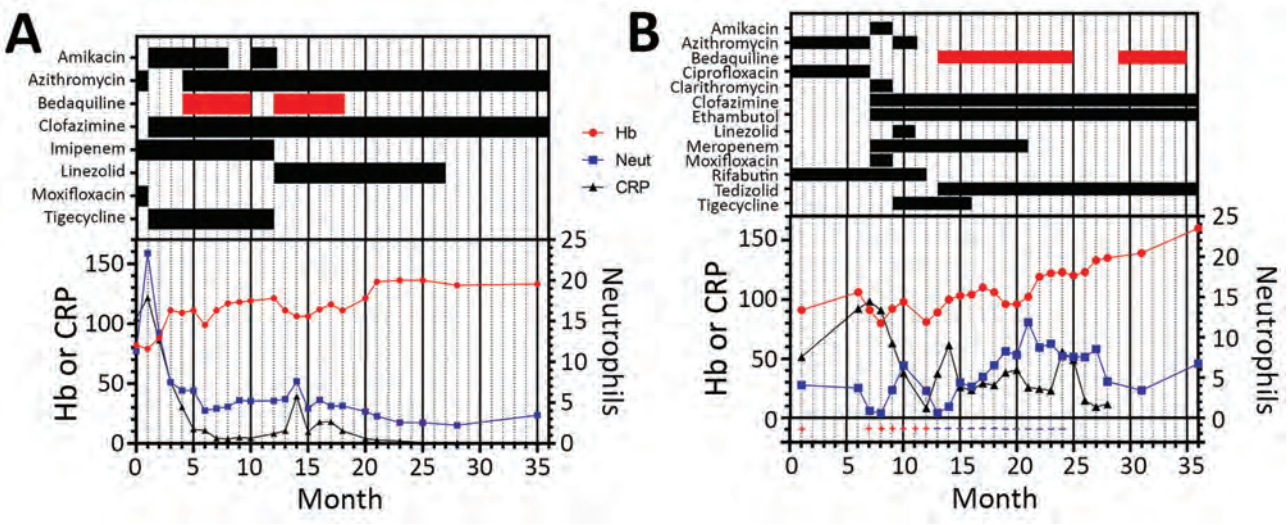

Figure 1. Summary of treatment and monitoring of 2 HIV-positive persons who had disseminated *Mycobacterium abscessus* infections, London, UK. A) Case-patient 1. B) Case-patient 2. The infection in case-patient 1 was secondary to fecal abdominal cavity contamination after rectal perforation. Bars in top section show timing of treatments; red indicates bedaquiline. Drug regimens and treatment responses were measured by using Hb (g/L), Neut ($\times 10^9$ cells/L), and CRP (mg/L). Values (+ and –) on the bottom of panel B are results for mycobacterial blood cultures. CRP, C-reactive protein; Hb, hemoglobin; Neut, neutrophils.

this drug was withheld until his renal function recovered. On its reinitiation at the same dose, tinnitus developed, prompting permanent withdrawal of amikacin. Because of excellent progress, tigecycline was replaced with linezolid at that time.

^{18}Fluorodeoxyglucose-positron emission tomography/computed tomography imaging was used to monitor disease response (Figure 2). Although pulmonary and hepatic lesions emerged intermittently, they were consistently culture negative and are believed to represent immune-mediated lesions. His most recent scan 36 months after treatment began showed ongoing, but greatly reduced, ^{18}fluorodeoxyglucose avidity in all areas. Therefore, he continues maintenance therapy with clofazimine and azithromycin, despite evidence of clarithromycin resistance in vitro. This combination (clofazimine and azithromycin) has been well tolerated, and the condition of the patient continues to be favorable.

Case-patient 2 was a 30-year-old man who had pyrexia, pancytopenia, and lymphadenopathy. Advanced HIV infection had been diagnosed 1 month earlier (CD4 count 10 cells/μL, viral load >1 million copies/mL). He started antiretroviral therapy 10 days before he came to the hospital. Culture of lymph node, peripheral blood, and sputum all yielded *M. avium*. Treatment with azithromycin, rifabutin, and ciprofloxacin was initiated. Ethambutol was excluded because of color blindness.

The patient initially transferred his care to another hospital but returned 6 months later because

Table 1. MICs and CLSI interpretation as reported by Public Health England reference laboratory for all drugs tested against *Mycobacterium abscessus* isolate from case-patient 1 (*5*)*

Drug	MIC, mg/L	CLSI interpretation
Amikacin	Month 0: 16	Sensitive
	Month 3: 32	Intermediate
Cefoxitin	128	Resistant
Ciprofloxacin	>4	Resistant
Clarithromycin	>16	Resistant (phenotype suggestive of inducible resistance)
Cotrimoxazole	>8/152	Resistant
Doxycycline	>16	Resistant
Imipenem	16	Intermediate
Linezolid	Month 0: 32	Resistant
	Month 3: 16	Intermediate
Moxifloxacin	>8	Resistant
Tigecycline	2	No defined breakpoints
Tobramycin	8	Resistant

*MICs were obtained for the initial isolate of the patient at month 0, and again at month 3. Where duplicated, values were consistent, except for amikacin and linezolid, where both MICs are included. CLSI, Clinical and Laboratory Standards Institute.

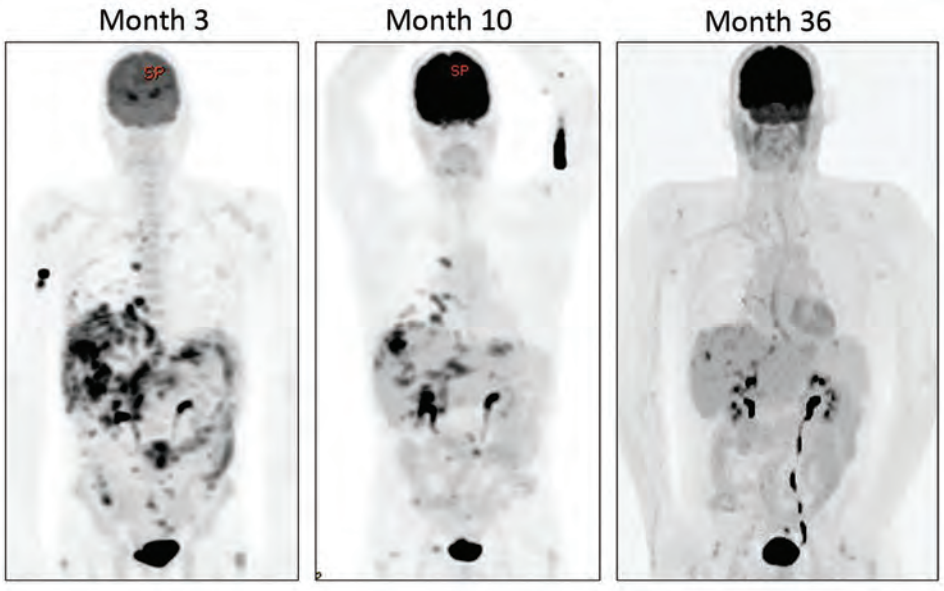

Figure 2. Serial ^{18}fluorodeoxyglucose-positron emission tomography/computed tomography imaging quantification of disease burden for an HIV-positive person (case-patient 1) given treatment for disseminated *Mycobacterium abscessus* infection, London, UK. Images demonstrate marked reduction in fluorodeoxyglucose avidity over time.

of abdominal pain. Mycobacterial blood cultures had remained persistently positive throughout the intervening period, and at his return cultures of blood, bone marrow, and lymph node were positive for *M. avium*. We performed sensitivity testing (Table 2). Few drugs have MIC values for *M. avium*, and the correlation between MIC and clinical outcomes for drugs other than clarithromycin is unclear (*5*). The isolate demonstrated new clarithromycin resistance, postulated to have emerged because of persistence through treatment with a macrolide-containing regimen without ethambutol (*6*). His treatment was intensified by addition of amikacin and, after discussion with ophthalmologists, ethambutol. Because he continued to have fevers, meropenem, which covered the possibility of bacterial sepsis, and clofazimine were initiated, leading to symptomatic improvement. Because his symptoms worsened again on brief cessation of meropenem, it was continued.

Treatment for this patient required multiple modifications because of adverse drug effects (Figure 1, panel B). Amikacin was stopped because of renal toxicity. Given the extensive in vitro resistance, best practice recommendation to add 2 drugs synchronously, lack of access to bedaquiline at this time, and evidence for a possible benefit of tigecycline in combination with a macrolide (*7*), tigecycline and linezolid were initiated in its place, causing nausea and anemia, respectively. He also had arthralgia secondary to moxifloxacin and QTc prolongation caused by azithromycin, which required their cessation.

Shortly after linezolid and azithromycin were discontinued, his fevers and neutropenia returned. Mycobacterial blood cultures again showed *M. avium* despite prolonged treatment and immune reconstitution. Although bedaquiline sensitivity of this isolate was not determined in vitro, compassionate access to bedaquiline was obtained from Janssen-Cilag, and treatment was initiated at month 13 (dosing as reported for case-patient 1), along with tedizolid. Rifabutin was discontinued because of concerns over its effect on bedaquiline pharmacokinetics.

Table 2. MICs and CLSI interpretation as reported by Public Health England reference laboratory for all drugs tested against *Mycobacterium abscessus* isolate from case-patient 2 (*5*)*

Drug	MIC, mg/L	CLSI interpretation
Amikacin intravenous	>64	Resistant
Ciprofloxacin	>16	No defined breakpoints
Clarithromycin	Not reported	Month 0: sensitive; month 6: high-level resistance
Doxycycline	>16	No defined breakpoints
Ethambutol	>16	No defined breakpoints
Linezolid	64	Resistant
Moxifloxacin	>8	Resistant
Rifampin	>8	No defined breakpoints

*MICs were calculated for the isolate at the initial presentation (month 0) of the patient and again at his representation 6 mo later. The second testing identified a new high level of resistance. CLSI, Clinical and Laboratory Standards Institute.

After bedaquiline and tedizolid were initiated, his fevers resolved, and he made a steady recovery and had no side effects. Given his high risk for relapse, he received bedaquiline for 18 months on the advice of the British Thoracic Society panel, ensuring a year of effective therapy since his last positive blood culture. He has successfully immune reconstituted, continues to receive only antiretroviral therapy, and remains healthy.

Conclusions

Treating disseminated NTM infections is challenging and often complicated by antimicrobial resistance and adverse effects of combination drug therapy. In multidrug-resistant *M. tuberculosis*, bedaquiline has been shown to decrease the time to sputum culture negativity and improve outcomes (*8*), leading to interest in its use for NTM infections.

In vitro sensitivity of NTM to bedaquiline has been demonstrated (*9*,*10*), although several species, including *M. novocastrense*, *M. shimodei*, and *M. xenopi*, are intrinsically resistant (*11*). In addition, although bedaquiline is bactericidal against many mycobacterial species, it might only be bacteriostatic against *M. avium* (*12*). Despite this feature, bedaquiline has been used in salvage treatment for pulmonary infections with NTM (*13*), but little experience regarding its use for disseminated NTM infections has been published.

These 2 case-patients were given bedaquiline on compassionate grounds, given the lack of alternative options because of drug resistance and toxicity. For both patients, bedaquiline enabled construction of an antimicrobial drug regimen that included >2 drugs to which the organism was susceptible in vitro and probably contributed to their positive outcomes. Both patients tolerated the drug and made good clinical progress after its initiation. Given the need for combination therapy, it is impossible to attribute the positive outcome of these cases to a single drug. Both patients received bedaquiline and clofazimine because there is evidence that this combination is synergistic against NTMs in vitro (*14*). Case-patient 2 only achieved sustained mycobacterial culture negativity after treatment with bedaquiline and tedizolid.

Use of bedaquiline as salvage therapy for pulmonary NTM infection is often complicated by the emergence of drug resistance and disease relapse (*15*). These case-patients received bedaquiline for ≥1 year, and neither showed evidence of the acquisition of drug resistance or disease relapse over that time or since. These case-patients provide support for use of bedaquiline for treatment of disseminated NTM infection, particularly when standard regimens cannot be used because of drug resistance or adverse drug effects.

About the Author

Dr. Gil is an infectious diseases and microbiology registrar at the North Middlesex Hospital, London, UK. Her primary research interests are tissue immunology, leukocyte recruitment, and immune deficiency.

References

1. Holland SM. Nontuberculous mycobacteria. Am J Med Sci. 2001;321:49–55. https://doi.org/10.1097/00000441-200101000-00008
2. Brown-Elliott BA, Nash KA, Wallace RJ Jr. Antimicrobial susceptibility testing, drug resistance mechanisms, and therapy of infections with nontuberculous mycobacteria. Clin Microbiol Rev. 2012;25:545–82. https://doi.org/10.1128/CMR.05030-11
3. Millar BC, Moore JE. Antimycobacterial strategies to evade antimicrobial resistance in the nontuberculous mycobacteria. Int J Mycobacteriol. 2019;8:7–21. https://doi.org/10.4103/ijmy.ijmy_153_18
4. Pym AS, Diacon AH, Tang S-J, Conradie F, Danilovits M, Chuchottaworn C, et al.; TMC207-C209 Study Group. Bedaquiline in the treatment of multidrug- and extensively drug-resistant tuberculosis. Eur Respir J. 2016;47:564–74. https://doi.org/10.1183/13993003.00724-2015
5. M24Ed3 susceptibility testing of mycobacteria, *Nocardia* spp., and other aerobic Actinomycetes, 3rd ed. Wayne (PA): Clinical and Laboratory Standards Institute [cited 2020 Nov 6]. https://clsi.org/standards/products/microbiology/documents/m24
6. Schön T, Chryssanthou E. Minimum inhibitory concentration distributions for *Mycobacterium avium* complex-towards evidence-based susceptibility breakpoints. Int J Infect Dis. 2017;55:122–4. https://doi.org/10.1016/j.ijid.2016.12.027
7. Benson CA, Williams PL, Currier JS, Holland F, Mahon LF, MacGregor RR, et al.; AIDS Clinical Trials Group 223 Protocol Team. A prospective, randomized trial examining the efficacy and safety of clarithromycin in combination with ethambutol, rifabutin, or both for the treatment of disseminated *Mycobacterium avium* complex disease in persons with acquired immunodeficiency syndrome. Clin Infect Dis. 2003;37:1234–43. https://doi.org/10.1086/378807
8. Bax HI, Bakker-Woudenberg IA, Ten Kate MT, Verbon A, de Steenwinkel JE. Tigecycline potentiates clarithromycin activity against *Mycobacterium avium* in vitro. Antimicrob Agents Chemother. 2016;60:2577–9. https://doi.org/10.1128/AAC.02864-15
9. Diacon AH, Pym A, Grobusch MP, de los Rios JM, Gotuzzo E, Vasilyeva I, et al.; TMC207-C208 Study Group. Multidrug-resistant tuberculosis and culture conversion with bedaquiline. N Engl J Med. 2014;371:723–32. https://doi.org/10.1056/NEJMoa1313865
10. Aguilar-Ayala DA, Cnockaert M, André E, Andries K, Gonzalez-Y-Merchand JA, Vandamme P, et al. In vitro activity of bedaquiline against rapidly growing nontuberculous mycobacteria. J Med Microbiol.

2017; 66:1140–3. https://doi.org/10.1099/jmm.0.000537
11. Martin A, Godino IT, Aguilar-Ayala DA, Mathys V, Lounis N, Villalobos HR. In vitro activity of bedaquiline against slow-growing nontuberculous mycobacteria. J Med Microbiol. 2019;68:1137–9. https://doi.org/10.1099/jmm.0.001025
12. Cholo MC, Mothiba MT, Fourie B, Anderson R. Mechanisms of action and therapeutic efficacies of the lipophilic antimycobacterial agents clofazimine and bedaquiline. J Antimicrob Chemother. 2017;72:338–53. https://doi.org/10.1093/jac/dkw426
13. Lounis N, Gevers T, Van den Berg J, Vranckx L, Andries K. ATP synthase inhibition of *Mycobacterium avium* is not bactericidal. Antimicrob Agents Chemother. 2009;53:4927–9. https://doi.org/10.1128/AAC.00689-09
14. Alexander DC, Vasireddy R, Vasireddy S, Philley JV, Brown-Elliott BA, Perry BJ, et al. Emergence of mmpT5 variants during bedaquiline treatment of *Mycobacterium intracellulare* lung disease. J Clin Microbiol. 2017;55:574–84. https://doi.org/10.1128/JCM.02087-16
15. Ruth MM, Sangen JJ, Remmers K, Pennings LJ, Svensson E, Aarnoutse RE, et al. A bedaquiline/clofazimine combination regimen might add activity to the treatment of clinically relevant non-tuberculous mycobacteria. J Antimicrob Chemother. 2019;74:935–43. https://doi.org/10.1093/jac/dky526

Address for correspondence: Eliza Gil, Hospital for Tropical Diseases, Maple House, 149 Tottenham Court Rd, Bloomsbury, London W1T 7NF, UK; email: eliza.gil@nhs.net

July 2020

Emerging Viruses

- Case Manifestations and Public Health Response for Outbreak of Meningococcal W Disease, Central Australia, 2017
- Transmission of Chikungunya Virus in an Urban Slum, Brazil
- Public Health Role of Academic Medical Center in Community Outbreak of Hepatitis A, San Diego County, California, USA, 2016–2018
- Macrolide-Resistant *Mycoplasma pneumoniae* Infections in Pediatric Community-Acquired Pneumonia
- Efficient Surveillance of *Plasmodium knowlesi* Genetic Subpopulations, Malaysian Borneo, 2000–2018
- Bat and Lyssavirus Exposure among Humans in Area that Celebrates Bat Festival, Nigeria, 2010 and 2013
- Rickettsioses as Major Etiologies of Unrecognized Acute Febrile Illness, Sabah, East Malaysia
- Meningococcal W135 Disease Vaccination Intent, the Netherlands, 2018–2019
- Risk for Coccidioidomycosis among Hispanic Farm Workers, California, USA, 2018
- Atypical Manifestations of Cat-Scratch Disease, United States, 2005–2014
- Survey of Parental Use of Antimicrobial Drugs for Common Childhood Infections, China

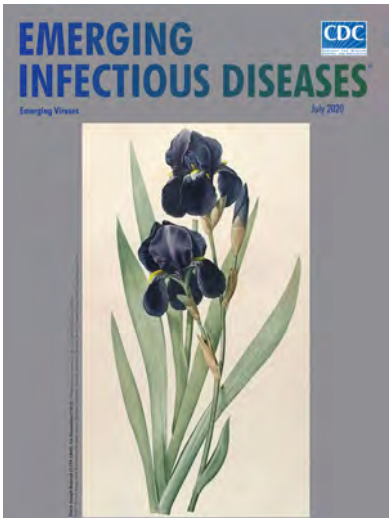

- Paradoxal Trends in Azole-Resistant *Aspergillus fumigatus* in a National Multicenter Surveillance Program, the Netherlands, 2013–2018
- Large Nationwide Outbreak of Invasive Listeriosis Associated with Blood Sausage, Germany, 2018–2019
- High Contagiousness and Rapid Spread of Severe Acute Respiratory Syndrome Coronavirus 2
- Identifying Locations with Possible Undetected Imported Severe Acute Respiratory Syndrome Coronavirus 2 Cases by Using Importation Predictions
- Severe Acute Respiratory Syndrome Coronavirus 2–Specific Antibody Responses in Coronavirus Disease Patients
- Burden and Cost of Hospitalization for Respiratory Syncytial Virus in Young Children, Singapore
- Human Adenovirus Type 55 Distribution, Regional Persistence, and Genetic Variability
- Policy Decisions and Use of Information Technology to Fight COVID-19, Taiwan
- Sub-Saharan Africa and Eurasia Ancestry of Reassortant Highly Pathogenic Avian Influenza A(H5N8) Virus, Europe, December 2019
- Serologic Evidence of Severe Fever with Thrombocytopenia Syndrome Virus and Related Viruses in Pakistan
- Shuni Virus in Wildlife and Nonequine Domestic Animals, South Africa
- Transmission of Legionnaires' Disease through Toilet Flushing
- Carbapenem Resistance Conferred by OXA-48 in K2-ST86 Hypervirulent *Klebsiella pneumoniae*, France
- Laboratory-Acquired Dengue Virus Infection, United States, 2018
- Linking Epidemiology and Whole-Genome Sequencing to Investigate *Salmonella* Outbreak, Massachusetts, USA, 2018

EMERGING INFECTIOUS DISEASES

To revisit the July 2020 issue, go to:
https://wwwnc.cdc.gov/eid/articles/issue/26/7/table-of-contents

Implementation of an Animal Sporotrichosis Surveillance and Control Program, Southeastern Brazil

Simone M. Moreira, Elisa H.P. Andrade, Marcelo T. Paiva, Hassan M. Zibaoui, Lauranne A. Salvato, Maria I. Azevedo, Camila S.F. Oliveira, Danielle F.M. Soares, Kelly M. Keller, Sérgio L. Magalhães, Maria H.F. Morais, José R.R. Costa, Camila V. Bastos

We report the implementation of an animal sporotrichosis surveillance and control program that evaluates strategies to identify suspected and infected cats in a municipality in southeastern Brazil. All adopted measures reinforced the program, although strategies had different abilities to detect the presence of infection.

Sporotrichosis, which is caused by the dimorphic fungi of the genus *Sporothrix*, affects several species of mammal. It often occurs in urban areas that have epidemic conditions (*1*). *Sporothrix brasiliensis* is an emerging species prevalent in Brazil (*2*).

Cats show peculiar signs of the disease and enable the agent to multiply, which favors transmission. Brazil has the highest incidence of sporotrichosis in Latin America because of hyperendemic human sporotrichosis, which is transmitted by cats, particularly in the state of Rio de Janeiro (*3*,*4*), in the southeastern region.

Since sporotrichosis is a zoonosis, in the absence of a specific program, the implementation of a surveillance system in animals that use public services can contribute to the identification of the disease and to the recommendation of practices related to control in municipalities. Thus, data produced are transformed into information and are a triggering factor of the information-decision-action triad, which fuels surveillance and constitutes a decision-making instrument (*5*).

Author affiliations: Instituto Federal de Minas Gerais, Bambuí, Brazil (S.M. Moreira); Universidade Federal de Minas Gerais, Belo Horizonte, Brazil (E.H.P. Andrade, M.T. Paiva, L.A. Salvato, M.I. Azevedo, C.S.F. Oliveira, D.F.M. Soares, K.M. Keller, C.V. Bastos); Prefeitura Municipal de Contagem, Contagem, Brazil (H.M. Zibaoui, S.L. Magalhães, M.H.F. Morais, J.R.R. Costa)

DOI: https://doi.org/10.3201/eid2703.202863

Because of the need to identify infected animals, an animal sporotrichosis surveillance and control program was implemented in a municipality of Minas Gerais state, Brazil. The objective of this study was to evaluate different measures and strategies for identification of cases as part of a feline sporotrichosis surveillance system in this municipality during 2017–2018.

The Study

We conducted the study in Contagem, a municipality located in the southeastern region of Brazil, in Minas Gerais, which borders Rio de Janeiro state. Contagem has an area of 194,746 km^2 and ≈663,855 inhabitants (*6*). During 2018, the feline population of this city was estimated to be 8,842 (Zoonosis Department, Health Department of Contagem, Minas Gerais, Brazil, 2019, unpub. data).

The cross-sectional observational analysis encompassed a convenience sample of 165 felines who had cutaneous lesions suggestive of sporotrichosis and resided in the municipality during May 2017–December 2018. Using different strategies, public service veterinarians, and endemic control agents (ECA) (Table), we identified animals that had cutaneous lesions suggestive of sporotrichosis. ECA are public health professionals who work in predefined territories, visiting properties regularly for the control of arboviruses. They were trained by veterinarians to pinpoint animals with lesions suggestive of sporotrichosis.

We collected samples in households and in the Center of Zoonosis Control (CZC) in Contagem, a public animal unit in which desexing services and programs for zoonosis control are provided. This study was approved by the Committee for

Table. Strategies of identifying suspected sporotrichosis cases by health surveillance professionals in Contagem, Minas Gerais, Brazil, May 2017–December 2018*

Category	Classification of identification strategy	Description
1	Euthanasia at CZC	Cats that had serious injuries suggestive of sporotrichosis were brought by owners for veterinary evaluation at CZC and euthanized because of illness or lack of financial resources for treatment. Sample collection for diagnosis confirmation was conducted at CZC after euthanasia.
2	Active surveillance	Cats that had suspicious skin lesions were identified by endemic control agents during routine home visits for control of arboviruses. Sample collection for diagnosis confirmation was conducted in households.
3	Passive surveillance	Cats with suspicious skin injuries were brought by owners to CZC for veterinary evaluation. Sample collection for diagnosis confirmation was conducted at CZC.
4	Public desexing service	Cats with suspicious skin injuries were identified during a clinical examination before the public desexing service at CZC requested by owners. Sample collection for diagnosis confirmation was conducted at CZC before desexing.

*CZC, Center of Zoonosis Control.

Ethics in Research of the Federal University of Minas Gerais (no. CAAE05012918.4.0000.5149), and use of data was approved by the Health Department of Contagem.

Characterization of cases positive for sporotrichosis was performed by collecting exudates from skin lesions of all suspected cases on sterile swab specimens that were placed in Stuart medium and sent to the Laboratory of Mycology and Mycotoxins of the School of Veterinary of the Federal University of Minas Gerais. Samples were cultivated on Sabouraud agar (KASVI, https://www.kasvi.com.br) containing chloramphenicol and cycloheximide and incubated at 25°C for growth of colonies for up to 10 days. Macroscopic and microscopic characteristics of the colonies were observed to identify fungi of the genus *Sporothrix*. Isolates were identified by PCR based on calmodulin gene sequences (*7*).

Of 165 cats that had cutaneous lesions suggestive of sporotrichosis, which represented 1.86% of the

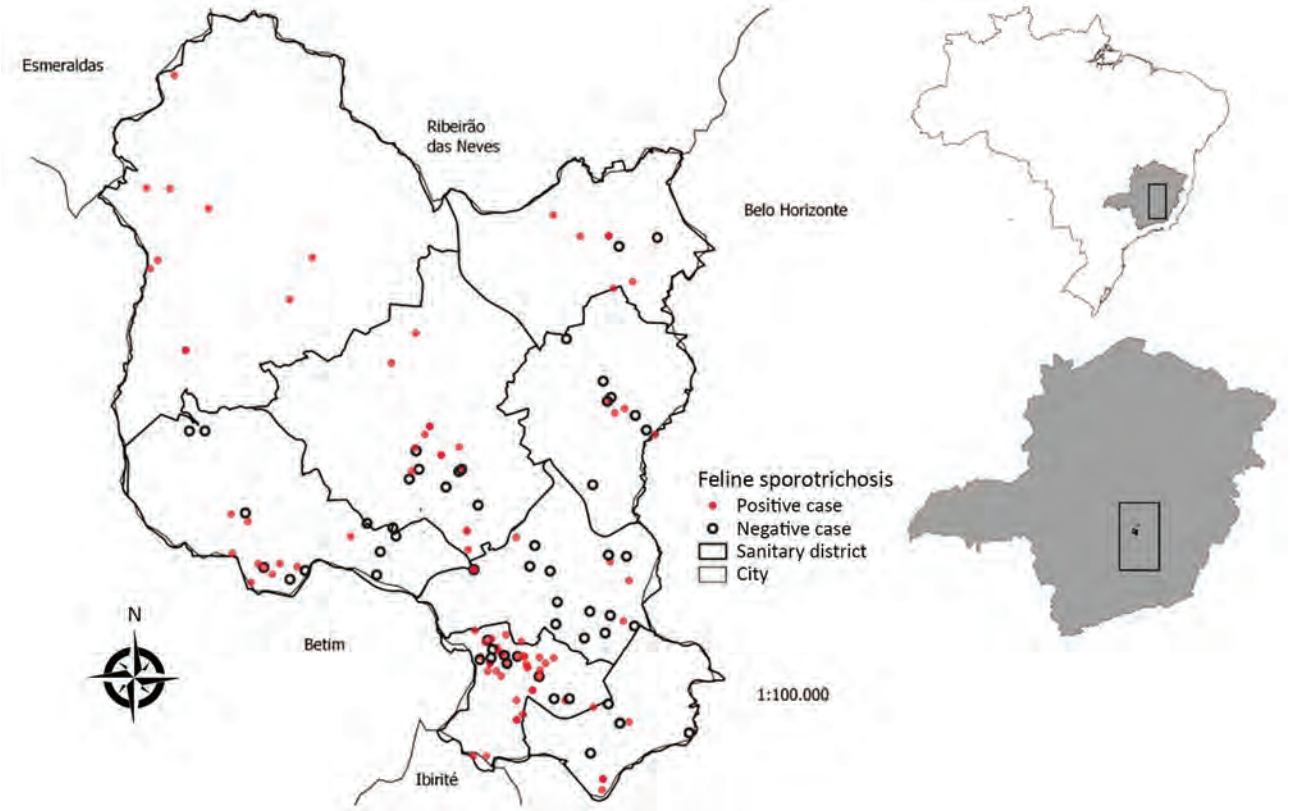

Figure 1. Spatial distribution of cats with cutaneous lesions suggestive of sporotrichosis, according to laboratory diagnosis, Contagem, Minas Gerais, Brazil, May 2017–December 2018. Map was created using QGIS version 3.10 software (https://qgis.org) and the database for Contagem. Inset maps show location of Contagem within Minas Gerais state and Brazil.

city´s estimated feline population, 103 (62.4%) were considered positive. All health districts (administrative division) had positive cases, demonstrating the spread of the disease throughout the studied territory (Figure 1). Among the positive samples sent for molecular identification (34.3%), all were confirmed as containing *S. brasiliensis*, a species often found in different regions of Brazil (*2*,*7*,*8*) and in parts of Latin America (*9*,*10*). The percentage of positive animals in this region was higher than that seen in other locations in Brazil that had epidemics (*1*,*11*).

The euthanasia service provided 36.9% (38/103) of positive cats. Passive surveillance provide 31.0% (32/103), active surveillance provided 26.2% (27/103) and the public desexing service provided 5.8% (6/103). The ability to detect the infection among the total number of suspected animals identified by each strategy varied (Figure 2). Active surveillance proved to be efficient for identification of infected cats because 84.4% (27/32) with cutaneous lesions suggestive of sporotrichosis obtained by this approach were laboratory positive. In this category, the role of ECA stands out because this group was able to identify animals that had suggestive lesions. This finding demonstrates that awareness and training of these professionals are essential for the early detection of cases in a surveillance program in the cities affected by this zoonosis.

During the study, 50 animals that had suggestive cutaneous lesions were taken to the CZC by inhabitants of Contagem. This action was characterized as passive surveillance. Of these 50 cats, 32 (64.0%) had laboratory confirmed infections. This finding might reflect the awareness of the program among the population, which was promoted mainly by ECA.

Of the 40 cats identified that had lesions suspected of being sporotrichosis by the public desexing service, 6 (15%) were laboratory positive. Among the strategies for obtaining cats suspected of having sporotrichosis, this strategy identified the lowest percentage of positive animals. However, this practice represents an additional form of passive surveillance, which is relevant because of the potential for early identification of the disease resulting from felines submitted for neutering that are clinically evaluated before the surgical procedure.

Conversely, the category of cats that had cutaneous lesions suggestive of sporotrichosis referred for euthanasia at CZC showed the highest positivity (38/43, 88.4%). Animals in this condition were in an advanced stage of the disease. However, the diagnosis made at the time of euthanasia is ineffective in blocking transmission of sporotrichosis because it is most likely that until they died, these animals disseminated the etiologic agent.

Conclusions

Identifying cats that had cutaneous lesions suggestive of sporotrichosis or that were identified as positive for sporotrichosis contributes to reduction of inappropriate disposal of corpses, which in Contagem are incinerated by an outsourced company. This measure helped reduce environmental

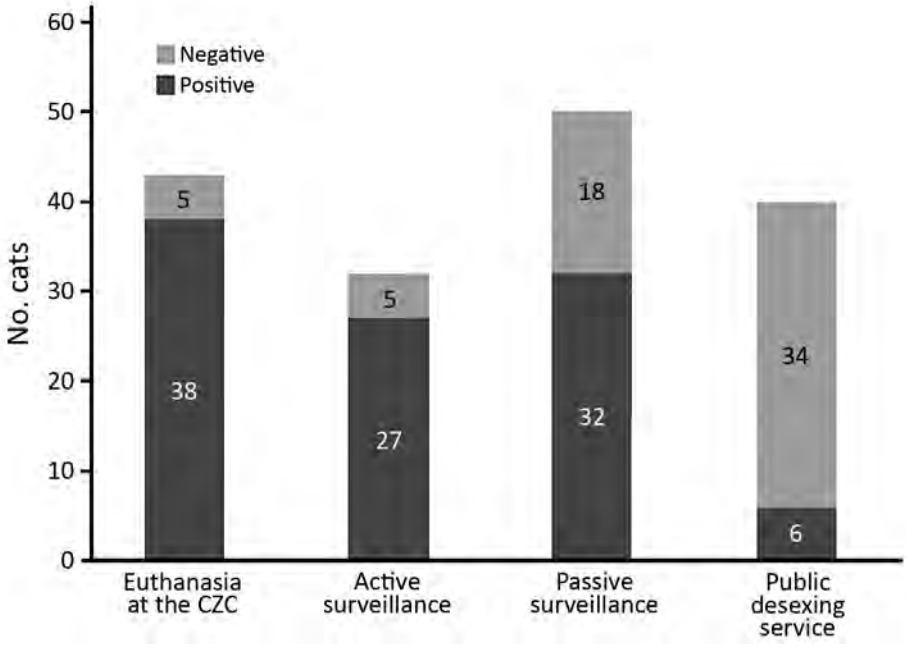

Figure 2. Proportion of cats laboratory-positive for sporotrichosis among animals with suspected disease, according to the strategy of identification, Contagem, Minas Gerais, Brazil, May 2017–December 2018.

contamination and should be part of an animal sporotrichosis control program. Decomposing abandoned dead cats or cats being buried in the domestic environment could represent a risk for increased fungal load in the soil (*12*).

If one considers the health program implemented in the municipality, access to free diagnosis associated with multiple strategies for identifying infected cats (active surveillance, passive surveillance, public desexing service, and euthanasia service) proved to be a useful tool for surveillance and control of feline sporotrichosis. It was possible to identify the disease distributed throughout the territory, and surveillance strategies can, if maintained continuously in the service routine, offer a better situational diagnosis of the disease over time. In our view, the current challenges to the sporotrichosis detection system consist of enhancing training programs and awareness of public health professionals regarding early diagnosis.

We showed relevant advances in the surveillance of feline sporotrichosis. This program is a useful instrument to ensure standardization and efficiency of field actions. Active and passive surveillance were necessary means for initial actions related to completion of the implemented program. Training public health professionals, providing free laboratory diagnosis for animals, and disposing of positive corpses appropriately represent the minimum requirements for support of surveillance and control in municipalities that have their first sporotrichosis cases.

Acknowledgments

We thank the Municipality of Contagem, Minas Gerais, Brazil, for participating in the study.

This study was supported by Conselho Nacional de Desenvolvimento Científico e Tecnológico (project no. 438936/2018) and Pró-Reitoria de Pesquisa da Universidade Federal de Minas Gerais (project no. 26048 * 65).

About the Author

Dr. Moreira is a veterinarian and professor at the Federal Institute of Minas Gerais, Bambuí, Minas Gerais, Brazil. Her primary research interest is veterinary public health.

References

1. Poester VR, Mattei AS, Madrid IM, Pereira JT, Klafke GB, Sanchotene KO, et al. Sporotrichosis in southern Brazil, towards an epidemic? Zoonoses Public Health. 2018;65:815–21. https://doi.org/10.1111/zph.12504
2. Rodrigues AM, de Hoog GS, de Camargo ZP. Sporothrix species causing outbreaks in animals and humans driven by animal–animal transmission. PLoS Pathog. 2016;12:e1005638. https://doi.org/10.1371/journal.ppat.1005638
3. Gremião ID, Miranda LH, Reis EG, Rodrigues AM, Pereira SA. Zoonotic pidemic of sporotrichosis: cat to human transmission. PLoS Pathog. 2017;13:e1006077. https://doi.org/10.1371/journal.ppat.1006077
4. Schubach A, Schubach TM, Barros MB, Wanke B. Cat-transmitted sporotrichosis, Rio de Janeiro, Brazil. Emerg Infect Dis. 2005;11:1952–4. https://doi.org/10.3201/eid1112.040891
5. Day MJ, Breitschwerdt E, Cleaveland S, Karkare U, Khanna C, Kirpensteijn J, et al. Surveillance of zoonotic infectious diseases transmitted by small companion animals [Online Report]. Emerg Infect Dis. 2012;18:22. https://doi.org/10.3201/eid1812.120664
6. Instituto Brasileiro de Geografia e Estatística (IBGE). Cities, 2010 [in Portuguese] [cited 2020 Nov 20]. https://cidades.ibge.gov.br/brasil/mg/contagem/panorama
7. Rodrigues AM, de Hoog GS, de Camargo ZP. Molecular diagnosis of pathogenic *Sporothrix* species. PLoS Negl Trop Dis. 2015;9:e0004190. https://doi.org/10.1371/journal.pntd.0004190
8. Sanchotene KO, Madrid IM, Klafke GB, Bergamashi M, Della Terra PP, Rodrigues AM, et al. *Sporothrix brasiliensis* outbreaks and the rapid emergence of feline sporotrichosis. Mycoses. 2015;58:652–8. https://doi.org/10.1111/myc.12414
9. Córdoba S, Isla G, Szusz W, Vivot W, Hevia A, Davel G, et al. Molecular identification and susceptibility profile of *Sporothrix schenckii* sensu lato isolated in Argentina. Mycoses. 2018;61:441–8. https://doi.org/10.1111/myc.12760
10. García-Duarte JM, Acosta VR, Viera PM, Caballero AA, Matiauda GA, de Oddone VB, et al. Sporotrichosis transmitted by domestic cat. A family case report [in Portuguese]. Revista de Nacional (Itauguá). 2017;9:35–48. https://doi.org/10.18004/rdn2017.0009.02.067-076
11. Montenegro H, Rodrigues AM, Dias MA, da Silva EA, Bernardi F, de Camargo ZP. Feline sporotrichosis due to *Sporothrix brasiliensis*: an emerging animal infection in São Paulo, Brazil. BMC Vet Res. 2014;10:269. https://doi.org/10.1186/s12917-014-0269-5
12. Téllez MD, Batista-Duharte A, Portuondo D, Quinello C, Bonne-Hernández R, Carlos IZ. *Sporothrix schenckii* complex biology: environment and fungal pathogenicity. Microbiology (Reading). 2014;160:2352–65. https://doi.org/10.1099/mic.0.081794-0

Address for correspondence: Camila V. Bastos, Escola de Veterinária, Universidade Federal de Minas Gerais, Av. Antônio Carlos 6627, Belo Horizonte, Minas Gerais 31270-901, Brazil; email: camilabastos@ufmg.br or camilavetmail@gmail.com

Addressing Reemergence of Diphtheria among Adolescents through Program Integration in India

Kiran Kumar Maramraj, M.L. Kavitha Latha, Rukma Reddy, Samir V. Sodha, Suneet Kaur, Tanzin Dikid, Sukrutha Reddy, S.K. Jain, Sujeet Kumar Singh

We report a diphtheria outbreak mostly among children (median 12 years; range 4–26 years) of a religious minority in urban India. Case-fatality rate (15%, 19/124) was higher among unimmunized patients (relative risk 4.1, 95% CI 1.5–11.7). We recommend mandating and integrating immunization into school health programs to prevent reemergence.

Diphtheria is a vaccine-preventable disease of the upper respiratory system caused by toxigenic strains of *Corynebacterium diphtheriae*. Global case-fatality rate (CFR) is estimated at 5%–10%; higher CFRs of up to 20% are reported in children <5 years of age (*1*). In 2016, with 78% national coverage for third-dose diphtheria-tetanus-pertussis (DTP) vaccine, India reported 48% of diphtheria cases and half of 350 deaths worldwide (*2*,*3*). In India, the 3 primary DTP doses are administered at 6, 10, and 14 weeks of age, and booster doses are given at 16–24 months and 5–6 years of age. Numerous states across India have reported diphtheria outbreaks, including Assam in 2010, Karnataka in 2011, and Andhra Pradesh in 2014 (*4*). In December 2017, the Integrated Disease Surveillance Program of Telangana state reported a rise in diphtheria cases. We investigated to describe the epidemiology of the outbreak, identify risk factors, assess trends in immunization coverage, and provide evidence-based recommendations.

Author affiliations: National Centre for Disease Control, New Delhi, India (K.K. Maramraj, S. Kaur, T. Dikid, S.K. Jain, S.K. Singh); Ronald Ross Institute of Tropical and Communicable Diseases, Hyderabad, India (M.L.K. Latha); State Health Department, Telangana, India (R. Reddy, S. Reddy); Centers for Disease Control and Prevention, Atlanta, Georgia, USA (S.V. Sodha)

DOI: https://doi.org/10.3201/eid2703.203205

The Study

For this study we defined a diphtheria case as an upper respiratory tract illness with an adherent pseudomembrane in the nasal cavity, pharynx, or larynx and *C. diphtheriae* isolated from a clinical specimen from a Telangana resident during January 1–December 31, 2017. Clinical specimens were cultured initially on blood tellurite medium followed by selective culture on cystinase medium. We identified 124 laboratory-confirmed diphtheria cases, for an annual incidence of 3.5 cases/1 million residents; the 19 deaths represented a CFR of 15%. This incidence was more than the mean incidence (±2 SD) of 2.9 cases/1 million residents during 2014–2016, which confirmed the 2017 cases as an outbreak. Age range for case-patients was 4–26 years (median 12 years). Adolescents 10–14 years of age had the highest annual incidence rate, 15/1 million residents. CFR decreased by age from 24% among children 4–9 years of age to no deaths in persons 20–29 years (odds ratio [OR] 1.9, 95% CI 1.1–3.4; p = 0.03). Only 11% (14/124) of laboratory-confirmed samples had an Elek test for toxigenic strain; 12 (86%) of those 14 samples were positive. Female patients accounted for 50% of cases but 63% of deaths. Children identified as Muslim, a religious minority in Telangana, accounted for 60% of cases, but 74% of deaths. Most cases (81%) and deaths (89%) occurred in the last half of 2017 (Figure 1). Urban Hyderabad makes up only 11.2% of the population of Telangana (https://www.telangana.gov.in/PDFDocuments/Statistical-Year-Book-2017.pdf) but accounted for 53% of diphtheria cases and 47% of deaths in the state; annual incidence in Hyderabad was 19 cases/1 million population, the highest among all geographic areas of Telangana.

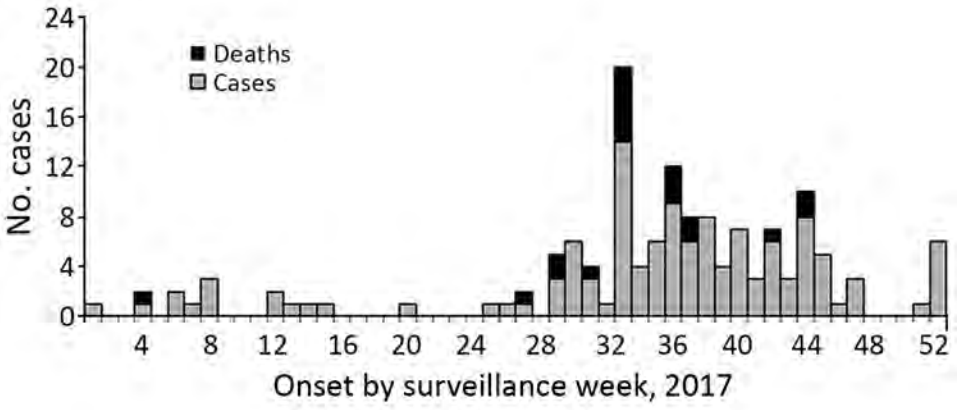

Figure 1. Epidemic curve by patient date of illness onset for 124 confirmed diphtheria cases, including 19 deaths, Telangana, India, 2017.

This investigation was a public health response to an outbreak. Requisite approvals were obtained from national and state health authorities.

We conducted a retrospective cohort study to assess factors associated with death among case-patients. We defined the cohort as all patients with laboratory-confirmed diphtheria in Telangana during January 1–December 31, 2017. Among 124 case-patients identified, 25 (20%) were not located or declined to provide immunization information; 99 (80%) patients participated in the cohort study. Among the 99 patients, immunization coverage for DTP3 was 53% and for DTP second booster was 36%, based on vaccination card or parental recall when the card was not available (Table 1). Case-patients without all 3 doses of the primary immunization series were more likely than those having had the full DPT3 to die from diphtheria (relative risk [RR] 4.1; 95% CI 1.5–11.7) with 60% attributable risk. Symptoms significantly associated with death were hoarseness (100%), dyspnea (100%), bull neck appearance (89%), and stridor (42%) (p <0.001 for all). Delayed hospital admission (i.e., >72 hours elapsed after sore throat onset) was also significantly associated with death (RR 2.8, 95% CI 1.2–6.8) (Table 2).

We reviewed DTP immunization coverage trends in Telangana during 1998–2016 by assessing National Family Health surveys conducted in 1998–1999, 2005–2006, and 2015–2016 (*5*) and District-Level Household and Facility Surveys conducted in 1998–1999, 2002–2004, 2007–2008, and 2012–2013 (*6*). DTP3 coverage showed a dip in 2005 (61% in 2005 vs. 75% mean during 1998–2016). The diphtheria cases reported in 2017 were hypothetically distributed according to their birth cohorts over the period 1998–2016, to compare with the immunization coverage of that year. Around half of these cases (48%, 60/124) occurred during 2005–2009, after a dip in immunization in 2005 (Figure 2).

We assessed the available records during 2014–2017 from 12 healthcare facilities in urban Hyderabad. None had periods when vaccines were out of stock, all had cold chain temperature logs maintained within the appropriate range, and all conducted >80% of the immunization sessions across all quarters; administrative immunization reported >90% DTP3 coverage. Interviews of health facility staff revealed that all 12 facilities had an immunization-tracking system in place for children <2 years of age. However, for children ≥2 years of age, there was no tracking mechanism, and they were not included in the routine coverage surveys and administrative coverage reports. Mission Indradhanush, a nationwide immunization drive by the government of India, has made major gains in improving immunization coverage; however, it did not target children ≥2 years of age (*7*).

Our study is limited because probable cases of diphtheria not confirmed by laboratory testing and asymptomatic cases were excluded, so the outbreak was likely underestimated. In addition, we did not conduct population immunization coverage surveys in the affected community and relied on published government estimates instead.

Table 1. Immunization status of 99 study patients with confirmed diphtheria cases, Telangana, India, 2017*

Diphtheria vaccine	Based on card information only, no. (%)	Based on card information or parental recall, no. (%)
Pentavalent 1 or DTP1	23 (23)	55 (56)
Pentavalent 2 or DTP2	23 (23)	53 (54)
Pentavalent 3 or DTP3	23 (23)	52 (53)
DTP booster 1	21 (21)	44 (44)
DTP booster 2†	17 (18)	35 (36)

*DTP, diphtheria-tetanus-pertussis vaccine.
†Denominator for DTP booster 2 = 96; three 4-year-olds were excluded because they were not eligible for DTP booster 2 based on age.

Conclusions

The age shift of diphtheria cases is of global concern. Case-based surveillance studies in India have

Table 2. Risk factors for mortality for 99 study patients with confirmed diphtheria cases, Telangana, India, 2017

Risk factor	Died, no. (%), n = 19	Survived, no. (%), n = 80	CFR, % Among exposed	CFR, % Among nonexposed	RR (95% CI)	p value
Not fully immunized with DTP3	15 (79)	32 (40)	32	8	**4.1 (1.5–11.7)**	0.002
Delayed hospital admission	13 (68)	30 (38)	30	11	**2.8 (1.2–6.8)**	0.01
<10 y of age	12 (63)	32 (37)	27	13	2.1 (0.9–4.9)	0.06
Muslim	14 (74)	48 (60)	23	14	1.7 (0.7–4.3)	0.27
Female	12 (63)	40 (50)	23	15	1.5 (0.7–3.6)	0.30
Rural residence	10 (53)	38 (47)	21	18	1.2 (0.5–2.6)	0.68

*Bold indicates statistical significance. CFR, case-fatality rate; DTP, diphtheria-tetanus-pertussis vaccine; RR, relative risk.

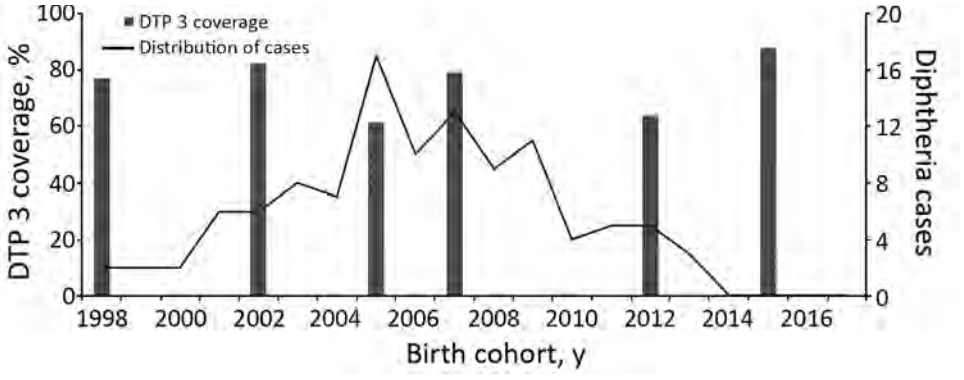

Figure 2. Distribution of DTP3 immunization coverage during 1998–2016 and hypothetical distribution of 2017 cases according to birth cohorts in Telangana, India. Data sources for DTP-3 coverage are National Family Health Surveys (NFHS; *5*) and District Level Household & Facility Surveys (DLHS; *6*), conducted by the government of India. Data source for coverage in 1998 was NFHS-2, in 2005 was NFHS-3, and in 2015 was NFHS-4. Data source for coverage in 2002 was DLHS-2, in 2007 was DLHS-3, and in 2012 was DLHS-4. DTP3, diphtheria-tetanus-pertussis.

suggested that areas with greater immunization coverage have experienced an age-shift with a higher incidence among older children (*8*,*9*). In this diphtheria outbreak, cases were primarily among adolescents and school-age children; no cases were reported in children <4 years of age, probably because of high (>90%) vaccine coverage in birth cohorts since 2014. Gaps in booster-dose coverage probably resulted in waning immunity provided by the primary series (*10*,*11*). This outbreak had a much higher CFR (15%) compared with the national CFR of 3% for diphtheria in 2017 (*12*). CFR was higher among underimmunized children and those with delayed hospital admission, similar to previously reported outbreaks (*13*–*15*). Hyderabad reported incidence 5 times higher than the average in the state. The Muslim community makes up only for 12% of Telangana's population but accounted for 60% of cases and 74% of deaths due to diphtheria reported in the state.

To address the factors leading to this outbreak and to prevent diphtheria outbreaks in the future, we recommended 2 main strategies. First, we recommend adding 2 adolescent booster doses at 10 and 16 years of age to the routine immunization schedule, which would address possible waning of immunity from the primary series. To help accomplish this, we recommend integrating the immunization program with school health programs. Schools annually identify and track eligible schoolchildren for administration of age-appropriate vaccine doses. The government could mandate that schools require a second DTP booster before students enter primary school (ages 5–6 years) and a tetanus-diphtheria booster as they leave primary school (ages 10–11 years) and secondary school (ages 15–16 years). Second, we recommend implementing focused immunization services in urban Muslim communities by engaging religious leaders and community stakeholders. Addressing gaps in routine delivery of immunization service in marginalized and underserved populations is essential for averting future vaccine-preventable disease outbreaks.

Acknowledgments

The authors acknowledge the leadership and staff of the Integrated Disease Surveillance Programme, State Health Department, Telangana, and Sir Ronald Ross Institute of Tropical and Communicable Diseases, Hyderabad. We also thank Rajesh Yadav and Ann M. Buff for providing technical assistance and manuscript review.

The India Epidemic Intelligence Service Program was funded by cooperative agreement 1U2G GH001904-04 between the National Centre for Disease Control, the Ministry of Health and Family Welfare, and the US Centers for Disease Control and Prevention.

About the Author

Dr. Maramraj is a public health specialist and Epidemic Intelligence Service officer for the National Centre for Disease Control, New Delhi, India. His primary research interest is in the epidemiology of emerging and reemerging infectious diseases and their impact on public health.

References

1. Centers for Disease Control and Prevention. Diphtheria [cited 2019 Sep 30]. https://www.cdc.gov/diphtheria/clinicians.html
2. World Health Organization. Vaccine-preventable diseases: monitoring system. 2019 global summary. Incidence time series for India [cited 2019 Sep 29]. https://apps.who.int/immunization_monitoring/globalsummary/incidences?c=IND
3. International Institute for Population Sciences, Ministry of Health and Family Welfare, Government of India. District level household and facility survey—3. 2008 [cited 2019 Oct 5]. http://rchiips.org/pdf/india_report_dlhs-3.pdf
4. Savaskar SV, Bandichhode ST, Chhajed PS. Diphtheria in children: are we even close to control the menace? IP Int J Med Paediatr Oncol. 2017;3:106–9 [cited 2019 Oct 5]. https://www.ipinnovative.com/journals/IJMPO/article-full-text/4886
5. International Institute for Population Sciences Mumbai, Ministry of Health and Family Welfare, Government of India. National family health survey, India [cited 2019 Oct 5]. http://rchiips.org/nfhs
6. Ministry of Health and Family Welfare, Government of India. District level household & facility survey [cited 2019 Oct 5]. http://rchiips.org
7. National Health Mission, Ministry of Health and Family Welfare, Government of India. Intensified Mission Indradhanush operational guidelines. 2017 [cited 2019 Oct 2]. https://nhm.gov.in/New_Updates_2018/NHM_Components/Immunization/Guildelines_for_immunization/Mission_Indradhanush_Guidelines.pdf
8. Sangal L, Joshi S, Anandan S, Balaji V, Johnson J, Satapathy A, et al. Resurgence of diphtheria in North Kerala, India, 2016: laboratory supported case-based surveillance outcomes. Front Public Health. 2017;5:218. https://doi.org/10.3389/fpubh.2017.00218
9. Clarke KEN, MacNeil A, Hadler S, Scott C, Tiwari TSP, Cherian T. Global epidemiology of diphtheria, 2000–2017. Emerg Infect Dis. 2019;25:1834–42. https://doi.org/10.3201/eid2510.190271
10. World Health Organization. Diphtheria vaccine: WHO position paper, August 2017—recommendations. Vaccine. 2018;36:199–201. https://doi.org/10.1016/j.vaccine.2017.08.024
11. Tiwari T, Wharton M. Diphtheria toxoid. In: Plotkin SA, Orenstein WA, Offit PA, editors. Vaccines, 6th ed. Edinburgh: Elsevier Saunders; 2013. p. 153–66.
12. Central Bureau of Health Intelligence, Ministry of Health and Family Welfare, Government of India. National Health Profile 2018 [cited 2019 Sep 30]. http://www.cbhidghs.nic.in/Ebook/National%20Health%20Profile-2018%20(e-Book)/files/assets/common/downloads/files/NHP%202018.pdf
13. Landazabal García N, Burgos Rodríguez MM, Pastor D. Diphtheria outbreak in Cali, Colombia, August–October 2000. Epidemiol Bull. 2001;22:13–5.
14. Besa NC, Coldiron ME, Bakri A, Raji A, Nsuami MJ, Rousseau C, et al. Diphtheria outbreak with high mortality in northeastern Nigeria. Epidemiol Infect. 2014;142:797–802. https://doi.org/10.1017/S0950268813001696
15. Meera M, Rajarao M. Diphtheria in Andhra Pradesh—a clinical-epidemiological study. Int J Infect Dis. 2014;19:74–8. https://doi.org/10.1016/j.ijid.2013.10.017

Address for correspondence: Kiran Kumar Maramraj, National Centre for Disease Control 151/304, Sekhon Vihar, Palam, New Delhi, 110010, India; email: kiran.maramraj@gmail.com

Trends in Untreated Tuberculosis in Large Municipalities, Brazil, 2008–2017

Melanie H. Chitwood, Daniele M. Pelissari, Gabriela Drummond Marques da Silva, Patricia Bartholomay, Marli Souza Rocha, Denise Arakaki-Sanchez, Mauro Sanchez, Ted Cohen, Marcia C. Castro, Nicolas A. Menzies

We adapted a mathematical modeling approach to estimate tuberculosis (TB) incidence and fraction treated for 101 municipalities of Brazil during 2008–2017. We found the average TB incidence rate decreased annually (0.95%), and fraction treated increased (0.30%). We estimated that 9% of persons with TB did not receive treatment in 2017.

Many countries that have considerable subnational variation in tuberculosis (TB) burden also have decentralized the management and implementation of control policies. In this context, local estimates of TB burden can convey actionable insights for these TB control decisions. Reported cases are commonly used as a proxy for TB burden; however, reported cases may not reflect the true burden because areas of apparently low burden may instead represent areas of inadequate case detection. Modeling approaches have been proposed to adjust for this bias and enable valid inference of TB incidence, but these approaches typically require primary data collection (*1*,*2*). Alternative methods make use of routinely collected data (*3*–*5*). We applied a recently developed Bayesian method to report unbiased estimates of TB incidence and the completeness of case detection in Brazil's state capitals and 100 most populous municipalities during 2008–2017 (Appendix, https://wwwnc.cdc.gov/EID/article/27/3/20-4094-App1.pdf). The Office of Human Research Administration at Harvard T.H. Chan School of Public Health reviewed the initial study submission (protocol no. IRB18-0759) and determined that it met the criteria for exemption from ethics board review.

Author affiliations: Yale School of Public Health, New Haven, Connecticut, USA (M.H. Chitwood, T. Cohen); Ministry of Health, Brasília, Brazil (D.M. Pelissari, P. Bartholomay, M.S. Rocha, D. Arakaki-Sanchez); Oswaldo Cruz Foundation, Minas Gerais, Brazil (G.D. Marques da Silva); University of Brasília, Brasília (M. Sanchez); Harvard T.H. Chan School of Public Health, Boston, Massachusetts, USA (M.C. Castro, N.A. Menzies)

DOI: https://doi.org/10.3201/eid2703.204094

The Study

We selected the 100 most populous municipalities in Brazil (on the basis of mean population between 2008–2017) plus Palmas, the 1 state capital that was not among those 100. We obtained TB treatment notifications from Brazil's National Notifiable Disease Information System (SINAN) (*5*) and death data from the Mortality Information System (SIM) (*6*), representing 438,163 notified TB cases and 45,984 TB-related deaths. Using these data, we estimated a Bayesian model of tuberculosis incidence (M.H. Chitwood et al., unpub. data, https://doi.org/10.2139/ssrn.3463278) in which incidence is approximated by the sum of 3 numbers: treatment initiations, deaths before treatment initiation, and disease resolutions before treatment initiation for a municipality in a given year. We reported the annual incidence rate as absolute incidence divided by population size and the fraction receiving treatment (fraction treated) as the number initiating treatment divided by incidence in a given year. The fraction treated differs from the case detection rate by considering loss to follow-up between diagnosis and treatment as an additional mechanism contributing to undertreatment. We also estimated the incidence of untreated TB (untreated TB rate) as the product (incidence rate) × (1 – fraction treated), to produce a combined measure of elevated incidence and inadequate case detection.

Across all 101 municipalities in 2017, there were 53.2 treatment notifications/100,000 population; we estimate a TB incidence rate of 58.6 (range 11.6–169) cases/100,000 population (Table). In 2017 São Vicente had the highest estimated TB incidence, 169 (95% CI 154–185) cases/100,000 population, and Palmas

Table. Reported cases and estimated burden of TB in state capitals of Brazil, 2017

Municipality	Case notifications/100,000 population*	Incidence/100,000 population (95% CI)	Fraction of cases treated (95% CI)	Untreated TB/100,000 population (95% CI)†
Rio Branco	82.7	83.5 (75.0–92.9)	0.940 (0.879–0.979)	5.07 (1.72–10.7)
Maceió	47.2	55.6 (50.5–61.6)	0.853 (0.779–0.908)	8.23 (4.80–13.4)
Manaus	114	125 (118–133)	0.910 (0.855–0.946)	11.4 (6.51–19.2)
Macapá	39.0	39.9 (34.7–46.3)	0.893 (0.798–0.956)	4.34 (1.64–8.92)
Salvador	54.6	65.3 (60.6–71.9)	0.842 (0.765–0.898)	10.4 (6.31–16.8)
Fortaleza	63.7	70.8 (66.7–75.8)	0.899 (0.849–0.938)	7.17 (4.25–11.3)
Vitória	36.3	39.4 (34.3–44.9)	0.947 (0.883–0.984)	2.10 (0.604–5.00)
Goiânia	17.1	19.4 (17.3–21.7)	0.895 (0.815–0.953)	2.05 (0.883–3.80)
São Luís	64.5	77.2 (70.8–85.0)	0.844 (0.771–0.902)	12.1 (7.20–19.1)
Belo Horizonte	23.6	25.3 (23.2–27.7)	0.926 (0.861–0.97)	1.88 (0.702–3.73)
Campo Grande	38.7	42.4 (38.3–47.2)	0.916 (0.847–0.964)	3.58 (1.45–6.98)
Cuiabá	68.6	79.6 (68.9–103)	0.854 (0.650–0.947)	12.2 (3.82–35.7)
Belém	103	125 (116–138)	0.818 (0.744–0.872)	23.0 (15.1–34.8)
João Pessoa	47.9	51.0 (45.8–57.1)	0.908 (0.824–0.962)	4.78 (1.83–9.80)
Recife	98.4	118 (110–129)	0.839 (0.770–0.892)	19.0 (12.1–29.5)
Teresina	27.6	32.3 (28.8–36.6)	0.906 (0.817–0.966)	3.07 (1.04–6.45)
Curitiba	17.0	19.3 (17.4–21.6)	0.909 (0.829–0.962)	1.78 (0.693–3.57)
Rio de Janeiro	99.8	104 (101–109)	0.953 (0.917–0.977)	4.93 (2.33–8.98)
Natal	54.0	58.3 (52.9–64.8)	0.884 (0.809–0.940)	6.81 (3.36–11.9)
Porto Velho	75.9	81 (73.6–89.5)	0.937 (0.869–0.978)	5.19 (1.71–11.2)
Boa Vista	44.0	41 (35.4–47.1)	0.934 (0.865–0.976)	2.73 (0.914–5.99)
Porto Alegre	92.9	106 (99.2–115)	0.879 (0.817–0.924)	12.9 (7.65–20.8)
Florianópolis	39.3	45.4 (40.5–51.1)	0.941 (0.868–0.983)	2.71 (0.752–6.51)
Aracaju	39.1	42 (37.6–47.3)	0.905 (0.829–0.960)	4.02 (1.59–7.77)
São Paulo	56.5	59.7 (57.5–62.5)	0.944 (0.904–0.972)	3.33 (1.6–6.04)
Palmas	6.28	11.6 (9.34–14.3)	0.910 (0.786–0.974)	1.06 (0.279–2.75)
Rio Branco	82.7	83.5 (75.0–92.9)	0.940 (0.879–0.979)	5.07 (1.72–10.7)

*Excluding notifications for misdiagnosis, reengagement in care, and deceased persons.
†Untreated TB is the product of incidence × (1 – fraction treated), rounded up.

had the lowest, 11.6 (95% CI 9.3–14.3) cases/100,000 population. We estimate that the fraction treated ranged from 0.778 (95% CI 0.687–0.852) to 0.969 (95% CI 0.934–0.990)/100,000 population and the untreated TB rate ranged from 0.723 (95% CI 0.231–1.61) to 23.0 (95% CI 15.1–34.8)/100,000 population (Figure 1).

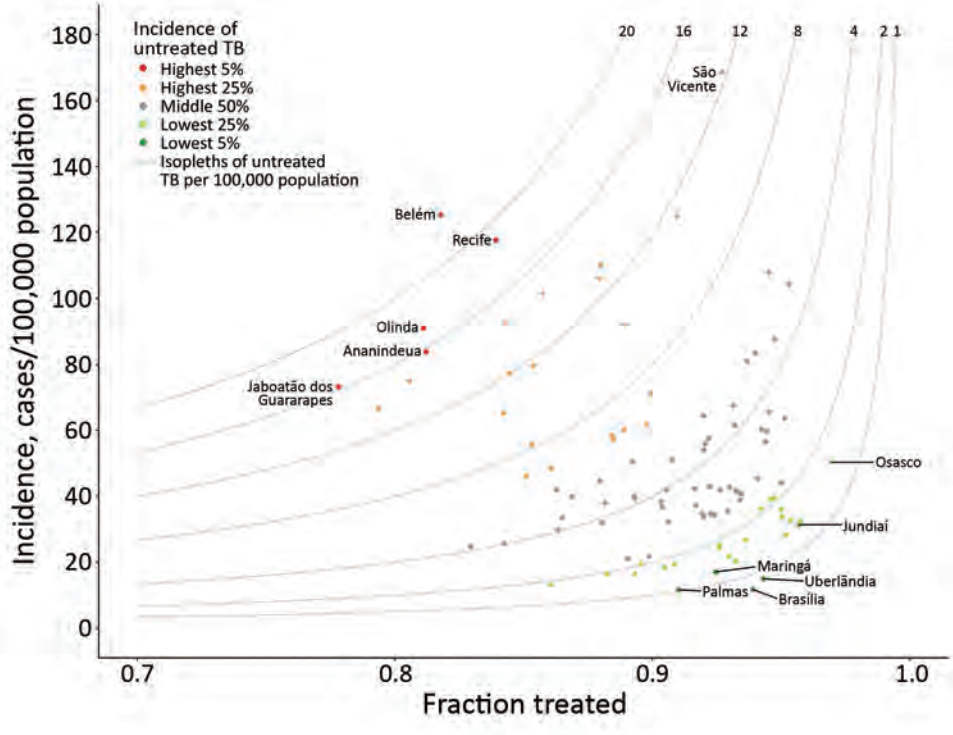

Figure 1. Modeled tuberculosis (TB) burden in 101 largest municipalities and state capitals of Brazil, 2017. Gray curves indicate isopleths of untreated TB: incidence × 1 – (fraction treated). Municipalities in the 5th and 95th percentiles of untreated TB, as well as those with the highest incidence (São Vicente) and highest fraction treated (Osasco), are labeled.

During 2008–2017, there were 438,163 TB treatment notifications; for this period we estimate that there were 488,329 (95% CI 474,715–507,676) incident TB cases, of which 49,778 (95% CI 36,072–69,217) did not initiate treatment. We observed a decrease in notifications from 56.6/100,000 population in 2008 to 53.2/100,000 population in 2017; over this period we estimate that average incidence decreased from 63.9 (range 13.7–138) to 58.6 (range 11.6–169)/100,000 population. Incidence decreased at an average annual rate of 0.95% (range –5.41% to 4.73%), the fraction treated increased at an average annual rate of 0.290% (range –0.966% to 3.55%), and the untreated TB rate decreased at an average annual rate of 2.88% (range –17.4% to 7.98%).

We compared the 10 municipalities with the largest absolute decrease and the 10 with the largest absolute increase in the untreated TB rate (Figure 2). In the municipalities with the largest decrease in untreated TB, the fraction of treated TB cases increased at an average annual rate of 1.23% (0.619–2.17), and incidence decreased at an average annual rate of 1.31% (–3.16 to 2.31) (Figure 2, panels A, B). We estimated that incidence increased in 2/10 municipalities, most notably São Vicente, which had an average annual rate of increase of 2.31% (95% CI 0.642%–3.89%).

In the 10 municipalities with the largest increase in untreated TB, the fraction treated decreased; average annual rate was 0.596% (0.252–0.985) and average incidence rate increased (0.732%; range –2.82 to 3.62) (Figure 2, panels C, D). Although the fraction treated decreased on average, CIs were wide and crossed 0 for the majority of estimates. The change in incidence was heterogenous in this group, ranging from an average decrease of 2.83% (95% CI 1.75%–3.93%) per year in Duque de Caxias to an average increase of 3.63% (95% CI 1.82%–5.35%) per year in Campos dos Goytacazes.

Conclusions

Using a recently developed Bayesian approach for subnational TB estimation (M.H. Chitwood et al.,

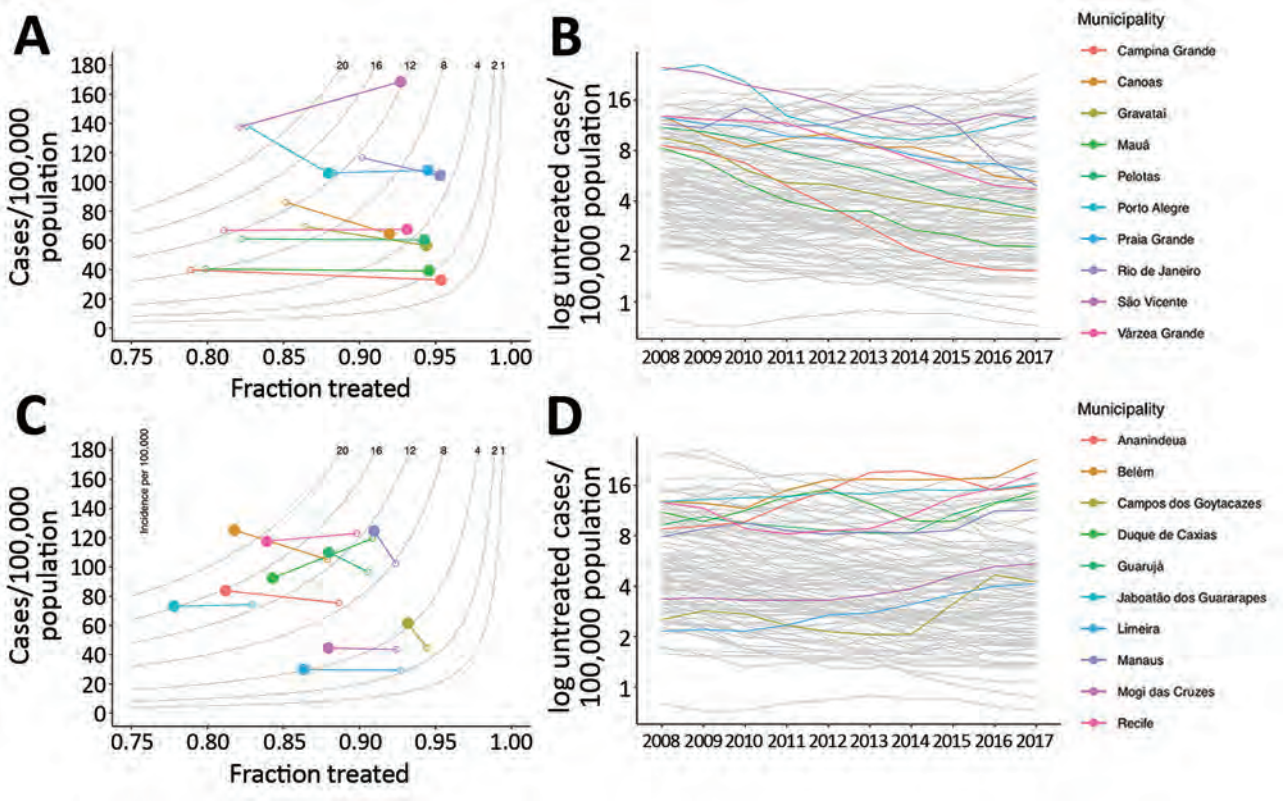

Figure 2. Municipalities of Brazil with the greatest decreases and increases in untreated tuberculosis (TB), 2008–2017. A, B) The 10 municipalities with the greatest decrease in untreated TB, showing the difference between modeled incidence and fraction treated (panel A) and time series of untreated TB (B). C) The 10 municipalities of Brazil with the greatest increase in untreated TB, showing the difference in modeled incidence of TB and fraction treated (C) and time series of untreated TB (D). In panels A and C, gray lines represent isopleths of untreated TB rate per 100,000 population, measured as the product of incidence and (1 – fraction treated); open circles indicate 2008 values, solid circles 2017 values. In panels B and D, gray lines represent other municipalities for comparison.

unpub. data), we estimated the TB incidence rate, fraction treated, and the untreated TB rate for 101 large municipalities in Brazil during 2008–2017. We found that the incidence rate decreased on average and the fraction treated increased on average over the study period. However, in several high-burden municipalities, TB incidence rose and the fraction treated declined, increasing the untreated-TB rate and indicating gaps in local TB control efforts. Comparing our results with a similar state-level analysis of TB trends in Brazil, we found that large municipalities are more heterogenous and have more volatile trends in incidence and fraction treated than states.

The rate of untreated TB communicates both the size of the epidemic and the strength of the response. Municipalities with the highest incidence or the lowest fraction treated may not be the same municipalities with the highest untreated TB rate; an area with a moderate TB incidence and a moderate fraction treated could have a nontrivial rate of untreated TB. If municipalities in need of additional programmatic support were identified based only on the estimated incidence or fraction treated, cities with moderate incidence may be overlooked.

Because we applied a common set of assumptions across all municipalities, our approach may not account for local factors that influence the ratio between reported TB cases and deaths attributed to TB. In our analysis, this ratio provides a signal of the completeness of case detection. If TB death reporting in a municipality were biased downwards (e.g., many TB deaths were misattributed to other causes), the result would be an upward bias in the estimate of the fraction of cases treated. We assume that differences between deaths of persons who have initiated treatment and deaths reported in SIM are due to deaths that occur before treatment. A records linkage of SIM and SINAN was not possible for this analysis. Such a linkage would enable more precise quantification of the frequency of death before treatment initiation. If the overlap between the systems was lower than expected (e.g., more deaths before treatment initiation), our model would underestimate TB burden.

In this analysis, we identified municipalities, such as São Vicente, in which both the fraction treated and incidence increased on average. If these estimates are correct, our findings suggest that factors other than treatment coverage, such as delays between disease onset and treatment initiation, low treatment completion rates, or worsening nutrition and housing quality, could be driving trends in TB incidence. Further analysis of municipalities with both increasing fraction treated and increasing incidence is warranted to elucidate which factors drive increasing TB incidence despite improvements in treatment coverage.

N.A.M. reports grants from Lemann Brazil Research Fund and National Institutes of Health (grant no. 1R01AI146555-01A1) during the conduct of the study.

About the Author

Ms. Chitwood is a doctoral student at the Yale School of Public Health. Her research interests include infectious disease epidemiology and mathematical modeling.

References

1. World Health Organization. Tuberculosis prevalence surveys: a handbook. WHO/HTM/TB/2010.17. Geneva: The Organization; 2011.
2. Glaziou P, Pavli A, Bloss E, Uplekar M, Floyd K. Assessing tuberculosis under-reporting through inventory studies. Geneva: World Health Organization; 2012.
3. Avilov KK, Romanyukha AA, Borisov SE, Belilovsky EM, Nechaeva OB, Karkach AS. An approach to estimating tuberculosis incidence and case detection rate from routine notification data. Int J Tuberc Lung Dis. 2015;19:288–94. https://doi.org/10.5588/ijtld.14.0317
4. Ross JM, Henry NJ, Dwyer-Lindgren LA, de Paula Lobo A, Marinho de Souza F, Biehl MH, et al. Progress toward eliminating TB and HIV deaths in Brazil, 2001–2015: a spatial assessment. BMC Med. 2018;16:144. https://doi.org/10.1186/s12916-018-1131-6
5. Ministério da Saúde. National Notifiable Disease Information System—Sinan. 2nd ed. [in Portuguese]. Brasília: The Ministry; 2007. http://bvsms.saude.gov.br/bvs/publicacoes/07_0098_M.pdf
6. Ministério da Saúde. SIM—Mortality Information System [in Portuguese]. 2008 [cited 2021 Jan 13]. http://www2.datasus.gov.br/DATASUS/index.php?area=060701

Address for correspondence: Melanie H. Chitwood, Yale School of Public Health, 60 College St, New Haven, CT 06511, USA; email: melanie.chitwood@yale.edu.

Without Mercy

Jordi Casabona[1]

Between electric gloom,
angels and demons dressed in plastic blue
have dragged me through the darkness,
to the infinite black stone,
where the origin and the end of time are lost.

There, in the immense dark solitude,
and in the imposed silence of word and thought,
She, in my breath, gazed at me
with her eyes of fire,
frosty and timeless,

without any mercy,
without any mercy.

About the Author

Dr. Casabona is a medical epidemiologist and scientific director of the Centre d'Estudis Epidemiològics de VIH/SIDA/ITS de Catalunya (CEEISCAT), Barcelona, Spain. He has devoted his career working on HIV/STIs both at the local and international level. He is also a writer, having published 3 poetry books.

Bibliography

1. Casabona J. The island of despair. Ann Infect Dis Epidemiol. 2020;5:1061.

Address for correspondence: Jordi Casabona, CEEISCAT, Josep Carreras Building, Ctra. de Can Ruti, Camí de les Escoles, s/n, Badalona 08916, Spain; email: jcasabona@iconcologia.net

Author affiliation: Campus de Can Ruti, Badalona, Spain

DOI: https://doi.org/eid10.3201/eid2703.203690

[1]The author wrote this poem, originally in Catalan, during the first days of his hospitalization because of coronavirus disease in March 2020 during the first wave in Spain.

Severe Pulmonary Disease Caused by *Mycolicibacter kumamotonensis*

Katerina Manika, Fanourios Kontos, Apostolos Papavasileiou, Dimitrios Papaventsis, Maria Sionidou, Ioannis Kioumis

Author affiliations: G. Papanikolaou Hospital, Thessaloniki, Greece (K. Manika, M. Sionidou, I. Kioumis); Attikon University Hospital, Athens, Greece (F. Kontos); Sotiria Chest Diseases Hospital, Athens (A. Papavasileiou, D. Papaventsis)

DOI: https://doi.org/10.3201/eid2703.191648

Severe *Mycolicibacter kumamotonensis*-pulmonary disease was diagnosed in a 68-year-old immunocompetent woman in Greece; the disease was initially treated as tuberculosis. The patient responded favorably to a new treatment regimen of azithromycin, amikacin, moxifloxacin, and linezolid. Complete symptom resolution and radiologic improvement resulted.

Species belonging to genus *Mycolicibacter* (formerly *Mycobacterium terrae complex*) are considered not pathogenic, with the exception of causing chronic tenosynovitis of the hand (*1*,*2*). We present a case of severe pulmonary disease caused by *Mycolicibacter kumamotonensis*, a pathogen that was described in 2006 (*3*).

A 68-year-old woman in Greece had had shortness of breath, productive cough, and low-grade fever for several weeks. The patient was from Georgia but had been living in Greece for the preceding 20 years; she had a history of breast cancer, which had been treated with chemotherapy and radiotherapy 7 years earlier, and bronchiectasis. During the preceding 3 years, the patient had recurrent chest infections and received multiple antimicrobial drug regimens. Based on a positive sputum acid-fast staining, standard antituberculosis treatment was initiated. Culture of the sputum sample was macroscopically suggestive of nontuberculous mycobacteria, but identification of the species was not feasible because of poor growth and technical problems. After 1 month the patient reported improvement of her symptoms and total resolution of fever. Her erythrocyte sedimentation rate (ESR) dropped from 46 to 25 mm/h (reference range 0–20 mm/h), and her weight was stable. Computed tomography (CT) scan of her chest showed multiple cavities, bronchiectasis, nodules, and tree-in-bud appearance (Figure, panels A–C). Bronchoscopy was performed, but PCR for *Mycobacterium tuberculosis*, acid-fast stain, and culture of the bronchial washing were all negative.

Five months into treatment, the patient's condition gradually worsened. She developed productive cough and shortness of breath with hypoxemia (SpO_2 of 91% breathing room air), and her ESR rose to 59 mm/h. A new bronchoscopy was performed. Acid-fast staining results were negative, whereas results of a culture on MGIT960 automated system (strain GR- 21075) (Becton Dickinson, http://www.bd.com) and Lowenstein-Jensen slants (bioMérieux, https://www.biomerieux.com) were positive. No other pathogens were isolated.

For molecular identification, we sequenced regions of 927 bp of 16S rDNA gene and of 440 bp of the 65-kDa heat shock protein (hsp65) gene (3730 DNA analyzer; Applied Biosystems, https://www.thermofisher.com) using the Big Dye Terminator Cycle Sequencing Kit (Applied Biosystems) and previously described primers (*4*). We compared sequences with those of validly published species in the National Center for Biotechnology Information (http://www.ncbi.nlm.nih.gov) using BLAST (http://hsp65blast.phsa.ca/blast/blast.html) and deposited them in GenBank (accession nos. MT491187 and MT491188).

The sequence of 16S rDNA and hsp65 genes showed 100% similarity with the type strain of *Mycolicibacter kumamotonensis* (strain CST7274). We then determined the MICs (SLOMYCOI; TREK Diagnostic Systems, http://www.trekds.com) (*5*). We found the strain had susceptibility to clarithromycin (MIC 1 μg/mL), amikacin (MIC 16 μg/mL), doxycycline (MIC ≤0.12 μg/mL), rifabutin (MIC ≤0.25 μg/mL), ethambutol (MIC 2 μg/mL), and trimethoprim/sulfamethoxazole (MIC 2/38 μg/mL); intermediate susceptibility to linezolid (MIC 16 μg/mL); and resistance to rifampin (MIC >8 μg/mL), ciprofloxacin (MIC 8 μg/mL), and moxifloxacin (MIC 4 μg/mL).

At the end of antituberculosis treatment, a second CT scan revealed slight improvement of the nodules and the tree-in-bud appearance but persistence of the cavities (Figure, panels D–F). Because of the patient's clinical deterioration and the isolation of *M. kumamotonensis* from bronchoalveolar lavage (*1*), we initiated treatment with azithromycin (500 mg 5 d/wk), amikacin (750 mg intramuscular, 5 d/wk), moxifloxacin (400 mg), and linezolid (600 mg). The patient reported complete resolution of symptoms and gained 2 kg of bodyweight, and her ESR dropped to 15 mm/h. One year after diagnosis, a new CT scan showed further improvement, with closure of cavities (Figure, panels G–I). However, many of the nodules persisted. The patient is now

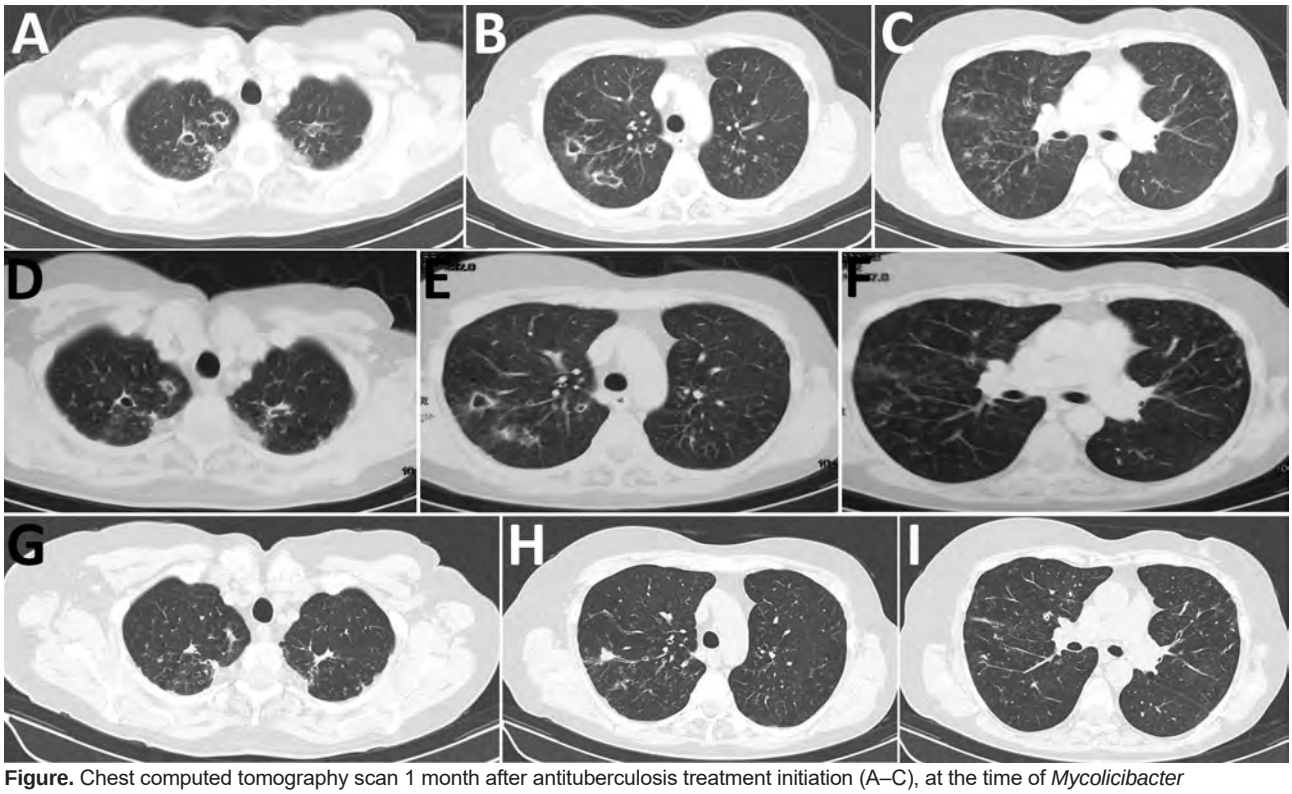

Figure. Chest computed tomography scan 1 month after antituberculosis treatment initiation (A–C), at the time of *Mycolicibacter kumamotonensis* identification (D–F), and 1 year after treatment initiation for *M. kumamotonensis* (G–I). Resolution of cavities and scar formation (A to D to G), resolution of pulmonary infiltrations (B to E to H), and hardening of the nodular appearances (C to F to I) are shown.

fully active and working. The plan is to continue treatment for another 6 months.

M. kumamotonensis has been isolated from respiratory specimens, lymph nodes, and soft tissue all over the world (*3*,*4*,*6*,*7*). Most of these reports, however, do not include data on the clinical implications of *M. kumamotonensis* identification. In their recent report, Iemura-Kashiwagi et al. (*7*) describe the case of soft tissue infection successfully treated with a combination of antimicrobial drugs and surgical debridement. Compared with that report, the MICs of our strain were higher for most of the drugs, possibly because of our patient's history of chest infections treated with multiple regimens.

In an older study, Smith et al. (*8*) reported that 14 out of 54 patients with *M. terrae* infection had pulmonary disease. Because *M. kumamotonensis* and *M. arupense* are the most frequently isolated species of the complex (*9*), some of these cases could in fact be attributed to *M. kumamotonensis.* On the other hand, *M. kumamotonensis* has recently been found in a hospital environment (*10*), so laboratory contamination of clinical specimens is a possibility. Based on the complete resolution of symptoms and the improvement after the appropriate treatment was initiated, we do not consider contamination to be the case with our patient.

The patient responded favorably to the selected regimen even though the strain was resistant to moxifloxacin and of borderline MIC to linezolid. Increase of moxifloxacin dose was not attempted because of fear of QT prolongation in an elderly woman. In conclusion, *M. kumamotonensis* infection should be included in the differential diagnosis of mycobacterial pulmonary disease with cavity formation in immunocompetent adults with bronchiectasis.

About the Author

Dr. Manika is an assistant professor of pneumonology at the Aristotle University of Thessaloniki, Thessaloniki, Greece. Her main focuses of interest are tuberculosis, cystic fibrosis in adults, and respiratory infections.

References

1. Griffith DE, Aksamit T, Brown-Elliott BA, Catanzaro A, Daley C, Gordin F, et al.; ATS Mycobacterial Diseases Subcommittee; American Thoracic Society; Infectious Disease Society of America. An official ATS/IDSA statement: diagnosis, treatment, and prevention of nontuberculous mycobacterial diseases. Am J Respir Crit Care Med. 2007; 175:367–416. https://doi.org/10.1164/rccm.200604-571ST
2. Gupta RS, Lo B, Son J. Phylogenomics and comparative genomic studies robustly support division of the genus *Mycobacterium* into an emended genus *Mycobacterium*

and four novel genera. Front Microbiol. 2018;9:67. https://doi.org/10.3389/fmicb.2018.00067
3. Masaki T, Ohkusu K, Hata H, Fujiwara N, Iihara H, Yamada-Noda M, et al. *Mycobacterium kumamotonense* sp. nov. recovered from clinical specimen and the first isolation report of *Mycobacterium arupense* in Japan: novel slowly growing, nonchromogenic clinical isolates related to *Mycobacterium terrae* complex. Microbiol Immunol. 2006;50:889–97. https://doi.org/10.1111/j.1348-0421.2006.tb03865.x
4. Kontos F, Mavromanolakis DN, Zande MC, Gitti ZG. Isolation of *Mycobacterium kumamotonense* from a patient with pulmonary infection and latent tuberculosis. Indian J Med Microbiol. 2016;34:241–4. https://doi.org/10.4103/0255-0857.180356
5. Clinical and Laboratory Standards Institute. Susceptibility testing of mycobacteria, Nocardia spp., and other aerobic actinomycetes. 3rd edition. CLSI Standard Document M24. Annapolis Junction (MD): The Institute; 2018.
6. Hoefsloot W, van Ingen J, Andrejak C, Angeby K, Bauriaud R, Bemer P, et al.; Nontuberculous Mycobacteria Network European Trials Group (NTM-NET). The geographic diversity of nontuberculous mycobacteria isolated from pulmonary samples: an NTM-NET collaborative study. Eur Respir J. 2013;42:1604–13. https://doi.org/10.1183/09031936.00149212
7. Iemura-Kashiwagi M, Ito I, Ikeguchi R, Kadoya M, Iemura T, Yoshida S, et al. Soft tissue infection caused by *Mycolicibacter kumamotonensis*. J Infect Chemother. 2019;26:136–9. https://doi.org/10.1016/j.jiac.2019.06.013
8. Smith DS, Lindholm-Levy P, Huitt GA, Heifets LB, Cook JL. *Mycobacterium terrae*: case reports, literature review and in vitro antibiotic susceptibility testing. Clin Infect Dis. 2000;30:444–53. https://doi.org/10.1086/313693
9. Tortoli E, Gitti Z, Klenk HP, Lauria S, Mannino R, Mantegani P, et al. Survey of 150 strains belonging to the *Mycobacterium terrae* complex and description of *Mycobacterium engbaekii* sp. nov., *Mycobacterium heraklionense* sp. nov. and *Mycobacterium longobardum* sp. nov. Int J Syst Evol Microbiol. 2013;63:401–11. https://doi.org/10.1099/ijs.0.038737-0
10. Davarpanah M, Azadi D, Shojaei H. Prevalence and molecular characterization of non-tuberculous mycobacteria in hospital soil and dust of a developing country, Iran. Microbiology. 2019;165:1306–14. https://doi.org/10.1099/mic.0.000857

Address for correspondence: Katerina Manika, Respiratory Infections Unit, Pulmonary Department, Aristotle University of Thessaloniki, G. Papanikolaou Hospital, Exohi 57010, Thessaloniki, Greece; email: ktmn05@yahoo.gr

Misidentification of *Burkholderia pseudomallei*, China

Bin Wu, Xinxin Tong, Haoyan He, Yinmei Yang, Huling Chen, Xiao Yang, Banglao Xu

Author affiliation: Guangzhou First People's Hospital, South China University of Technology, Guangzhou, China

DOI: https://doi.org/10.3201/eid2703.191769

We report a case of melioidosis in China and offer a comparison of 5 commercial detection systems for *Burkholderia pseudomallei*. The organism was misidentified by the VITEK 2 Compact, Phoenix, VITEK mass spectrometry, and API 20NE systems but was eventually identified by the Bruker Biotyper system and 16S rRNA sequencing.

Burkholderia pseudomallei is the cause of melioidosis, a serious disease endemic to Southeast Asia and northern Australia (*1*). Because of the increase in international travel, the disease is now occurring in areas to which *B. pseudomallei* is not endemic. In these previously unaffected areas, laboratory staff might be unfamiliar with the organism or use identification systems that are not suitable for its detection, potentially leading to misidentification (*2*). We report the misidentification of *B. pseudomallei* by various commercial detection systems.

On May 15, 2019, a man 33 years of age in Guangxi Province, China, sought treatment for leg pain at a local hospital in Guangxi Province. Physicians diagnosed his condition as gout and prescribed oral febuxostat. However, the pain progressively worsened, and the patient began to have difficulty walking. On June 10 he was admitted to Guangzhou First People's Hospital. Laboratory analysis of serum samples taken at admission showed moderate systemic inflammation with elevated levels of procalcitonin (0.296 ng/mL; reference value <0.05 ng/mL), C-reactive protein (61.7 mg/L; reference value <6.0 mg/L), erythrocyte sedimentation rate (120 mm/h; reference value <15 mm/h), leukocytes (13.87 × 10^9 cells/L; reference value 1.1–3.2 × 10^9 cells/L), and neutrophils (9.42 × 10^9 cells/L; reference value: 1.8–6.3 × 10^9 cells/L). His temperature fluctuated between 38.5°C and 39.8°C, peaking in the evening. Magnetic resonance imaging results suggested osteomyelitis. We conducted surgical debridement and collected pus from the lesion for microbiological analysis. We used the matrix-assisted laser desorption/ionization time-of-flight (MALDI-TOF) mass spectrometry VITEK 2 Compact system (bioMérieux,

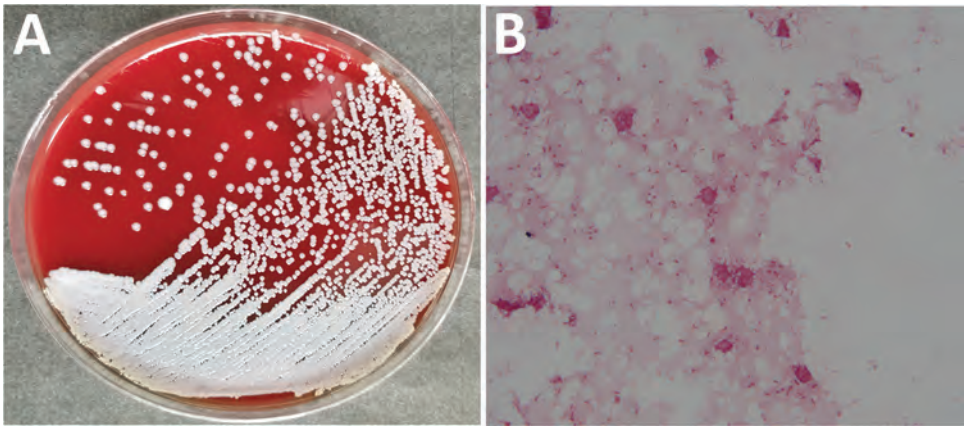

Figure. *Burkholderia pseudomallei* isolated from patient, China, 2019. A) Culture on sheep blood agar. B) Gram-stained smear. Original magnification ×1,000.

https://www.biomerieux.com) to identify the isolate as *Aeromonas sobria* with 93% probability. According to the VITEK 2 Compact system, the isolate was sensitive to amikacin, meropenem, imipenem, ceftazidime, ciprofloxacin, trimethoprim/sulfamethoxazole, and piperacillin/tazobactam but resistant to cefepime and aztreonam. We made a preliminary diagnosis of *Aeromonas* infection and treated the patient with piperacillin/tazobactam (500 mg, 4×/d) and levofloxacin (500 mg/d). However, we doubted the accuracy of this identification because *Aeromonas sobria* rarely causes extraintestinal disease (*3*). To examine this suspicion, we collected blood samples and incubated them in the Bact/ALERT 3D automated microbial detection system (bioMérieux). We cultured the samples on sheep blood and chocolate agar, revealing gram-negative rod-shaped bacteria (Figure; Appendix Figure 1, https://wwwnc.cdc.gov/EID/article/27/3/19-1769-App1.pdf). We then tested the samples with a variety of commercial detection systems. The VITEK 2 Compact system again identified the blood sample as *Aeromonas sobria* with 90% probability. However, the Bruker MALDI-TOF Biotyper system (Bruker Daltonics, https://www.bruker.com) identified the isolate as *B. pseudomallei* with an identification score of 2.18 (a score of >2.0 is considered an accurate identification). BD Phoenix M50 (Becton Dickinson, http://www.bd.com) identified it as *Alcaligenes faecalis* with 98% probability; VITEK MS (bioMérieux) identified it as *B. thailandensis* with an identification score of 2.23; API 20NE (bioMérieux) identified it as *Pseudomonas fluorescens* with 75.8% probability (Table).

To confirm the identity of the organism, we extracted DNA from blood cultures using a bacterial genomic DNA isolation kit (Sangon Biotech Co., Ltd, https://www.sangon.com). The 16S rRNA gene was amplified and sequenced by Sangon Biotech Co., Ltd. The isolate showed 100% identity and 100% coverage with a sequence of *B. pseudomallei* collected in India in 2019 (GenBank accession no. CP040552.1). On June 25, we diagnosed melioidosis in the patient. The patient recovered and was discharged after 14 days of the original piperacillin/tazobactam and levofloxacin treatment regimen. The global recommendations from the US Public Health Emergency Medical Countermeasures Enterprise suggest that physicians treat melioidosis with intravenous ceftazidime or meropenem, according to the severity of the disease; alternatively, physicians can prescribe oral trimethoprim/sulfamethoxazole or amoxicillin/clavulanic acid (*4*).

We conducted multilocus sequence typing as described previously (*5*). This isolate belongs to sequence type (ST) 550, corresponding with isolates previously documented in Vietnam in 2005 (*6*). The patient in this study had never been to Vietnam, but Guangxi Province borders that country. We constructed a phylogenetic tree with 1,000 bootstrap replicates using the unweighted pair group method with arithmetic averages in MEGA X software

Table. Identification of *Burkholderia pseudomallei* by various detection systems, China, 2019

Detection method	Identification result	Characteristics
Vitek 2 Compact	*Aeromonas sobria*	90% probability
Phoenix	*Alcaligenes faecalis*	98% probability
Bruker Biotyper MS	*Burkholderia pseudomallei*	2.18 score*
Vitek MS	*Burkholderia thailandensis*	2.23 score*
API 20NE	*Pseudomonas fluorescens*	75.8% probability
16S rRNA	*Burkholderia pseudomallei*	GenBank accession no.CP040552.1

*An identification score >2.0 indicates an accurate identification.

(https://www.megasoftware.net). This tree included isolates from other countries in Asia downloaded from PubMLST (https://pubmlst.org); the isolate in this study was most closely related to ST175 from Thailand (Appendix Figure 2) (*6*).

The accuracy of the identifications made by VITEK 2 (63%–81%), Phoenix (0%–28%), and API 20NE (37%–99%) systems varied substantially (*7*,*8*). Zakharova et al. found that commercially available biochemical identification systems commonly misidentified *B. pseudomallei* as *Chromobacterium violaceum* or *B. cepacia* complex (*9*). We found that although the isolate in this study was misidentified by multiple systems, most systems accurately identified the genus. MALDI-TOF mass spectrometry is a rapid, accurate, and highly reproducible technique for bacterial identification. Several studies have explored the potential of MALDI-TOF mass spectroscopy for the identification of *B. pseudomallei*. We prefer the Bruker Biotyper system, which is more accurate because the VITEK databases lack reference spectra for *B. pseudomallei* (*10*). In conclusion, scientists must be aware of the potential misidentification of *B. pseudomallei* by automated identification systems, especially those in regions to which *B. pseudomallei* is not endemic.

About the Author

Mr. Wu is a member of the Department of Laboratory Medicine of Guangzhou First People's Hospital, Guangzhou. His primary research interest is bacterial infections.

References

1. Chewapreecha C, Holden MT, Vehkala M, Valimaki N, Yang Z, Harris SR, et al. Global and regional dissemination and evolution of *Burkholderia pseudomallei*. Nat Microbiol. 2017;2:16263. https://doi.org/10.1038/nmicrobiol.2016.263
2. Kiratisin P, Santanirand P, Chantratita N, Kaewdaeng S. Accuracy of commercial systems for identification of *Burkholderia pseudomallei* versus *Burkholderia cepacia*. Diagn Microbiol Infect Dis. 2007;59:277–81. https://doi.org/10.1016/j.diagmicrobio.2007.06.013
3. Kobayashi H, Seike S, Yamaguchi M, Ueda M, Takahashi E, Okamoto K, et al. *Aeromonas sobria* serine protease decreases epithelial barrier function in T84 cells and accelerates bacterial translocation across the T84 monolayer in vitro. PLoS One. 2019;14:e0221344. https://doi.org/10.1371/journal.pone.0221344
4. Lipsitz R, Garges S, Aurigemma R, Baccam P, Blaney DD, Cheng AC, et al. Workshop on treatment of and postexposure prophylaxis for *Burkholderia pseudomallei* and *B. mallei* Infection, 2010. Emerg Infect Dis. 2012;18:e2. https://doi.org/10.3201/eid1812.120638
5. Godoy D, Randle G, Simpson AJ, Aanensen DM, Pitt TL, Kinoshita R, et al. Multilocus sequence typing and evolutionary relationships among the causative agents of melioidosis and glanders, *Burkholderia pseudomallei* and *Burkholderia mallei*. J Clin Microbiol. 2003;41:2068–79. https://doi.org/10.1128/JCM.41.5.2068-2079.2003
6. Kamthan A, Shaw T, Mukhopadhyay C, Kumar S. Molecular analysis of clinical *Burkholderia pseudomallei* isolates from southwestern coastal region of India, using multi-locus sequence typing. PLoS Negl Trop Dis. 2018;12:e0006915. https://doi.org/10.1371/journal.pntd.0006915
7. Zong Z, Wang X, Deng Y, Zhou T. Misidentification of *Burkholderia pseudomallei* as *Burkholderia cepacia* by the VITEK 2 system. J Med Microbiol. 2012;61:1483–4. https://doi.org/10.1099/jmm.0.041525-0
8. Hoffmaster AR, AuCoin D, Baccam P, Baggett HC, Baird R, Bhengsri S, et al. Melioidosis diagnostic workshop, 2013. Emerg Infect Dis. 2015;21.
9. Zakharova IB, Lopasteyskaya YA, Toporkov AV, Viktorov DV. Influence of biochemical features of *Burkholderia pseudomallei* strains on identification reliability by Vitek 2 System. J Glob Infect Dis. 2018;10:7–10. https://doi.org/10.4103/jgid.jgid_39_17
10. Lau SK, Sridhar S, Ho CC, Chow WN, Lee KC, Lam CW, et al. Laboratory diagnosis of melioidosis: past, present and future. Exp Biol Med (Maywood). 2015;240:742–51. https://doi.org/10.1177/1535370215583801

Address for correspondence: Banglao Xu, Guangzhou First People's Hospital, School of Medicine, South China University of Technology, Department of Laboratory Medicine, 1 Panfu Rd, Guangzhou, 510180, China; email: eyxubl@scut.edu.cn

Autochthonous Case of Pulmonary Histoplasmosis, Switzerland

Yvonne Schmiedel,[1] Annina E. Büchi,[1] Sabina Berezowska, Alexander Pöllinger, Konrad Mühlethaler, Manuela Funke-Chambour

Author affiliations: Basel University Hospital, Basel, Switzerland (Y. Schmiedel); Hôpital du Jura, Delémont, Switzerland (Y. Schmiedel); Inselspital, Bern University Hospital, University of Bern, Bern, Switzerland (Y. Schmiedel, A.E. Büchi, A. Pöllinger, M. Funke-Chambour); Lausanne University Hospital and University of Lausanne Lausanne, Switzerland (S. Berezowska); Institute of Pathology, University of Bern, Bern, Switzerland (S. Berezowska); Institute for Infectious Diseases, University of Bern, Bern (K. Mühlethaler)

DOI: https://doi.org/10.3201/eid2703.191831

[1]These authors contributed equally to this article.

In Europe, pulmonary histoplasmosis is rarely diagnosed except in travelers. We report a probable autochthonous case of severe chronic pulmonary histoplasmosis in an immunocompetent man in Switzerland without travel history outside of Europe. Diagnosis was achieved by histopathology, fungal culture, and serology, but the source of the infection remains speculative.

A 48-year-old man in Switzerland sought treatment for a 1-year history of progressive dyspnea, cough, 20-kg weight loss, and increased sweating; he was receiving oxygen therapy. Results of previous consultations had been inconclusive. An HIV screening test was negative. Medical history included hyperreflexia, depression, and chronic hepatitis B. The man had stopped cocaine inhalation and heroin consumption 20 years earlier but continued smoking cigarettes and cannabis. Regular medications included omeprazole and trimipramine. Except for a short trip to Greece and Italy many years before, the patient reported no foreign travel.

In the absence of travel history to an endemic area, histoplasmosis was not initially considered at the time this patient sought treatment. A prolonged diagnostic process and delayed treatment initiation had meanwhile resulted in significant deterioration of health, including need for home oxygen therapy, and loss of ability to work. Meanwhile, the patient was cachectic and had clubbing on his fingers and toes. Spirometry revealed nearly normal dynamic lung volumes. Forced expiratory volume was 3 L (75%) and forced vital capacity 4.1 L (83%), but diffusion capacity was severely impaired; diffusing capacity for carbon monoxide was 20%. A 6-minute walking test was limited to 400 m (59% predicted), initial oxygen saturation dropping from 90% to 78%. A chest computed tomography (CT) scan showed a diffuse reticulonodular pattern with predominantly upper lung opacifications and bronchiectases indicating fibrotic lung disease (Figure, panels A, B). Reversed halo signs and right upper lobe nodules were found. Bronchoscopy results including bronchoalveolar lavage were unremarkable. Initial sampling with microbiological screening was negative.

Differential diagnoses included toxic lung damage or other interstitial lung disease, (e.g. atypical presentation of Langerhans cell histiocytosis or sarcoidosis). A wedge biopsy showed predominantly upper-lobe fibrosis and multiple, confluent, necrotizing granulomas harboring yeasts, establishing the diagnosis of pulmonary histoplasmosis (Appendix Figure, https://wwwnc.cdc.gov/EID/article/27/3/19-1831-App1.pdf).

A qualitative immunodiffusion test (IMMY, https://www.immy.com) was positive for antibodies in plasma, but an antigen immunoassay for *Histoplasma* in urine (IMMY) was negative; a beta-1,3-D glucan test (Fungitell, https://www.fungitell.com) was highly positive (>500 pg/mL; limit <80 pg/mL). At

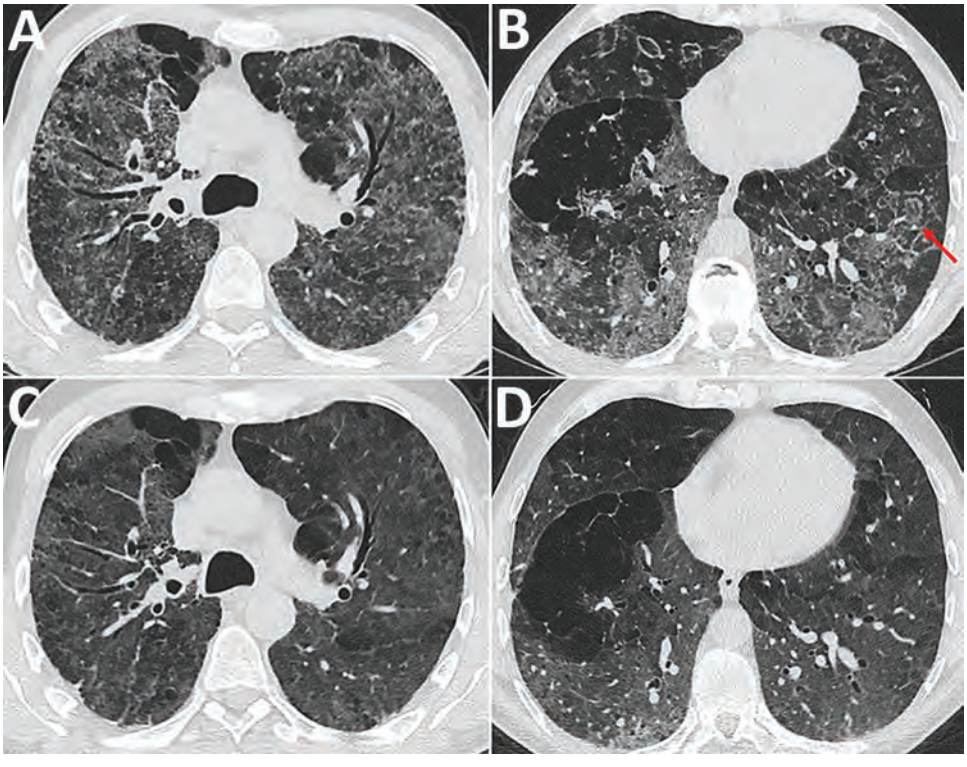

Figure. Chest computed tomography (CT) images at the level of the upper third and the lower third of the lung in a patient with pulmonary histoplasmosis, Switzerland. A, B) Initial CT shows diffuse reticulonodular pattern with ground glass opacifications, predominantly located in the upper two thirds of the lungs, and several areas with reverse halo signs (red arrows). C, D) Follow-up CT scan exhibited reduced ground-glass opacities and a regression of the micronodules. The reversed halos showed complete regression. CT, computed tomography.

prolonged incubation (14 days, 30°C), a fungal culture on BD Difco dehydrated culture media Sabouraud brain heart infusion agar base (with chloramphenicol and cycloheximide) (https://www.bd.com) showed flat, floccose to powdery, whitish growth. We found microscopically large, tuberculated macroconidia (7–12 μM) and small round microconidia on short, lateral pegs consistent with *Histoplasma capsulatum*. Matrix-assisted laser desorption/ionization time-of-flight mass spectrometry (MALDI Biotyper, https://www.bruker.com) results confirmed the diagnosis. Molecular identification was done using an in-house panfungal PCR assay with consecutive sequence analysis. We used the internal transcribed spacer region as target and internal transcribe sequences 1 and 2 for amplification primers (*1*,*2*). Microsynth AG (https://www.microsynth.ch) performed DNA sequencing. Sequences produced alignments of *H. capsulatum* in BLAST (https://blast.ncbi.nlm.nih.gov/Blast.cgi) and CBS (Centraalbureau voor Schimmelcultures; Westerdijk Institute, https://wi.knaw.nl) databases.

Some radiologic features were unusual. There was no cavity formation (*3*), and the reverse halo sign has rarely been described in chronic pulmonary histoplasmosis (*4*). However, bullae seen on the scan, previously observed in patients with heavy tobacco use and underlying lung disease, were compatible with the diagnosis. Despite slow growth, cultures for histoplasmosis together with histopathology remain the diagnostic standard (*1*). Panfungal PCR is sensitive, but its performance depends on internal validation processes (*2*). Immunocompetence and lack of dissemination could explain repeatedly negative urine antigen testing. (*1*).

Underlying lung disease likely predisposed this patient for severe disease. However, his clinical response to treatment was remarkable. We initiated antifungal treatment with liposomal amphotericin B and oral prednisolone. After a few days, the patient improved substantially, and oxygen supplementation was stopped. At 10 days, therapy was switched to oral itraconazole. Steroid treatment was continued at a tapered dosage over 3 months, with trimethoprim/sulfamethoxazole used as *Pneumocystis jirovecii* pneumonia prophylaxis. At 3-month follow-up, the patient had improved considerably. Repeated spirometry was nearly normal, showing persistent impairment of diffusion capacity. Follow-up chest CT scan (Figure 1, panels C, D) showed regression of ground-glass opacities and micronodules; the reversed halos had disappeared. Overall, optimal treatment duration remains unclear (*5*), but because of probable underlying preexisting lung disease, persistent pathological findings from CT, and continued desaturation under exercise, continuing treatment for >12 months seemed necessary.

The source of infection for this patient remains speculative. However, possible risk exposures were guano from flying bats in the garden (*6*), previous use of organic fertilizer possibly containing histoplasma (*7*), and regular work-related unpacking of fruits and spices from straw-filled boxes from West Africa, although *H. capsulatum* var. *capsulatum* is less common in that region (*8*).

In addition to previous findings of histoplasmosis in badgers (*9*), this case confirms the likely environmental occurrence of *H. capsulatum* in Switzerland. Although diagnoses of autochthonous histoplasmosis have been rare, and few autochthonous cases have been described (*10*), our finding of a probable autochthonous case of chronic pulmonary histoplasmosis in an immunocompetent male in Switzerland highlights the incomplete understanding of histoplasmosis endemicity and indicates that it has likely been underestimated in Europe.

About the Author

Ms. Schmiedel has a masters degree in epidemiology and a diploma in tropical medicine from Cayetano Heredia Universidad in Lima, Peru, and has completed specialized training in infectious diseases and internal medicine. She currently works as a senior infectious disease consultant at Hôpital du Jura (affiliated with Basel University Hospital) and has a strong interest in infection control and tropical medicine. Ms. Büchi has a masters degree in immunology and microbiology from Bern University in Switzerland and is studying to become an internist at the Inselspital in Bern. She has a primary research interest in bloodstream infection.

References

1. Hage CA, Ribes JA, Wengenack NL, Baddour LM, Assi M, McKinsey DS, et al. A multicenter evaluation of tests for diagnosis of histoplasmosis. Clin Infect Dis. 2011;53:448–54. https://doi.org/10.1093/cid/cir435
2. Kauffman CA. Histoplasmosis: a clinical and laboratory update. Clin Microbiol Rev. 2007;20:115–32. https://doi.org/10.1128/CMR.00027-06
3. Wheat LJ, Conces D, Allen SD, Blue-Hnidy D, Loyd J. Pulmonary histoplasmosis syndromes: recognition, diagnosis, and management. Semin Respir Crit Care Med. 2004;25:129–44. https://doi.org/10.1055/s-2004-824898
4. Marchiori E, Melo SMD, Vianna FG, Melo BSD, Melo SSD, Zanetti G. Pulmonary histoplasmosis presenting with the reversed halo sign on high-resolution CT scan. Chest. 2011;140:789–91. https://doi.org/10.1378/chest.11-0055
5. Wheat LJ, Freifeld AG, Kleiman MB, Baddley JW, McKinsey DS, Loyd JE, et al.; Infectious Diseases Society of America. Clinical practice guidelines for the management of patients with histoplasmosis: 2007 update by the Infectious Diseases Society of America. Clin Infect Dis. 2007;45:807–25. https://doi.org/10.1086/521259

6. Staffolani S, Buonfrate D, Angheben A, Gobbi F, Giorli G, Guerriero M, et al. Acute histoplasmosis in immunocompetent travelers: a systematic review of literature. BMC Infect Dis. 2018;18:673. https://doi.org/10.1186/s12879-018-3476-z
7. Gómez LF, Torres IP, Jiménez-A MDP, McEwen JG, de Bedout C, Peláez CA, et al. Detection of *Histoplasma capsulatum* in organic fertilizers by Hc100 nested polymerase chain reaction and its correlation with the physicochemical and microbiological characteristics of the samples. Am J Trop Med Hyg. 2018;98:1303–12. https://doi.org/10.4269/ajtmh.17-0214
8. Azar MM, Hage CA. Laboratory diagnostics for histoplasmosis. J Clin Microbiol. 2017;55:1612–20. https://doi.org/10.1128/JCM.02430-16
9. Akdesir E, Origgi FC, Wimmershoff J, Frey J, Frey CF, Ryser-Degiorgis MP. Causes of mortality and morbidity in free-ranging mustelids in Switzerland: necropsy data from over 50 years of general health surveillance. BMC Vet Res. 2018;14:195. https://doi.org/10.1186/s12917-018-1494-0
10. Ashbee HR, Evans EG, Viviani MA, Dupont B, Chryssanthou E, Surmont I, et al.; European Confederation of Medical Mycology Working Group on Histoplasmosis. Histoplasmosis in Europe: report on an epidemiological survey from the European Confederation of Medical Mycology Working Group. Med Mycol. 2008;46:57–65. https://doi.org/10.1080/13693780701591481

Address for correspondence: Yvonne Schmiedel, Inselspital University Hospital Bern, Department of Infectious Diseases, Freiburgstrasse Bern 3010, Switzerland; email: yvonneschmiedel@gmail.com

etymologia

Histoplasma capsulatum [hĭs′tə-plăz′mə kăp′sə-lā′təm]

Monika Mahajan

In 1905, Samuel Taylor Darling serendipitously identified a protozoan-like microorganism in an autopsy specimen while trying to understand malaria, which was prevalent during the construction of the Panama Canal. He named this microorganism *Histoplasma capsulatum* because it invaded the cytoplasm (plasma) of histiocyte-like cells (Histo) and had a refractive halo mimicking a capsule (capsulatum), a misnomer.

Histoplasma capsulatum, a dimorphic fungus, now belongs to Kingdom Fungi and causes histoplasmosis (Darling's disease) through inhalation of spores found in soil and bird droppings. The fungus thrives in the central and eastern parts of United States, especially around the Ohio and Mississippi River valleys, and in South America, Africa, Asia, and Australia. Three varieties exist globally: *H. capsulatum* var. *capsulatum, H. capsulatum* var. *duboisii,* and *H. capsulatum* var. *farciminosum.*

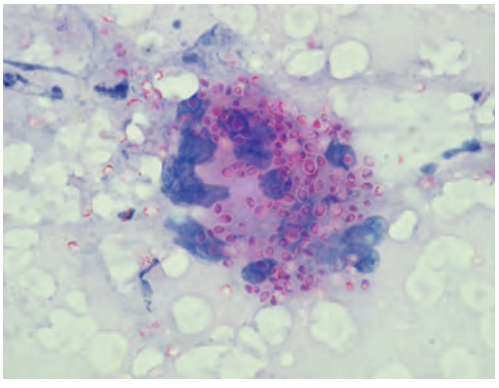

Figure. Numerous, capsulated yeast cells (shown in pink) of *Histoplasma capsulatum* in a bone marrow aspirate (Giemsa-stained, original magnification ×400). Source: Shivaprakash Rudramurthy, PGIMER, Chandigarh, India.

Sources

1. Darling ST. A protozoon general infection producing pseudotubercules in the lungs and focal necrosis in the liver, spleen, and lymphnodes. JAMA. 1906;46:1283. https://doi.org/10.1001/jama.1906.62510440037003
2. Hagan T. The discovery and naming of histoplasmosis: Samuel Taylor Darling. JAMA. 1903;40:1905–7 [cited 2020 Nov 19]. http://www.antimicrobe.org/hisphoto/history/Discovery%20of%20Histoplasmosis-Darling.asp
3. Histoplasmosis, types of diseases, fungal diseases, CDC [cited 2020 Aug 21]. https://www.cdc.gov/fungal/diseases/histoplasmosis/
4. Ramsey TL, Applebaum AA. Histoplasmosis "darling." Am J Clin Pathol. 1942;12:85–94. https://doi.org/10.1093/ajcp/12.2.85
5. Slavin MA, Chakrabarti A. Opportunistic fungal infections in the Asia–Pacific region. Med Mycol. 2012;50:18–25. https://doi.org/10.3109/13693786.2011.602989

Author affilation: Post Graduate Institute of Medical Education and Research, Chandigarh, India

Address for correspondence: Monika Mahajan, Department of Medical Microbiology, Post Graduate Institute of Medical Education and Research, Research Block A, Sector 12, UT Chandigarh 160012, India; email: monideepmj@yahoo.com

DOI: https://doi.org/10.3201/eid2703.ET2703

Local Transmission of SARS-CoV-2 Lineage B.1.1.7, Brazil, December 2020

Ingra Morales Claro,[1] Flavia Cristina da Silva Sales,[1] Mariana Severo Ramundo, Darlan S. Candido, Camila A.M. Silva, Jaqueline Goes de Jesus, Erika R. Manuli, Cristina Mendes de Oliveira, Luciano Scarpelli, Gustavo Campana, Oliver G. Pybus, Ester Cerdeira Sabino,[2] Nuno Rodrigues Faria,[2] José Eduardo Levi[2]

Author affiliations: University of São Paulo, São Paulo, Brazil (I.M. Claro, F.C.S. Sales, M.S. Ramundo, D.S. Candido, C.A.M. Silva, J.G. de Jesus, E.R. Manuli, E.C. Sabino, N.R. Faria, J.E. Levi); University of Oxford, Oxford, UK (D.S. Candido, O.G. Pybus, N.R. Faria); Diagnósticos da América SA (DASA), Baueri, Brazil (C.M. de Oliveira, L. Scarpelli, G. Campana, J.E. Levi); Imperial College London, London, UK (N.R. Faria)

DOI: https://doi.org/10.3201/eid2703.210038

In December 2020, research surveillance detected the B.1.1.7 lineage of severe acute respiratory syndrome coronavirus 2 in São Paulo, Brazil. Rapid genomic sequencing and phylogenetic analysis revealed 2 distinct introductions of the lineage. One patient reported no international travel. There may be more infections with this lineage in Brazil than reported.

Genomic sequencing and analysis during the severe acute respiratory syndrome coronavirus 2 (SARS-CoV-2) pandemic have led to identification of ≈800 distinct SARS-CoV-2 lineages worldwide. A new phylogenetic cluster, B.1.1.7 lineage or variant of concern 202012/01, is characterized by 17 unique mutations and was first detected in southeastern England in late September 2020 (A. Rambaut et al., unpub. data, https://virological.org/t/preliminary-genomic-characterisation-of-an-emergent-sars-cov-2-lineage-in-the-uk-defined-by-a-novel-set-of-spike-mutations/563). As of January 17, 2021, this lineage had been confirmed in 38 countries (https://cov-lineages.org/global_report_B.1.1.7.html). Epidemiologic and phylogenetic studies suggest that the rapid epidemic growth of B.1.1.7 in the United Kingdom is caused by its higher transmissibility (E. Volz et al., unpub. data, https://www.medrxiv.org/content/10.1101/2020.12.30.20249034v2; N. Davies, unpub. data, https://cmmid.github.io/topics/covid19/uk-novel-variant.html), which could lead to increased incidence and higher peaks in hospitalizations and deaths (N. Davies, unpub. data, https://cmmid.github.io/topics/covid19/uk-novel-variant.html).

We confirm 2 cases of infection with SARS-CoV-2 B.1.1.7 lineage in Latin America. On December 30, 2020, we received saliva samples from 2 patients for genomic sequencing as part of research surveillance activities. Patient 1 was a woman 20–30 years of age residing in São Paulo, Brazil, who reported no travel outside of Brazil. Her symptoms began on December 21, and testing was conducted the next day. Patient 2 was a man 30–40 years of age who was tested in São Paulo on December 22 after having traveled from London on December 19. Ethics approval for this study was confirmed by the national ethics review board (Comissão Nacional de Ética em Pesquisa, protocol no. CAAE 30127020.0.0000.0068).

PCR testing (TaqPath COVID-19 PCR; ThermoFisher Scientific, https://www.thermofisher.com) performed as previously described (*1*) indicated that patient 1 was positive for the open reading frame 1ab (cycle threshold [C_t] 25.8) and nucleoprotein (C_t 24.5) gene targets and patient 2 was positive for open reading frame 1ab (C_t 28.1) and nucleoprotein (C_t 27.29), but both were negative for the spike gene target. The 2 spike-gene dropout samples were identified among 400 samples collected during November 4–December 25, 2020.

For each sample, we conducted nanopore sequencing in duplicate by using the ARTIC protocol (https://www.protocols.io/view/ncov-2019-sequencing-protocol-bbmuik6w). Concentrations of double-stranded DNA for the library-negative controls were below detection levels, indicating no contamination. We conducted whole-genome sequencing of SARS-CoV-2 by using the MinION platform (Oxford Nanopore Technologies, https://nanoporetech.com). By December 31, sequencing statistics revealed 56,565 mapped reads for patient 1 and 51,761 for patient 2. Consequently, 28,023 bases for patient 1 and 26,339 for patient 2 were covered at >25× depth. Consensus sequences covered 92.4% of the Wuhan Hu-1 reference genome (GenBank accession no. MN908947.3) for patient 1 and 87.1% for patient 2. For the 2 newly generated genome sequences, we identified the B.1.1.7 lineage (assignment probability = 1.0) by using the pangolin COVID-19 Lineage Assigner version 2.1.6 (*2*) (https://pangolin.cog-uk.io). The 2 genomes were made publicly available on GISAID (http://www.gisaid.org) on December 31, 2020 (identification nos. EPI_ISL_754236 for patient 1 and EPI_ISL_754237 for patient 2).

We next estimated a rapid maximum-likelihood phylogenetic tree (*3*,*4*) for a multiple sequence align-

[1]These first authors contributed equally to this article.

[2]These senior authors contributed equally to this article.

ment (*5*) with the new sequences and 127 publicly available B.1.1.7 genomes from around the world available on GISAID (*6*) as of December 31, 2020 (https://github.com/CADDE-CENTRE/VOC-Lineage-Brazil). The virus genome recovered from patient 1 grouped within a well-supported cluster (bootstrap 85%) of 10 sequences (60% from the United Kingdom) (Figure). This finding is consistent with the travel history of an asymptomatic family member who was positive for SARS-CoV-2 (according to a rapid test performed on December 23, 2020), who arrived in São Paulo on December 17 after traveling from Italy to the United Kingdom and, after a short stay, from London to São Paulo, and who was in close contact with patient 1. The sequence from patient 2 clustered with good statistical support (bootstrap 79.4%) with a sequence collected in the United Kingdom on November 27. Patient 2 had traveled from London to São Paulo on December 19 and was symptomatic when saliva was collected on December 22. Phylogenetic analysis suggests that this infection represents a second, independent introduction of the B.1.1.7 lineage from the United Kingdom to Brazil; patient 2 was not epidemiologically linked to patient 1.

Because information about this lineage from locations outside the United Kingdom is limited, our interpretations based on phylogenetic data might be biased by the different numbers of available genome sequences shared around the globe. Moreover, the samples that we analyzed were selected from only 2 cases confirmed by reverse transcription PCR in São Paulo; thus, our genomes were obtained from a small fraction of targeted spike-gene failure, and frequency of detection in our nonrandom sample does not represent prevalence of this lineage at the population level.

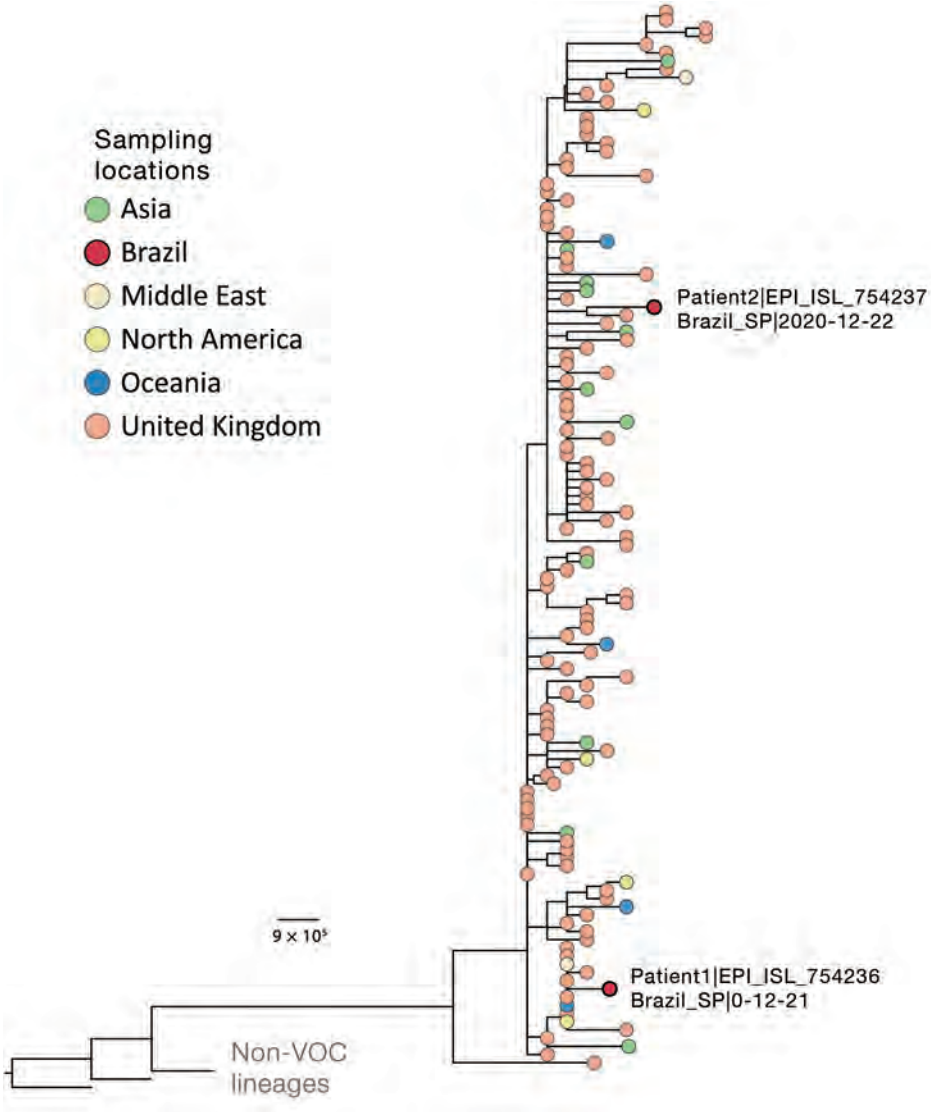

Figure. Phylogenetic context of novel severe acute respiratory syndrome coronavirus 2 B.1.1.7 genomes isolated from 2 patients in Brazil (labeled on figure), December 2020. Downsampling for the phylogenetic analysis of the B.1.1.7 SARS-CoV-2 variant (n = 4,693, December 31, 2020) was performed by selecting 1 sequence per country per day. As outgroups, we included 2 B.1.1 sequences from the United Kingdom that were closely related to the lineage of interest and sequence WH04 from Wuhan, China (GISAID identification no. EPI_ISL_406801; http://www.gisaid.org). Details on multiple alignment and phylogenetic tree reconstruction are described elsewhere (*4*). Tree file, aligned sequences, and GISAID acknowledgment tables are available at https://github.com/CADDE-CENTRE/VOC-Lineage-Brazil. Scale bar indicates nucleotide substitutions per site. VOC, variant of concern.

Despite temporary suspension of all flights to or from Brazil from or through the United Kingdom as of December 25, 2020 (http://www.gov.uk/foreign-travel-advice/brazil), it is likely that the number of SARS-CoV-2 lineage B.1.1.7 infections in Brazil is higher than that reported. Increasing genomic surveillance of B.1.1.7 and other variants of concern that carry mutations of potential biological significance (e.g., E484K in the spike protein; C.M. Voloch, unpub data, https://www.medrxiv.org/content/10.1101/2020.12.23.20248598v1) is imperative for monitoring vaccination effectiveness and contextualizing the epidemiology and evolution of SARS-CoV-2 in Latin America.

Acknowledgments

We thank all researchers who are working around the clock to generate and share genome data worldwide on GISAID (http://www.gisaid.org). GISAID acknowledgment tables are available at https://github.com/CADDE-CENTRE/VOC-Lineage-Brazil.

This project was supported by a Medical Research Council-São Paulo Research Foundation (FAPESP) CADDE partnership award (MR/S0195/1 and FAPESP 18/14389-0) (http://caddecentre.org/). N.R.F. is supported by a Wellcome Trust and Royal Society Sir Henry Dale Fellowship (204311/Z/16/Z).

About the Author

Mrs. Claro is a PhD student at the Department of Infectious Disease, School of Medicine & Institute of Tropical Medicine, University of São Paulo, São, Paulo, Brazil. She is a part of the Centre for Arbovirus Discovery, Diagnostics, Genomics and Epidemiology team and has primary research interests in real-time epidemiologic surveillance of viruses of public importance for Brazil.

References

1. Vogels CBF, Watkins AE, Harden CA, Brackney DE, Shafer J, Wang J, et al. SalivaDirect: a simplified and flexible platform to enhance SARS-CoV-2 testing capacity. Med. 2020 Dec 26 [Epub ahead of print]. https://doi.org/10.1016/j.medj.2020.12.010
2. Rambaut A, Holmes EC, O'Toole Á, Hill V, McCrone JT, Ruis C, et al. A dynamic nomenclature proposal for SARS-CoV-2 lineages to assist genomic epidemiology. Nat Microbiol. 2020;5:1403–7. https://doi.org/10.1038/s41564-020-0770-5
3. Minh BQ, Schmidt HA, Chernomor O, Schrempf D, Woodhams MD, von Haeseler A, et al. IQ-TREE 2: new models and efficient methods for phylogenetic inference in the genomic era. Mol Biol Evol. 2020;37:1530–4. https://doi.org/10.1093/molbev/msaa015
4. Candido DS, Claro IM, de Jesus JG, Souza WM, Moreira FRR, Dellicour S, et al. Evolution and epidemic spread of SARS-CoV-2 in Brazil. Science. 2020;369:1255–60. https://doi.org/10.1126/science.abd2161
5. Katoh K, Standley DM. MAFFT multiple sequence alignment software version 7: improvements in performance and usability. Mol Biol Evol. 2013;30:772–80. https://doi.org/10.1093/molbev/mst010
6. Shu Y, McCauley J. GISAID: Global Initiative on Sharing All Influenza Data—from vision to reality. Euro Surveill. 2017;30;22:30494.

Address for correspondence: Nuno R. Faria, St Mary's Hospital, Praed St, Paddington, London W2 1NY, UK; email: nfaria@ic.ac.uk; and José Eduardo Levi, Avenida Juruá 548, Alphaville, Barueri, SP 06455-010, Brazil; email: jose.levi.ext@dasa.com.br

Mycobacterium bovis Pulmonary Tuberculosis, Algeria

Fatah Tazerart, Jamal Saad, Abdellatif Niar, Naima Sahraoui,[1] Michel Drancourt[1]

Author affiliations: Université Ibn Khaldoun de Tiaret, Tiaret, Algeria (F. Tazerart); Université de Blida, Blida, Algeria (F. Tazerart, N. Sahraoui); Institut Hospitalo-Universitaire Méditerranée Infection, Marseille, France (F. Tazerart, J. Saad, M. Drancourt); Aix-Marseille-University, Marseille (J. Saad, M. Drancourt); Laboratoire de Reproduction des Animaux de la Ferme, Université Ibn Khaldoun de Tiaret, Tiaret (A. Niar)

DOI: https://doi.org/10.3201/eid2703.191823

We analyzed 98 *Mycobacterium tuberculosis* complex isolates collected in 2 regions of Algeria in 2015–2018 from 93 cases of pulmonary tuberculosis. We identified 93/98 isolates as *M. tuberculosis* lineage 4 and 1 isolate as *M. tuberculosis* lineage 2 (Beijing). We confirmed 4 isolates as *M. bovis* by whole-genome sequencing.

In Algeria, interpreting tuberculosis (TB) incidence, estimated at 53–88 cases/100,000 population in 2017 (*1*), is limited by the fact that the diagnosis relies on microscopic examination of clinical samples. Iso-

[1]These authors equally contributed to this work.

lates are presumptively identified as *Mycobacterium tuberculosis* complex based on colony phenotype.

We analyzed 98 sputum isolates identified as *M. tuberculosis* complex by 5 Tuberculosis and Respiratory Disease Control Service facilities in 2015–2018 (Appendix Table 1, Figure, https://wwwnc.cdc.gov/EID/article/27/3/19-1823-App1.pdf). Exact tandem repeat D analysis (*2*) confirmed these 98 isolates as *M. tuberculosis* complex. Large-sequence polymorphism analysis using PCR sequencing of genomic regions RD105, RD239, and RD750 and of the polyketide synthase gene *pks*15/1 (*3*) yielded 88 (89.8%) *M. tuberculosis* sensu stricto Euro-American lineage 4 isolates and 1 East Asian lineage 2 (Beijing) isolate. Whole-genome sequencing (WGS) of 5 RD deletion–free unidentified isolates indicated that these 5 isolates, P9982(ERR3588223), P9983(ERR3588225), P9985(ERR3588243), P9984(ERR3588246), and P9986(ERR3588247), were *M. tuberculosis* sensu stricto Euro-American lineage 4. We conducted WGS analysis using TB-profiler for *M. tuberculosis* online tool (https://tbdr.lshtm.ac.uk/upload) for lineage and sublineage determination. Altogether, *M. tuberculosis* lineage 4 was the predominant lineage in the 5 Algerian departments and the sole lineage documented in Bgayet, Tizi-Ouzou, and Medea (Appendix Table 2); it was found to be the cause of pulmonary TB in 79/93 (85%) cases, pleural TB in 11 (12%) cases, and lymph node TB in 3 (3%) cases. These observations updated those issued from a previous study conducted in 14 departments including 114 (88%) cases of pulmonary localization and 15 cases (12%) of extrapulmonary localization (*4*). In a later study, spoligotyping revealed that most isolates belonged to *M. tuberculosis* Euro-American lineage 4; the Haarlem clade accounted for 29.5% of studied isolates; the Latin American-Mediterranean clade, 25.6%; and the T clade, 24.8% (*4*). In our study, 1 *M. tuberculosis* Beijing strain was isolated from a bronchial fluid sample collected in Blida from the location at which 15 *M. tuberculosis* Beijing isolates had been identified ≈10 years earlier from 14 workers from Algeria and 1 from China (*5*). Our observation suggests that 10-year circulation of *M. tuberculosis* Beijing strain in the community in Blida area most probably followed immigration of workers from China employed in the construction sector.

WGS analysis of 4 additional isolates exhibiting a 6-bp deletion in the *pks*15/1 gene identified them as *M. bovis*. Using a Roary pangenome pipeline (https://sanger-pathogens.github.io/Roary), we found that *M. bovis* CSURP9981 grouped with *M. bovis* CSURP9979 and that *M. bovis* CSURP9980 grouped with *M. bovis* CSURP9978 (Figure). Further analysis based on the 3,732,808-bp core genome detected 3,761-bp (0.1%) of single-nucleotide polymorphisms (SNPs) between the 4 isolate genomes. Whole-genome sequences of *M. bovis* strains in the study have been deposited in GenBank (sequence P9978, accession no. ERR3587501; P9979, no. ERR3587591; P9980, no. ERR3587597; and P9981, no. ERR3588222).

All 4 patients had pulmonary TB and had no detectable lymph node swelling and no scrofula (*6*). Two case-patients in Blida were a 27-year-old unemployed man and a 60-year-old taxi driver who both declared that they did not consume raw milk and had no contacts with cattle; a neighbor of the 60-year-old patient was a butcher with whom he

Figure. Pangenome-based tree of 4 human *Mycobacterium bovis* isolates, Algeria. The tree was generated by Roary (https://sanger-pathogens.github.io/Roary) from binary gene presence or absence in the accessory genome. Scale bar indicates 10% sequence divergence.

spent a lot of time. Two case-patients in Ain Defla were 18-year-old and 43-year-old housewives living in 2 different rural areas. The interviews of these patients did not reveal contacts with cattle. Identification of human cases of *M. bovis* was unexpected because in 50 years, only 7 cases of *M. bovis* human infection have been reported in Algeria: 3 cases of pulmonary TB and 2 cases of cervical lymphatic TB detected in a total of 1,183 (0.4%) phenotypically identified *M. bovis* isolates (*7*), and 2 additional cases reported in 2009 (*8*).

M. bovis TB is clinically, pathologically, and radiologically indistinguishable from *M. tuberculosis*; diagnosis requires accurate identification of the causative mycobacterium, most efficiently by using WGS. Our report illustrates pitfalls in precisely tracing the natural history of *M. bovis* TB in patients, including sources, routes of transmission, and primary route of entry, which may determine the pathology of the infection. Zoonotic *M. bovis* TB was most often transmitted to humans by the consumption of *M. bovis*–contaminated dairy products that caused lymphatic TB, eventually becoming pulmonary TB (*9*). We previously reported a hidden circumstance for contacts with *M. bovis*–infected animals, tracing 1 *M. bovis* pulmonary TB case in a patient in Tunisia to contacts with an infected sheep during religious festivities in 2018 (*10*). In the case we report here, foodborne transmission cannot be ruled out, but it is possible that this may be a rare case of aerosol transmission.

Algeria is a bovine TB–enzootic country. We recommend comparing the genome sequences from the 4 patients reported here with those of future bovine isolates in the same departments to trace zoonotic *M. bovis* TB in Algeria and contribute to the understanding of its natural history.

Acknowledgments

We thank Graba L., Lamri Zahir, Cherair Ali, and Kerrouche Moussa and those who are responsible for the Tuberculosis and Respiratory Disease Control Service facilities of Tizi Ouzou for their valuable assistance. We also thank Mohamed Rahal, Asma Aiza, and especially Sofiane Tahrikt.

About the Author

Dr. Tazerart is a veterinarian with a magister degree in animal epidemiology. He is an instructor at Blida University and is a PhD student at Tiaret University, Algeria. His research interests include bovine and human tuberculosis in Algeria, with a focus on characterization of animal and human *M. bovis* strains.

References

1. Bouziane F, Allem R, Sebaihia M, Kumanski S, Mougari F, Sougakoff W, et al.; CNR-MyRMA. First genetic characterisation of multidrug-resistant *Mycobacterium tuberculosis* isolates from Algeria. J Glob Antimicrob Resist. 2019;19:301–7. https://doi.org/10.1016/j.jgar.2019.05.010
2. Djelouadji Z, Raoult D, Daffé M, Drancourt M. A single-step sequencing method for the identification of *Mycobacterium tuberculosis* complex species. PLoS Negl Trop Dis. 2008;2:e253. https://doi.org/10.1371/journal.pntd.0000253
3. Gagneux S, Small PM. Global phylogeography of *Mycobacterium tuberculosis* and implications for tuberculosis product development. Lancet Infect Dis. 2007;7:328–37. https://doi.org/10.1016/S1473-3099(07)70108-1
4. Ifticene M, Kaïdi S, Khechiba MM, Yala D, Boulahbal F. Genetic diversity of *Mycobacterium tuberculosis* strains isolated in Algeria: results of spoligotyping. Int J Mycobacteriol. 2015;4:290–5. https://doi.org/10.1016/j.ijmyco.2015.06.004
5. Ifticene M, Gacem FZ, Yala D, Boulahbal F. *Mycobacterium tuberculosis* genotype Beijing: about 15 strains and their part in MDR-TB outbreaks in Algeria. Int J Mycobacteriol. 2012;1:196–200. https://doi.org/10.1016/j.ijmyco.2012.10.006
6. Forget N, Challoner K. Scrofula: emergency department presentation and characteristics. Int J Emerg Med. 2009;2:205–9. https://doi.org/10.1007/s12245-009-0117-8
7. de Beco O, Boulahbal F, Grosset J. Incidence of the bovine bacillus in human tuberculosis at Algiers in 1969 [in French]. Arch Inst Pasteur Alger. 1970;48:93–101.
8. Gharnaout M, Bencharif N, Abdelaziz R, Douagui H. Tuberculosis from *Mycobacterium bovis*: about two cases [in French]. Rev. Mal. Respir. 2009;26:141. https://www.em-consulte.com/rmr/article/197004
9. Michel AL, Müller B, van Helden PD. *Mycobacterium bovis* at the animal–human interface: a problem, or not? Vet Microbiol. 2010;140:371–81. https://doi.org/10.1016/j.vetmic.2009.08.029
10. Saad J, Baron S, Lagier JC, Drancourt M, Gautret P. *Mycobacterium bovis* pulmonary tuberculosis after ritual sheep sacrifice in Tunisia. Emerg Infect Dis. 2020;26:1605–7. https://doi.org/10.3201/eid2607.191597

Address for correspondence: Michel Drancourt, Aix Marseille Université, Institut Hospitalo-Universitaire Méditerranée Infection, 19-21 Bd Jean Moulin, 13005 Marseille, France; email: michel.drancourt@univ-amu.fr

COVID-19–Associated *Fusobacterium nucleatum* Bacteremia, Belgium

Louis Wolff, Delphine Martiny, Véronique Yvette Miendje Deyi, Evelyne Maillart, Philippe Clevenbergh, Nicolas Dauby

Author affiliations: Université Libre de Bruxelles, Brussels, Belgium (L. Wolff, D. Martiny, V.Y. Miendje Deyi, E. Maillart, P. Clevenbergh, N. Dauby); Saint-Pierre University Hospital Brussels, Brussels (L. Wolff, N. Dauby); Université de Mons, Mons, Belgium (D. Martiny); Laboratoire Hospitalier Universitaire de Bruxelles–Universitair Laboratorium Brussel, Brussels, (D. Martiny, V.Y. Miendje Deyi); Brugmann University Hospital, Brussels (E. Maillart, P. Clevenbergh)

DOI: https://doi.org/10.3201/eid2703.202284

We report 4 cases of *Fusobacterium nucleatum* bacteremia associated with coronavirus disease (COVID-19). Three cases occurred concomitantly with COVID-19 diagnosis; 1 occurred on day 15 of intensive care. None of the patients had known risk factors for *F. nucleatum* bacteremia. *F. nucleatum* infection could represent a possible complication of COVID-19.

Fusobacterium nucleatum is a gram-negative anaerobic rod member of the oral and digestive microbiota (*1*). *F. nucleatum* is an uncommon cause of bacteremia; annual reported incidence is 0.22–0.34 cases/100,000 population (*1*,*2*). Risk factors for *F. nucleatum* bacteremia include malignancy, older age, alcohol abuse, immunosuppression, and dialysis; infection is often hospital-acquired (*1*,*2*). Mortality rates for *F. nucleatum* bacteremia can reach 10% (*1*,*2*).

In March and April 2020, 2 major hospitals in Brussels, Belgium, observed 4 cases of monomicrobial *F. nucleatum* bacteremia, all associated with severe acute respiratory syndrome coronavirus 2 (SARS-CoV-2) infection among patients with coronavirus disease (COVID-19). In contrast, the same hospitals reported a total of 4 *F. nucleatum* cases in 2019, 3 in 2018, 2 in 2017, 1 in 2016, and 2 in 2015. However, the hospital emergency plan initiated on March 14 during the first wave of the COVID-19 pandemic in Belgium prohibited all nonurgent medical care. Thus, the 2020 *F. nucleatum* incidence cannot be extrapolated and compared with previous years because of modifications of patient characteristics.

F. nucleatum was cultured from patients' blood specimens by using a BD BACTEC FX blood culture system (Becton Dickinson, https://www.bd.com) and pure isolates were successfully identified by using matrix-assisted laser desorption/ionization time-of-flight mass spectrometry (Bruker Daltonics, https://www.bruker.com). Cross-contamination was formally excluded because blood cultures became positive on different days and bacterial identifications were performed on separate sets of experiments (Table 1).

Nasopharyngeal swab samples were collected from the 4 patients. Three patients tested positive for SARS-CoV-2 by reverse transcription PCR (RT-PCR) using the RealStar SARS-CoV-2 RT-PCR kit (Altona Diagnostics, https://www.altona-diagnostics.com) and 1 by a COVID-19 Ag Respi-Strip rapid antigen test (Coris Bioconcept, https://www.corisbio.com). All 4 patients had concomitant pneumonia compatible with COVID-19 on chest computed tomography (CT) scans. The patients were 34, 51, 52, and 70 years of age (median 51.5 years); the median age was lower than in previously reported *F. nucleatum* bacteremia (*1*,*2*), but the sample size is too small for statistical analysis. None of the patients had any classical risk factors for *F. nucleatum* bacteriemia. The youngest patient had no underlying conditions. Three patients had abdominal symptoms and 2 underwent abdominal CT with contrast, but both had unremarkable results. Three patients had symptoms of bacteremia at the time of COVID-19 diagnosis; bacteremia was diagnosed in the other patient after 15 days in the hospital intensive care unit (ICU). The ICU patient received a single 800-mg intravenous dose of tocilizumab (TCZ) to treat COVID-19–associated hyperinflammatory syndrome. Increased risk for severe infection, including bacteremia, has been associated with long-term TCZ treatment when administered for non-COVID-19 indications (*3*). To our knowledge, no previous *F. nucleatum* infection has been reported with TCZ use in general. The patient died of COVID-19–related severe respiratory failure on day 21 in the ICU, but the other 3 patients were discharged to home without complications.

Although SARS-CoV-2 infection initially was described as an agent of severe pneumonia, other organ involvements are now well described. Other studies among hospitalized COVID-19 patients have shown that 18%–48% had digestive complaints ranging from anorexia to diarrhea and abdominal pain (*4*,*5*). RT-PCR detected the virus in the feces of 48%–53% of patients with abdominal complaints and feces remained positive in 20%–33% of patients even after respiratory samples converted from RT-PCR–positive to negative (*4*,*6*). The propensity of SARS-CoV-2 to infect digestive organs might be explained by the fact that

Table. Characteristics of 4 cases of *Fusobacterium nucleatum* bacteremia in patients with COVID-19, Belgium*

Characteristic	Patient 1	Patient 2	Patient 3	Patient 4
Age, y	52	51	34	70
COVID-19 diagnosis	Day of admission	Day of admission	Day of admission	Day of admission
Symptoms at diagnosis	Dry cough and sore throat for 7 d	Cough, abdominal pain, and diarrhea for 7 d	Cough, abdominal pain, and diarrhea for 7 d	Fever (38.5°C), vomiting for 1 d
Underlying conditions	Hypertension	Diabetes, hypertension, obesity	None	Diabetes, hypertension, hypothyroidism, history of stroke
Radiological findings				
Chest CT	Ground glass opacities in all lobes	Diffuse infiltrates in all lobes	Ground glass opacities in 10% of lungs	Ground glass opacities in 10% of lungs
Abdominal CT with contrast	NA	NA	Unremarkable	Unremarkable
Blood culture collection	Day 1	Day 15	Day 1	Day 1
Time to positivity (no. sets)	96 h (1 of 2)	55 h (1 of 2)	72 h (1 of 2)	72 h (1 of 2)
COVID-19 therapy	HCQ 400 mg oral 2×/d on day 1, then 200 mg 2×/d for 4 d	HCQ 400 mg oral 2×/d on day 1, then 200 mg 2×/d for 4 d; TCZ 800 mg IV once; and RDV 200 mg IV loading dose, then 100 mg 4×/d for 4 d	None	None
Antimicrobial drug therapy	None	TZP 4 g IV 4×/d for 6 d	MTZ 500 mg orally 3×/d for 7 d	None
F. nucleatum antimicrobial susceptibility testing				
Amoxicillin/clavulanic	S	S	S	S
Clindamycine	S	S	S	S
Imipenem	S	S	S	S
Metronidazole	S	S	S	S
Piperacilline/tazobactam	S	S	S	S
Outcome	Discharged home	Died	Discharged home	Discharged home

*COVID-19, coronavirus disease; CT, computed tomography; HCQ, hydroxychloroquine; IV, intravenous; MTZ, metronidazole; RDV, remdesivir; S, susceptible; TCZ, tocilizumab; TZP, piperacilline-tazobactam.

angiotensin converting enzyme 2, a known receptor used by the virus to enter human cells, has been found to be highly expressed in enterocytes (*4*,*7*).

The reservoir of *F. nucleatum* is generally considered to be the oral cavity (*8*). Only 1 of these patients had oral symptoms, but no oral lesions were observed. The 3 other patients had abdominal symptoms, suggesting that bacteremia might be the consequence of translocation from the digestive tract (*9*). *F. nucleatum* has been shown to colonize colon mucus with associated mucosal inflammation (*10*).

In conclusion, digestive tract invasion by SARS-CoV-2 and secondary inflammatory response might promote translocation of opportunistic pathogens, such as *F. nucleatum*, and further research could elucidate this interaction. Nonetheless, our observations suggest that anaerobe bacteremia should be considered as a complication of COVID-19.

Acknowledgments

We thank Adrian Griffiths for English language revision.

About the Author

Dr. Wolff is a resident in internal medicine at Saint-Pierre University Hospital Brussels, Belgium. His research interests include immunology and medical education.

References

1. Afra K, Laupland K, Leal J, Lloyd T, Gregson D. Incidence, risk factors, and outcomes of *Fusobacterium* species bacteremia. BMC Infect Dis. 2013;13:264. https://doi.org/10.1186/1471-2334-13-264
2. Nohrström E, Mattila T, Pettilä V, Kuusela P, Carlson P, Kentala E, et al. Clinical spectrum of bacteraemic *Fusobacterium* infections: from septic shock to nosocomial bacteraemia. Scand J Infect Dis. 2011;43:463–70. https://doi.org/10.3109/00365548.2011.565071
3. Bykerk VP, Östör AJK, Alvaro-Gracia J, Pavelka K, Román Ivorra JA, Nurmohamed MT, et al. Long-term safety and effectiveness of tocilizumab in patients with rheumatoid arthritis and inadequate responses to csDMARDs and/or TNF inhibitors: an open-label study close to clinical practice. Clin Rheumatol. 2019;38:2411–21. https://doi.org/10.1007/s10067-019-04535-z
4. Xiao F, Tang M, Zheng X, Liu Y, Li X, Shan H. Evidence for gastrointestinal infection of SARS-CoV-2. Gastroenterology. 2020; 158:1831–1833.e3. https://doi.org/10.1053/j.gastro.2020.02.055
5. Pan L, Mu M, Yang P, Sun Y, Wang R, Yan J, et al. Clinical characteristics of COVID-19 patients with digestive symptoms in Hubei, China: a descriptive, cross-sectional, multicenter study. Am J Gastroenterol. 2020;115:766–73. https://doi.org/10.14309/ajg.0000000000000620
6. Cheung KS, Hung IFN, Chan PPY, Lung KC, Tso E, Liu R, et al. Gastrointestinal manifestations of SARS-CoV-2 infection and virus load in fecal samples from a Hong Kong cohort: systematic review and meta-analysis. Gastroenterology. 2020;159:81–95. https://doi.org/10.1053/j.gastro.2020.03.065

7. Lamers MM, Beumer J, van der Vaart J, Knoops K, Puschhof J, Breugem TI, et al. SARS-CoV-2 productively infects human gut enterocytes. Science. 2020;369:50–4. https://doi/10.1126/science.abc1669
8. Abed J, Maalouf N, Manson AL, Earl AM, Parhi L, Emgård JEM, et al. Colon cancer-associated *Fusobacterium nucleatum* may originate from the oral cavity and reach colon tumors via the circulatory system. Front Cell Infect Microbiol. 2020;10:400. https://doi.org/10.3389/fcimb.2020.00400
9. Han YW. *Fusobacterium nucleatum*: a commensal-turned pathogen. Curr Opin Microbiol. 2015;23:141–7. https://doi.org/10.1016/j.mib.2014.11.013
10. Strauss J, Kaplan GG, Beck PL, Rioux K, Panaccione R, Devinney R, et al. Invasive potential of gut mucosa-derived *Fusobacterium nucleatum* positively correlates with IBD status of the host. Inflamm Bowel Dis. 2011;17:1971–8. https://doi.org/10.1002/ibd.21606

Address for correspondence: Nicolas Dauby, Department of Infectious Diseases, CHU Saint-Pierre, Brussels, Belgium; email: nicolas_dauby@stpierre-bru.be

Drug-Resistant Tuberculosis in Pet Ring-Tailed Lemur, Madagascar

Marni LaFleur, Kim E. Reuter, Michael B. Hall, Hoby H. Rasoanaivo, Stuart McKernan, Paulo Ranaivomanana, Anita Michel, Marie Sylvianne Rabodoarivelo, Zamin Iqbal, Simon Grandjean Lapierre, and Niaina Rakotosamimanana

Author affiliations: Lemur Love Inc., San Diego, California, USA (M. LaFleur); University of San Diego, San Diego (M. LaFleur, K.E. Reuter); University of Utah, Salt Lake City, Utah, USA (K.E. Reuter); European Bioinformatics Institute, Cambridge, UK (M.B. Hall, Z. Iqbal); University of Antananarivo, Antananarivo, Madagascar (H.H. Rasoanaivo); Wildlife One Health, Mtunzini, South Africa (S. McKernan); Institut Pasteur de Madagascar, Antananarivo (P. Ranaivomanana, M.S. Rabodoarivelo, S. Grandjean Lapierre, N. Rakotosamimanana); University of Pretoria, Pretoria, South Africa (A. Michel); Université de Montréal, Montréal (S. Grandjean Lapierre)

DOI: https://doi.org/10.3201/eid2703.202924

We diagnosed tuberculosis in an illegally wild-captured pet ring-tailed lemur manifesting lethargy, anorexia, and cervical lymphadenopathy. Whole-genome sequencing confirmed the *Mycobacterium tuberculosis* isolate belonged to lineage 3 and harbored streptomycin resistance. We recommend reverse zoonosis prevention and determination of whether lemurs are able to maintain *M. tuberculosis* infection.

Tuberculosis (TB) is an ancient disease affecting a plethora of domestic and wild animals, including humans. In primates, TB can cause severe multisystemic disease. The prevalence of TB in lemurs within Madagascar is unknown; the most recent documented case occurred in 1973 (*1*). Reverse zoonotic transmission of TB can occur when nonhuman primates are in close contact with humans (*1*). We report a clinical case and genomic analysis of TB infection in a female subadult ring-tailed lemur (*Lemur catta*) held at a nongovernmental organization facilty in Southwestern Madagascar. The University of San Diego (San Diego, CA, USA) provided ethics authorization (no. IACUC 0619-01).

The lemur was born in the wild in September or October 2018 and was surrendered to the facility in April 2019. On July 12, the animal was emaciated, anorexic, and lethargic; it had a large fistulated mass on the left cervical region. The mass was surgically removed and found to be caseous and necrotic (Figure). Despite rehydration and systemic antimicrobial therapy, the lemur died on July 16.

We confirmed TB infection by PCR on the lymph node sample using GeneXpert MTB/RIF assay (Cepheid, https://www.cepheid.com) (*2*). We cultured on Löwenstein-Jensen solid medium to confirm streptomycin resistance using the proportions method, enabling phenol chloroform DNA extraction and genomic DNA sequencing using Oxford Nanopore Technologies (ONT) (https://www.nanoporetech.com) long-read sequencing. We basecalled raw data using ONT Guppy software version 3.4.5. We performed read mapping using minimap2 version 2.17. For decontamination, we used a manually curated database including viral nontuberculosis mycobacteria and human sequences, augmented with *L. catta* genome (GenBank accession no. PVHV00000000) to improve host DNA filtering. Decontaminated reads were mapped to the *M. tuberculosis* H37Rv reference genome (accession no. NC_000962.3); we called single-nucleotide polymorphisms (SNPs) using bcftools version 1.10 (http://samtools.github.io/bcftools/bcftools.html) and masked repetitive regions (*3*). We performed genotypic resistance testing using Mykrobe Predict version 0.8.2 (https://www.mykrobe.

Figure. Lymph node removed from ring-tailed lemur in Madagascar that exhibited advanced clinical symptoms consistent with tuberculosis. Blade is 44 mm by 22 mm.

com) and confirmed streptomycin resistance (causative variant R83P/CCG4407954CGG) (*4*). For lineage identification, we used both SNP-based method, which uses known lineage-defining SNPs, and k-mer–based methods, which rely on an in-silico equivalent of PCR probes analyzing each SNP alleles' 20bp flanking regions (*5*–*7*). Both methods confirmed the isolate as lineage 3.1.1 (Central Asian sublineage Kilimanjaro, CASI-KILI). We ruled out laboratory cross-contamination and assessed relative genomic distance of this isolate compared with other human TB isolates from Madagascar by reanalyzing all lineage 3 TB isolates cultured in the laboratory during March 2017–June 2019 for which lineage typing and genomic sequencing data were available, and created a SNP distance matrix and phylogenetic tree (Appendix Figures 1, 2, https://wwwnc.cdc.gov/EID/article/27/3/20-2924-App1.pdf). The lemur's isolate was substantially distant from other isolates by a closest SNP distance of 63 SNPs (mada_116), ruling out laboratory contamination or transspecies transmission within the samples processed on site (*3*). We submitted *M. tuberculosis* lineage 3 consensus sequence to GenBank (accession no. PRJNA659624).

Human TB isolates in the region of Toliara most frequently belong to lineage 1 (Institut Pasteur de Madagascar, unpub. data). However, lineage 3 isolates were previously isolated in humans from other regions of Madagascar (*7*). Pet lemurs are transported over vast distances (*8*,*9*); this lemur may have originated or been transferred from another region of Madagascar. The Malagasy lineage 3 profile shares similarities with strains found in Tanzania and the Indo-Pakistanese subcontinent (*7*).

Human activities, including trade and translocation of wild animals and keeping of wildlife as pets, have resulted in reverse zoonotic TB and spillover into wild populations in, among others, meerkats (*Suricata suricatta*), banded mongoose (*Mungos mungo*), and Asian elephants (*Elephas maximus*) (*10*). Although the risks of transmitting emerging diseases from wildlife to humans have received much attention, the risks that human diseases present to wildlife are not well described. In addition to other anthropogenic activities that imperil wildlife (e.g., deforestation, bushmeat consumption, animal trafficking), the effects of human disease reservoirs may become increasingly detrimental (*10*).

Illegal trade of wild-captured lemurs is rampant in Madagascar (*8*,*9*). Moreover, humans are frequently in close contact with pet or tourist facility–based lemurs. Some resorts encourage tourists to feed lemurs from their mouths, whereby pathogens could be transferred. Because lemurs make poor pets and often become aggressive, many are discarded as adults, some by release into forests with wild conspecific populations (*8*,*9*).

We present anatomopathologic and molecular diagnostics evidence that wild-born lemurs can become infected with and die from complications of TB. To minimize risk for transmission of TB between humans and lemurs, we recommend enforced prohibition of keeping wild-captured lemurs as pets, systematic clinical screening and microbiological testing of facility-based animals and staff who become ill, and necropsy of deceased lemurs. Because we do not know if lemurs are able to maintain *M. tuberculosis* infection, we recommend quarantine and testing at lemur facilities and caution against release of captive lemurs into the wild. We also warn against close proximity or contact between humans and lemurs (captive or wild) in Madagascar, given the potential for reverse zoonotic and zoonotic transmission of TB and other infectious diseases.

Acknowledgments

We thank Madagascar Ministry of the Environment and Forests for permission to study ring-tailed lemurs (no. 155/19/MEDD/SG/DGEF/DGRNE) and the lemur facility for permission to conduct surgery and sample the sick ring-tailed lemurs.

The University of San Diego and Lemur Love, Inc. provided funding for this study.

About the Author

Dr. LaFleur is an assistant professor at the University of San Diego, California, USA, and the founder and director of Lemur Love, a US-based nonprofit organization conducting research, conservation, and small-scale development in Madagascar. Her research examines the ecology of wild ring-tailed lemurs and the legal and illegal trades of wild-captured lemurs in Madagascar.

References

1. Blancou J, Rakotoniaina P, Cheneau Y. Types of TB bacteria in humans and animals in Madagascar [in French]. Arch Inst Pasteur Madagascar. 1974;43:31–38.
2. Ligthelm LJ, Nicol MP, Hoek KGP, Jacobson R, van Helden PD, Marais BJ, et al. Xpert MTB/RIF for rapid diagnosis of tuberculous lymphadenitis from fine-needle-aspiration biopsy specimens. J Clin Microbiol. 2011; 49:3967–70. https://doi.org/10.1128/JCM.01310-11
3. Hunt M, Bradley P, Lapierre SG, Heys S, Thomsit M, Hall MB, et al. Antibiotic resistance prediction for *Mycobacterium tuberculosis* from genome sequence data with Mykrobe. Wellcome Open Res. 2019;4:191. https://doi.org/10.12688/wellcomeopenres.15603.1
4. Shitikov E, Kolchenko S, Mokrousov I, Bespyatykh J, Ischenko D, Ilina E, et al. Evolutionary pathway analysis and unified classification of East Asian lineage of *Mycobacterium tuberculosis*. Sci Rep. 2017;7:9227. https://doi.org/10.1038/s41598-017-10018-5
5. Rutaihwa LK, Menardo F, Stucki D, Gygli SM, Ley SD, Malla B, et al. Multiple introductions of *Mycobacterium tuberculosis* lineage 2–Beijing into Africa over centuries. Front Ecol Evol. 2019;7:112. https://doi.org/10.3389/fevo.2019.00112
6. Stucki D, Brites D, Jeljeli L, Coscolla M, Liu Q, Trauner A, et al. *Mycobacterium tuberculosis* lineage 4 comprises globally distributed and geographically restricted sublineages. Nat Genet. 2016;48:1535–43. https://doi.org/10.1038/ng.3704
7. Ferdinand S, Sola C, Chanteau S, Ramarokoto H, Rasolonavalona T, Rasolofo-Razanamparany V, et al. A study of spoligotyping-defined *Mycobacterium tuberculosis* clades in relation to the origin of peopling and the demographic history in Madagascar. Infect Genet Evol. 2005;5:340–8. https://doi.org/10.1016/j.meegid.2004.10.002
8. LaFleur M, Clarke TA, Reuter KE, Schaefer MS, terHorst C. Illegal trade of wild-captured *Lemur catta* within Madagascar. Folia Primatol (Basel). 2019;90:199–214. https://doi.org/10.1159/000496970
9. Reuter KE, LaFleur M, Clarke TA, Holiniaina Kjeldgaard F, Ramanantenasoa I, Ratolojanahary T, et al. A national survey of household pet lemur ownership in Madagascar. PLoS One. 2019;14:e0216593. https://doi.org/10.1371/journal.pone.0216593
10. Chomel BB, Belotto A, Meslin FX. Wildlife, exotic pets, and emerging zoonoses. Emerg Infect Dis. 2007;13:6–11. https://doi.org/10.3201/eid1301.060480

Address for correspondence: Marni LaFleur, Department of Anthropology, University of San Diego, Saints Tekawitha-Serra Hall, Suite 218C, 5998 Alcala Park, San Diego, CA 92110-2492, USA; email: marni.lafleur@gmail.com

Genomic and Pathologic Findings for *Prototheca cutis* Infection in Cat

Grazieli Maboni,[1] Jessica A. Elbert,[1] Justin M. Stilwell, Susan Sanchez

Author affiliations: University of Guelph, Guelph, Ontario, Canada (G. Maboni); Athens Veterinary Diagnostic Laboratory, Athens, Georgia, USA (G. Maboni, S. Sanchez); University of Georgia, Athens (J.A. Elbert, J.M. Stilwell)

DOI: https://doi.org/10.3201/eid2703.202941

Severe nasal *Prototheca cutis* infection was diagnosed postmortem for an immunocompetent cat with respiratory signs. Pathologic examination and whole-genome sequencing identified this species of algae, and susceptibility testing determined antimicrobial resistance patterns. *P. cutis* infection should be a differential diagnosis for soft tissue infections of mammals.

Prototheca spp. (phylum Chlorophyta, order Chlorellales, family *Chlorellaceae*) are ubiquitous algal organisms that represent emerging infectious agents of humans and animals (*1*). Protothecosis has been increasingly reported for immunocompromised human and animal patients (*1*,*2*). At least 14 species of *Prototheca* have been recognized; 1 case of *P. cutis*–associated dermatitis in an immunocompromised man has been reported (*3*,*4*). We describe a case of *P. cutis* in a domestic cat in Georgia, USA.

In January 2020, an 11-year-old, 5.8-kg, neutered male, domestic cat was examined for sneezing, wheezing, congestion, and rhinitis. This indoor/outdoor cat was negative for feline leukemia and feline immunodeficiency viruses. The cat showed no response to treatment with steroids and cefovecin sodium (Convenia; Zoetis, https://www.zoetis.com). From June 2019 through January 2020, the nasal planum became rounded and disfigured. A biopsy sample submitted to a private diagnostic laboratory indicated a fungal infection containing organisms suggestive of *Cryptococcus* spp. Because of concerns over the zoonotic potential of *Cryptococcus* spp., the cat was euthanized and submitted for postmortem examination.

Gross reflection of the skin revealed that a locally extensive area of connective tissue and musculature overlying ≈70% of the nasal bridge and dorsal nasal planum was diffusely soft, variably tan to light orange, and mildly gelatinous (Appendix Figure 1, https://wwwnc.cdc.gov/EID/article/27/3/20-2941-App1.pdf).

[1]These authors contributed equally to this article.

Microscopic evaluation revealed a severe granulomatous nodular dermatitis, panniculitis, cellulitis, pyogranulomatous osteomyelitis, and rhinitis (Figure). Disseminated throughout the nasal turbinates were numerous free and intrahistiocytic sporangia with and without endospores (Figure). Although these findings suggest previously resolved infection in the skin, subcutis, and muscle and active infection in the nasal turbinates, the initial site of infection (cutaneous vs. nasal turbinates) and disease pathogenesis could not be definitively determined (Appendix).

Fungal culture yielded white colonies growing in the presence and absence of light at 30°C (Appendix Figure 2). Cytologic examination revealed colonies of round cells with internal septations and thick walls resembling sporangia and endospores, which were identified with lactophenol cotton blue stain (Appendix Figure 2). Sporangia were gram positive, although they appeared to be unevenly stained (Appendix Figure 2). Genus and species were not identified by matrix-assisted laser desorption ionization/time-of-flight mass spectrometry and GEN III Microbial identification (Biolog, https://www.biolog.com). Partial sequencing of the internal transcribed spacer region and the D1/D2 region of the 28S rRNA gene yielded sequences 96% and 99% homologous to those from *P. cutis* available in BLAST (https://blast.ncbi.nlm.nih.gov) and CBS-KNAW (https://www.knaw.nl, currently Westerdijk Fungal Biodiversity Institute) databases.

Because the mitochondrial *cytb* gene potentially represents a new standard method for identifying *Prototheca* species (*5*), we performed whole-genome sequencing to investigate *cytb* as well as other genes by using Illumina MiSeq (https://www.illumina.com) (Appendix). The nuclear genome was 19,237,076-bp long, and the plastid genome was 51,673-bp long, which corresponds to genome sizes obtained from sequencing of *P. cutis* JCM15793 strain ATCC PRA-138 (https://www.atcc.org) (*6*). We

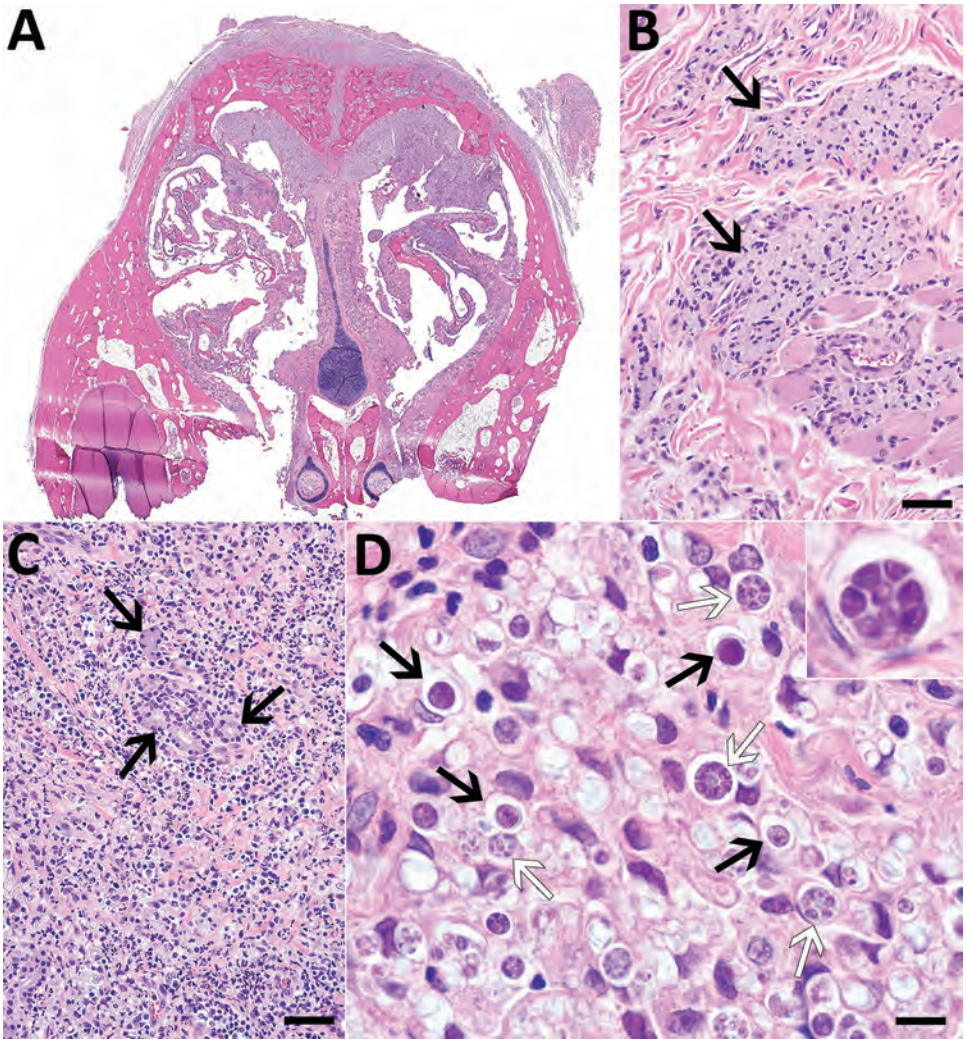

Figure. Histologic lesions associated with protothecosis caused by *Prototheca cutis* in a cat. A) Subgross cross-section of the nasal turbinates showing marked expansion of the nasal epithelium and overlying subcutaneous tissue. B) Epithelioid macrophages (arrows) with abundant, intracytoplasmic, gray material multifocally dissecting through subdermal collagen and musculature. Hematoxylin and eosin (H&E) stain; scale bar indicates 50 µm. C) Submucosal glands (arrows), markedly displaced by myriad macrophages, neutrophils, lymphocytes, plasma cells, and algal sporangia. H&E stain; scale bar indicates 50 µm. D) Algal sporangia (black arrows), which sometimes endosporulate (white arrows), producing up to 8 endospores (inset). H&E stain; scale bar indicates 10 µm and does not apply to inset.

submitted the genome assembly to GenBank (accession no. JABBYS000000000). The in silico–targeted gene alignment revealed genes homologous with available *P. cutis* sequences including *cytB* (99.8%, accession no. MT363977), chloroplast genome DNA (99.54%), 18S rRNA gene (100%, accession no. MT360051), ITS (99.12%, accession no. MT359908), and 28S rRNA (D1/D2 domain) (100%, accession no. MT360265), which were deposited in GenBank.

We performed susceptibility testing for antifungal and antimicrobial drugs because both have been used against *Prototheca* spp. infections in animals (*7*,*8*). The isolate showed high MICs for fluconazole and itraconazole and a low MIC for amphotericin B (Table). Resistance to fluconazole and susceptibility to amphotericin B are well recognized for other *Prototheca* species (*9*); however, resistance to itraconazole could be unique to *P. cutis*. MICs were high for most antimicrobial drugs, including cefovecin, which had been unsuccessful in treating the cat (Table). Oxacillin, pradofloxacin, and trimethoprim/sulfamethoxazole inhibited growth at the lowest concentrations, indicating in vitro sensitivity to these drugs. We further investigated whether resistance genes from the whole-genome sequence corresponded to phenotypic resistance. We used the Comprehensive Antibiotic Resistance Database (https://card.mcmaster.ca) to identify genes conferring resistance to β-lactams, tetracyclines, aminoglycosides, chloramphenicol, and vancomycin. Consistent with MICs, no resistance genes corresponded to pradofloxacin and trimethoprim/sulfamethoxazole (Table). The MIC data provided here may be helpful for establishing future clinical breakpoints for *Prototheca* spp.

Our primary concern with regard to this case was determining the zoonotic potential of the agent, which was initially misdiagnosed as *Cryptococcus* spp. Although *Prototheca* spp. are widely considered to be zoonotic agents, reports of definitive cases of

Table. Antimicrobial and antifungal MICs and resistance genes identified by whole-genome sequencing of *Prototheca cutis* isolated from a nasal lesion in a cat*

Class	MIC, μg/mL	AMR genes
Antimicrobial testing†		
β-lactams		*Oxa-168*, *NmcA*, *OXA-198*, *IMP-8*
Amoxicillin/clavulanate	8	
Ampicillin	>8	
Oxacillin	≤0.25	
Penicillin G	8	
Cefazolin	>4	
Cefovecin	>8	
Cefpodoxime	>8	
Cephalothin	>4	
Imipenem	4	
Tetracyclines		*tet(31)*
Doxycycline	>0.5	
Minocycline	1	
Tetracycline	>1	
Quinolones		None found
Enrofloxacin	>4	
Marbofloxacin	2	
Pradofloxacin	≤0.25	
Aminoglycosides		*AAC(6')-Ij*, *AAC(3)-Xa*, *AAC(3)-VIIIa*
Amikacin	>32	
Gentamicin	8	
Lincosamides: clindamycin	4	None found
Macrolides: erythromycin	>4	None found
Rifamycins: rifampin	>2	None found
Nitrofurans: nitrofurantoin	>64	None found
Phenicols: chloramphenicol	>32	*catB10*
Sulfonamides: trimethoprim/sulfamethosoxazole	≤2	None found
Vancomycin	>16	*vanA*, *vanRO*
Antifungal testing‡		Not investigated
Azoles		
Fluconazol	>256	
Itraconazol	>32	
Polyenes: amphotericin B	0.19	

*AMR genes were identified by using the Comprehensive Antibiotic Resistance Database (https://card.mcmaster.ca). Interpretation of MICs was not included in this table because clinical breakpoints for *Prototheca* spp. are not available. AMR, antimicrobial resistance.
†Antimicrobial susceptibility testing was performed by using a Trek Sensititre Gram Positive panel (TREK Diagnostic Systems, http://www.trekds.com).
‡Antifungal susceptibility testing was performed by using MIC test strips (Liofilchem, https://www.liofilchem.com).

zoonotic transmission are lacking in the literature. Zoonotic transmission from bovids is thought to occur via consumption of contaminated milk (*10*). The zoonotic potential of *P. cutis* is unclear; infectivity is probably similar to that of other *Prototheca* spp.

Our report of *P. cutis* isolation from a cat reinforces protothecosis as an emerging infectious disease of humans and animals. We emphasize the potential of *P. cutis* to infect presumably immunocompetent hosts. The veterinary and human medical communities should be aware of the unusual clinical, pathologic, and microbiological manifestations of protothecosis.

Acknowledgments

We thank the talented histology and microbiology technicians at the Athens Veterinary Diagnostic Laboratory for their technical assistance, especially Paula Bartlett and Amy McKinney.

About the Author

Dr. Maboni is a board-certified veterinary microbiologist working as an assistant professor at the University of Guelph, Canada. Her primary research interests are medical diagnosis of bacterial and fungal diseases.

References

1. Pal M, Abraha A, Rahman MT, Dave P. Protothecosis: an emerging algal disease of humans and animals [cited 2020 Jun 17]. https://www.researchgate.net/publication/266359627_Protothecosis_an_emerging_algal_disease_of_humans_and_animals
2. Lanotte P, Baty G, Senecal D, Dartigeas C, Bailly E, Duong TH, et al. Fatal algaemia in patient with chronic lymphocytic leukemia. Emerg Infect Dis. 2009;15:1129–30. https://doi.org/10.3201/eid1507.090373
3. Jagielski T, Bakula Z, Gawor J, Maciszewski K, Kusber WH, Dylag M, et al. The genus *Prototheca* (Trebouxiophyceae, Chlorophyta) revisited: implications from molecular taxonomic studies. Algal Res. 2019;43:101639. https://doi.org/10.1016/j.algal.2019.101639
4. Satoh K, Ooe K, Nagayama H, Makimura K. *Prototheca cutis* sp. nov., a newly discovered pathogen of protothecosis isolated from inflamed human skin. Int J Syst Evol Microbiol. 2010;60:1236–40. https://doi.org/10.1099/ijs.0.016402-0
5. Jagielski T, Gawor J, Bakuła Z, Decewicz P, Maciszewski K, Karnkowska A. *cytb* as a new genetic marker for differentiation of *Prototheca* species. J Clin Microbiol. 2018;56:e00584–18. https://doi.org/10.1128/JCM.00584-18
6. Suzuki S, Endoh R, Manabe RI, Ohkuma M, Hirakawa Y. Multiple losses of photosynthesis and convergent reductive genome evolution in the colourless green algae *Prototheca*. Sci Rep. 2018;8:940. https://doi.org/10.1038/s41598-017-18378-8
7. Pressler BM, Gookin JL, Sykes JE, Wolf AM, Vaden SL. Urinary tract manifestations of protothecosis in dogs. J Vet Intern Med. 2005;19:115–9. https://doi.org/10.1111/j.1939-1676.2005.tb02669.x
8. Vince AR, Pinard C, Ogilvie AT, Tan EO, Abrams-Ogg AC. Protothecosis in a dog. Can Vet J. 2014;55:950–4.
9. Marques S, Silva E, Carvalheira J, Thompson G. Short communication: in vitro antimicrobial susceptibility of *Prototheca wickerhamii* and *Prototheca zopfii* isolated from bovine mastitis. J Dairy Sci. 2006;89:4202–4. https://doi.org/10.3168/jds.S0022-0302(06)72465-1
10. Melville PA, Watanabe ET, Benites NR, Ribeiro AR, Silva JA, Garino Junior F, et al. Evaluation of the susceptibility of *Prototheca zopfii* to milk pasteurization. Mycopathologia. 1999;146:79–82. https://doi.org/10.1023/A:1007005729711

Address for correspondence: Grazieli Maboni, Department of Pathobiology, Ontario Veterinary College, University of Guelph, 50 Stone Rd E, Guelph, ON N1G 2W1, Canada; email: grazieli.maboni@gmail.com

Validity of Diagnosis Code–Based Claims to Identify Pulmonary NTM Disease in Bronchiectasis Patients

Jennifer H. Ku, Emily M. Henkle, Kathleen F. Carlson, Miguel Marino, Kevin L. Winthrop

Author affiliations: Oregon Health & Science University–Portland State University School of Public Health, Portland, Oregon, USA (J.H. Ku, E.M. Henkle, K.F. Carlson, M. Marino, K.L. Winthrop); Veterans Affairs Portland Healthcare System, Portland (K.F. Carlson)

DOI: https://doi.org/10.3201/eid2703.203124

Nontuberculous mycobacteria infection is increasing in incidence and can lead to chronic, debilitating pulmonary disease. We investigated the accuracy of diagnosis code–based nontuberculous mycobacteria lung disease claims among Medicare beneficiaries in the United States. We observed that these claims have moderate validity, but given their low sensitivity, incidence might be underestimated.

Nontuberculous mycobacteria (NTM) infection is an illness of increasing incidence caused by environmental organisms and can lead to chronic pulmonary disease (*1*–*5*). The accuracy of International

Classification of Diseases (ICD) diagnosis codes for NTM infection has been evaluated only in limited fashion (*6*) and is unknown in the context of bronchiectasis, which most patients with pulmonary NTM infection have (*7*,*8*). We investigated the accuracy of ICD diagnosis codes for NTM infection among Medicare beneficiaries in the United States by using the Bronchiectasis and NTM Research Registry (BRR) as the reference standard.

We identified persons with a diagnosis of bronchiectasis (ICD Ninth Revision, Clinical Modification [ICD-9-CM], codes 494.0 or 494.1) from 2006–2014 Medicare data. BRR is a database of persons with bronchiectasis, NTM infection, or both at 13 US medical institutions (*8*). BRR captures clinical data from the 24-month period before enrollment and at annual follow-ups. We matched study participants enrolled at 7 BRR sites to Medicare data (*9*). Medicare observation began on the later date of either enrollment or data-start (January 1, 2006) and ended on the earlier date of either coverage-end or data-end (December 31, 2014). We included study participants with an overlap in BRR and Medicare observation, excluding claims or cultures outside this overlap.

We established a primary case definition of an NTM infection as ≥1 inpatient discharge or outpatient visit coded 031.0 (pulmonary mycobacterial infection) assigned by a clinician; we also established alternative definitions (Table). For the primary and each alternative case definition, we calculated positive predictive value (PPV) as the proportion of Medicare claim–based NTM infections meeting the BRR case definition ±12 months of the first claim. Sensitivity was calculated as the proportion of patients meeting the BRR case definition who had a claim for NTM infection within ±12 months of meeting that definition. All analyses were performed by using SAS statistical software 9.4 (SAS Institute Inc., https://www.sas.com). This study was approved by the Institutional Review Board at Oregon Health & Science University.

Of the 530 Medicare beneficiaries also enrolled in BRR at the 7 sites, 457 (86.2%) were matched (Figure). Our final analytic sample included 403 participants who averaged 73.5 years of age (range 62–98 years, SD 6.2) and were mostly women (80.4%) and White (95.8%). Of the 403 participants, 205 (50.9%) had ≥1 NTM infection claim based on a diagnosis code assigned by a clinician.

We observed that diagnosis code–based claims have moderate validity for identifying NTM infection. Our primary case definition had a PPV of 63.2% (95% CI 57.1%–69.4%) (Table) and was 69.9% (95% CI 63.9%–75.9%) sensitive in detecting NTM infection within ±12 months of the first claim date. PPV was maximized when a second claim was required and codes restricted to those assigned by an infectious disease specialist. In a previous study, the microbiologic NTM infection case definition (*1*) had a high PPV (77%) and yielded maximized sensitivity and PPV when combined with ICD-9-CM codes (*6*). Our results were similar in that NTM infection codes had fairly high PPVs but lower sensitivity.

Table. Positive predictive value and sensitivity of ICD-9-CM diagnosis code–based case definitions for NTM infection in 2006–2014 Medicare data by using Bronchiectasis and NTM Research Registry as reference standard, United States*

NTM case definition†	No. participants with diagnosis-based Medicare claim for NTM infection	PPV (95% CI)‡	No. participants meeting BRR case definition for NTM infection§	Sensitivity (95% CI)¶
Primary definition: ICD-9-CM 031.0				
All clinician-given codes#	234	63.2 (57.1–69.4)	226	69.9 (63.9–75.9)
ID specialist– and pulmonologist-given codes only	205	65.4 (58.9–71.9)	226	61.5 (55.2–67.9)
ID specialist–given codes only	127	70.1 (62.1–78.0)	226	39.8 (33.4–46.2)
Pulmonologist-given codes only	133	60.9 (52.6–69.2)	226	36.7 (30.4–43.0)
Secondary definition: ICD-9-CM 031.0, requiring a second 031.0 claim >30 d but <12 m of first claim				
All clinician-given codes	122	72.1 (63.3–79.9)	226	41.6 (35.2–48.0)
ID specialist– and pulmonologist-given codes only	100	74.0 (64.3–82.3)	226	33.2 (27.1–39.7)
ID specialist–given codes only	45	82.2 (71.1–93.4)	226	16.4 (11.6–21.2)
Pulmonologist-given codes only	44	70.5 (57.0–83.9)	226	13.3 (30.4–43.0)

*BRR, Bronchiectasis and NTM Research Registry; NTM, nontuberculous mycobacteria; ICD-9-CM, International Classification of Disease, Ninth Version, Clinical Modification; ID, infectious disease; PPV, positive predictive value.
†Only ICD-9-CM 031.0 code (pulmonary mycobacterial infection) was considered; other codes for NTM (031.8 [other specified mycobacterial diseases] and 031.9 [unspecified disease due to mycobacteria]) were not considered.
‡PPV for meeting a case definition for NTM infection in BRR within ±12 months of first ICD-9-CM NTM code-cased claim (code 031.0).
§NTM cases were identified in BRR on the basis of culture positivity on ≥1 respiratory specimen or antibiotic treatment for NTM during follow-up (a macrolide plus ≥1 antibiotic drugs).
¶Sensitivity for an ICD-9-CM NTM code–based claim within ±12 months of meeting a case definition for NTM infection in BRR.
#Clinician types include physicians, physician assistants, and nurse practitioners, excluding radiology or laboratory-associated claims.

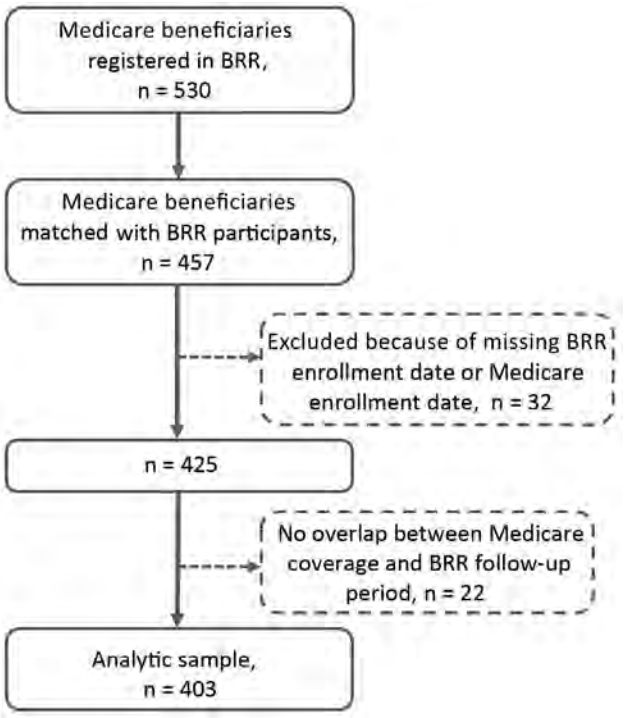

Figure. Flow diagram of the analytic sample (n = 403) of Medicare beneficiaries and persons from BRR matched during 2006–2014, United States. Original pool of Medicare beneficiaries (n = 530) included beneficiaries of Medicare parts A, B, and D but not C and excluded those with cystic fibrosis and a history of HIV or organ transplant. BRR, Bronchiectasis and NTM Research Registry.

False-positive diagnosis codes could be caused by several factors. The Medicare population includes persons with chronic illness whose records might include codes from previous NTM infections, but we could not evaluate this possibility because of limited claims data before BRR baseline. More than half of study participants with false-positive codes had negative cultures, indicating that the code was applied for NTM evaluation or monitoring in the absence of active disease. Higher PPVs, when restricted to specialist-assigned codes, imply that general clinicians might be more likely to assign the disease code when disease criteria are not met. The poor sensitivity was not unexpected; NTM infection is frequently underdiagnosed and miscoded as a nonpulmonary NTM or other infection. Our case definition required 1 positive culture, whereas current diagnostic guidelines require 2; of study participants meeting our case definition, 35% had a second positive culture within 12 months.

A limitation of our study is that we only included Medicare beneficiaries ≥65 years of age with bronchiectasis; also, BRR collects data from specialized NTM centers, which might differ from general clinic settings. Our Medicare data ended in 2014, limiting the sample size and overlap with BRR observation time. Last, we only evaluated ICD-9-CM codes, although ICD Tenth Revision, Clinical Modification (ICD-10-CM), codes have been required since 2015 (*10*). However, understanding the validity of ICD-9-CM codes is essential for interpretation of the existing literature that is based on ICD-9-CM codes and to inform future research using ICD-10-CM codes. Further, ICD-9-CM codes for NTM map directly to ICD-10-CM codes (ICD-9-CM 031.0 equates to ICD-10-CM A31.0 [pulmonary mycobacterial infection]), helping guide future comparisons.

Our results indicate that a case definition of ≥2 claims given 30 days apart within 12 months of each other accurately identifies pulmonary NTM infection in patients who also have bronchiectasis. Given low sensitivity, incidence might be severely underestimated in claims-based epidemiologic research. Claims data provide critical information about the epidemiology of NTM infection when clinical data are not available, but findings should be interpreted with awareness of the potential for misclassification.

This work was funded by Insmed Incorporated.

About the Author

Ms. Ku is a doctoral candidate in public health in epidemiology at the Oregon Health & Science University–Portland State University School of Public Health. Her research interests include the epidemiology of pulmonary nontuberculous mycobacterial disease and the pharmacoepidemiology of therapy targeting pulmonary NTM disease.

References

1. Griffith DE, Aksamit T, Brown-Elliott BA, Catanzaro A, Daley C, Gordin F, et al.; ATS Mycobacterial Diseases Subcommittee; American Thoracic Society; Infectious Disease Society of America. An official ATS/IDSA statement: diagnosis, treatment, and prevention of nontuberculous mycobacterial diseases. Am J Respir Crit Care Med. 2007; 175:367–416. https://doi.org/10.1164/rccm.200604-571ST
2. Bodle EE, Cunningham JA, Della-Latta P, Schluger NW, Saiman L. Epidemiology of nontuberculous mycobacteria in patients without HIV infection, New York City. Emerg Infect Dis. 2008;14:390–6. https://doi.org/10.3201/eid1403.061143
3. Cassidy PM, Hedberg K, Saulson A, McNelly E, Winthrop KL. Nontuberculous mycobacterial disease prevalence and risk factors: a changing epidemiology. Clin Infect Dis. 2009;49:e124–9. https://doi.org/10.1086/648443
4. Prevots DR, Shaw PA, Strickland D, Jackson LA, Raebel MA, Blosky MA, et al. Nontuberculous mycobacterial lung disease prevalence at four integrated health care delivery systems. Am J Respir Crit Care Med. 2010;182:970–6. https://doi.org/10.1164/rccm.201002-0310OC
5. Adjemian J, Olivier KN, Seitz AE, Holland SM, Prevots DR. Prevalence of nontuberculous mycobacterial lung disease

in U.S. Medicare beneficiaries. Am J Respir Crit Care Med. 2012;185:881–6. https://doi.org/10.1164/rccm.201111-2016OC
6. Winthrop KL, Baxter R, Liu L, McFarland B, Austin D, Varley C, et al. The reliability of diagnostic coding and laboratory data to identify tuberculosis and nontuberculous mycobacterial disease among rheumatoid arthritis patients using anti-tumor necrosis factor therapy. Pharmacoepidemiol Drug Saf. 2011;20:229–35. https://doi.org/10.1002/pds.2049
7. Koh WJ, Kwon OJ. Bronchiectasis and non-tuberculous mycobacterial pulmonary infection. Thorax. 2006;61:458, author reply 458.
8. Aksamit TR, O'Donnell AE, Barker A, Olivier KN, Winthrop KL, Daniels MLA, et al.; Bronchiectasis Research Registry Consortium. Adult patients with bronchiectasis: a first look at the US Bronchiectasis Research Registry. Chest. 2017;151:982–92. https://doi.org/10.1016/j.chest.2016.10.055
9. Henkle E, Curtis JR, Chen L, Chan B, Aksamit TR, Daley CL, et al. Comparative risks of chronic inhaled corticosteroids and macrolides for bronchiectasis. Eur Respir J. 2019;54:1801896. https://doi.org/10.1183/13993003.01896-2018
10. Centers for Medicare & Medicaid Services. ICD-10: official CMS industry resources for the ICD-10 transition [cited 2020 Apr 4]. https://www.cms.gov/ICD10

Address for correspondence: Jennifer H. Ku, Oregon Health & Science University Hospital, 3181 SW Sam Jackson Park Rd, GH104, Portland, OR 97239-3098, USA; email: kuj@ohsu.edu

Limited Capability for Testing *Mycobacterium tuberculosis* for Susceptibility to New Drugs

Hamzah Z. Farooq,[1] Daniela M. Cirillo, Doris Hillemann, David Wyllie, Marieke J. van der Werf, Csaba Ködmön, Vlad Nikolayevskyy

Author affiliations: Public Health England, London, UK (H.Z. Farooq, D. Wyllie, V. Nikolayevskyy); San Raffaele Scientific Institute, Milan, Italy (D.M. Cirillo); Research Centre for Mycobacteria, Borstel, Germany (D. Hillemann); European Centre for Disease Prevention and Control, Stockholm, Sweden (M.J. van der Werf, C. Ködmön)

DOI: https://doi.org/10.3201/eid2703.204418

[1]Current affiliation: University of Manchester, Manchester, UK.

We surveyed availability of phenotypic drug susceptibility testing for drug-resistant *Mycobacterium tuberculosis* in Europe. Of 27 laboratories, 17 tested for linezolid, 11 for clofazimine, 9 for bedaquiline, and 6 for delamanid during 2019. Our findings indicate that testing capacity for newer and repurposed tuberculosis drugs exists, but its availability is limited.

Mycobacterium tuberculosis is a major cause of death globally, and increasing predicted deaths from tuberculosis (TB) are caused by delays in diagnosis and treatment of new cases associated with coronavirus disease containment measures (*1*). Drug-resistant, multidrug-resistant (MDR), and extensively drug-resistant (XDR) TB remain major public health issues (*1*).

In the World Health Organization European Region, the proportion of rifampin-resistant and MDR TB is greater than the global average. New drug regimens incorporating bedaquiline, clofazimine, linezolid, and delamanid to treat MDR and XDR TB have been recommended by the World Health Organization and are being implemented globally (*2*). For newer and repurposed drugs (NRDs), phenotypic drug susceptibility testing (pDST) is not yet fully standardized because of a lack of data for epidemiologic cutoff values. In addition, genomic DST (gDST) lacks sensitivity, and genetic mechanisms of drug resistance have yet to be fully established for NRDs (*3*).

There have been issues with procuring pure substances for testing and availability of resistant isolates (non-XDR strains) for validation of assays. The widely used BACTEC mycobacteria growth indicator tube (MGIT) technology (Becton Dickinson, https://www.bd.com) has not been calibrated against a reference standard protocol and is not fully validated for second-line drugs, highlighting the need for sustainable external quality assessment (EQA) schemes. For well-tolerated compounds, (i.e., moxifloxacin), phenotypic and genotypic resistance prediction using current interpretive guidance might be discordant, leading to uncertainty about clinical efficacy.

Availability of pDST for bedaquiline, clofazimine, linezolid, and delamanid in Europe is unknown, which is of concern in areas that have higher incidences of drug resistance, such as eastern Europe. Within a framework of EQA schemes implemented by the European TB Reference Laboratory Network and coordinated by the European Centre for Disease Prevention and Control, we performed a survey on the availability and performance of pDST for NRDs in European Union/European Economic Area laboratories during 2018–2019.

EQA is one of the key components of the European TB Reference Laboratory Network, which uses an interlaboratory comparison to enable objectivity in auditing the performance of a laboratory (*4*). For the EQA panels, 5 well-characterized *M. tuberculosis* isolates that have varying drug susceptibility profiles, including those resistant to ≥1 NRDs (n = 3), were sent to participating laboratories. These laboratories were requested to test samples for phenotypic susceptibility to drugs routinely tested in their laboratory. Reports received were analyzed against reference results by using established protocols (*4*).

A total of 28 laboratories participated and reported results within the deadline of the EQA (2018–2019). In this EQA panel, results were reported for 15 drugs, including NRDs. Of 28 laboratories, 15 tested for linezolid, 6 for clofazimine, 6 for bedaquiline, and 4 for delamanid during 2018. This increased to 17 tested for linezolid, 11 for clofazimine, 9 for bedaquiline, and 6 for delamanid during 2019 (Figure). All but 1 laboratory used MGIT methods for NRDs (*5*).

During 2019, a total of 17 laboratories reported 100% correct results and 9 laboratories reported 96%–99% correct results. One laboratory scored 85%, and 1 laboratory scored only 69% (i.e., below the threshold for certification). There were 3 very major errors (false-susceptible results) for clofazimine (n = 2) and bedaquiline (n = 1), and 1 major error (false-resistant result) for linezolid. Other errors included very major errors for protionamide (n = 4), isoniazid (n = 3), moxifloxacin (n = 1), and streptomycin (n = 1) and major errors for moxifloxacin (n = 3), rifampin (n = 2), isoniazid (n = 1), and protionamide (n = 1).

Our findings show that availability of pDST is increasing in Europe but remains limited. With the increasing availability of the NRDs for TB, standardized and validated pDST of *M. tuberculosis* in culture isolates to NRDs is crucial for appropriate use of new drugs in treatment regimens.

Ongoing global efforts to define a set of quality control strains and standardize MGIT methods against a reference to overcome variability (*6*) are

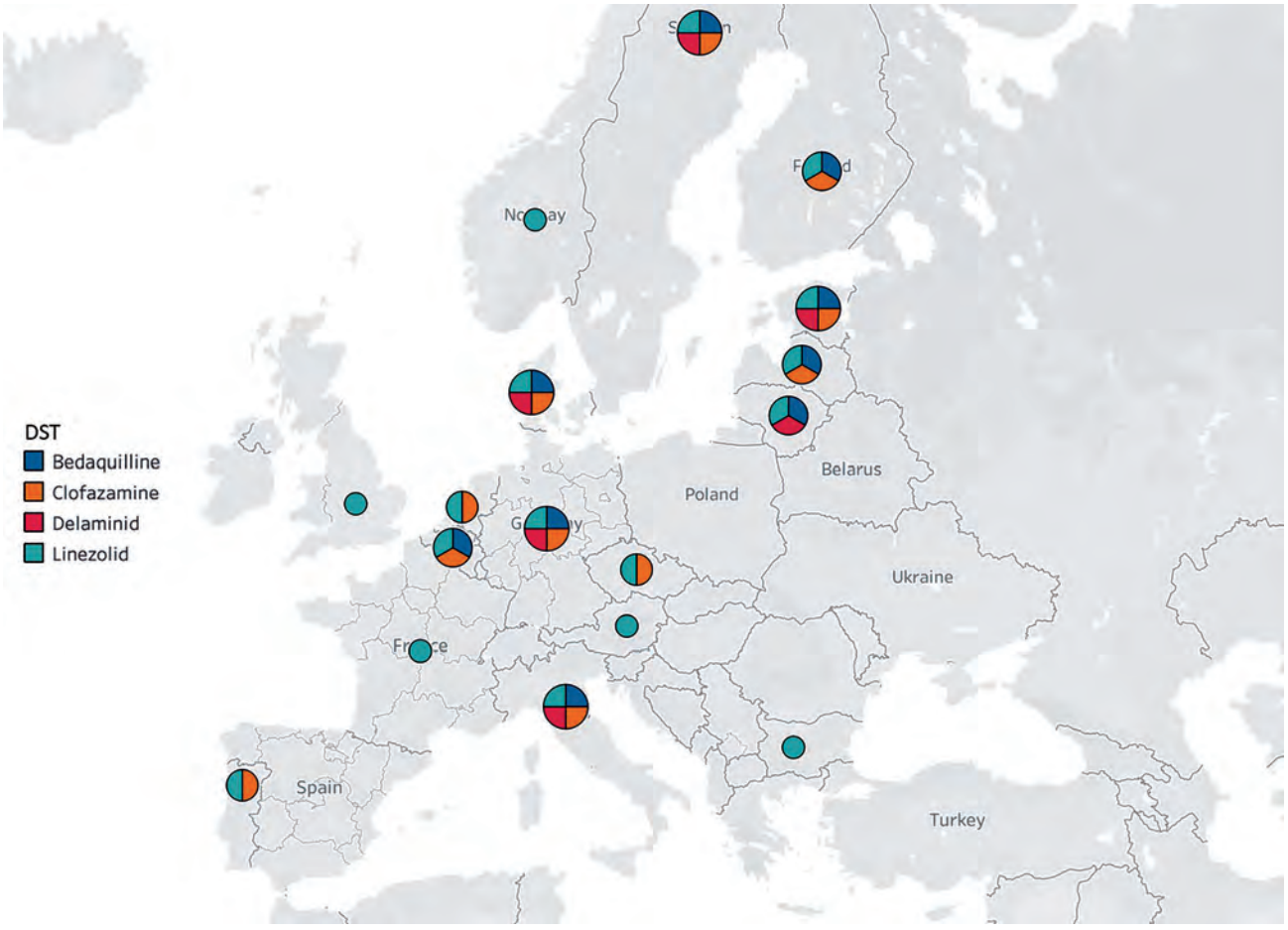

Figure. European Union laboratories performing phenotypic DST of new tuberculosis drugs, 2019. Map courtesy of Mapbox OpenStreet Map (https://www.mapbox.com). DST, drug susceptibility testing.

being complemented by ensuring clear rules on when pDST is required and to ensure that gDST is fully used. Appropriate use of pDST and gDST is essential for clinical management of MDR and XDR TB to limit transmission and prevent development of further resistance (*7*). Use of bedaquiline and delamanid requires special approval in certain countries because of substantial cost of this drug (*8*). Thus, performing pDST for NRDs is essential to ensure that isolates are susceptible to the newer agents.

Validated and quality-controlled pDST, including automated liquid culture systems and microtiter plate-based assays for NRDs, might be used to improve accuracy of prediction of resistance and susceptibility to NRDs by using whole-genome sequencing (*9*). Although pDST is considered the standard for susceptibility testing for NRDs, using whole-genome sequencing will help to detect and characterize new mutations and insertions/deletions associated with drug resistance and also analyze strain relatedness rapidly, resulting in prompt public health actions, and thus will be highly useful. Use of data from multicenter EQA sites (*10*) can help develop standardized guidelines for pDSTs for global use. In addition, pDST data for isolates can be used for additional studies to validate predicting resistance to gDSTs for NRDs.

Acknowledgments

We thank the staff of the EQA participant laboratories and the National Mycobacterial Reference Service, UK, for their contributions to the study.

This study was supported by the European Centre for Disease Prevention and Control (grant no. ECDC/GRANT/2018/001).

About the Author

Dr. Farooq is a specialist registrar in infectious diseases and virology in the Department of Virology and Infectious Diseases, University of Manchester, Manchester, UK. His primary research interest is emerging infections, such as MDR TB and Crimean-Congo hemorrhagic fever.

References

1. World Health Organization. Global tuberculosis report, 2019. Geneva: The Organization [cited 2020 Nov 30]. https://www.who.int/teams/global-tuberculosis-programme/tb-reports/global-report-2019
2. Prasad R, Gupta N, Banka A. Shorter and cheaper regimen to treat multidrug-resistant tuberculosis: a new hope. Indian J Med Res. 2017;146:301–3.
3. Köser CU, Maurer FP, Kranzer K. 'Those who cannot remember the past are condemned to repeat it': drug-susceptibility testing for bedaquiline and delamanid. Int J Infect Dis. 2019;80S:S32–5. https://doi.org/10.1016/j.ijid.2019.02.027
4. Nikolayevskyy V, Hillemann D, Richter E, Ahmed N, van der Werf MJ, Kodmon C, et al.; ERLTB-Net Network. External quality assessment for tuberculosis diagnosis and drug resistance in the European Union: a five year multicentre implementation study. PLoS One. 2016;11:e0152926. https://doi.org/10.1371/journal.pone.0152926
5. World Health Organzation. WHO consolidated guidelines on drug-resistant tuberculosis treatment; 2019. Geneva: The Organization [cited 2020 Nov 30]. https://www.who.int/tb/publications/2019/consolidated-guidelines-drug-resistant-TB-treatment/en
6. Schön T, Miotto P, Köser CU, Viveiros M, Böttger E, Cambau E. *Mycobacterium tuberculosis* drug-resistance testing: challenges, recent developments and perspectives. Clin Microbiol Infect. 2017;23:154–60. https://doi.org/10.1016/j.cmi.2016.10.022
7. Drobniewski F, Nikolayevskyy V, Balabanova Y, Bang D, Papaventsis D. Diagnosis of tuberculosis and drug resistance: what can new tools bring us? Int J Tuberc Lung Dis. 2012;16:860–70. https://doi.org/10.5588/ijtld.12.0180
8. Manalan K, Green N, Arnold A, Cooke GS, Dedicoat M, Lipman M, et al. A cost comparison of amikacin therapy with bedaquiline, for drug-resistant tuberculosis in the UK. J Infect. 2020;80:38–41. https://doi.org/10.1016/j.jinf.2019.09.006
9. Allix-Béguec C, Arandjelovic I, Bi L, Beckert P, Bonnet M, Bradley P, et al.; CRyPTIC Consortium and the 100,000 Genomes Project. Prediction of susceptibility to first-line tuberculosis drugs by DNA sequencing. N Engl J Med. 2018;379:1403–15.
10. Kaniga K, Aono A, Borroni E, Cirillo DM, Desmaretz C, Hasan R, et al. Validation of bedaquiline phenotypic drug susceptibility testing methods and breakpoints: a multilaboratory, multicountry study. J Clin Microbiol. 2020;58:e01677-19. https://doi.org/10.1128/JCM.01677-19

Address for correspondence: Vlad Nikolayevskyy, National Mycobacterial Reference Service, National Infection Service, Public Health England Colindale, 61 Colindale Ave, London NW9 5EQ, UK: email: vlad.nikolayevskyy@phe.gov.uk

SARS-CoV-2 Exposure in Escaped Mink, Utah, USA

Susan A. Shriner, Jeremy W. Ellis, J. Jeffrey Root, Annette Roug, Scott R. Stopak, Gerald W. Wiscomb, Jared R. Zierenberg, Hon S. Ip,[1] Mia K. Torchetti,[1] Thomas J. DeLiberto[1]

Author affiliations: US Department of Agriculture (USDA) National Wildlife Research Center, Fort Collins, Colorado, USA (S.A. Shriner, J.W. Ellis, J.J. Root, T.J. DeLiberto); Utah Division of Wildlife Resources, Salt Lake City, Utah, USA (A. Roug); USDA Wildlife Services, Boise, Idaho, USA (S.R. Stopak); USDA Wildlife Services, Billings, Montana, USA (G.W. Wiscomb); USDA Wildlife Services, Salt Lake City (J.R. Zierenberg); US Geological Survey National Wildlife Health Center, Madison, Wisconsin, USA (H.S. Ip); USDA Veterinary Services, Ames, Iowa, USA (M.K. Torchetti)

DOI: https://doi.org/10.3201/eid2703.204444

In August 2020, outbreaks of coronavirus disease were confirmed on mink farms in Utah, USA. We surveyed mammals captured on and around farms for evidence of infection or exposure. Free-ranging mink, presumed domestic escapees, exhibited high antibody titers, suggesting a potential severe acute respiratory syndrome coronavirus 2 transmission pathway to native wildlife.

We report a wildlife epidemiologic investigation of mammals captured on or near properties in Utah, USA, where outbreaks of severe acute respiratory syndrome coronavirus 2 (SARS-CoV-2) infection occurred in farmed mink. Mink farms are relatively common in the United States, and most are small family farms. The US Department of Agriculture's National Veterinary Services Laboratories (Ames, IA, USA) confirmed SARS-CoV-2 in mink at 2 Utah farms on August 17, 2020, after an investigation by the Utah Veterinary Diagnostic Laboratory and the Washington Animal Disease Diagnostic Laboratory (*1*). SARS-CoV-2 outbreaks have subsequently been confirmed at multiple farms in Utah, Michigan, Wisconsin, and Oregon. Although epidemiologic investigations are ongoing, infected workers are the probable source of the virus's introduction (*2*).

The first reported SARS-CoV-2 infection in mink occurred in the Netherlands in April 2020 (*3*). Since then, dozens of farms in Europe have experienced outbreaks, and more than a million mink have been culled (*2*). Genetic analyses suggest spillover from human infections, and potential zoonotic transmission from mink to a worker is suspected (*4*). Clinical data from mink infected with SARS-CoV-2 indicate the species is highly susceptible and that infections can range from asymptomatic to peracute (*5*).

We captured free-roaming mammals during August 22–30, 2020, by using Sherman (rodents) and Tomahawk (mesocarnivores) traps placed outside of barns and barrier fences on outbreak premises and public lands within a 3.5-km buffer zone. Sample collection included oral, nasal (washes for mice), and rectal swab specimens; tissue specimens; and blood specimens. Swabs were placed in cryovials filled with 0.5 mL viral transport medium, and tissue specimens were placed in plastic sample bags or cryovials. Serum and swab samples were stored on ice, and tissue specimens were flash frozen on dry ice. Most samples were shipped within 24 hours. Swabs and serum samples were shipped to the National Veterinary Services Laboratories, and tissue specimens were sent to the US Geological Survey National Wildlife Health Center (Madison, WI, USA) for testing. All swabs and tissue specimens were tested for SARS-CoV-2 viral RNA by real-time reverse transcription PCR (rRT-PCR) targeting the N1 and N2 genes, and serum samples were tested by virus neutralization assay (*6*). A positive rRT-PCR result was defined as detection of both N1 and N2.

We captured 102 mammals (78 rodents and 24 mesocarnivores). Rodent captures consisted of 45 deer mice (*Peromyscus maniculatus*), 5 *Peromyscus* spp. mice, 25 house mice (*Mus musculus*), and 3 rock squirrels (*Otospermophilus variegatus*). Mesocarnivore captures consisted of 11 presumed escaped American mink (*Neovison vison*), 2 presumed wild American mink, 5 raccoons (*Procyon lotor*), and 6 striped skunks (*Mephitis mephitis*). Presumed escaped mink were closely associated with barns and designated as domestic escapees on the basis of location, behavior, and appearance. We identified wild mink by brown coat color and smaller size compared with farmed mink. All escaped mink and rodents, except for 4 deer mice and 1 rock squirrel, were caught on farm premises. All raccoons, the 2 presumed wild mink, and all but 1 striped skunk were captured off-property but within the buffer zone.

Serum samples from the 11 mink escapees tested positive for SARS-CoV-2 antibodies by virus neutralization (Table). No other animal had a detectable antibody response. Of the antibody-positive escaped mink, 3 also had high cycle threshold (C_t) detections by rRT-PCR of nasal swabs (range C_t 35.89–38.95) and 1 lung tissue specimen (C_t 39.2 for N1). A rectal swab specimen from a house mouse had a high C_t detection by rRT-PCR but was negative for SARS-CoV-2 antibodies. N1 alone was

[1]These senior authors contributed equally to this article.

Table. Virus neutralization titers and rRT-PCR cycle thresholds for samples collected from captured mammals in study of SARS-CoV-2 exposure in escaped mink, Utah, USA, August 2020

Animal ID	Animal	Capture date	Site	Virus neutralization titer	rRT-PCR C_t†	rRT-PCR sample type
ID000003	Escaped mink	2020 Aug 23	A	128	ND	ND
ID000004	Escaped mink	2020 Aug 23	A	128	ND	ND
ID000101	Escaped mink	2020 Aug 24	A	512	ND	ND
ID000010	Escaped mink	2020 Aug 24	A	512	38.80	Nasal swab
ID000011	Escaped mink	2020 Aug 24	A	512	ND	ND
ID000012	Escaped mink	2020 Aug 24	A	512	38.95	Nasal swab
ID000013	Escaped mink	2020 Aug 24	A	128	ND	ND
ID000014	Escaped mink	2020 Aug 24	A	256	‡	Nasal swab, lung tissue
ID000052	Escaped mink	2020 Aug 30	B	64	‡	Nasal swab
ID000053	Escaped mink	2020 Aug 30	B	256	37.38	Nasal swab
ID000054	Escaped mink	2020 Aug 30	B	128	ND	ND
ID000030	Feral or wild mink	2020 Aug 26	C	Negative	ND	ND
ID000051	Feral or wild mink	2020 Aug 28	C	Negative	ND	ND
ID000017	House mouse	2020 Aug 25	C	Negative	35.89	Rectal swab
ID000064	Deer mouse	2020 Aug 30	B	Negative	‡	Oral swab
ID000093	Deer mouse	2020 Aug 31	B	Negative	‡	Rectal swab

*C_t, cycle threshold; rRT-PCR, real-time reverse transcription PCR; SARS-CoV-2, severe acute respiratory syndrome coronavirus 2; ND, not detected.
†Mean C_t across the N1- and N2-genes; a positive result is defined as detection of both N1 and N2.
‡C_t detection of N1-gene only.

detected by rRT-PCR in 2 samples from deer mice (C_t 37.55 and 39.57).

Experimental studies of rodents suggest that Old World rodents (e.g., *Mus*) are resistant to SARS-CoV-2 infection (*7*) and New World species (e.g., *Peromyscus*) are susceptible (A. Fagre, unpub. data, https://doi.org/10.1101/2020.08.07.241810; B.D. Griffin, unpub. data, https://doi.org/10.1101/2020.07.25.221291). Given the demonstrated resistance of house mice to SARS-CoV-2 infection, the high-C_t rectal swab specimen, in absence of other positive results, suggests potential ingestion and excretion of contaminated material (e.g., food, carcasses) rather than infection. In contrast, the antibody responses of all escaped mink combined with high-C_t swab specimens for some animals suggests recent SARS-CoV-2 infections. These exposures in escaped mink are unsurprising given biosecurity practices on some premises did not exclude incursions of escaped mink into barns.

Although we did not find evidence for SARS-CoV-2 establishment in wildlife, the discovery of escaped mink with the opportunity to disperse and interact with susceptible wildlife, such as wild mink or deer mice, is concerning. In Utah, mink farms often overlap with designated critical mink habitats. Interactions or shared resources between escaped mink and wild mink or other wildlife species represent potential transmission pathways for spillover of SARS-CoV-2 into wildlife and could lead to health consequences or establishment of new reservoirs in susceptible wildlife (*8*; A. Fagre, unpub. data, https://doi.org/10.1101/2020.08.07.241810). Heightened biosecurity and best management practices would help prevent accidental releases of infected animals or spillover of SARS-CoV-2 from susceptible species to native wildlife.

Acknowledgments

We thank the private landowners who generously provided land access. We also thank the Utah Veterinary Diagnostic Laboratory for significant support by providing expertise, space, and access to their facility and the Viral Special Pathogens Branch of the Centers for Disease Control and Prevention for sampling protocols and expertise. We thank the dedicated and skilled staff at state and federal agency laboratories that contributed to this study. We additionally thank the One Health Federal Interagency COVID-19 Coordination Team for efforts to facilitate this work.

This research was supported by the US Department of Agriculture, Wildlife Services.

Any use of trade, firm, or product names is for descriptive purposes only and does not imply endorsement by the US Government.

About the Author

Dr. Shriner is a wildlife epidemiologist at the US Department of Agriculture, Animal and Plant Health Inspection Service, Wildlife Services, National Wildlife Research Center. Her primary research interests are wildlife epidemiology and disease ecology.

References

1. Animal and Plant Health Inspection Service. Cases of SARS-CoV-2 in animals in the United States. 2020 Sep 14 [cited 2020 Sep 19]. https://www.aphis.usda.gov/aphis/ourfocus/animalhealth/sa_one_health/sars-cov-2-animals-us
2. Cahan E. COVID-19 hits U.S. mink farms after ripping through Europe. Science. 2020 Aug 18 [cited 2020 Jan 8]. https://www.sciencemag.org/news/2020/08/covid-19-hits-us-mink-farms-after-ripping-through-europe

3. ProMed. Coronavirus disease 2019 update (135): Netherlands (North Brabant) animal, farmed mink. 2020 Apr 27 [cited 2020 Jan 8]. http://www.promedmail.org, archive no. 20200427.7272289.
4. Oreshkova N, Molenaar RJ, Vreman S, Harders F, Oude Munnink BB, Hakze-van der Honing RW, et al. SARS-CoV-2 infection in farmed minks, the Netherlands, April and May 2020. Euro Surveill. 2020;25. https://doi.org/10.2807/1560-7917.ES.2020.25.23.2001005
5. Molenaar RJ, Vreman S, Hakze-van der Honing RW, Zwart R, de Rond J, Weesendorp E, et al. Clinical and pathological findings in SARS-CoV-2 disease outbreaks in farmed mink (*Neovison vison*). Vet Pathol. 2020;57:653–7. https://doi.org/10.1177/0300985820943535
6. McAloose D, Laverack M, Wang L, Killian ML, Caserta LC, Yuan F, et al. From people to *Panthera*: natural SARS-CoV-2 infection in tigers and lions at the Bronx Zoo. MBio. 2020;11:e02220–20. https://doi.org/10.1128/mBio.02220-20
7. Bao L, Deng W, Huang B, Gao H, Liu J, Ren L, et al. The pathogenicity of SARS-CoV-2 in hACE2 transgenic mice. Nature. 2020;583:830–3. https://doi.org/10.1038/s41586-020-2312-y
8. Olival KJ, Cryan PM, Amman BR, Baric RS, Blehert DS, Brook CE, et al. Possibility for reverse zoonotic transmission of SARS-CoV-2 to free-ranging wildlife: a case study of bats. PLoS Pathog. 2020;16:e1008758. https://doi.org/10.1371/journal.ppat.1008758

Address for correspondence: Susan A. Shriner, USDA APHIS Wildlife Services National Wildlife Research Center, 4101 LaPorte Ave, Fort Collins, CO, 80521, USA; email: Susan.A.Shriner@usda.gov

Mycobacterium bovis Infection in Free-Ranging African Elephants

Michele A. Miller, Tanya J. Kerr, Candice R. de Waal, Wynand J. Goosen, Elizabeth M. Streicher, Guy Hausler, Leana Rossouw, Tebogo Manamela, Louis van Schalkwyk, Léanie Kleynhans, Robin Warren, Paul van Helden, Peter E. Buss

Author affiliations: Stellenbosch University, Cape Town, South Africa (M.A. Miller, T.J. Kerr, C.R. de Waal, W.J. Goosen, E.M. Streicher, G. Hausler, L. Kleynhans, P. van Helden); South African National Parks, Skukuza, South Africa (L. Rossouw, T. Manamela, P.E. Buss); Skukuza State Veterinarian Office, Skukuza (L. van Schalkwyk); South African Medical Research Council Centre for Tuberculosis Research, Cape Town (R. Warren)

DOI: https://doi.org/10.3201/eid2703.204729

Mycobacterium bovis infection in wildlife species occurs worldwide. However, few cases of *M. bovis* infection in captive elephants have been reported. We describe 2 incidental cases of bovine tuberculosis in free-ranging African elephants (*Loxodonta africana*) from a tuberculosis-endemic national park in South Africa and the epidemiologic implications of these infections.

Tuberculosis (TB), caused by the human pathogen *Mycobacterium tuberculosis*, is a recognized disease in human-managed and wild Asian elephants (*Elephas maximus*) and African elephants (*Loxodonta africana*) (*1*–*3*). Previous findings demonstrate the importance of human-elephant interfaces for transmission. However, range countries for African and Asian elephants also have high burdens of bovine TB, caused by *M. bovis*. The World Organisation for Animal Health (OIE) records cases of bovine TB; in the 49 elephant range countries in Africa and Asia, only Namibia is declared free of *M. bovis* (*4*). Therefore, the paucity of cases of *M. bovis* infection in elephants is unexpected. The lack of *M. bovis* cases in elephants may be caused by rare or sporadic exposure, innate resistance of the species, or limited surveillance, especially in environments to which bovine TB is endemic.

Kruger National Park (KNP) in South Africa has recorded *M. bovis* infection in >20 wildlife species and is considered a bovine TB–endemic area. Although cases of *M. bovis* infection have been reported in other large herbivores, such as black rhinoceros (*Diceros bicornis*) and white rhinoceros (*Ceratotherium simum*) (*5*,*6*), only 1 case of *M. tuberculosis* infection has been found in an elephant in KNP (*3*), despite hundreds of individual animals examined during 1967–1994 when elephants were harvested (*7*). After the discovery of an *M. tuberculosis*–infected adult bull elephant in 2016 (*3*), opportunistic sampling of elephants was implemented by park veterinarians.

In May 2018, a young bull elephant (E1; estimated age 18–20 years) was fatally shot in the southern part of KNP. In addition, a young bull elephant (E2; estimated age 3 years) in KNP was euthanized in October 2019 after being found moribund. Postmortem examination of E1 revealed rare small, consolidated masses in the lung. Elephant 2 had several focal firm masses (1–2 cm^2) scattered in the lung containing caseous material and some mineralization. We took representative samples from the peripheral (prescapular, inguinal, popliteal), head (parotid, retropharyngeal), thoracic (tracheobronchial), and abdominal (mesenteric) lymph nodes; lung lesions were also sampled. We froze samples at −20°C and

Table. *Mycobacterium bovis* information and spoligotype patterns for isolates from 2 African elephants, South Africa*

Sample no.	Year	Species	Spoligotype pattern	Spoligotype no.
E1	2018	*M. bovis*	■■□■■■■■□■■■■■■□■■■■□■■■■■■■■■■■■■■■□□□□□	SB0121
E2	2019	*M. bovis*	■■□■■■■■□■■■■■■□■■■■□■■■■■■■■■□■■■■■■■□□□□□	SB1681

*Isolates were identified by mycobacterial culture and speciation.

transported them for mycobacterial culture and speciation in the Biosafety Level 3 laboratories at Stellenbosch University (Cape Town, South Africa) and ARC-Onderstepoort Veterinary Institute (Pretoria, South Africa).

We prepared tissues for mycobacterial culture as previously described (*8*) using the BD BACTEC MGIT 960 Mycobacterial Detection System (Becton Dickinson, https://www.bd.com). We performed mycobacterial speciation by region-of-difference PCR (*8*) and spoligotyping (*9*) on Ziehl-Neelsen stain positive cultures. We isolated *M. bovis* from both tracheobronchial lymph node cultures from E1. Culture results from E2 confirmed the presence of *M. bovis* in 2 lung samples in 2 different laboratories, and in a tracheobronchial lymph node cultured in the second laboratory. We characterized the *M. bovis* spoligotype pattern from E1 as SB0121, which is the most common strain found in KNP (*9*) (Table). In contrast, in E2 we found a novel spoligotype pattern (SB1681) not previously reported in KNP (Table). However, this pattern varied by 1 spacer, and it is possible that this strain evolved from the common SB0121 strain in KNP.

The finding of *M. bovis* infection in 2 free-ranging African elephants in KNP has significance for other elephant populations in bovine TB–endemic areas. In South Africa, the Department of Agriculture, Land Reform, and Rural Development has the authority to place *M. bovis*–infected premises under quarantine. Previously, elephants and rhinoceros were excluded from movement restrictions placed on other species in bovine TB–endemic populations. However, our findings require revisiting this assumption and investigating disease transmission risks for these species. Kerr et al., in a retrospective study investigating antibodies to *M. tuberculosis* complex antigens in KNP elephants, has estimated seroprevalence at 6%–9% (*10*), suggesting that *M. bovis* and possibly *M. tuberculosis* infection is more common in KNP than previously thought. However, no additional samples were available to confirm infection in the individual elephants studied. It is more likely that these seropositive responses in elephants represent infection with *M. bovis* because all the cases of TB in rhinoceros to date have been due to *M. bovis* infection (*5*,*6*). Isolation and speciation of pathogenic mycobacteria are essential for understanding the epidemiology of these infections, especially in areas where human–livestock–wildlife interfaces occur.

Our findings emphasize the importance of surveillance using molecular and bacteriological tools for detection of bovine TB in elephants because serologic assays and visual assessment of gross and histopathological lesions cannot differentiate between infection with *M. bovis* and *M. tuberculosis*. In areas where elephants may have indirect (through shared forage and water sources) or direct contact with animal and human populations with high burdens of *M. bovis* and *M. tuberculosis*, such as African and Asian range countries, it is crucial that surveillance and diagnostic tools are readily available to distinguish these pathogens to improve our understanding of epidemiology of TB at human–livestock–wildlife interfaces.

Acknowledgments

We thank the South African National Parks (SANParks) Veterinary Wildlife Services for providing the samples.

Financial support for this research was provided by the South African Medical Research Council (SAMRC) Centre for Tuberculosis Research, the National Research Foundation (NRF) South African Research Chair Initiative (SARChI; grant no. 86949), Harry Crossley Foundation (HCF; 2018–2020), and Stellenbosch University Faculty of Medicine and Health Science. Funding to T.J.K. was provided through NRF SAMRC Centre for TB Research Postdoctoral Fellowship. Funding to W.J.G. was provided by a National Geographic Society Explorer Grant (no. S006337). Funding to C.R.D. was provided through NRF Innovation Master's Scholarship (grant no. 113511).

The content is the sole responsibility of the authors and does not necessarily represent the official views of the South African Medical Research Council or National Research Foundation. Ethics approval for the sample acquisition and testing of these animals was granted by the Stellenbosch University Animal Care and Use Committee (SU-ACU 2018-6308), and South African National Parks Animal Care and Use Committee (SANParks Research Agreement BUSP1511). Section 20 approval was granted by the South African Department of Agriculture, Land Reform and Rural Development (DALRRD) formerly the Department of Agriculture, Forestry, and Fisheries (DAFF Section 20: 12/11/1/7/6).

About the Author

Prof. Miller is the South African Research Chair in Animal TB in the Department of Science and Innovation—National Research Foundation Centre of Excellence for Biomedical TB Research and South African Medical Research Council Centre for TB Research at Stellenbosch University. Her research interests include TB in animals and One Health approaches to multi-species pathogens.

References

1. Chandranaik BM, Shivashankar BP, Umashankar KS, Nandini P, Giridhar P, Byregowda SM, et al. *Mycobacterium tuberculosis* infection in free-roaming wild Asian elephant. Emerg Infect Dis. 2017;23:555–7. https://doi.org/10.3201/eid2303.161439
2. Mikota SK, Maslow JN. Tuberculosis at the human–animal interface: an emerging disease of elephants. Tuberculosis (Edinb). 2011;91:208–11. https://doi.org/10.1016/j.tube.2011.02.007
3. Miller MA, Buss P, Roos EO, Hausler G, Dippenaar A, Mitchell E, et al. Fatal tuberculosis in a free-ranging African elephant and One Health implications of human pathogens in wildlife. Front Vet Sci. 2019;6:18. https://doi.org/10.3389/fvets.2019.00018
4. World Organisation for Animal Health. Bovine tuberculosis [cited 2020 Dec 8]. https://www.oie.int/en/animal-health-in-the-world/animal-diseases/bovine-tuberculosis
5. Miller M, Buss P, van Helden P, Parsons S. *Mycobacterium bovis* in a free-ranging black rhinoceros, Kruger National Park, South Africa, 2016. Emerg Infect Dis. 2017;23:557–8. https://doi.org/10.3201/eid2303.161622
6. Miller MA, Buss P, Parsons SDC, Roos E, Chileshe J, Goosen WJ, et al. Conservation of white rhinoceroses threatened by bovine tuberculosis, South Africa, 2016–2017. Emerg Infect Dis. 2018;24:2373–5. https://doi.org/10.3201/eid2412.180293
7. van Aarde R, Whyte I, Pimm S. Culling and the dynamics of the Kruger National Park African elephant population. Anim Conserv. 1999;2:287–94. https://doi.org/10.1111/j.1469-1795.1999.tb00075.x
8. Goosen WJ, Miller MA, Chegou NN, Cooper D, Warren RM, van Helden PD, et al. Agreement between assays of cell-mediated immunity utilizing *Mycobacterium bovis*–specific antigens for the diagnosis of tuberculosis in African buffaloes (*Syncerus caffer*). Vet Immunol Immunopathol. 2014;160:133–8. https://doi.org/10.1016/j.vetimm.2014.03.015
9. Dippenaar A, Parsons SDC, Miller MA, Hlokwe T, Gey van Pittius NC, Adroub SA, et al. Progenitor strain introduction of *Mycobacterium bovis* at the wildlife–livestock interface can lead to clonal expansion of the disease in a single ecosystem. Infect Genet Evol. 2017;51:235–8. https://doi.org/10.1016/j.meegid.2017.04.012
10. Kerr TJ, de Waal CR, Buss PE, Hofmeyr J, Lyashchenko KP, Miller MA. Seroprevalence of *Mycobacterium tuberculosis* complex in free-ranging African elephants (*Loxodonta africana*) in Kruger National Park, South Africa. J Wildl Dis. 2019;55:923–7. https://doi.org/10.7589/2018-12-292

Address for correspondence: M.A. Miller, Department of Science and Innovation—National Research Foundation Centre of Excellence for Biomedical Tuberculosis Research, South African Medical Research Council Centre for Tuberculosis Research, Division of Molecular Biology and Human Genetics, Faculty of Medicine and Health Sciences, Stellenbosch University, PO Box 241, Cape Town 8000, South Africa; email: miller@sun.ac.za

Bats and Viruses: Current Research and Future Trends

Eugenia Corrales-Aguilar and Martin Schwemmle, editors; Caister Academic Press, Poole, UK; Bats and Viruses: Current Research and Future Trends, 2020; ISBN: 978-1-912530-14-4 (paperback); 978-1-912530-15-1 (e-book); Pages: 230; Price: $319

DOI: http://doi.org/10.3201/eid2703.204561

Fluttering above us at dusk, bats evoke awe and wonder as they signal the coming of the night. Bats are native to every continent but Antarctica, and they often live in or enter human-occupied spaces. They are highly diverse, both phylogenetically and ecologically. Bats also carry zoonotic diseases, including many of the viruses discussed in the new book *Bats and Viruses*, edited by Eugenia Corrales-Aguilar and Martin Schwemmle. Bats' diversity, frequent proximity to humans, and carriage of zoonotics make them an important and often poorly understood component of public health and infectious disease.

Bats and Viruses sets out to review hot topics in current research, and it also provides background information accessible to those without specific expertise in this particular field. It is a highly technical volume that is unlikely to be readily accessible to a general audience. It is, however, understandable to a reader outside of the immediate technical area of bats and viruses, especially those with technical backgrounds in zoonotics and infectious disease; wildlife biology, including wildlife ecology; evolutionary biology, and phylogenetics; and molecular and cellular biology.

In addition to a review of current topics, the book provides background in bat biology and virology; this is of great value to a reader who is not deeply experienced in this technical area. Each chapter includes an extensive references section, providing even more opportunity to delve deeply into the background.

The organization of the book is logical. About half of the chapters are organized by taxonomy of the viruses being covered: flaviviruses, alphaviruses, influenza A–like viruses, coronaviruses, hantaviruses, polyomaviruses. Two chapters cover immunity in bats: one on innate immunity, the other on adaptive immunity. Three chapters address techniques used to study virology of bats: isolation of viruses; in vivo techniques, including coverage of bat husbandry; metagenomics.

Given the current pandemic, the chapter that many will open up to first is "Bats and Coronaviruses," by Susanna K. P. Lau, et al. This chapter is clearly understandable to a reader without expertise in the field of bat biology and virology, contains a lucid history of coronaviruses, and focuses in on some of the more well-known coronaviruses, such as severe acute respiratory syndrome and Middle East respiratory syndrome viruses. Although other chapters cover coronaviruses, this information is not indicated in the index; a more comprehensive index would be helpful to guide the reader across the multiplicity of topics covered in this multiauthored volume.

This book would be useful for scientific libraries seeking a technical overview of current topics in bats and viruses with an emphasis on human health effects. It is accessible to readers with backgrounds in infectious disease, wildlife biology, and molecular or cellular biology and would be of interest to those readers who want to know more about how those different fields interact.

David Hewitt

Author affiliation: US Department of Housing and Urban Development, Washington, DC, USA

Address for correspondence: David Hewitt, 4835 Cordell Ave, Bethesda, MD 20814-3156, USA; email: davidhewitt@post.harvard.edu

Strange Case of a Sojourn in Saranac

Terence Chorba

Robert Louis Stevenson, the renowned Scottish author and poet, was born in 1850 in Edinburgh, Scotland. From childhood onward, he suffered from frequent chest infections, fevers, and hemoptysis. This master who gave us *Treasure Island* (1881–83), *A Child's Garden of Verses* (1885), *Kidnapped* (1886), and *Strange Case of Dr Jekyll and Mr Hyde* (1886) lived his brief 44 years in an era when tuberculosis (then called consumption) was widespread in Europe but laboratory and radiologic diagnostics were not available.

On March 24, 1882, the date on which World TB Day is based, Robert Koch announced his discovery of the causative organism of tuberculosis, *Mycobacterium tuberculosis*. Through Koch's use of alkalinized methylene blue stain and a brown counterstain for contrast, this discovery laid to rest the theory that tuberculosis was congenital, a belief stemming from its extensive occurrence in families. In 1895, Wilhelm Röntgen first described the potential medical application of radiography when he captured the image of the bony and soft-tissue structures of his wife's hand on a photographic plate. Without bacteriology or radiography, Stevenson's persistently cachectic body habitus and pulmonary symptoms were thought to be consistent with tuberculosis, although other diagnoses have been proposed. These have included chronic idiopathic bronchiectasis, sarcoidosis, and hereditary hemorrhagic telangiectasia, any of which could potentially have been exacerbated by residual scarring from the bouts of pneumonia he experienced as a child and by his chain-smoking as an adult.

By 1887, Stevenson had achieved considerable wealth from his writings and acted on medical advice to seek a climate drier than that of the British Isles. He and his family set out for Colorado, but upon arriving in Massachusetts, he learned of the growing reputation of physician Edward Livingston Trudeau, who founded the Adirondack Cottage Sanatorium at Saranac Lake, New York, for the cure of pulmonary tuberculosis. In October 1887, Stevenson, together with his wife, his mother, his stepson, and a family servant, moved into Baker Cottage, a house adjacent to the sanatorium. Stevenson remained there through the winter and produced many essays for *Scribner's Magazine* and completed most of a novel, *The Master of Ballantrae*. Trudeau was unable to demonstrate the presence of tubercle bacilli in Stevenson's sputum. Stevenson left the sanatorium in April 1888 and travelled to San Francisco, Hawaii, and the Samoan Islands, where he died in 1894.

In 1915, the Saranac Chapter of the Stevenson Society commissioned John Gutzon Borglum, an American sculptor, to create the bronze bas-relief featured on the cover of this month's journal, to adorn the wall of Baker Cottage in memory of Stevenson. Relief is the term used to describe sculptural images that remain attached to a solid background plane of the material out of which the images themselves have been sculpted. Bas-relief is relief in which images of faces or figures are rendered with less depth than they possess in life and in which no aspect of the image is cut away from the underside. The master of this technique in America was Augustus Saint-Gaudens (1848–1907), an inspiration to Borglum and fellow alumnus of the École des Beaux-Arts in Paris. Saint-Gaudens created the exquisite $20 US gold coin with the standing female figure of Liberty set in bas-relief, minted from 1907 through 1933 (Figure 1). Of the Saranac bas-relief, the *New York Times* article from the day of the unveiling described the intent of the artist: "[Stevenson is] shown walking on the veranda where…he says in his letters he gained inspiration for Ballantrae and the great Scribner essays. The figure, in fur cap and coat,

Figure 1. Double Eagle, US $20 gold (fineness 0.9000) coin, 34 mm, 33.436 g, designed by Augustus Saint-Gaudens, 1907. Obverse: Bas relief representation of Liberty, personified by a tall, robed woman striding forward, bearing a torch in her right hand and an olive branch in her left hand. Rays of a sunrise in the background. Reverse: Young eagle in flight, silhouetted by the rays of a sunrise. National Numismatic Collection, National Museum of American History, Washington, DC., USA. Photograph by Jaclyn Nash.

Author affiliation: Centers for Disease Control and Prevention, Atlanta, Georgia, USA

DOI: https://doi.org/10.3201/eid2703.AC2703

Figure 2. Gutzon Borglum. Statue of E.L. Trudeau, 1918. Bronze. From Historic Saranac Lake Wiki. Originally erected at the Adirondack Cottage Sanatorium. Moved to the Trudeau Institute, Saranac Lake, New York, 1964. The statue is a representation of E. L. Trudeau as a male tuberculosis patient with a blanket folded on his lap. In the pedestal is an inscription with a folk-saying favorite of Trudeau, "*Guerir quelquefois, soulager souvent, consoler toujours*" (To cure sometimes, to relieve often, to comfort always). Trudeau started the facility, which has been credited with being the first sanatorium in the United States, at Saranac Lake in 1885, at the dawn of the nation's sanatorium movement, which peaked with over 108,000 beds in 1954. Sanatoriums remained the standard of care for tuberculosis for over half a century in the United States; after streptomycin was discovered in 1943 and antimicrobial drugs were subsequently used to treat and cure tuberculosis, sanatoriums closed or were transformed into general hospitals.

a thin hand clutching the collar together in the face of the zero blast, breathes the spirit of the sick man out of doors, and the lift of the head as he says 'Come, let us make a tale!' reveals the rare spirit of the heroic in physical adversity." After Edward Trudeau died in 1915, Borglum was also commissioned to craft a life-size statue of the founder for the Saranac sanatorium (Figure 2).

Borglum was born to Mormons in Idaho in 1867, but grew up in Nebraska and Kansas, where he began his formal art training. At age 22, he enrolled at the Académie Julian and the École des Beaux-Arts, where sculptor Auguste Rodin (1840–1917) was one of his instructors. Over the next several years, Borglum developed more skills and success as a sculptor in Spain and England. In 1901, he embarked on a prolific period in America; his works include the equestrian bronze in Sheridan Circle in Washington, DC, some of the statuary of the Cathedral of St. John the Divine in New York City, a memorial to the fallen North Carolina infantry from Pickett's Charge at Gettysburg, and a bust of Abraham Lincoln now in the United States Capitol crypt. He had white supremacist leanings, and in 1915, the same year he made the Saranac bronze bas-relief, he also was hired to begin a granite bas-relief carving to honor the Confederacy on Stone Mountain, Georgia. In 1925, controversy with the committee who gave him the commission ended with his being fired and his work being blasted off the mountain's face, but the experience gave him knowledge of the methods for sculpting on a scale that made possible his subsequent creation of the national monument at Mount Rushmore. From 1927 until his death in 1941, Borglum labored on that project, his greatest opus. Carved into granite in the Black Hills of South Dakota on land that had been illegally seized from the Lakota tribe during a gold rush in the 1870s, this national memorial has also been the subject of criticism for aspects of the actions of each of the men it memorializes. Even there, a bas-relief quality informs the work, especially in the image of Abraham Lincoln, rising out from within the rock toward the viewer.

The Saranac bas-relief was a piece of genius for Borglum. Stevenson emerges from the flat plane of the bronze to convey the image of *spes phthisica*, a storied term used in the nineteenth century to refer to an elated mental state thought to be experienced by creative people with consumption, which inspired them to produce great works.

Bibliography

1. Furnas JC. Voyage to windward: the life of Robert Louis Stevenson. New York: William Sloane Associates; 1951.
2. Guttmacher AE, Callahan JR. Did Robert Louis Stevenson have hereditary hemorrhagic telangiectasia? Am J Med Genet. 2000;91:62–5. https://doi.org/10.1002/(SICI)1096-8628(20000306)91:1<62::AID-AJMG11>3.0.CO;2-3
3. Harman C. Myself and the other fellow: a life of Robert Louis Stevenson. New York: HarperCollins Publishers; 2006.
4. Koch R. The etiology of tuberculosis [in German]. Berliner Klinische Wochenschrift 1882;19:221–30. (English version available as Pinner M, Pinner BR, Krause AK. Koch R. The aetiology of tuberculosis: a translation) [cited 2021 Feb 3]. https://www.worldcat.org/title/aetiology-of-tuberculosis/oclc/14746066
5. Morens DM. At the deathbed of consumptive art. Emerg Infect Dis. 2002;8:1353–8. https://doi.org/10.3201/eid0811.020549
6. Saranac unveils Stevenson tablet. New York Times. October 31, 1915. p. 12 [cited 2021 Jan 25]. https://timesmachine.nytimes.com/timesmachine/1915/ 10/31/101570271.html?pageNumber=12
7. Peters P. W.C. Roentgen and the discovery of x-rays. In: Textbook of radiology. New York: GE Healthcare; 1995 [cited 2021 Jan 25]. https://archive.is/20080511205052/http:/www.medcyclopaedia.com/library/radiology/chapter01.aspx
8. Shaff H, Shaff AK. Six wars at a time: the life and times of Gutzon Borglum, sculptor of Mt. Rushmore. 5th ed. Sioux Falls (SD): Center for Western Studies; 1985.
9. Sharma OP. Murray Kornfeld, American College of Chest Physician, and sarcoidosis: a historical footnote: 2004 Murray Kornfeld Memorial Founders Lecture. Chest. 2005;128:1830–5. https://doi.org/10.1016/S0012-3692(15)52223-X
10. Woodhead R. The strange case of R.L. Stevenson. Edinburgh (UK): Luath Press; 2001.

Address for correspondence: Terence Chorba, Centers for Disease Control and Prevention, 1600 Clifton Rd NE, Mailstop US 12-4, Atlanta, GA 30329-4027, USA; email: tlc2@cdc.gov

EMERGING INFECTIOUS DISEASES®

Upcoming Issue

- Systematic Review of Reported HIV Outbreaks, Pakistan, 2000–2019
- Animal Reservoirs and Hosts for Emerging Alphacoronavirsuses and Betacoronaviruses
- Emergence of Human Monkeypox and Declining Population Immunity in the Context of Urbanization, Nigeria, 2017–2020
- Characteristics of COVID-19 among Meat Processing Industry Workers in Nebraska and the Effectiveness of Select Risk Mitigation Measures
- Blastomycosis Surveillance in 5 States, United States, 1987–2018
- Infections with Tickborne Pathogens after Tick Bite, Austria, 2015–2018
- Epidemiologic and Genomic Reidentification of Yaws, Liberia
- Dynamic Public Perceptions of the Coronavirus Disease Crisis, the Netherlands, 2020
- Identifying Sexual Contact as a Risk Factor for Campylobacter Infection
- COVID-19–Associated Pulmonary Aspergillosis, March–August 2020
- Improving Treatment and Outcomes for Melioidosis in Children, Northern Cambodia, 2009–2018
- Characteristics and Risk Factors of Hospitalized and Nonhospitalized COVID-19 Patients, Atlanta, Georgia, USA, March–April 2020
- Rare Norovirus GIV Foodborne Outbreak, Wisconsin, USA
- Venezuelan Equine Encephalitis Complex Alphavirus in Bats, French Guiana
- Post-Vaccination COVID-19 among Healthcare Workers, Israel
- SARS-CoV-2 Seropositivity among US Marine Recruits Attending Basic Training, United States, Spring–Fall 2020
- High Human Anthrax Case Fatality Rate in Northern Ghana, 2005–2016
- Genomic Analysis of Novel Poxvirus Brazilian Porcupinepox Virus, Brazil, 2019
- Surveillance of COVID-19–Associated Multisystem Inflammatory Syndrome in Children, South Korea
- Fatal Case of Crimean-Congo Hemorrhagic Fever Caused by Reassortant Virus, Spain, 2018
- Stability of SARS-CoV-2 RNA in Nonsupplemented Saliva
- Increasing SARS-CoV-2 Testing Capacity with Pooled Saliva Samples
- Persistence of SARS-CoV-2 N-Antibody Response in Healthcare Workers, London, UK
- Increased Likelihood of Detecting Ebola Virus RNA in Semen by Using Sample Pelleting
- Experimental SARS-CoV-2 Infection of Bank Voles
- Inguinal Ulceroglandular Tularemia Caused by *Francisella tularensis* Subspecies *holarctica*, Canada
- Risk for Fomite-Mediated Transmission of SARS-CoV-2 in Child Daycares, Schools, and Offices
- Novel SARS-CoV-2 Variant Identified in Travelers from Brazil to Japan
- Imported SARS-COV-2 Variant P.1 Detected in Traveler Returning from Brazil to Italy

Complete list of articles in the April issue at http://www.cdc.gov/eid/upcoming.htm

Earning CME Credit

To obtain credit, you should first read the journal article. After reading the article, you should be able to answer the following, related, multiple-choice questions. To complete the questions (with a minimum 75% passing score) and earn continuing medical education (CME) credit, please go to http://www.medscape.org/journal/eid. Credit cannot be obtained for tests completed on paper, although you may use the worksheet below to keep a record of your answers.

You must be a registered user on http://www.medscape.org. If you are not registered on http://www.medscape.org, please click on the "Register" link on the right hand side of the website.

Only one answer is correct for each question. Once you successfully answer all post-test questions, you will be able to view and/or print your certificate. For questions regarding this activity, contact the accredited provider, CME@medscape.net. For technical assistance, contact CME@medscape.net. American Medical Association's Physician's Recognition Award (AMA PRA) credits are accepted in the US as evidence of participation in CME activities. For further information on this award, please go to https://www.ama-assn.org. The AMA has determined that physicians not licensed in the US who participate in this CME activity are eligible for AMA PRA Category 1 Credits™. Through agreements that the AMA has made with agencies in some countries, AMA PRA credit may be acceptable as evidence of participation in CME activities. If you are not licensed in the US, please complete the questions online, print the AMA PRA CME credit certificate, and present it to your national medical association for review.

Article Title

Fluconazole-Resistant *Candida glabrata* Bloodstream Isolates, South Korea, 2008–2018

CME Questions

1. You are advising an infectious disease practice about management of fluconazole-resistant (FR) *Candida glabrata* bloodstream isolates (BSI). On the basis of the study of South Korean multicenter surveillance cultures collected during an 11-year period (2008–2018) by Won and colleagues, which one of the following statements about mortality and antifungal resistance of *C. glabrata* BSI is correct?

A. 2.7% of collected isolates were FR (minimum inhibitory concentration [MIC] ≥64 mg/L)
B. 30- and 90-day mortality rates were significantly higher in patients with FR vs fluconazole-susceptible dose-dependent (F-SDD) isolates
C. Appropriate antifungal therapy was not an independent protective factor against mortality in patients with FR isolates
D. The rate of FR remained stable from 2008 to 2018

2. According to the study of South Korean multicenter surveillance cultures collected during an 11-year period (2008–2018) by Won and colleagues, which one of the following statements about antifungal resistance molecular mechanisms of FR *C. glabrata* BSI isolates is correct?

A. 98.5% of FR isolates, but only 0.9% of F-SDD isolates, had 1 to 2 additional Pdr1p amino-acid substitutions (AAS) except genotype-specific Pdr1p AAS, based on PDR1 sequencing
B. Multilocus sequence typing (MLST) showed that one quarter of FR isolates belonged to ST 7
C. AAS in FR isolates occurred only in the inhibition domain of Pdr1p
D. The P76S and P143T AAS were specific to FR isolates

3. On the basis of the study of South Korean multicenter surveillance cultures collected during an 11-year period (2008–2018) by Won and colleagues, which one of the following statements about clinical and public health implications of outcomes and antifungal resistance molecular mechanisms of FR *C. glabrata* BSI isolates is correct?

A. Although FR increased from 2008 to 2018, echinocandin resistance decreased
B. The findings suggest that the high mortality rate of FR *C. glabrata* BSIs is caused solely by FR
C. The findings suggest that 5 MLST genotype-specific Pdr1p AAS are responsible for azole resistance
D. Increasing prevalence of FR BSI isolates of *C. glabrata* worldwide mandates efforts to improve their detection and implement appropriate antifungal therapy

Earning CME Credit

To obtain credit, you should first read the journal article. After reading the article, you should be able to answer the following, related, multiple-choice questions. To complete the questions (with a minimum 75% passing score) and earn continuing medical education (CME) credit, please go to http://www.medscape.org/journal/eid. Credit cannot be obtained for tests completed on paper, although you may use the worksheet below to keep a record of your answers.

You must be a registered user on http://www.medscape.org. If you are not registered on http://www.medscape.org, please click on the "Register" link on the right hand side of the website.

Only one answer is correct for each question. Once you successfully answer all post-test questions, you will be able to view and/or print your certificate. For questions regarding this activity, contact the accredited provider, CME@medscape.net. For technical assistance, contact CME@medscape.net. American Medical Association's Physician's Recognition Award (AMA PRA) credits are accepted in the US as evidence of participation in CME activities. For further information on this award, please go to https://www.ama-assn.org. The AMA has determined that physicians not licensed in the US who participate in this CME activity are eligible for AMA PRA Category 1 Credits™. Through agreements that the AMA has made with agencies in some countries, AMA PRA credit may be acceptable as evidence of participation in CME activities. If you are not licensed in the US, please complete the questions online, print the AMA PRA CME credit certificate, and present it to your national medical association for review.

Article Title

Effectiveness of Preventive Therapy for Persons Exposed at Home to Drug-Resistant Tuberculosis, Karachi, Pakistan

CME Questions

1. You are seeing a 45-year-old man diagnosed recently with a pulmonary infection with multidrug-resistant tuberculosis (MDR TB). What can you tell him about the epidemiology and prognosis of MDR TB?

A. Tuberculosis trails only infection with Shigella species as the leading infectious cause of death globally
B. The success rate for treatment of MDR TB is approximately 55%
C. MDR TB is defined by resistance to isoniazid and ethambutol
D. MDR TB is unlikely to spread to household contacts

2. The patient lives with 5 other people in a 2-bedroom apartment. Which one of the following variables are risk factors for incident infection with tuberculosis among his contacts?

A. Age 20 to 25 years and obesity
B. Age 10 to 19 years and underweight
C. Age 5 to 10 years and obesity
D. Age less than 5 years and underweight

3. You decide to treat several members of this patient's family with levofloxacin and ethambutol to prevent incident tuberculosis. In the main study analysis of the current study, what were the incidence rate ratio (IRR) and number needed to treat (NNT) comparing observed vs expected cases of tuberculosis associated with preventive therapy?

A. IRR, 0.87; NNT 412
B. IRR, 0.40; NNT 64
C. IRR, 0.22; NNT 16
D. IRR, 0.08; NNT 4

4. What did the additional analyses of the efficacy of preventive therapy in the prevention of incident tuberculosis in the current study show?

A. They reinforced that preventive therapy was effective
B. They demonstrated that preventive therapy was not significantly effective
C. They demonstrated that preventive therapy was only effective among adults
D. They demonstrated that only combinations which included moxifloxacin were effective